Heinrich-Heine-Universität Düsseldorf

Universitätsklinikum Düsseldorf

ADULT NEUROGENESIS AND COGNITIVE TRAINING AS IMPACT FACTORS ON THE RECEPTOR ARCHITECTURE OF THE MOUSE OLFACTORY SYSTEM

INAUGURAL-DISSERTATION

zur Erlangung des Doktorgrades

der Mathematisch-Naturwissenschaftlichen Fakultät

der Heinrich-Heine-Universität Düsseldorf

vorgelegt von

Kimberley Lothmann

aus Ludwigsburg

Düsseldorf, Oktober, 2022

aus dem Cécile und Oskar Vogt Institut für Hirnforschung

der Heinrich-Heine-Universität Düsseldorf

Gedruckt mit der Genehmigung der

Mathematisch-Naturwissenschaftlichen Fakultät der

Heinrich-Heine-Universität Düsseldorf

Berichterstatter:

1. Prof. Dr. Katrin Amunts

2. Prof. Dr. Dieter Willbold

Tag der mündlichen Prüfung: 28. 02. 2023

I'm still standing.

Sir Elton John

Index

Publications

Lothmann, K., Amunts, K., and Herold, C. (2021). **The Neurotransmitter Receptor Architecture of the Mouse Olfactory System.** *Front Neuroanat* 15, 632549. doi: 10.3389/fnana.2021.632549.

Author contribution statement

Kimberley Lothmann performed the analysis of the receptor autoradiograms, designed the figures, evaluated the results and wrote the draft of the manuscript. Prof. Dr. Katrin Amunts provided critical feedback and expertise for the manuscript. Dr. Christina Herold designed the study, verified the methods and supervised the project. Prof. Dr. Katrin Amunts and Dr. Christina Herold acquisitioned funding for the project. All authors reviewed and edited the manuscript during each stage and approved the final manuscript.

Lothmann, K., Deitersen, J., Zilles, K., Amunts, K., and Herold, C. (2020). **New boundaries and dissociation of the mouse hippocampus along the dorsal-ventral axis based on glutamatergic, GABAergic and catecholaminergic receptor densities.** *Hippocampus* n/a(n/a). doi: 10.1002/hipo.23262.

List of abbreviations

α_1	Alpha-1 adrenergic receptor
α_2	Alpha-2 adrenergic receptor
AC	Astrocyte
AIC	5-amino-imidazole-4-carboxamide
AMPA	Alpha-amino-3-hydroxy-5-methyl-4-isoxazolepropionic acid
AOB	Accessory olfactory bulb
AOC	Anterior olfactory cortex
AR	Autoradiogram
A_S	Specific activity
BC	Astrocyte-like B-type stem cell
BrdU	Bromodeoxyuridine, 5-bromo-2'-deoxyuridine
BV	Blood vessel
CC	Corpus callosum
CG	Control group
C_{KB}	Adjusted receptor concentration
CG_{TMZ}	Experimental group with suppressed adult neurogenesis
DP	Dorsal peduncular cortex
EC	Ependymal cell
ENTl	Entorhinal cortex, lateral
ENTm	Entorhinal cortex, medial
EPd	Endopiriform nucleus, dorsal
epl	External plexiform layer
GABA	γ-aminobutyric acid
$GABA_A$	γ-aminobutyric acid, type A
$GABA_{A(BZ)}$	γ-aminobutyric acid, type A, benzodiazepine binding sites
$GABA_B$	γ-aminobutyric acid, type B
GC	Granule cell
GFAP	Glial fibrillary acidic protein
Gl	glomerular cell layer
GL	Glomeruli olfactorii
ipl	Internal plexiform layer
Kainate	kainic acid receptor
K_D	dissociation constant

L	Ligand
lot	lateral olfactory tract
LV	lateral ventricle
MC	Mitral cell
mi	mitral cell layer
MOB	Main olfactory bulb
MTIC	3-methyl-(triazen-1-yl)imidazole-4-carboxamide
MWM	Morris water maze
MWM_{CG}	Experimental group with cognitive training
MWM_{TMZ}	Cognitively trained group with suppressed adult neurogenesis
$mGlu_{2/3}$	Metabotropic glutamate receptor 2/3
N	Neuroblast
NaCl	Sodium chloride
NB	Nonspecific binding
NeuN	neuronal nuclear protein
NMDA	N-Methyl-D-Aspartate
NSC	Neuronal stem cell
onl	Olfactory nerve layer
opl	Outer plexiform layer
ORBm	Orbitofrontal cortex, medial
ORBvl	Orbitofrontal cortex, ventrolateral
ORBl	Orbitofrontal cortex, lateral
ORN	Olfactory receptor/sensory neuron
PC	Transient amplifying progenitor cell
PFA	Paraformaldehyde
PGC	Periglomerular cell
PIR	Piriform cortex
RMS	Rostral migratory stream
sAC	Short axon cell
SB	Specific binding
SEM	standard error of the mean
SGZ	Subgranular zone
SVZ	Subventricular zone
TB	Total binding
TC	Tufted cell

TMZ	Temozolomide
TTd	taenia tecta, dorsal
TTv	taenia tecta, ventral
vnl	Vomeronasal nerve layer
VRN	Vomeronasal receptor/sensory neuron

List of Figures

Zusammenfassung

Die olfaktorische Wahrnehmung ist für eine Vielzahl von Funktionen von großer Bedeutung, beispielsweise für die Identifizierung, Kategorisierung und Diskriminierung von Gerüchen, die Nahrungsselektion oder Fortpflanzung. Zur Aufnahme der Geruchsmoleküle dienen Geruchsrezeptoren der Nase, deren Aktivierung eine Signalkaskade zum zentralnervösen olfaktorischen System auslöst. Das System verarbeitet die Reize über funktional unterschiedliche Regionen, deren Zytoarchitektur im Nagergehirn aktuell größtenteils bekannt ist. Die funktionalen Unterschiede der Regionen hängen jedoch darüber hinaus mit den unterschiedlichen Rezeptorarchitekturen zusammen, die bisher kaum untersucht wurden.

Um die Funktionalität, Plastizität und Zellerneuerung des olfaktorischen Systems im adulten Gehirn zu gewährleisten, werden im Prozess der adulten Neurogenese in der subventrikulären Zone neue Neuronen generiert, die über den rostralen migratorischen Strom direkt zum Riechkolben migrieren. Studien zeigten, dass sich die Proliferationsrate durch kognitives Training erhöhte. Inwiefern sich die adulte Neurogenese und kognitives Training jedoch auf die Rezeptorarchitektur der olfaktorischen Regionen auswirken, ist bislang nicht bekannt. Um diese Frage zu beantworten, wurden in der vorliegenden Arbeit Rezeptorprofile aller olfaktorisch relevanter Regionen von adulten männlichen C57BL/6-Mäusen untersucht. Dazu wurden die Dichten glutamaterger (AMPA, Kainate, $mGlu_{2/3}$ und NMDA), GABAerger ($GABA_A$, $GABA_{A(BZ)}$ und $GABA_B$), noradrenerger (α_1 und α_2) und dopaminerger ($D_{1/5}$) Neurotransmitterrezeptoren mittels quantitativer in-vitro-Rezeptor-Autoradiographie in Kombination mit der Zyto- und Myelo-Architektur analysiert. Temozolomid wurde zur Supprimierung der adulten Neurogenese verabreicht, die post-mortem quantitativ und qualitativ mittels immunhistochemischer BrdU-Färbung überprüft wurde.

Besonders im olfaktorischen Bulbus wurden nach Unterdrückung der adulten Neurogenese abnehmende Rezeptordichten erwartet, da Neuroblasten der subventrikulären Zone hierhin migrieren. Beim kognitiven Training wurde aufgrund der zusätzlich gesteigerten Motorik eine Verschiebung zu einem inhibitorischeren Rezeptorprofil vermutet. Für trainierte Tiere mit unterdrückter Neurogenese wurde von einer Annäherung an die Werte der Kontrolltiere ausgegangen. Besonders in Hippocampus-assoziierten Regionen (z.B. die taenia tecta und der entorhinale Kortex) wurde mit signifikanten Veränderungen gerechnet.

Die Experimente ergaben eine heterogene Rezeptordichtverteilung in den untersuchten olfaktorischen Regionen. Generell wurden hohe Rezeptordichten von $mGlu_{2/3}$, $GABA_{A(BZ)}$ und $GABA_B$ festgestellt. Noradrenerge Rezeptoren zeigten eine sehr heterogene Verteilung, während der dopaminerge Rezeptor $D_{1/5}$ niedrige Konzentrationen aufwies, mit Ausnahme des Tuberculum

olfactorium und Nucleus endopiriformis. Signifikante Veränderungen der Rezeptorprofile wurden durch kognitives Training beobachtet, bei denen Zunahmen von $GABA_A$- (+135 % im akzessorischen Bulbus) und $mGlu_{2/3}$-Rezeptoren (168 % im Nucleus endopiriformis) bei simultaner Abnahme der NMDA-Rezeptordichten verzeichnet wurden. Die Supprimierung der adulten Neurogenese im untrainierten Tier veränderte die olfaktorische Rezeptorarchitektur teilweise signifikant, während sie im trainierten Tier nur geringe Veränderungen bewirkte. Ausgenommen davon war ein Anstieg noradrenerger α-Rezeptoren in trainierten Tieren (α_1: +30%; α_2: +40%), die in untrainierten Tieren nach Supprimierung der adulten Neurogenese signifikant anstiegen. $mGlu_{2/3}$-Rezeptoren zeigten keine Zunahme in trainierten Tieren mit supprimierter adulter Neurogenese, obwohl erhöhte Rezeptordichten durch kognitives Training und die Suppression der adulten Neurogenese beobachtet wurden.

Die multimodalen rezeptor-architektonischen Analysen der vorliegenden Arbeit bietet neue Einblicke in die neurochemische Organisation des olfaktorischen Systems der Maus. Anhand der Multirezeptorprofile konnten die Regionen in Cluster eingeteilt werden, die auf funktionale Gemeinsamkeiten hinweisen. Dies kann als Basis für zukünftige funktionale Untersuchungen der weniger bekannten olfaktorischen Regionen dienen. Da diverse neurologische Erkrankungen mit einer Veränderung von Rezeptordichten einhergehen (z. B. Parkinson-Krankheit), könnten diese Ergebnisse Ansätze bei verschiedenen psychiatrischen (z. B. Depression, Angststörungen) und kognitiven (z. B. Alzheimer-Krankheit) Erkrankungen bieten, bei denen eine gestörte adulte Neurogenese beobachtet werden kann. Außerdem bieten die Ergebnisse eine Basis für zukünftige Vergleichsstudien in Tiermodellen spezifischer Erkrankungen. Zusätzliche Untersuchungen der mRNA der Rezeptoren und deren Splice-Varianten könnten für pharmakologische Analysen neue Ansätze bieten.

Abstract

Olfactory perception is essential for a variety of brain functions, such as odor identification, categorization, and discrimination, food selection, and reproduction. Odorants bind on olfactory receptors of the nose, inducing a signaling cascade to olfactory system in the brain. This system processes the stimuli via functionally distinct regions, whose cytoarchitecture has been largely studied in the rodent brain. The functional differences of the regions are based on distinct receptor architectures, that have hardly been analyzed.

To ensure the functionality, plasticity, and cell renewal of the olfactory system in the adult brain, the process of adult neurogenesis generates new neurons in the subventricular zone that migrate directly to the olfactory bulb via the rostral migratory stream. Studies showed that cognitive training has an enhancing effect on the proliferation rate in this process. Whether adult neurogenesis and cognitive training affect the receptor architecture of the olfactory regions, remains unclear. To address this question, the present work examined receptor profiles of all olfactory relevant regions from adult male C57BL/6 mice. Therefore, densities of glutamatergic (AMPA, kainate, $mGlu_{2/3}$, and NMDA), GABAergic ($GABA_A$, $GABA_{A(BZ)}$, and $GABA_B$), noradrenergic (α_1 and α_2), and dopaminergic ($D_{1/5}$) neurotransmitter receptors were analyzed by quantitative in vitro receptor autoradiography in combination with the analysis of the cyto- and myelo-architecture. Temozolomide was applied to suppress adult neurogenesis, which was quantitatively and qualitatively verified post-mortem by BrdU immunohistochemical staining.

Upon suppression of adult neurogenesis, decreasing receptor densities were generally expected, especially in the olfactory bulb, since newly generated neurons specifically arrive here. During cognitive training, a shift to a more inhibitory receptor profile was suspected due to the additional increase in motor activity. For trained animals with suppressed neurogenesis, an approximation to the levels of control animals was assumed. Significant changes were expected especially in the regions that are also associated with the hippocampus (e.g., the taenia tecta and the entorhinal cortex).

The experiments revealed a heterogeneous receptor density distribution in the distinct olfactory regions. In general, high receptor densities of $mGlu_{2/3}$, $GABA_{A(BZ)}$, and $GABA_B$ were revealed. Noradrenergic receptors showed a very heterogeneous distribution, whereas the dopaminergic receptor $D_{1/5}$ showed low concentrations, except in the olfactory tubercle and endopiriform nucleus. Significant changes in receptor profiles were observed by cognitive training, in which general increases of $GABA_A$ (+135% in the accessory olfactory bulb) and $mGlu_{2/3}$ receptors (168% in the endopiriform nucleus) were observed with a simultaneous decrease in NMDA receptor densities. Suppression of adult neurogenesis in the untrained animal significantly altered

the olfactory receptor architecture partially, while trained animals showed only minor alterations upon suppression. This excluded an increase in noradrenergic α-receptors in trained animals (α_1: +30%; α_2: +40%), which increased significantly in untrained animals after suppression of adult neurogenesis. $mGlu_{2/3}$-receptors showed no increase here, although increased densities were observed by cognitive training and suppression of adult neurogenesis.

The multimodal receptor architectonic analyses of the present work provide new insights into the neurochemical organization of the mouse olfactory system. Based on the multireceptor profiles, regions could be classified into clusters indicating functional similarities. This may provide a basis for future functional studies of the less studied olfactory regions. Since diverse neurological diseases are associated with alterations in receptor densities (e.g., Parkinson's disease), these results may provide approaches in various psychiatric (e.g., depression, anxiety disorders) and cognitive (e.g., Alzheimer's disease) disorders where an impaired adult neurogenesis might be considered. Furthermore, the results provide a basis for future comparative studies in experimental animal models of specific conditions. Additional studies of the receptors' mRNA and their splice variants could yield to new approaches for pharmacological studies.

1. Introduction

The sense of smell is considered to be one of the phylogenetically oldest senses in vertebrates. It is a chemical sense, as it is activated by the binding of chemical substances, the odorants. These are bound by special receptors in the upper part of the nasal cavities, the olfactory epithelium, whereupon a signal cascade is triggered. The signals are transmitted by the olfactory nerve through several regions in the brain that form the olfactory system. The olfactory system is closely connected to the limbic system, thus enabling subjective sensations of chemical stimuli. The human sense of smell has long been thought to be rather *underdeveloped*, especially when compared to rodents. However, the human olfactory system has almost the same density of neurons as found in brains of other mammals. Humans can perceive and distinguish a wide range of odors which can, among other things, affect our memories, behavior and appetite and are thus just as sensitive as in other mammals (McGann, 2017).

Medical studies in the 21st century have shown that chemical senses are affected in multiple disorders. For example, olfactory dysfunction was found to be an early indicator of neurodegenerative diseases and schizophrenia (Albers et al., 2006). Since the olfactory pathway is the only afferent tract that does not project directly to the thalamus, subconscious and instinctive responses are facilitated (Courtiol and Wilson, 2015). In this way, the olfactory system performs numerous functions, for example the hedonics, identification, categorization, and discrimination of olfactory impressions. Particularly in the animal kingdom, food selection, early predator perception, reproduction and other social interactions are linked to the subconscious processing of olfactory.

The present work will focus on the mouse olfactory system, which is finely structured. Odorants can be detected by more than 1000 olfactory receptors, allowing odors to be categorized very accurately. Mice are a popular model organism for experimental studies since they are uncomplicated to keep, reproduce quickly, have a rapid life cycle and the complete genome is known to be 95% similar to that of humans (Chinwalla et al., 2002). Due to their similar genome, they contract many diseases for the same genetic reasons, which can be caused by genetic manipulation in experimental animal models (Simmons, 2008). Thus, especially in the mouse model, it is important to achieve a comprehensive understanding of the olfactory system. The detailed anatomy and summary of the distinct olfactory regions is given in chapter 1.1.

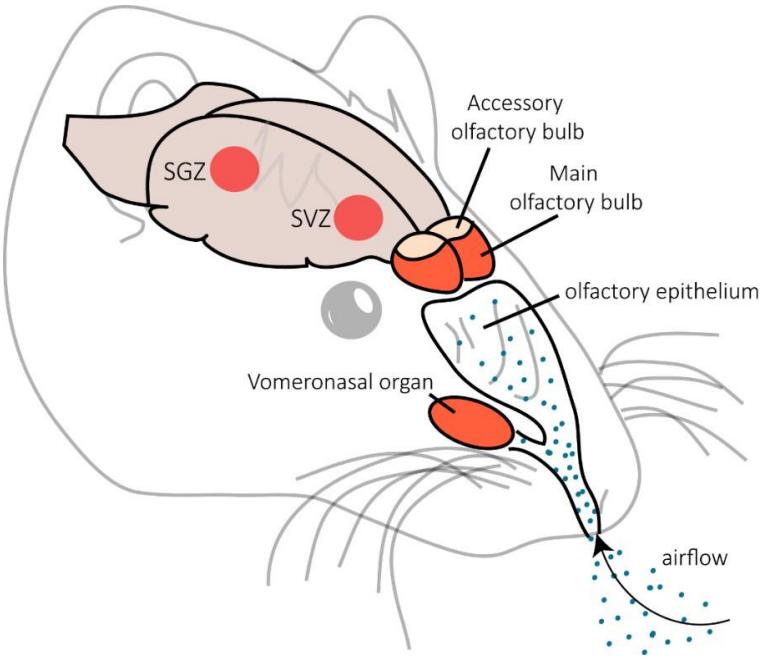

Figure 1: The olfactory systems in the mouse brain

Schematic representation of the mouse nasal cavities and the central and peripheral olfactory regions. In the mouse nasal cavities, primary olfactory sensory neurons receive odorants and convert them into chemical signals that are projected directly via neurotransmitter release into the first procession station of the olfactory system in the central nervous system. Initially, olfactory signals are detected via the olfactory epithelium and the vomeronasal organ in the nasal cavities. The signals are directly transmitted via the respiratory air. For odor transduction, olfactory sensory neurons (ORNs) are located in the olfactory epithelium. ORNs are bipolar primary sensory neurons of the olfactory system. They have an apical dendrite with G-protein-coupled receptors in the olfactory epithelium and an axon projecting to the main olfactory bulb. Each ORN, approximately 6 - 10 million in total, contains only one type of receptor. They are embedded in the olfactory epithelium by supporting cells and replaced by basal cells after apoptosis in four to eight weeks. Axons of the olfactory and vomeronasal sensory neurons project to their corresponding regions in the brain (main- and accessory olfactory bulbs). As ORNs are in permanent contact with the odor molecules in respiratory air, particles and pathogens, their continual replacement is necessary. Therefore, adult neurogenesis produces new neurons that are generated by neurogenic niches, the subventricular zone (SVZ) and subgranular zone (SGZ) in the adult brain (Ming and Song, 2005).

After Ramon y Cajal concluded that ‘once development was ended, the founts of growth and regeneration of the axons and dendrites dried up irrevocably’, the dogma that neurogenesis was limited to the young, developing organism persisted (Ramon y Cajal, 1913b; Gross, 2000; Colucci-D'Amato et al., 2006). Subsequent studies showed in rhesus monkeys that olfactory receptor cells of the olfactory epithelium were able to regenerate after damage (Schultz, 1960), and further findings suggested that neuronal regeneration is not unique to olfaction but is possible

in multiple nervous systems (Farbman, 1992). Moreover, proliferation of neurons in the subventricular zone (SVZ; Figure 1, Figure 5) along the lateral ventricles has been demonstrated in the mouse brain (Lois and Alvarez-Buylla, 1993) and new neurons in the subgranular zone of the dentate gyrus (SGZ; Figure 1) in the primate (Gould et al., 1999; Kornack and Rakic, 1999), and human (Eriksson et al., 1998) brains were demonstrated. These studies ended the long-held central dogma of neurogenesis in the adult brain. A detailed summary of the historical discovery of adult neurogenesis and the process are given in chapter 1.2.

Now it is known that adult neurogenesis plays a crucial role in the olfactory system. Thousands of adult neurons are integrated into existing neuronal circuits of the olfactory bulb every day (Alvarez-Buylla et al., 2001). It is debated whether this process serves to maintain the olfactory bulb circuitry, aids in the shaping of sensory information, supports olfactory learning processes, and/or mediates odor memory (Lazarini and Lledo, 2011). Also unknown is the impact of adult neurogenesis on the receptor architecture of the olfactory system, e.g., whether it can be seen as an adaptive process that has a compensatory effect on altered receptor architecture during aging.

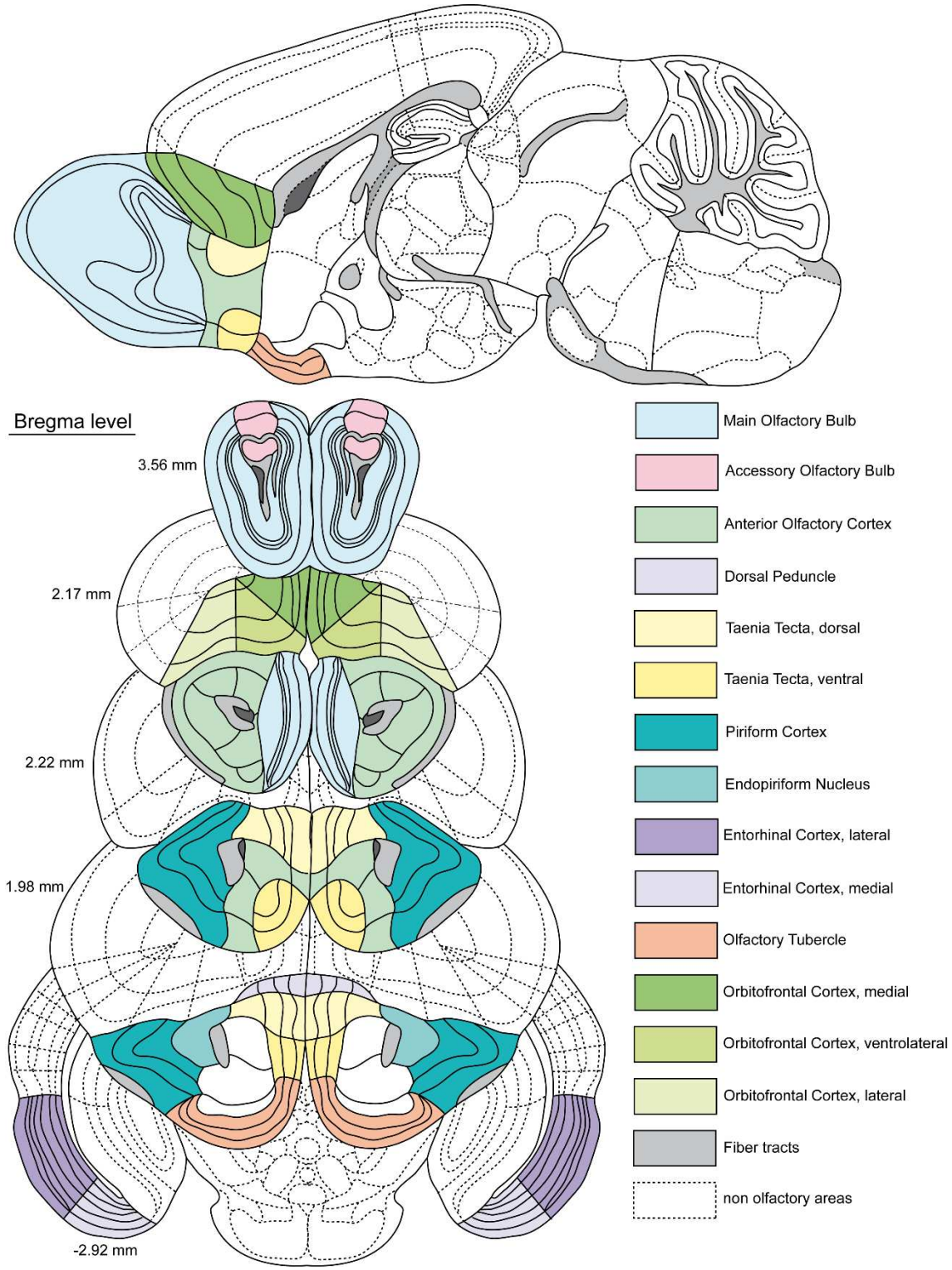

Figure 2: Schematic representation of the investigated olfactory areas

Coronal sections of the mouse (C57BL/6) brain along the anterior-posterior axis (related Bregma levels alongside). The sagittal section is used for orientation of a particular area more locally. The areas examined are marked with different colors (see legend). Dashed lines indicate non-olfactory areas. The gray areas represent the fibrous pathways, whereas dark gray areas represent the subventricular zone. Boundaries adapted by the Allen Brain Reference Atlas (Lothmann et al., 2021).

1.1 Structure and connectivity of the mouse olfactory system

Odorants are absorbed by olfactory sensory cells in the nasal epithelium. These sensory cells project subsequently to the main olfactory bulb (Figure 3), where the information is gathered in glomeruli to synapse onto mitral/tufted cells (Ennis et al., 2007; Ennis, 2008a). These project via the lateral olfactory tract to the cortical and subcortical regions of the olfactory system, that is divided into a primary and a secondary cortex (Figure 2). The primary olfactory cortex includes regions that receive direct input from the main and accessory olfactory bulb via the lateral olfactory tract. These comprise (Figure 2) the taenia tecta (dorsal and ventral parts), the dorsal peduncular cortex, the piriform cortex, the endopiriform nucleus, the anterior olfactory cortex, the entorhinal cortex (medial and lateral parts), and the olfactory tubercle. The secondary olfactory cortex consists of the olfactory network of the orbitofrontal cortex (medial, ventrolateral, and lateral parts) (Shepherd, 1972; Haberly and Price, 1978; Haberly, 1985; Barbas, 1993; Ennis et al., 2007; Ennis, 2008a; Doty, 2015; Ennis et al., 2015). In the following paragraphs, an overview of the anatomy of the olfactory system is provided.

1.1.1 The main olfactory bulb

The main olfactory bulb is a paired bulge of the frontal wall of the prosencephalon and has evolutionarily been shown to be a highly conserved structure. It is the first relay station of the central nervous integration of odor information, while downstreaming brain regions provide the subsequent interpretation of the incoming information (Shipley and Ennis, 1996). The main olfactory bulb is located between Bregma level 4.28 mm and Bregma 2.8 mm at the rostral pole of the nasal cavity, where it is connected with the olfactory epithelium via olfactory sensory neurons for transmission of the received olfactory information. In rodents it is organized into six circular layers (Figure 3A, D).

The outermost layer is the olfactory nerve layer. This is where the bundled axons of the ORNs from the olfactory epithelium pass through, that collected and processed the odor information. The layer consists of axons, glial cells, and astrocytes (Cajal, 1911b; Cajal, 1911a; Doucette, 1989; Bailey and Shipley, 1993; Ennis et al., 2007). The axons of the olfactory sensory neurons form spherical, neuropil-containing, round structures called glomeruli in the glomeruli layer. There are up to 2000 glomeruli per bulb (50 – 100 µm in diameter), isolated from each other by astrocytes. In the glomeruli, the axons of the olfactory sensory receptor neurons synapse on mitral, tufted, juxtaglomerular, periglomerular, and short axon cells (Cajal, 1911b; Cajal, 1911a; Pinching and Powell, 1971a; b; 1972; Ennis et al., 2007). Importantly for the diversity of scents, the

axons of each olfactory sensory receptor type only converge on one to three specific glomeruli. These activate selectively up to 30 mitral and 80 tufted cells per glomerulus (Shepherd, 1972), so an odor-specific activity pattern is provided. Here and in the adjacent external plexiform layer, olfactory information is processed for the first time. The external plexiform layer consists mainly of tufted cells while the neighboring mitral layer contains mainly mitral cells (Cajal, 1890; Ennis et al., 2007).

The relatively cell-poor internal plexiform layer contains axons and dendrites of granule cells and mitral/tufted cells (de Olmos et al., 1978; Ennis et al., 2007). The soma of the granule cells are located in the granule cell layer (Figure 3B, D), while the dendrites form the lateral olfactory tract that projects to the olfactory cortex where the olfactory information is processed further (Figure 3A, C).

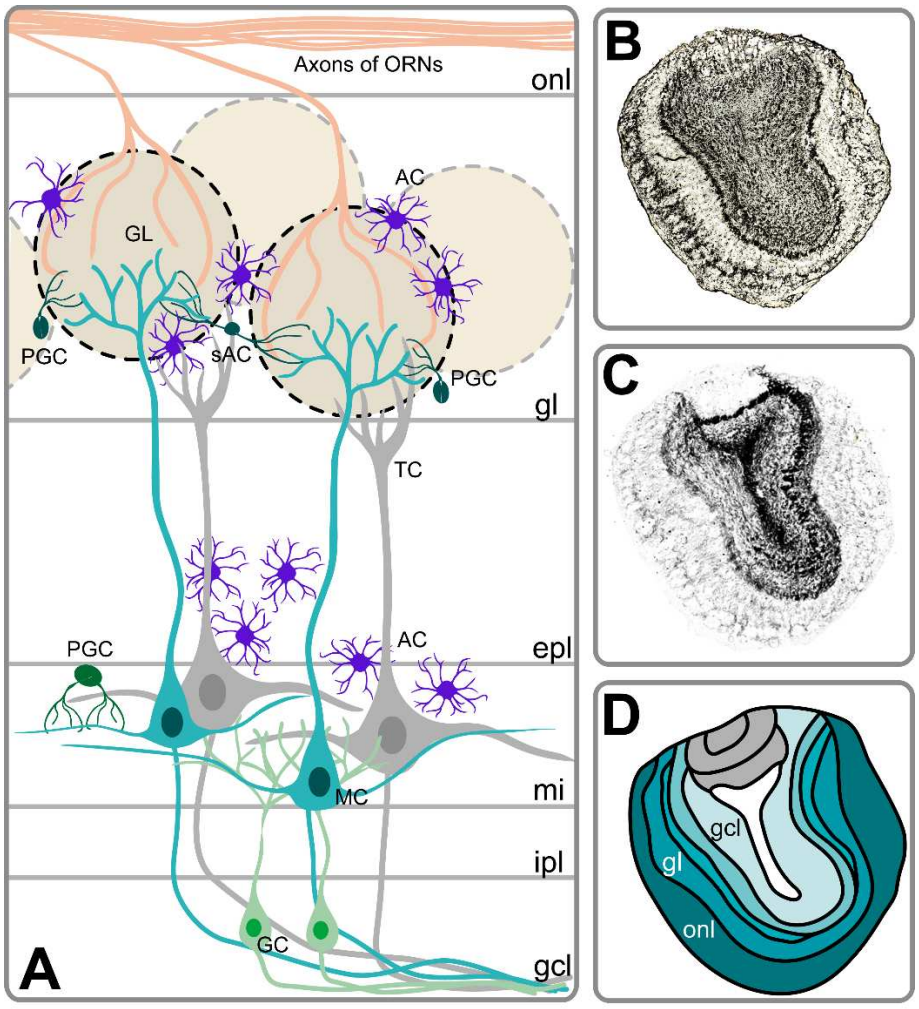

Figure 3: Connectivity scheme of the main olfactory bulb

The main olfactory bulb is the primary relay center for circuitry and transmission of olfactory information from the olfactory epithelium to the olfactory system. **A** Cellular organization of the main olfactory bulb. Axons of the olfactory receptor neurons (ORNs) enter the main olfactory bulb via the olfactory nerve layer (onl) and project to the apical dendrites of the main neurons (mitral (MC) and tufted cells (TC)) of the glomerular layer (gl). The gl contains different interneurons (periglomerular cells (PGC), short axon cells (sAC) and astrocytes (AC) that process the information. The formation of synapses on the neurons of the gl results in the appearance of spheroid nerve networks (Glomeruli olfactorii (GL)). In the external plexiform layer (epl), the second processing level, additional interneurons such as granule cells (GC) and form dendrodendritic synapses with lateral dendrites of the projection neurons. Across the mitral cell layer (mi) are cell bodies of mitral cells, whose axons pass through the internal plexiform layer (ipl). The somata of granule cells are located in the gcl, where the axons of mitral and tufted cells form the lateral olfactory tract that exits the main olfactory bulb and projects to the olfactory cortex. Schematic overview based on data of Ennis et al., 2007. **B** Nissl-stained section of the main olfactory bulb (Bregma level 3.92 mm). **C** Myelin sheath staining of the main olfactory bulb (Bregma level 3.92 mm) **D** Schematic illustration of the main olfactory bulb. Olfactory nerve layer (onl), glomerular cell layer (gl), granule cell layer (gcl).

1.1.2 The accessory olfactory bulb

The peripheral sensory organ of the accessory olfactory system of the mouse is the vomeronasal organ, that is located in the vomer bone (Halpern and Martínez-Marcos, 2003). The relay station of the vomeronasal organ is the accessory olfactory bulb, which is located between Bregma level 3.56 mm and 2.96 mm in the mouse brain. It is also referred to as the Jacobson organ, based on its discovery by the Danish anatomist Ludvig Jacobson (Jacobson et al., 1998). The accessory olfactory system can be found in most vertebrates, but it has been assumed that there is no accessory olfactory system in the adult human (Smith and Bhatnagar, 2000; Trotier et al., 2000; Meredith, 2001). Studies demonstrated, that the vomeronasal organ has been lost in various taxa like crocodiles, whales, some bats, and some primates (Eisthen, 1992; Meisami and Bhatnagar, 1998; Halpern and Martínez-Marcos, 2003). Because of its connection to the vomeronasal organ and the amygdala, the accessory olfactory bulb has been reported to impact behavior, including social, sexual/reproductive, and aggressive habits (Jacobson et al., 1998). However, the exact role is still not entirely understood. Previous studies suggested that the accessory olfactory system had a function in pheromone detection. This hypothesis has been debated, as the main olfactory bulb also processes pheromones (Meredith, 1998; Halpern and Martínez-Marcos, 2003; Mucignat-Caretta, 2010).

The accessory olfactory bulb (from superficial to deep) consists of the glomerular layer, the mitral cell layer, and the granular layer (Figure 4). The axons of the vomeronasal receptor neurons are bundled across the vomeronasal organ nerve layer and enter the glomerular layer of the accessory olfactory bulb. The projections and architecture are similar to the main olfactory bulb (Jia and Halpern, 1997; Meisami and Bhatnagar, 1998). Below the glomerular layer lies the mitral and subjacent the granular cell layer. The mitral cell layer contains the mitral/tufted cells and axons of granule cells. The mitral/tufted cell axons project through the glomerular layer directly to the bed nucleus of the accessory olfactory tract, the medial and posteromedial nuclei of the amygdala and the bed nucleus of the stria terminalis (Winans and Scalia, 1970; Scalia and Winans, 1975; von Campenhausen and Mori, 2000; Salazar and Brennan, 2001; Mucignat-Caretta, 2010). The amygdala projects back to the accessory olfactory bulb via the stria terminalis, regulating primary olfactory and social odor processing (Raisman, 1972; Oboti et al., 2018). The bed nucleus of the stria terminalis sends GABAergic projections to the mitral layer of the accessory olfactory bulb, while the amygdaloid nuclei maintain glutamatergic connections to the granule layer of the accessory olfactory bulb (Mucignat-Caretta, 2010). The granule cell layer contains the soma of the granule cells (Figure 4).

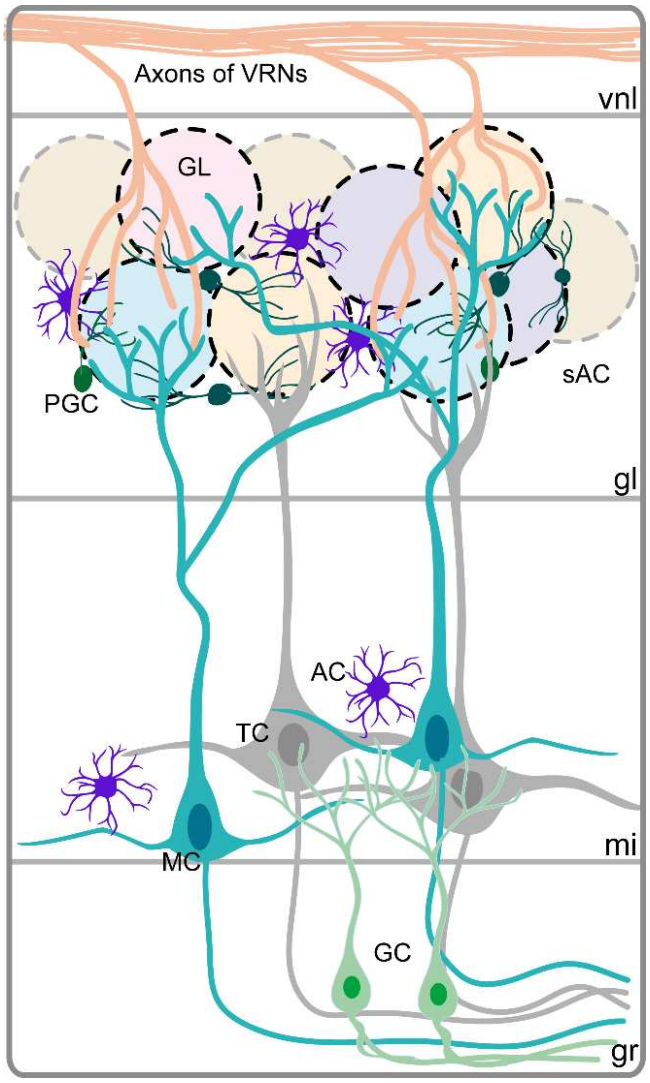

Figure 4: Connectivity scheme of the accessory olfactory bulb

The laminar patterns of the main and accessory olfactory bulb are very similar. Axons of the vomeronasal receptor neurons (VRNs) enter the accessory olfactory bulb via the vomeronasal nerve layer (vnl) and project on the apical dendrites of the mitral cells of the mitral cell layer (gl), forming glomeruli (GL). Periglomerular cells (PGC), astrocytes (AC) and short axon cells (sAC) connect the cells and glomeruli in this layer. Astrocytes (AC) and soma of mitral (MC) and tufted cells (TC) are located in the mitral cell layer (mi). Axons of mitral cells pass through the granule cell layer (gr) and form the lateral olfactory tract with the axons of the main olfactory bulb. Soma of granule cells (GC) are located in the gr. Schematic overview based on the data of Mucignat-Caretta, 2010.

1.1.3 The taenia tecta

The taenia tecta is composed of a dorsal and a ventral part. Dorsomedially to the anterior olfactory cortex and the piriform cortex, the four-layered dorsal taenia tecta (also termed *anterior hippocampal continuation*) adjoins (Haberly and Price, 1978). Caudally of the anterior olfactory cortex, the three-layered ventral taenia tecta is located rostromedially (Haberly and Price, 1978). The dorsal part is located between Bregma 2.46 mm and Bregma 1.34 mm and the ventral part between Bregma level 2.46 mm and Bregma 1.98 mm.

Recent studies in mice have revealed that the dorsal part plays a role in the processing of olfactory information and in communicating between the olfactory system and the hippocampal formation. Overall, it is only known that the taenia tecta regions encode specific stimuli attributes. The ventral taenia tecta has been suggested to play a role in the transformation of olfactory signals into reward-directed behaviors (Shiotani et al., 2020). Further functional studies are still needed to understand the function of this region (Cousens, 2020).

The dorsal taenia tecta receives olfactory input from the entorhinal cortex, the main olfactory bulb and septal nuclei and projects to the hippocampal formation and back to the main olfactory bulb (Wyss and Sripanidkulchai, 1983; Cleland and Linster, 2019). The ventral part receives information from the main olfactory bulb, anterior olfactory cortex (lateral part), the lateral entorhinal cortex and the piriform cortex and projects back to the main olfactory bulb, piriform cortex, lateral anterior olfactory cortex and to the olfactory tubercle.

The Allen Brain reference atlas that was used for this work divided the layers of the dorsal taenia tecta into layer I, layer II, layer III and layer IV, and the ventral taenia tecta into layer I, layer II and layer III (Dong, 2008).

1.1.4 The dorsal peduncular cortex

The four-layered dorsal peduncular cortex is located in the medial prefrontal cortex between Bregma level 1.98 mm and Bregma 0.98 mm dorsal to the dorsal taenia tecta.

There is only a limited knowledge available for the dorsal peduncular cortex. It maintains strong reciprocal projections with the lateral entorhinal cortex and piriform cortex and projects to the olfactory tubercle, the main olfactory bulb (Haberly and Price, 1978), to lower brainstem regions and to the trigeminal brainstem sensory nuclear complex (Akhter et al., 2014). Due to its connections, it plays a role in blood pressure regulation and the suppression of conditioned anxiety following extinction and addiction (Owens and Verberne, 2001; Vidal-Gonzalez et al., 2006; Peters et al., 2009). The taenia tecta together with the dorsal peduncular cortex are often combined as *ventralmost prefrontal cortex*, regulating the extinction learning (Peters et al., 2009). Extinction learning is essential for the treatment of anxiety disorders, which have become more prevalent and relevant in the past years.

The cytoarchitecture has been defined in previous studies in rats (Paxinos et al., 1980; Peyron et al., 1997; Zilles, 2012; Akhter et al., 2014) to distinguish the dorsal peduncular cortex from adjacent regions. Accordingly, the region can be divided into four layers: Layer I is slightly broader than the adjacent regions. Layer II displays (layer II/III) densely packed cells, which facilitates the distinction from the dorsal taenia tecta. The Allen Brain reference atlas divided the layers of the dorsal peduncular cortex into layer I, layer II/III, layer V and layer Va (Dong, 2008).

1.1.5 The piriform cortex

The three-layered piriform cortex is located laterally to the anterior olfactory cortex between Bregma level 2.46 mm and Bregma -2.8 mm.

Functionally, the region could be divided into an anterior part for encoding molecular features of the odorant and a posterior part for odor quality (Gottfried et al., 2006). In this work, the region is not distinguished into two parts. With respect to the literature, the anterior piriform cortex was analyzed. The piriform cortex plays a crucial role as a node for the distribution of olfactory information to other brain regions (Nigri et al., 2013). This is reflected in its connectivity to other olfactory regions like the main olfactory bulb (Collins et al., 1981), olfactory tubercle, lateral entorhinal cortex, anterior olfactory cortex (lateral, dorsal, medial, posteroventral), ventral taenia tecta and dorsal peduncular cortex (Haberly and Price, 1978). The piriform cortex is active during memory and imagination (Bensafi et al., 2007) or associations with an odor (Gottfried et al., 2004; González et al., 2006) and links representations to olfactory inputs (Johnson et al., 2000). Connections to the taenia tecta and the dorsal peduncular cortex maintain the integrity of sensory inputs with behavior (Luskin and Price, 1983). Emotional and motivational sensory input is subjectively evaluated through the connection to the amygdala and the olfactory tubercle (Luskin and Price, 1983; Ikemoto, 2007). The connection with the hippocampal formation is essential in olfactory working memory (Luskin and Price, 1983; Zelano et al., 2009). Projections to the anterior olfactory cortex provide the spatial orientation of the odor origin (Schoenfeld and Macrides, 1984; Kikuta et al., 2010) to discriminate odors (Howard et al., 2009). There are also cortical projections to the insula and the orbitofrontal cortex, which are associated with the piriform cortex in taste perception (Ennis et al., 2007; Veldhuizen and Small, 2011). Due to connections to the substantia nigra, the locus coeruleus, VTA and the raphe nuclei (Fallon and Loughlin, 1982; Datiche and Cattarelli, 1996; Ennis et al., 2007), the piriform cortex represents the value of the odors, but not the source (Zelano et al., 2007).

Layer I contains excitatory afferent and intrinsic granule cell connections. Layer II is characterized by cell bodies of pyramidal cells that branch into layer III (Linster and Hasselmo, 2001).

1.1.6 The endopiriform nucleus

The endopiriform nucleus is located lateral to the piriform cortex between Bregma level 2.46 mm and -2.8 mm. It consists of a large group of densely packed multipolar neurons (Behan and Haberly, 1999).

As a part of the primary olfactory cortex, the dorsal endopiriform nucleus receives projections from the main olfactory bulb, the piriform, entorhinal and perirhinal cortex and projects to the piriform, entorhinal, insular, orbital, perirhinal cortices, the olfactory tuberculum, and the hippocampal formation. Both the piriform cortex and the dorsal endopiriform nucleus share common target regions and play a role in epileptogenesis in the temporal lobe (Behan and Haberly, 1999; Sugai et al., 2012; Vaughan and Jackson, 2014). The amygdala is directly connected to the dorsal endopiriform nucleus (Ottersen, 1982; Luskin and Price, 1983; Canteras et al., 1992). The dorsal endopiriform nucleus is thought to play a role in memory consolidation (Behan and Haberly, 1999) and behaviors depending on olfactory convergence (Canteras et al., 1992).

1.1.7 The anterior olfactory cortex

The anterior olfactory cortex is located caudally to the main olfactory bulb between Bregma level 3.08 mm and 1.98 mm. The region has barely been studied and is also controversial in its nomenclature. Pigache defined the olfactory region as the *anterior olfactory nucleus* since it had neither columnar structures nor a three-layered structure and was instead divided into two zones (Pigache, 1970). Arguments for the designation as a cortex were given by Haberly, since the region showed cortical features (Haberly, 2001). For review see Brunjes et al., 2005. In this work, the structure is referred to as the anterior olfactory cortex, in order to use the most recent terminology.

The anterior olfactory cortex is a two-layered structure consisting of the superficial Pars externa and the underlying Pars principalis. The pars principalis can be further subdivided into a medial, lateral, dorsal and posteroventral part. All subregions of the anterior olfactory cortex provide ipsi- and contralateral projections via the anterior commissure to the main olfactory bulb. Fibers project to the piriform cortex, olfactory tubercle, ventral taenia tecta, orbitofrontal cortex, and hypothalamus. The anterior olfactory cortex receives projections from the piriform cortex, entorhinal cortex, orbitofrontal cortex and CA1 from the hippocampal formation (Haberly and Price, 1978; Brunjes et al., 2005; Brunjes and Kenerson, 2010; Brunjes et al., 2011; Cleland and Linster, 2019). Functionally, the anterior olfactory cortex plays a role in the top-down regulation of the main olfactory bulb odor processing, odor learning and spatial coding for odor quality (Brunjes et al., 2005; Rothermel and Wachowiak, 2014; Cleland and Linster, 2019).

1.1.8 The entorhinal cortex

The entorhinal cortex borders medially and rostrally to the piriform cortex, dorsally and caudally to the postrhinal cortex and caudally and laterally to the presubiculum and hippocampus between Bregma level -2.80 mm and Bregma -5.34 mm. It is divided into a lateral and a medial part.

The medial entorhinal cortex plays a role in the spatial processing domain of the cortex through connections to the presubiculum, parasubiculum, retrosplenial and postrhinal cortex (Witter et al., 2017). It receives olfactory input via connections to the hippocampus (Biella and de Curtis, 2000).

The lateral entorhinal cortex is part of the inhibitory control of the olfactory memory trace and plays a role in conditioned odor and context aversions (Ferry et al., 2006; Ferry et al., 2015; Leitner et al., 2016). This is reflected by its connections with the amygdaloid complex, the dorsal endopiriform cortex, the main olfactory bulb, the piriform cortex, the dorsal peduncular cortex, the insular, the medial- and orbitofrontal regions and the prepiriform cortex (Krettek and Price, 1977; Haberly and Price, 1978; Witter et al., 2017). It is involved in the processing of object information, attention, and motivation due to connections to the insula, the medial and orbitofrontal cortex and the perirhinal cortex (Witter et al., 2017). Projections to the hippocampus are essential for the integration of olfactory information (Stäubli et al., 1984; Chapuis et al., 2013; Leitner et al., 2016).

The entorhinal cortex shows a homogenous distribution of neurons over six layers. Layer II of the medial part contains medium-sized excitatory pyramidal cells and stellate cells, while layer II of the lateral part consists of large and medium-sized multipolar neurons and pyramidal cells. Some of these cells cluster into sublayers (Witter et al., 2017). Layer III in both parts comprises spiny excitatory pyramidal neurons (Tahvildari and Alonso, 2005) while layer IV and Va comprise larger pyramidal neurons. In contrast to layer Va, layer Vb consists of smaller pyramidal cells (Canto and Witter, 2012; Witter et al., 2017). In this work, the layers II and VI are not further subdivided because of a discontinuity in the finding of a border.

1.1.9 The olfactory tubercle

The olfactory tubercle is located ventrally to the piriform cortex and medially to the ventral taenia tecta between Bregma level 1.98 mm and Bregma 0.14 mm.

The region contributes to the state and attention-dependent odor discrimination by modulating the behavioral odor discrimination (Gadziola et al., 2015), determining the odor source (Zelano et al., 2005) and by participating in early attention processes of the olfactory code (Zelano et al., 2005; Wesson and Wilson, 2010; 2011). Upon the conscious perception of odors, neurons of the olfactory tubercle encode goal-directed behaviors (Gadziola and Wesson, 2016; Carlson et al., 2018).

The olfactory tubercle receives projections from the main olfactory bulb, the piriform cortex (Wesson and Wilson, 2011), dorsal endopiriform nucleus (Behan and Haberly, 1999), the entorhinal cortex (Haberly and Price, 1978) and via the vomeronasal pathway from the amygdala (Fallon et al., 1978). Non-olfactory inputs are provided by the hippocampus and the reward system, the ventral tegmental region, and the nucleus accumbens (Wesson and Wilson, 2011; Cleland and Linster, 2019). The olfactory tubercle projects back to the nucleus accumbens and is therefore considered to be part of the ventral striatum (Cleland and Linster, 2019). It projects bilaterally to the anterior olfactory cortex (Brunjes et al., 2005) and main olfactory bulb (Mohedano-Moriano et al., 2012). The ventral tegmental region projects dopaminergic to the olfactory tubercle (Haberly and Price, 1978).

It is a three-layered structure consisting of layer I, the plexiform or molecular layer, where projections from the main olfactory bulb enter (Scott et al., 1980). The second layer, often referred to as the pyramidal or dense cell layer, is the most densely populated layer, which includes the Islands of Calleja. Layer III is the polymorphic layer. It is the thickest layer and receives input from the piriform cortex (Luskin and Price, 1983; Schwob and Price, 1984; Unnerstall et al., 1984; Cansler et al., 2020).

1.1.10 The orbitofrontal cortex

The three parts of the orbitofrontal cortex (lateral, ventrolateral, dorsal) are located dorsal to the accessory olfactory bulb and the anterior olfactory cortex between Bregma level 2.96 mm and Bregma 1.98 mm.

It is activated by olfactory stimuli (Jones-Gotman and Zatorre, 1988; Zatorre et al., 1992; Francis et al., 1999) and plays a role in olfactory associated learning by learning and reversing stimulus-reinforcement associations and the integration of olfactory identity (Rolls, 2004). The medial orbitofrontal cortex determines the level of accommodation for subjectively pleasant odors while the lateral orbitofrontal cortex is active upon subjectively unpleasant odors (Rolls, 2004). Lesions of the orbitofrontal cortex lead to impairments in odorant-discrimination learning (Eichenbaum et al., 1980; Zatorre and Jones-Gotman, 1991; Ongür and Price, 2000).

The orbitofrontal cortex is strongly connected to the basolateral amygdala (Aggleton et al., 1980; McDonald et al., 1996; Orsini et al., 2015) to process and integrate stimulus-reward associations and cue-outcome associations (Schoenbaum and Roesch, 2005; Lucantonio et al., 2015; Sharpe and Schoenbaum, 2016). While the lateral part of the orbitofrontal cortex contains the secondary taste region (Baylis et al., 1995), the medial part includes the olfactory region (Tanabe et al., 1975; Rolls and Baylis, 1994). Thus, the lateral orbitofrontal cortex is innervated by the primary taste cortex (Baylis et al., 1995) and the medial orbitofrontal cortex by fibers of the primary olfactory cortex (Johnson et al., 1968; Tanabe et al., 1975; Rolls, 2004). Overall, the orbitofrontal cortex receives somatosensory, gustatory, auditory, visual (Barbas, 1988; 1993; Cavada et al., 2000; Rolls, 2004) and spatial localization inputs (Lipton et al., 1999). It sends projections to the entorhinal cortex (Insausti et al., 1987), the ventral tegmental region (Takahashi et al., 2009), the dorsal striatum (Johnson et al., 1968; Zimmermann et al., 2018) and reciprocally to the mediodorsal nucleus of the thalamus (Krettek and Price, 1977; Ongür and Price, 2000).

1.2 Adult neurogenesis

The generation of new neurons in the adult brain is termed as adult neurogenesis. In the early and middle 20th century, neuron generation was thought to occur exclusively during embryonic and early postnatal development (His, 1904; Ramon y Cajal, 1913a). Joseph Altman was the first to detect adult generated neurons in the rat hippocampus using [^{3}H]-thymidine (Altman, 1962a; b; Altman and Das, 1965). This phenomenon was also confirmed by electron microscopy in the hippocampus of cats and guinea pigs (Altman and Das, 1967; Das and Altman, 1971) and in the olfactory bulb in the rodent brain (Kaplan and Hinds, 1977). Later, newly generated adult neurons were also detected in the primate and human brain (Eriksson et al., 1998; Gould et al., 1999).

Subsequent studies of adult neurogenesis were enabled by a new immunofluorescence method to detect proliferating cells by 5'-bromo-3'-deoxyuridine (BrdU), a synthetic thymidine analogue (Eriksson et al., 1998). BrdU was first developed to visualize the proliferative index of gliomas (Hoshino et al., 1989; Struikmans et al., 1997). Thereby, adult neurogenesis was revealed in the human brain. Here, neuroblasts were not restricted to the subventricular zone (SVZ) and could additionally be detected in the adjacent striatum (Bergmann et al., 2012; Ernst et al., 2014).

The properties of stem cells for self-renewal and multipotency are provided by specific microenvironments, the neurogenic niches. Mammalian adult neurogenesis occurs in two germinal regions, the SVZ and the subgranular zone of the hippocampal formation (SGZ). In both neurogenic niches, neurogenesis involves the division of progenitor cells, including differentiation and functional integration into the particular region: in the olfactory bulbar circuit via the SVZ or into the hippocampal formation via the SGZ. While the SGZ provides new excitatory granule cells, the SVZ generates GABAergic neuroblasts that differentiate into interneurons in the olfactory bulb (Ming and Song, 2005).

The basis of adult neurogenesis are multipotent neural stem cells (NSCs). Multipotency means that NSCs can differentiate into various neuronal and glial subtypes because they are undifferentiated and mitotically active cells (Gage et al., 1995; Weiss et al., 1996; McKay, 1997; Gage, 2000; van der Kooy and Weiss, 2000; Garthe et al., 2009). Furthermore, stem cells exhibit the property of an unlimited ability to divide. When NSCs divide, a differentiation is made between symmetric and asymmetric division. Symmetric division results in two identical daughter cells, whereas asymmetric division results in a replicate of the parent stem cell and a differentiated daughter cell. Because of their high proliferative activity, the direct descendants of stem cells (lineage-specific progenitor cells) are called transient-amplifying cells. However, in contrast to stem cells, they have a limited ability to divide and are predetermined to a specific differentiation (neurons, astroglia, glia or oligodendroglia).

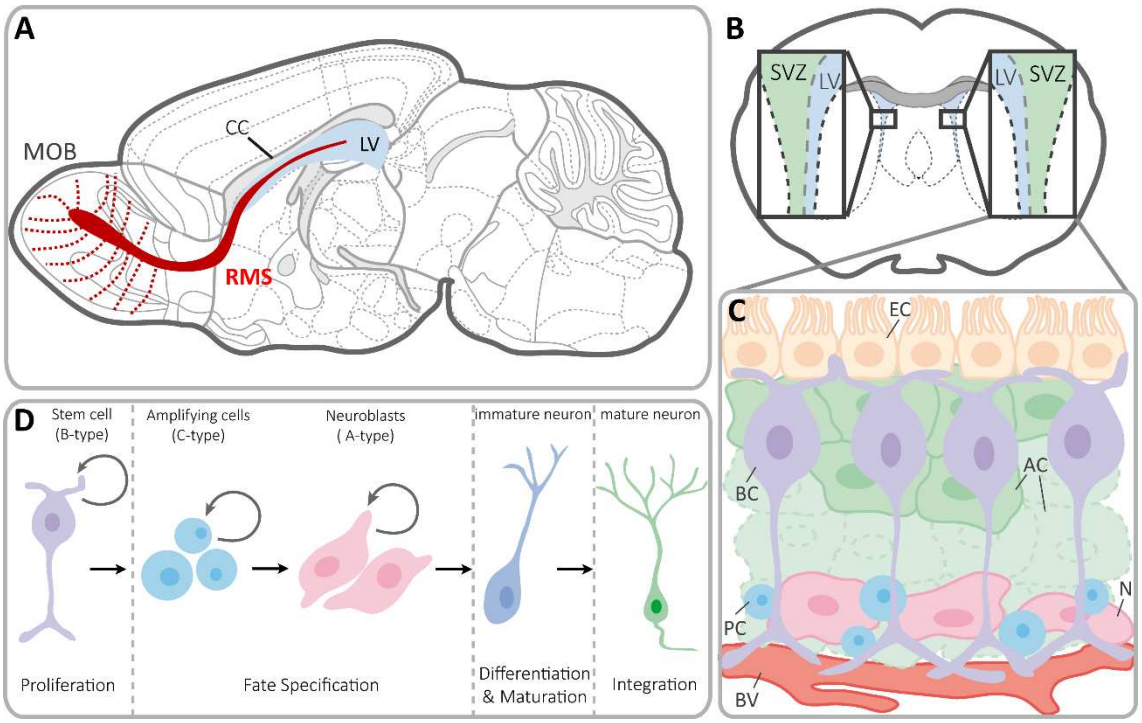

Figure 5: Location, anatomy, and neurogenesis of the adult SVZ

A Schema of a sagittal section of the mouse brain. Subjacent to the corpus callosum (CC) is the location of the lateral ventricle (LV) where the SVZ is located at the outer wall. SVZ-generated neuroblasts migrate through the rostral migratory stream (RMS) to the main olfactory bulb (MOB) where they migrate radially and differentiate into new interneurons. **B** Schema of a coronal section of the mouse brain (bregma level 1.18 mm). The SVZ is located laterally of the LV. **C** Cellular organization of the SVZ. The SVZ is composed of different cell types: Ependymal cells (EC) separate the LV from the SVZ, astrocytes (AC), astrocyte-like B-type stem cells (BC), transient amplifying C-type progenitor cells (PC), A-type neuroblasts (N) and blood vessels (BV). **D** Stages of adult SVZ-neurogenesis. Neural stem cells (B-Type) proliferate and divide into transient amplifying cells (C-Type) that differentiate into neuroblasts (A-Type). A- and B-cells form a tube-like structure, the RMS, through which neuroblasts migrate in chains, differentiate, and maturate into interneurons. At the MOB, the new mature neurons integrate in the granule and glomerular cell layers. The figure is based on the data of Ming and Song, 2005.

1.2.1 Adult neurogenesis in the subventricular zone

The SVZ is located along the lateral wall of the lateral ventricles (Figure 5). Here, adult neurogenesis takes place in four developmental stages (Figure 5D): In the first stage (proliferation) arise transient amplifying cells from multipotent stem cells at a low division rate (B-cells). The second stage of development describes the fate specification. Here, the transient amplifying cells (C-cells) differentiate into neuroblasts (A-cells) and immature neurons. Inhibitors of gliogenesis are contributed by adjacent ependymal cells of the lateral ventricle and participate in determining the neuronal fate. The third stage describes the migration of the immature neurons. Astrocytes sheath the neurons, that are migrating through the rostral migratory stream into the main olfactory bulb (Figure 5A). Here, they migrate radially into the glomerular and granule cell layers. Adult neurogenesis also occurs in the accessory olfactory bulb, as interneurons are also renewed here (Halpern and Martínez-Marcos, 2003; Nunez-Parra et al., 2011). The fourth developmental stage is the synaptic integration. Immature neurons differentiate into interneurons of the main olfactory bulb, including GABAergic granule cells, GABAergic and dopaminergic periglomerular cells, or glutamatergic juxtaglomerular cells (Ming and Song, 2005).

1.2.2 Determinants of subventricular zone adult neurogenesis

Adult neurogenesis is regulated by various factors and molecular mechanisms, for example the neurogenic niche as a specific microenvironment (Louissaint et al., 2002; Licht and Keshet, 2015). Here, a cascade of signaling effectors constitutes the major impact on the sustainment of adult neurogenesis (Shohayeb et al., 2018). Hormones, neurotropic growth factors, transcription factors and neuro-inflammation also play critical roles in adult neurogenesis (for review see Shohayeb et al., 2018). The glutamatergic signaling from astrocytes to neuroblasts with a concomitant GABAergic control from neuroblasts to astrocytes exert the homeostatic control of adult interneuron production and development (Platel et al., 2007). Glutamate receptors (ionotropic and metabotropic) are expressed on NSCs in the SVZ, where they promote cell proliferation, differentiation, and survival (Castiglione et al., 2008; Platel et al., 2010; Young et al., 2011). GABA regulates the stem cell quiescence and neural progenitor cell fate decisions. $GABA_AR$s are critical in the SVZ for proper maturation of granule cells and synaptic integration into the main olfactory bulb. GABAergic modulation controls the increased plasticity in developing NSCs (Alfonso et al., 2012; Pallotto and Deprez, 2014). Dopaminergic receptors (D_1 and D_2) control the proliferation and differentiation fate of neural progenitor cells in the SVZ (Baker et al., 2004; Freundlieb et al., 2006; O'Keeffe et al., 2009). The understanding of the interrelationship of neurotransmitters and adult neurogenesis could provide an important basis for pharmacological approaches in disease models.

Extrinsic factors also affect adult neurogenesis. For example, physical activity increases adult neurogenesis through an increase in the proliferation rate of progenitor cells in the SGZ (van Praag et al., 1999a; van Praag et al., 1999b; Kronenberg et al., 2006) and SVZ (Jin et al., 2010; Chae et al., 2014). However, only voluntary activity improved cell proliferation according to a study in mice (van Praag et al., 1999b), whereas in rats, regular swim training caused an increase in progenitor cell proliferation and maturation of the SVZ (Chae et al., 2014).

1.2.3 Suppression of adult neurogenesis

The SVZ is the largest neurogenic niche of the adult mammalian brain, containing a large pool of NSCs. SVZ-NSCs revealed similarities to proliferative glioblastoma stem cells in the tumorigenesis of glioblastoma multiforme and are therefore evaluated as initiators of this aggressive type of cancer (Beiriger et al., 2022). Studies demonstrated the migratory pattern of NSCs from the SVZ to the tumor and clinical studies achieved success by irradiating the ipsilateral SVZ (Gupta et al., 2012). Active NSCs can be eliminated by antimitotic treatments (Doetsch et al., 1999a; Ihrie and Alvarez-Buylla, 2011). Therefore, the antimitotic alkylating agent Temozolomide (TMZ) has been applied in the past to treat recurrent or progressive glioblastoma in the progress of cancer research since it is capable of transcending the blood-brain barrier (Stevens et al., 1987). For detailed reviews on glioblastoma multiforme and adult neurogenesis see Capdevila et al. (2017).

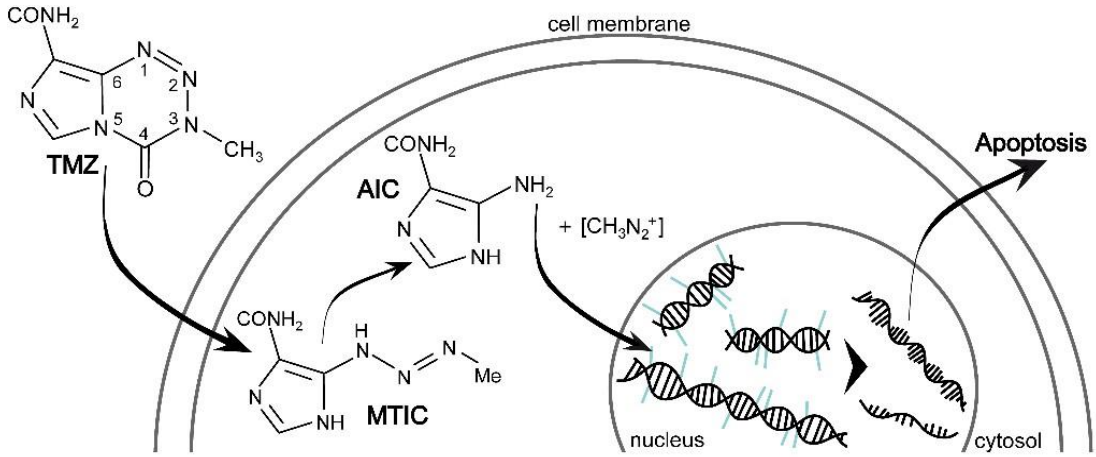

Figure 6: Mechanism of the effect of Temozolomide

TMZ is hydrolyzed to MTIC (3-methyl-(triazen-1-yl)imidazole-4-carboxamide), the active metabolite that translocated through the cell membrane into the cell nucleus. Here, MTIC transfers methyl groups on guanine, leading to a break of double-strand DNA during replication. This leads to apoptosis (Schreck and Grossman, 2018). Figure based on the work of Schreck and Grossman.

The imidazotetrazine derivative is a member of a class of polycyclic compounds consisting of a tetrazine ring and an imidazole ring. As a precursor to the agent, TMZ hydrolyzes at physiological pH to the pharmacologically significant alkylane 5-(3-methyltriazen-1-yl)imidazole-4-carboxamide (MTIC) (Wilman, 1986; Darkes et al., 2002). MTIC further hydrolyzes to 5-amino-imidazole-4-carboxamide (AIC) and methylhydrazine (Figure 6).

The addition of methyl groups at the N7 and O6 positions of guanine and the O3 position of adenine, results in the incorporation of thymine in place of cytosine during DNA replication (Brindley et al., 1986; Tisdale, 1987; Marzolini et al., 1998; Garthe et al., 2009; Lee, 2016). This induces cell cycle arrest at G2/M, resulting in rapid apoptosis-inducing effects in transient-amplifying cells. Methylation of non-proliferative active cells is considered to be improbable (Zucchetti et al., 1989).

However, only active NSCs that express the epidermal growth factor receptor can be eliminated by TMZ, so quiescent NSCs remain as a regeneration pool for SVZ neuroblasts (Giachino and Taylor, 2009).

1.2.4 Adult neurogenesis in other brain regions

Adult neurogenesis has been demonstrated in several brain regions (for review see Jurkowski et al. (2020)), e.g., the SGZ of the dentate gyrus of the hippocampal formation. In contrast to the SVZ, five developmental stages have been identified here. NSCs spread from the subgranular zone of the dentate gyrus with their radial projections into the granular cell layer and their tangential projections along the granule cell layer and the hilus. In stage one (proliferation), these NSCs give rise to transient amplification cells that further differentiate into immature neurons in stage two (fate specification). During migration in developmental stage three, these immature neurons migrate a short distance into the granule cell layer, where they align their axons/dendrites during stage four (axon/dendrite targeting). Axon alignment occurs along the mossy fiber tracts in the CA3 pyramidal cell layer, whereas dendrites extend to the molecular layer. In the final stage (synaptic integration), new granule neurons are synaptically integrated into the hippocampal formation (Altman and Das, 1965; Ming and Song, 2005; Kempermann et al., 2015; Abbott and Nigussie, 2020).

Evidence for a hypothalamic neurogenesis has been found on the lateral wall of the third ventricle in the adult rat brain (Evans et al., 2002; Markakis et al., 2004). This neurogenic niche exhibits distinct zones with different degrees of proliferation (Pérez-Martín et al., 2010). Other studies discussed the hypothalamic adult neurogenesis in social and metabolic functions and sexual/mating behavior, but not in humans (Bernstein et al., 1993; Cheng et al., 2011; Lee and Blackshaw, 2012; Recabal et al., 2017). Postnatally generated neurons have also been detected in the striatum (Schlösser et al., 1999; Ernst et al., 2014).

In the cerebellum, the external germinal layer contributes to neurogenesis postnatally (Altman and Bayer, 1997; Lee et al., 2005). Purkinje cells are thought to originate from the ventricular zone of the cerebellum, whereas granule cells originate from the external germ layer. Transplantation studies demonstrated the generation of other cell types (e.g., astrocytes, oligodendrocytes, and various interneurons) from ventricular zone progenitor cells that migrate postnatally to the cerebellar cortex (Hallonet et al., 1990; Zhang and Goldman, 1996; Lee et al., 2005).

1.3 Neurotransmitter receptors in the olfactory system

Over the past few years, knowledge of neurotransmitter receptors has expanded through cellular, electrophysiological, and molecular techniques. The development of selective antagonists and agonists enabled the identification of different receptor types and subtypes in neuropharmacological experiments and radioactive ligand binding studies. Neurotransmitter receptors can be found, for example, in the synaptic membrane of neurons. Because they are not homogeneously distributed, they can be used in receptor autoradiography to determine region boundaries. Thus, a change in distribution patterns could indicate a border of distinct regions (Zilles et al., 1991; Zilles and Schleicher, 1991). Neurotransmitter receptors are frequently used as targets in therapeutic treatment (Bonuccelli et al., 2009; Cremer et al., 2015a; Cremer et al., 2015b).

In the olfactory system, glutamatergic receptors have been shown to regulate mitral and tufted cell excitability (Salin et al., 2001; Urban and Sakmann, 2002; Christie and Westbrook, 2006; Blakemore et al., 2018). Metabotropic GABA receptors have been implicated in odor contrast and odor discrimination learning (Smith and Jahr, 2002; McGregor et al., 2004; Shepherd, 2004; Panzanelli et al., 2005; Sokolic and McGregor, 2007) and catecholaminergic receptors exhibit a function in the reward response to odors (Doucette et al., 2011; Zhang et al., 2017).

In the following, the receptors of this work will be summarized concerning their classification in glutamatergic, GABAergic, and catecholaminergic receptors.

1.3.1 Glutamatergic receptors

Glutamate is the most important excitatory neurotransmitter in the mammalian brain. Glutamate receptors are several receptor families and multiple subtypes, each with individual pharmacological and physiological properties. There are three families of ionotropic glutamate receptors with intrinsic cation-permeable channels: NMDA, AMPA, and kainate receptors (Sommer and Seeburg, 1992) and eight receptor families of metabotropic G-protein coupled glutamate receptors, mGlu1 to mGlu8 (Pin and Duvoisin, 1995; Cartmell and Schoepp, 2000). Overall, ionotropic and metabotropic receptors are positive regulators of adult neurogenesis (Platel et al., 2007). Glutamatergic neurotransmitters are stored in synaptic vesicles and are released into the synaptic cleft in a Ca^{2+}-dependent manner upon depolarization (Greenamyre and Porter, 1994). From here, they are released by Na^{+}-dependent uptake carriers from neurons and glia (Tapiero et al., 2002).

The AMPA receptor

The AMPA (α-Amino-3-hydroxy-5-methyl-4-isoxazole propionic acid) receptor (AMPAR) consists of four subunits (GluR1, GluR2, GluR3, and GluR4) that form homo- and heterotetramers (Hollmann et al., 1989; Ozawa et al., 1998) including sodium- and potassium-dependent channels. The receptor function is already active at the first synapse of olfaction. This is located between the olfactory sensory neurons and the postsynaptic targets (mitral cells, tuft cells, and periglomerular cells) in the olfactory bulb. This transition is subject to ongoing anatomical plasticity provided by an increase in AMPA versus NMDA receptors (Grubb et al., 2008). AMPARs promote synchronous mitral cell activity (Usrey, 2002) to ensure signal transduction between the glomeruli.

Glutamate is a positive regulator of adult SVZ neurogenesis (Platel et al., 2007). After assuming that neuroblasts do not express AMPA and NMDA receptors (Carleton et al., 2003), Platel and colleagues showed that neuroblasts already express functional AMPA/kainate receptors in the SVZ (Platel et al., 2007). Upon inhibition of NMDARs, AMPARs/kainateRs showed increased cell proliferation with decreased apoptosis rates (Brazel et al., 2005). In the pathological brain, AMPARs modulated adult neurogenesis by promoting survival and proliferation of neural stem cells (Lauterborn et al., 2000; Hachem et al., 2017).

The kainate receptor

The kainate (2-carboxy-4-(1-isopropenyl)-3-pyrrolidine acetate) receptors (kainateR) consist of three low affinity (GluR5, GluR6, GluR7) and two high affinity (Ka1 and Ka2) groups. Previously, these receptors were grouped together with AMPARs. In the olfactory bulb, kainate agonists modulate excitatory and inhibitory transmission and are involved in olfactory information coding circuits (Blakemore et al., 2018). Here, they are expressed on mitral/tufted and periglomerular cells (Petralia et al., 1994; Davila et al., 2007).

In adult neurogenesis, kainateRs have been shown to be responsible for the proper functionality of newborn neurons in the dentate gyrus (Zhu et al., 2021).

The NMDA receptor

The NMDA (N-methyl-D-aspartate) receptor (NMDAR) is composed of NR1, NR2A-D, and NR3A subunits that act voltage-charged by ligand binding. Due to the slower release of glutamate from the NR2A subunit (Lester et al., 1990) and the second binding site at the NR1 subunit (Johnson and Ascher, 1987), the kinetics of NMDARs are slower than AMPARs and kainateRs. Another unique feature of this receptor family is that it can be inhibited under resting conditions via physiological Mg^{2+}-ion (Ascher et al., 1988). NMDARs play a central role in the induction of long-term potentiations (LTP) and long-term depression, leading to a major importance in learning and memory (Collingridge et al., 2013). In the olfactory system, NMDARs are involved in olfactory learning and memory (Xia et al., 2005) and odor preference learning (Lethbridge et al., 2012).

In adult neurogenesis, only 20 % of SVZ-Neuroblasts express functional NMDARs in the neurogenic niche. However, upon entering the main olfactory bulb, the number increases to 100 %, which demonstrates the receptor function for the synaptic integration of neuroblasts (Platel et al., 2010). In the process of synaptic integration, NMDARs support the morphological differentiation of granule cells of the main olfactory bulb (Kelsch et al., 2012). Up to now, NMDARs are known to be involved in all developmental stages of adult-born neurons in a activity-dependent manner (Platel and Kelsch, 2013).

The metabotropic glutamate 2/3 receptor

Metabotropic glutamate receptors (mGluR) belong to the family of G-protein-coupled receptors that can modulate excitability via a second-messenger mechanism. G-proteins are

membrane-bound proteins that are activated by extracellular ligands. These include, for example, neurotransmitters, light, peptides, or intracellular. Stimulus binding results in a conformational change of the mGluR, which activates the G-protein. This activation leads to the functional activation of transcription factors, enzymes, and ion channels. The activation results in an exchange of G-protein-bound guanosine-5-triphosphate (GTP) to guanosine-5-diphosphate (GDP). Upon G-protein inactivation, GTP is hydrolyzed back to GDP. Different G-protein couplings and ligand selectivity divide mGluRs into eight subtypes. Group I consist of mGluR and mGluR5, which are mainly localized at postsynaptic sites. Group II consists of mGluR2 and 3, and group III consists of mGluRs 4, 6, 7, and 8 (Conn and Pin, 1997). Both groups are mostly expressed presynaptically (Pinheiro and Mulle, 2008).

The nomenclature of the groups resulted from their chronological detection, starting at mGluR1 (Houamed et al., 1991). Group I receptors are bound to G_q proteins and stunt phospholipase C. This results in a Ca^{2+} increase inside the cell and activation of protein kinase C (Fagni et al., 2000). Group II and III are coupled to G_i/G_o-proteins, which inhibit adenylate cyclase. This inhibition leads to a decrease in cAMP and inactivates protein kinase A (Niswender and Conn, 2010; Willard and Koochekpour, 2013; Suh et al., 2018).

The ligand LY341495 ((2S)-2-amino-2-[(1S,2S)-2-carboxycycloprop-1-yl]-3-(xanth-9-yl) propanoic acid), is an orthosteric antagonist of group II and III (Niswender et al., 2008). In therapeutic form, it has an antidepressant effect and can lower the effective dose of ketamine (Pilc et al., 2008; Pałucha-Poniewiera et al., 2021).

In the olfactory system, knowledge about the $mGlu_{2/3}$ receptor is unclear. It plays a role in olfactory habituation, one of the oldest forms of sensory system learning (McNamara et al., 2008). The receptor impacts mitral and granule cell signals in the external plexiform layer, implicating the receptor in contrasting stimuli in the main olfactory bulb (Ennis et al., 2006; Heinbockel et al., 2007). In general, $mGlu_2Rs$ activity suppresses glutamatergic excitability of mitral/tufted cells in the main and accessory olfactory bulb (Dong and Ennis, 2018).

In adult neurogenesis, it has been shown that activation of $mGlu_3$ and $mGlu_5$ receptors stimulates stem cell proliferation and neural progenitor cell survival (Di Giorgi-Gerevini et al., 2005; Melchiorri et al., 2007; Dindler et al., 2018). Proliferating cells express active $mGlu_{2/3}Rs$, demonstrating a function in the regulation of NSCs (Dindler et al., 2018).

1.3.2 GABAergic receptors

Gamma-aminobutyric acid (GABA) is the primary inhibitory neurotransmitter in the central nervous system. Two classes of receptors mediate the binding of GABA neurotransmitters: $GABA_A$ and $GABA_B$. $GABA_A$Rs are ionotropic receptors, while $GABA_B$Rs are metabotropic receptors. Benzodiazepine binding sites are present on subunits of $GABA_A$Rs ($GABA_{A(BZ)}$Rs).

GABAergic signals are the major inhibitory regulators in the SVZ and RMS. In general, GABA is considered here as a negative regulator of SVZ-neuroblasts (Nguyen et al., 2003; Liu et al., 2005; Platel et al., 2007). Migration rates are also reduced by GABAergic signaling pathways (Bolteus and Bordey, 2004).

The $GABA_A$ receptor

$GABA_A$Rs are composed of different subunits (α-, β-, γ-, Δ-, ε-, π-, θ-, and ρ-subunits as well as splice variants), whose different compositions lead to distinct pharmacological and physiological properties (Hevers and Lüddens, 1998; Simon et al., 2004). The subunits form chloride ion channels that open upon binding. When the receptors are activated, negatively charged ion influx into the cell, impeding the cell's excitability. In the olfactory system, $GABA_A$Rs are involved in contrasting similar odor information in the main olfactory bulb (Wilson and Laurent, 2005). This process is triggered via the inhibitory effect of $GABA_A$Rs on granule cells interacting with mitral/tufted cells. Periglomerular cells have a self-inhibitory effect induced by $GABA_A$Rs that leads to an all-or-nothing response, thus making a crucial contribution to the contrasting of odors (Smith and Jahr, 2002).

$GABA_A$Rs in the entorhinal cortex regulate the duration of up-down states that are involved in epileptiform bursts (Mann et al., 2009). A reduction in receptor density was observed in temporal lobe epilepsy (Stefanits et al., 2019). The receptor is involved in the inhibition of anxiety (Lewis and Gould, 2007) and reveal decreased densities in the entorhinal cortex of Alzheimer's disease patients (Kwakowsky et al., 2018).

Upon their activation in neuroblasts, the rate of migration in the RMS (Bolteus and Bordey, 2004; Heck et al., 2007) and number of proliferative SVZ neuroblasts (Nguyen et al., 2003; Liu et al., 2005) is reduced. Due to the amount of GABAergic signals, NSCs receive information about the available neuroblast pool, since $GABA_A$Rs increase with increasing amounts of neuroblasts (Platel et al., 2007).

The $GABA_A$-Benzodiazepine binding sites

Ligands with benzodiazepine binding sites modulate the inhibitory action of GABA allosterically. The binding of a ligand results in a conformational change, which conversely exhibits altered GABA affinity. In pharmacology, diazepam and flunitrazepam are well-known ligands of the benzodiazepine binding sites. When bound, they enhance GABAergic action on $GABA_ARs$ (Hunt, 1983; Sieghart, 1995).

In the olfactory system, $GABA_{A(BZ)}Rs$ have been implicated in selectively impairing olfactory discrimination learning (Sokolic and McGregor, 2007). While these receptors are increased in the orbitofrontal cortex of schizophrenic patients (Kiuchi et al., 1989), they, are decreased by 40% in the brains of Alzheimer's disease patients (Jansen et al., 1990).

Flumazenil, a ligand for $GABA_{A(BZ)}Rs$, is an antagonist of midazolam, a drug that is used in pediatric anesthesia (Yu et al., 1990). It has been shown that a too-early intake limits the proliferation of NSCs in adulthood, exerting a negative effect on adult neurogenesis (Doi et al., 2021). On the other hand, type 2 progenitor cells in the adult hippocampus express $GABA_ARs$, which can stimulate neuronal differentiation (Deisseroth and Malenka, 2005; Wang et al., 2005).

The $GABA_B$ receptors

$GABA_BRs$ are G-protein-coupled proteins that produce slow and long-lasting inhibition via G_i/G_o-protein activation. This effect is mediated by the activation of K^+-ion channels, which in turn leads to inactivation of Ca^{2+}-ion channels and thus inhibition of adenylate cyclase. The receptors are heterodimers that are composed of R1 and R2 subunits (Bettler et al., 2004).

In the olfactory bulb, $GABA_BRs$ regulate the sustained currents of Na^+- and K^+ to mitral cells, thereby increasing the efficacy of synaptic potentials (Li et al., 2017). Periglomerular cells exhibit presynaptic inhibition on olfactory sensory neurons, accessing them via $GABA_BRs$ at axonal terminals (Aroniadou-Anderjaska et al., 2000; Murphy et al., 2005; Wachowiak et al., 2005). Thus, $GABA_BRs$ modulate sensory inputs to the main olfactory bulb. Growing axons of olfactory receptor neurons also express $GABA_BRs$ to control their own growth upon entry into the glomerular layer (Priest and Puche, 2004). $GABA_BRs$ control feedback from the primary olfactory cortex to the main olfactory bulb (Mazo et al., 2016).

In adult neurogenesis, an inhibition of $GABA_BRs$ leads to an increase in proliferation (Felice et al., 2012). In general, in the adult hippocampus, $GABA_BRs$ were found to act as inhibitors of adult neurogenesis and thus proliferation of NSCs (Giachino et al., 2014; Song et al., 2021).

1.3.3 Catecholaminergic receptors

Catecholaminergic receptors can be subdivided in adrenergic α-receptors and dopaminergic receptors. The receptors are G-protein-coupled and thus have an effect on adenylyl cyclase and stimulation of phosphatidylinositol hydrolysis (Caron and Lefkowitz, 1993).

The Alpha-1 adrenergic receptor

α_1-receptors (α_1R) consist of subtypes α_{1A}, α_{1B}, and α_{1C} (Bylund, 1992). They are activated upon the binding of norepinephrine and epinephrine. They are involved in the modulation of attention and memory (Sirviö and MacDonald, 1999) and in the activation of GABAergic interneurons (Papay et al., 2006; Gupta et al., 2009).

In the olfactory system, α_1Rs increase the excitatory response of mitral cells to a low input from olfactory nerves (Ennis, 2008a; Ennis, 2008b), so α_1Rs regulate weaker olfactory stimuli in the main olfactory bulb. Higher concentrations of norepinephrine at α_1Rs increase excitability, whereas low concentrations seem to have no effect (Nai et al., 2010). The concentration of norepinephrine varies with the neuronal activity of the locus coeruleus, which causes an increase in norepinephrine cell activity upon excitation by novel odors (Linster et al., 2011). In synchronous mitral/tufted cells, their activity is important in excitatory-rewarding or inhibitory non-rewarding olfactory responses (Doucette et al., 2011). Thus, α_1Rs are essential for the discrimination of chemically similar odors (Mandairon et al., 2008). In the entorhinal cortex, α_1Rs block epileptiform activity induced by norepinephrine (Stanton et al., 1987).

To date, the function of the receptor in adult neurogenesis is unclear. A study has shown that it plays a regulatory role in the survival of new neurons and the apoptosis of astrocytes in adult neurogenesis (Gupta et al., 2009). Activation of α_1Rs has a positive effect on vascular endothelial growth factors (Gonzalez-Cabrera et al., 2003), which in turn increase proliferation of neuronal progenitor cells (Jin et al., 2002).

The Alpha-2 adrenergic receptor

α_2-Receptors (α_2R) consist of the three pharmacological subtypes α_{2A}, α_{2B}, and α_{2C}. All subtypes inhibit adenylate cyclase via G_i/G_o proteins. This activates K^+-ion channels and inhibits Ca^{2+}-channels so that the concentration level of cAMP is reduced (Limbird, 1988; Bylund, 1992). α_2Rs acts inhibitory in blood pressure regulation and pain perception (Starke et al., 1989; Ruffolo

et al., 1993). Norepinephrine, acting at α_2Rs, is involved in the formation of the partner recognition memory of the accessory olfactory bulb by facilitating NMDA-dependent LTPs at the mitral cell-to-granule cell synapse by disinhibition of mitral cells (Huang et al., 2018) and granule cells of the main olfactory bulb (Nai et al., 2010). In the entorhinal cortex, adrenergic receptors have been shown to inhibit excitatory synaptic transmission (Pralong and Magistretti, 1995) and reduce induced epileptiform discharges (Stoop et al., 2000).

The receptor is essential for the plasticity of adult neurogenesis by promoting differentiation (Karkoulias et al., 2006). In the SGZ, α_2Rs expressed on progenitor cells decrease adult neurogenesis, leading to a positive effect in chronic antidepressant treatments (Yanpallewar et al., 2010). In the SVZ, the receptor has an effect in the protection against neuronal death and thus at promoting function in the survival of neuroblasts (Bauer et al., 2003; Jhaveri et al., 2014).

The Dopamine receptor

Dopamine receptors can be divided in two types: the D1-type includes D_1 and D_5 receptors. The D2-type includes D_2, D_3, and D_4 receptors (Andersen et al., 1990; Sibley and Monsma, 1992; Vallone et al., 2000). D1- and D2-type receptors differ mainly on their modulation of adenylate cyclase. While D1- types are positively coupled to adenylate cyclase and lead to an activation, D2-types are negatively coupled (Spano et al., 1978; Kebabian and Calne, 1979).

Dopamine is involved in a variety of neural functions, such as cognition, working memory, attention, emotion, reward, feeding, motor function, sleep, et cetera. (Snyder et al., 1970; Missale et al., 1998; Sibley, 1999). In the olfactory system, D1- type receptors co-modulate olfactory conditioning (Weldon et al., 1991). The receptors play a key role in Parkinson's disease, in which striatal dopaminergic innervations are degraded (Ehringer and Hornykiewicz, 1960; Pasquini and Pavese, 2021). Thereby, they are of pharmacological interest in the treatment of brain diseases due to their diversity (Beaulieu and Gainetdinov, 2011).

It was shown that a D1- type agonist causes the survival of newborn neurons in the SGZ, whereas the D2-type agonist had no effect on either proliferation or survival (Takamura et al., 2014). In the SVZ, dopamine exerts an impact on the proliferation rate of adult neurogenesis (Baker et al., 2004; O'Keeffe et al., 2009; Doze and Perez, 2012; Mishra et al., 2019; Garcia-Garrote et al., 2021).

1.4 Receptor autoradiography

The methodology of autoradiography is used to visualize radioactively labeled targets. Receptor autoradiography is a form of this technique that involves the labeling of receptor-specific ligands via radioactive isotopes in order to subsequently visualize the binding sites of a receptor. The radiation from radioisotopes produces a latent image the so-called receptor-autoradiogram. The weaker the radiation, the longer exposure times are required. In its subsequent photographic processing, the radiation is detectable by a darkening similar to a black-and-white photograph. The amount of radiolabeled detected receptors corresponds to the amount of receptors in the tissue. Thus, receptor autoradiography is an imaging technique that is used to localize and quantify receptor binding sites (Zilles and Schleicher, 1991).

In the 1970s, receptor binding techniques were established for opiate and dopamine receptors (Kuhar et al., 1973; Seeman et al., 1975), which, together with computer-assisted imaging techniques, represented a milestone in imaging research (Zilles et al., 1986; Schleicher and Zilles, 1988). In vitro receptor autoradiography provided an imaging technique that combined quantitative and qualitative features. Especially in brain research, the method is appropriate to visualize the chemoarchitectonic organization of regions, especially of the cortex (Zilles et al., 1986). The different receptor distribution patterns in distinct regions of the brain can be used to define borders between regions of interest (Zilles et al., 1991; Scheperjans et al., 2005) and provides evidence of functionally (dis-)similar brain regions (Zilles et al., 1991; Zilles and Palomero-Gallagher, 2001; Zilles et al., 2002a; Zilles et al., 2004). The method generates high spatial resolution images (< 100 µm) of whole tissues. Thus, a receptor can be visualized directly in several brain regions in one slice (whole hemisphere autoradiography) Hall et al. (1998). Due to the fact that the brain sections are very thin, the successive tissue sections can be incubated with different radioligands, resulting in multiple receptor autoradiograms for one region. In this context, the method is most useful in combination with histological stained sections.

Since it is a postmortem technique, pre- and postmortem factors may influence ligand binding, which should be mentioned as an individual hypothetical limitation. In particular, the postmortem extraction and handling of the brain are a crucial factor for the quality of the method. Here, vacuum freeze-drying of unfixed tissue sections turned out to be suitable in order to avoid damaging of the receptor protein structure (Stumpf and Roth, 1964; Zilles et al., 2002b). In addition, there is a need for selective and highly sensitive radiolabeled receptor ligands with low nonspecific binding, which makes the method very cost intensive. Receptor autoradiography was chosen for this work as it provided the visualization of the ten different receptors, has a high resolution and the images remain available for analysis in the future due to digitization.

1.5 Aims and objectives

The present thesis is part of a larger project, therefore the autoradiograms were already present, and provided for analysis in the context of this work. The aim of this work is the investigation of the impact of adult neurogenesis and cognitive training on the receptor architecture of the mouse olfactory system.

Considering the functional heterogeneity of the mouse olfactory system, the first experiment is conducted to analyze the receptor architecture of the olfactory regions. The anatomy and receptor distribution should be visualized by receptor autoradiographic analyses in combination with cytoarchitectonic mapping. Based on the correlation of receptor architecture and functionality of a region, further analyses aim to provide a functional interpretation of less known regions (taenia tecta, dorsal peduncular cortex, anterior olfactory cortex). A distinct receptor profile is expected for each olfactory region, which will subsequently be classified into clusters based on its (dis-)similarities in the receptorarchitecture. Hierarchical cluster analysis and a heat map will reveal which receptors contributed most to the cluster formations.

The functional role of receptors in adult neurogenesis has been a growing part of investigations. To date, the impact of adult neurogenesis on the receptor profiles has not been addressed. Therefore, mouse brains with suppressed adult neurogenesis should demonstrate the alterations of receptor densities in olfactory regions. In a second experiment, the successful suppression of adult neurogenesis should be verified by a quantitative evaluation of immunohistochemically BrdU-labeled cells in the main olfactory bulb. The number of labeled cells should be collected for every experimental group. The cell quantity of untreated animals to TMZ-treated animals should then reflect a successful inhibition. Based on the results of this experiment, the third step of this work will determine the alterations in the olfactory receptor architecture upon the suppression of adult neurogenesis. The receptor densities of 14 olfactory regions of ten control animals will be compared to the respective densities of ten TMZ-treated animals by receptor autoradiography. A general pattern alteration in the treated animals is expected, particularly for inhibitory receptors. In all subsequent experiments, receptor densities should be determined by receptor autoradiography with subsequent data computation and statistical evaluation.

In the fourth experiment, the impact of cognitive training on the receptor architecture of the olfactory system should be analyzed. Receptor densities of ten trained animals will be compared to the densities of control animals. Higher GABAR concentrations are expected in trained animals. The fifth experiment will determine if the olfactory receptor architecture of trained mice will be altered after suppression of adult neurogenesis. The olfactory receptor

densities of trained, untreated mice will be compared to concentrations of trained, TMZ-treated animals. Cognitive training and adult neurogenesis are expected to exert a contrary impact, so minor changes are expected. In this comparison, a long-time study could be of great interest since the impact of a lack in proliferating cells could increase over time.

The sixth experiment should reveal the impact of both determinants on the olfactory receptor concentrations. Densities of trained animals with suppressed adult neurogenesis will be compared against densities of control animals. A regulating and stabilizing effect of cognitive training on the receptor architecture in the TMZ-treated animals is expected, so only minor differences are supposed. In the seventh experiment, cognitive training will be analyzed as a modifying factor in suppressed adult neurogenesis. The receptor patterns of both TMZ-treated groups will be examined. If cognitive training has a greater effect on the receptor architecture than adult neurogenesis, the values of the trained animals should be more similar to those of the control animals. In general, higher receptor levels are expected for trained TMZ-treated animals.

The final, eighth experiment will further evaluate the impact of cognitive training on receptor densities of the olfactory system in adult mice with impaired neurogenesis. Therefore, the relative data of the third experiment will be compared against those of the fifth experiment. Graphical plotting of both relative receptor alterations in a fingerprint will display whether the effect of an absent adult neurogenesis is reduced in the trained animal due to cognitive training. A heat map should visualize which receptors or regions differ the most. GABAergic receptors are expected to exert the most differences in this comparison.

2. Material and Methods

The present work focused on the analysis of immunohistochemical and receptor autoradiographic data of the olfactory system in mice. It is based on receptor autoradiographic and immunohistochemical images as well the performance of behavioral tests and treatment of animals that were performed earlier. It is part of a large experiment and included the histology and digitization of receptor autoradiographs and immunohistochemical images for half of the experimental animals. In this chapter, the whole spectrum of applied methods is briefly summarized, in order to provide the necessary context for interpreting the results of the study.

2.1 Animals

The project included 180 mice of strain C57BL/6 (Janvier Labs, Germany) 60 animals were part of the present thesis. To exclude possible sex effects, only male animals were examined (Ormerod et al., 2004; Tanapat et al., 2005; Bowers et al., 2010; Hyer et al., 2017; Hyer et al., 2018; Yagi and Galea, 2019).

The animals (eight weeks old, approximately 30 g body weight) were kept in groups of five mice each in a cage (37x22x15 cm) in enriched environment (van Praag et al., 2000; Würbel, 2001; Wolfer et al., 2004). They were kept in a 12-h dark-light rhythm with food and water ad libitum. All experiments were performed according to the German Animal Welfare Act (Az.87-51.04.2010.A250) and the guidelines of the State Office for Nature, Environment and Consumer Protection (LANUV, NRW, Germany) and in agreement with the National Institute of Health Guide for Care and Use of Laboratory Animals.

As shown in Table 1, the project included three categories of animals: the control animals, the animals that underwent cognitive training and the animals for immunohistochemical control of the suppression of adult neurogenesis. Every category included two groups: the control group (CG) and the group with suppressed adult neurogenesis (TMZ).

This resulted in the following groups for receptor autoradiography:

- Control animals in enriched environment (control group; **CG**; n = 10)
- Animals in enriched environment with suppressed neurogenesis (**CG_{TMZ}**; n = 10)
- Animals in enriched environment, that received cognitive training (**MWM_{CG}**; n = 10)
- Animals in enriched environment with suppressed neurogenesis, that received cognitive training (**MWM_{TMZ}**; n = 10)

Table 1: Overview of the group design

	Control groups (+ NaCl)		Treatment groups (+ TMZ)	
control	10 animals	**CG**	10 animals	**CG_{TMZ}**
training	10 animals	**MWM_{CG}**	10 animals	**MWM_{TMZ}**
+ BrdU	10 **CG** animals 10 **MWM_{CG}** animals		10 **CG_{TMZ}** animals 10 **MWM_{TMZ}** animals	

2.1.1 Treatments

Following the protocol of Garthe and colleagues, four TMZ treatment cycles were performed (Garthe et al., 2009): animals in the TMZ group were injected intraperitoneal with a dose of 25 mg/kg body weight for four weeks on three consecutive days, followed by a four-day rest period for convalescence (Figure 7). 20 animals were treated with NaCl according to the same schedule and volume as TMZ. Animals were weighted before each application and the amount of TMZ was adjusted to the current weights.

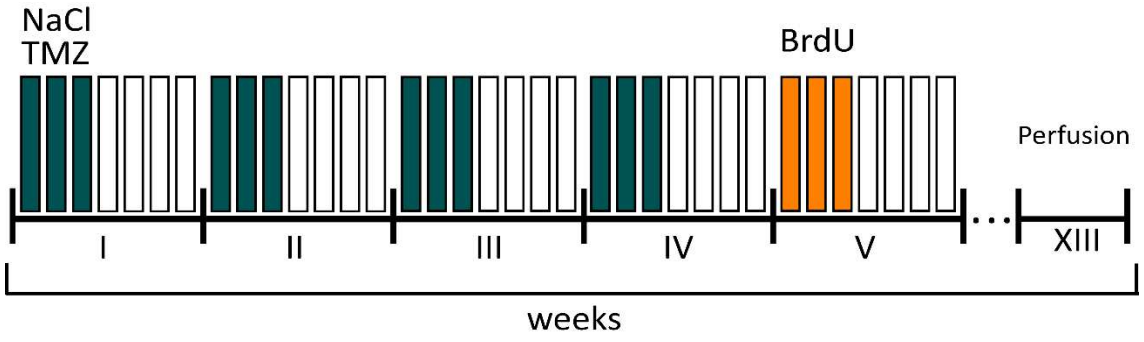

Figure 7: Application scheme of experimental procedures in animal studies.

Application of TMZ (dark green) on three consecutive days (rectangles) over a period of four weeks (x-axis). Following application of BrdU for another three consecutive days. Eight weeks after the last TMZ administration (13 weeks after the start of pharmaceutical application), the animals were perfused.

Adult neurogenesis was detected by labelling proliferating cells using 5'-bromo-2'-deoxyuracil (BrdU). Animals were treated with BrdU at a daily dose of 50 mg/kg for three consecutive days by intraperitoneal injection 5 weeks after initial inhibition of adult neurogenesis (Figure 7).

2.1.2 Training

20 animals underwent cognitive training in form of well standardized behavioral tests (Zilles et al., 2000; Deacon and Rawlins, 2006; Vorhees and Williams, 2006; Garthe and Kempermann, 2013). The direct analysis of these tests (time duration, paths, performance) was part of another thesis (Jordens, 2012). First, the animals underwent cognitive training in the Y-maze. Second, T-maze studies were conducted. Both tests provided food rewards (Froot Loops, Kellogg's). For social facilitation, all animals of the same home cage were placed together during cognitive training. Third, Morris Water Maze was performed in a daily inter-trial interval.

2.1.3 Brain preparation

Animals were anesthetized intraperitoneal with 60 mg/ml pentobarbital. Subsequently, animals were perfused transcardially with 0.9% NaCl followed by paraformaldehyde (PFA, 4% in 0.1 M phosphate buffer pH 7.4). Animals were decapitated, brains were removed from the skull, and shock-frozen using isopentane (2-methylbutane) at -40 °C, and stored at -70 °C. For this thesis, there were 60 brains in total. 40 brains were used for receptor autoradiography and 20 brains for immunohistochemistry.

2.2 Tissue processing

The brains were mounted on a block in a cryostat microtome (-20 °C; CM 3050, Leica; 2800 Frigocut, Reichert-Jung). At -13 °C, the preparation was subsequently cut into coronal sections. Coverslips were coated with chromium-potassium gelatin and refrigerated to melt the sections onto these slides after they were cut. Thereafter, sections were freeze-dried overnight at -25 °C under vacuum in a desiccator containing silica gel. Subsequently, the sections were stained differently depending on the following experiments.

The brains for receptor autoradiography were sectioned at a thickness of 15 µm, from Bregma level 3.8 mm to Bregma -3.6 mm in about 30 series. Each series included 14 sections. This resulted

in approximately 400 sections per animal and up to 700 sections per ligand. Series 6, 11, 16 and 21 were stained alternately with unbound ligands to control the staining quality. The cutting scheme can be found in Supp. Tab. 1. Brains for immunohistochemical methods were cut with a section thickness of 32 µm and were stained with a triplicate stain BrdU/NeuN/GFAP.

2.2.1 Histology

Silver staining of cell bodies was performed according to an established protocol (Merker, 1983; Uylings et al., 1999). Cryo-sections were fixed at room temperature in neutral buffered formalin (4%) overnight. After immersion in distilled water for 1 min, sections were incubated in 4% formic acid for 3 hours and then in formic acid/H_2O_2 overnight (Supp. Tab 2). The following day, the sections were rinsed (1 min, distilled water, flowing) and incubated 2 times for 5 min in 1% acetic acid in distilled water. After preparation of developer solutions A, B, and C (see Supp. Tab. 2), the sections were developed for 15-30 min by a continuously dipping the slide in developer solution C. When the desired intensity was achieved the staining procedure was stopped in 1% acetic acid (5 min) and the sections were rinsed for 5 min under running distilled aqua. Subsequently, the sections were fixed with fixative solution (Supp. Tab. 2; T-max, Kodak, Germany) for 2 min, again immersed in distilled water for 5 min, and finally dehydrated in an ascending alcohol series (70%, 80%, 90%, 96%, 100%) and xylene (2 times) for 2-5 min each. DPX (Sigma, Germany) was used to cover the tissue sections. Details are provided in Supp. Tab. 2.

Staining of myelin was performed according to an established protocol of a modified silver staining method (Gallyas, 1971) as outlined in Supp. Tab. 3.

2.2.2 Immunohistochemistry

BrdU-Immunohistochemical labeling was carried out as described previously (Kempermann et al., 2003) to detect adult neurogenesis in the olfactory bulb and simultaneously control its suppression using TMZ. In short (Supp. Tab. 4): Following preparation, brains were post-fixed in 4% PFA for 24 hours and then incubated in 30% sucrose solution for an additional 24 hours at 4 °C. The fixed brains were frozen at -70 °C and finally cut into 32 µm thick coronal tissue sections using a freezing microtome (Leica, Bensheim; Germany). For further processing, the sections were stored at 4 °C in glycol solution.

For immunohistochemical detection of BrdU-positive cells (BrdU+), the tissue sections were first incubated in 0.5% H_2O_2 in phosphate-buffered saline (0.12 M, pH 7.4; PBS) for 30 min to block tissue peroxidase activities. To denature DNA and thus facilitate accessibility to BrdU, the sections were incubated in 2 M HCl (30 min, 45 °C). This was followed by neutralization in 0.1 M borate buffer (pH 8.5). After repeated rinses (5 – 20 times) with PBS, the sections were incubated overnight at 4 °C with the primary antibody in PBS, 0.1% Triton X-100, and 0.1 % sodium azide. Further rinsing (5 – 20 times, PBS) was followed by one-hour incubation with the second antibody in PBS and TritonX-100 (0.12 M, pH 7.4) at room temperature.

A one-hour incubation in ABC reagent (Vectastain, Vector Laboratories, Burlingame, CA) was used for amplification according to the avidin-biotin principle. The final staining reaction was performed with 0.5 mg/ml 3.3'-diaminobenzidine (DAB, Sigma, Germany), 0.0025 mg/ml ammonium nickel sulfate (Sigma, Germany), 2 mg/ml D-glucose (Sigma, Germany), 0. 4 mg/ml ammonium chloride (VWR Merck, Germany), 0.4 mg/ml cobalt chloride-6-hydrate (Merck) in sodium buffer (pH 6.0), and 1 mg/ml glucose oxidase (Sigma, Germany). The tissue sections were subsequently rinsed in PBS (5 – 20 times) again and then mounted on microscope slides.

2.2.3 Receptor autoradiography

Quantitative receptor autoradiography was used to detect receptor densities in a region of interest in histological sections. Ligands bound to [^{3}H]-tritium were used for optical labelling of neurotransmitter receptors. Tritium is a stable isotope hydrogen that is present in all receptors, it does not cause structural changes, and it is comparatively safe to handle due to its low-energy irradiation (Zilles and Schleicher, 1991).

[^{3}H] radioligands

The following ten receptors were studied including their ligands:

Glutamatergic receptors:

- Agonist [^{3}H]-AMPA for the ionotropic receptor α-Amino-3-hydroxy-5-methyl-4-isoxazol-Propionic acid (AMPAR)
- Agonist [^{3}H]-Kainate for the ionotropic receptor Kainate (KainateR)
- Antagonist [^{3}H]-MK-801 for the ionotropic receptor N-Methyl-D-Aspartate (NMDAR)
- Antagonist [^{3}H]-LY-341495 for the metabotropic group II receptor ($mGlu_{2/3}R$)

GABAergic receptors:

- Agonist [^{3}H]-Muscimol(5-(Aminomethyl)-isoxazol-3-ol) for the ionotropic receptor γ-Amino-butyric acid A ($GABA_AR$)
- Agonist [^{3}H]-flumazenil for the ionotropic $GABA_A$ receptor associated benzodiazepine binding site ($GABA_{A(BZ)}R$).
- Agonist [^{3}H]-CGP54626 for the metabotropic receptor γ-Amino-butyric acid B ($GABA_BR$)

Noradrenergic receptors:

- Agonist [^{3}H]-Prazosin for the metabotropic alpha-1 adrenergic receptor (α_1R)
- Antagonist [^{3}H]-RX-821002 for the metabotropic alpha-2 adrenergic receptor (α_2R)

Dopaminergic receptor:

- Antagonist [^{3}H]-SCH23390 for the metabotropic group I/V dopaminergic receptor ($D_{1/5}R$)

Binding protocol

Details of concentrations (ligands, competitor, buffers), incubation conditions (time, temperature) and washing procedures are given in Supp. Tab. 5. Radiolabeling of neurotransmitter receptors followed a standardized protocol consisting of three steps (Zilles et al., 2002a; Schleicher et al., 2005; Palomero-Gallagher et al., 2009; Zilles et al., 2015; Zilles and Palomero-Gallagher, 2017; Palomero-Gallagher and Zilles, 2018; Lothmann et al., 2020; Lothmann et al., 2021).

During preincubation (1), endogenous substances that prevent binding of the tritium-labelled ligands with the target receptor were removed from the tissue section and the tissue was rehydrated. In the subsequent main incubation (2), the sections were incubated with [^{3}H] radioligands. Nonspecific binding sites were occupied, so simultaneous co-incubation with a nonlabelled displacer was performed on sections of each series. When specific and nonspecific binding of the [^{3}H]-ligand occurred, the binding was referred to as total binding (TB). If the radioligand was displaced by the displacer due to higher affinity, the nonspecific binding (NB) became visible. The specific binding (SB) resulted from the difference of the total binding and the non-specific binding. Upon completion of binding (3), a washing step was performed to prevent artifacts. Subsequent drying was followed by exposure to film sheets, revealing receptor binding.

2.3 Data analysis

2.3.1 Quantification of $BrdU^+$ cells

Three to five sections of the main olfactory bulb with the lateral olfactory tract of each animal (n = 20) were chosen for quantification. In each section, the three fluorescence channels (BrdU: red, NeuN: blue; GFAP: green) were selected individually or in combination to ensure that all BrdU-labeled cells were captured. In addition, cells labeled only with NeuN or/and GFAP were also counted but are not part of this work. BrdU-labeled cells could be detected using the NeuN-BrdU double staining by overlapping both fluorescence (blue and red) channels. For cell counting, ZEN digital imaging software (blue edition, Zeiss, Germany) was used. The immunopositive cells were marked in the image processing step of the software using the "Draw point of interest" function. A color was specified in advance for each labelling. Once all signals were marked by hand, the points of interest were counted by the software and reported as a table.

2.3.2 Quantification of receptor densities

Receptor autoradiographs were digitized using the AxioVision 4.8 imaging system with an AxioCamHR (Carl Zeiss MicroImaging, Göttingen, Germany). Illumination was restricted to the size of a tissue section by black foil to ensure constant and homogeneous light scatter. To exclude further inhomogeneity due to differences in brightness, a reference image was generated at an unexposed location. The correction of the subsequent image acquisitions based on the reference image was done automatically by the image processing program.

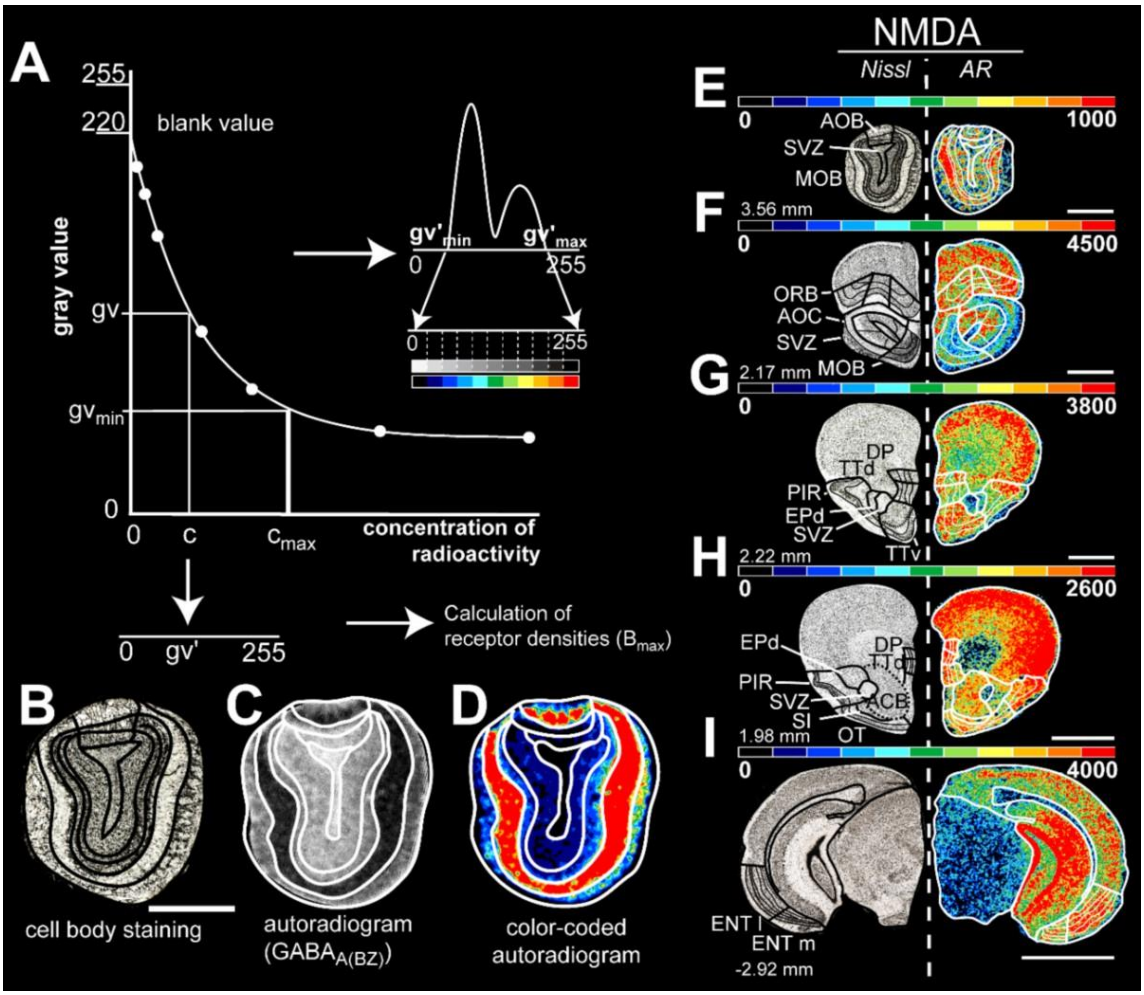

Figure 8: Computing densities in receptor autoradiographs

A Calibration curve of known radioactive co-exposure isotope standards used to calculate the concentration of bound ligand. It provides a non-linear dependence of gray value and radioactive decay concentration. This allows you to convert the gray value of the autoradiogram to the corresponding radioactive decay concentration on a pixel-by-pixel basis. A gray level histogram of the converted autoradiogram (**C**) was generated, followed by a linear contrast enhancement procedure. Here, the grayscale histogram is converted into an array of 11 colors to visualize the density pattern in the autoradiograph (**D**). Boundaries are defined by simultaneously using brain sections of the same level using cell body staining (**B**). **A** adapted by Zilles and Schleicher, 1995 and Herold et al., 2014. **E-I** Illustrative diagram of border identification of color-coded images showing the distribution and density of NMDA glutamate receptors at various Bregma levels (left, in mm). The color scale of 11 equally distributed colors corresponds to the receptor density of the fmol/mg protein. The color scale of each image is optimized to provide optimal visualization for different densities of receptors. Therefore, the red ends correspond to the best visual fit for the examined structure, but this is not necessarily the maximum density. Scale bars: B-E, 1.3 mm; F-H, 1.5 mm; I, 2 mm (Lothmann et al., 2021)

The autoradiographs were saved as 8-bit gray-scale images. The different shades of gray in an image allowed to compute the intensity of the binding (Figure 8). On each slide with receptor

autoradiographs, so-called microscales with known concentrations were applied and recorded. Through these recordings, transformation curves can be generated for each slide showing the non-linear correlation between gray levels and concentration of radioactivities in fmol/mg protein. Processing was performed using MATLAB (MathWorks, USA).

To allow precise delineation of regions, histologically stained sections corresponding to the same Bregma level of each autoradiograph of a series were compared. Subsequently, borders were digitally plotted using a digital tablet, and receptor density values were correlated with the image matrix based on the reference point system. To account for the specific saturation conditions of the receptors, the values were individually corrected using the following equation:

$$C_{KB} = \frac{(K_D + L)}{(A_S \cdot L)}$$

The adjusted receptor concentration C_{KB} depends on the dissociation constant K_D, the incubation concentration of the ligand L and its specific activity A_S. By using this equation, it is possible to convert the gray values of the autoradiograph pixel by pixel into the absolute receptor concentration for the investigated regions.

2.4 Statistics and Visualizations

A total of 18 olfactory regions were examined, 14 were analyzed as part of this work. Values for the anterior commissure/olfactory limb, lateral olfactory tract, the subependymal zone, and substantia innominata were not included in the analyses. When evaluating the receptor architectural sections, the mean and cortical receptor densities were determined for one hemisphere per animal. For each olfactory region (n = 14), at least three sections per receptor (n = 10) and animal (n = 10 per group) were selected. Laminar receptor densities were determined directly, and all individual region results were averaged per brain. To obtain an average region value, the laminar results per region were summarized and averaged.

For further steps and optimal comparability between groups, the obtained values were normalized over the number of animals per group. Thus, an overall mean value of one region was obtained for each receptor per group.

2.4.1 Receptor Fingerprints

Receptor fingerprints (also known as net plots) were created to graphically display the mean values of a region for each receptor in a group. Polar plots were also generated to graphically display the mean values of all receptors for each region. Absolute polar plots were used for category-internal comparisons (control versus TMZ-treated), whereas receptor fingerprints were used to represent relative values for cross-category group comparisons.

Receptor fingerprints were standardized to a uniform coordinate system to provide comparability of receptor architectural characteristics of a region in terms of shape and size. Similarities in the fingerprints suggest similar characteristics in function and were therefore created for the mean region values only, not for the laminar mean values.

2.4.2 Cluster Analysis

To examine the similarities and dissimilarities, of the receptor fingerprints in control animals, the normalized averaged mean receptor concentrations were further analyzed using multivariate distance analysis. Hierarchical cluster analysis (SPSS Statistics 26) was used to quantify the level of similarity between the multireceptor balance of the olfactory region pairwise by Euclidean distance. Subsequently, the result was visualized in 2D using nonlinear multidimensional scaling. Via hierarchical cluster analysis (Ward linkage with Euclidean distances), the normalized

mean values of the receptor densities were displayed in their relationships to each other in clusters as a phylogenetic tree and as a heat map. As a measure of the stability of the clusters, a silhouette analysis was performed, whose coefficient was intended to provide an evaluation of this analysis.

2.4.3 Statistical analyses

For statistical analysis (SPSS Statistics 26) of receptor densities of the control group, a Friedman ANOVA was performed for each receptor across all subregions and layers. This was followed by a Wilcoxon rank test for pairwise inter-subregion comparisons (Supp. Tab. 9 – Supp. Tab. 21). For regional differences, a Dunn-Bonferroni post-hoc test was used for multiple comparisons (Supp. Tab. 7).

The difference between BrdU-positive cells in a two-independent-groups comparison (control vs. TMZ-treated) was tested with the non-parametrical Mann-Whitney-U-test, since the variables were not normally distributed.

For group comparisons, a Friedman ANOVA with repeated measurements was performed across all subregions and layers for each receptor to detect general differences in the chemoarchitecture of the different regions of the olfactory system (categorial factors: Grouping [e.g.: CG vs. CG_{TMZ}] and receptor-groups; variables: regions). The Shapiro-Wilk-Test was used to check for normal distribution. The distributions were significantly non-normal for most regions (p value > .05). A pairwise, non-parametrically multifactorial Mann-Whitney-U-test was then performed for pairwise inter-subregion comparisons. Differences were considered significant if they were larger than 95% of the values under random distribution (null hypothesis; $p < .05$).

3. Results

The following regions of the main and accessory olfactory bulb (Bregma level 3.56 mm), the taenia tecta (dorsal, ventral) and piriform cortex (Bregma level 2.22 to 1.98 mm), the anterior olfactory cortex and the orbitofrontal cortex (medial, ventrolateral, lateral; Bregma level 2.17 mm), the dorsal peduncular cortex (Bregma level 1.98 mm) and the entorhinal cortex (Bregma level -2.92 mm) were mapped receptor-architectonically and analyzed for the different conditions. In detail, these olfactory regions were examined in control animals, untrained animals with suppressed adult neurogenesis, trained animals, and trained animals with suppressed adult neurogenesis. In general, effects of adult neurogenesis and cognitive training on receptor architecture were observed on regional and laminar levels.

3.1 The neurotransmitter receptor architecture of the mouse olfactory system

The analysis of the receptor architecture of the olfactory system revealed a varying density distribution of glutamatergic, GABAergic and catecholaminergic receptors in the main and accessory olfactory bulb, dorsal peduncular cortex, anterior olfactory cortex, olfactory tubercle, taenia tecta, entorhinal cortex, piriform cortex, endopiriform nucleus, and orbitofrontal cortex. $mGlu_{2/3}Rs$, benzodiazepine binding sites and $GABA_BRs$ showed high densities, while low densities for α_1Rs and $D_{1/5}Rs$ (except in the olfactory tubercle) were observed and presented as multi-receptor density profiles (see Figure 9 – Figure 11). Mean neurotransmitter receptor densities (fmol/mg protein) ± SEM in all 14 investigated olfactory regions of the mouse olfactory system of control mice (CG) are provided in Supp. Tab. 6. For statistical comparisons between these groups see Supp. Tab. 7. Each receptor type was tested with Friedman ANOVA and further with pairwise Dunn-Bonferroni post hoc test. Supp. Tab. 7 provides the significance and adjusted significance with $*p < .05$.

Results were published in Lothmann et al., 2021.

3.1.1 Receptor-specific differentiation of olfactory regions

Subdivisions of the olfactory system were identified in the images of Nissl-stained sections according to the criteria by Lein et al. and used as a basis to analyze the receptor architecture of the olfactory regions (Figure 9 – Figure 11; Supp. Tab. 6, Supp. Tab. 7).

Glutamatergic receptors

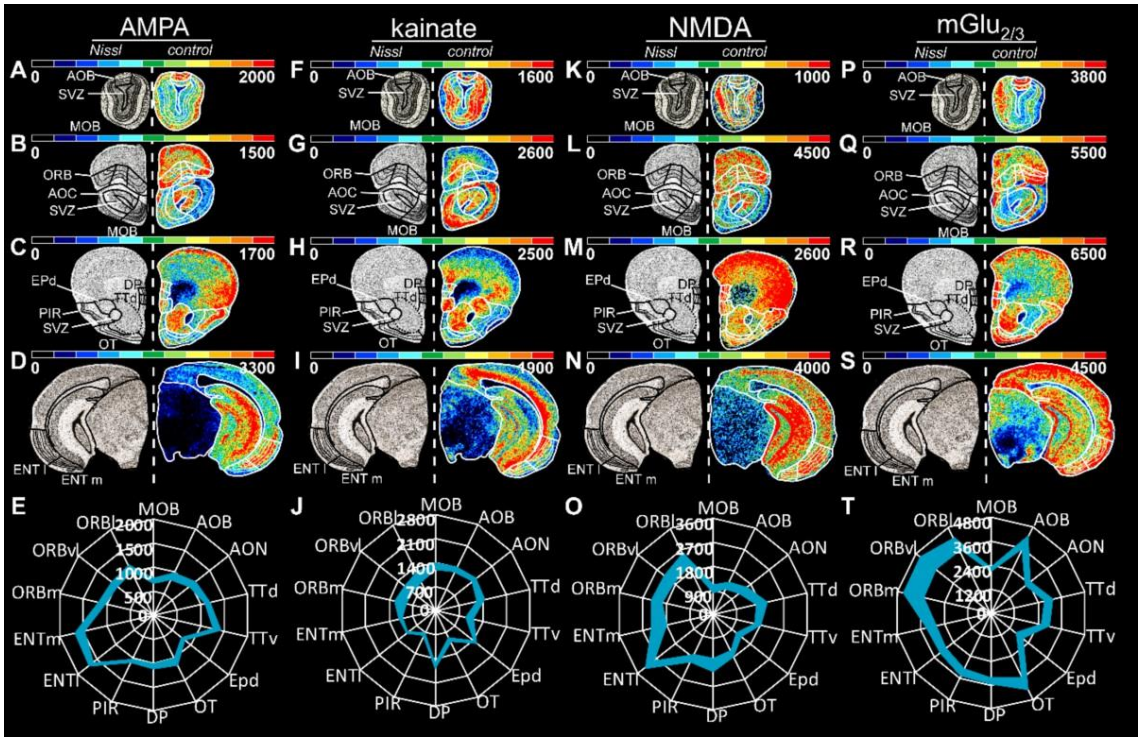

Figure 9: Distribution of glutamatergic receptors

Nissl stained and color-coded autoradiographs revealed the distribution pattern of glutamatergic receptor (AMPA **A-E**, kainate **F-J**, NMDA **K-O**, $mGlu_{2/3}$ **P-T**). Combination of Nissl stained sections on the left and the corresponding color-coded autoradiographs on the right. Bregma levels and region boundaries (black and white lines) according to Figure 2. Receptor densities (fmol/mg protein) are demonstrated by the color scale, maximum receptor concentration of the section alongside the autoradiograph. Red color represents the exemplary optimized representation, not the maximum receptor density of the region, while black indicates the absence of receptor expression. Polar plots (**E, J, O, T**) show absolute density values with upper (mean density + SEM) and lower (mean density – SEM) densities as color filled region. Receptor concentrations in Supp. Tab. 6; statistical data in Supp. Tab. 7. Main olfactory bulb (MOB); accessory olfactory bulb (AOB), anterior olfactory nucleus (AOC); taenia tecta, dorsal (TTd); taenia tecta, ventral (TTv); dorsal peduncular cortex (DP); piriform cortex (PIR), dorsal endopiriform nucleus (EPd); entorhinal cortex, lateral (ENTl), entorhinal cortex, medial (ENTm); orbitofrontal cortex, medial (ORBm); orbitofrontal cortex, lateral (ORBl), orbitofrontal cortex, ventrolateral (ORBvl); olfactory tubercle (OT); nucleus accumbens (ACB).

Glutamatergic receptors revealed a heterogenous picture in the olfactory system: while $mGlu_{2/3}Rs$ were highly expressed in the endopiriform nucleus (1836 ± 224 fmol/mg protein) and the ventrolateral orbitofrontal cortex (4024 ± 511 fmol/mg protein), AMPARs, kainateRs and NMDARs displayed lower distributions than $mGlu_{2/3}Rs$ (Figure 9). Except for the orbitofrontal cortex (Figure 9B, G), AMPARs (Figure 9A-E) and kainateRs (Figure 9F-J) consistently differed in their concentrations in a contrary relationship. The lateral entorhinal cortex had the highest concentration of AMPARs (1664 ± 59 fmol/mg protein), while the endopiriform nucleus showed the highest density of kainateRs (1624 ± 95 fmol/mg protein). Except for the main olfactory bulb (954 ± 158 fmol/mg protein), NMDARs were found in high quantities (up to 3037 ± 224 fmol/mg protein in the lateral entorhinal cortex, for example). The medial (2091 ± 301 fmol/mg protein) and lateral entorhinal cortex (3037 ± 224 fmol/mg protein) could be clearly subdivided by NMDAR concentrations. In the orbitofrontal cortex, $mGlu_{2/3}Rs$ were found in high concentrations (4024 ± 511 fmol/mg protein). The $mGlu_{2/3}R$ distinguished the accessory olfactory bulb (3948 ± 376 fmol/mg protein) from the main olfactory bulb (2180 ± 121 fmol/mg protein) and anterior olfactory cortex (2365 fmol/mg protein, Supp. Tab. 6, 7).

GABAergic receptors

GABAergic receptors showed generally high concentrations in the olfactory system (Figure 10). While $GABA_AR$ densities were relatively low (803 ± 93 fmol/mg protein) in the main olfactory bulb and in the medial orbitofrontal cortex (1553 ± 105 fmol/mg protein Supp. Tab. 6), they showed high concentrations in the accessory olfactory bulb (2791 ± 257 fmol/mg protein up to 6409 ± 664 fmol/mg protein, Supp. Tab. 6). The accessory olfactory bulb revealed the highest density of benzodiazepine binding sites, which indicated the border to the main olfactory bulb and the border of the anterior olfactory cortex to the ventral part of the taenia tecta (Supp. Tab. 6). The medial entorhinal cortex (6201 ± 200 fmol/mg protein) displayed the highest $GABA_BR$ expression. Low densities of $GABA_BRs$ (5003 ± 404 fmol/mg protein) and $GABA_ARs$ (1393 ± 172 fmol/mg protein) in the lateral region of the orbitofrontal cortex revealed changes in GABAR densities across the regions of the orbitofrontal cortex (Supp. Tab. 6, Supp. Tab. 7).

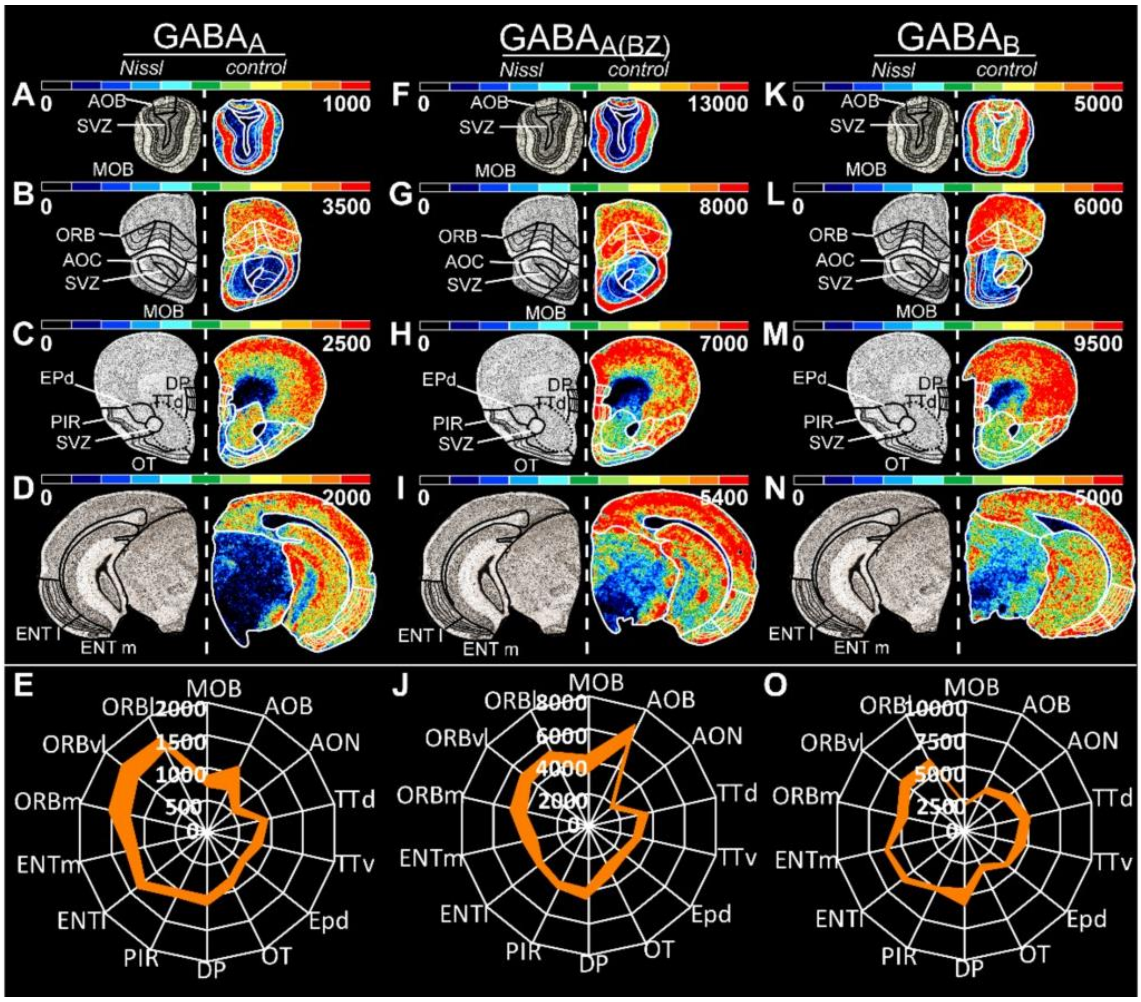

Figure 10: Distribution of GABAergic receptors

Nissl stained, and color-coded autoradiographs revealed the distribution patterns of GABAergic receptors (GABA$_A$, GABA$_{A(BZ)}$, GABA$_B$). Designations and figure structure as in Figure 9. Receptor concentrations in Supp. Tab. 6; statistical data in Supp. Tab. 7.

Catecholaminergic receptors

Our data revealed that a heterogenous distribution of noradrenergic receptors in the olfactory system (Figure 11). The primary and secondary olfactory cortices had comparatively low concentrations of α_1Rs, ranging from 513 ± 67 fmol/mg protein in the lateral orbitofrontal cortex to 675 ± 50 fmol/mg protein in the accessory olfactory bulb. Compared to the main olfactory bulb (497 ± 32 fmol/mg protein, Supp. Tab. 6), α_2Rs were high in density in the olfactory cortices (up to 1809 ± 160 fmol/mg protein). When compared to the other studied receptors, $D_{1/5}$Rs (61 ± 6 fmol/mg protein in the main olfactory bulb) were less distributed (Figure 11). Only the olfactory tubercle showed high expression patterns (5340 ± 439 fmol/mg protein). The olfactory tubercle's

boundary with the piriform cortex was clearly highlighted by high concentrations of $D_{1/5}$Rs in the olfactory tubercle (Supp. Tab. 6, Supp. Tab. 7).

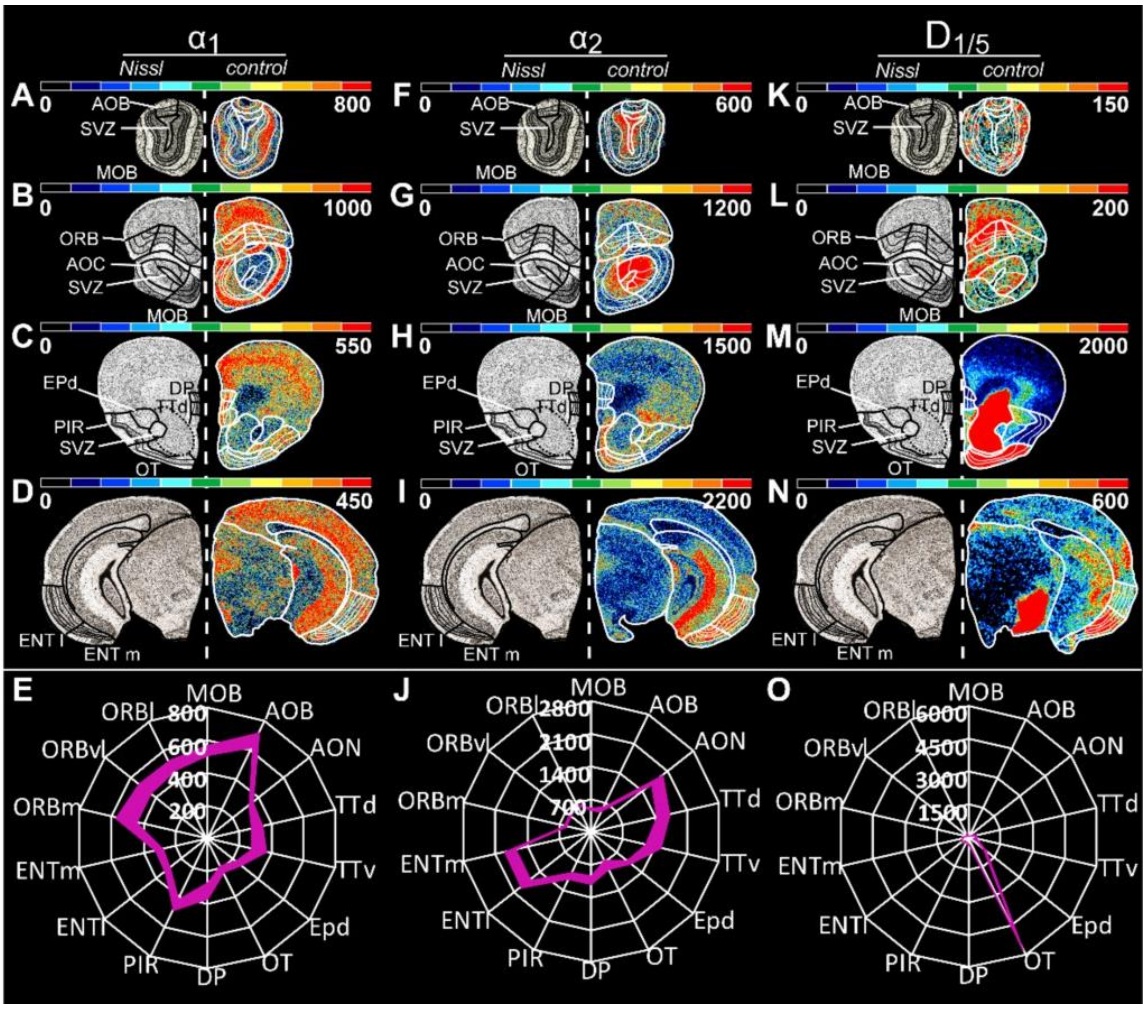

Figure 11: Distribution of catecholaminergic receptors

Nissl stained, and color-coded autoradiographs revealed the distribution patterns of catecholaminergic receptors (α_1, α_2, $D_{1/5}$). Designations and figure structure as in Figure 9. Receptor concentrations in Supp. Tab. 6; statistical data in Supp. Tab. 7.

3.1.2 Layer-specific receptor distributions

Individual receptor densities for each layer of all layered olfactory regions (all regions except the dorsal endopiriform nucleus) and subregions (for the anterior olfactory cortex) were calculated, resulting in specific receptor profile for each region (Figure 12 – Figure 18). Mean neurotransmitter receptor densities (fmol/mg protein ± SEM) in the layers of all 14 investigated olfactory regions of the mouse olfactory system of control mice (CG) are provided in Supp. Tab. 8.

For statistical comparisons of the laminar comparisons in every investigated region see further Supp. Tab. 9 – Supp. Tab. 21.

The main and accessory olfactory bulb

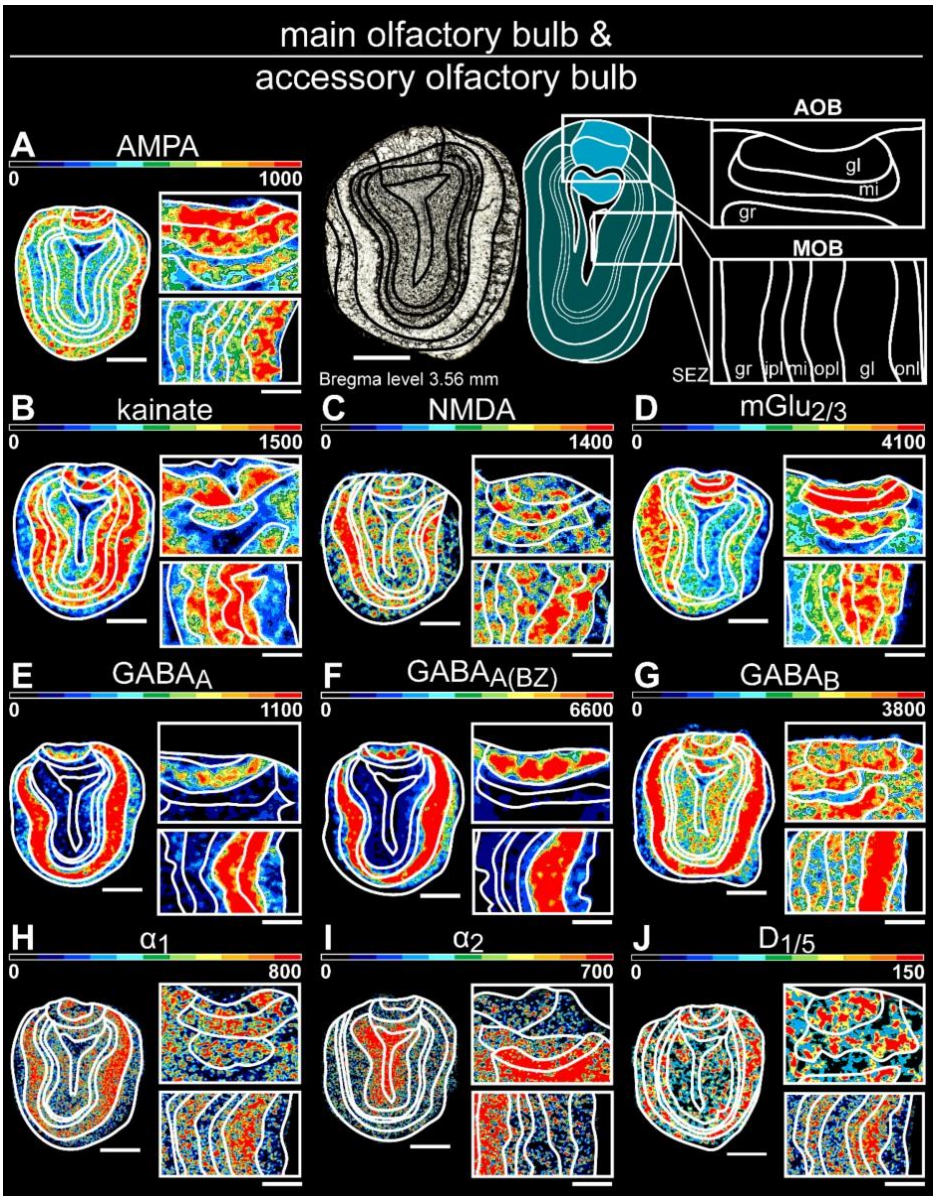

Figure 12: Color-coded layer-specific receptor distributions of the main and accessory olfactory bulbs

In the main olfactory bulb (**A-J**), the borders of the glomerular layer (gl) to the olfactory nerve layer (onl) were revealed by high densities of NMDARs ($p < .05$), $GABA_ARs$ ($p < .05$), $GABA_{A(BZ)}Rs$ ($p < .05$), and $GABA_BRs$ ($p < .05$). High receptor densities of α_2Rs demarked the border of the granular layer (gr) to the inner plexiform layer (ipl; $p < .05$). In the accessory olfactory bulb (**K-T**), the distribution of kainateRs clearly revealed the border of the mitral cell layer (mi) to the gr ($p < .05$) and glomerular layers (gl; $p < .05$). $GABA_{A(BZ)}Rs$ were highly expressed in the gr in contrast to the gl ($p < .05$). Densities in fmol/mg protein. Designations and figure structure as in Figure 9. For detailed receptor densities see Supp. Tab. 8. Statistical analysis in Supp. Tab. 9 (MOB) and 10 (AOB). Scale bars: Nissl-Image, 1 mm; A-J, 400 µm

Except for AMPARs and α_2Rs, all receptors were highly expressed in the glomerular layer of the main olfactory bulb and the mitral layer of the accessory olfactory bulb (Supp. Tab. 8). $GABA_{A(BZ)}$Rs showed the highest densities in the deeper layers of the main olfactory bulb, while $mGlu_{2/3}$Rs (Figure 12D) and $GABA_B$Rs (Figure 12G) showed significantly high concentrations in the superficial layers (Figure 12F).

The accessory olfactory bulb's granular layer showed the highest expression of α_2Rs and $D_{1/5}$Rs (Figure 12I, J).

The primary and secondary olfactory cortices

$GABA_B$Rs (4223 ± 345 fmol/mg protein; Figure 13G) and $mGlu_{2/3}$Rs (2365 ± 165 fmol/mg protein) were found in high concentrations throughout the anterior olfactory cortex (for layer-specific statistical analysis, see Supp. Tab. 11; Figure 13D).

The pars externa and pars principalis were separated by high $mGlu_{2/3}$ (Figure 13D), $GABA_{A(BZ)}$ (Figure 13F), and α_1 (Figure 13H) receptor densities. The medial region was characterized by high densities of AMPARs (1226 ± 81 fmol/mg protein, Figure 13A) and $GABA_B$Rs (4608 ± 423 fmol/mg protein, Figure 13G). High concentrations of α_2Rs (2296 ± 165 fmol/mg protein, Figure 13I) and $D_{1/5}$Rs (234 ± 69 fmol/mg protein, Figure 13J) and low densities of $GABA_{A(BZ)}$Rs (1414 ± 146 fmol/mg protein) clearly differentiated the dorsal part of the anterior olfactory cortex from the other surrounding subregions (Figure 13F).

The posteroventral subregion showed high kainateR (1783 ± 138 fmol/mg protein, Figure 13B) expression levels and low densities of $mGlu_{2/3}$Rs (1846 ± 115 fmol/mg protein, Figure 13D) and α_1Rs (Figure 13H). High NMDA (996 ± 62 fmol/mg protein, Figure 13C) and $GABA_B$ (3629 ± 328 fmol/mg protein, Figure 13G) receptor densities, as well as low $GABA_A$R (565 ± 21 fmol/mg protein) concentrations (Figure 13E), separated the posteroventral subregion from the rest of the pars principalis.

Except for kainateRs (1860 ± 129 fmol/mg protein, Figure 13L) and $D_{1/5}$Rs (509 ± 61 fmol/mg protein, Figure 13T), the dorsal peduncular cortex (Supp. Tab. 8, Supp. Tab. 12) had low receptor concentrations in deep layer VI compared to layers I – III.

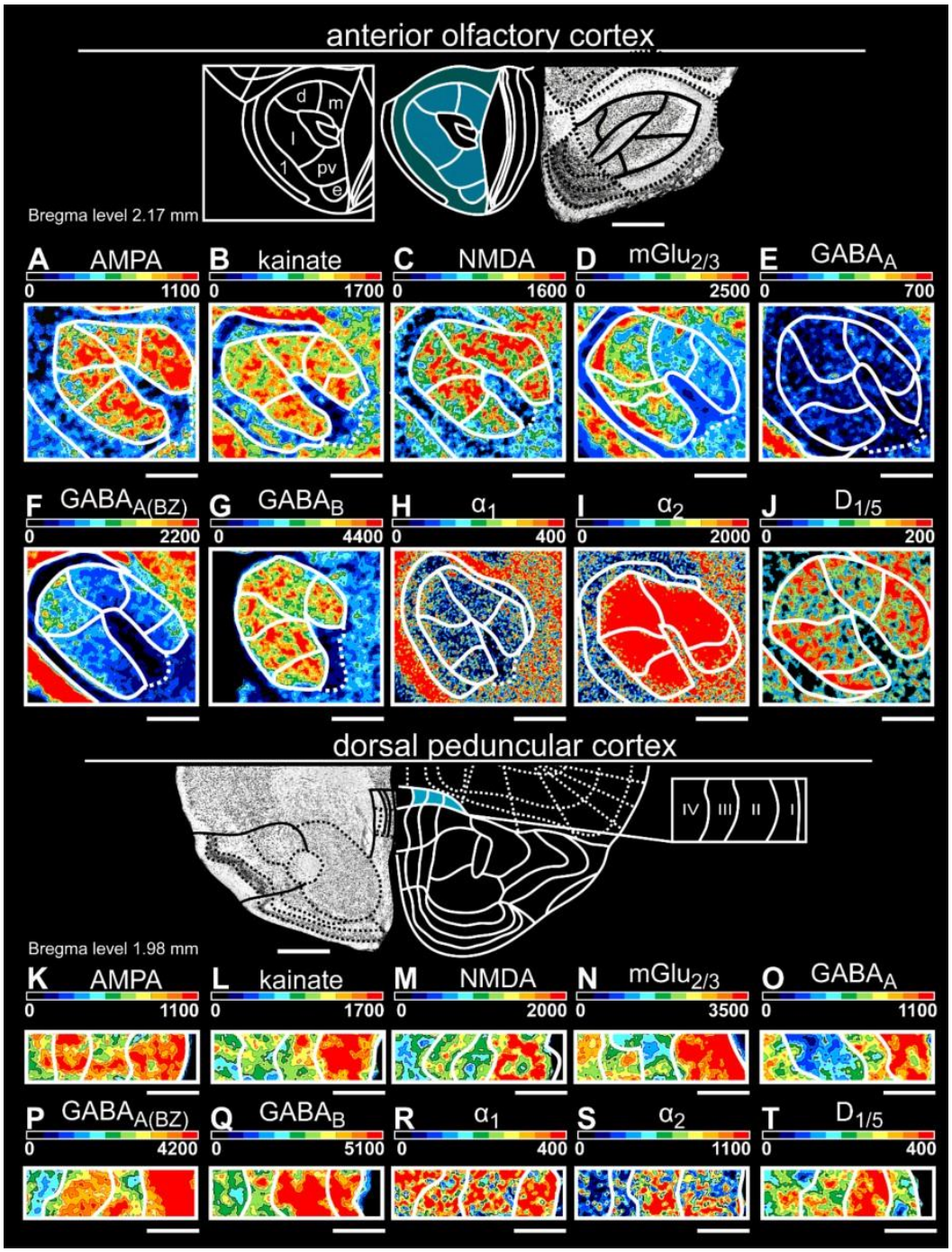

Figure 13: Color-coded layer-specific receptor distributions of the anterior olfactory cortex and dorsal peduncular cortex

In the anterior olfactory cortex (A-J), high receptor densities for AMPARs were observed, especially in the medial part, compared to the adjacent dorsal region ($p < .05$). In the dorsal peduncular cortex (K-T), $mGlu_{2/3}$Rs were seen to be higher expressed in layer I than layer II/III ($p < .05$). Densities in fmol/mg protein. Designations and figure structure as in Figure 9. For detailed receptor densities see Supp Tab. 8. Statistical analysis in Supp. Tab. 11 (AOC) and Supp. Tab. 12 (DP). Scale bars: Nissl-Image, 1 mm; A-J, 400 µm.

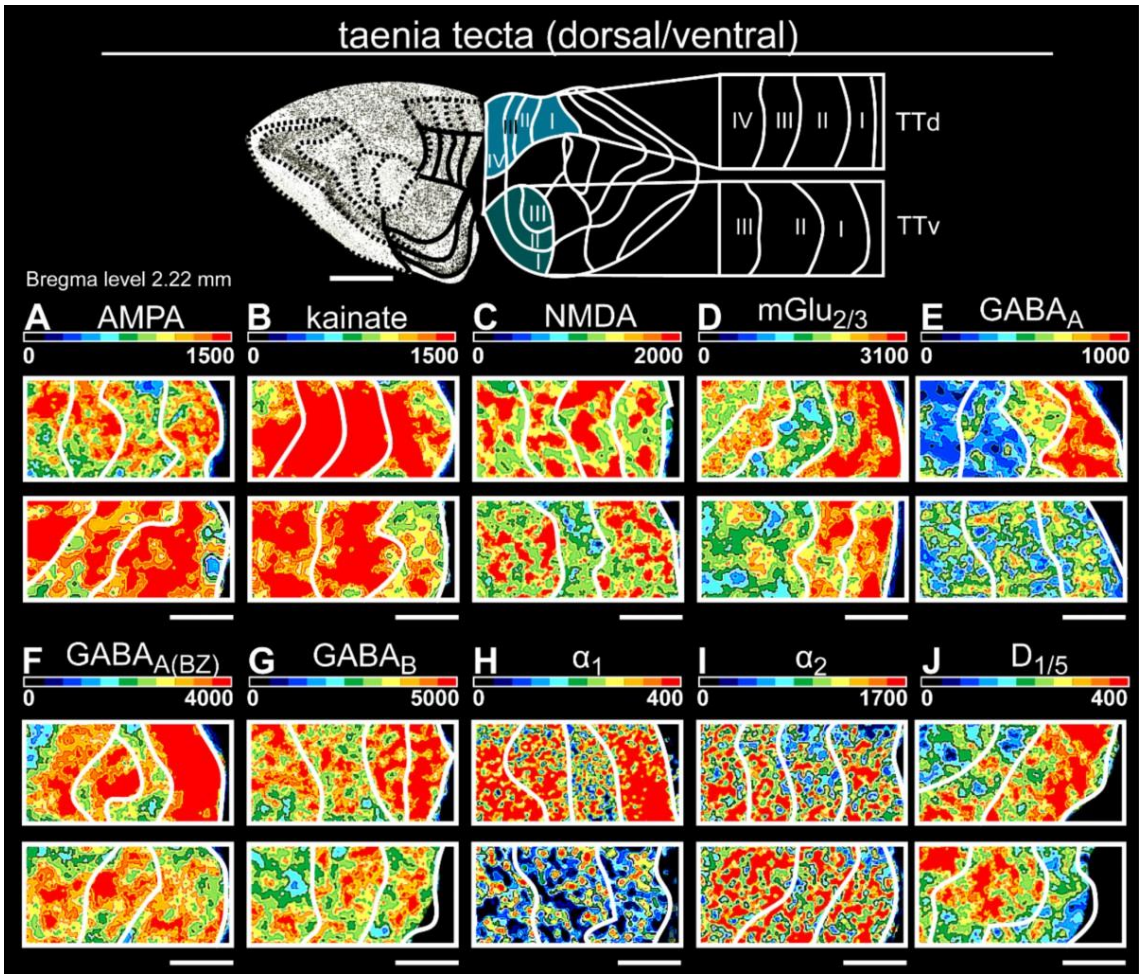

Figure 14: Color-coded layer-specific receptor distributions of the taenia tecta (dorsal/ventral)

In the dorsal part (TTd), the border of layer I to layer II was demonstrated by AMPARs ($p < .05$) and $GABA_{A(BZ)}$Rs ($p < .05$). In the ventral part, a clear difference from layer I to II was revealed by kainateRs ($p < .05$). Designations and figure structure as in Figure 9. For detailed receptor densities see Supp Tab. 8. Statistical analysis in Supp. Tab. 13 (TTd) and Supp. Tab. 14 (TTv). Scale bars: Nissl-Image, 1 mm; A-J, 400 µm

In both parts of the taenia tecta, glutamatergic receptors were high in expression levels (Supp. Tab. 8). Glutamatergic (excluding kainateRs, Figure 14A-D) and GABAergic receptors (Figure 14E-F) were prominent in superficial layers I/II, while α_1Rs (341 ± 43 fmol/mg protein) and $D_{1/5}$Rs (594 ± 62 fmol/mg protein) were abundant in deep layer IV (Figure 14I). $GABA_B$Rs showed the highest densities in both regions' layer II and were considerably more expressed in the dorsal compared to ventral regions (dorsal: 4999 ± 570 fmol/mg protein, ventral: 876 ± 512 fmol/mg protein, Figure 14G).

The superficial layer I of the piriform cortex (Supp. Tab. 8) displayed high densities of glutamatergic (NMDARs [2103 ± 165 fmol/mg protein, Figure 14C], $mGlu_{2/3}Rs$ [4400 ± 283 fmol/mg protein Figure 14D]) and GABAergic ($GABA_ARs$ [1169 ± 77 fmol/mg protein, Figure 14E], $GABA_{A(BZ)}Rs$ [4193 ± 205 fmol/mg protein, Figure 14F]) receptors, whereas deep layer III had the highest concentrations of α_2Rs (1159 ± 99 fmol/mg protein, Figure 14I) and $D_{1/5}Rs$ (368 ± 51 fmol/mg protein, Figure 14J).

GABAergic receptors ($GABA_A$: 695 ± 61 fmol/mg protein, $GABA_{A(BZ)}$: 2791 ± 257 fmol/mg protein, $GABA_B$: 4059 ± 211 fmol/mg protein, Figure 15E-G) were prevalent in the endopiriform nucleus (Supp. Tab. 6, Supp. Tab. 8). AMPARs (789 ± 51 fmol/mg protein, Figure 15A) and α_1Rs (238 ± 23 fmol/mg protein, Figure 15H) were low distributed, compared to other olfactory related regions.

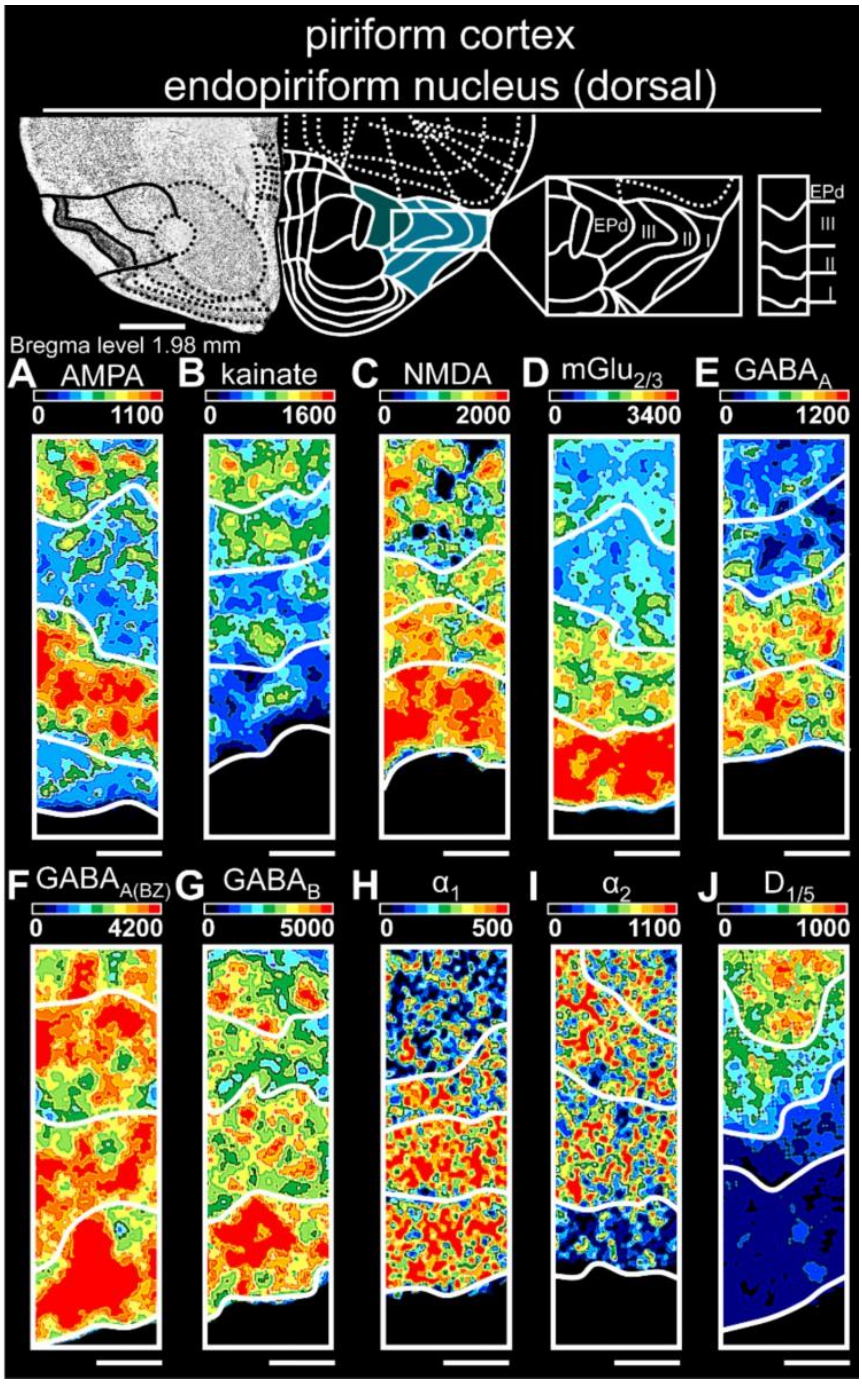

Figure 15: Color-coded layer-specific receptor distributions in the piriform cortex and endopiriform nucleus
The border between layer I and II was demonstrated by AMPARs ($p < .05$) and $mGlu_{2/3}Rs$ ($p < .05$). AMPARs were higher in layer II, compared to layer III ($p < .05$). $D_{1/5}Rs$ were highly expressed in layer III, compared to layer II ($p < .005$). Lower receptor densities of α_1Rs ($p < .013$) contrasted layer III from layer II. Densities in fmol/mg protein. Designations and figure structure as in Figure 9. For detailed receptor densities see Supp Tab. 8. Statistical analysis in Supp. Tab. 16. Scale bars: Nissl-Image, 1.2 mm; A-J, 400 µm

The highest receptor densities were found in layer II of the medial and lateral entorhinal cortex. Layers II/III of both regions (Supp. Tab. 8) displayed high densities of glutamatergic receptors (NMDA [lateral: 3401 ± 274 fmol/mg protein, medial: 2698 ± 163 fmol/mg protein, Figure 16C], $mGlu_{2/3}Rs$ [lateral: 3431 ± 194 fmol/mg protein, medial: 3512 ± 432 fmol/mg protein, Figure 16D]) and GABAergic receptors (particularly $GABA_B$ medial with 7038 ± 286 fmol/mg protein, Figure 16E-G). The deep layers V/VI had high expression rates of kainateRs (lateral: up to 1710 ± 112 fmol/mg protein in layer VIa, medial: up to 1309 ± 107 fmol/mg protein in layer VI, Figure 16B) and α_2Rs (lateral: 2061 ± 168 fmol/mg protein in layer V, medial: 2127 ± 146 fmol/mg protein in layer V, Figure 16H-J). Despite the low expression of NMDARs (lateral: 2123 ± 187 fmol/mg protein, medial: 1360 ± 155 fmol/mg protein, Figure 16C) and $GABA_BRs$ (lateral: 4258 ± 155 fmol/mg protein, medial: 5276 ± 471 fmol/mg protein, Figure 16G) in layer VI of both subdivisions (compared to the expression densities in the other layers), their concentration in the medial part was higher than the lateral part.

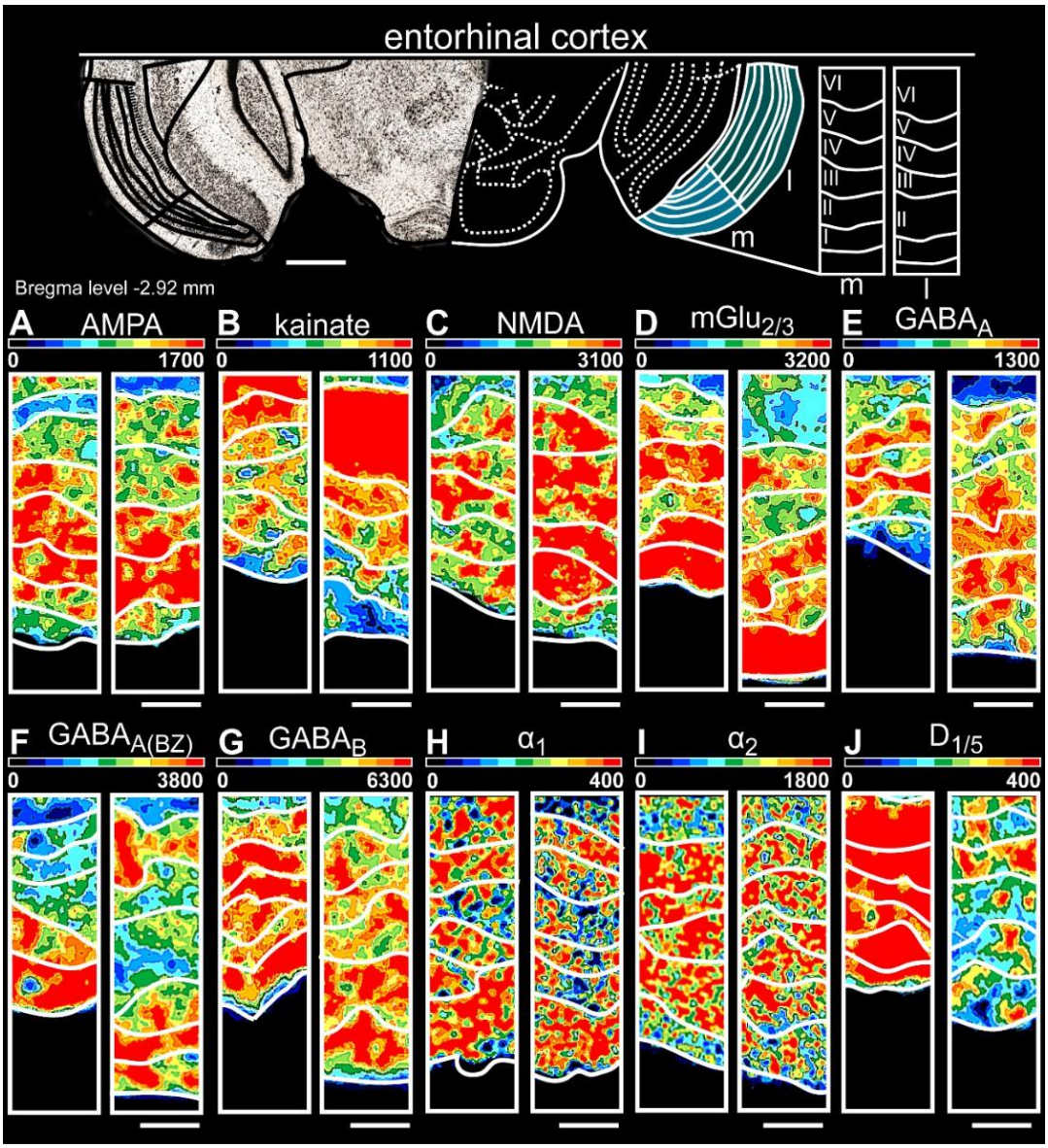

Figure 16: Color-coded layer-specific receptor distribution of the entorhinal cortex

In the lateral part, NMDARs revealed the border of layer I to II/III ($p < .05$). AMPARs were highly expressed in layer II/III, compared to layer I ($p < .05$) and V ($p < .05$). Layer V showed lower receptor densities of kainateRs than layer VI ($p < .05$). In the medial part, $GABA_A$Rs revealed a border of layer V to VI ($p = .04$). Layer I displayed a lower density of α_2Rs in contrast to layer II ($p < .05$). Densities in fmol/mg protein. Designations and figure structure as in Figure 9. For detailed receptor densities see Supp Tab. 8. Statistical analysis in Supp. Tab. 17 (ENTl) and Supp. Tab. 18 (ENTm). Scale bars: Nissl-Image, 1.5 mm; A-J, 200 µm

Except for kainateRs in layer VI (up to 1609 ± 126 fmol/mg protein in the lateral part, Figure 17B), the three regions of the orbitofrontal cortex (Supp. Tab. 8) showed high receptor densities in layers I/II for glutamatergic AMPA (up to 1253 ± 75 fmol/mg protein in the medial part), NMDA (2741 ± 237 fmol/mg protein in the medial part), $mGlu_{2/3}$ (5193 ± 110 fmol/mg protein in the lateral part) receptors (Figure 17A-D) and GABAergic $GABA_{A(BZ)}$ (5491 ± 443 fmol/mg protein in the lateral part) and $GABA_B$ (6482 ± 530 fmol/mg protein in the ventrolateral part) receptors (Figure 17E-G). While the medial and lateral parts showed high densities of noradrenergic α_1 (up to 575 ± 84 fmol/mg protein in medial layer II/III) and α_2 (up to 802 ± 35 fmol/mg protein in the lateral layer I) receptors, the ventrolateral region had high amounts (α_1: 505 ± 52 fmol/mg protein, α_2: 767 ± 35 fmol/mg protein) in layer I (Figure 17H-I). In deep layer VI, $D_{1/5}$ receptors were generally low in concentration but highly expressed (up to 276 ± 44 fmol/mg protein in the medial part, Figure 17J).

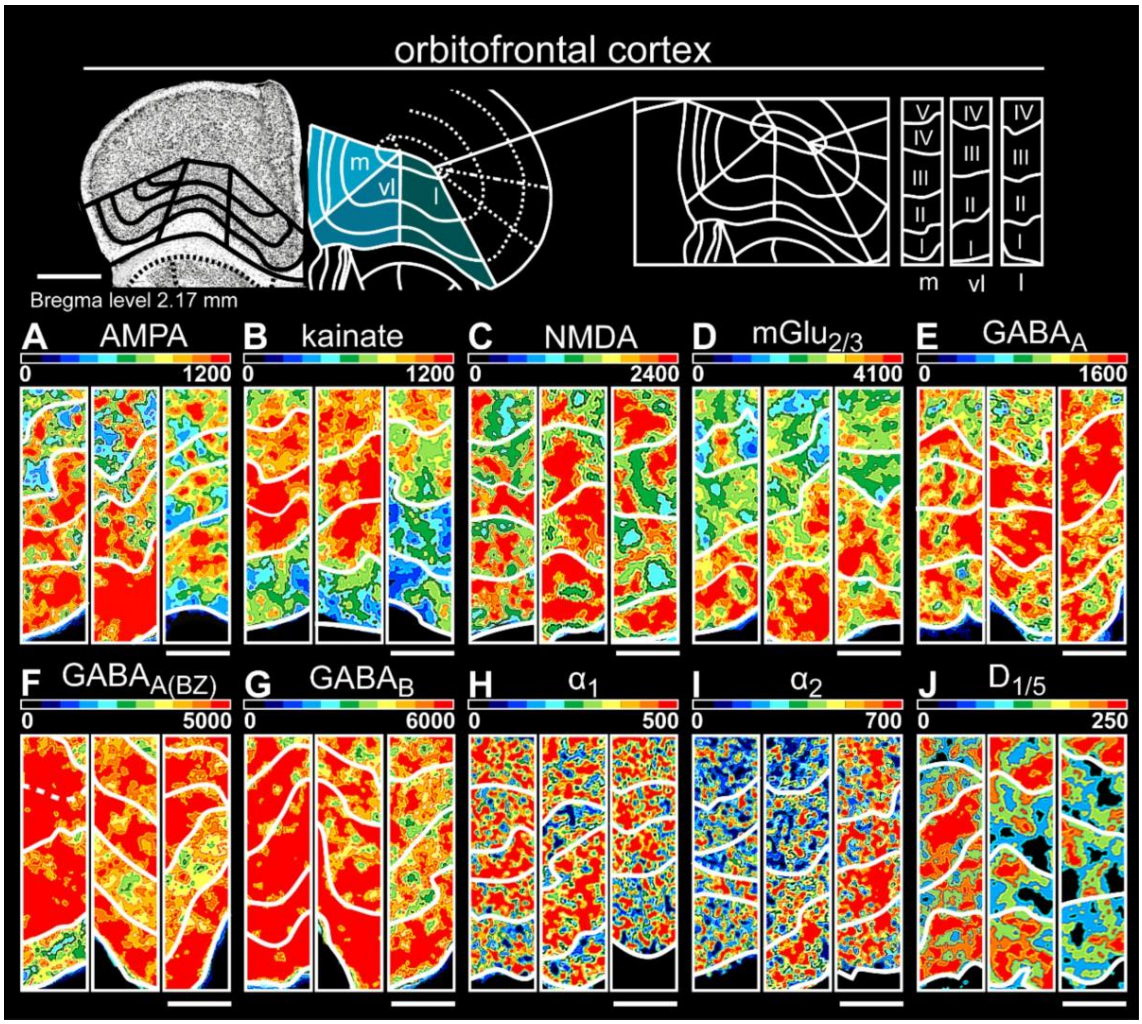

Figure 17: Color-coded layer-specific receptor distribution of the orbitofrontal cortex

In the medial part, particularly for kainateR and $GABA_{A(BZ)}R$, layer I expressed less receptor densities than layer II, whereas NMDARs clearly revealed the border between layer III and IV ($p < .05$). In the ventrolateral part, AMPARs ($p < .05$) and α_2Rs ($p < .05$) showed the border of layer I to layer II. $GABA_BRs$ ($p < .05$) were highly expressed in layer III compared to layer IV, while kainateRs ($p < .05$) showed the border of layer III to IV. In the lateral part, the differences of $GABA_BRs$ revealed the border of layer I to II ($p < .05$). KainateRs were lower in densities in layer III than in layer V ($p < .05$), while $D_{1/5}Rs$ were denser in layer VI than in layer V ($p < .05$). Densities in fmol/mg protein. Designations and figure structure as in Figure 9. For detailed receptor densities see Supp. Tab. 8. Statistical analysis in Supp. Tab. 19 (ORBm), Supp. Tab. 20 (ORBvl) and Supp. Tab. 21 (ORBl). Scale bars: Nissl-Image, 800 µm; A-J, 300 µm

The olfactory tubercle

Low receptor concentrations (excluding $mGlu_{2/3}Rs$ [4837 ± 283 fmol/mg protein, Figure 18D) separated the molecular layer I from the pyramidal layer II in the olfactory tubercle (Supp. Tab. 8). AMPA (layer I: 757 ± 44 fmol/mg protein, layer II: 1381 ± 98 fmol/mg protein; $p < .05$), $GABA_B$ (layer I: 2131 ± 286 fmol/mg protein, layer II: 3344 ± 316 fmol/mg protein; $p < .05$) and $D_{1/5}$ (layer I: 4529 ± 404 fmol/mg protein, layer II: 6451 ± 563 fmol/mg protein; $p < .05$) showed high concentration differences between layer I and layer II.

High NMDA (1768 ± 116 fmol/mg protein, Figure 18C) and $GABA_A$ (973 ± 91 fmol/mg protein, Figure 18E) receptor densities characterized the pyramidal layer II. The polymorphic layer III was characterized by a comparison with layer II for AMPARs (layer II: 1381 ± 44 fmol/mg protein, layer III: 1092 ± 80 fmol/mg protein; $p < .05$), $mGlu_{2/3}Rs$ (layer II: 4090 ± 409 fmol/mg protein, layer III: 3487 ± 248 fmol/mg protein; $p = .028$) and $D_{1/5}Rs$ (layer II: 6451 ± 563 fmol/mg protein, layer III: 5041 ± 503 fmol/mg protein; $p < .05$).

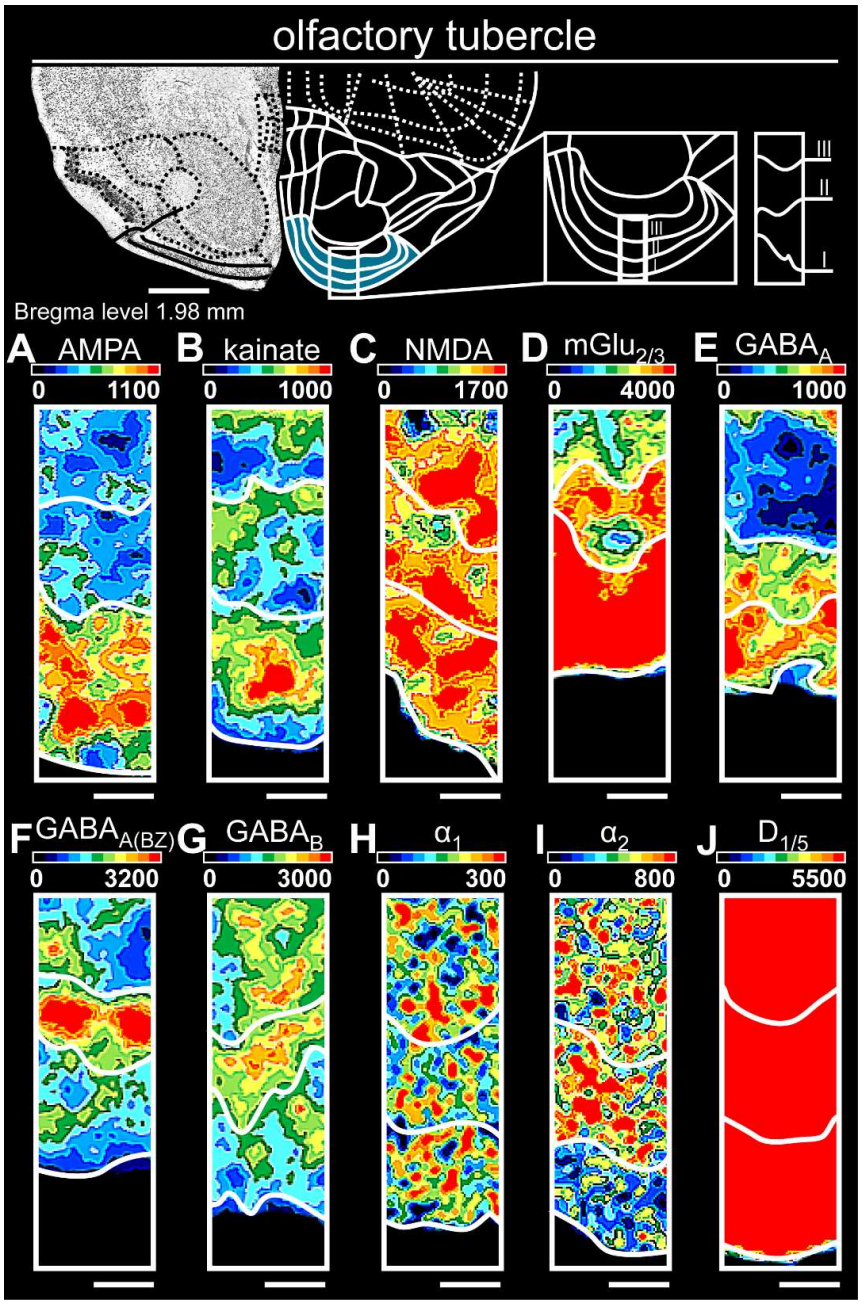

Figure 18: Color-coded layer-specific receptor distribution of the olfactory tubercle

The border from layer I to II was clearly seen for $mGlu_{2/3}$Rs and α_2Rs ($p < .05$), as layer I expressed higher receptor densities than layer II. $D_{1/5}$Rs were strongly expressed in all layers of the olfactory tubercle, so the layers were visually indistinguishable for the calculated maximal receptor expression (J). Densities in fmol/mg protein. Designations and figure structure as in Figure 9. For detailed receptor densities see Supp Tab. 8. Statistical analysis in Supp. Tab. 14. Scale bars: Nissl-Image, 1.2 mm; A-J, 400 µm.

3.1.3 Receptor fingerprints of the olfactory regions

To provide a direct comparison between the analyzed regions, so called receptor fingerprints (Zilles et al., 2002a) were calculated for each region where densities were averaged over all cortical layers or subdivisions (Figure 19, Supp. Tab. 6, Supp. Tab. 7).

Initially, fingerprints were created for each individual region, and revealed a number of similarities: each fingerprint showed high values for GABAergic receptors, but different concentrations of glutamatergic and catecholaminergic receptors. While the main and accessory olfactory bulb were high in densities of $GABA_{A(BZ)}$Rs, the remaining regions were dominated by $GABA_B$Rs. In contrast, the olfactory tubercle showed similar concentrations for the GABAergic receptors $GABA_{A(BZ)}$ and $GABA_B$. Glutamatergic $mGlu_{2/3}$Rs were prominent in most regions. The endopiriform nucleus and lateral entorhinal cortex differed because the concentration of $mGlu_{2/3}$Rs was not as high, compared to the remaining receptors. $D_{1/5}$Rs were low in concentration in all olfactory regions when compared to the other investigated receptors. Here, the olfactory tubercle showed the highest concentrations of $D_{1/5}$Rs.

Based on these fingerprints and the observed similarities, multidimensional scaling has been performed (Figure 19). It showed three large clusters (silhouette coefficient 0.4): (1) the olfactory bulbs (main and accessory olfactory bulb), (2) regions of the primary and secondary cortex, excluding the olfactory tubercle (3), which formed its own cluster. A heat map showed region-specific densities and revealed the contribution of the examined receptors to the clustering of the subdivisions as a color-coded graph based on mean densities (Figure 19).

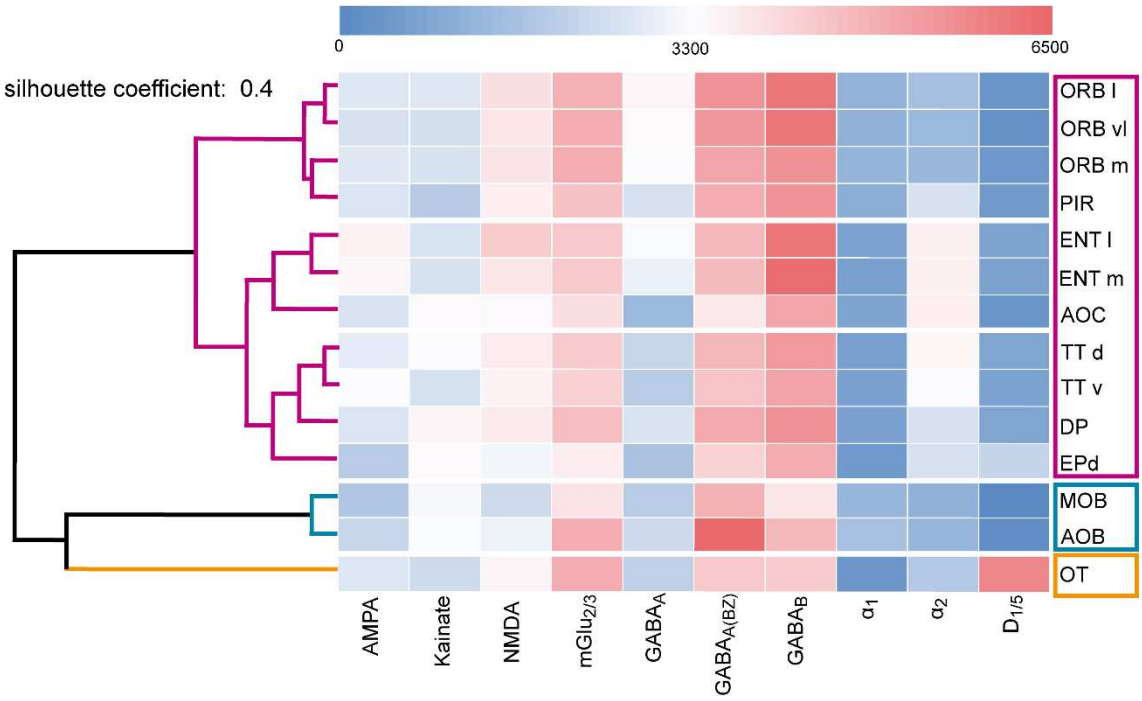

Figure 19: Dendrogram of the hierarchical cluster analysis

The heat map displays region-specific receptor densities according to their clusters (Figure 20). Receptor densities (fmol/mg protein) are displayed by a color legend from blue (low) to red (high). Red color indicates high values (> 3300 fmol/mg protein), while blue color displays lower values (< 3300 fmol/mg protein). Designations in Figure 9 (Lothmann et al., 2021).

The cluster from the main olfactory bulb and accessory olfactory bulb resulted mainly from similar values for AMPARs, kainateRs, $GABA_A$Rs, and catecholaminergic receptors. In addition, the remaining receptors $mGlu_{2/3}$, $GABA_{A(BZ)}$, and $GABA_B$ showed the same tendency. The high density of $GABA_{A(BZ)}$Rs in the accessory olfactory bulb was striking. The levels in the main olfactory bulb were high and almost higher than in the remaining olfactory regions. The receptors AMPA and α_2 were lower expressed in the main and accessory olfactory bulb cluster than in the other regions. This revealed a cluster for main and accessory olfactory bulb.

The cluster of the olfactory tubercle differed mainly in the high concentration of dopaminergic $D_{1/5}$ receptors. While this receptor was only marginally present in the olfactory system, it is strongly expressed in the olfactory tubercle. This contrasts with the GABAergic receptors, which were less distributed in the olfactory tubercle than in other regions. Also, kainateRs occurred significantly less in their density in this region. α_1Rs exhibited their lowest distribution in the olfactory tubercle.

The remaining regions were combined as one large cluster that could be further subdivided into three smaller clusters. This resulted in a cluster of both parts of taenia tecta, the dorsal

peduncular cortex and the dorsal endopiriform nucleus. The cluster differed mainly by an equal concentration of $GABA_B$, α_1 and $D_{1/5}$Rs. In general, the densities of the receptors in this group were similar, but there were differences in the glutamatergic receptors and α_2Rs within the cluster.

There is a cluster of both parts of the entorhinal cortex and the anterior olfactory cortex. This subcluster showed similar concentrations of $mGlu_{2/3}$Rs, $GABA_B$Rs, α_1Rs, α_2Rs, and $D_{1/5}$Rs in both regions. The density of α_2Rs in this subcluster was different from the other regions. The regions of the orbitofrontal cortex clustered together with the piriform cortex. Only the low concentrations of kainateRs and $GABA_A$Rs distinguished the piriform cortex from the orbitofrontal cortex here. A strong similarity in receptor distributions was observed in their total density values and in their ratios to each other.

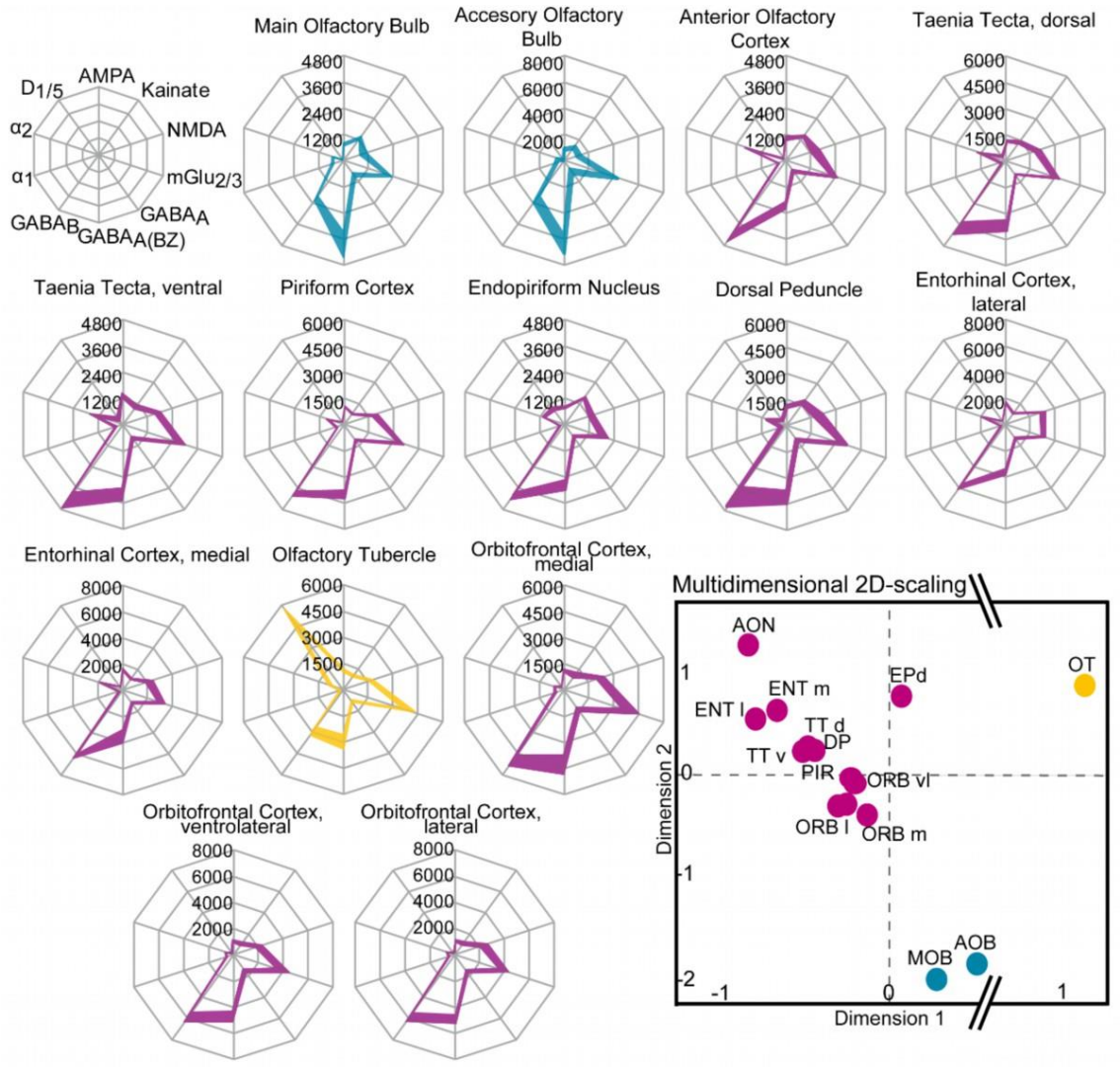

Figure 20: Receptor fingerprints of 14 olfactory regions.

Mean densities (in fmol/mg protein) are provided for each individual receptor type, connected by a colored line (colors are similar to the multidimensional 2D-scaling analysis). Receptor location of each fingerprint is outlined in the first graph. The filled regions show the standard error between the upper and lower limits of the mean receptor densities (± SEM). Lower right: Receptor-driven multidimensional 2D-scaling of the olfactory system. Based on the region-specific multi-receptor balance of all investigated receptors (averaged over ten animals/hemispheres), the dots were created, representing the feature vector of each region. In case the dots are closely arranged, a small Euclidean distance is represented. This shows a high similarity of the receptor architecture of the investigated regions. The hierarchical cluster analysis resulted in a three-cluster solution: the olfactory relay centers (blue), the cortical olfactory regions (violet) and the olfactory tubercle (yellow). The olfactory tubercle shows the highest Euclidean distance (interruption of the X-axis, dimension 1). For abbreviations see Figure 2; Lothmann et al. (2021).

3.2 Suppression of adult neurogenesis

To prove the successful suppression of adult neurogenesis, fluorescence-labeled BrdU-NeuN-double-labeled cells were counted for ten brains of every group and compared in both categories (see 2.1.3). Cell proliferation was significantly decreased in TMZ-treated animals (Figure 21).

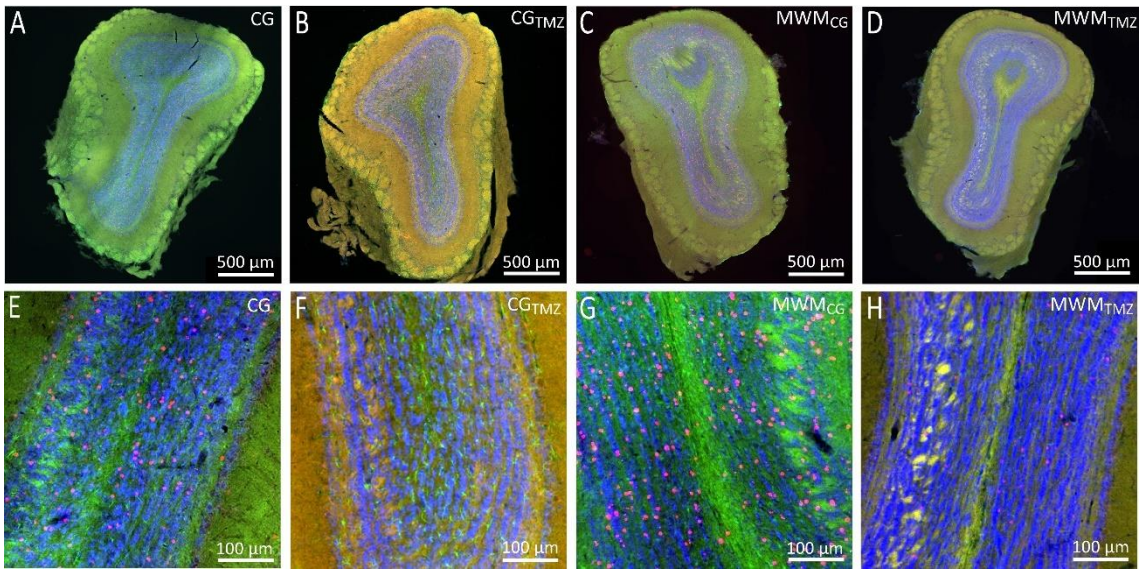

Figure 21: Evidence for an effective inhibition of adult neurogenesis in the mouse olfactory bulb

Immunofluorescence staining of the mouse main olfactory bulb with BrdU (red), NeuN (blue) and GFAP (green) for control mice (CG; **A,** close up in **E**), mice with suppressed adult neurogenesis (CG_{TMZ}; **B**, close up in **F**), trained animals with intact adult neurogenesis (MWM_{CG}; **C**, close up in **G**) and trained mice with suppressed adult neurogenesis (MWM_{TMZ}; **D**, close up in **H**).

Control animals (Figure 21A, E) expressed a higher total number of BrdU-positive cells, with an average of 156 BrdU-positive cells in the main olfactory bulb, whereas TMZ-treated animals (Figure 21B, F) had an average of 73 cells. Co-expression of BrdU-NeuN was also significantly higher in control animals (301 ± 43 positive cells) than in treated animals with suppressed adult neurogenesis (115 ± 39 positive cells). Double labeling BrdU-GFAP showed equivalent values in both animals (control: 27 ± 5; TMZ: 22 ± 4; Figure 22). Thus, TMZ resulted in a significant decrease in proliferative cells in the main olfactory bulb.

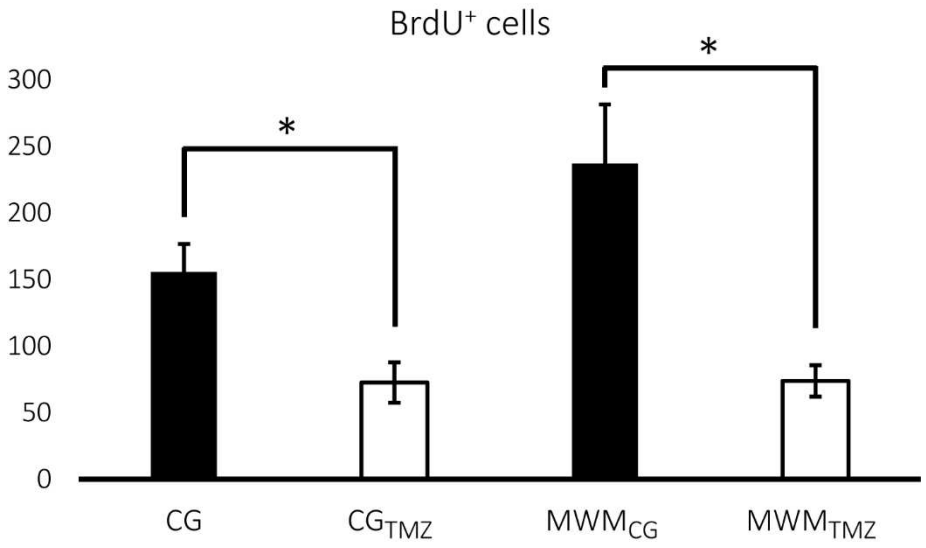

Figure 22: Statistical proof of suppression of adult neurogenesis.

BrdU-positive cells shows the counted BrdU-expressing cells per section of the olfactory bulb. Only immunohistochemical images of the main olfactory bulb were acquired, n = 3 per animal. The data show the mean values of counted cells in untrained animals (left two bars) and trained animals (right two bars). Tested were animals with intact adult neurogenesis (black bars) against animals with suppressed adult neurogenesis (white bars). Error bars were calculated using ± SEM. A nonparametric Mann-Whitney-U-test was used for pairwise comparison (*p < .05). See Supp. Tab. 22 for detailed protein concentrations with associated p-values.

The same was shown for cognitively trained animals. With 237 ± 45 cells (mean cell number) in the main olfactory bulb, trained animals (Figure 21C, G) expressed more BrdU-positive cells than trained animals with suppressed adult neurogenesis (Figure 21D, H; 74 ± 12 cells). The number of cells that co-expressed BrdU-NeuN was significantly higher in MWM_{CG} (511 ± 104 positive cells) than in MWM_{TMZ} (140 ± 30). Like in untrained animals, the double-labeling of BrdU-GFAP showed similar cell counts in both trained groups (MWM_{CG}: 21 ± 5; MWM_{TMZ}: 27 ± 4 positive cells; Figure 22). So, there was a significant decrease in proliferative cells in untrained and trained TMZ-treated animals.

3.3 The impact of inhibited adult neurogenesis on the receptor architecture of the olfactory system

The mean densities (fmol/mg protein) of receptor binding sites for glutamate, GABA, noradrenaline, and dopamine in the brains of control mice (CG) and mice with suppressed adult neurogenesis (CG_{TMZ}) were evaluated by quantitative receptor autoradiography. The quantity of GABAergic receptors increased significantly ($GABA_ARs$ and $GABA_BRs$; $p < .05$) with the suppression of adult neurogenesis, while less NMDARs were detected in CG_{TMZ}. Noradrenergic receptors revealed significant receptor increases in certain regions (dorsal peduncular cortex, medial entorhinal cortex, olfactory tubercle, Supp. Tab. 23) of CG_{TMZ}. In general, the olfactory tubercle, anterior olfactory bulb, the ventral taenia tecta and the medial entorhinal cortex proved showed the largest changes among olfactory regions (Supp. Tab. 23, Supp. Tab. 24).

3.3.1 Neurogenesis suppression alters the olfactory receptor architecture

Mean neurotransmitter receptor densities (fmol/mg protein) ± SEM in all 14 investigated olfactory regions of the mouse olfactory system of control mice (CG) and mice with suppressed adult neurogenesis (CG_{TMZ}) are provided in Supp. Tab. 23. For statistical comparisons between these groups see further Supp. Tab. 24. Each receptor type was tested with non-parametric Mann-Whitney-U test. Supp. Tab. 24 provides the percentage difference of absolute receptor concentrations, the p-value, and correlation coefficient r. The data showed differences in receptor concentrations in TMZ-treated mice, except for $mGlu_{2/3}$ receptors that revealed no significant differences in any olfactory region. Some receptors decreased in concentration (AMPARs, NMDARs, $D_{1/5}Rs$) while most receptor densities increased (kainateRs, $GABA_ARs$, $GABA_{A(BZ)}Rs$, $GABA_BRs$, α_1Rs, α_2Rs) in concentration densities.

Glutamatergic receptors

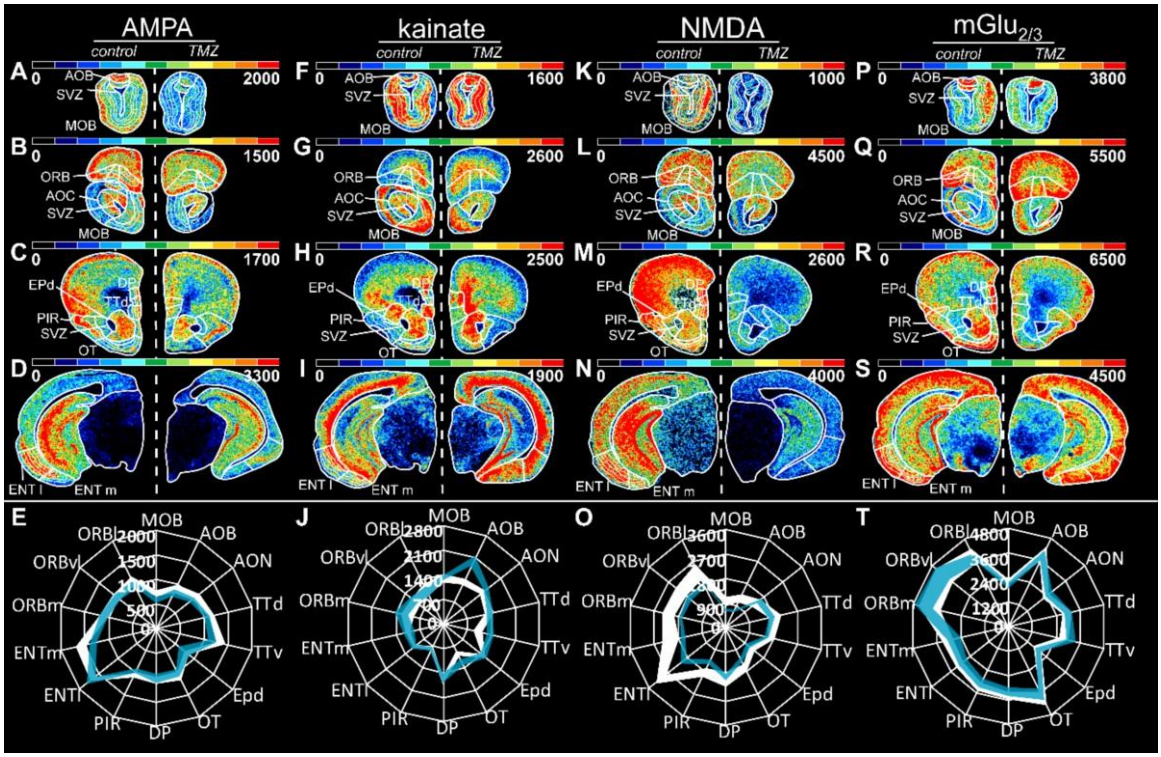

Figure 23: Color-coded autoradiographs revealed the distribution patterns of glutamatergic receptors in control animals (left, control) and animals with suppressed adult neurogenesis (right, TMZ). The indicated receptors (AMPA **A-D**, kainate **F-I**, NMDA **K-N**, $mGlu_{2/3}$ **P-S**) refer to the respective row of the following sections. AMPA receptors showed a decrease in density in the main olfactory bulb (-20.5%; $p < .05$). While kainateRs increased in receptor concentration in the accessory olfactory bulb (+48.6%; $p < .05$), NMDARs decreased here (-42.1%; $p < .05$). Bregma levels and region borders (black and white lines) like figure 2. Specific receptor densities (fmol/mg protein) are encoded by the color scale, maximum receptor concentration of the section alongside the autoradiograph. Red represents the ideal representation, not the maximum receptor density of the region, while black indicates the absence of receptor expression. Polar plots (**E**, **J**, **O**, **T**) display the mean densities (fmol/mg protein) of the measured receptor densities for control (white) and animals with suppressed adult neurogenesis (blue). Filled regions mark the upper and lower standard errors of the mean (± SEM). Densities in fmol/mg protein. Designations and figure structure as in Figure 9. For detailed receptor densities see Supp Tab. 22. Statistical analysis in Supp. Tab. 24.

Significant differences in AMPA receptor densities between control and TMZ animals could only be observed in the medial entorhinal cortex (-15.9%, $p < .05$) and the ventrolateral orbitofrontal cortex (-20.5%, $p < .05$; Figure 23, Supp. Tab. 23, Supp. Tab. 24). Especially the medial entorhinal cortex revealed low values for AMPARs after inhibition of adult neurogenesis (-15.9%, $p < .05$; Figure 23, Figure 26, Supp. Tab. 23).

The mean densities of kainate receptors were similar in most of the analyzed regions in both groups, with exception of three regions: the accessory olfactory bulb, the ventral taenia tecta and the olfactory tubercle. In these regions, significant differences in kainate receptor densities were found ($p < .05$). In the accessory olfactory bulb, the concentration was increased by 48% in the TMZ group, while the densities were increased by 34.6%; $p < .05$ in the ventral taenia tecta and by 26.9%; $p < .05$ in the olfactory tubercle (Figure 23, Figure 26, Supp. Tab. 23, Supp. Tab. 24).

NMDA receptors were the only glutamate receptor displaying descending values in receptor densities in the TMZ animal. Significant differences were found between the densities of NMDA receptors in the brains of TMZ and control mice: in the accessory olfactory bulb (-42.1%; $p < .05$), the entorhinal cortex (medial: -23.1%; $p < .05$, lateral: -34.6%; $p < .05$), the olfactory tubercle (-19.9%; $p < .05$), and the orbitofrontal cortex (medial: -21.9%; $p < .05$, lateral: -22.9%; $p < .05$; Figure 23, Figure 26, Supp. Tab. 23, Supp. Tab. 24).

Mean densities of $mGlu_{2/3}Rs$ showed generally high receptor densities. However, no significant differences were found between the densities of $mGlu_{2/3}Rs$ in the brains of TMZ and control mice (Figure 23, Figure 26, Supp. Tab. 23, Supp. Tab. 24).

GABAergic receptors

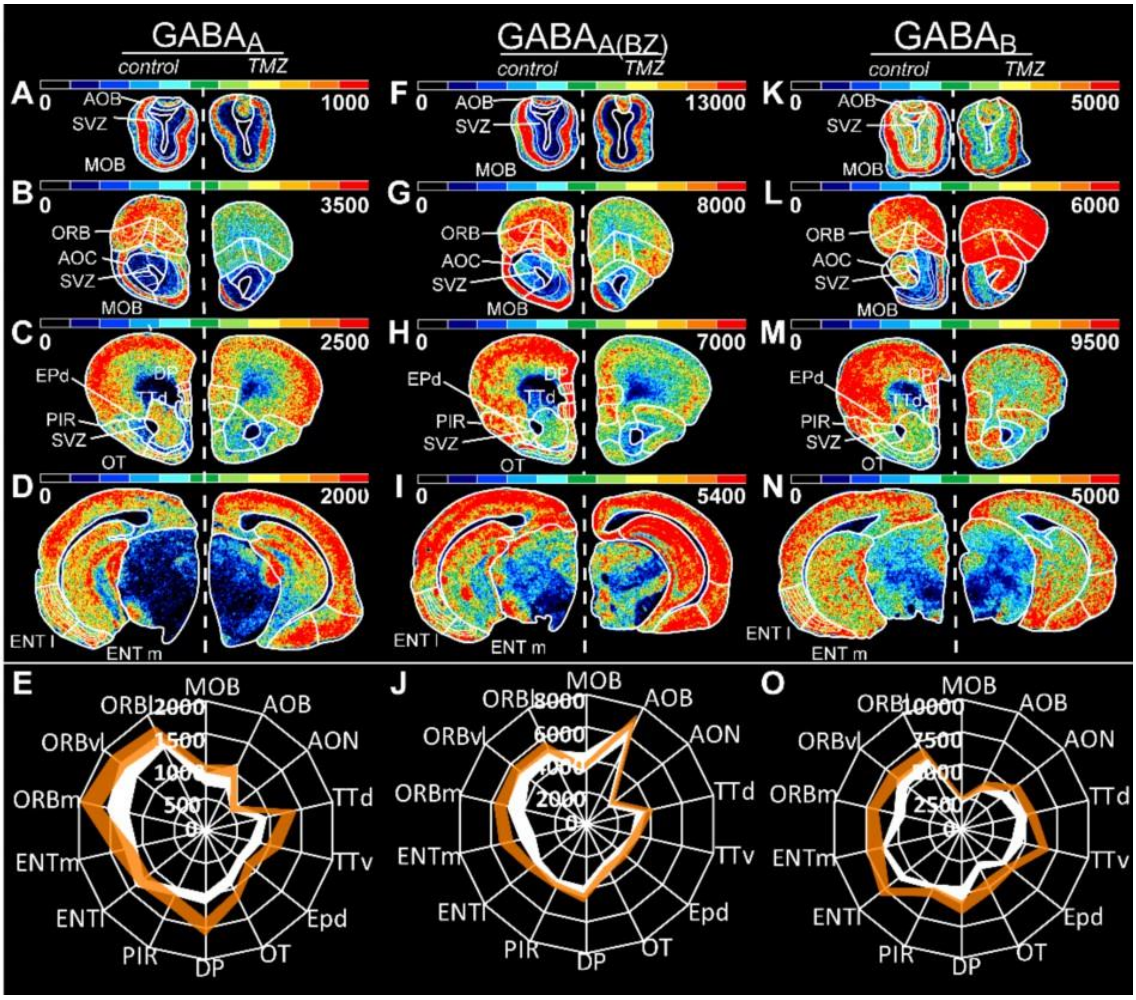

Figure 24: Color-coded autoradiographs reveal the distribution and density of GABAergic receptors in control animals (left, control) and animals with suppressed adult neurogenesis (right, TMZ). The indicated receptors ($GABA_A$ **A-D**, $GABA_{A(BZ)}$ **F-I**, $GABA_B$ **K-N**) refer to the respective row of the following sections. GABAergic receptors generally showed increases in concentrations in CG_{TMZ}, for example $GABA_A$Rs in the dorsal taenia tecta (+47.4%; $p < .05$), $GABA_{A(BZ)}$Rs in the medial entorhinal cortex (+37.3%; $p < .05$), and $GABA_B$Rs in the olfactory tubercle (+57.6%; $p < .05$). Information about the color scale and polar plots (**E, J, O**) in Figure 23. Densities in fmol/mg protein. Designations and figure structure as in Figure 9. For detailed receptor densities see Supp. Tab. 23. Statistical analysis in Supp. Tab. 24.

$GABA_A$ binding sites showed heterogeneous differences between olfactory regions (Figure 24). Significant increases in receptor densities were observed in the dorsal taenia tecta (+47.3%; $p < .05$), endopiriform nucleus (+24.4%; $p < .05$), dorsal peduncular cortex (+42.2%; $p < .05$), olfactory tubercle (+31.37%; $p < .05$), and medial orbitofrontal cortex (+30.8%; $p < .05$) of CG_{TMZ} (Figure 24, Figure 26, Supp. Tab. 23, Supp. Tab. 24).

BZ-binding sites revealed a tendency to increase in receptor concentration in CG_{TMZ} animals (Figure 24). The increases were not significant for most of the olfactory regions, except the medial entorhinal cortex (+37.3%; $p< .05$; Figure 24, Figure 26, Supp. Tab. 23, Supp. Tab. 24).

In general, $GABA_B$ receptors in most ROIs showed high receptor densities after suppression of adult neurogenesis. Notably were the high receptor concentrations in the anterior olfactory bulb (+25.8%; $p < .05$), the ventral taenia tecta (+49.6%; $p < .05$), the entorhinal cortex (lateral: +29.3%; $p < .05$, medial: +10.9%; $p < .05$), the medial orbitofrontal cortex (+41.4%; $p < .05$) and the olfactory tubercle (+57.6%; $p < . 05$; Figure 24, Figure 26, Supp. Tab. 23, Supp. Tab. 24) of CG_{TMZ}.

Catecholaminergic receptors

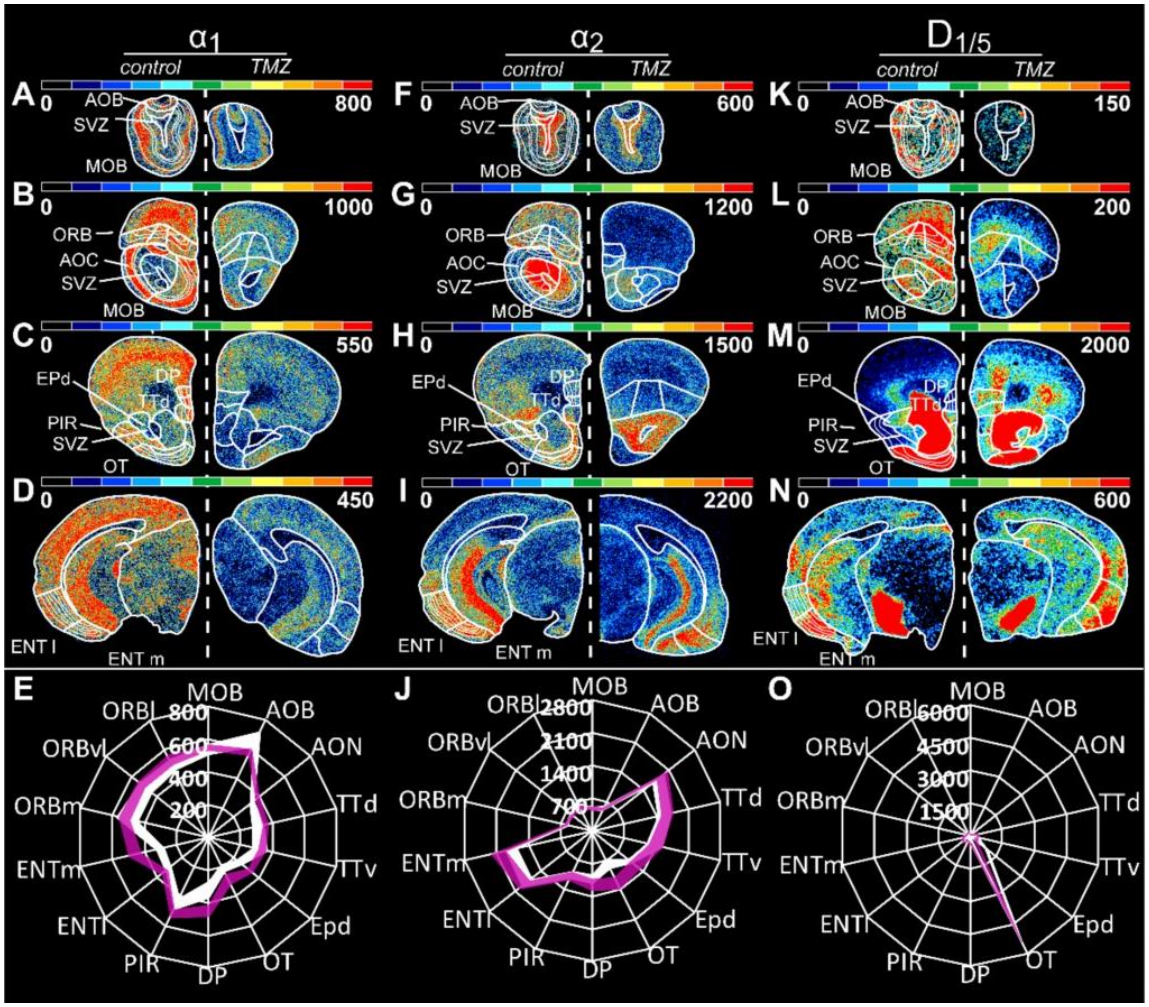

Figure 25: Color-coded autoradiographs revealed the distribution patterns of catecholaminergic receptors in control animals (left, control) and animals with suppressed adult neurogenesis (right, TMZ). The indicated receptors (α_1 **A-D**, α_2 **F-I**, $D_{1/5}$ **K-N**) refer to the respective row of the following sections. Catecholaminergic receptors showed a heterogenous picture, as α1Rs increased in the medial entorhinal cortex (+52.2%; $p < .05$), whereas α_2Rs increased in the olfactory tubercle (+59.8%; $p < .05$) of TMZ-treated animals. Dopaminergic receptors decreased significantly in the dorsal endopiriform nucleus (-63.6%; $p < .05$). Densities in fmol/mg protein. Designations and figure structure as in Figure 9. Information about the color scale and polar plots (**E, J, O**) in Figure 23. For detailed receptor densities see Supp. Tab. 23. Statistical analysis in Supp. Tab. 24.

The analyzed noradrenergic receptors (Figure 25, Figure 26) revealed a few differences between CG and CG_{TMZ} animals. While the agonist α_1 decreased in concentrations exclusively in the accessory olfactory bulb (-13.5%; $p < .05$), significant increases were observed in the endopiriform nucleus (+35.6%; $p < .05$) and the medial entorhinal cortex (+52.2%; $p < .05$) of the CG_{TMZ} animals. The antagonist α_2 revealed a significant increase in receptor concentration in CG_{TMZ} animals only in

the olfactory tubercle (+59.8%; $p < .05$) at generally high receptor densities (Figure 25, Figure 26, Supp. Tab. 23, Supp. Tab. 24).

The mean concentrations of the $D_{1/5}$Rs were particularly low compared to the other receptors. Statistical tests indicated significantly decreased densities in the accessory olfactory bulb (-32.7%; $p < .05$) and endopiriform nucleus (-63.6%; $p < .05$) in CG_{TMZ} animals (Figure 25, Figure 26, Supp. Tab. 23, Supp. Tab. 24).

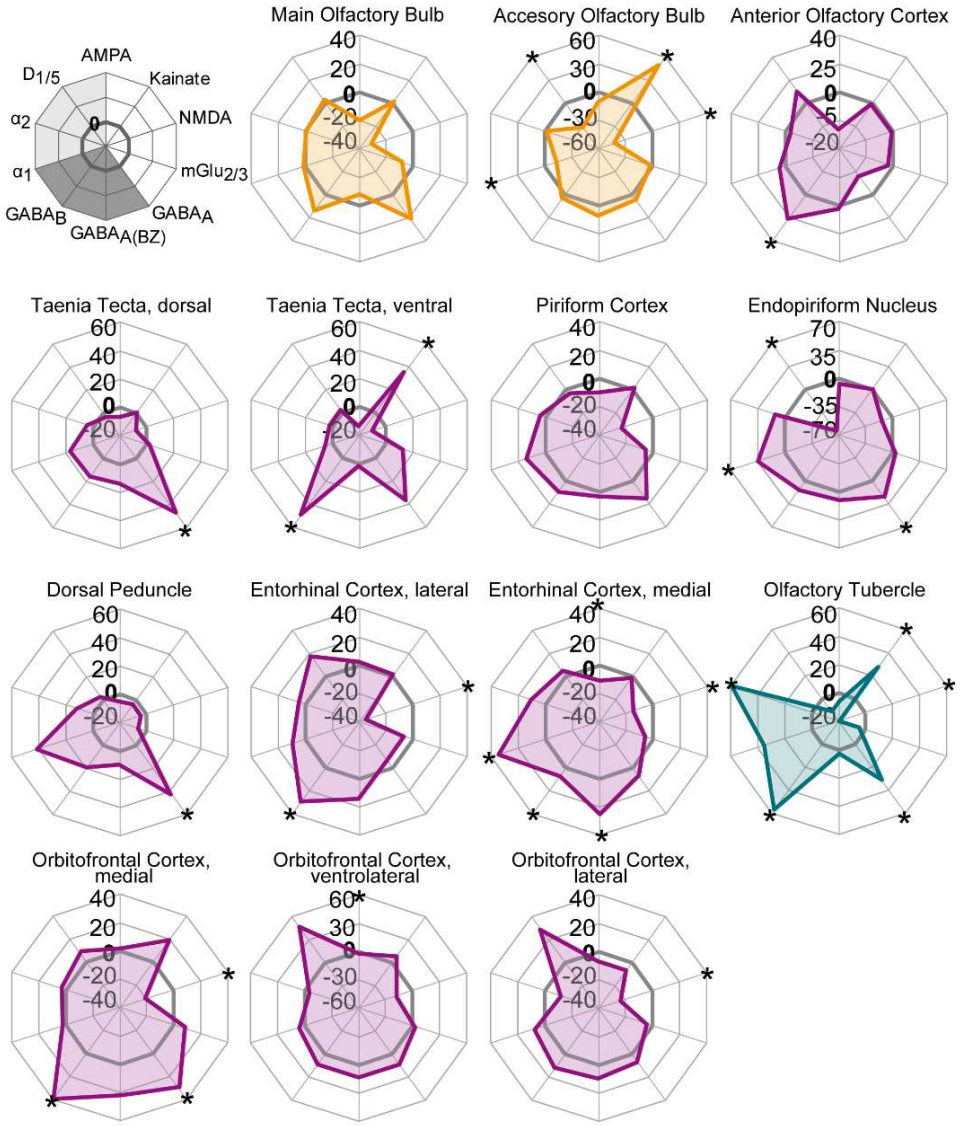

Figure 26: Receptor fingerprints of the 14 investigated olfactory regions

Relative differences of mean densities [%] of CG versus CG_{TMZ}. Colors are similar to clusters of the multidimensional 2D-scaling analysis. The positions of the receptors are shown schematically in the first graph. The thicker dark gray loop marks the 0% level. Asterisks describe statistical significance (*$p < .05$).

3.3.2 Layer-specific alterations of the receptor architecture

Mean neurotransmitter receptor densities (fmol/mg protein) ± SEM in the layers of all 14 investigated olfactory regions of the mouse olfactory system of control mice (CG) and mice with suppressed adult neurogenesis (CG_{TMZ}) are provided in Supp. Tab. 25. For statistical comparisons between these groups see further Supp. Tab. 26. Each receptor type was tested with non-parametric Mann-Whitney-U test. Supp. Tab. 26 provides the percentage difference of absolute receptor concentrations, the p-value, and the sum of ranks W for the investigated layers and receptors. Most receptors decreased in concentrations upon the direct comparison of the concentration of the layers, but, overall, every layer showed an individual difference that is represented Supp. Tab. 25.

Main olfactory bulb and accessory olfactory bulb

While AMPARs in the main olfactory bulb of CG_{TMZ} mice (Figure 31) showed a significant decrease in the inner plexiform (-27.3%; $p < .05$), mitral cell (-19.3%; $p < .05$) and olfactory nerve layer (-11.2%; $p < .05$), no significant changes were seen in the accessory olfactory bulb (Supp. Tab. 25, Supp. Tab. 26). KainateRs showed a receptor increase in the glomerular layer of the main olfactory bulb (+11.4%; $p < .05$) and the accessory olfactory bulb (+216.1%; $p < .05$; Figure 32) due to suppression of the adult neurogenesis. NMDARs decreased significantly in all layers of the accessory olfactory bulb (all $p < .05$) in CG_{TMZ}. $GABA_{A(BZ)}$Rs showed an concentration increase in the inner plexiform layer of the main olfactory bulb (+25.8%; $p < .05$) and the mitral (+35.9%; $p < .05$) and glomerular layers (+28.1%; $p < .05$) of the accessory olfactory bulb. While α_1Rs in the mitral cell layer (main: -11.8%; $p < .05$, accessory: -17.9%; $p < .05$) showed receptor decreases in both regions, $D_{1/5}$Rs were significantly less distributed in the inner/outer plexiform layer (inner: -28.2%; $p < .05$; outer: -28.7%; $p < .05$) of the main olfactory bulb and the granular (-42.4%; $p < .05$) and mitral cell layer (-33.1%; $p < .05$) of the accessory olfactory bulb (Supp. Tab. 25, Supp. Tab. 26) in CG_{TMZ}.

Primary olfactory cortex

In the anterior olfactory cortex (Figure 33), only the pars externa showed a strong receptor decrease of AMPARs (-31.6%; $p < .05$) and kainateRs (-15.5%; $p < .05$) in CG_{TMZ}. In the same layer, $GABA_BRs$ (+31.2%; $p < .05$) were significantly higher expressed. KainateRs (+24.4%; $p < .05$) and $GABA_BRs$ (+22.8%; $p < .05$) increased in the medial part. NMDARs (+81.8%; $p < .05$) and $GABA_BRs$ (+49.2%; $p < .05$) showed a strong increase in density in the postero-ventral part. In the dorsal part, significantly less $mGlu_{2/3}Rs$ (-19.9%; $p < .05$) were expressed in CG_{TMZ}, while the concentration of α_1Rs (+38.5%; $p < .05$) increased. The lateral part revealed a receptor decrease in $GABA_{A(BZ)}Rs$ (-12.9%; $p < .05$) and concentration increases of $GABA_BRs$ (+30.7%; $p < .05$) and $D_{1/5}Rs$ (+7.5%; $p < .05$; Supp. Tab. 25, Supp. Tab. 26).

In the dorsal taenia tecta (Figure 34), receptor densities of $GABA_ARs$ (+118.3%; $p < .05$) and α_1Rs (+40.1%; $p < .05$) increased in layer II in CG_{TMZ}. In layer III, $GABA_ARs$ (+74.2%; $p < .05$) also increased in concentration. Layer IV showed density increases of $GABA_ARs$ (+100.5%; $p < .05$) and $GABA_BRs$ (+35.3%; $p < .05$; Supp. Tab. 25, Supp. Tab. 26).

In the ventral taenia tecta (Figure 35), layer I showed a decrease of NMDARs (-19.3%; $p < .05$) with a simultaneous increase of $mGlu_{2/3}Rs$ (+61.4%; $p < .05$) in CG_{TMZ} animals. Layer II showed high densities of kainateRs (+36.8%; $p < .05$), while layer III expressed significantly higher $GABA_ARs$ (+154.1%; $p < .05$; Supp. Tab. 25, Supp. Tab. 26) upon suppression of adult neurogenesis.

In layer II/III of the dorsal peduncular cortex (Figure 37), NMDARs (-23.4%; $p < .05$) decreased significantly in concentration with a simultaneous increase in $GABA_ARs$ (+88.9%; $p < .05$) and α_2Rs (+34.3%; $p < .05$) CG_{TMZ}. Layer V showed decreasing concentrations of $mGlu_{2/3}Rs$ (-13.4%; $p < .05$) and increases of α_1Rs (+85.8%; $p < .05$) . $GABA_ARs$ increased in all layers (up to +92.5%; $p < .05$ in layer I; Supp. Tab. 25, Supp. Tab. 26). In layer I of the piriform cortex (Figure 38), only NMDARs showed significant differences (-35.7%; $p < .05$).

In both parts of the entorhinal cortex (lateral: Figure 39, medial: Figure 40) of CG_{TMZ} animals, AMPARs decreased in concentrations in the superficial layers and highly in the deeper layers. Layer VI of the lateral entorhinal cortex (Figure 39) revealed a strong decrease in AMPAR concentration (-21.9%; $p < .05$), while the medial entorhinal cortex (Figure 40) decreased in layer I (-49.5%; $p < .05$) and layer II (-29.6%; $p < .05$), while it increased in layer V (+20.8%; $p < .05$). NMDARs generally showed a strong, significant decrease ($p < .05$). $GABA_{A(BZ)}Rs$ increased in density, particularly in layers II, (+29.0%; $p < .05$), III (+26.7%; $p < .05$) and IV (+21.9%; $p < .05$) of the lateral part and layer III (+72.4%; $p < .05$) and IV (+76.3%; $p < .05$) of the medial part. $GABA_BRs$ increased in the lateral part ($p < .05$) of CG_{TMZ}. While α_1Rs showed a strong increase in the medial part ($p < .05$),

α_2Rs showed an increase in the deeper layers (IV: +22.1%; $p < .05$; V: +34.2%; $p < .05$; VI: +42.5%; $p < .05$). $D_{1/5}$Rs showed an increase in concentration in layer III of the lateral part of the entorhinal cortex (+36.3%; $p < .05$; Supp. Tab. 25, Supp. Tab. 26) upon suppression of adult neurogenesis.

Layer I of the olfactory tubercle (Figure 36) showed strong receptor decreases of NMDARs upon suppression of adult neurogenesis (-35.1%; $p < .05$), while $GABA_A$Rs (+21.3 $p < .05$) increased. NMDARs were decreased in layers II/III (-23.0%; $p < .05$) of CG_{TMZ}. Layer III also revealed concentration increases of α_1Rs (+19.6%; $p < .05$) and α_2Rs (+58.0%; $p < .05$; Supp. Tab. 25, Supp. Tab. 26).

Secondary olfactory cortex

KainateRs (-27.3%; $p < .05$) and $mGlu_{2/3}$Rs (-12.6%; $p < .05$) showed a significant decrease in layer II/III of the lateral orbitofrontal cortex, while NMDARs (I: -27.6%; $p < .05$; II/III: -30.7%; $p < .05$; VI: -24.9%; $p < .05$) were generally lower expressed in CG_{TMZ}. In the medial part, GABAergic receptors showed a significant increase; $GABA_A$Rs in layer II (+38.3%; $p < .05$) and II/III (+48.9%; $p < .05$), $GABA_{A(BZ)}$Rs in layer II (+23.7%; $p < .05$) and V (+37.3%; $p < .05$) and all layers for $GABA_B$Rs ($p < .05$). In layer I (+20.2%; $p < .05$) of the lateral part, α_1Rs showed high densities while α_2Rs revealed low concentrations in layer I (-8.9%; $p < .05$) and VI (-16.8%; $p < .05$). $D_{1/5}$Rs revealed significant increases in the ventrolateral part (layer I: +98.9%; $p < .05$; V: +62.2%; $p < .05$; VI: +27.1%; $p < .05$; Figure 41; Supp. Tab. 25, Supp. Tab. 26) upon suppression of adult neurogenesis.

3.4 Cognitive training and adult neurogenesis impact the olfactory receptor-architecture

In this chapter, the impact of cognitive training on the receptor architecture of the olfactory system will be described. First, the direct influence for the individual olfactory regions (3.4.1) and their respective layers (3.4.1.1) were determined by comparing MWM_{CG} against CG (chapter 3.4.1).

Subsequently, the impact of adult neurogenesis in the trained (MWM_{CG} and MWM_{TMZ}) animals was examined for the olfactory regions (3.4.2) and their respective layers (3.4.2.1). Next, both factors were examined concurrently by comparing the receptor concentrations of trained animals with suppressed adult neurogenesis (MWM_{TMZ}) against the concentrations of control animals (CG), each at the olfactory regional level (3.4.3) as well as on the laminar level (3.4.3.1). To compare the receptor concentrations of suppressed adult neurogenesis in untrained and trained animals, the regional (3.4.4.) and laminar (3.4.4.1) olfactory receptor densities of both groups with suppressed adult neurogenesis (CG_{TMZ} vs. MWM_{TMZ}) were compared. Finally, the different impacts of adult neurogenesis were compared using relative data to analyze the impact of cognitive training (CG/CG_{TMZ} vs. MWM_{CG}/MWM_{TMZ}; 3.4.5).

Receptor fingerprints were generated for each type of comparison (Figure 26 – Figure 30). In addition, figures were generated for each region showing all four studied groups (CG, CG_{TMZ}, MWM_{CG}, MWM_{TMZ}, Figure 31 – Figure 41).

3.4.1 Cognitive training alters the olfactory receptor profiles

Mean neurotransmitter receptor densities (fmol/mg protein) ± SEM of all 14 investigated olfactory regions of the mouse olfactory system of control mice (CG) and cognitively trained mice (MWM_{CG}) are provided in Supp. Tab. 27. For statistical comparisons between these groups see further Supp. Tab. 28. Each receptor type was tested with non-parametric Mann-Whitney-U test. Supp. Tab. 28 provides the percentage difference of absolute receptor concentrations, the *p*-value, and correlation coefficient *r*. The data showed a difference in receptor concentration in trained mice. Most receptors increased in concentration ($mGlu_{2/3}$, $GABA_ARs$, $GABA_{A(BZ)}Rs$, $GABA_BRs$, α_1Rs) due to cognitive training, while the other receptor densities decreased (AMPARs, kainateRs, NMDARs, α_2Rs, $D_{1/5}Rs$) in densities.

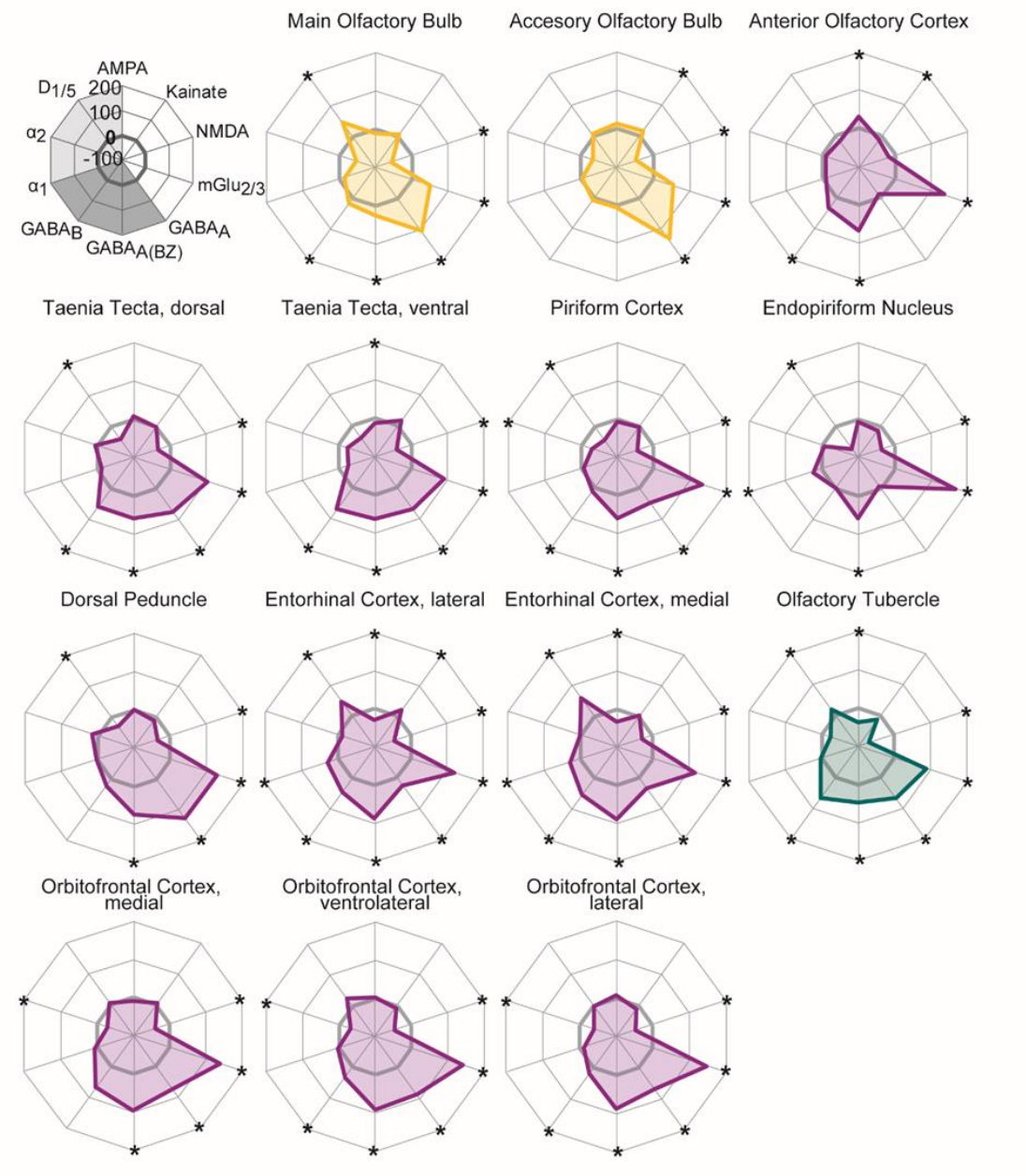

Figure 27: Receptor fingerprints of the 14 investigated olfactory regions

Relative differences of mean densities [%] of CG and MWM_{CG}. Colors are similar to the multidimensional 2D-scaling analysis. The positions of the receptors are shown schematically in the first graph. Asterisks describe statistical significance (*$p < .05$, Supp. Tab. 28).

Glutamatergic receptors

Different effects for glutamatergic receptors could be observed. AMPARs and NMDARs exhibited decreasing concentrations due to cognitive training. While AMPARs decreased in densities in the olfactory tubercle (-38.0%, $p < .05$) and the entorhinal cortex (medial: -32.6%, $p < .05$; lateral: -29.8%, $p < .05$) they increased in the anterior olfactory cortex (29.9%, $p < .05$) in the MWM_{CG} animals (Figure 27; Supp. Tab. 27, Supp. Tab. 28). KainateRs revealed an opposite picture to AMPARs, as they showed an increase in receptor densities in the accessory olfactory bulb (+15.5%, $p < .05$) and the lateral entorhinal cortex (+20.6%, $p < .05$) upon cognitive training, while the anterior olfactory cortex showed a significant decrease (-12.4%, $p < .05$; Figure 27; Supp. Tab. 27, Supp. Tab. 28).

Also, in NMDARs, the olfactory tubercle revealed a significantly low receptor concentration (-70.0%, $p < .05$) in MWM_{CG}, similar to AMPARs. In general, NMDARs tended to decrease in concentration due to cognitive training. Due to this, NMDARs appeared different from the other three investigated glutamatergic receptors (Figure 27, Supp. Tab. 27, Supp. Tab. 28). Like AMPARs and kainateRs, $mGlu_{2/3}Rs$ also showed a general significant increase. Here, the orbitofrontal cortex was most prominent (+ 140.0%, $p < .05$; Figure 27; Supp. Tab. 27, Supp. Tab. 28).

GABAergic receptors

GABAergic receptors showed a heterogenous picture: strong receptor increases were observed in all three receptor subtypes in brains of MWM_{CG} animals. For $GABA_ARs$, the increase was prominent in the accessory olfactory bulb (+134.0%, $p < .05$), and the dorsal peduncular cortex (+126.7%, $p < .05$). The main olfactory bulb (+104.6%, $p < .05$) also showed a particularly strong receptor increase. The entorhinal cortex demonstrated little differences in receptor concentration (Figure 27, Supp. Tab. 27, Supp. Tab. 28).

For $GABA_{A(BZ)}Rs$, the orbitofrontal (lateral: +87.4%; $p < .05$, ventrolateral: +91.7% $p < .05$, medial: +94.5%; $p < .05$) and entorhinal cortex (lateral: +87.2% $p < .05$, medial: +88.2% $p < .05$) revealed highly increased receptor concentrations by cognitive training (Figure 27; Supp. Tab. 27, Supp. Tab. 28). For $GABA_BRs$, the strongest increases were found in the receptor densities of the taenia tecta (dorsal: +58.3% $p < .05$, ventral: +70.8%; $p < .05$), the olfactory tubercle (+67.0%;$p < .05$) and the medial orbitofrontal cortex (+67.2%; $p < .05$) of MWM_{CG} animals (Figure 27; Supp. Tab. 27, Supp. Tab. 28), compared to CG animals.

Catecholaminergic receptors

Catecholaminergic receptors revealed different patterns of alterations in MWM_{CG} animals: While α_1Rs showed an increase in the endopiriform nucleus (+25.4%; $p < .05$), and the entorhinal cortex (lateral: +29.0%; $p < .05$; medial: +28.7%; $p < .05$), α_2Rs revealed a significant decrease in receptor densities in the main olfactory bulb (-46.7%; $p < .05$), the piriform cortex (-28.7%; $p < .05$) and all subregions of the orbitofrontal cortex (lateral: -39.1%; $p < .05$, ventrolateral: -32.4%; $p < .05$, medial: -29.0%; $p < .05$, Figure 27; Supp. Tab. 27, Supp. Tab. 28) of MWM_{CG} animals.

In $D_{1/5}$Rs, the main olfactory bulb (+46.8%; $p < .05$), the olfactory tubercle (-23.9%; $p < .05$), the entorhinal cortex (lateral: +46.7%; $p < .05$, medial: +58.3%; $p < .05$) showed an increase in receptor density with cognitive training, whereas the dorsal taenia tecta (-40.7%; $p < .05$), the endopiriform nucleus (-71.1%; $p < .05$), the dorsal peduncular cortex (-29.5%; $p < .05$), and the piriform cortex (-43.5%; $p < .05$) were increased in concentration (Figure 27; Supp. Tab. 27, Supp. Tab. 28).

3.4.1.1 Layer-specific alterations upon cognitive training

Mean neurotransmitter receptor densities (fmol/mg protein) ± SEM in the layers of all 14 investigated olfactory regions of the olfactory system of control mice (CG) and trained mice (MWM_{CG}) are provided in Supp. Tab. 29. For statistical comparisons between these groups see Supp. Tab. 30. Each receptor type was tested with non-parametric Mann-Whitney-U test. Supp. Tab. 30 provides the percentage difference in receptor concentrations, the p-value, and the Z-value for the investigated layers and receptors. All receptors revealed alterations in the layers of olfactory regions, without demonstrating a general effect. For example, $GABA_{A(BZ)}$Rs were decreased in the granule layer of the accessory olfactory bulb, while the concentration was increased in the mitral and glomerular layer (Supp. Tab. 30) of MWM_{CG} animals.

Main and accessory olfactory bulb

Glutamatergic receptors showed significant changes in the olfactory nerve layer of the main olfactory bulb (AMPA: -46.2%; $p < .05$; kainate: -42.7%; $p < .05$; NMDA: -60.1%; $p < .05$; Figure 31) and the glomerular layer of the accessory olfactory bulb (AMPA: +56.4%; $p < .05$; kainate: +101.6%; $p < .05$; NMDA: -53.7%; $p < .05$; $mGlu_{2/3}$: + 224.6%; $p < .05$; Figure 32) of MWM_{CG} animals. GABAergic receptors were significantly increased in the glomerular layer of the accessory olfactory bulb by cognitive training ($GABA_A$: +538.7%; $p < .05$; $GABA_{A(BZ)}$: +129.3%; $p < .05$; $GABA_B$: +18.7%; $p < .05$). Dopaminergic $D_{1/5}$R were altered in the glomerular layer of the accessory olfactory bulb (+76.8%; $p < .05$). The opposite was true for noradrenergic receptors: they were strongly altered in the olfactory nerve layer in the main olfactory bulb (α_1: -45.6%; $p < .05$; α_2: -47.8%; $p < .05$) but not in the glomerular layer of the accessory olfactory bulb (α_2: -46.7%; $p < .05$). The strongest changes occurred in the glomerular layer of both regions. NMDARs (main: -60.1%; $p < .05$; accessory: -55.3%; $p < .05$), $GABA_A$Rs (main: +163.9%; $p < .05$; accessory: +538.7%; $p < .05$), $GABA_{A(BZ)}$Rs (main: +49.7%; $p < .05$; accessory: +129.3%; $p < .05$), and $GABA_B$Rs (main: +94.7%; $p < .05$; accessory: +18.7%; $p < .05$) showed changes in both olfactory bulbs (Figure 31, Figure 32, Supp. Tab. 29, Supp. Tab. 30) of MWM_{CG} animals.

Primary olfactory cortex

Changes in the dorsal part of the anterior olfactory cortex (Figure 33) in brains of MWM_{CG} animals were significant. AMPARs (+45.7%; $p < .05$), NMDARs (-20.7%; $p < .05$), $mGlu_{2/3}Rs$ (+162.9%; $p < .05$), $GABA_{A(BZ)}Rs$ (+120.7%; $p < .05$), $GABA_BRs$ (28.2%; $p < .05$), α_1Rs (-17.6%; $p < .05$), and α_2Rs (-21.5%; $p < .05$) differed from the densities of CG animals. The lateral part showed significant deviations from CG animals in NMDARs (-50.2%; $p < .05$), $mGlu_{2/3}Rs$ (+127.8%; $p < .05$), $GABA_{A(BZ)}Rs$ (+43.2%; $p < .05$), and $GABA_BRs$ (+32.5%; $p < .05$); catecholaminergic receptors did not differ significantly.

In the dorsal (Figure 34) and ventral (Figure 35) subregions of taenia tecta, the superficial layers showed significant changes in NMDARs (dorsal: -45.5%; $p < .05$ (layer I), -30.7%; $p < .05$ (layer II); ventral: -56.7%; $p < .05$ (layer I), -38.0%; $p < .05$ (layer II)) and $mGlu_{2/3}Rs$ (dorsal: +100.4%; $p < .05$ (layer I); +116.5%; $p < .05$ (layer II); ventral: +106.2%; $p < .05$ (layer I); +103.8%; $p < .05$ (layer II). $GABA_ARs$ (dorsal: +91.8%; $p < .05$; ventral: +70.4%; $p < .05$) and $GABA_{A(BZ)}Rs$ (dorsal: +73.9%; $p < .05$; ventral: +76.5%; $p < .05$) were mostly altered in layer II, but $GABA_BRs$ displayed little changes here (dorsal: +50.2%; $p < .05$; ventral: +66.4%; $p < .05$) and significant differences in layer I (dorsal: +63.1%; $p < .05$; ventral: +91.9%; $p < .05$) and IV (+55.8%; $p < .05$) of MWM_{CG} animals. $D_{1/5}Rs$ revealed significant changes only in layer IV of the dorsal taenia tecta (-55.6%; $p < .05$; Supp. Tab. 29, Supp. Tab. 30).

The olfactory tubercle (Figure 36) showed significant changes in receptor densities of GABAergic ($GABA_A$: +70.2%; $p < .05$; $GABA_{A(BZ)}$: +48.3%; $p < .05$; $GABA_B$: +80.6%; $p < .05$) receptors, AMPARs (-46.9%; $p < .05$), and NMDARs (-67.8%; $p < .05$) in layer II of MWM_{CG} animals. Layer I showed changes in kainateRs (-61.2%; $p < .05$), NMDARs (-85.8%; $p < .05$), and $D_{1/5}Rs$ (+27.4%; $p < .05$).

In layer I of the dorsal peduncular cortex of MWM_{CG} animals, strong changes were observed in $mGlu_{2/3}Rs$ (-44.2%; $p < .05$) and $GABA_BRs$ (+60.0%; $p < .05$), with little alterations of $GABA_{A(BZ)}Rs$ (+42.1%; $p < .05$). Layer VI exhibited alterations in α_2Rs (+36.5%; $p < .05$), and $D_{1/5}Rs$ (-46.7%; $p < .05$; Supp. Tab. 29, Supp. Tab. 30) in MWM_{CG} animals.

In the piriform cortex (Figure 38), layer III showed differences for $mGlu_{2/3}Rs$ (+173.0%; $p < .05$) and $D_{1/5}Rs$ (-57.5%; $p < .05$). In AMPARs (-28.2%; $p < .05$) and $GABA_{A(BZ)}Rs$ (+70.1%; $p < .05$), the highest differences were observed in layer II (Supp. Tab. 29, Supp. Tab. 30) of cognitively trained animals.

In the lateral part of the entorhinal cortex (Figure 39), the highest difference in layer I was detected for $mGlu_{2/3}Rs$ (+161.5%; $p < .05$), and the lowest in $GABA_{A(BZ)}Rs$ (+55.9%; $p < .05$), and

NMDARs (-43.1%; $p < .05$). AMPARs and kainateRs differed here, with changes in AMPARs running from high (layer II: -42.6%; $p < .05$; III: -35.4%; $p < .05$) to low concentration differences (layer V: -22.5%; $p < .05$), whereas kainateRs showed low (layer II: -24.5%; $p < .05$) to high (layer VI; 62.5%; $p < .05$) differences in densities for MWM_{CG} animals. In layer I and layer II, opposite changes were observed in noradrenergic receptors, as α_1Rs showed the highest changes here (layer I: +59.9%; $p < .05$; II: +55.7%; $p < .05$), while α_2Rs revealed almost no alterations. In layer III - VI, the same was observed in catecholaminergic receptors, except for α_2Rs that showed high (up to -25.4%; $p < .05$ in layer VI) and α_1Rs low (+15.4%; $p < .05$) differences (Supp. Tab. 29, Supp. Tab. 30) in the MWM_{CG}.

In the medial part (Figure 40), $mGlu_{2/3}$Rs (+116.2%; $p < .05$) and $GABA_B$Rs (+63.6%; $p < .05$) changed significantly in layer II. Layer V showed high differences in kainateRs (+35.4%; $p < .05$) and NMDARs (-36.6%; $p < .05$). Layer IV revealed low noticeable differences in α_1R density (+47.2%; $p < .05$) in cognitively trained animals (Supp. Tab. 29, Supp. Tab. 30).

Secondary olfactory cortex

In the orbitofrontal cortex (Figure 41), medially $mGlu_{2/3}$Rs (layer I: +127.1%; $p < .05$; II: +161.2%; $p < .05$) and $GABA_B$Rs (layer I: 91.3%; $p < .05$; II: 83.1%; $p < .05$) were altered in the superficial layers of cognitively trained animals. $GABA_{A(BZ)}$Rs differed in the deeper layers (layer V: +118.8%; $p < .05$; layer VI: +124.0%; $p < .05$), AMPARs (II/III: +23.0%; $p < .05$) and $GABA_A$Rs (II: +72.4%; $p < .05$; II/III: +92.6%; $p < .05$) in layer II, and II/III of MWM_{CG} animals. In the ventrolateral part of the orbitofrontal cortex, $mGlu_{2/3}$Rs (V: +147.2%; $p < .05$; VI: +131.5%; $p < .05$) showed low differences in layers V and VI, whereas kainateRs (V: -24.7%; $p < .05$) and $GABA_{A(BZ)}$Rs (V: +89.2%; $p < .05$; VI: +143.3%; $p < .05$) displayed significant differences similarly to the medial part. The lateral part revealed high differences in the receptor density of $mGlu_{2/3}$Rs (I: +154.5%; $p < .05$; VI: +163.3%; $p < .05$), $GABA_{A/B}$Rs (I: +31.4%; $p < .05$), and NMDARs (I: -52.5%; $p < .05$; VI: -50.1%; $p < .05$), in trained animals.

3.4.2 Impaired adult neurogenesis alters the olfactory receptor densities of trained animals

Mean neurotransmitter receptor densities (fmol/mg protein ± SEM) in all 14 investigated olfactory regions of the olfactory system of MWM_{CG} and MWM_{TMZ} are provided in Supp. Tab. 31. For statistical comparisons between these groups see Supp. Tab. 32. Each receptor type was tested with non-parametric Mann-Whitney-U test. Supp. Tab. 32 provides the percentage difference in absolute receptor concentrations, the *p*-value, and correlation coefficient *r*. The data showed a few differences in receptor concentration in MWM_{TMZ}. For example, the accessory olfactory bulb decreased in receptor concentrations of kainateRs and $mGlu_{2/3}$Rs, while densities for $GABA_B$Rs increased significantly. Receptor Fingerprints are provided in Figure 28 for every olfactory region and show the relative differences of the comparison in trained animals.

Glutamatergic receptors

There were no significant differences in AMPA receptor densities between MWM_{CG} and MWM_{TMZ} (Figure 28, Supp. Tab. 31, Supp. Tab. 32). KainateRs revealed a significant difference in the accessory olfactory bulb (-13.5%; $p < .05$; Figure 32), otherwise, there was no general difference for this receptor in the olfactory system of the MWM_{TMZ} group. For NMDARs, only the ventrolateral orbitofrontal cortex displayed a significant increase of receptor concentration (+32.3%; $p < .05$; Figure 41). Metabotropic $mGlu_{2/3}$R revealed two significant decreases in densities for the piriform cortex (-13.3%; $p < .05$; Figure 38) and the accessory olfactory bulb (-22.3%; $p < .05$; Figure 32;Figure 28; Supp. Tab. 31, Supp. Tab. 32) in MWM_{TMZ} animals.

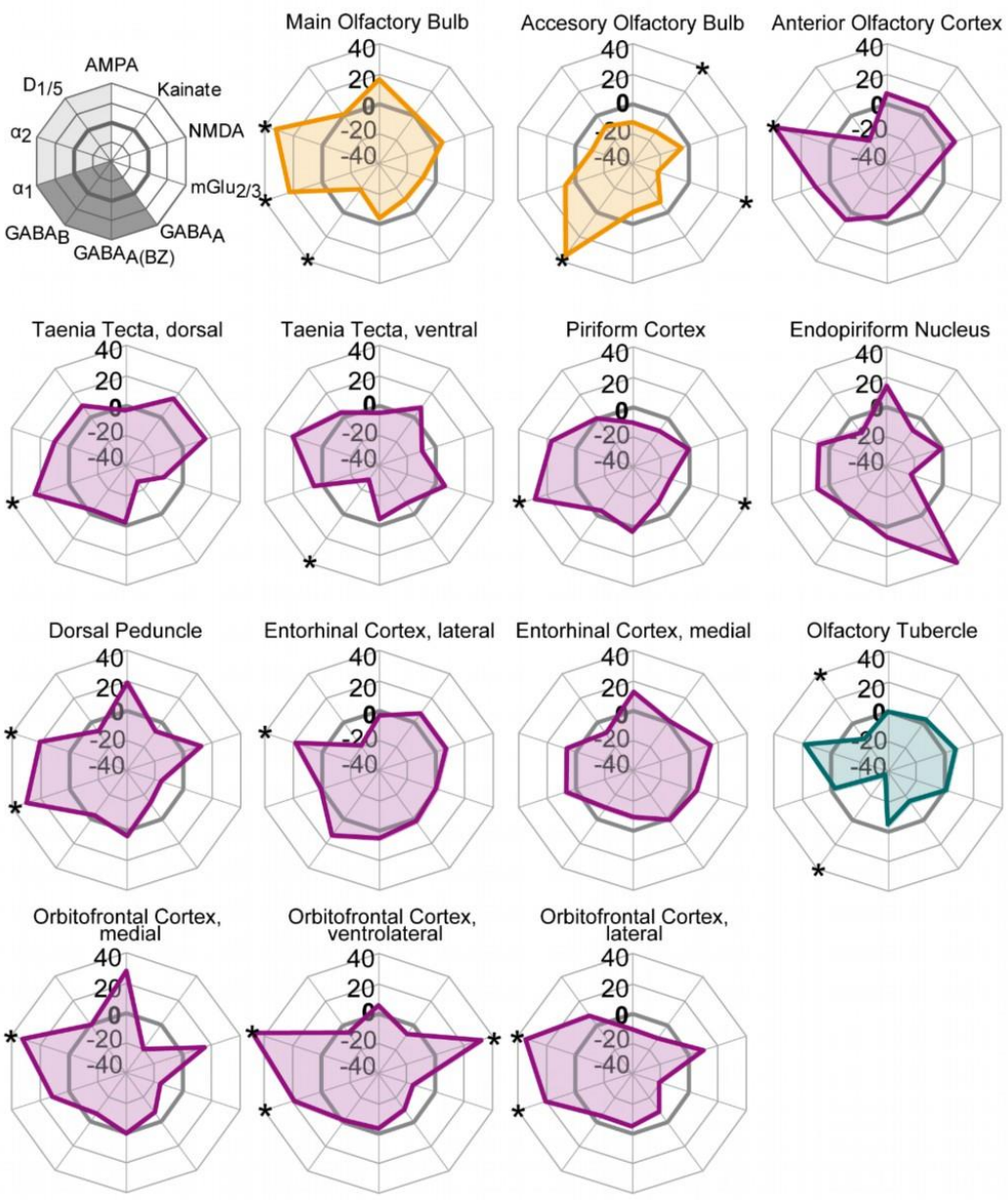

Figure 28: Receptor fingerprints of 14 olfactory regions

Relative differences of mean densities [%] of trained animals with active (MWM_{CG}) against trained animals with suppressed adult neurogenesis (MWM_{TMZ}). Colors are similar to the multidimensional 2D-scaling analysis. The positions of the receptors are shown schematically in the first row. Asterisks describe statistical significance (*p < .05, Supp. Tab. 32).

GABAergic receptors

There were no significant differences in receptor concentrations for $GABA_AR$s and $GABA_{A(BZ)}$Rs in the comparison of MWM_{CG} and MWM_{TMZ} (Figure 28, Supp. Tab. 31). However, the results were different for $GABA_BR$s: There were significant increases in receptor densities for the olfactory bulbs (main: -18.2%; $p < .05$; Figure 31; accessory: 35.6%; $p < .05$; Figure 32), the ventral taenia tecta (-27.8%; $p < .05$; Figure 35) and the olfactory tubercle (-37.1%; $p < .05$; Figure 36; Figure 28; Supp. Tab. 31, Supp. Tab. 32) in the MWM_{TMZ} group.

Catecholaminergic receptors

Upon examination of adult neurogenesis in trained animals, noradrenergic receptors showed an increase in their receptor densities in the TMZ-treated group (Figure 28). The agonist α_1R revealed significant increases in densities especially in the main olfactory bulb (+22.8%; $p < .05$; Figure 31), the dorsal taenia tecta (+23.4%; $p < .05$; Figure 34), the dorsal peduncular cortex (+30.6%; $p < .05$; Figure 37), the piriform cortex (+28.1%; $p < .05$; Figure 38) and the orbitofrontal cortex (ventrolateral: +19.0%; $p < .05$; lateral: +20.1%; $p < .05$; Figure 41). Also, the antagonist α_2R displayed significant increases in the main olfactory bulb (+32.5%; $p < .05$; Figure 31), the anterior olfactory cortex (+38.2%; $p < .05$; Figure 33), the dorsal peduncular cortex (+30.6%; $p < .05$; Figure 37), the lateral entorhinal cortex (+18.6%; $p < .05$; Figure 39), and the orbitofrontal cortex (Figure 41; lateral: +34.2%; $p < .05$; ventrolateral: +48.4%; $p < .05$; medial: +32.7%; $p < .05$; Figure 28; Supp. Tab. 31, Supp. Tab. 32) in MWM_{TMZ}.

The dopaminergic receptor $D_{1/5}$ decreased in receptor densities but showed one significant difference between MWM_{CG} and MWM_{TMZ} in the olfactory tubercle (-13.4%; $p < .05$; Figure 28; Figure 36; Supp. Tab. 31, Supp. Tab. 32).

3.4.2.1 Layer-specific alterations of the receptor architecture

Mean neurotransmitter receptor densities (fmol/mg protein ± SEM) in the layers of all 14 investigated olfactory regions of the olfactory system of MWM_{CG} and MWM_{TMZ} are provided in Supp. Tab. 33. For statistical comparisons between these groups see Supp. Tab. 34. Each receptor type was tested with non-parametric Mann-Whitney-U test. Supp. Tab. 34 provides the percentage difference in receptor concentrations, the *p*-value, and the sum of ranks W for the investigated layers and receptors. All receptors revealed differences in the layers of olfactory regions, without demonstrating a general effect.

Main and accessory olfactory bulb

Most of the analyzed receptors showed differences in the inner plexiform layer of the main olfactory bulb of MWM_{TMZ} animals (Figure 31): NMDA (+33.4%; $p < .05$), $mGlu_{2/3}$ (-16.1%; $p < .05$), $GABA_A$ (-20.6%; $p < .05$), $GABA_B$ (-16.4%; $p < .05$), α_1 (+25.8%; $p < .05$) and α_2 (+50.7%; $p < .05$). Simultaneously, the glomerular layer revealed differences for $GABA_ARs$ (-29.0%; $p < .05$), $GABA_BRs$ (-112.0%; $p < .05$), α_1Rs (+26.7%; $p < .05$) and α_2Rs (+32.0%; $p < .05$). In the accessory olfactory bulb (Figure 32), AMPARs (-28.1%; $p < .05$), $GABA_{A(BZ)}Rs$ (+22.4%; $p < .05$) and $GABA_BRs$ (-19.1%; $p < .05$) were altered in the mitral cell layer, while $mGlu_{2/3}Rs$ (-39.4%; $p < .05$) and $GABA_BRs$ (+86.3%; $p < .05$) revealed differences in the glomerular layer, due to suppression of adult neurogenesis in the trained animals (Supp. Tab. 33, Supp. Tab. 34).

Primary olfactory cortex

The anterior olfactory cortex (Figure 33) displayed alterations in the dorsal subregion for NMDARs (+21.4%; $p < .05$), $mGlu_{2/3}Rs$ (-26.7%; $p < .05$), $GABA_ARs$ (-28.3%; $p < .05$), $GABA_BRs$ (+16.0%; $p < .05$), α_1Rs (+17.2%; $p < .05$), and α_2Rs (+54.5%; $p < .05$). The posteroventral part showed differences for kainateRs (+20.1%; $p < .05$) and α_2Rs (+40.9%; $p < .05$), while the lateral subregion exhibited increases in receptor concentrations of NMDARs (+33.6%; $p < .05$) and $D_{1/5}Rs$ (-22.9%; $p < .05$; Supp. Tab. 33, Supp. Tab. 34).

While layer II of the dorsal taenia tecta (Figure 34) revealed alterations for α_1Rs (+27.9%; $p < .05$), layer IV showed differences for a_2Rs (+15.9%; $p < .05$) in MWM_{TMZ}. Differences for NMDARs (+35.5%; $p < .05$) and α_1Rs (+20.2%; $p < .05$) were prominent in layer III, whereas $GABA_BRs$ (-4.9%; $p < .05$) and α_1Rs (+24.9%; $p < .05$) were altered in layer I. The ventral taenia tecta (Figure 35) displayed concentration differences for AMPARs (-16.1%; $p < .05$) and $GABA_BRs$ (-34.7%; $p < .05$) in layer I and NMDARs in layer III (-16.7%; $p < .05$; Supp. Tab. 33, Supp. Tab. 34) in TMZ-treated

trained animals. In the olfactory tubercle (Figure 36), only $GABA_A$Rs (-24.4%; $p < .05$), $GABA_B$Rs (-40.9%; $p < .05$) and $D_{1/5}$Rs (-21.6%; $p < .05$) were decreased in layer I of MWM_{TMZ}. The dorsal peduncular cortex (Figure 37) revealed a few alterations in the investigated receptors. AMPARs (+24.0%; $p < .05$) and $mGlu_{2/3}$Rs (-17.3%; $p < .05$) differed in layer I, while layer V showed alterations for noradrenergic α_1Rs (+36.3%; $p < .05$) and α_2Rs (+26.4%; $p < .05$; Supp. Tab. 33, Supp. Tab. 34).

The piriform cortex (Figure 38) increased in density for α_1Rs in layer I (+30.5%; $p < .05$) and layer II (+35.0%; $p < .05$). Otherwise, glutamatergic $mGlu_{2/3}$Rs decreased in densities in layer II (-15.5%; $p < .05$) and layer III (-27.1%; $p < .05$). Also, AMPARs altered in layer II (-20.2%; $p < .05$) and kainateRs in layer I (-29.8%; $p < .05$; Supp. Tab. 33, Supp. Tab. 34) in TMZ-treated trained animals.

Only a few changes were observed in the lateral entorhinal cortex (Figure 39) of MWM_{TMZ}. In layer I, $D_{1/5}$Rs decreased upon suppression of adult neurogenesis in the trained animal (-25.5%; $p < .05$). Layer II showed a decrease for $D_{1/5}$Rs (-32.5%; $p < .05$) and an increase for $GABA_B$Rs (+23.8%; $p < .05$). The most alterations were increases of α_2Rs in layer III (+24.2%; $p < .05$), layer IV (+21.8%; $p < .05$) and layer V (+21.0%; $p < .05$). Eventually, AMPARs decreased in layer V (-22.2%; $p < .05$). In the medial entorhinal cortex (Figure 40), only $GABA_B$Rs (-15.8%; $p < .05$) revealed a decrease and α_2Rs an increase (+25.0%; $p < .05$) in receptor concentrations, due to the suppression of adult neurogenesis (Supp. Tab. 33, Supp. Tab. 34).

Secondary olfactory cortex

In the medial part of the orbitofrontal cortex (Figure 41) of MWM_{TMZ}, noradrenergic receptors revealed increases in receptor densities: α_1Rs in layer II/III (+14.5%; $p < .05$) and layer VI (+16.5%; $p < .05$), α_2Rs in layer II/III (+36.1%; $p < .05$), layer V (+33.5%; $p < .05$) and layer VI (+45.3%; $p < .05$). Glutamatergic receptors decreased in layer II (kainate: -24.0%; $p < .05$) and increased in layer V (NMDA: +20.7%; $p < .05$). The ventrolateral part showed significant alterations in layer I (NMDA: +30.7%; $p < .05$; α_1: +29.1%; $p < .05$; α_2: +35.7%; $p < .05$) and layer VI ($GABA_{A(BZ)}$: -15.8%; $p < .05$; α_1: +22.6%; $p < .05$; α_2: +24.4%; $p < .05$). Otherwise, NMDARs and α_2 were increased in layer II/III (NMDA: +20.8%; $p < .05$; α_2: +59.6%; $p < .05$) and layer V (NMDA: +37.4%; $p < .05$; α_2: +71.3%; $p < .05$; Supp. Tab. 33, Supp. Tab. 34) in MWM_{TMZ}.

The lateral subregion showed increased noradrenergic receptors in all layers: layer I (α_2: +27.7%; $p < .05$), layer II/III (α_1: +31.9%; $p < .05$; α_2: +37.4%; $p < .05$), layer V (α_1: +19.0%; $p < .05$; α_2: +42.8%; $p < .05$) and layer VI (α_1: +19.9%; $p < .05$; Supp. Tab. 33, Supp. Tab. 34).

3.4.3 Neurogenesis and training alter the olfactory receptor profiles

Mean neurotransmitter receptor densities (fmol/mg protein ± SEM) in all 14 investigated olfactory regions of the olfactory system of CG and MWM_{TMZ} are provided in Supp. Tab. 35. For statistical comparisons between these groups see Supp. Tab. 36. Each receptor type was tested with non-parametric Mann-Whitney-U test. Supp. Tab. 36 provides the percentage difference in absolute receptor concentrations, the *p*-value, and correlation coefficient *r*. The data showed multiple differences in receptor concentration in trained mice with suppressed adult neurogenesis. For example, $mGlu_{2/3}Rs$ increased significantly in every region except the accessory olfactory bulb. Also, GABAergic receptors increased significantly in most of the investigated areas. AMPARs, kainateRs and dopaminergic $D_{1/5}Rs$ decreased in concentrations for most of the investigated regions in MWM_{TMZ} animals.

Glutamatergic receptors

There were significant differences in AMPA receptor densities between CG and MWM_{TMZ} (Figure 29; Supp. Tab. 35, Supp. Tab. 36). The concentrations in the anterior olfactory cortex (+38.8%; $p < .05$; Figure 33), the ventral taenia tecta (-17.5%; $p < .05$; Figure 35), the piriform cortex (-16.0%; $p < .05$; Figure 38), the entorhinal cortex (medial: -24.4%; $p < .05$; Figure 40; lateral: -32.3%; $p < .05$; Figure 39) and the olfactory tubercle (-38.1%; $p < .05$; Figure 36) revealed a lower concentration of AMPARs in MWM_{TMZ} (Figure 29; Supp. Tab. 35, Supp. Tab. 36).

Except for three olfactory regions, the mean densities of kainate receptors in both groups were identical in most of the studied regions in MWM_{TMZ}. In MWM_{TMZ} the concentration was increased in the endopiriform nucleus (-22.3%; $p < .05$; Figure 38) and the medial orbitofrontal cortex (-14.4%; $p < .05$; Figure 41), while densities increased (+28.7%; $p < .05$; Figure 39) in the lateral entorhinal cortex (Figure 29; Supp. Tab. 35, Supp. Tab. 36) of MWM_{TMZ}.

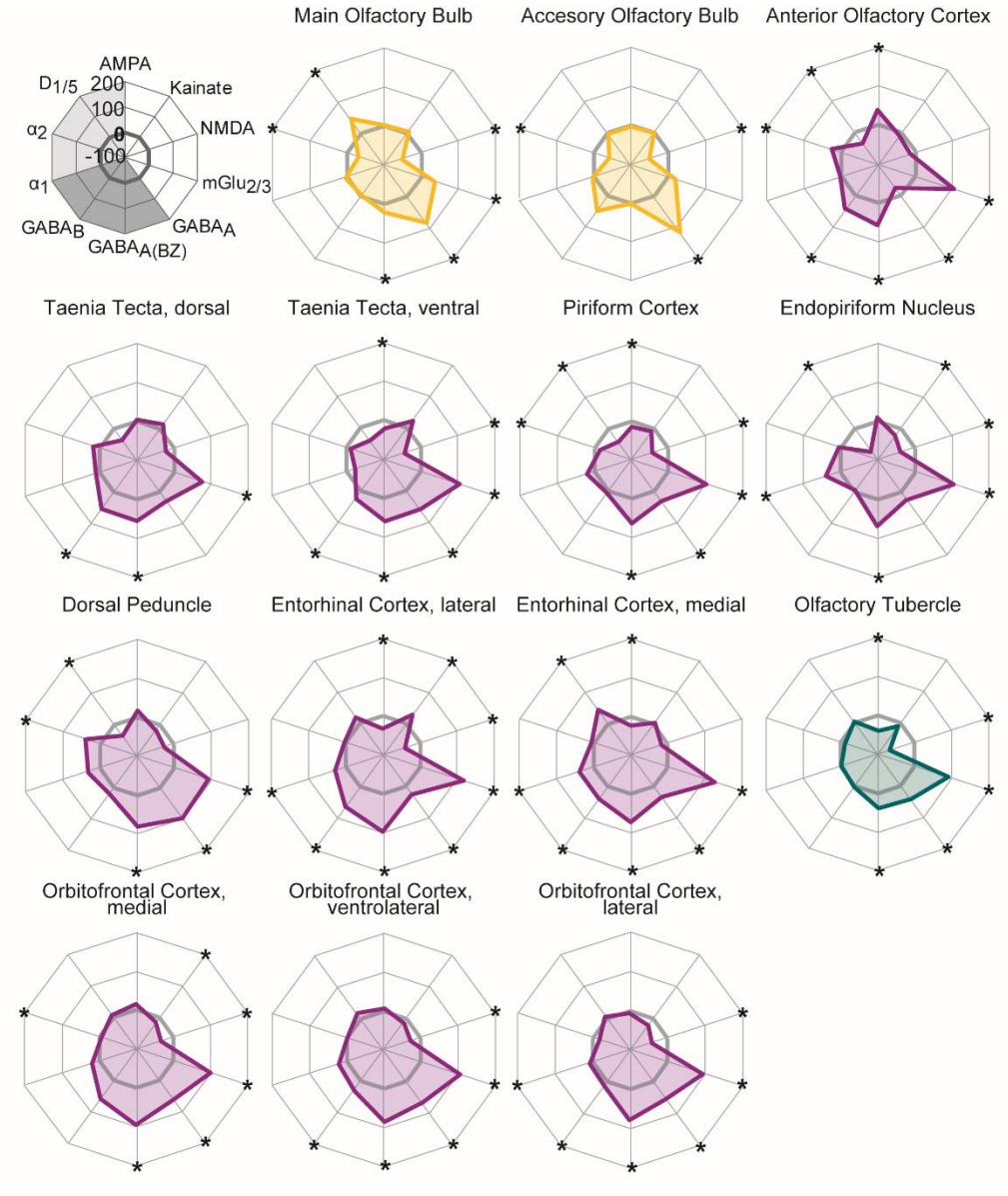

Figure 29: Receptor fingerprints of the 14 investigated olfactory regions

Relative differences of mean densities [%] of CG (control, active adult neurogenesis) and MWM$_{TMZ}$ (trained animals with suppressed adult neurogenesis). Colors are similar to the multidimensional 2D-scaling analysis. The positions of the receptors are shown schematically in the first row. Asterisks describe statistical significance (*p < .05, Supp. Tab. 36).

In MWM_{TMZ}, NMDA receptors were the only glutamate receptors with decreasing receptor densities (Figure 29Figure 39). The concentrations of NMDA receptors in brains of MWM_{TMZ} and CG were revealed to be significantly different: in the olfactory bulbs (main: -53.7%; $p < .05$; Figure 31; accessory: -50.5%; $p < .05$; Figure 32), the ventral taenia tecta (-47.0%; $p < .05$; Figure 35); the piriform cortex (-43.8%; $p < .05$; Figure 38); the endopiriform nucleus (-36.0%; $p < .05$; Figure 38), the lateral entorhinal cortex (-41.0%; $p < .05$; Figure 39), the olfactory tubercle (-67.7%; $p < .05$; Figure 36), and the orbitofrontal cortex (medial: -31.7%; $p < .05$; ventrolateral: -29.2%; $p < .05$; lateral: -41.5%; $p < .05$; Figure 41; Figure 29; Supp. Tab. 35, Supp. Tab. 36) of MWM_{TMZ}.

The mean densities of $mGlu_{2/3}Rs$ revealed increasing differences in MWM_{TMZ} compared to CG in all investigated regions except the accessory olfactory bulb (Figure 29). Statistical tests revealed the highest differences in receptor densities in the anterior olfactory cortex (+105.8%; $p < .05$; Figure 33), the endopiriform nucleus (+106.8%; $p < .05$; Figure 38) and the entorhinal cortex (lateral: +118.2%; $p < .05$; Figure 39; medial: +125.5%; $p < .05$; Figure 40; Figure 29; Supp. Tab. 35, Supp. Tab. 36).

GABAergic receptors

$GABA_A$ receptors differed significantly between the investigated brain regions. Significant increases were observed in the main olfactory bulb (+83.8%; $p < .05$; Figure 31), the accessory olfactory bulb (+114.2%; $p < .05$; Figure 32) and the dorsal peduncular cortex (+96.1%; $p < .05$; Figure 37) in the brains of MWM_{TMZ} (Figure 29; Supp. Tab. 35, Supp. Tab. 36).

In all studied regions, BZ-binding sites demonstrated increasing concentrations in MWM_{TMZ} animals, except for the accessory olfactory bulb (Figure 29). The highest differences were observed in the dorsal peduncular cortex (+81.0%; $p < .05$; Figure 37), the lateral entorhinal cortex (+97.1%; $p < .05$; Figure 39), and the orbitofrontal cortex (medial: +95.6%; $p < .05$; ventrolateral: +84.9%; $p < .05$; Figure 41; Figure 29; Supp. Tab. 35, Supp. Tab. 36).

$GABA_B$ receptor densities increased in most regions after adult neurogenesis was suppressed. The high concentration in the anterior olfactory cortex (+42.5%; $p < .05$; Figure 33), the dorsal taenia tecta (+54.0%; $p < .05$; Figure 34), the lateral entorhinal cortex (+65.5%; $p < .05$; Figure 39) and the medial orbitofrontal cortex (+56.8%; $p < .05$; Figure 41) was significant (Figure 29; Supp. Tab. 35, Supp. Tab. 36) in MWM_{TMZ}.

Catecholaminergic receptors

Low changes in noradrenergic receptors were found between CG and MWM_{TMZ} animals (Figure 29). The agonist α_1R revealed decreased concentrations primarily in the endopiriform nucleus (+35.9%; $p < .05$; Figure 38), the entorhinal cortex (medial: +39.0%; $p < .05$; Figure 40; lateral: +30.2%; $p < .05$; Figure 39), and the medial orbitofrontal cortex (+19.7%; $p < .05$; Figure 41). The antagonist α_2R demonstrated a significant increase in receptor concentration in the MWM_{TMZ} group in the olfactory bulbs (main: -29.4%; $p < .05$; Figure 31; accessory: -41.9%; $p < .05$; Figure 32), the anterior olfactory cortex (+24.5%; $p < .05$; Figure 33), the piriform cortex (-16.7%; $p < .05$; Figure 38), the dorsal peduncular cortex (+40.3%; $p < .05$; Figure 37) and the lateral orbitofrontal cortex (-18.3%; $p < .05$; Figure 41; Figure 29; Supp. Tab. 35, Supp. Tab. 36) in MWM_{TMZ}.

The olfactory regions of the MWM_{TMZ} animals revealed a heterogenous picture: while the main olfactory bulb (+46.7%; $p < .05$; Figure 31) and the medial entorhinal cortex (+43.8%; $p < .05$; Figure 40) revealed increasing concentrations, the endopiriform nucleus (-74.6%; $p < .05$; Figure 38) and piriform cortex (-43.2%; $p < .05$; Figure 38) exhibited decreasing receptor densities in brains of MWM_{TMZ} (Figure 29; Supp. Tab. 35, Supp. Tab. 36).

3.4.3.1 Layer-specific alterations of the receptor architecture

Mean neurotransmitter receptor densities (fmol/mg protein ± SEM) in the layers of all 14 investigated olfactory regions of the olfactory system of CG and MWM_{TMZ} are provided in Supp. Tab. 37. For statistical comparisons between these groups see Supp. Tab. 38. Each receptor type was tested with non-parametric Mann-Whitney-U test. Supp. Tab. 38 provides the percentage difference in receptor concentrations, the p-value, and the Z-value for the investigated layers and receptors. All receptors revealed differences in the layers of olfactory regions, without demonstrating a general effect. For example, AMPARs showed increasing concentrations in the anterior olfactory cortex of MWM_{TMZ} while the densities decreased in the layers of the other analyzed regions.

Main and accessory olfactory bulb

The most severe changes were found in the glomerular layer in both bulbs (Figure 31; Figure 32) in the group comparison of GC versus MWM_{TMZ}. GABAergic $GABA_A$ (main: +87.5%; $p < .05$; accessory: +310.2%; $p < .05$), $GABA_{A(BZ)}$ (main: +50.0%; $p < .05$; 125.0%; $p < .05$), $GABA_B$ (main: +71.4%; $p < .05$; accessory: +121.1%; $p < .05$) receptors as well as NMDARs (main: -65.6%; $p < .05$; accessory: -60.8%; $p < .05$) and $mGlu_{2/3}Rs$ (main: +21.5%; $p < .05$; accessory: +96.7%; $p < .05$) revealed high differences in the trained animal with suppressed adult neurogenesis. However, whereas NMDARs decreased, the other receptors increased in concentration. The mitral and granule layers also demonstrated significant alterations, significantly $GABA_{A(BZ)}Rs$ in the main (mitral: +147.4%; $p < .05$; granule: +71.5%; $p < .05$) and accessory olfactory bulb (mitral: +115.1%; $p < .05$; granule: -85.8%; $p < .05$). $GABA_ARs$ showed little change in the mitral layer of the accessory olfactory bulb, although the increase in receptor densities in the other two layers was high (Supp. Tab. 37, Supp. Tab. 38).

Primary olfactory cortex

The lateral anterior olfactory cortex (Figure 33) showed differences in α_1Rs (-8.3%; $p < .05$) in MWM_{TMZ}. In contrast, AMPARs were increased in the dorsal (+36.0%; $p < .05$) and posteroventral (+55.1%; $p < .05$) regions in the trained animal, as well as in the pars externa (+35.3%; $p < .05$). Here and in the lateral part, α_2Rs (+28.4%; $p < .05$) were significantly higher in the trained animal. NMDARs in the lateral part revealed a significant decrease in receptor density in the trained animal (-33.4%; $p < .05$), whereas they increased in the posteroventral part (+24.8%; $p < .05$; Supp. Tab. 37, Supp. Tab. 38) of MWM_{TMZ}.

The dorsal peduncular cortex (Figure 37) revealed huge differences among its layers. While layer I showed a decrease in AMPARs (+23.2%; $p < .05$) in the trained animal, the receptor increased in layer V (+57.3%; $p < .05$). The pattern was opposite for α_2Rs, that were increased in MWM_{TMZ} in the other three layers (II/III: +52.6%; $p < .05$; V: +63.3%; $p < .05$; VI: +71.5%; $p < .05$; Supp. Tab. 37, Supp. Tab. 38).

In the taenia tecta (dorsal: Figure 34; ventral: Figure 35), α_1Rs showed no difference in the layers of both parts. The strongest changes were seen in NMDARs, that showed a significant decrease in receptor density in layer I (-49.7%; $p < .05$) and layer II (-26.6%; $p < .05$) of the dorsal taenia tecta and in all layers of the ventral part (I: -71.0%; $p < .05$; II: -40.3%; $p < .05$; III: -32.4%; $p < .05$). Layer III of both parts increased in kainateRs (dorsal: +41.6%; $p < .05$; ventral: +34.2%; $p < .05$). In layer IV, the decrease in $D_{1/5}$Rs in the trained animal was significant (-53.4%; $p < .05$), whereas $GABA_A$Rs increased here (+42.7%; $p < .05$) and in layer I (+57.3%; $p < .05$) of the ventral part (Supp. Tab. 37, Supp. Tab. 38).

The piriform cortex (Figure 38) displayed a decrease in NMDAR densities in all three layers (I: -55.1%; $p < .05$; II: -39.8%; $p < .05$; III: -38.9%; $p < .05$). AMPARs changed inconsistently in MWM_{TMZ}, as the receptor decreased in layer II (-42.7%; $p < .05$) but increased in layer III (+31.1%; $p < .05$). $D_{1/5}$Rs also showed different changes, as the receptor hardly changed in layer I but decreased significantly in layer III (-55.8%; $p < .05$; Supp. Tab. 37, Supp. Tab. 38).

In the medial entorhinal cortex (Figure 40) in MWM_{TMZ}, AMPARs decreased in layer I (-55.7%; $p < .05$), II (-26.0%; $p < .05$), and VI (-25.8%; $p < .05$). NMDARs also decreased, but in layer II (-30.8%; $p < .05$), III (-17.2%; $p < .05$), and V (-29.3%; $p < .05$). KainateR decreased in layer III (-18.2%; $p < .05$) and increased in layer V (+34.6%; $p < .05$), and VI (+39.1%; $p < .05$) but showed little alteration in layer II. In the lateral part (Figure 39), NMDARs (layer II: -41.3%; $p < .05$) and AMPARs (layer I: -44.1%; $p < .05$) decreased simultaneously in the superficial layers, whereas $GABA_{A(BZ)}$Rs (layer III: +96.6%; $p < .05$) and $GABA_A$ (layer V: +29.1%; $p < .05$) increased in MWM_{TMZ}. In contrast,

layer VI revealed no change in AMPARs but an increase in KainateRs (+67.5%; $p < .05$) in MWM_{TMZ} (Supp. Tab. 37, Supp. Tab. 38).

In the olfactory tubercle (Figure 36), all layers revealed decreases in the receptor densities of AMPARs (layer I: -34.3%; $p < .05$; II: -40.7%; $p < .05$; III: -37.1%; $p < .05$) and NMDARs (layer I: -79.8%; $p < .05$; II: -64.2%; $p < .05$; -59.4%; $p < .05$) in MWM_{TMZ}. KainateRs decreased in layer I (-51.9%; $p < .05$) in the trained animal. Layer III exhibited increases in $mGlu_{2/3}Rs$ (+88.7%; $p < .05$), $GABA_A$ (+49.2%; $p < .05$), and $GABA_{A(BZ)}Rs$ (+73.8%; $p < .05$; Supp. Tab. 37, Supp. Tab. 38).

Secondary olfactory cortex

In the orbitofrontal cortex of MWM_{TMZ} (Figure 41), the medial part showed a decrease of NMDARs in layer I (-60.0%; $p < .05$), II (-36.0%; $p < .05$), and VI (-32.3%; $p < .05$). Catecholaminergic receptors remained almost unchanged in all layers. Whereas layer I showed little alteration in AMPARs and kainateRs, AMPARs increased in layer II/III (+28.6%; $p < .05$) while kainateRs decreased in layer V (-30.7%; $p < .05$) simultaneously. Similar shifts were seen in the ventrolateral part. Catecholaminergic receptors showed no change, whereas NMDARs decreased significantly (layer I: -41.8%; $p < .05$). KainateRs were reduced in density only in the deeper layers (layer V: -42.7%; $p < .05$), whereas they showed no alterations in the superficial layers. $GABA_BRs$ revealed a significant increase in layer I (+74.9%; $p < .05$), as well as in the lateral part (+47.0%; $p < .05$). Here, $GABA_ARs$ also increased sharply (+74.7%; $p < .05$), but minor with increasing layer depth (layer VI: +30.1%; $p < .05$). KainateRs exhibited a decrease in layer II/III (-32.0%; $p < .05$) and layer V (-36.1%; $p < .05$) in MWM_{TMZ}. Notably, α_1Rs only differed in the lateral orbitofrontal cortex with a stronger decrease in layer I (-15.0%; $p < .05$) to layer VI (-24.6%; $p < .05$; Supp. Tab. 37, Supp. Tab. 38).

3.4.4 Training revealed alterations in animals with suppressed neurogenesis

Mean neurotransmitter receptor densities (fmol/mg protein ± SEM) in all 14 investigated olfactory regions of the olfactory system of CG_{TMZ} and MWM_{TMZ} are provided in Supp. Tab. 39. For statistical comparisons between these groups see Supp. Tab. 40. Each receptor type was tested with non-parametric Mann-Whitney-U test. Supp. Tab. 40 provides the percentage difference in absolute receptor concentrations, the *p*-value, and correlation coefficient *r*. The data showed multiple differences in receptor concentration in MWM_{TMZ} without a general effect.

Glutamatergic receptors

There were significant differences in glutamate receptor densities between CG_{TMZ} and MWM_{TMZ} (Figure 30, Supp. Tab. 39, Supp. Tab. 40).

Trained animals exhibited a high concentration of AMPA receptor in the anterior olfactory cortex (+53.4%; $p < .05$; Figure 33) and dorsal peduncular cortex (+23.8%; $p < .05$; Figure 37) with suppressed adult neurogenesis compared to untrained animals with suppressed adult neurogenesis. Receptor decreases were higher in MWM_{TMZ}, for example in the olfactory tubercle (-34.0%; $p < .05$; Figure 36), and lateral entorhinal cortex (-33.8%; $p < .05$; Figure 39). KainateRs showed higher densities in the lateral entorhinal cortex (+21%, $p < .05$; Figure 39) in the trained animal, while there were decreased densities in the accessory olfactory bulb (-32.8%; $p < .05$; Figure 32), the anterior olfactory cortex (-15.4%, $p < .05$; Figure 33), the endopiriform nucleus (-22.5%, $p < .05$; Figure 38), and olfactory tubercle (-30.0%, $p < .05$; Figure 36). The densities of NMDARs were significantly lower in MWM_{TMZ} than in CG_{TMZ}, for example, in the main olfactory bulb (-32.6%, $p < .05$; Figure 31), the olfactory tubercle (-59.7%, $p < .05$; Figure 36), the piriform cortex (-26.3%, $p < .05$; Figure 38), the medial (-12.5%, $p < .05$), and ventrolateral (-13.7.%, $p < .05$; Figure 41) orbitofrontal cortex. $mGlu_{2/3}Rs$ revealed contrary density changes, as there were high receptor densities in MWM_{TMZ}, especially in the anterior olfactory cortex (+91.4%, $p < .05$; Figure 33), the endopiriform nucleus (+101.9%, $p < .05$; Figure 38), the dorsal peduncular cortex (+105.1%, $p < .05$; Figure 37), the piriform cortex (+116.4%, $p < .05$; Figure 38), and lateral orbitofrontal cortex (+102.97%, $p < .05$; Figure 30; Figure 41; Supp. Tab. 39, Supp. Tab. 40).

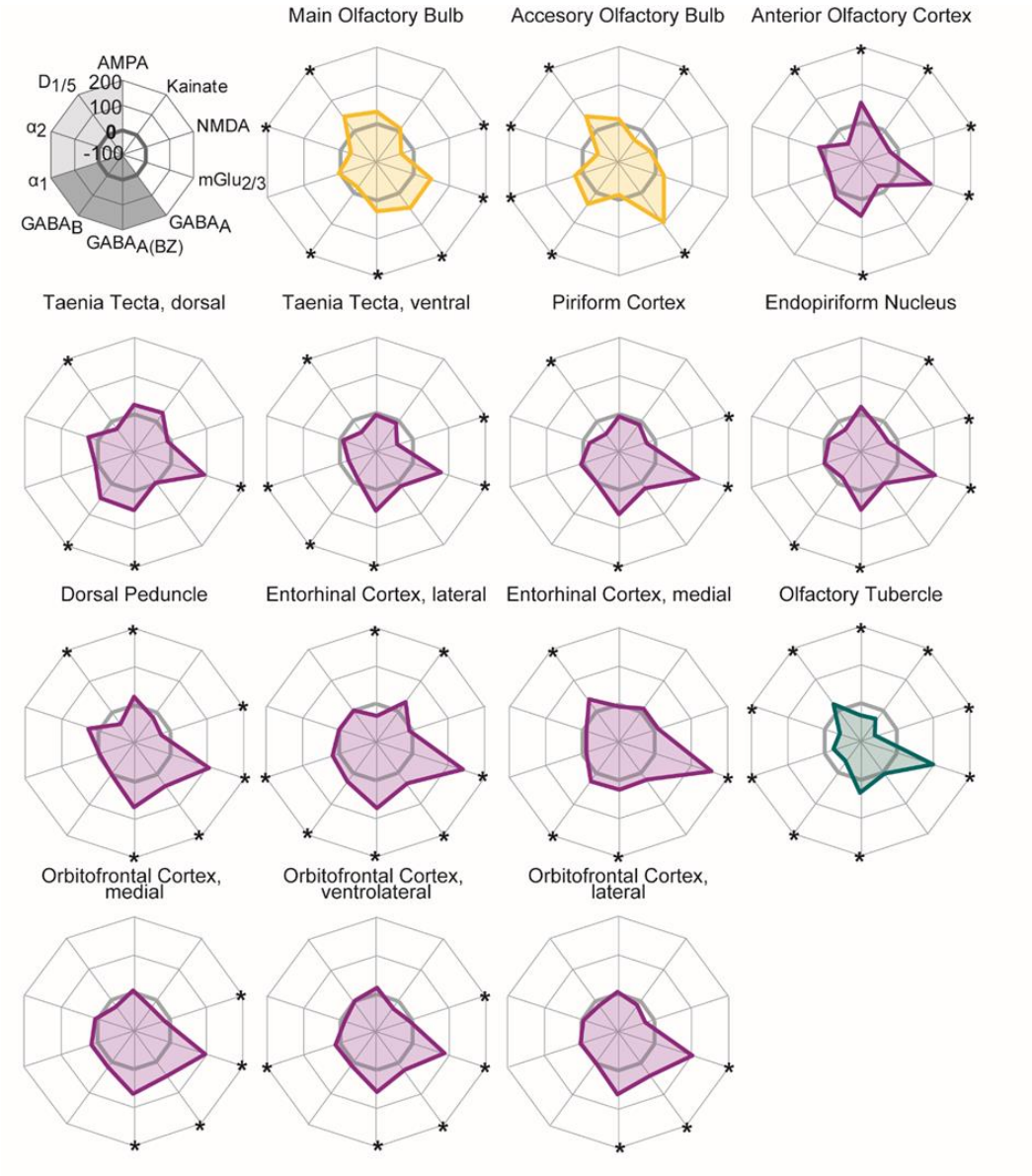

Figure 30 Receptor fingerprints of the 14 investigated olfactory regions

Relative differences of mean densities [%] of CG_{TMZ} and MWM_{TMZ}. Colors are similar to the multidimensional 2D-scaling analysis. The positions of the receptors are shown schematically in the first row. Asterisks describe statistical significance (*p < .05, Supp. Tab. 40).

GABAergic receptors

GABAergic receptors were present in higher concentration in MWM_{TMZ} than in CG_{TMZ}. For example, $GABA_A$Rs in the main olfactory bulb (+51.3%, $p < .05$; Figure 31), the accessory olfactory bulb (+98.4%, $p < .05$; Figure 32), the dorsal peduncular cortex (+37.8%, $p < .05$; Figure 37), and the orbitofrontal cortex (lateral: +43.2%, $p < .05$; ventrolateral: +46.9%, $p < .05$; medial: +22.6%, $p < .05$; Figure 41) were significantly high in the trained animals than in the untrained group. Nearly the same showed BZ-binding sites: $GABA_{A(BZ)}$Rs revealed significantly high concentrations in MWM_{TMZ} in the anterior olfactory cortex (+42.5%, $p < .05$; Figure 33), the taenia tecta (dorsal: +37.3%, $p < .05$; Figure 34; ventral: +55.0%, $p < .05$; Figure 35), the dorsal peduncular cortex (+65.5%, $p < .05$; Figure 37), the entorhinal cortex (lateral: +72.9%, $p < .05$; Figure 39; medial: +25.2%, $p < .05$; Figure 40) and the ventrolateral orbitofrontal cortex (+63.8%, $p < .001$; Figure 41; Figure 30; Supp. Tab. 39, Supp. Tab. 40).

$GABA_B$Rs were also significantly increased in the taenia tecta (dorsal: +33.0%, $p < .05$; Figure 34; ventral: -17.6%, $p < .05$; Figure 35), the olfactory tubercle (-33.4%, $p < .05$; Figure 36), and the entorhinal cortex (medial: +26.5%, $p < .05$; Figure 40; lateral: +27.9%, $p < .05$; Figure 39; Figure 30; Supp. Tab. 39, Supp. Tab. 40).

Catecholaminergic receptors

Noradrenergic receptors showed low receptor concentrations in MWM_{TMZ}. α_1Rs, for example, were significantly increased in the accessory olfactory bulb (+20.3%, $p < .05$; Figure 32) and the ventral taenia tecta (-25.1%, $p < .05$; Figure 35). In the lateral entorhinal cortex, there was an increase in density (+19.2%, $p < .05$; Figure 39). α_2Rs were particularly decreased in the main olfactory bulb (-28.9%, $p < .05$; Figure 31), the accessory olfactory bulb (-40.5%, $p < .05$; Figure 32), and the olfactory tubercle (-43.8%, $p < .05$; Figure 36) of the MWM_{TMZ} group (Figure 30; Supp. Tab. 39, Supp. Tab. 40).

Dopaminergic $D_{1/5}$Rs revealed a mixed picture: concentrations increased in the main olfactory bulb (+43.7%, $p < .05$; Figure 31), the olfactory tubercle (+17.1%, $p < .05$; Figure 36) and the medial entorhinal cortex (+34.7%, $p < .05$; Figure 40), while they decreased in the taenia tecta (dorsal: -33.0%, $p < .05$; Figure 34; ventral: -38.0%, $p < .05$; Figure 35), the dorsal peduncular cortex (-36.3%, $p < .05$; Figure 37) and the piriform cortex (-41.2%, $p < .05$; Figure 38; Figure 30; Supp. Tab. 39, Supp. Tab. 40).

3.4.4.1 Layer-specific alterations of the receptor architecture

Mean neurotransmitter receptor densities (fmol/mg protein ± SEM) in the layers of all 14 investigated olfactory regions of the olfactory system of CG_{TMZ} and MWM_{TMZ} are provided in Supp. Tab. 41. For statistical comparisons between these groups see Supp. Tab. 42. Each receptor type was tested with non-parametric Mann-Whitney-U test. Supp. Tab. 42 provides the percentage difference in receptor concentrations, the *p*-value, and the Z-value for the investigated layers and receptors. All receptors revealed differences in the layers of olfactory regions, without demonstrating a general effect.

Main and accessory olfactory bulb

In the main olfactory bulb of MWM_{TMZ} (Figure 31), the outer plexiform layer showed significant differences in $mGlu_{2/3}Rs$ (-42.1%; $p < .05$) whereas the glomerular layer revealed high changes in receptor concentration in GABAergic receptors ($GABA_A$: -34.0%; $p < .05$; $GABA_{A(BZ)}$: -29.2%; $p < .05$; $GABA_B$: -46.7%; $p < .05$; Figure 31). Minor differences were observed in both groups in the olfactory nerve layer of the main olfactory bulb for $mGlu_{2/3}Rs$, $GABA_ARs$, and $GABA_{A(BZ)}Rs$ (Supp. Tab. 41, Supp. Tab. 42).

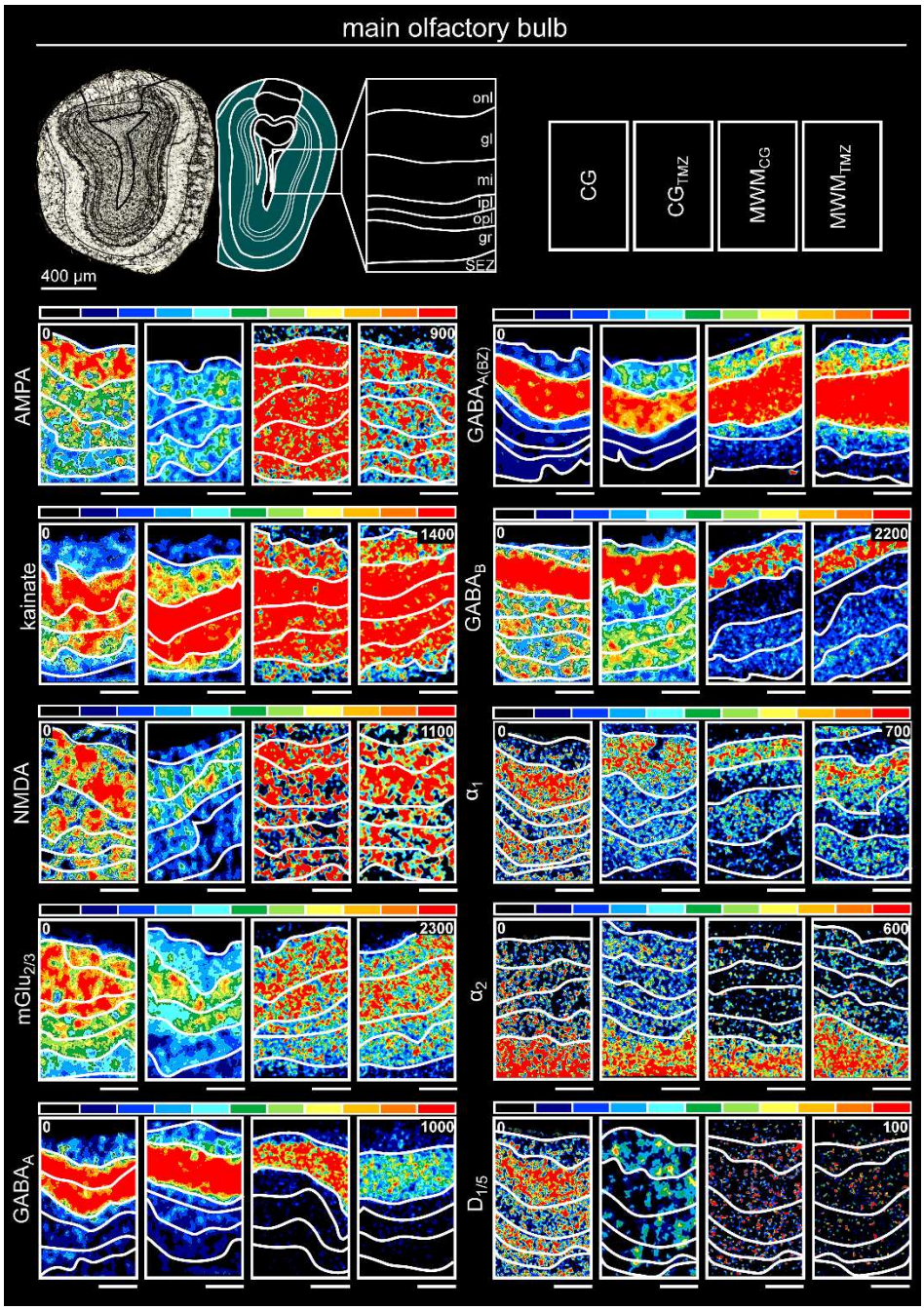

Figure 31: Color-coded layer-specific autoradiographs of the main olfactory bulb

The receptor densities of all investigated receptors in the main olfactory bulb represented in color-coded autoradiographs [in fmol/mg protein]. Color scale: Red represents the exemplary optimized representation, not the maximum receptor density of the region, while black indicates the absence of receptor expression. All results of the four groups are shown: Control (left), mice with suppressed adult neurogenesis (CG_{TMZ}, second column from left), trained mice (MWM_{CG}, third column from left), and trained mice with suppressed adult neurogenesis (MWM_{TMZ}, right). Nissl-stained section with corresponding scheme in the upper left. The layers of the region are represented next to the scheme. Scale bars: A-J, Coronal slice: 1.3 mm; color coded sections: 400 µm; onl, olfactory nerve layer; gl, glomerular layer; mi, mitral layer; ipl, inner plexiform layer; opl, outer plexiform layer; gr, granular layer; SEZ subependymal zone.

High differences were observed in the glomerular layer of the accessory olfactory bulb of MWM_{TMZ}, significantly in kainateRs (Figure 32; +137.6%; $p < .05$) and $GABA_BRs$ (-63.0%; $p < .05$; Figure 32). The mitral cell layer of the accessory olfactory bulb displayed differences in $mGlu_{2/3}Rs$ (-40.6%; $p < .05$) and $GABA_{A(BZ)}Rs$ (-36.8%; $p < .05$; Supp. Tab. 41, Supp. Tab. 42) in MWM_{TMZ}.

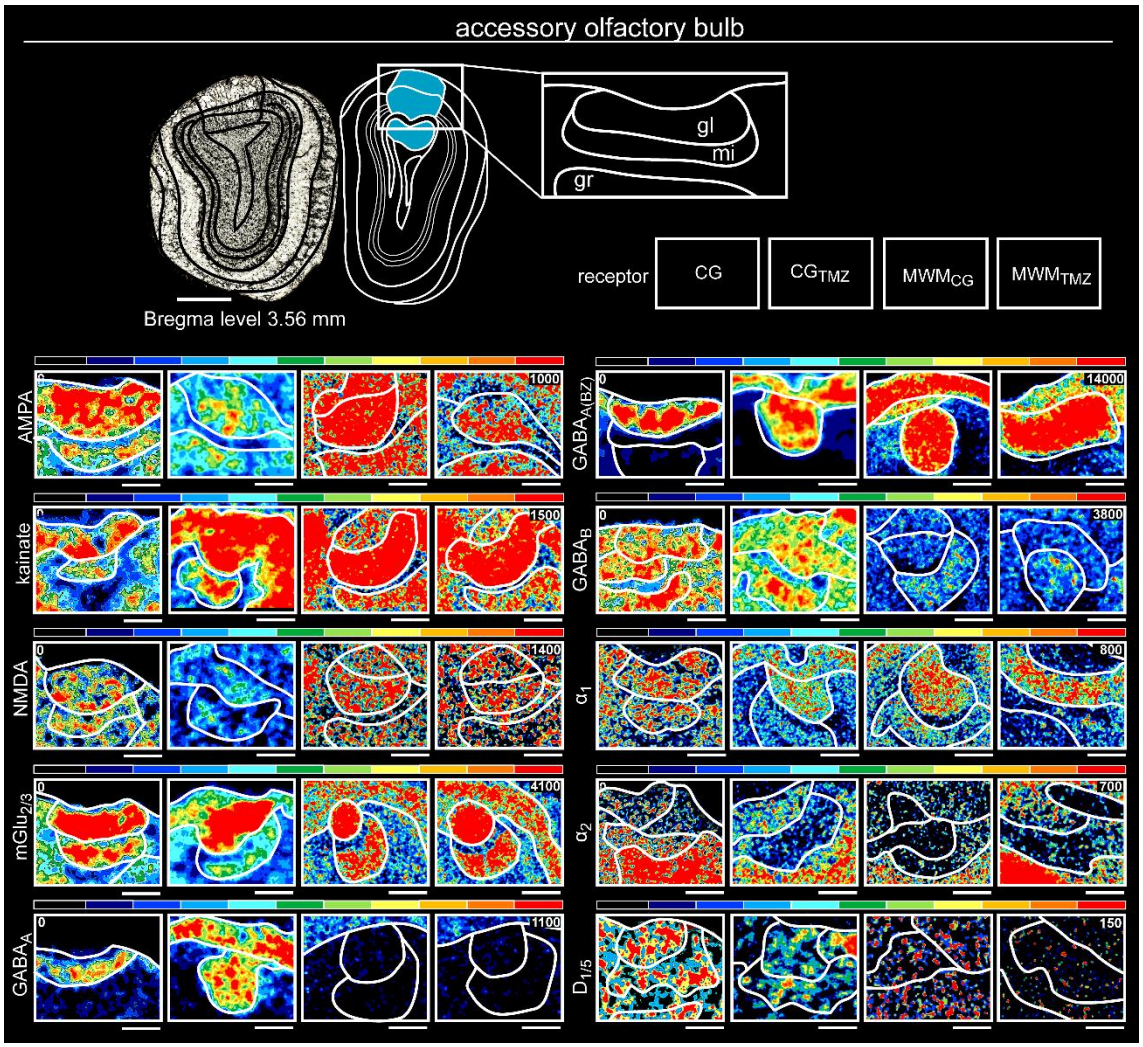

Figure 32: Color-coded layer-specific autoradiographs of the accessory olfactory bulb

The receptor distribution of all investigated receptors in the accessory olfactory bulb represented in color-coded autoradiographs [in fmol/mg protein]. Figure structure according to Figure 31. Scale bars: Coronal slice: 1.3 mm; Magnifications: 400 µm; gl, glomerular layer; mi, mitral layer; gr, granular layer.

Primary olfactory cortex

In the anterior olfactory cortex of MWM_{TMZ} (Figure 33), significant changes were seen in the lateral and posteroventral subregions. In the lateral part, $mGlu_{2/3}$Rs and $GABA_{A(BZ)}$Rs (-44.1%; $p < .05$) were altered, otherwise only little changes in α_1Rs (+23.3%; $p < .05$), and $D_{1/5}$Rs (+18.5%; $p < .05$) were observed. In the posteroventral part, AMPARs (-40.7%; $p < .05$), NMDARs (+45.7%; $p < .05$), and $GABA_B$Rs (-10.5%; $p < .05$) showed significant differences. In the pars externa, AMPARs (-49.5%; $p < .05$), $mGlu_{2/3}$Rs (-42.7%; $p < .05$), $GABA_{A(BZ)}$Rs (-39.4%; $p < .05$) and $GABA_B$Rs (-18.3%; $p < .05$) showed high decreases (+41.9%; $p < .05$; Supp. Tab. 41, Supp. Tab. 42), except for NMDARs.

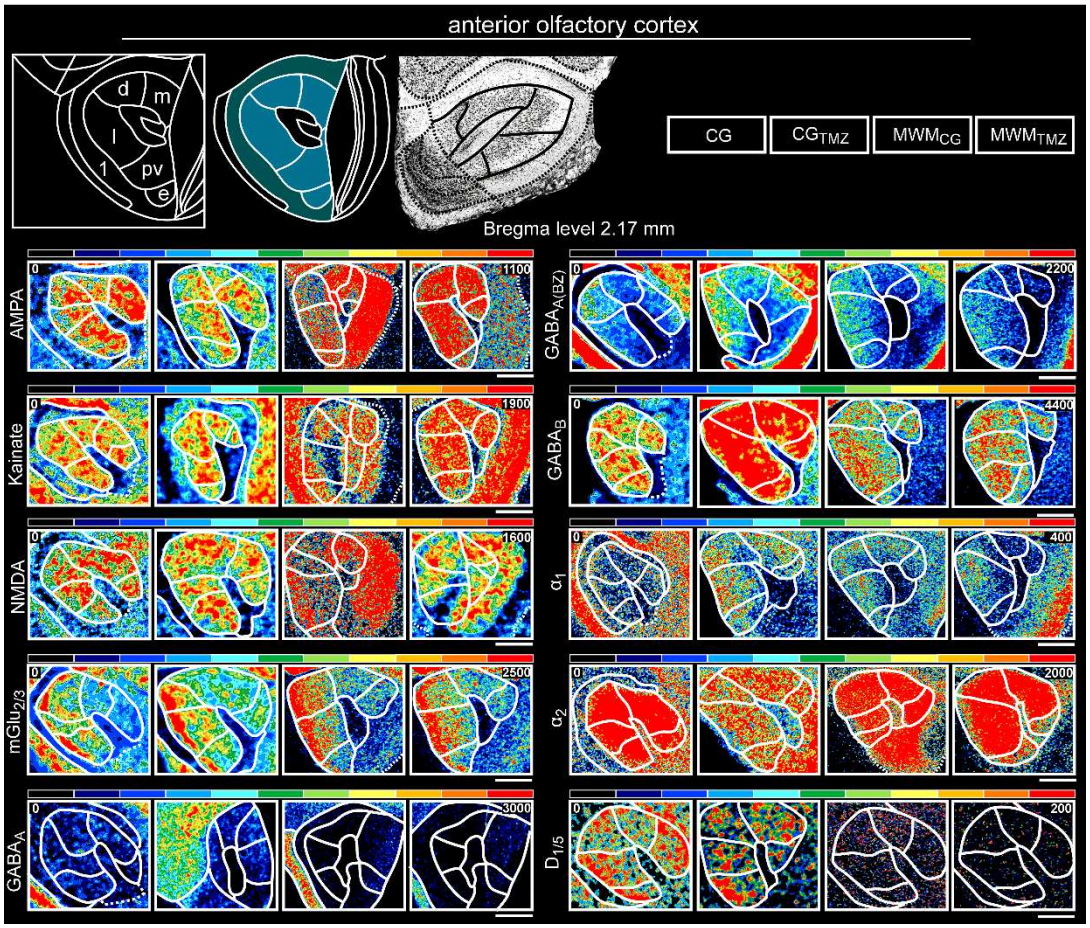

Figure 33: Color-coded layer-specific autoradiographs of the anterior olfactory cortex

The receptor distribution of all investigated receptors in the anterior olfactory cortex represented in color-coded autoradiographs [in fmol/mg protein]. Figure structure according to Figure 31. Scale bars: Nissl-Image, 800 µm; A-J, 600 µm; K-T, 200 µm; m, medial; d, dorsal; l, lateral; pv, posteroventral; 1, pars externa.

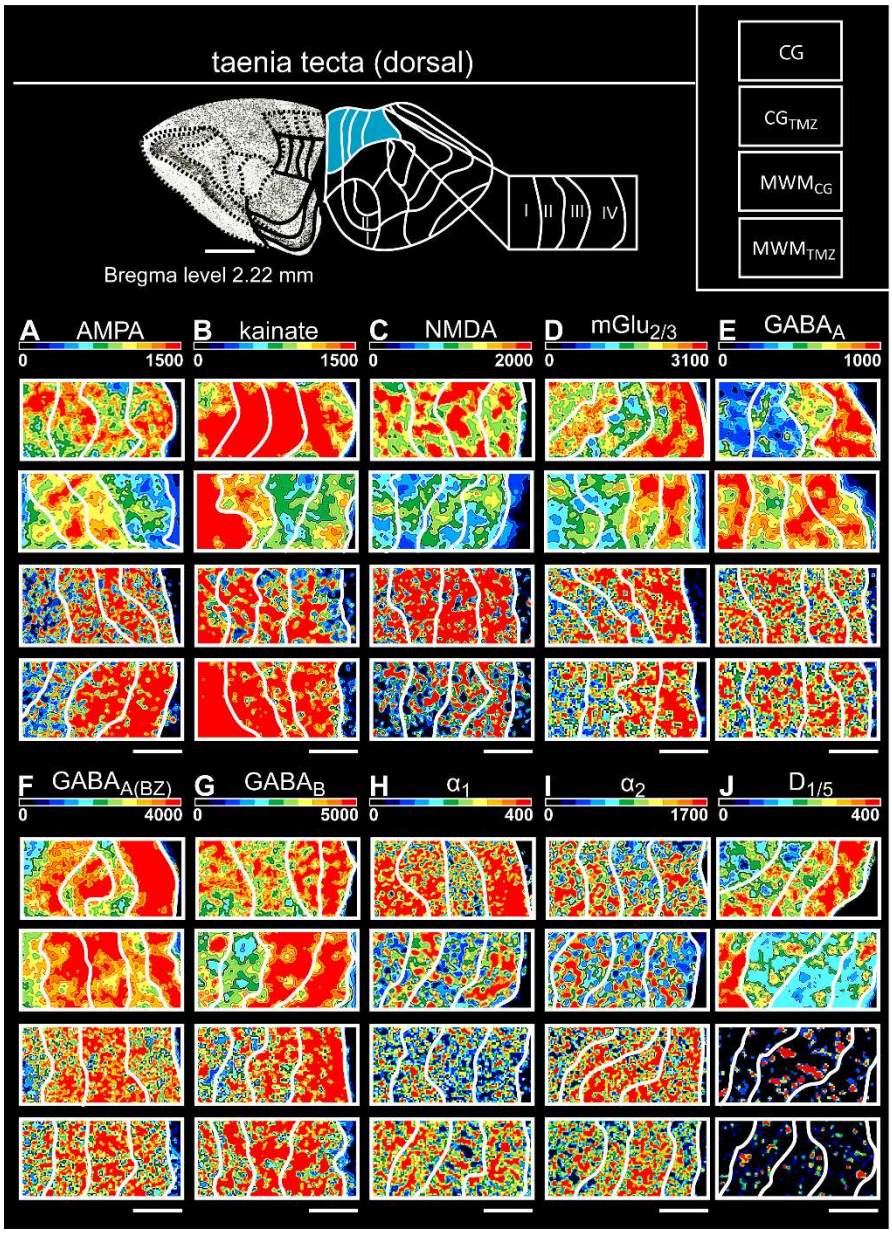

Figure 34: Color-coded layer-specific autoradiographs of the taenia tecta (dorsal)

The receptor distribution of all investigated receptors in the dorsal taenia tecta represented in color-coded autoradiographs [in fmol/mg protein]. Figure structure according to Figure 31. Scale bars: Nissl-Image, 1 mm; A-J, 400 µm.

The dorsal part of taenia tecta (Figure 34) increased in concentrations of NMDARs (+66.3%; $p < .05$) and decreasing densities of $mGlu_{2/3}$Rs (-33.0%; $p < .05$), $GABA_{A(BZ)}$Rs (-20.6%; $p < .05$), and $GABA_B$Rs (-19.2%; $p < .05$) in layer I of MWM_{TMZ}. The same receptors also decreased in layer II ($mGlu_{2/3}$Rs: -49.7%; $p < .05$; $GABA_{A(BZ)}$Rs: -26.7%; $p < .05$; $GABA_B$Rs: -20.6%; $p < .05$), layer III ($mGlu_{2/3}$Rs: -49.0%; $p < .05$; $GABA_{A(BZ)}$Rs: -27.4%; $p < .05$; $GABA_B$Rs: -38.6%; $p < .05$), and layer IV ($mGlu_{2/3}$Rs: -43.1%; $p < .05$; $GABA_{A(BZ)}$Rs: -30.2%; $p < .05$; $GABA_B$Rs: -25.1%; $p < .05$), where also α_2Rs (-33.7%; $p < .05$) and $D_{1/5}$Rs (+87.7%; $p < .05$) displayed alterations in MWM_{TMZ} (Supp. Tab. 41, Supp. Tab. 42).

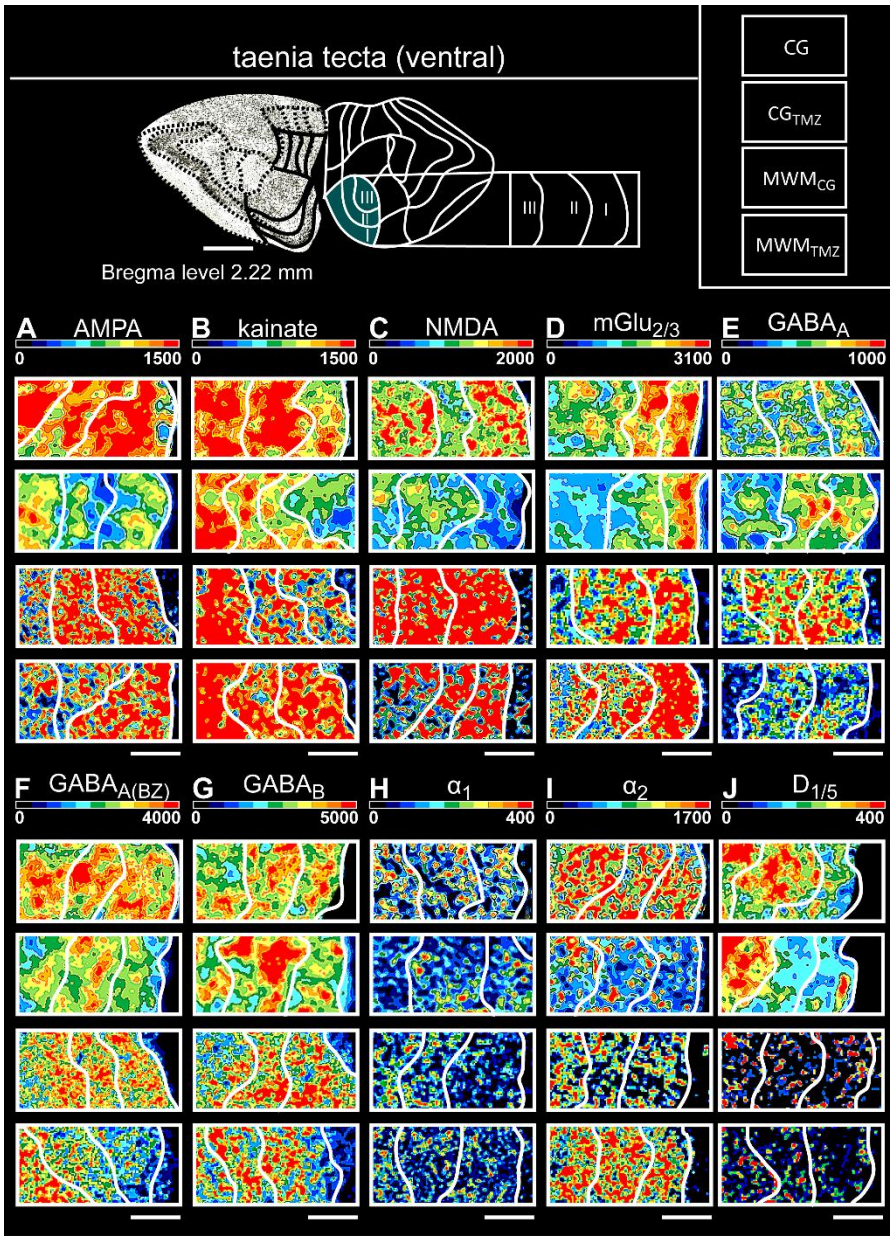

Figure 35: Color-coded layer-specific autoradiographs of the taenia tecta (ventral)

The receptor distribution of all investigated receptors in the ventral taenia tecta represented in color-coded autoradiographs [in fmol/mg protein]. Figure structure according to Figure 31.Scale bars: Nissl-Image, 1 mm; A-J, 400 µm.

The ventral part of taenia tecta (Figure 35) presented high receptor concentration differences in layer I for NMDARs (+177.9%; $p < .05$), $GABA_{A(BZ)}$Rs (-40.5%; $p < .05$), $GABA_B$Rs (+41.9%; $p < .05$) and α_1Rs (+68.6%; $p < .05$) of MWM_{TMZ}. Layer II revealed increased receptor densities for NMDARs (+49.8%; $p < .05$) and $D_{1/5}$Rs (+54.5%; $p < .05$) and decreased concentrations for $mGlu_{2/3}$Rs (-49.4%; $p < .05$) and $GABA_{A(BZ)}$Rs (-33.1%; $p < .05$). Layer III of the trained animals increased densities for NMDARs (+51.3%; $p < .05$), $GABA_B$Rs (+14.8%; $p < .05$) and $D_{1/5}$Rs (+95.2%; $p < .05$) and decreased concentrations of $mGlu_{2/3}$Rs (-43.1%; $p < .05$) and $GABA_{A(BZ)}$Rs (-41.2%; $p < .05$; Supp. Tab. 41, Supp. Tab. 42) in MWM_{TMZ}.

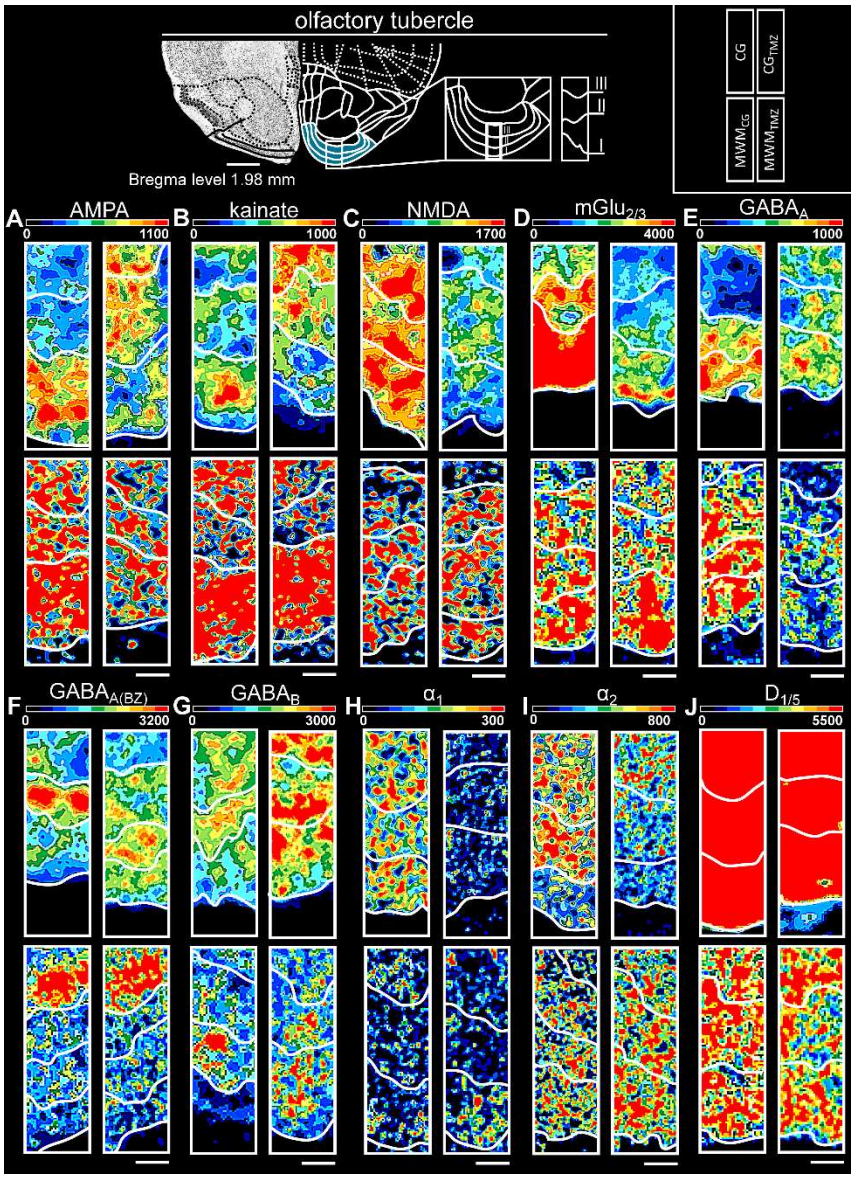

Figure 36: Color-coded layer-specific autoradiographs of the olfactory tubercle

The receptor distribution of all investigated receptors in the olfactory tubercle represented in color-coded autoradiographs [in fmol/mg protein]. Figure structure according to Figure 31. Scale bars: Nissl-Image, 1.2 mm; A-J, 400 µm.

In the olfactory tubercle (Figure 36), significant alterations of $GABA_{A(BZ)}$Rs (-41.6%; $p < .05$) and $D_{1/5}$Rs (-23.2%; $p < .05$) were seen in layer III, whereas the same receptors were less altered in layer I. Here, AMPARs (+36.8%; $p < .05$), kainateRs (+160.5%; $p < .05$), NMDARs (+221.1%; $p < .05$), $mGlu_{2/3}$Rs (-40.6%; $p < .05$), $GABA_B$Rs (+60.4%; $p < .05$) and α_2Rs (+63.5%; $p < .05$) increased significantly in concentrations in MWM_{TMZ}. In layer II, the highest differences were observed in NMDARs (+115.2%; $p < .05$), $mGlu_{2/3}$Rs (-49.0%; $p < .05$), $GABA_B$Rs (+40.7%; $p < .05$) and α_2Rs (+65.9%; $p < .05$; Supp. Tab. 41, Supp. Tab. 42).

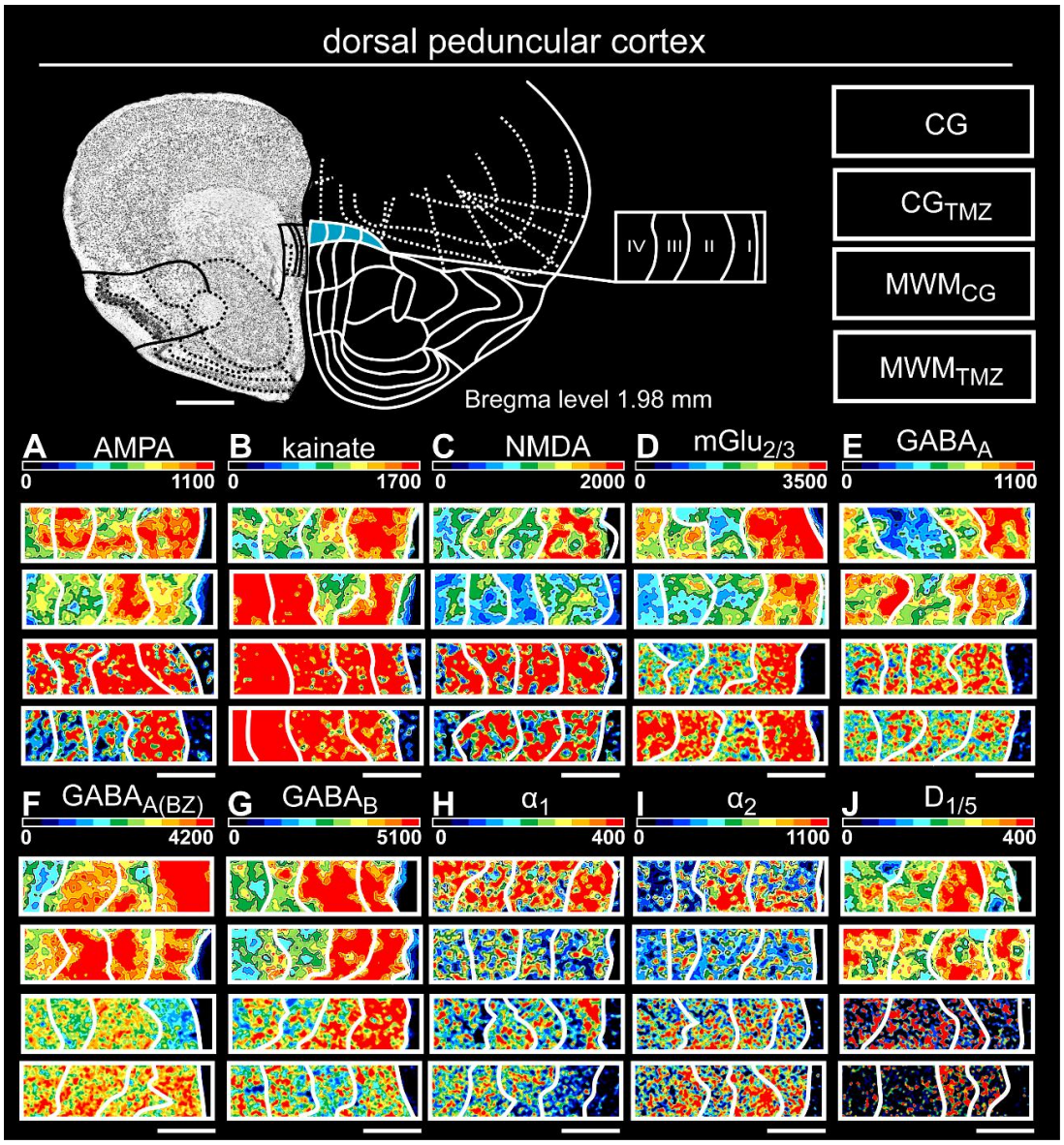

Figure 37: Color-coded layer-specific autoradiographs of the dorsal peduncular cortex

The receptor distribution of all investigated receptors in the dorsal peduncular cortex represented in color-coded autoradiographs [in fmol/mg protein]. Figure structure according to Figure 31. Scale bars: Nissl-Image, 800 µm; A-J, 600 µm; K-T, 200 µm.

In the dorsal peduncular cortex (Figure 37), layer I showed the highest alterations in receptor concentration for AMPARs (-30.3%; $p < .05$), NMDARs (+32.0%; $p < .05$); $mGlu_{2/3}Rs$ (-41.1%; $p < .05$), $GABA_ARs$ (-29.5%; $p < .05$), and $GABA_{A(BZ)}Rs$ (-32.9%; $p < .05$) in MWM_{TMZ}. Layer II/III decreased in concentrations of $mGlu_{2/3}Rs$ (-56.5%; $p < .05$), $GABA_ARs$ (-23.8%; $p < .05$), $GABA_{A(BZ)}Rs$ (-39.8%; $p < .05$) and increased in $D_{1/5}Rs$ (+43.3%; $p < .05$). Layer V showed decreasing densities for AMPARs (-37.0%; $p < .05$), $mGlu_{2/3}Rs$ (-61.0%; $p < .05$), $GABA_ARs$ (-27.4%; $p < .05$), $GABA_{A(BZ)}Rs$ (-41.5%; $p < .05$), α_2Rs (-37.3%; $p < .05$) and increasing concentrations for $D_{1/5}Rs$ (+87.0%; $p < .05$) in MWM_{TMZ}. Overall, all receptors except $GABA_BRs$ and α_1Rs revealed significant differences in layer VI of MWM_{TMZ} (Supp. Tab. 41, Supp. Tab. 42).

The piriform cortex (Figure 38) increased concentrations for AMPARs (+19.1%; $p < .05$), kainateRs (+43.5%; $p < .05$), NMDARs (+43.0%; $p < .05$), $mGlu_{2/3}Rs$ (-54.2%; $p < .05$), $GABA_{A(BZ)}Rs$ (-37.6%; $p < .05$) and α_2Rs (+49.6%; $p < .05$) in layer I relative to the other two layers. AMPARs were highly increased in layer II (+73.5%; $p < .05$), same as kainateRs (+33.8%; $p < .05$) and $D_{1/5}Rs$ (+59.8%; $p < .05$), while $mGlu_{2/3}Rs$ (-50.5%; $p < .05$) and $GABA_{A(BZ)}Rs$ (-37.6%; $p < .05$) decreased in densities. Layer III decreased in densities of AMPARs (-27.3%; $p < .05$), $mGlu_{2/3}Rs$ (-54.7%; $p < .05$), and $GABA_{A(BZ)}Rs$ (-41.2%; $p < .05$) and increases of NMDARs (+31.2%; $p < .05$) and $D_{1/5}Rs$ (+116.1%; $p < .05$) in MWM_{TMZ} (Supp. Tab. 41, Supp. Tab. 42).

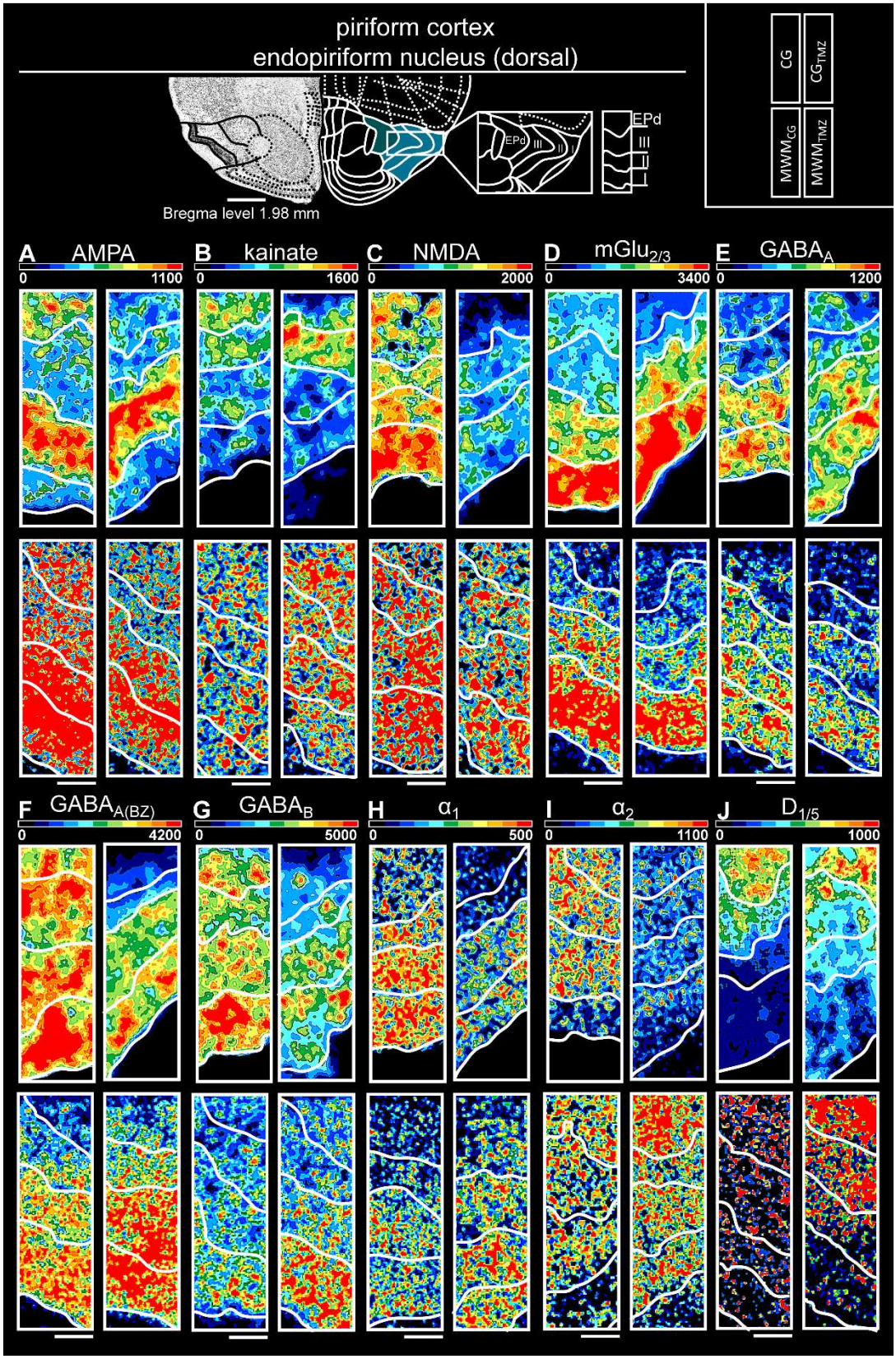

Figure 38: Color-coded layer-specific autoradiographs of the piriform cortex and the endopiriform nucleus

The receptor distribution of all investigated receptors in the piriform cortex and endopiriform nucleus (dorsal) represented in color-coded autoradiographs [in fmol/mg protein]. Figure structure according to Figure 31. Scale bars: Nissl-Image, 1.2 mm; A-J, 400 µm; EPd, dorsal endopiriform nucleus

In all layers of the lateral entorhinal cortex (Figure 39) significant alterations of AMPARs (from layer I: +39.7%; $p < .05$ to layer V: +89.0%; $p < .05$), $mGlu_{2/3}Rs$ (from layer I: -60.8%; $p < .05$ to layer VI: -48.7%; $p < .05$), $GABA_{A(BZ)}Rs$ (from layer II: -21.4%; $p < .05$ to layer VI: 49.2%; $p < .05$) and $GABA_BRs$ (from layer I: -25.4%; $p < .05$ to layer VI: -20.8%; $p < .05$) were observed in MWM_{TMZ}. KainateRs increased in concentration in layer I (+61.6%; $p < .05$) and II (+28.3%; $p < .05$) and decreased in layer V (-28.4%; $p < .05$) and VI (-39.9%; $p < .05$). α_1Rs decreased in layer II (-20.7%; $p < .05$), III (-20.7%; $p < .05$) and VI (-10.2%; $p < .05$) while $D_{1/5}Rs$ increased their densities in MWM_{TMZ} in layer II (+32.2%; $p < .05$) and layer III (+26.9%; $p < .05$; Supp. Tab. 41, Supp. Tab. 42).

In the medial part of the entorhinal cortex (Figure 40), $mGlu_{2/3}Rs$ were decreased in concentration in all layers in the trained animals (from layer I: -47.8%; $p < .05$ to layer VI: -59.6%; $p < .05$). Also, $GABA_BRs$ decreased in all layers, except layer I (from layer II: -15.9%; $p < .05$ to layer VI: -20.5%; $p < .05$). $GABA_{A(BZ)}Rs$ only differed in concentrations in the deeper layers IV to VI (layer IV: -10.03%; $p < .05$; layer V: -37.6%; $p < .05$; layer VI: -46.3%; $p < .05$). Layer I of the medial entorhinal cortex showed an increase in densities for kainateRs (+42.6%; $p < .05$) and a decrease for $GABA_ARs$ (-25.1%; $p < .05$). Layer III showed significant alterations for kainateRs (+29.0%; $p < .05$) and decreased in concentrations of NMDARs (-13.8%; $p < .05$), while layer V showed altered differences for AMPARs (+28.7%; $p < .05$), α_2Rs (+21.1%; $p < .05$) and $D_{1/5}Rs$ (-27.9%; $p < .05$) in MWM_{TMZ}. Layer VI revealed decreased densities of α_1Rs (-18.4%; $p < .05$) in the medial entorhinal cortex (Supp. Tab. 41, Supp. Tab. 42).

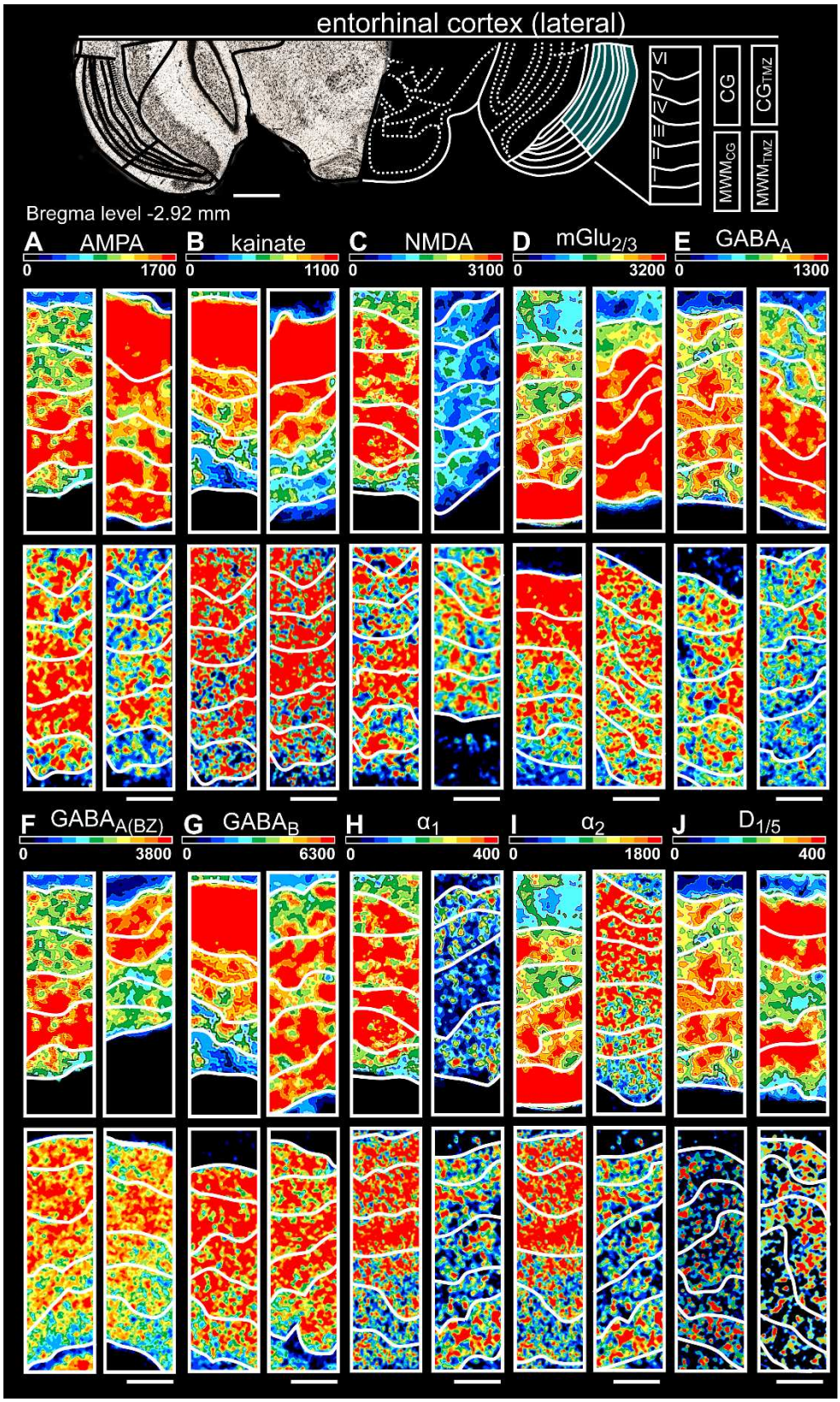

Figure 39: Color-coded layer-specific autoradiographs of the lateral entorhinal cortex

The receptor distribution of all investigated receptors in the lateral entorhinal cortex represented in color-coded autoradiographs [in fmol/mg protein]. Figure structure according to Figure 31. Scale bars: Nissl-Image, 1.5 mm; A-J, 200 µm

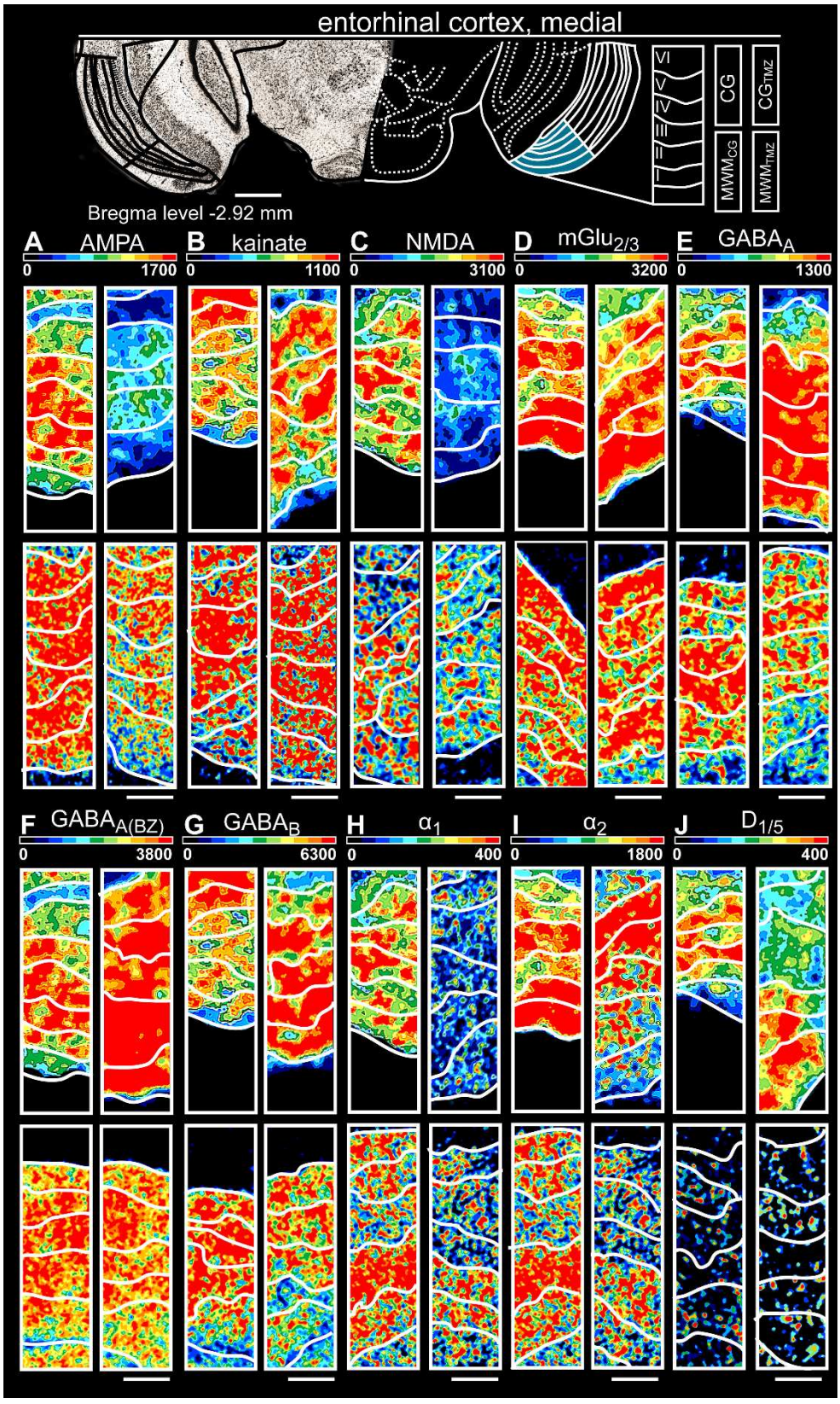

Figure 40: Color-coded layer-specific autoradiographs of the medial entorhinal cortex

The receptor distribution of all investigated receptors in the medial entorhinal cortex represented in color-coded autoradiographs [in fmol/mg protein]. Figure structure according to Figure 31. Scale bars: Nissl-Image, 1.5 mm; A-J, 200 µm

Secondary olfactory cortex

The medial part of the orbitofrontal cortex (Figure 41) revealed differences in the investigated receptor concentrations in all layers for $mGlu_{2/3}$ (from layer I: -34.4%; $p < .05$ to layer VI: -57.8%; $p < .05$) and $GABA_{A(BZ)}$ (from layer I: -32.0%; $p < .05$ to layer VI: -46.3%; $p < .05$) in MWM_{TMZ}. Layer I showed altered receptor concentrations for NMDARs (+55.1%; $p < .05$) and $GABA_A$Rs (-29.2%; $p < .05$), while layer II increased in concentration of NMDARs (+19.2%; $p < .05$). Layer II/III displayed significant decreases in densities of AMPARs (-24.4%; $p < .05$), $GABA_B$Rs (-18.4%; $p < .05$) and α_1Rs (-16.5%; $p < .05$). Concentrations of α_1Rs were decreased in the trained animals (-22.6%; $p < .05$; Supp. Tab. 41, Supp. Tab. 42).

The ventrolateral part (Figure 41) also revealed alterations in concentrations of $mGlu_{2/3}$Rs (from layer I: -53.3%; $p < .05$ to layer VI: -52.5%; $p < .05$) and $GABA_{A(BZ)}$Rs (from layer I: -35.5%; $p < .05$ to layer VI: -38.4%; $p < .05$) in all layers. While layer I and II increased in receptor density for NMDARs (layer I: +32.3%; $p < .05$; II/III: +19.9%; $p < .05$), $GABA_A$Rs decreased here (layer I: -48.0%; $p < .05$; II/III: -35.5%; $p < .05$). $GABA_B$Rs decreased in concentration in layer I (-24.6%; $p < .05$) and α_1Rs in layer II/III (-15.0%; $p < .05$). $GABA_A$Rs decreased in density in layer V (-34.6%; $p < .05$) and $D_{1/5}$Rs increased in layer VI (+29.6%; $p < .05$) in MWM_{TMZ} (Supp. Tab. 41, Supp. Tab. 42).

The lateral orbitofrontal cortex (Figure 41) showed alterations in receptor concentrations in all layers for $mGlu_{2/3}$Rs (from layer I: -50.2%; $p < .05$ to layer VI: -54.2%; $p < .05$), NMDARs (from layer I: +33.1%; $p < .05$ to layer VI: +30.9%; $p < .05$) and $GABA_{A(BZ)}$Rs (from layer I: -31.1%; $p < .05$ to layer VI: -42.0%; $p < .05$). $GABA_A$Rs were decreased in all layers (layer I: -46.6%; $p < .05$ to layer VI: -33.7%; $p < .05$), except layer VI. $GABA_B$Rs decreased in concentrations in layer I (-16.7%; $p < .05$) of the trained animals, while α_2Rs increased in their densities in layer V (+24.5%; $p < .05$). $D_{1/5}$Rs showed alterations with an increase of receptor concentrations in layer V (+44.9%; $p < .05$) in MWM_{TMZ} (Supp. Tab. 41, Supp. Tab. 42).

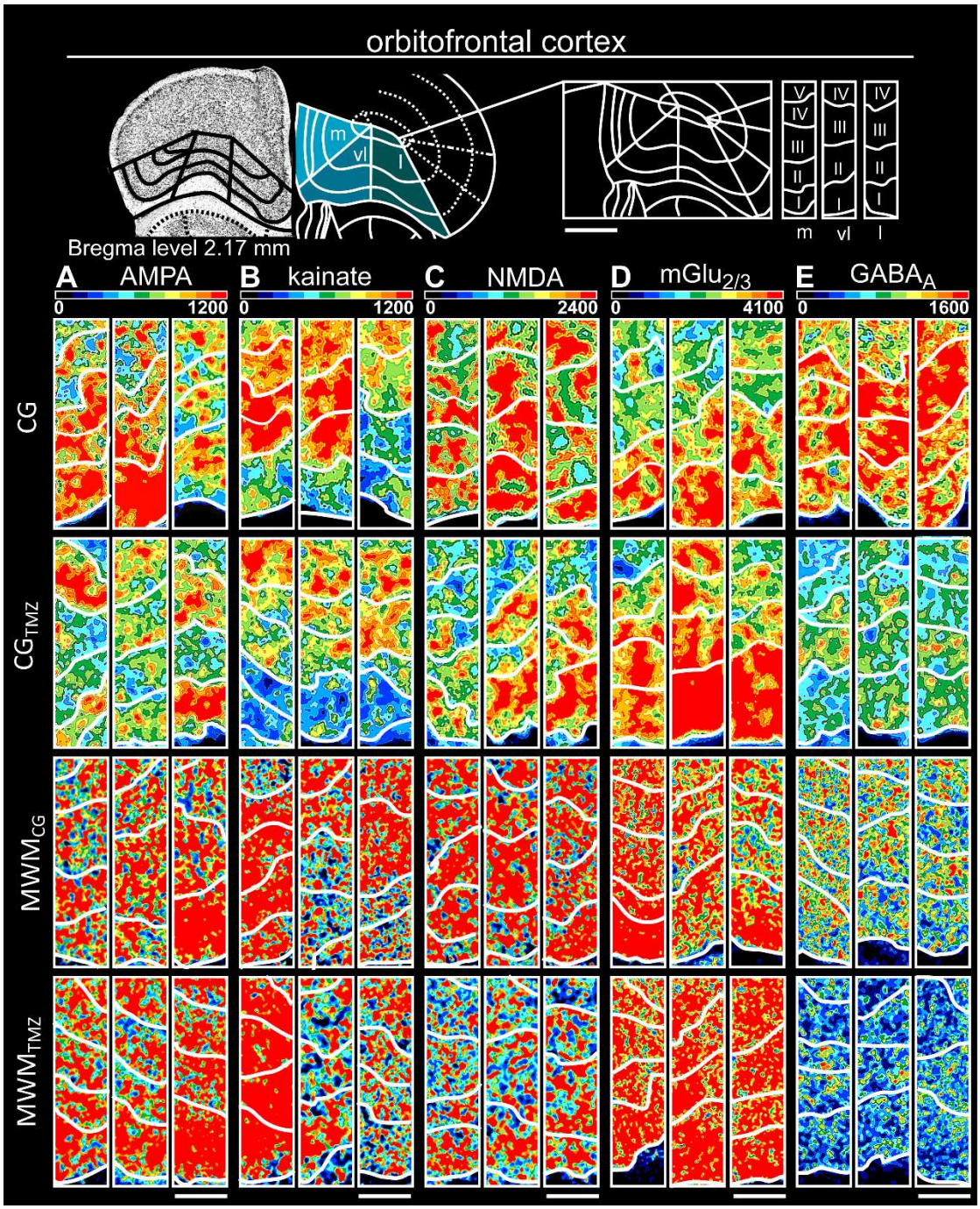
orbitofrontal cortex
m
vl
l
V
IV
III
II
I
Bregma level 2.17 mm
A AMPA
B kainate
C NMDA
D mGlu2/3
E GABAA
0
1200
2400
4100
1600
CG
CGTMZ
MWMCG
MWMTMZ

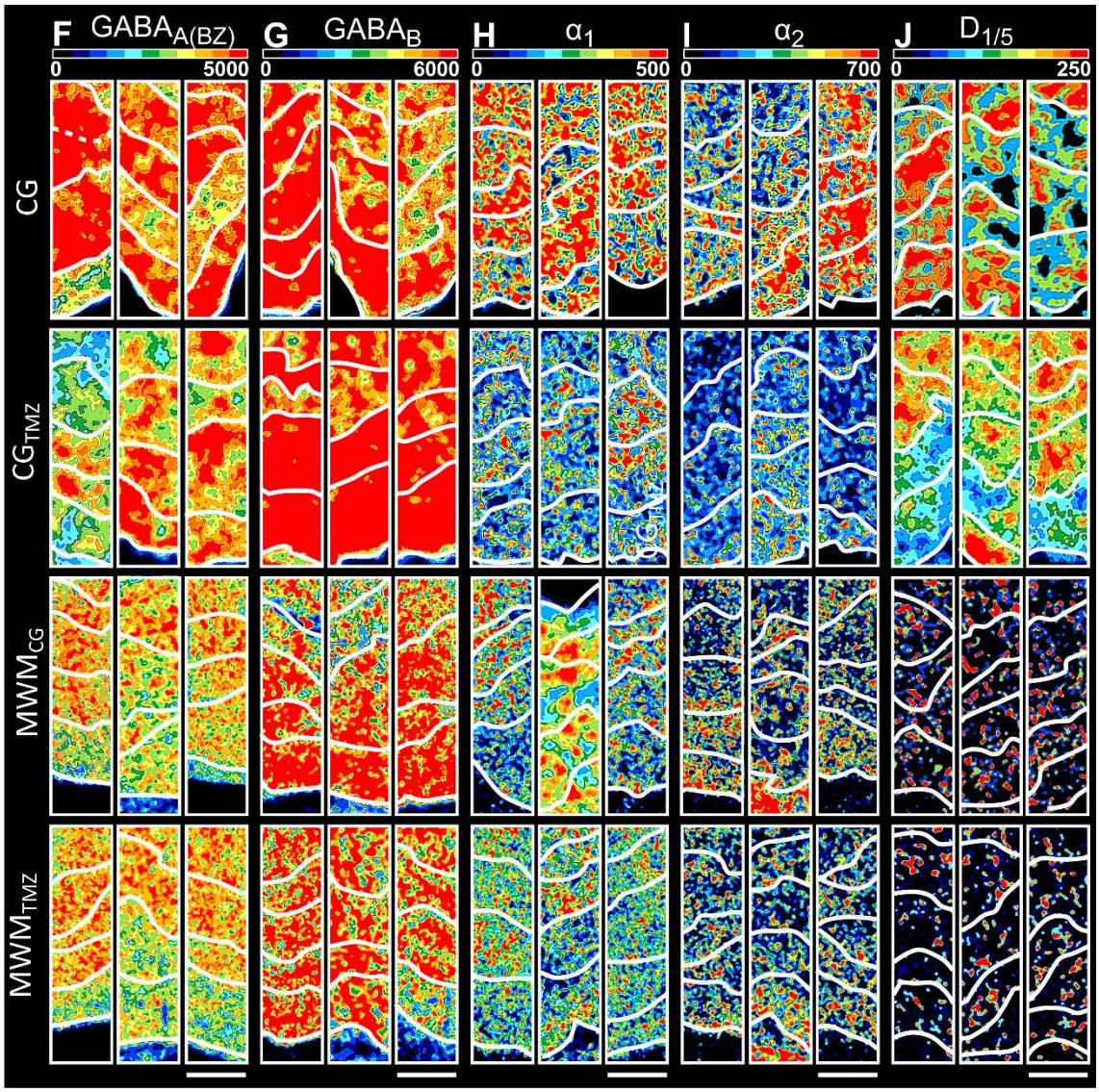

Figure 41: Color-coded layer-specific autoradiographs of the orbitofrontal cortex

The receptor distribution of all investigated receptors in the orbitofrontal cortex (l, lateral; m, medial; vl, ventrolateral) represented in color-coded autoradiographs [in fmol/mg protein]. Figure structure according to Figure 31. Scale bars: Nissl-Image, 800 µm; A-J, 300 µm

3.4.5 Comparison of alterations in trained and untrained animals

Among all investigated receptors, significant differences in concentrations were observed for NMDARs, $GABA_ARs$, $GABA_BRs$, and α_2Rs in both category comparisons (Figure 42). The difference in the concentration of NMDARs was higher in untrained animals than in the trained animals. $GABA_ARs$ displayed high differences in their concentration alterations, significantly in the dorsal taenia tecta (73%) and dorsal peduncular cortex (56%) of untrained animals. While $GABA_ARs$ in untrained animals displayed an increase in receptor densities in these regions, the difference was smaller in trained animals. $GABA_BRs$ and α_2Rs also revealed this picture: While $GABA_BRs$ were altered significantly high in the ventral taenia tecta (77%) and olfactory tubercle (95%), α_2Rs showed a high difference in density alteration in the ventrolateral orbitofrontal cortex. The same was true for kainateRs in the accessory olfactory bulb (62%) and $D_{1/5}Rs$ in the ventrolateral orbitofrontal cortex (54%). In untrained animals, $D_{1/5}Rs$ in the dorsal endopiriform nucleus showed a decrease in receptor concentration due to suppression of adult neurogenesis but showed an increase in concentration in trained animals (Figure 42).

AMPARs and $GABA_{A(BZ)}Rs$ showed minor alteration in concentrations, here the differences between control and TMZ treatment are the same in both group comparisons. This was true for the main olfactory bulb, taenia tecta, dorsal endopiriform nucleus, olfactory tubercle, piriform cortex, the lateral entorhinal cortex, ventrolateral and lateral orbitofrontal cortex (Figure 42).

A heat map (Figure 42) showed the most significant percentages of changes for all regions, regardless of increasing or decreasing values. This revealed that $GABA_BRs$ had the most significant differences. When compared to the fingerprints, it can be seen that this is because $GABA_BRs$ in untrained animals increased significantly in some cases due to suppression of adult neurogenesis, while in trained animals they showed a decrease to stagnation.

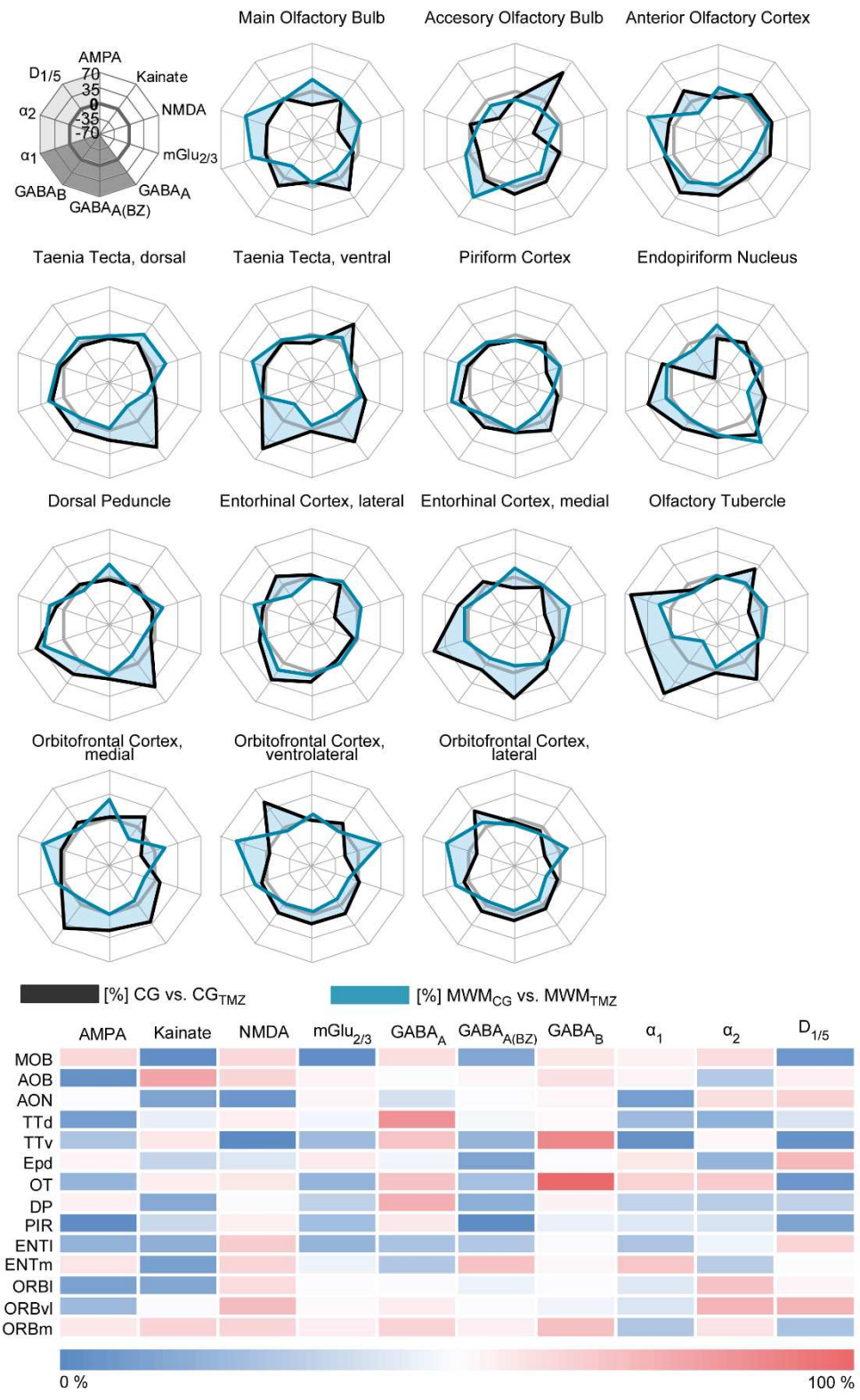

Figure 42: Heat map and dendrogram of all four groups

Differences between the untrained experimental group (**CG** vs. **CG$_{TMZ}$**, Figure 26) versus the trained experimental group (**MWM$_{CG}$** and **MWM$_{TMZ}$**, Figure 28). The relative differences of the respective group comparisons [%] were compared with each other to highlight the effect of cognitive training in suppressed adult neurogenesis. Red color indicates high different values, while blue color displays low differences.

4. Discussion

The present studies show an impact of adult neurogenesis and cognitive training on the receptor architecture of the mouse olfactory system. Instead of a general effect, individual regional and laminar alterations of each receptor could be observed.

In the following, the receptor architecture of the olfactory system will be discussed regarding glutamatergic, GABAergic, and catecholaminergic receptor densities of the olfactory regions (chapter 4.1). It could be shown that the entire olfactory system can be classified into three potentially functional groups and that the olfactory tubercle occupies a special position, so the special role of the olfactory tubercle will be discussed (chapter 4.1.1). The other regions of the olfactory system will be analyzed due to their clustering in functional similar groups (chapter 4.1.2).

The impact of cognitive training on the receptor level of the olfactory system will be analyzed (chapter 4.2). Following, the influence of adult neurogenesis on the receptor architecture of the olfactory system will be discussed for untrained (chapter 4.3) and trained (chapter 4.4) animals. In these comparisons, the receptors are discussed in separate chapters according to their excitatory (AMPA, kainate, NMDA, $mGlu_{2/3}$, α_1, $D_{1/5}$) or inhibitory ($GABA_A$, $GABA_{A(BZ)}$, $GABA_B$, α_2) characteristics.

4.1 The receptor architecture of the mouse olfactory system

Major parts of this chapter 4.1 including subchapters were published in Lothmann et al., 2021.

Previous studies primarily focused on the receptor distributions in the main olfactory bulb and the piriform cortex (for reviews see Shepherd, 2004; Ennis et al., 2007). Until now, the receptor architecture of the dorsal and ventral taenia tecta, the dorsal peduncular cortex, and the endopiriform nucleus have scarcely been analyzed. Additionally, the olfactory regions that were identified so far have not yet been discussed as a comprehensive system. As a result, there is no solid basis for the identification of changes in receptor balance associated with disorders in the olfactory system. Several types of receptors are involved in neurodegenerative diseases (Armstrong et al., 1994; Hawkes, 2006; Zhang et al., 2015; Kwakowsky et al., 2018) and dysfunctions (Thompson et al., 2006; Yuan and Slotnick, 2014; Münster et al., 2020). Therefore, region- and layer-specific receptor balances could provide evidence for pharmacological targets. For instance, adrenoceptors serve as potential pharmacological targets for neurodegenerative and neuropsychiatric disorders like depression and schizophrenia (Arponen et al., 2014). In the PET tracer study by Arponen and colleagues, the highest α_2C receptor concentration was thought to be in the human olfactory tubercle and striatum, while our data and other studies revealed the highest expression in the anterior olfactory cortex and entorhinal cortex in rodents (Scheinin et al., 1994; Holmberg et al., 2003). In this work, receptor autoradiography was chosen for its higher resolution compared to PET tracing.

4.1.1 The special role of the olfactory tubercle in the olfactory system

Based on the cluster analysis (see section 3.1.3), the olfactory tubercle constitutes a single cluster due to its significant concentration of dopaminergic receptors, a result confirmed by earlier studies (Wamsley et al., 1991; Duffy et al., 2000). In general, dopaminergic receptors become active upon reward-promising odor stimuli, evidencing the role of the olfactory tubercle as a motivational evaluation region for odor preferences (Ikemoto, 2007; Zhang et al., 2017; Murata et al., 2019). The neurochemical structure of the olfactory tubercle (Cansler et al., 2020) is of actual interest. Its special role in olfaction originates from its function in the ventral striatum (de Olmos and Heimer, 1999; Cansler et al., 2020), that is highly dopaminergic. Therefore, the categorization of the olfactory tubercle to the striatal system was assumed (Knable et al., 1994; Sulzer et al., 2016). However, further studies of the motor system are necessary to point to a definite classification. As a multisensory region, the olfactory tubercle is also involved in odor-guided

behavior (Fitzgerald et al., 2014; Murata et al., 2015; Murata, 2020). It also differs from the other olfactory regions in its cytoarchitecture, since the trilaminar cortex contains special clusters of granule cells, the islands of Calleja (Pigache, 1970) in layers II and III, where they receive input from the main olfactory bulb (Bayer, 1985; Xiong and Wesson, 2016). The receptor architecture of the olfactory tubercle showed lower receptor concentrations in its layer I than in layers II and III. Only $mGlu_{2/3}Rs$ were expressed highly in layer I, evidencing the direct input from the tufted cells of the main olfactory bulb (Scott et al., 1980; Imamura et al., 2011; Xiong and Wesson, 2016).

The olfactory tubercle also exhibits significantly closer similarities to the ventral striatum in embryogenesis (Bayer, 1985). Astrocytes of the olfactory tubercle and the ventral striatum arise from subpallial progenitor cells of the ventricular zone (Torigoe et al., 2015). Together with the piriform cortex, the olfactory tubercle evolves its striata chronologically prior to the olfactory cortex (Schwob and Price, 1984b; a), so both regions might show advanced maturation and function at early developmental stages (Wesson and Wilson, 2011). So, the distinct receptor architecture of the olfactory tubercle may be due to its different embryogenesis. Whether a clear affiliation of a multisensory area is needed remains open. Only the molecular architecture should be known in order to be able to target or assess a region that is active in numerous functions.

4.1.2 Molecular organization of the olfactory cortex in comparison to function

Regional receptor fingerprints indicate functional characteristics, if further receptor profiles with related functional data is available (Zilles et al., 2002; Eickhoff et al., 2008; Palomero-Gallagher et al., 2009; Zilles et al., 2015; Zilles and Palomero-Gallagher, 2017; Impieri et al., 2019). Increasing amounts of available receptor fingerprints could evidence yet unknown functional networks (Palomero-Gallagher et al. 2009; Palomero-Gallagher and Zilles 2018; Zilles et al. 2015).

The receptor fingerprints of the main and accessory olfactory bulbs were highly similar and differed significantly from the receptor profiles of the cortical olfactory regions. Probably because of their similar function, since both regions enable the uptake and processing of olfactory stimuli (Mucignat-Caretta, 2010; Cleland and Linster, 2019). Cytoarchitectonic similarities could also lead to this cluster, since both bulbs are similar in their prenatal development (Martín-López et al., 2012). Additionally, the laminar structure of the accessory olfactory bulb is similar to the main olfactory bulb, but less distinctive (Larriva-Sahd, 2008). Up to now, only limited data on the receptor architecture of the main olfactory bulb is available.

The primary and secondary olfactory cortex are involved in olfactory processing (Ennis et al., 2015). They formed one cluster in the hierarchical cluster analysis, consisting of three smaller clusters, that will following be discussed in detail: (1) the taenia tecta, the dorsal peduncular cortex and the endopiriform nucleus; (2) the entorhinal cortex and the anterior olfactory cortex and (3) the orbitofrontal cortex and the piriform cortex.

First cluster: the taenia tecta, dorsal peduncular cortex and endopiriform nucleus

The dorsal peduncular cortex and the tecta taenia differed from other analyzed regions due to their concentrations of glutamatergic receptors and densities of α_2Rs. Until now, only limited data for group II mGluRs (McOmish et al., 2016), subunits of $GABA_A$Rs (Zhang et al., 1991) and D_1Rs in pyramidal and GABAergic neurons of the taenia tecta (Santana et al., 2009) is available, so comprehensive receptor profiles to address possible functions or system affiliations are missing. Another problem is that the data of earlier studies cannot explicitly be related to the taenia tecta or the dorsal peduncular cortex since all prefrontal regions were analyzed as one structure. Knowledge regarding their functions is incomplete. The dorsal peduncular cortex and the taenia tecta participate in extinction and associative learning and have connections to the piriform cortex, the lateral entorhinal cortex, the olfactory tubercle, and the main olfactory bulb (Haberly and Price,

1978; Ottersen, 1982; Wyss and Sripanidkulchai, 1983; Santiago and Shammah-Lagnado, 2005; Peters et al., 2009; Cleland and Linster, 2019). High concentrations of kainateRs are characteristic for both regions and contributed to the clustering. KainateRs are known in the etiology of epilepsy (Falcón-Moya et al., 2018) and may act as pharmaceutical targets. For this reason, it is appropriate to particularly investigate the endopiriform nucleus with regard on its possible kainate-related role in epilepsy. The function of the endopiriform nucleus also remains unclear but previous studies assumed that it integrates olfactory information of the piriform cortex with gustatory information of the gustatory cortex (Sugai et al., 2012). It is very similar to the piriform cortex (Hoffman and Haberly, 1993; 1996; Demir et al., 1998), also in its strongly epileptogenic character. However, it differs significantly in its receptor architecture, presumably due to its connection to the insular cortex and the claustrum, thereby also processing non-olfactory information (Sugai et al., 2012). Both regions are considered to be part of the limbic circuitry and originate in the lateral pallium (Watson and Puelles, 2017; Bruguier et al., 2020). Further studies could provide insights in the study of epilepsy and extinction learning.

Second cluster: the entorhinal cortex and the anterior olfactory cortex

The entorhinal cortex connects the olfactory system with the hippocampus (Haberly and Price, 1978; Stäubli et al., 1984; Chapuis et al., 2013; Leitner et al., 2016) and the anterior olfactory cortex (Luskin and Price, 1983; Wyss and Sripanidkulchai, 1983; Mason et al., 2016; Cleland and Linster, 2019). Dysfunctionality of the entorhinal cortex leads to memory loss, known from Alzheimer's disease (Van Hoesen et al., 1986; Braak and Braak, 1991). AMPARs were highly concentrated in layer II and III of the lateral entorhinal cortex, whereas their densities differed slightly across the layers of the medial entorhinal cortex. Here, AMPAR-mediated synaptic responses are facilitated by dopaminergic D_1Rs (Glovaci et al., 2014), that were present, but not highly concentrated (layer VI). The high receptor densities might relate to the significant role of AMPARs in the pathology of Alzheimer's disease (Armstrong et al., 1994).

Also, NMDARs were highly present in layer II/III, probably because they are involved in generating theta oscillations in the hippocampus and the entorhinal cortex to provide the encoding spatial memory (Battaglia et al., 2011; Buzsáki and Moser, 2013; Gu et al., 2017). In the medial entorhinal cortex, NMDARs affect the temporal transfer of information in the hippocampal formation by gamma rhythm-generating microcircuits (Middleton et al., 2008). Also, NMDARs showed increased concentrations in layer V of the medial entorhinal cortex compared to the other layers, presumably because they participate in short-term plasticity here (Chamberlain et al., 2008). High concentrations of $mGlu_{2/3}$Rs were observed in the entorhinal cortex, comparative to

other studies (Ohishi et al., 1993; Fotuhi et al., 1994; Wright et al., 2013). Local functions of the receptor remain unclear (Yoshida et al., 2008).

$GABA_{A(BZ)}$Rs play an important role in learning and the physiological regulation of the memory storage (Venault et al., 1986; Lal et al., 1988; Izquierdo and Medina, 1991). In line with these studies, $GABA_{A(BZ)}$Rs were highly expressed in the superficial layers II/III of both entorhinal subregions, which may be involved in the consolidation of memory. Additionally, $GABA_B$Rs were high in densities throughout the entorhinal cortex. Here, $GABA_B$Rs suppress quantitative, activity-independent glutamate release (Thompson et al., 2006) and thereby control spatial memory (Deng et al., 2009).

Catecholaminergic receptors were mainly concentrated in the deep layers of the entorhinal cortex, with the exception of $D_{1/5}$Rs, that were highly expressed in layer III of the medial entorhinal cortex. D_1Rs suppress the up-state of spontaneous slow oscillations in layer II of the lateral entorhinal cortex, thereby regulating the dendritic excitability of neurons in layer V (Rosenkranz and Johnston, 2006; Batallán-Burrowes and Chapman, 2018). Due to the observed density patterns of $D_{1/5}$Rs and $GABA_A$Rs in layer III of the medial entorhinal cortex, a regulation of $GABA_A$ release by $D_{1/5}$Rs could also be supposed here.

To date, the receptor level of the anterior olfactory cortex is barely analyzed. NMDARs (Zhao et al., 2017) and kainateRs (Wisden and Seeburg, 1993) were observed, but information on the subregions is missing. However, NMDARs are involved in the adaptation of olfactory input in the anterior olfactory cortex (Zhao et al., 2017). Interestingly, glutamatergic receptors showed high expression rates in distinct parts of the anterior olfactory cortex: AMPARs (medial), kainateRs (posteroventral), NMDARs (lateral) and $mGlu_{2/3}$Rs (lateral and external).

$GABA_A$Rs and $GABA_B$Rs were observed in the anterior olfactory cortex (Bowery et al., 1987; Zhang et al., 1991), but this thesis demonstrated that $GABA_B$Rs are significantly higher concentrated than $GABA_A$Rs here. Microinjections of muscimol into the anterior olfactory cortex eliminated inhalation- and odor-evoked signals in the main olfactory bulb and therefore $GABA_A$Rs are more likely to be attributed to indirect modulation in the anterior olfactory cortex (Rothermel and Wachowiak, 2014). The anterior olfactory cortex is connected with the hippocampus (Cleland and Linster, 2019), suspecting the receptor function in memory regulation. It is part of the local determination of the odor source (Kikuta et al., 2010), so it is evident that $GABA_B$Rs are involved in spatial cognition in the entorhinal cortex and play a role in the odor-induced activity of mitral/tufted cells of the main olfactory bulb through anterior olfactory cortex-to-granule cell connection (Mazo et al., 2016). High densities were observed in the lateral and medial parts of the anterior olfactory cortex, supporting their contribution to spatial orientation of odor sources.

Contrary to the hypothesis of an equal receptor distribution (Meyer et al., 2006), there were high differences in the subregions of the anterior olfactory cortex regarding the distribution of noradrenergic receptors. α_1Rs were particularly concentrated in the pars externa, while high levels of α_2Rs were observed in parts of the pars principalis (dorsal, medial, and posteroventral). Up to now, there are no functional studies regarding catecholaminergic receptors in the anterior olfactory cortex. However, a highly similar distribution pattern similar to the entorhinal cortex, could indicate similar regulatory functions. The anterior olfactory cortex and the entorhinal cortex play a key role in the development of neurodegenerative diseases, so further research is of particular interest. Neurofibrillary tangles and neuritic plaques correlate with cell loss in the anterior olfactory cortex (Esiri and Wilcock, 1984; Ohm and Braak, 1987; Ubeda-Bañon et al., 2020), while memory impairment in Alzheimer's disease is associated with the pathological dysfunctionality of the entorhinal cortex (Van Hoesen et al., 1986; Braak and Braak, 1991). Consequently, the cluster of entorhinal and anterior olfactory cortex could be interesting in the research field of Alzheimer's disease.

Third cluster: the orbitofrontal cortex and the piriform cortex

Both regions are functionally involved in olfactory discrimination (Staubli et al., 1987; Critchley and Rolls, 1996; Schoenbaum et al., 1999; Lazic et al., 2007). Connections from the piriform cortex to the orbitofrontal cortex and the amygdaloid complex (Illig, 2006) contribute to olfactory dysfunction in Parkinson's disease (Lee et al., 2020). However, little is known about this area cluster, so further research is necessary for additional conclusions at the organizational level (Li et al., 2010; Xu et al., 2012; Cremer et al., 2015a; Cremer et al., 2015b; Zhang and Manahan-Vaughan, 2015; Perez-Lloret and Barrantes, 2016; Kwakowsky et al., 2018)

AMPARs and NMDARs are necessary for the generation of LTPs in the piriform cortex (Shepherd, 2004) and the early learning of olfactory preferences (Morrison et al., 2013; Mukherjee and Yuan, 2016). Layer II showed high levels of AMPARs (Petralia and Wenthold, 1992) NMDARs (Petralia et al., 1994) and $mGlu_{2/3}$Rs (Wada et al., 1998). NMDARs and $mGlu_{2/3}$Rs are the only glutamatergic receptors that are highly concentrated in layer I, presumably because the activity of NMDARs increases by metabotropic agonists (Collins, 1993; Shepherd, 2004).

While the lateral and ventrolateral orbitofrontal cortices were similar in their receptor profiles, the medial orbitofrontal cortex differed. KainateRs were significantly high in layer III, while AMPARs were highly concentrated in layer I of all three orbitofrontal parts where simultaneously the minimum concentration of kainateRs was present. The cluster of these two regions needs to be

studied on a more functional level, as both regions have strong connections to multiple systems and thus have an impact on information processing. The orbitofrontal cortex is not part of the primary olfactory cortex because it has no direct connection to the main olfactory bulb. The region processes sensory information on a secondary level. Although the piriform cortex is part of the primary olfactory cortex, it also maintains several connections to regions of various systems. Thus, the piriform as well as the orbitofrontal cortex show extensive processing pathways at the secondary level, whose disturbance may have extensive consequences.

4.2 Training enhanced regional GABAergic and $mGlu_{2/3}$ receptor distributions in the olfactory system

The cognitive training led to numerous alterations. In the following, only the strongest changes are reviewed: Among glutamatergic receptors, AMPARs were observed to significantly decrease in densities in the olfactory tubercle, whereas kainateRs increased in the lateral entorhinal cortex. NMDARs decreased in the main and accessory olfactory bulbs. GABAergic receptors generally showed increases, such as $GABA_ARs$ in the dorsal peduncular cortex, $GABA_{A(BZ)}Rs$ in the medial orbitofrontal cortex, and $GABA_BRs$ in the ventral taenia tecta. Catecholaminergic receptors showed a heterogenous picture, as α_1Rs increased in the entorhinal cortex, whereas α_2Rs decreased in the main olfactory bulb and orbitofrontal cortex. Dopaminergic receptors decreased significantly in the dorsal endopiriform nucleus while they increased in the entorhinal cortex. This chapter is divided into excitatory and inhibitory receptors.

Excitatory receptors

There was a striking decrease of AMPARs and NMDARs in the olfactory tubercle and the entorhinal cortex of trained animals. NMDARs and AMPARs are known to be involved in the completing of spatial memory tasks, mainly in the hippocampal formation (Liang et al., 1994; Stecher et al., 1997). Here, NMDARs are expressed in high amounts particularly in CA1 and dentate gyrus, where the receptor is essential for the induction of plasticity (long-term potentiation) (Collingridge, 1985; Collingridge, 1992; Nicolle et al., 1996). All studied olfactory regions showed a reduction of NMDARs. These decreases may suggest a possible prioritization, as an increase in receptor would be more urgent in hippocampal regions. This assumption requires further analysis of the receptor concentrations in the hippocampus for NMDARs in another experiment. However, it is known that NMDA-antagonism negatively affects working memory in mice, so cognitive training could have degraded binding sites for MK-801 (Kumar et al., 2015; Hurtubise et al., 2017).

AMPARs primarily decreased densities in the taenia tecta, olfactory tubercle, and entorhinal cortex upon cognitive training. In the anterior olfactory cortex, AMPARs increased significantly, which may be due to the relay of new olfactory stimuli by the experimental design: In the animal's new environment are new sensory stimuli to be classified for the animal's orientation by bilateral olfactory perception via the anterior olfactory cortex. Excitatory kainateRs, $mGlu_{2/3}Rs$ and $D_{1/5}Rs$ increased in densities after cognitive training in the entorhinal cortex. Higher concentrations of kainateRs are in line with their functional significance in spatial memory acquisition and recall (Lowry et al., 2013). In contrast to the general decrease of NMDARs,

$mGlu_{2/3}$Rs increased in the analyzed olfactory regions. It was previously shown in the mouse model of schizophrenia that LY-379268 compensates excitatory and inhibitory deficits and thus can serve as a pharmaceutical target (Engel et al., 2016). This leads to the question of a time-related adaptation of receptors to multi-day cognitive training that resulted in an increase in $mGlu_{2/3}$R binding sites for LY-341495 due to the reduction of NMDARs.

In the hippocampus, $D_{1/5}$Rs are involved in spatial memory processing (da Silva et al., 2012), confirming increasing receptor densities in the entorhinal cortex. The olfactory tubercle is known to be a motivational evaluation region for olfactory preferences, since dopamine receptors get activated in response to reward-promising olfactory signals (Ikemoto, 2007; Zhang et al., 2017; Murata et al., 2019). In the olfactory system, the dopamine increase could be triggered by the motoric exercise, or goal attainment (reaching the platform of the MWM). Additionally, the food reward of the performed T- and Y-maze experiments emitted odor stimuli, that could have led to the receptor increase in the main olfactory bulb. This effect could be important in Parkinson disease research, where dopamine depletion leads to a decrease in the proliferation rate in the mouse olfactory bulb as well as in the dentate gyrus (Höglinger et al., 2004). Thus, it would be interesting to observe the receptor activity in brains of affected mice. Based on this, investigations into preventive therapies prior to neurodegenerative loss might be initiated.

Inhibitory receptors

Cognitive training resulted in a significant increase of $GABA_A$Rs. The training had a particularly strong effect on the main olfactory bulb, accessory olfactory bulb, taenia tecta, olfactory tubercle, dorsal peduncular cortex, and orbitofrontal cortex. A knockout study of a subunit of $GABA_A$Rs in mice revealed that a low concentration of $GABA_A$ receptors in the hippocampus resulted in better performance in the MWM (Collinson et al., 2002), so training was more likely to decrease the amount of receptor. Since GABAergic afferents and $GABA_A$ receptor activation favor neural stem cell differentiation in the adult hippocampus (Ge et al., 2007), an increase in active $GABA_A$R binding sites could also be expected in the main olfactory bulb as a location of adult neurogenesis. Increased densities were also observed in the entorhinal cortex (both parts), where patients with temporal lobe epilepsy (Stefanits et al., 2019) or Alzheimer's disease (Kwakowsky et al., 2018) lack in $GABA_A$R concentration. The significant receptor increases in the orbitofrontal cortex might also be related to the increased amount of decisions the animal had to make during the tasks, as the receptor is active in the orbitofrontal cortex during impulsive choices (Swanson et al., 2015; Ucha et al., 2019). Briefly: Cognitive training could increase adult

neurogenesis as indicated by a sharp increase of GABARs. Alternatively, cognitive training could increase the receptor density which could favor an increased proliferation rate.

$GABA_{A(BZ)}$Rs were observed to be upregulated in all analyzed regions, except the accessory olfactory bulb. Since $GABA_A$Rs generally had a strong increase in concentration due to cognitive training, an increase in $GABA_{A(BZ)}$Rs was assumed. The increase in $GABA_{A(BZ)}$Rs might be explained by the modulation of BZ agonists on $GABA_A$R responses, that can increase the affinity of the receptors (Gielen et al., 2012). This potentiation of the $GABA_A$R response results in rapid synaptic inhibition, an effect that made benzodiazepine binding sites a pharmacological target for the treatment of anxiety disorders, epilepsy, and sleep disorders (Rudolph and Möhler, 2004; Jacob et al., 2012). Nevertheless, the research on $GABA_{A(BZ)}$Rs continues since they are known to have a modulatory effect in learning and memory related processes (Rudolph and Knoflach, 2011; Hipp et al., 2021). Therefore, knowledge about increasing receptor densities may be beneficial, especially in pharmacological research.

$GABA_B$Rs increased in regions of the olfactory system due to cognitive training, consistent with the receptors' positive effect on spatial memory (Sahraei et al., 2019). Since the taenia tecta, entorhinal cortex, and olfactory tubercle showed significant increases, the results are consistent with the memory-specific training in the mazes. The increase in receptor in the anterior olfactory cortex and piriform cortex is in line with a study that investigated the $GABA_B$ antagonist CGP55845 as a positive influence in odor discrimination learning (LaSarge et al., 2007; LaSarge et al., 2009). Thus, the response of the receptor to cognitive training is of particular interest for research in aging, as spatial reference memory and olfactory discrimination become progressively impaired with ongoing age (LaSarge et al., 2007).

With the increase of $GABA_A$Rs in the main olfactory bulb of trained animals, a decrease of α_2R-density could be observed. This effect goes in line with the suppressive effect of α_2Rs on the GABAergic inhibition of mitral cells (Nai et al., 2009; Nai et al., 2010). Also striking was the decrease in receptor density in the ventral taenia tecta, that is active in odor-driven reward-oriented tasks (Shiotani et al., 2020). A striking aspect of these results was that the decreases of α_2Rs in both regions were in the same ratio to the increases of $GABA_A$Rs: when $GABA_A$Rs doubled in concentration, α_2Rs decreased by 50%.

In summary, this experiment revealed that cognitive training could cause a change in receptor architecture. Certainly, motor control, individual anxiety perception, and sensory external stimuli play a crucial role in this context.

4.3 Impaired adult neurogenesis led to heterogenic alterations in olfactory receptor profiles

Adult neurogenesis was successfully suppressed using TMZ. In CG_{TMZ} animals, AMPARs were observed to significantly decrease densities in the main olfactory bulb, whereas kainateRs increased here. Concentrations of NMDARs decreased in the accessory olfactory bulb. GABAergic receptors generally showed higher densities: $GABA_AR$s in the dorsal taenia tecta, $GABA_{A(BZ)}$Rs in the medial entorhinal cortex, and $GABA_BR$s in the olfactory tubercle. Catecholaminergic α_1Rs increased in their concentrations in the medial entorhinal cortex, while α_2Rs increased in the olfactory tubercle. Dopaminergic receptors decreased significantly in the endopiriform nucleus.

Excitatory receptors

Glutamate is a positive regulator of adult SVZ neurogenesis since AMPARs and kainateRs increase cell proliferation and reduce apoptosis when NMDARs are blocked (Platel et al., 2007). $mGlu_{2/3}$Rs were highly expressed in the olfactory system (Lothmann et al., 2021) and on SVZ-neuroblasts, where they support proliferation and survival of neuronal progenitor cells (Di Giorgi-Gerevini et al., 2005). Additionally, excitatory subtypes of dopaminergic receptors increased the proliferation rate as previously demonstrated (Baker et al., 2004; Doze and Perez, 2012).

The administration of TMZ decreased the densities of the investigated excitatory receptors in all analyzed olfactory regions, except for kainateRs that increased. AMPARs decreased in density in the accessory olfactory bulb, ventral taenia tecta, and the olfactory tubercle, while kainateRs increased here. AMPA/KainateRs are expressed by neuroblasts in the SVZ and the granule cell layer of the main olfactory bulb where kainateRs reduce neuroblast migration rates upon activation (Carleton et al., 2003; Platel et al., 2007). KainateRs were the only glutamatergic receptors that showed an increase in concentration. This might be due to the homeostatic control of neuroblast production by GABA and glutamate: Astrocytes generate neuroblasts (Doetsch et al., 1999a) and proliferate considerably stronger when the neuroblasts are eliminated (Doetsch et al., 1999b). The amount of GABAergic receptors could be increased, as SVZ astrocytes do not express glutamate receptors (Platel and Bordey, 2016) like AMPA (Plested and Mayer, 2007), kainate (Platel et al., 2008), NMDA (Platel et al., 2010), or $mGlu_5$ (Platel et al., 2008). As a consequence, the density of kainate receptors might also increase, consistent with the hypothesis of Platel and colleagues (Platel et al., 2008) that kainateRs act as a "backup mechanism" equal to GABAergic receptors in order to regulate neuroblast migration. As a result, kainateRs act different than the other studied glutamatergic receptors upon suppression of adult neurogenesis. However, densities of kainateRs

did not change significantly in in the main olfactory bulb of CG_{TMZ} mice, but in hippocampus-related regions (taenia tecta and entorhinal cortex). This demonstrated the impact of adult neurogenesis on KainateRs in the taenia tecta, speculating if this region is modulated by the SGZ, or SVZ, since it is related to the hippocampal system where the SGZ provides proliferative stem cells. Thus, kainateRs increased in response to the suppression. This could be due to the fact that fewer GABAergic neuroblasts are replenished, so that kainateRs react as a glutamatergic backup for GABA.

Adult hippocampal neurogenesis is modulated either negatively (Hu et al., 2008) or positively (Hu et al., 2009) by NMDARs (Nacher and McEwen, 2006). In this work, the selective non-competitive NMDAR antagonist MK-801 was used, a ligand which is known to inhibit cell proliferation in the SVZ (Fan et al., 2012). Thus, the decrease of NMDARs upon suppression of adult neurogenesis could demonstrate a direct impact of adult neurogenesis on the receptor and hypothesizes a neurogenesis-supporting effect. Furthermore, NMDARs showed a significant decrease in concentration in the entorhinal cortex, which also may indicate the influence of SGZ neurogenesis. To date, it is not known if the neurogenic niches cooperate. Since the taenia tecta and the entorhinal cortex are both parts of the hippocampal and olfactory systems, further experiments could be done to determine the impact of both niches.

There were no significant effects of adult neurogenesis on the $mGlu_{2/3}R$ density in the olfactory system. The treatment with an $mGlu_{2/3}R$ antagonist also failed to demonstrate a change in proliferation (Di Giorgi-Gerevini et al., 2005).

Excitatory catecholaminergic receptors revealed significant alterations upon inhibition of adult neurogenesis: The densities of α_1Rs decreased in the accessory olfactory bulb, where α_1Rs increase the GABAergic inhibition of mitral cells (Araneda and Firestein, 2006). A reduction of α_1Rs upon suppression of adult neurogenesis could lead to a neurogenesis-dependent effect of α_1Rs on the functionality of the accessory olfactory bulb. Conditioning to diverse odor preferences is also formed by noradrenergic input in the main olfactory bulb, where α_1Rs increase the excitability of granule cells by GABAergic inhibition of mitral cells (Nai et al., 2010). The concentrations of $D_{1/5}$Rs were too low to display significant effects. However, the olfactory tubercle had a receptor profile that corresponded more to the dopaminergic striatal profile than to that of the olfactory system (Knable et al., 1994; Sulzer et al., 2016). Nevertheless, an influence of adult neurogenesis on the receptor profile could be demonstrated here, which could either be related to the SVZ or supports the hypothesis of striatal adult neurogenesis.

It is striking that only a few olfactory regions differed significantly in CG_{TMZ} animals. In regions of the primary olfactory cortex, receptor concentrations decreased after suppression of

adult neurogenesis (accessory olfactory bulb, endopiriform nucleus), whereas a part of the secondary olfactory cortex (ventrolateral orbitofrontal cortex) displayed a significant increase in dopaminergic receptor density. Dopamine has the potential to alter the functional connectivity of the orbitofrontal cortex to other regions and thus act neuromodulatory in the dynamic reconfiguration of functional networks (Clarke et al., 2014; Kahnt and Tobler, 2017). Therefore, it is possible that the suppression of adult neurogenesis increased dopamine concentrations in the orbitofrontal cortex, that resulted in decreased densities in the accessory olfactory bulb and endopiriform nucleus.

In summary, excitatory receptors decreased in densities due to suppression of adult neurogenesis, except kainateRs that increased in concentration. There was no region that showed a difference in all excitatory receptors, and there was no excitatory receptor that was altered in all olfactory regions in CG_{TMZ} mice.

Inhibitory receptors

GABAergic receptors play a modulatory role in all stages of adult neurogenesis. They have an excitatory effect in immature neurons and an inhibitory effect in mature neurons (Pontes et al., 2013). $GABA_ARs$ increased in their concentration due to suppression of adult neurogenesis mainly in the primary olfactory cortex and less in the olfactory bulbs, since neuroblasts are GABAergic. The dorsal taenia tecta, olfactory tubercle, and dorsal peduncular cortex in particular revealed a significant receptor increase. In contrast to this, adult neurogenesis seemed to have only a small effect on the receptor density of $GABA_{A(BZ)}Rs$. Only the medial entorhinal cortex revealed a strong increase in density.

In contrast to $GABA_{A(BZ)}Rs$, $GABA_BRs$ increased the densities in several olfactory regions. The increase in concentration was interesting in the anterior olfactory cortex, where presynaptic $GABA_BRs$ are involved in the odorant-induced activity of mitral and tufted cells of the main olfactory bulb by a special connection (Mazo et al., 2016). An increase in concentration could be seen in the piriform cortex where $GABA_BRs$ regulate NMDARs, which in turn modulate the formation of LTPs (Olpe et al., 1993; Truong et al., 2002). $GABA_BRs$ increased simultaneously to the decreasing concentrations of NMDARs in the piriform cortex. The inhibitory effect of $GABA_BRs$ could thereby lead to a reduced pattern separation between odor categories in the orbitofrontal cortex (Bao et al., 2016). So, a suppressed adult neurogenesis could result in an altered perception of olfactory stimuli.

An increase of $GABA_BRs$ was also seen in the entorhinal cortex. $GABA_BRs$ in the medial part could suppress the glutamate release (Thompson et al., 2006), allowing $GABA_BRs$ to control the entorhinal cortex excitability and thereby exert control over spatial awareness (Deng et al., 2009). An increase in $GABA_BR$ densities could lead to a reduction in anxiety disorder and depression, since a reduced receptor concentration could lead to anxiolytic behavior in mice (Jacobson et al., 2007; Bravo et al., 2011; Fogaça and Duman, 2019). An anti-depressant effect has been demonstrated via $GABA_BR$ antagonists (Slattery et al., 2005), while a knockout study of the $GABA_{B1b}$ receptor subunit demonstrated that it plays an important role in anxiety-associated cognitive processes (Jacobson et al., 2007). Further studies in rats showed that the absence of adult neurogenesis led to depressive-like symptoms that could be reversed by antidepressants (Malberg et al., 2000; Sahay and Hen, 2007; Mateus-Pinheiro et al., 2013; Micheli et al., 2018). However, the selection of an appropriate mouse model in the field of psychiatric disorders is debatable, since clinical symptoms in anxiety disorders and depression are of multifactorial character. Nevertheless, the change in receptor patterns observed here may provide further evidence in the field of mental illness.

α_2Rs increased in the olfactory tubercle and entorhinal cortex. In the entorhinal cortex, α_2Rs inhibit excitatory synaptic transmission (Pralong and Magistretti, 1995), which means that increasing α_2R densities could result in a high inhibition rate. α_2Rs show support in cognitive functions of the prefrontal cortex, specifically working memory and attention, assuming a role in the treatment of ADHD (Arnsten, 2010). Thus, increasing densities in the olfactory tubercle and the entorhinal cortex could affect the motivational-striatal system. Furthermore, the concomitant strong decrease in NMDARs supports the decline in excitatory transmission, further enhancing the inhibitory influence.

In summary, densities of inhibitory receptors, especially GABAergic receptors, increased due to the suppression of adult neurogenesis. This increase would be interesting for further research on depression and anxiety disorders, as these psychiatric disorders continue to increase in society. On the basis of this project, knowledge about the function of SVZ-neurogenesis could be one of the hallmarks for psychological diseases.

4.4 The effect of cognitive training in mice with impaired adult neurogenesis

Cognitive training is widely known to be a positive support for a *healthy lifestyle*. Our results confirm a huge impact on the olfactory regions, seen in chapter 4.2. Contrary, an impaired adult neurogenesis is described in the pathology of various disorders. This leads to the question to what extent both factors act simultaneously if a counterbalance could be achieved or if one factor predominates. In this chapter, untrained animals and trained (MWM) animals, each with suppressed adult neurogenesis, are analyzed. The chapter is divided into excitatory and inhibitory receptors.

Excitatory receptors

Only a few differences between the group of control animals with impaired adult neurogenesis (CG_{TMZ}) and the group of trained animals with impaired adult neurogenesis (MWM_{TMZ}) were statistically significant. Among the excitatory receptors, differences were only evident for kainateRs in the accessory olfactory bulb, NMDARs in the ventrolateral orbitofrontal cortex, $mGlu_{2/3}Rs$ in the accessory olfactory bulb, piriform cortex, α_1Rs in the main olfactory bulb, dorsal taenia tecta, dorsal peduncular cortex, piriform cortex, orbitofrontal cortex, and $D_{1/5}Rs$ in the olfactory tubercle. No general effect was observed. Decreasing concentrations were seen for kainateRs, $D_{1/5}Rs$, $mGlu_{2/3}Rs$, whereas increasing receptor densities were seen for NMDARs and α_1Rs.

The comparing of both group comparisons with each other (Figure 42), indicated that the suppressed adult neurogenesis had a higher impact in the untrained animal than in the trained group. The excitatory receptors revealed significant differences in the main olfactory bulb. While AMPARs, NMDARs, and α_1Rs increased in MWM animals, they showed decreasing concentrations or no alterations in untrained CG animals. Particularly in the main olfactory bulb, the impact of adult neurogenesis would be noticeable since neuroblasts arrive here by the RMS. In the main olfactory bulb, only AMPARs decreased in untrained animals, whereas no statistically significant changes were seen in trained animals. So cognitive training had a stabilizing effect on the densities of AMPARs. Contrary to this, concentrations of α_1Rs were increased in MWM_{TMZ} animals, but not in CG_{TMZ} animals. The fact that cognitive training itself caused highly significant changes in the receptor profile of the main olfactory bulb suggests that adult neurogenesis is enhanced by cognitive training.

Trained animals showed a higher stability in their receptor architecture (MWM_{CG} vs MWM_{TMZ}), compared to untrained animals (CG vs CG_{TMZ}). These results may show a positive effect

of cognitive training in the affected brain. In the accessory olfactory bulb, the MWM animals showed decreasing tendencies of excitatory receptors upon TMZ administration. In particular, kainateRs exhibited increasing densities in CG_{TMZ}, while the concentration decreased in MWM_{TMZ} animals. Since increased KainateRs are associated with epilepsy, these results may suggest a positive effect of cognitive training on the affected brain.

NMDARs were barely altered in MWM_{TMZ}, while they decreased in the CG_{TMZ} animals, particularly in the accessory olfactory bulb and the entorhinal cortex. However, densities of NMDARs were strongly decreased due to cognitive training (see chapter 4.2), but not altered (except increased densities in the entorhinal cortex) in MWM_{TMZ}. Contrary to this is the decrease of NMDARs in every group comparison, except for MWM_{CG} vs. MWM_{TMZ}. This could evidence that cognitive training prevents the effect of a suppressed adult neurogenesis on the NMDAR population in the olfactory system. $mGlu_{2/3}$Rs were unaltered in the CG group, whereas they decreased in densities in the accessory olfactory bulb and piriform cortex of the MWM group.

α_1Rs were hardly comparable since both groups showed increasing tendencies. However, if regions without alterations in receptor density were observed in MWM animals, the densities were increased in the CG animals and vice versa. E.g., in the CG animal, TMZ-administration did not reveal changes in receptor densities in the orbitofrontal cortex and main olfactory bulb, whereas trained animals showed increased concentrations of α_1Rs here. Only the lateral entorhinal cortex and the ventral taenia tecta were unaltered in both groups. This suggests that both cognitive training and adult neurogenesis have an impact on catecholaminergic receptors. More functional data would be needed to assess this.

While $D_{1/5}$Rs barely revealed any changes in MWM_{TMZ}, they decreased in CG_{TMZ} (except for the increase in the olfactory tubercle). Nevertheless, the density of $D_{1/5}$Rs is still on the same density level as $D_{1/5}$Rs in the CG animals. This indicates that even with inhibited adult neurogenesis, cognitive training maintains the density of $D_{1/5}$Rs at a constant level, at least in the olfactory tubercle. Thus, an important supportive impact of cognitive training could be assumed.

In general, cognitive training seemed to stabilize the level of excitatory receptors. These results are essential for the support of the brain by cognitive training in, e.g., memory processes that are affected in dementia, Alzheimer's, and Huntington's disease due to impaired adult neurogenesis. Additionally, it is also interesting in the context of anxiety disorders, since the chemical balance of the associated regions (in this case the dorsal peduncular cortex) could be modulated by cognitive training either for prevention or complementary to therapeutic methods.

Inhibitory receptors

Upon suppression of adult neurogenesis, the inhibitory receptors $GABA_A$, $GABA_{A(BZ)}$, GABAB, and α_2Rs revealed significant alterations in concentrations in trained and untrained animals. However, $GABA_A$ and $GABA_{A(BZ)}$Rs did not show statistically significant differences in the comparison of MWM_{CG} to MWM_{TMZ}, suggesting the facilitation and simultaneous stabilization of adult neurogenesis with cognitive training. The results of $GABA_B$Rs and α_2Rs complemented each other in the group comparisons: In CG animals, $GABA_B$Rs were significantly increased in the anterior olfactory cortex, the ventral taenia tecta, the olfactory tubercle, the entorhinal cortex, and the lateral orbitofrontal cortex. On the contrary, in MWM animals, $GABA_B$Rs decreased in the main olfactory bulb, accessory olfactory bulb, the ventral taenia tecta, and olfactory tubercle. This may be due to the fact that the receptor increased highly by cognitive training (see chapter 4.2). In general, densities of $GABA_B$R in CG_{TMZ} were on the same level as in MWM_{CG}. This could lead to two hypothesis: the increased number of $GABA_B$Rs could indicate a deficient state of the olfactory system, or the receptor adapted to the suppressed neuroblast supply by limiting itself to a lower receptor number to ensure a stability of the system. Interestingly, a previous study demonstrated $GABA_B$Rs antidepressant-like phenotypes that occurred after blocking $GABA_B$Rs (Cryan and Slattery, 2010), suggesting that low levels of $GABA_B$Rs could be used to prevent depression as a mental illness through cognitive training (Chan et al., 2020).

The increasing densities of α_2Rs were striking in the anterior olfactory cortex, taenia tecta, and dorsal peduncular cortex. This result could lead to new approaches in extinction learning, due to the function of the taenia tecta and the dorsal peduncular cortex (Peters et al., 2009). The anterior olfactory cortex supports odor processing and odor learning through connections to other olfactory structures (Rothermel and Wachowiak, 2014; Cleland and Linster, 2019). Whether the increase in density of the receptor could has a positive effect on the olfactory odor learning aspect is uncertain.

In conclusion, the cognitive training stabilized the receptor density pattern, so the profiles didn't alter significantly after adult neurogenesis was suppressed. Consequently, cognitive training was more likely to affect the receptor architecture of the olfactory system than adult neurogenesis. Nevertheless, this hypothesis relates to a limited study time frame. In long-term studies, the deficiency of new proliferative cells could probably not be compensated by cognitive training in the long term.

4.5 Sex differences in the rodent receptor architecture and impact on adult neurogenesis

Only male mice were selected in the planning of this project. However, based on the findings of the recent years, the problem of sex choices in experimental animals should be highlighted. Pharmaceutical products are mainly based on male animals in most studies, which might result in different outcomes in the female organism. According to the current state of knowledge, it is known that female laboratory animals are also suitable for any kind of experiment and their characteristics, such as a changing hormonal cycle, do not represent a limitation in the analysis of the results. Therefore, an extension of the project with female experimental animals would be beneficial for the conclusions of this project. In the process of these reflections, this chapter will briefly summarize the studies regarding sex difference in adult neurogenesis and neurotransmitter profiles of the brain.

Males and females have strong physiological differences due to their hormonal inequality. Sex hormones, including gonadal hormones (androgens and estrogens) fluctuate and are known to be the origin of sexual dimorphism with respect to behavior and adult neurogenesis in the hippocampus (Mahmoud et al., 2016). In particular, the estrus cycle of females is responsible for a strong cyclic fluctuation in hormone levels that is not observed in males in any comparable form. Sexual experience, gestation, parturition, and lactation are special features of the female organism that induce permanent alterations in the adult brain, including the hippocampal adult neurogenesis. In general, gonadal hormones (progesterone, luteinizing hormone, estrogen, estradiol) modulate the different stages of adult neurogenesis of the SGZ and SVZ, such as cell proliferation and cell survival, in both male and female rodents (Mak et al., 2007; Galea, 2008; Barha and Galea, 2010; Bowers et al., 2010; Leuner et al., 2010; Liu et al., 2010; Cheng et al., 2013; Galea et al., 2013; Chan et al., 2014; Barth et al., 2015). Also, studies concerning stress hormones that occur increased by the hormonal balance of female animals show that rats have 50% higher proliferation throughout their estrous cycle during the proestrus phase than in the diestrus and estrus phases (Westenbroek et al., 2004). Stress responses fluctuate more in cyclically altered hormonal levels (Marques et al., 2016) and result in a substantial shift in neuroplasticity in the prenatal phase that negatively affects cell proliferation in the adult brain (Mandyam et al., 2008).

Further, female sex hormones modulate synaptic transmission, which may lead to altered responsiveness of hippocampal receptors (Yankova et al., 2001; Maejima et al., 2013) or presynaptic neurotransmitter release (Yokomaku et al., 2003). Serotonin and dopamine in particular are reported to be impaired in premenstrual dysphoric disorder, which is exclusively dispositioned in females (Schmidt et al., 1998; Bäckström et al., 2003; Epperson et al., 2012). The

effect of sex hormones on neurotransmitter systems varies. For instance, progesterone exerts excitatory effects on glutamate responses (Hausmann and Güntürkün, 2000) and $GABA_AR$s (van Wingen et al., 2008), whereas estrogen has suppressive effects on GABA responses and also exerts excitatory effects on glutamate transmission (Smith and Woolley, 2004). In particular, NMDARs (Gazzaley et al., 1996; Woolley et al., 1997; Adams et al., 2004) and indirectly dopamine receptors (Barth et al., 2015) are promoted by estrogen.

Also, at the level of receptor architecture, a significant sex-specific distinction in their densities was found for the glutamatergic receptors AMPA, kainate, and NMDA in the rat hippocampus (Palomero-Gallagher et al., 2003). Accordingly, male rats displayed higher densities of these receptors than females. In addition, this study also showed a significant increase in receptor concentrations in the female rodent brain in estrus, compared to diestrus. Thus, modulation of sex-specific hormones on synaptic transmission and receptor architecture is evident. In summary, there is a significant demand for comparative data from female experimental animals and the current state of research is able to consider the hormonal cycle. Therefore, this work provides a basis to look at comparative data from other sexes.

4.6 Adult neurogenesis, learning and epilepsy

For a long time, only the hippocampus was the focus of research on the important topic of epilepsy. It remained unconsidered that, just like the hippocampus, the olfactory system is composed of regions with three- to five-layered allocortical structures. The piriform cortex and the endopiriform nucleus are two of the regions now known for their high epileptogenic susceptibility.

The symptomatology of temporal lobe epilepsy lists early olfactory hallucinations (olfactory auras) that are experienced subjectively and cannot be clearly localized (neuro)anatomically. Olfactory ictal symptoms as an initial symptom of a focal seizure may vary, since it might be mis-correlated to the environmental stimulus (Jacek et al., 2007; Elliott et al., 2009). Because of surgical difficulties to study the regions of the olfactory system, progress in research is difficult to achieve, although the olfactory system is of central scientific interest. However, a more accessible region is the piriform cortex, which is predisposed to epileptic seizures because of its anatomy and its central function in the olfactory system (Vaughan and Jackson, 2014). Injections into (among others) this region of $GABA_A$ antagonists or kainic acid and other glutamatergic concentrations resulted in bilateral tonic-clonic seizures. Therefore, prevention of an overexcitation of AMPARs or NMDARs might prevent seizure (Piredda and Gale, 1986; Halonen et al., 1994; Tortorella et al., 1997).

Moreover, kainic-acid-induced epilepsy caused an increased but abnormal neurogenesis in the SGZ (Parent et al., 2007), thus a link between kainateRs, adult neurogenesis, and epilepsy has already been demonstrated. Our data revealed no alteration of KainateR concentration by TMZ administration in the control animal. However, upon the impact of cognitive training, receptor alteration occurred in the lateral entorhinal cortex that is involved in the initiation of seizures (Bernasconi et al., 1999; Xu et al., 2016). The effect of cognitive training on the initiation and duration of epileptic seizures is part of current epilepsy research (Goldstein et al., 2004; Gorantla et al., 2016; Leeman-Markowski and Schachter, 2017).

Cognitive training showed a reduction of NMDARs in the piriform cortex and endopiriform nucleus, but also a blockade of NMDARs was found to be non-successful in the treatment of epileptic seizures (Vaughan and Jackson, 2014). AMPARs did not reveal changes in their concentration, so cognitive training cannot serve as a form of therapy to limit excitation of glutamatergic AMPARs in this case. However, suppression of adult neurogenesis in the endopiriform nucleus demonstrated a significant increase of $GABA_A$Rs, while cognitive training increased the concentration only in the piriform cortex. Since GABAergic receptors regulate NMDAR concentrations by blockade during low-frequency transmissions through hyperpolarization, an increase in the receptor may be beneficial in the case of seizure reduction.

$GABA_ARs$ exhibit increased receptor densities in the trained animal, while $GABA_BRs$ increased in regions where $GABA_ARs$ were less altered (especially in the anterior olfactory cortex and entorhinal cortex).

The endopiriform nucleus, although functionally barely studied, is a region with a crucial role in temporal lobe epilepsy (Behan and Haberly, 1999; Majak and Moryś, 2007). Here, an increase in receptor densities of $GABA_A$ and α_1 could be observed, whereas $D_{1/5}Rs$ recorded a strong decrease. A significantly low receptor density was evident during cognitive training. Interestingly, increased D_1R and decreased D_2R function is involved in limbic epilepsy (Bozzi and Borrelli, 2013), and therefore, a low receptor concentration of D_1Rs in the epileptogenic endopiriform nucleus could be beneficial for patients to control epileptic seizures. Accordingly, cognitive training and suppression of adult neurogenesis in this region may affect epileptogenic activity.

The entorhinal cortex plays a role in seizure generation and propagation in temporal lobe epilepsy through cell loss (Bernasconi et al., 1999). Our data showed a reduction in AMPARs (medial part) and NMDARs (both) with a concomitant increase in the densities of $GABA_{A(BZ)}Rs$ (medial), $GABA_BRs$ (both), and α_1Rs (medial) upon suppression of adult neurogenesis in the entorhinal cortex. $GABA_BRs$ are responsible in shortening the duration of persistent states of epileptic outbreaks in the entorhinal cortex (Mann et al., 2009; Nibber et al., 2017), thus an increase could have a positive effect on epileptogenic seizures. Furthermore, since α_1Rs block norepinephrine-induced epileptic activity in the entorhinal cortex (Stanton et al., 1987), an increase in concentration by TMZ administration may represent a positive impact on the clinical profile of epilepsy.

4.7 Conclusion and outlook

The findings on the receptor architecture of the olfactory system in the rodent brain initiate further discussions. Since the olfactory system is responsible for a sense that shows first symptoms in various neuronal diseases, the question about the chemical architecture of the regions in the human brain emerges. The first part of the present work therefore provides a comparative basis for future investigations in the human brain. Hierarchical cluster analysis of the autoradiographic data revealed three functionally distinct cluster. Further functional experiments are needed to confirm these clusters on a functional level.

This project revealed an impact of adult neurogenesis on the receptor architecture of the olfactory system. There was no prove whether the differences were merely due to the absence of ongoing neuronal plasticity, or whether a modulatory effect took place to compensate the lack of new neurons. Further experiments are necessary to prove whether the neurogenic niches are interconnected to compensate upon changes in the brain structure or whether certain regions can be exclusively assigned to one niche. In general, most of the regions were altered in their receptor profiles. A comparison of these profiles to those of experimental mouse models of human diseases would be a useful next step for the interpretation of the data of this work. This could be essential in the search for pharmaceutical research. Furthermore, an all-encompassing understanding of adult neurogenesis is of great interest in regard to an increasingly aging population.

Cognitive training was shown to have a significant impact on the receptor architecture of the olfactory system. Whether these alterations have a general positive effect on the olfactory regions needs to be shown in further experiments. However, this observation is of interest for neurodegenerative diseases, as often functional deficits of the olfactory system are part of the early diagnosis of e.g., Alzheimer's or Parkinson's disease.

The extent to which cognitive training has a regulatory effect on the affected brain and its neurotransmitter systems could be elucidated by the last part of this work. Behavioral data from the trained animals from this project will need to be discussed and contextualized with the results of this work.

5. References

Abbott, L.C., and Nigussie, F. (2020). Adult neurogenesis in the mammalian dentate gyrus. *Anat Histol Embryol* 49(1), 3-16. doi: 10.1111/ahe.12496.

Adams, M.M., Fink, S.E., Janssen, W.G., Shah, R.A., and Morrison, J.H. (2004). Estrogen modulates synaptic N-methyl-D-aspartate receptor subunit distribution in the aged hippocampus. *J Comp Neurol* 474(3), 419-426. doi: 10.1002/cne.20148.

Aggleton, J.P., Burton, M.J., and Passingham, R.E. (1980). Cortical and subcortical afferents to the amygdala of the rhesus monkey (Macaca mulatta). *Brain Res* 190(2), 347-368. doi: 10.1016/0006-8993(80)90279-6.

Akhter, F., Haque, T., Sato, F., Kato, T., Ohara, H., Fujio, T., et al. (2014). Projections from the dorsal peduncular cortex to the trigeminal subnucleus caudalis (medullary dorsal horn) and other lower brainstem areas in rats. *Neuroscience* 266, 23-37. doi: 10.1016/j.neuroscience.2014.01.046.

Albers, M.W., Tabert, M.H., and Devanand, D.P. (2006). Olfactory dysfunction as a predictor of neurodegenerative disease. *Curr Neurol Neurosci Rep* 6(5), 379-386. doi: 10.1007/s11910-996-0018-7.

Alfonso, J., Le Magueresse, C., Zuccotti, A., Khodosevich, K., and Monyer, H. (2012). Diazepam binding inhibitor promotes progenitor proliferation in the postnatal SVZ by reducing GABA signaling. *Cell Stem Cell* 10(1), 76-87. doi: 10.1016/j.stem.2011.11.011.

Altman, J. (1962a). Are new neurons formed in the brains of adult mammals? *Science* 135(3509), 1127-1128. doi: 10.1126/science.135.3509.1127.

Altman, J. (1962b). Autoradiographic study of degenerative and regenerative proliferation of neuroglia cells with tritiated thymidine. *Exp Neurol* 5, 302-318. doi: 10.1016/0014-4886(62)90040-7.

Altman, J., and Bayer, S.A. (1997). Relation to Its Evolution, Structure and Functions. *CRC Press, Boca Raton; Florida, USA*.

Altman, J., and Das, G.D. (1965). Autoradiographic and histological evidence of postnatal hippocampal neurogenesis in rats. *J Comp Neurol* 124(3), 319-335. doi: 10.1002/cne.901240303.

Altman, J., and Das, G.D. (1967). Postnatal neurogenesis in the guinea-pig. *Nature* 214(5093), 1098-1101. doi: 10.1038/2141098a0.

Alvarez-Buylla, A., García-Verdugo, J.M., and Tramontin, A.D. (2001). A unified hypothesis on the lineage of neural stem cells. *Nat Rev Neurosci* 2(4), 287-293. doi: 10.1038/35067582.

Andersen, P.H., Gingrich, J.A., Bates, M.D., Dearry, A., Falardeau, P., Senogles, S.E., et al. (1990). Dopamine receptor subtypes: beyond the D1/D2 classification. *Trends Pharmacol Sci* 11(6), 231-236. doi: 10.1016/0165-6147(90)90249-8.

Anholt, R.R., Murphy, K.M., Mack, G.E., and Snyder, S.H. (1984). Peripheral-type benzodiazepine receptors in the central nervous system: localization to olfactory nerves. *J Neurosci* 4(2), 593-603. doi: 10.1523/jneurosci.04-02-00593.1984.

Araneda, R.C., and Firestein, S. (2006). Adrenergic enhancement of inhibitory transmission in the accessory olfactory bulb. *J Neurosci* 26(12), 3292-3298. doi: 10.1523/jneurosci.4768-05.2006.

Armstrong, D.M., Ikonomovic, M.D., Sheffield, R., and Wenthold, R.J. (1994). AMPA-selective glutamate receptor subtype immunoreactivity in the entorhinal cortex of

non-demented elderly and patients with Alzheimer's disease. *Brain Res* 639(2), 207-216. doi: 10.1016/0006-8993(94)91732-9.

Arnsten, A.F. (2010). The use of a-2A adrenergic agonists for the treatment of attention-deficit/hyperactivity disorder. *Expert Rev Neurother* 10(10), 1595-1605. doi: 10.1586/ern.10.133.

Aroniadou-Anderjaska, V., Zhou, F.M., Priest, C.A., Ennis, M., and Shipley, M.T. (2000). Tonic and synaptically evoked presynaptic inhibition of sensory input to the rat olfactory bulb via GABA(B) heteroreceptors. *J Neurophysiol* 84(3), 1194-1203. doi: 10.1152/jn.2000.84.3.1194.

Arponen, E., Helin, S., Marjamäki, P., Grönroos, T., Holm, P., Löyttyniemi, E., et al. (2014). A PET Tracer for Brain α2C Adrenoceptors, (11)C-ORM-13070: Radiosynthesis and Preclinical Evaluation in Rats and Knockout Mice. *J Nucl Med* 55(7), 1171-1177. doi: 10.2967/jnumed.113.135574.

Ascher, P., Bregestovski, P., and Nowak, L. (1988). N-methyl-D-aspartate-activated channels of mouse central neurones in magnesium-free solutions. *J Physiol* 399, 207-226. doi: 10.1113/jphysiol.1988.sp017076.

Bäckström, T., Andreen, L., Birzniece, V., Björn, I., Johansson, I.M., Nordenstam-Haghjo, M., et al. (2003). The role of hormones and hormonal treatments in premenstrual syndrome. *CNS Drugs* 17(5), 325-342. doi: 10.2165/00023210-200317050-00003.

Bailey, M.S., and Shipley, M.T. (1993). Astrocyte subtypes in the rat olfactory bulb: morphological heterogeneity and differential laminar distribution. *J Comp Neurol* 328(4), 501-526. doi: 10.1002/cne.903280405.

Baker, S.A., Baker, K.A., and Hagg, T. (2004). Dopaminergic nigrostriatal projections regulate neural precursor proliferation in the adult mouse subventricular zone. *Eur J Neurosci* 20(2), 575-579. doi: 10.1111/j.1460-9568.2004.03486.x.

Bao, X., Raguet, L.L., Cole, S.M., Howard, J.D., and Gottfried, J. (2016). The role of piriform associative connections in odor categorization. *Elife* 5. doi: 10.7554/eLife.13732.

Barbas, H. (1988). Anatomic organization of basoventral and mediodorsal visual recipient prefrontal regions in the rhesus monkey. *J Comp Neurol* 276(3), 313-342. doi: 10.1002/cne.902760302.

Barbas, H. (1993). Organization of cortical afferent input to orbitofrontal areas in the rhesus monkey. *Neuroscience* 56(4), 841-864. doi: 10.1016/0306-4522(93)90132-y.

Barha, C.K., and Galea, L.A. (2010). Influence of different estrogens on neuroplasticity and cognition in the hippocampus. *Biochim Biophys Acta* 1800(10), 1056-1067. doi: 10.1016/j.bbagen.2010.01.006.

Barth, C., Villringer, A., and Sacher, J. (2015). Sex hormones affect neurotransmitters and shape the adult female brain during hormonal transition periods. *Front Neurosci* 9, 37. doi: 10.3389/fnins.2015.00037.

Batallán-Burrowes, A.A., and Chapman, C.A. (2018). Dopamine suppresses persistent firing in layer III lateral entorhinal cortex neurons. *Neurosci Lett* 674, 70-74. doi: 10.1016/j.neulet.2018.03.012.

Battaglia, F.P., Benchenane, K., Sirota, A., Pennartz, C.M., and Wiener, S.I. (2011). The hippocampus: hub of brain network communication for memory. *Trends Cogn Sci* 15(7), 310-318. doi: 10.1016/j.tics.2011.05.008.

Bauer, S., Moyse, E., Jourdan, F., Colpaert, F., Martel, J.C., and Marien, M. (2003). Effects of the alpha 2-adrenoreceptor antagonist dexefaroxan on neurogenesis in the olfactory bulb of the adult rat in vivo: selective protection against neuronal death. *Neuroscience* 117(2), 281-291. doi: 10.1016/s0306-4522(02)00757-1.

Bayer, S.A. (1985). Neurogenesis in the olfactory tubercle and islands of Calleja in the rat. *Int J Dev Neurosci* 3(2), 135-147. doi: 10.1016/0736-5748(85)90004-8.

Baylis, L.L., Rolls, E.T., and Baylis, G.C. (1995). Afferent connections of the caudolateral orbitofrontal cortex taste area of the primate. *Neuroscience* 64(3), 801-812. doi: 10.1016/0306-4522(94)00449-f.

Beaulieu, J.M., and Gainetdinov, R.R. (2011). The physiology, signaling, and pharmacology of dopamine receptors. *Pharmacol Rev* 63(1), 182-217. doi: 10.1124/pr.110.002642.

Behan, M., and Haberly, L.B. (1999). Intrinsic and efferent connections of the endopiriform nucleus in rat. *J Comp Neurol* 408(4), 532-548.

Beiriger, J., Habib, A., Jovanovich, N., Kodavali, C.V., Edwards, L., Amankulor, N., et al. (2022). The Subventricular Zone in Glioblastoma: Genesis, Maintenance, and Modeling. *Front Oncol* 12, 790976. doi: 10.3389/fonc.2022.790976.

Bensafi, M., Sobel, N., and Khan, R.M. (2007). Hedonic-specific activity in piriform cortex during odor imagery mimics that during odor perception. *J Neurophysiol* 98(6), 3254-3262. doi: 10.1152/jn.00349.2007.

Bergmann, O., Liebl, J., Bernard, S., Alkass, K., Yeung, M.S., Steier, P., et al. (2012). The age of olfactory bulb neurons in humans. *Neuron* 74(4), 634-639. doi: 10.1016/j.neuron.2012.03.030.

Bernasconi, N., Bernasconi, A., Andermann, F., Dubeau, F., Feindel, W., and Reutens, D.C. (1999). Entorhinal cortex in temporal lobe epilepsy. *A quantitative MRI study* 52(9), 1870-1870. doi: 10.1212/WNL.52.9.1870 %J Neurology.

Bernstein, P.L., Zuo, M., and Cheng, M.F. (1993). Social condition affects the courtship behavior of male ring doves with posterior medial hypothalamic lesions. *Behav Neural Biol* 59(2), 120-125. doi: 10.1016/0163-1047(93)90834-5.

Bettler, B., Kaupmann, K., Mosbacher, J., and Gassmann, M. (2004). Molecular structure and physiological functions of GABA(B) receptors. *Physiol Rev* 84(3), 835-867. doi: 10.1152/physrev.00036.2003.

Biella, G., and de Curtis, M. (2000). Olfactory inputs activate the medial entorhinal cortex via the hippocampus. *J Neurophysiol* 83(4), 1924-1931. doi: 10.1152/jn.2000.83.4.1924.

Blakemore, L.J., Corthell, J.T., and Trombley, P.Q. (2018). Kainate Receptors Play a Role in Modulating Synaptic Transmission in the Olfactory Bulb. *Neuroscience* 391, 25-49. doi: 10.1016/j.neuroscience.2018.09.002.

Bolteus, A.J., and Bordey, A. (2004). GABA release and uptake regulate neuronal precursor migration in the postnatal subventricular zone. *J Neurosci* 24(35), 7623-7631. doi: 10.1523/jneurosci.1999-04.2004.

Bonuccelli, U., Del Dotto, P., and Rascol, O. (2009). Role of dopamine receptor agonists in the treatment of early Parkinson's disease. *Parkinsonism Relat Disord* 15 Suppl 4, S44-53. doi: 10.1016/s1353-8020(09)70835-1.

Bowers, J.M., Waddell, J., and McCarthy, M.M. (2010). A developmental sex difference in hippocampal neurogenesis is mediated by endogenous oestradiol. *Biol Sex Differ* 1(1), 8. doi: 10.1186/2042-6410-1-8.

Bowery, N.G., Hudson, A.L., and Price, G.W. (1987). GABAA and GABAB receptor site distribution in the rat central nervous system. *Neuroscience* 20(2), 365-383. doi: 10.1016/0306-4522(87)90098-4.

Bozzi, Y., and Borrelli, E. (2013). The role of dopamine signaling in epileptogenesis. *Front Cell Neurosci* 7, 157. doi: 10.3389/fncel.2013.00157.

Braak, H., and Braak, E. (1991). Neuropathological stageing of Alzheimer-related changes. *Acta Neuropathol* 82(4), 239-259. doi: 10.1007/bf00308809.

Bravo, J.A., Forsythe, P., Chew, M.V., Escaravage, E., Savignac, H.M., Dinan, T.G., et al. (2011). Ingestion of Lactobacillus strain regulates emotional behavior and central GABA receptor expression in a mouse via the vagus nerve. *Proc Natl Acad Sci U S A* 108(38), 16050-16055. doi: 10.1073/pnas.1102999108.

Brazel, C.Y., Nuñez, J.L., Yang, Z., and Levison, S.W. (2005). Glutamate enhances survival and proliferation of neural progenitors derived from the subventricular zone. *Neuroscience* 131(1), 55-65. doi: 10.1016/j.neuroscience.2004.10.038.

Brindley, C.J., Antoniw, P., and Newlands, E.S. (1986). Plasma and tissue disposition of mitozolomide in mice. *Br J Cancer* 53(1), 91-97. doi: 10.1038/bjc.1986.13.

Bruguier, H., Suarez, R., Manger, P., Hoerder-Suabedissen, A., Shelton, A.M., Oliver, D.K., et al. (2020). In search of common developmental and evolutionary origin of the claustrum and subplate. *J Comp Neurol* 528(17), 2956-2977. doi: 10.1002/cne.24922.

Brunjes, P.C., Illig, K.R., and Meyer, E.A. (2005). A field guide to the anterior olfactory nucleus (cortex). *Brain Res Brain Res Rev* 50(2), 305-335. doi: 10.1016/j.brainresrev.2005.08.005.

Brunjes, P.C., Kay, R.B., and Arrivillaga, J.P. (2011). The mouse olfactory peduncle. *J Comp Neurol* 519(14), 2870-2886. doi: 10.1002/cne.22662.

Brunjes, P.C., and Kenerson, M.C. (2010). The anterior olfactory nucleus: quantitative study of dendritic morphology. *J Comp Neurol* 518(9), 1603-1616. doi: 10.1002/cne.22293.

Buzsáki, G., and Moser, E.I. (2013). Memory, navigation and theta rhythm in the hippocampal-entorhinal system. *Nat Neurosci* 16(2), 130-138. doi: 10.1038/nn.3304.

Bylund, D.B. (1992). Subtypes of alpha 1- and alpha 2-adrenergic receptors. *Faseb j* 6(3), 832-839. doi: 10.1096/fasebj.6.3.1346768.

Cajal, R. (1890). The origins and terminations of the olfactory, optic, and acoustic nerves in vertebrates. In studies on the cerebral cortex [Limbic structures]. Translated by Kraft LM (1955). *Chicago, IL: The Year Book Publishers*, 1-27.

Cajal, R. (1911a). Histologie du Systeme Nerveux de l'Hommes et des Vertebres. *Maloine: Paris*.

Cajal, R. (1911b). Olfactory apparatus: Olfactory mucosa and olfactory bulb or first-order olfactory center. Histology of the nervous system, Vol. II. Translated by Swanson N, Swanson L (1995). *New York: Oxford Univ Press, London*, 532-554.

Cansler, H.L., Wright, K.N., Stetzik, L.A., and Wesson, D.W. (2020). Neurochemical organization of the ventral striatum's olfactory tubercle. *J Neurochem* 152(4), 425-448. doi: 10.1111/jnc.14919.

Canteras, N.S., Simerly, R.B., and Swanson, L.W. (1992). Connections of the posterior nucleus of the amygdala. *J Comp Neurol* 324(2), 143-179. doi: 10.1002/cne.903240203.

Canto, C.B., and Witter, M.P. (2012). Cellular properties of principal neurons in the rat entorhinal cortex. I. The lateral entorhinal cortex. *Hippocampus* 22(6), 1256-1276. doi: 10.1002/hipo.20997.

Capdevila, C., Rodríguez Vázquez, L., and Martí, J. (2017). Glioblastoma Multiforme and Adult Neurogenesis in the Ventricular-Subventricular Zone: A Review. *J Cell Physiol* 232(7), 1596-1601. doi: 10.1002/jcp.25502.

Carleton, A., Petreanu, L.T., Lansford, R., Alvarez-Buylla, A., and Lledo, P.M. (2003). Becoming a new neuron in the adult olfactory bulb. *Nat Neurosci* 6(5), 507-518. doi: 10.1038/nn1048.

Carlson, K.S., Gadziola, M.A., Dauster, E.S., and Wesson, D.W. (2018). Selective Attention Controls Olfactory Decisions and the Neural Encoding of Odors. *Curr Biol* 28(14), 2195-2205.e2194. doi: 10.1016/j.cub.2018.05.011.

Caron, M.G., and Lefkowitz, R.J. (1993). Catecholamine receptors: structure, function, and regulation. *Recent Prog Horm Res* 48, 277-290. doi: 10.1016/b978-0-12-571148-7.50014-2.

Cartmell, J., and Schoepp, D.D. (2000). Regulation of neurotransmitter release by metabotropic glutamate receptors. *J Neurochem* 75(3), 889-907. doi: 10.1046/j.1471-4159.2000.0750889.x.

Castiglione, M., Calafiore, M., Costa, L., Sortino, M.A., Nicoletti, F., and Copani, A. (2008). Group I metabotropic glutamate receptors control proliferation, survival and differentiation of cultured neural progenitor cells isolated from the subventricular zone of adult mice. *Neuropharmacology* 55(4), 560-567. doi: 10.1016/j.neuropharm.2008.05.021.

Cavada, C., Compañy, T., Tejedor, J., Cruz-Rizzolo, R., and Reinoso-Suárez, F. (2000). The anatomical connections of the macaque monkey orbitofrontal cortex. A Review. *Cerebral cortex (New York, N.Y. : 1991)* 10, 220-242. doi: 10.1093/cercor/10.3.220.

Chae, C.H., Jung, S.L., An, S.H., Park, B.Y., Kim, T.W., Wang, S.W., et al. (2014). Swimming exercise stimulates neuro-genesis in the subventricular zone via increase in synapsin I and nerve growth factor levels. *Biol Sport* 31(4), 309-314. doi: 10.5604/20831862.1132130.

Chamberlain, S.E., Yang, J., and Jones, R.S. (2008). The role of NMDA receptor subtypes in short-term plasticity in the rat entorhinal cortex. *Neural Plast* 2008, 872456. doi: 10.1155/2008/872456.

Chan, J.Y.C., Chan, T.K., Kwok, T.C.Y., Wong, S.Y.S., Lee, A.T.C., and Tsoi, K.K.F. (2020). Cognitive training interventions and depression in mild cognitive impairment and dementia: a systematic review and meta-analysis of randomized controlled trials. *Age Ageing* 49(5), 738-747. doi: 10.1093/ageing/afaa063.

Chan, M., Chow, C., Hamson, D.K., Lieblich, S.E., and Galea, L.A. (2014). Effects of chronic oestradiol, progesterone and medroxyprogesterone acetate on hippocampal neurogenesis and adrenal mass in adult female rats. *J Neuroendocrinol* 26(6), 386-399. doi: 10.1111/jne.12159.

Chapuis, J., Cohen, Y., He, X., Zhang, Z., Jin, S., Xu, F., et al. (2013). Lateral entorhinal modulation of piriform cortical activity and fine odor discrimination. *J Neurosci* 33(33), 13449-13459. doi: 10.1523/jneurosci.1387-13.2013.

Cheng, M.F., Alexander, K., Zhou, S., Bonder, E., and Chuang, L.S. (2011). Newborn GnRH neurons in the adult forebrain of the ring dove. *Horm Behav* 60(1), 94-104. doi: 10.1016/j.yhbeh.2011.03.008.

Cheng, Y., Su, Q., Shao, B., Cheng, J., Wang, H., Wang, L., et al. (2013). 17 β -Estradiol attenuates poststroke depression and increases neurogenesis in female ovariectomized rats. *Biomed Res Int* 2013, 392434. doi: 10.1155/2013/392434.

Chinwalla, A.T., Cook, L.L., Delehaunty, K.D., Fewell, G.A., Fulton, L.A., Fulton, R.S., et al. (2002). Initial sequencing and comparative analysis of the mouse genome. *Nature* 420(6915), 520-562. doi: 10.1038/nature01262.

Christie, J.M., and Westbrook, G.L. (2006). Lateral excitation within the olfactory bulb. *J Neurosci* 26(8), 2269-2277. doi: 10.1523/jneurosci.4791-05.2006.

Clarke, H.F., Cardinal, R.N., Rygula, R., Hong, Y.T., Fryer, T.D., Sawiak, S.J., et al. (2014). Orbitofrontal dopamine depletion upregulates caudate dopamine and alters behavior via changes in reinforcement sensitivity. *J Neurosci* 34(22), 7663-7676. doi: 10.1523/jneurosci.0718-14.2014.

Cleland, T.A., and Linster, C. (2019). Central olfactory structures. *Handb Clin Neurol* 164, 79-96. doi: 10.1016/b978-0-444-63855-7.00006-x.

Collingridge, G.L. (1985). Long term potentiation in the hippocampus: mechanisms of initiation and modulation by neurotransmitters. *Trends in Pharmacological Sciences* 6, 407-411. doi: https://doi.org/10.1016/0165-6147(85)90192-0.

Collingridge, G.L. (1992). The Sharpey-Schafer Prize Lecture. The mechanism of induction of NMDA receptor-dependent long-term potentiation in the hippocampus. *Exp Physiol* 77(6), 771-797. doi: 10.1113/expphysiol.1992.sp003645.

Collingridge, G.L., Volianskis, A., Bannister, N., France, G., Hanna, L., Mercier, M., et al. (2013). The NMDA receptor as a target for cognitive enhancement. *Neuropharmacology* 64, 13-26. doi: 10.1016/j.neuropharm.2012.06.051.

Collins, G.G. (1993). Actions of agonists of metabotropic glutamate receptors on synaptic transmission and transmitter release in the olfactory cortex. *Br J Pharmacol* 108(2), 422-430. doi: 10.1111/j.1476-5381.1993.tb12820.x.

Collins, G.G., Anson, J., and Probett, G.A. (1981). Patterns of endogenous amino acid release from slices of rat and guinea-pig olfactory cortex. *Brain Res* 204(1), 103-120. doi: 10.1016/0006-8993(81)90655-7.

Collinson, N., Kuenzi, F.M., Jarolimek, W., Maubach, K.A., Cothliff, R., Sur, C., et al. (2002). Enhanced learning and memory and altered GABAergic synaptic transmission in mice lacking the alpha 5 subunit of the GABAA receptor. *J Neurosci* 22(13), 5572-5580. doi: 10.1523/jneurosci.22-13-05572.2002.

Colucci-D'Amato, L., Bonavita, V., and di Porzio, U. (2006). The end of the central dogma of neurobiology: stem cells and neurogenesis in adult CNS. *Neurol Sci* 27(4), 266-270. doi: 10.1007/s10072-006-0682-z.

Conn, P.J., and Pin, J.P. (1997). Pharmacology and functions of metabotropic glutamate receptors. *Annu Rev Pharmacol Toxicol* 37, 205-237. doi: 10.1146/annurev.pharmtox.37.1.205.

Courtiol, E., and Wilson, D.A. (2015). The olfactory thalamus: unanswered questions about the role of the mediodorsal thalamic nucleus in olfaction. *Front Neural Circuits* 9, 49. doi: 10.3389/fncir.2015.00049.

Cousens, G.A. (2020). Characterization of odor-evoked neural activity in the olfactory peduncle. *IBRO Rep* 9, 157-163. doi: 10.1016/j.ibror.2020.07.010.

Cremer, J.N., Amunts, K., Graw, J., Piel, M., Rösch, F., and Zilles, K. (2015a). Neurotransmitter receptor density changes in Pitx3ak mice--a model relevant to Parkinson's disease. *Neuroscience* 285, 11-23. doi: 10.1016/j.neuroscience.2014.10.050.

Cremer, J.N., Amunts, K., Schleicher, A., Palomero-Gallagher, N., Piel, M., Rösch, F., et al. (2015b). Changes in the expression of neurotransmitter receptors in Parkin and DJ-1 knockout mice--A quantitative multireceptor study. *Neuroscience* 311, 539-551. doi: 10.1016/j.neuroscience.2015.10.054.

Critchley, H.D., and Rolls, E.T. (1996). Olfactory neuronal responses in the primate orbitofrontal cortex: analysis in an olfactory discrimination task. *J Neurophysiol* 75(4), 1659-1672. doi: 10.1152/jn.1996.75.4.1659.

Cryan, J.F., and Slattery, D.A. (2010). GABAB receptors and depression. Current status. *Adv Pharmacol* 58, 427-451. doi: 10.1016/s1054-3589(10)58016-5.

da Silva, W.C., Köhler, C.C., Radiske, A., and Cammarota, M. (2012). D1/D5 dopamine receptors modulate spatial memory formation. *Neurobiol Learn Mem* 97(2), 271-275. doi: 10.1016/j.nlm.2012.01.005.

Darkes, M.J.M., Plosker, G.L., and Jarvis, B. (2002). Temozolomide: A Review of its Use in the Treatment of Malignant Gliomas, Malignant Melanoma and Other Advanced Cancers. *American Journal of Cancer* 1, 55-80.

Das, G.D., and Altman, J. (1971). Postnatal neurogenesis in the cerebellum of the cat and tritiated thymidine autoradiography. *Brain Res* 30(2), 323-330. doi: 10.1016/0006-8993(71)90082-5.

Datiche, F., and Cattarelli, M. (1996). Catecholamine innervation of the piriform cortex: a tracing and immunohistochemical study in the rat. *Brain Res* 710(1-2), 69-78. doi: 10.1016/0006-8993(95)01279-6.

Davila, N.G., Houpt, T.A., and Trombley, P.Q. (2007). Expression and function of kainate receptors in the rat olfactory bulb. *Synapse* 61(5), 320-334. doi: 10.1002/syn.20376.

de Olmos, J., Hardy, H., and Heimer, L. (1978). The afferent connections of the main and the accessory olfactory bulb formations in the rat: an experimental HRP-study. *J Comp Neurol* 181(2), 213-244. doi: 10.1002/cne.901810202.

Deacon, R.M., and Rawlins, J.N. (2006). T-maze alternation in the rodent. *Nat Protoc* 1(1), 7-12. doi: 10.1038/nprot.2006.2.

Deisseroth, K., and Malenka, R.C. (2005). GABA excitation in the adult brain: a mechanism for excitation- neurogenesis coupling. *Neuron* 47(6), 775-777. doi: 10.1016/j.neuron.2005.08.029.

Demir, R., Haberly, L.B., and Jackson, M.B. (1998). Voltage imaging of epileptiform activity in slices from rat piriform cortex: onset and propagation. *J Neurophysiol* 80(5), 2727-2742. doi: 10.1152/jn.1998.80.5.2727.

Deng, P.Y., Xiao, Z., Yang, C., Rojanathammanee, L., Grisanti, L., Watt, J., et al. (2009). GABA(B) receptor activation inhibits neuronal excitability and spatial learning in the entorhinal cortex by activating TREK-2 K+ channels. *Neuron* 63(2), 230-243. doi: 10.1016/j.neuron.2009.06.022.

Di Giorgi-Gerevini, V., Melchiorri, D., Battaglia, G., Ricci-Vitiani, L., Ciceroni, C., Busceti, C.L., et al. (2005). Endogenous activation of metabotropic glutamate receptors supports the proliferation and survival of neural progenitor cells. *Cell Death Differ* 12(8), 1124-1133. doi: 10.1038/sj.cdd.4401639.

Dindler, A., Blaabjerg, M., Kamand, M., Bogetofte, H., and Meyer, M. (2018). Activation of Group II Metabotropic Glutamate Receptors Increases Proliferation but does not Influence Neuronal Differentiation of a Human Neural Stem Cell Line. *Basic Clin Pharmacol Toxicol* 122(4), 367-372. doi: 10.1111/bcpt.12920.

Doetsch, F., Caillé, I., Lim, D.A., García-Verdugo, J.M., and Alvarez-Buylla, A. (1999a). Subventricular zone astrocytes are neural stem cells in the adult mammalian brain. *Cell* 97(6), 703-716. doi: 10.1016/s0092-8674(00)80783-7.

Doetsch, F., García-Verdugo, J.M., and Alvarez-Buylla, A. (1999b). Regeneration of a germinal layer in the adult mammalian brain. *Proc Natl Acad Sci U S A* 96(20), 11619-11624. doi: 10.1073/pnas.96.20.11619.

Doi, H., Matsuda, T., Sakai, A., Matsubara, S., Hoka, S., Yamaura, K., et al. (2021). Early-life midazolam exposure persistently changes chromatin accessibility to impair adult hippocampal neurogenesis and cognition. *Proc Natl Acad Sci U S A* 118(38). doi: 10.1073/pnas.2107596118.

Dong, H.W. (2008). *The Allen reference atlas: A digital color brain atlas of the C57Bl/6J male mouse.* Hoboken, NJ, US: John Wiley & Sons Inc.

Dong, H.W., and Ennis, M. (2018). Activation of Group II Metabotropic Glutamate Receptors Suppresses Excitability of Mouse Main Olfactory Bulb External Tufted and Mitral Cells. *Front Cell Neurosci* 11, 436. doi: 10.3389/fncel.2017.00436.

Doty, R.L. (2015). *Handbook of Olfaction and Gustation, 3rd Edition.* John Wiley & Sons.

Doucette, R. (1989). Development of the nerve fiber layer in the olfactory bulb of mouse embryos. *J Comp Neurol* 285(4), 514-527. doi: 10.1002/cne.902850407.

Doucette, W., Gire, D.H., Whitesell, J., Carmean, V., Lucero, M.T., and Restrepo, D. (2011). Associative cortex features in the first olfactory brain relay station. *Neuron* 69(6), 1176-1187. doi: 10.1016/j.neuron.2011.02.024.

Doze, V.A., and Perez, D.M. (2012). G-protein-coupled receptors in adult neurogenesis. *Pharmacol Rev* 64(3), 645-675. doi: 10.1124/pr.111.004762.

Duffy, R.A., Hunt, M.A., Wamsley, J.K., and McQuade, R.D. (2000). In vivo autoradiography of [3H]SCH 39166 in rat brain: selective displacement by D1/D5 antagonists. *J Chem Neuroanat* 19(1), 41-46. doi: 10.1016/s0891-0618(00)00045-4.

Ehringer, H., and Hornykiewicz, O. (1960). [Distribution of noradrenaline and dopamine (3-hydroxytyramine) in the human brain and their behavior in diseases of the extrapyramidal system]. *Klin Wochenschr* 38, 1236-1239. doi: 10.1007/bf01485901.

Eichenbaum, H., Shedlack, K.J., and Eckmann, K.W. (1980). Thalamocortical mechanisms in odor-guided behavior. I. Effects of lesions of the mediodorsal thalamic nucleus and frontal cortex on olfactory discrimination in the rat. *Brain Behav Evol* 17(4), 255-275. doi: 10.1159/000121803.

Eisthen, H.L. (1992). Phylogeny of the vomeronasal system and of receptor cell types in the olfactory and vomeronasal epithelia of vertebrates. *Microsc Res Tech* 23(1), 1-21. doi: 10.1002/jemt.1070230102.

Elliott, B., Joyce, E., and Shorvon, S. (2009). Delusions, illusions and hallucinations in epilepsy: 1. Elementary phenomena. *Epilepsy Res* 85(2-3), 162-171. doi: 10.1016/j.eplepsyres.2009.03.018.

Engel, M., Snikeris, P., Matosin, N., Newell, K.A., Huang, X.F., and Frank, E. (2016). mGluR2/3 agonist LY379268 rescues NMDA and GABAA receptor level deficits induced in a two-hit mouse model of schizophrenia. *Psychopharmacology (Berl)* 233(8), 1349-1359. doi: 10.1007/s00213-016-4230-0.

Ennis, M., Hamilton, K., and Hayar, A. (2007). "Neurochemistry of the Main Olfactory System."), 137-204.

Ennis, M., Hayar, A. (2008a). Physiology of the Main Olfactory Bulb. *In: Basbaum A. I., Shepherd G. M., Kaneko A., Westheimer, G. (2008) The Senses: A Comprehensive Reference. Elsevier* 4, 641-686.

Ennis, M., Puche, A.C., Holy, T., and Shipley, M.T. (2015). "Chapter 27 - The Olfactory System," in *The Rat Nervous System (Fourth Edition),* ed. G. Paxinos. (San Diego: Academic Press), 761-803.

Ennis, M., Zhu, M., Heinbockel, T., and Hayar, A. (2006). Olfactory nerve-evoked, metabotropic glutamate receptor-mediated synaptic responses in rat olfactory bulb mitral cells. *J Neurophysiol* 95(4), 2233-2241. doi: 10.1152/jn.01150.2005.

Ennis, M.a.H., A. (2008b). Physiology of the Olfactory Bulb. In *The Senses: A Comprehensive Reference*, Basbaum, A., Kaneko, A., and Shepherd, G. (Eds.-In Chief). *Olfaction and Taste, Firestein, S. and Beauchamp, G. (Eds.). San Diego: Academic Press* 4, 641-686.

Epperson, C.N., Steiner, M., Hartlage, S.A., Eriksson, E., Schmidt, P.J., Jones, I., et al. (2012). Premenstrual dysphoric disorder: evidence for a new category for DSM-5. *Am J Psychiatry* 169(5), 465-475. doi: 10.1176/appi.ajp.2012.11081302.

Eriksson, P.S., Perfilieva, E., Björk-Eriksson, T., Alborn, A.M., Nordborg, C., Peterson, D.A., et al. (1998). Neurogenesis in the adult human hippocampus. *Nat Med* 4(11), 1313-1317. doi: 10.1038/3305.

Ernst, A., Alkass, K., Bernard, S., Salehpour, M., Perl, S., Tisdale, J., et al. (2014). Neurogenesis in the striatum of the adult human brain. *Cell* 156(5), 1072-1083. doi: 10.1016/j.cell.2014.01.044.

Esiri, M.M., and Wilcock, G.K. (1984). The olfactory bulbs in Alzheimer's disease. *J Neurol Neurosurg Psychiatry* 47(1), 56-60. doi: 10.1136/jnnp.47.1.56.

Evans, J., Sumners, C., Moore, J., Huentelman, M.J., Deng, J., Gelband, C.H., et al. (2002). Characterization of mitotic neurons derived from adult rat hypothalamus and brain stem. *J Neurophysiol* 87(2), 1076-1085. doi: 10.1152/jn.00088.2001.

Fagni, L., Chavis, P., Ango, F., and Bockaert, J. (2000). Complex interactions between mGluRs, intracellular Ca2+ stores and ion channels in neurons. *Trends Neurosci* 23(2), 80-88. doi: 10.1016/s0166-2236(99)01492-7.

Falcón-Moya, R., Sihra, T.S., and Rodríguez-Moreno, A. (2018). Kainate Receptors: Role in Epilepsy. *Front Mol Neurosci* 11, 217. doi: 10.3389/fnmol.2018.00217.

Fallon, J.H., and Loughlin, S.E. (1982). Monoamine innervation of the forebrain: collateralization. *Brain Res Bull* 9(1-6), 295-307. doi: 10.1016/0361-9230(82)90143-5.

Fallon, J.H., Riley, J.N., Sipe, J.C., and Moore, R.Y. (1978). The islands of Calleja: organization and connections. *J Comp Neurol* 181(2), 375-395. doi: 10.1002/cne.901810209.

Fan, H., Gao, J., Wang, W., Li, X., Xu, T., and Yin, X. (2012). Expression of NMDA receptor and its effect on cell proliferation in the subventricular zone of neonatal rat brain. *Cell Biochem Biophys* 62(2), 305-316. doi: 10.1007/s12013-011-9302-5.

Farbman, A.I. (1992). *Cell biology of olfaction.* Cambridge University Press.

Felice, D., O'Leary, O.F., Pizzo, R.C., and Cryan, J.F. (2012). Blockade of the GABA(B) receptor increases neurogenesis in the ventral but not dorsal adult hippocampus: relevance to antidepressant action. *Neuropharmacology* 63(8), 1380-1388. doi: 10.1016/j.neuropharm.2012.06.066.

Ferry, B., Ferreira, G., Traissard, N., and Majchrzak, M. (2006). Selective involvement of the lateral entorhinal cortex in the control of the olfactory memory trace during conditioned odor aversion in the rat. *Behav Neurosci* 120(5), 1180-1186. doi: 10.1037/0735-7044.120.5.1180.

Ferry, B., Herbeaux, K., Javelot, H., and Majchrzak, M. (2015). The entorhinal cortex is involved in conditioned odor and context aversions. *Front Neurosci* 9, 342. doi: 10.3389/fnins.2015.00342.

Fitzgerald, B.J., Richardson, K., and Wesson, D.W. (2014). Olfactory tubercle stimulation alters odor preference behavior and recruits forebrain reward and motivational centers. *Front Behav Neurosci* 8**,** 81. doi: 10.3389/fnbeh.2014.00081.

Fogaça, M.V., and Duman, R.S. (2019). Cortical GABAergic Dysfunction in Stress and Depression: New Insights for Therapeutic Interventions. *Front Cell Neurosci* 13**,** 87. doi: 10.3389/fncel.2019.00087.

Fotuhi, M., Standaert, D.G., Testa, C.M., Penney, J.B., Jr., and Young, A.B. (1994). Differential expression of metabotropic glutamate receptors in the hippocampus and entorhinal cortex of the rat. *Brain Res Mol Brain Res* 21(3-4)**,** 283-292. doi: 10.1016/0169-328x(94)90259-3.

Francis, S., Rolls, E.T., Bowtell, R., McGlone, F., O'Doherty, J., Browning, A., et al. (1999). The representation of pleasant touch in the brain and its relationship with taste and olfactory areas. *Neuroreport* 10(3)**,** 453-459. doi: 10.1097/00001756-199902250-00003.

Freundlieb, N., François, C., Tandé, D., Oertel, W.H., Hirsch, E.C., and Höglinger, G.U. (2006). Dopaminergic substantia nigra neurons project topographically organized to the subventricular zone and stimulate precursor cell proliferation in aged primates. *J Neurosci* 26(8)**,** 2321-2325. doi: 10.1523/jneurosci.4859-05.2006.

Gadziola, M.A., Tylicki, K.A., Christian, D.L., and Wesson, D.W. (2015). The olfactory tubercle encodes odor valence in behaving mice. *J Neurosci* 35(11)**,** 4515-4527. doi: 10.1523/jneurosci.4750-14.2015.

Gadziola, M.A., and Wesson, D.W. (2016). The Neural Representation of Goal-Directed Actions and Outcomes in the Ventral Striatum's Olfactory Tubercle. *J Neurosci* 36(2)**,** 548-560. doi: 10.1523/jneurosci.3328-15.2016.

Gage, F.H. (2000). Mammalian neural stem cells. *Science* 287(5457)**,** 1433-1438. doi: 10.1126/science.287.5457.1433.

Gage, F.H., Coates, P.W., Palmer, T.D., Kuhn, H.G., Fisher, L.J., Suhonen, J.O., et al. (1995). Survival and differentiation of adult neuronal progenitor cells transplanted to the adult brain. *Proc Natl Acad Sci U S A* 92(25)**,** 11879-11883. doi: 10.1073/pnas.92.25.11879.

Galea, L.A. (2008). Gonadal hormone modulation of neurogenesis in the dentate gyrus of adult male and female rodents. *Brain Res Rev* 57(2)**,** 332-341. doi: 10.1016/j.brainresrev.2007.05.008.

Galea, L.A., Wainwright, S.R., Roes, M.M., Duarte-Guterman, P., Chow, C., and Hamson, D.K. (2013). Sex, hormones and neurogenesis in the hippocampus: hormonal modulation of neurogenesis and potential functional implications. *J Neuroendocrinol* 25(11)**,** 1039-1061. doi: 10.1111/jne.12070.

Gallyas, F. (1971). A principle for silver staining of tissue elements by physical development. *Acta Morphol Acad Sci Hung* 19(1)**,** 57-71.

Garcia-Garrote, M., Parga, J.A., Labandeira, P.J., Labandeira-Garcia, J.L., and Rodriguez-Pallares, J. (2021). Dopamine regulates adult neurogenesis in the ventricular-subventricular zone via dopamine D3 angiotensin type 2 receptor interactions. *Stem Cells* 39(12)**,** 1778-1794. doi: 10.1002/stem.3457.

Garthe, A., Behr, J., and Kempermann, G. (2009). Adult-generated hippocampal neurons allow the flexible use of spatially precise learning strategies. *PLoS One* 4(5)**,** e5464. doi: 10.1371/journal.pone.0005464.

Garthe, A., and Kempermann, G. (2013). An old test for new neurons: refining the Morris water maze to study the functional relevance of adult hippocampal neurogenesis. *Front Neurosci* 7**,** 63. doi: 10.3389/fnins.2013.00063.

Gazzaley, A.H., Weiland, N.G., McEwen, B.S., and Morrison, J.H. (1996). Differential regulation of NMDAR1 mRNA and protein by estradiol in the rat hippocampus. *J Neurosci* 16(21)**,** 6830-6838. doi: 10.1523/jneurosci.16-21-06830.1996.

Ge, S., Pradhan, D.A., Ming, G.L., and Song, H. (2007). GABA sets the tempo for activity-dependent adult neurogenesis. *Trends Neurosci* 30(1)**,** 1-8. doi: 10.1016/j.tins.2006.11.001.

Giachino, C., Barz, M., Tchorz, J.S., Tome, M., Gassmann, M., Bischofberger, J., et al. (2014). GABA suppresses neurogenesis in the adult hippocampus through GABAB receptors. *Development* 141(1)**,** 83-90. doi: 10.1242/dev.102608.

Giachino, C., and Taylor, V. (2009). Lineage analysis of quiescent regenerative stem cells in the adult brain by genetic labelling reveals spatially restricted neurogenic niches in the olfactory bulb. *Eur J Neurosci* 30(1)**,** 9-24. doi: 10.1111/j.1460-9568.2009.06798.x.

Gielen, M.C., Lumb, M.J., and Smart, T.G. (2012). Benzodiazepines modulate GABAA receptors by regulating the preactivation step after GABA binding. *J Neurosci* 32(17)**,** 5707-5715. doi: 10.1523/jneurosci.5663-11.2012.

Glovaci, I., Caruana, D.A., and Chapman, C.A. (2014). Dopaminergic enhancement of excitatory synaptic transmission in layer II entorhinal neurons is dependent on D_1-like receptor-mediated signaling. *Neuroscience* 258**,** 74-83. doi: 10.1016/j.neuroscience.2013.10.076.

Goldstein, L.H., Deale, A.C., Mitchell-O'Malley, S.J., Toone, B.K., and Mellers, J.D. (2004). An evaluation of cognitive behavioral therapy as a treatment for dissociative seizures: a pilot study. *Cogn Behav Neurol* 17(1)**,** 41-49. doi: 10.1097/00146965-200403000-00005.

Gonzalez-Cabrera, P.J., Gaivin, R.J., Yun, J., Ross, S.A., Papay, R.S., McCune, D.F., et al. (2003). Genetic profiling of alpha 1-adrenergic receptor subtypes by oligonucleotide microarrays: coupling to interleukin-6 secretion but differences in STAT3 phosphorylation and gp-130. *Mol Pharmacol* 63(5)**,** 1104-1116. doi: 10.1124/mol.63.5.1104.

González, J., Barros-Loscertales, A., Pulvermüller, F., Meseguer, V., Sanjuán, A., Belloch, V., et al. (2006). Reading cinnamon activates olfactory brain regions. *Neuroimage* 32(2)**,** 906-912. doi: 10.1016/j.neuroimage.2006.03.037.

Gorantla, V.R., Pemminati, S., Bond, V., Meyers, D.G., and Millis, R.M. (2016). Effects of Swimming Exercise on Learning and Memory in the Kainate-Lesion Model of Temporal Lobe Epilepsy. *J Clin Diagn Res* 10(11)**,** Cf01-cf05. doi: 10.7860/jcdr/2016/22100.8835.

Gottfried, J.A., Smith, A.P., Rugg, M.D., and Dolan, R.J. (2004). Remembrance of odors past: human olfactory cortex in cross-modal recognition memory. *Neuron* 42(4)**,** 687-695. doi: 10.1016/s0896-6273(04)00270-3.

Gottfried, J.A., Winston, J.S., and Dolan, R.J. (2006). Dissociable codes of odor quality and odorant structure in human piriform cortex. *Neuron* 49(3)**,** 467-479. doi: 10.1016/j.neuron.2006.01.007.

Gould, E., Reeves, A.J., Fallah, M., Tanapat, P., Gross, C.G., and Fuchs, E. (1999). Hippocampal neurogenesis in adult Old World primates. *Proc Natl Acad Sci U S A* 96(9)**,** 5263-5267. doi: 10.1073/pnas.96.9.5263.

Greenamyre, J.T., and Porter, R.H. (1994). Anatomy and physiology of glutamate in the CNS. *Neurology* 44(11 Suppl 8), S7-13.

Gross, C.G. (2000). Neurogenesis in the adult brain: death of a dogma. *Nat Rev Neurosci* 1(1), 67-73. doi: 10.1038/35036235.

Grubb, M.S., Nissant, A., Murray, K., and Lledo, P.M. (2008). Functional maturation of the first synapse in olfaction: development and adult neurogenesis. *J Neurosci* 28(11), 2919-2932. doi: 10.1523/jneurosci.5550-07.2008.

Gu, Z., Alexander, G.M., Dudek, S.M., and Yakel, J.L. (2017). Hippocampus and Entorhinal Cortex Recruit Cholinergic and NMDA Receptors Separately to Generate Hippocampal Theta Oscillations. *Cell Rep* 21(12), 3585-3595. doi: 10.1016/j.celrep.2017.11.080.

Gupta, M.K., Papay, R.S., Jurgens, C.W., Gaivin, R.J., Shi, T., Doze, V.A., et al. (2009). alpha1-Adrenergic receptors regulate neurogenesis and gliogenesis. *Mol Pharmacol* 76(2), 314-326. doi: 10.1124/mol.109.057307.

Gupta, T., Nair, V., Paul, S.N., Kannan, S., Moiyadi, A., Epari, S., et al. (2012). Can irradiation of potential cancer stem-cell niche in the subventricular zone influence survival in patients with newly diagnosed glioblastoma? *J Neurooncol* 109(1), 195-203. doi: 10.1007/s11060-012-0887-3.

Haberly, L.B. (1985). Neuronal circuitry in olfactory cortex: Anatomy and functional implications. *Chemical Senses* 10(2), 219-238. doi: 10.1093/chemse/10.2.219.

Haberly, L.B. (2001). Parallel-distributed processing in olfactory cortex: new insights from morphological and physiological analysis of neuronal circuitry. *Chem Senses* 26(5), 551-576. doi: 10.1093/chemse/26.5.551.

Haberly, L.B., and Price, J.L. (1978). Association and commissural fiber systems of the olfactory cortex of the rat. II. Systems originating in the olfactory peduncle. *J Comp Neurol* 181(4), 781-807. doi: 10.1002/cne.901810407.

Hachem, L.D., Mothe, A.J., and Tator, C.H. (2017). Positive Modulation of AMPA Receptors Promotes Survival and Proliferation of Neural Stem/Progenitor Cells from the Adult Rat Spinal Cord. *Stem Cells Dev* 26(23), 1675-1681. doi: 10.1089/scd.2017.0182.

Hall, H., Halldin, C., Farde, L., and Sedvall, G. (1998). Whole hemisphere autoradiography of the postmortem human brain. *Nucl Med Biol* 25(8), 715-719. doi: 10.1016/s0969-8051(98)00053-5.

Hallonet, M.E., Teillet, M.A., and Le Douarin, N.M. (1990). A new approach to the development of the cerebellum provided by the quail-chick marker system. *Development* 108(1), 19-31.

Halonen, T., Tortorella, A., Zrebeet, H., and Gale, K. (1994). Posterior piriform and perirhinal cortex relay seizures evoked from the area tempestas: role of excitatory and inhibitory amino acid receptors. *Brain Res* 652(1), 145-148. doi: 10.1016/0006-8993(94)90328-x.

Halpern, M., and Martínez-Marcos, A. (2003). Structure and function of the vomeronasal system: an update. *Prog Neurobiol* 70(3), 245-318. doi: 10.1016/s0301-0082(03)00103-5.

Hausmann, M., and Güntürkün, O. (2000). Steroid fluctuations modify functional cerebral asymmetries: the hypothesis of progesterone-mediated interhemispheric decoupling. *Neuropsychologia* 38(10), 1362-1374. doi: 10.1016/s0028-3932(00)00045-2.

Hawkes, C. (2006). Olfaction in neurodegenerative disorder. *Adv Otorhinolaryngol* 63, 133-151. doi: 10.1159/000093759.

Heck, N., Kilb, W., Reiprich, P., Kubota, H., Furukawa, T., Fukuda, A., et al. (2007). GABA-A receptors regulate neocortical neuronal migration in vitro and in vivo. *Cereb Cortex* 17(1), 138-148. doi: 10.1093/cercor/bhj135.

Heinbockel, T., Laaris, N., and Ennis, M. (2007). Metabotropic glutamate receptors in the main olfactory bulb drive granule cell-mediated inhibition. *J Neurophysiol* 97(1), 858-870. doi: 10.1152/jn.00884.2006.

Hevers, W., and Lüddens, H. (1998). The diversity of GABAA receptors. *Molecular neurobiology* 18(1), 35-86.

Hipp, J.F., Knoflach, F., Comley, R., Ballard, T.M., Honer, M., Trube, G., et al. (2021). Basmisanil, a highly selective GABA(A)-α5 negative allosteric modulator: preclinical pharmacology and demonstration of functional target engagement in man. *Sci Rep* 11(1), 7700. doi: 10.1038/s41598-021-87307-7.

His, W. (1904). *Die Entwickelung des menschlichen Gehirns: während der ersten Monate.* S. Hirzel.

Hoffman, W.H., and Haberly, L.B. (1993). Role of synaptic excitation in the generation of bursting-induced epileptiform potentials in the endopiriform nucleus and piriform cortex. *J Neurophysiol* 70(6), 2550-2561. doi: 10.1152/jn.1993.70.6.2550.

Hoffman, W.H., and Haberly, L.B. (1996). Kindling-induced epileptiform potentials in piriform cortex slices originate in the underlying endopiriform nucleus. *J Neurophysiol* 76(3), 1430-1438. doi: 10.1152/jn.1996.76.3.1430.

Höglinger, G.U., Rizk, P., Muriel, M.P., Duyckaerts, C., Oertel, W.H., Caille, I., et al. (2004). Dopamine depletion impairs precursor cell proliferation in Parkinson disease. *Nat Neurosci* 7(7), 726-735. doi: 10.1038/nn1265.

Hollmann, M., O'Shea-Greenfield, A., Rogers, S.W., and Heinemann, S. (1989). Cloning by functional expression of a member of the glutamate receptor family. *Nature* 342(6250), 643-648. doi: 10.1038/342643a0.

Holmberg, M., Fagerholm, V., and Scheinin, M. (2003). Regional distribution of alpha(2C)-adrenoceptors in brain and spinal cord of control mice and transgenic mice overexpressing the alpha(2C)-subtype: an autoradiographic study with [(3)H]RX821002 and [(3)H]rauwolscine. *Neuroscience* 117(4), 875-898. doi: 10.1016/s0306-4522(02)00966-1.

Hoshino, T., Nagashima, T., Cho, K.G., Davis, R.L., Donegan, J., Slusarz, M., et al. (1989). Variability in the proliferative potential of human gliomas. *J Neurooncol* 7(2), 137-143. doi: 10.1007/bf00165098.

Houamed, K.M., Kuijper, J.L., Gilbert, T.L., Haldeman, B.A., O'Hara, P.J., Mulvihill, E.R., et al. (1991). Cloning, expression, and gene structure of a G protein-coupled glutamate receptor from rat brain. *Science* 252(5010), 1318-1321. doi: 10.1126/science.1656524.

Howard, J.D., Plailly, J., Grueschow, M., Haynes, J.D., and Gottfried, J.A. (2009). Odor quality coding and categorization in human posterior piriform cortex. *Nat Neurosci* 12(7), 932-938. doi: 10.1038/nn.2324.

Hu, M., Sun, Y.J., Zhou, Q.G., Auberson, Y.P., Chen, L., Hu, Y., et al. (2009). Reduced spatial learning in mice treated with NVP-AAM077 through down-regulating neurogenesis. *Eur J Pharmacol* 622(1-3), 37-44. doi: 10.1016/j.ejphar.2009.09.031.

Hu, M., Sun, Y.J., Zhou, Q.G., Chen, L., Hu, Y., Luo, C.X., et al. (2008). Negative regulation of neurogenesis and spatial memory by NR2B-containing NMDA receptors. *J Neurochem* 106(4), 1900-1913. doi: 10.1111/j.1471-4159.2008.05554.x.

Huang, G.Z., Taniguchi, M., Zhou, Y.B., Zhang, J.J., Okutani, F., Murata, Y., et al. (2018). α(2)-Adrenergic receptor activation promotes long-term potentiation at excitatory synapses in the mouse accessory olfactory bulb. *Learn Mem* 25(4), 147-157. doi: 10.1101/lm.046391.117.

Hunt, W.A. (1983). The effect of ethanol on GABAergic transmission. *Neurosci Biobehav Rev* 7(1), 87-95. doi: 10.1016/0149-7634(83)90009-x.

Hurtubise, J.L., Marks, W.N., Davies, D.A., Catton, J.K., Baker, G.B., and Howland, J.G. (2017). MK-801-induced impairments on the trial-unique, delayed nonmatching-to-location task in rats: effects of acute sodium nitroprusside. *Psychopharmacology (Berl)* 234(2), 211-222. doi: 10.1007/s00213-016-4451-2.

Hyer, M.M., Khantsis, S., Venezia, A.C., Madison, F.N., Hallgarth, L., Adekola, E., et al. (2017). Estrogen-dependent modifications to hippocampal plasticity in paternal California mice (Peromyscus californicus). *Horm Behav* 96, 147-155. doi: 10.1016/j.yhbeh.2017.09.015.

Hyer, M.M., Phillips, L.L., and Neigh, G.N. (2018). Sex Differences in Synaptic Plasticity: Hormones and Beyond. *Front Mol Neurosci* 11, 266. doi: 10.3389/fnmol.2018.00266.

Ihrie, R.A., and Alvarez-Buylla, A. (2011). Lake-front property: a unique germinal niche by the lateral ventricles of the adult brain. *Neuron* 70(4), 674-686. doi: 10.1016/j.neuron.2011.05.004.

Ikemoto, S. (2007). Dopamine reward circuitry: two projection systems from the ventral midbrain to the nucleus accumbens-olfactory tubercle complex. *Brain Res Rev* 56(1), 27-78. doi: 10.1016/j.brainresrev.2007.05.004.

Illig, K.R. (2006). Projections from orbitofrontal cortex to anterior piriform cortex in the rat suggest a role in olfactory information processing. *The Journal of comparative neurology* 488(2), 224-231. doi: 10.1002/cne.20595.

Imamura, F., Ayoub, A.E., Rakic, P., and Greer, C.A. (2011). Timing of neurogenesis is a determinant of olfactory circuitry. *Nat Neurosci* 14(3), 331-337. doi: 10.1038/nn.2754.

Insausti, R., Amaral, D.G., and Cowan, W.M. (1987). The entorhinal cortex of the monkey: II. Cortical afferents. *J Comp Neurol* 264(3), 356-395. doi: 10.1002/cne.902640306.

Izquierdo, I., and Medina, J.H. (1991). GABAA receptor modulation of memory: the role of endogenous benzodiazepines. *Trends Pharmacol Sci* 12(7), 260-265. doi: 10.1016/0165-6147(91)90567-c.

Jacek, S., Stevenson, R.J., and Miller, L.A. (2007). Olfactory dysfunction in temporal lobe epilepsy: a case of ictus-related parosmia. *Epilepsy Behav* 11(3), 466-470. doi: 10.1016/j.yebeh.2007.05.016.

Jacob, T.C., Michels, G., Silayeva, L., Haydon, J., Succol, F., and Moss, S.J. (2012). Benzodiazepine treatment induces subtype-specific changes in GABA(A) receptor trafficking and decreases synaptic inhibition. *Proc Natl Acad Sci U S A* 109(45), 18595-18600. doi: 10.1073/pnas.1204994109.

Jacobson, L., Trotier, D., and Døving, K.B. (1998). Anatomical description of a new organ in the nose of domesticated animals by Ludvig Jacobson (1813). *Chem Senses* 23(6), 743-754. doi: 10.1093/chemse/23.6.743.

Jacobson, L.H., Bettler, B., Kaupmann, K., and Cryan, J.F. (2007). Behavioral evaluation of mice deficient in GABA(B(1)) receptor isoforms in tests of unconditioned anxiety. *Psychopharmacology (Berl)* 190(4), 541-553. doi: 10.1007/s00213-006-0631-9.

Jansen, K.L., Faull, R.L., Dragunow, M., and Synek, B.L. (1990). Alzheimer's disease: changes in hippocampal N-methyl-D-aspartate, quisqualate, neurotensin, adenosine, benzodiazepine, serotonin and opioid receptors--an autoradiographic study. *Neuroscience* 39(3), 613-627. doi: 10.1016/0306-4522(90)90246-z.

Jhaveri, D.J., Nanavaty, I., Prosper, B.W., Marathe, S., Husain, B.F., Kernie, S.G., et al. (2014). Opposing effects of α2- and β-adrenergic receptor stimulation on quiescent neural precursor cell activity and adult hippocampal neurogenesis. *PLoS One* 9(6), e98736. doi: 10.1371/journal.pone.0098736.

Jia, C., and Halpern, M. (1997). Segregated populations of mitral/tufted cells in the accessory olfactory bulb. *Neuroreport* 8(8), 1887-1890. doi: 10.1097/00001756-199705260-00019.

Jin, J., Kang, H.M., and Park, C. (2010). Voluntary exercise enhances survival and migration of neural progenitor cells after intracerebral haemorrhage in mice. *Brain Inj* 24(3), 533-540. doi: 10.3109/02699051003610458.

Jin, K., Zhu, Y., Sun, Y., Mao, X.O., Xie, L., and Greenberg, D.A. (2002). Vascular endothelial growth factor (VEGF) stimulates neurogenesis in vitro and in vivo. *Proc Natl Acad Sci U S A* 99(18), 11946-11950. doi: 10.1073/pnas.182296499.

Johnson, D.M., Illig, K.R., Behan, M., and Haberly, L.B. (2000). New features of connectivity in piriform cortex visualized by intracellular injection of pyramidal cells suggest that "primary" olfactory cortex functions like "association" cortex in other sensory systems. *J Neurosci* 20(18), 6974-6982. doi: 10.1523/jneurosci.20-18-06974.2000.

Johnson, J.W., and Ascher, P. (1987). Glycine potentiates the NMDA response in cultured mouse brain neurons. *Nature* 325(6104), 529-531. doi: 10.1038/325529a0.

Johnson, T.N., Rosvold, H.E., and Mishkin, M. (1968). Projections from behaviorally-defined sectors of the prefrontal cortex to the basal ganglia, septum, and diencephalon of the monkey. *Exp Neurol* 21(1), 20-34. doi: 10.1016/0014-4886(68)90030-7.

Jones-Gotman, M., and Zatorre, R.J. (1988). Olfactory identification deficits in patients with focal cerebral excision. *Neuropsychologia* 26(3), 387-400. doi: 10.1016/0028-3932(88)90093-0.

Jordens, K. (2012). Untersuchung zur Veränderung von kognitiven Funktionen nach Hemmung der adulten Neurogenese im Hippocampus der Maus. *Masterarbeit*.

Jurkowski, M.P., Bettio, L., E, K.W., Patten, A., Yau, S.Y., and Gil-Mohapel, J. (2020). Beyond the Hippocampus and the SVZ: Adult Neurogenesis Throughout the Brain. *Front Cell Neurosci* 14, 576444. doi: 10.3389/fncel.2020.576444.

Kahnt, T., and Tobler, P.N. (2017). Dopamine Modulates the Functional Organization of the Orbitofrontal Cortex. *J Neurosci* 37(6), 1493-1504. doi: 10.1523/jneurosci.2827-16.2016.

Kaplan, M.S., and Hinds, J.W. (1977). Neurogenesis in the adult rat: electron microscopic analysis of light radioautographs. *Science* 197(4308), 1092-1094. doi: 10.1126/science.887941.

Karkoulias, G., Mastrogianni, O., Ilias, I., Lymperopoulos, A., Taraviras, S., Tsopanoglou, N., et al. (2006). Alpha 2-adrenergic receptors decrease DNA replication and cell proliferation and induce neurite outgrowth in transfected rat pheochromocytoma cells. *Ann N Y Acad Sci* 1088, 335-345. doi: 10.1196/annals.1366.017.

Kebabian, J.W., and Calne, D.B. (1979). Multiple receptors for dopamine. *Nature* 277(5692), 93-96. doi: 10.1038/277093a0.

Kelsch, W., Li, Z., Eliava, M., Goengrich, C., and Monyer, H. (2012). GluN2B-containing NMDA receptors promote wiring of adult-born neurons into olfactory bulb circuits. *J Neurosci* 32(36), 12603-12611. doi: 10.1523/jneurosci.1459-12.2012.

Kempermann, G., Gast, D., Kronenberg, G., Yamaguchi, M., and Gage, F.H. (2003). Early determination and long-term persistence of adult-generated new neurons in the hippocampus of mice. *Development* 130(2), 391-399. doi: 10.1242/dev.00203.

Kempermann, G., Song, H., and Gage, F.H. (2015). Neurogenesis in the Adult Hippocampus. *Cold Spring Harb Perspect Biol* 7(9), a018812. doi: 10.1101/cshperspect.a018812.

Kikuta, S., Sato, K., Kashiwadani, H., Tsunoda, K., Yamasoba, T., and Mori, K. (2010). From the Cover: Neurons in the anterior olfactory nucleus pars externa detect right or left localization of odor sources. *Proc Natl Acad Sci U S A* 107(27), 12363-12368. doi: 10.1073/pnas.1003999107.

Kiuchi, Y., Kobayashi, T., Takeuchi, J., Shimizu, H., Ogata, H., and Toru, M. (1989). Benzodiazepine receptors increase in post-mortem brain of chronic schizophrenics. *Eur Arch Psychiatry Neurol Sci* 239(2), 71-78. doi: 10.1007/bf01759578.

Knable, M.B., Hyde, T.M., Herman, M.M., Carter, J.M., Bigelow, L., and Kleinman, J.E. (1994). Quantitative autoradiography of dopamine-D1 receptors, D2 receptors, and dopamine uptake sites in postmortem striatal specimens from schizophrenic patients. *Biol Psychiatry* 36(12), 827-835. doi: 10.1016/0006-3223(94)90593-2.

Kornack, D.R., and Rakic, P. (1999). Continuation of neurogenesis in the hippocampus of the adult macaque monkey. *Proc Natl Acad Sci U S A* 96(10), 5768-5773. doi: 10.1073/pnas.96.10.5768.

Krettek, J.E., and Price, J.L. (1977). Projections from the amygdaloid complex and adjacent olfactory structures to the entorhinal cortex and to the subiculum in the rat and cat. *J Comp Neurol* 172(4), 723-752. doi: 10.1002/cne.901720409.

Kronenberg, G., Bick-Sander, A., Bunk, E., Wolf, C., Ehninger, D., and Kempermann, G. (2006). Physical exercise prevents age-related decline in precursor cell activity in the mouse dentate gyrus. *Neurobiol Aging* 27(10), 1505-1513. doi: 10.1016/j.neurobiolaging.2005.09.016.

Kuhar, M.J., Pert, C.B., and Snyder, S.H. (1973). Regional distribution of opiate receptor binding in monkey and human brain. *Nature* 245(5426), 447-450. doi: 10.1038/245447a0.

Kumar, G., Olley, J., Steckler, T., and Talpos, J. (2015). Dissociable effects of NR2A and NR2B NMDA receptor antagonism on cognitive flexibility but not pattern separation. *Psychopharmacology (Berl)* 232(21-22), 3991-4003. doi: 10.1007/s00213-015-4008-9.

Kwakowsky, A., Calvo-Flores Guzmán, B., Pandya, M., Turner, C., Waldvogel, H.J., and Faull, R.L. (2018). GABA(A) receptor subunit expression changes in the human Alzheimer's disease hippocampus, subiculum, entorhinal cortex and superior temporal gyrus. *J Neurochem* 145(5), 374-392. doi: 10.1111/jnc.14325.

Lal, H., Kumar, B., and Forster, M.J. (1988). Enhancement of learning and memory in mice by a benzodiazepine antagonist. *Faseb j* 2(11), 2707-2711. doi: 10.1096/fasebj.2.11.3135223.

Larriva-Sahd, J. (2008). The accessory olfactory bulb in the adult rat: a cytological study of its cell types, neuropil, neuronal modules, and interactions with the main olfactory system. *J Comp Neurol* 510(3), 309-350. doi: 10.1002/cne.21790.

LaSarge, C.L., Bañuelos, C., Mayse, J.D., and Bizon, J.L. (2009). Blockade of GABA(B) receptors completely reverses age-related learning impairment. *Neuroscience* 164(3), 941-947. doi: 10.1016/j.neuroscience.2009.08.055.

LaSarge, C.L., Montgomery, K.S., Tucker, C., Slaton, G.S., Griffith, W.H., Setlow, B., et al. (2007). Deficits across multiple cognitive domains in a subset of aged Fischer 344 rats. *Neurobiol Aging* 28(6), 928-936. doi: 10.1016/j.neurobiolaging.2006.04.010.

Lauterborn, J.C., Lynch, G., Vanderklish, P., Arai, A., and Gall, C.M. (2000). Positive modulation of AMPA receptors increases neurotrophin expression by hippocampal and cortical neurons. *J Neurosci* 20(1), 8-21. doi: 10.1523/jneurosci.20-01-00008.2000.

Lazarini, F., and Lledo, P.M. (2011). Is adult neurogenesis essential for olfaction? *Trends Neurosci* 34(1), 20-30. doi: 10.1016/j.tins.2010.09.006.

Lazic, S.E., Goodman, A.O., Grote, H.E., Blakemore, C., Morton, A.J., Hannan, A.J., et al. (2007). Olfactory abnormalities in Huntington's disease: decreased plasticity in the primary olfactory cortex of R6/1 transgenic mice and reduced olfactory discrimination in patients. *Brain Res* 1151, 219-226. doi: 10.1016/j.brainres.2007.03.018.

Lee, A., Kessler, J.D., Read, T.A., Kaiser, C., Corbeil, D., Huttner, W.B., et al. (2005). Isolation of neural stem cells from the postnatal cerebellum. *Nat Neurosci* 8(6), 723-729. doi: 10.1038/nn1473.

Lee, D.A., and Blackshaw, S. (2012). Functional implications of hypothalamic neurogenesis in the adult mammalian brain. *Int J Dev Neurosci* 30(8), 615-621. doi: 10.1016/j.ijdevneu.2012.07.003.

Lee, S.Y. (2016). Temozolomide resistance in glioblastoma multiforme. *Genes Dis* 3(3), 198-210. doi: 10.1016/j.gendis.2016.04.007.

Lee, Y.H., Bak, Y., Park, C.H., Chung, S.J., Yoo, H.S., Baik, K., et al. (2020). Patterns of olfactory functional networks in Parkinson's disease dementia and Alzheimer's dementia. *Neurobiol Aging* 89, 63-70. doi: 10.1016/j.neurobiolaging.2019.12.021.

Leeman-Markowski, B.A., and Schachter, S.C. (2017). Cognitive and Behavioral Interventions in Epilepsy. *Curr Neurol Neurosci Rep* 17(5), 42. doi: 10.1007/s11910-017-0752-z.

Leitner, F.C., Melzer, S., Lutcke, H., Pinna, R., Seeburg, P.H., Helmchen, F., et al. (2016). Spatially segregated feedforward and feedback neurons support differential odor processing in the lateral entorhinal cortex. *Nat Neurosci* 19(7), 935-944. doi: 10.1038/nn.4303.

Lester, R.A., Clements, J.D., Westbrook, G.L., and Jahr, C.E. (1990). Channel kinetics determine the time course of NMDA receptor-mediated synaptic currents. *Nature* 346(6284), 565-567. doi: 10.1038/346565a0.

Lethbridge, R., Hou, Q., Harley, C.W., and Yuan, Q. (2012). Olfactory bulb glomerular NMDA receptors mediate olfactory nerve potentiation and odor preference learning in the neonate rat. *PLoS One* 7(4), e35024. doi: 10.1371/journal.pone.0035024.

Leuner, B., Glasper, E.R., and Gould, E. (2010). Sexual experience promotes adult neurogenesis in the hippocampus despite an initial elevation in stress hormones. *PLoS One* 5(7), e11597. doi: 10.1371/journal.pone.0011597.

Lewis, M.C., and Gould, T.J. (2007). Reversible inactivation of the entorhinal cortex disrupts the establishment and expression of latent inhibition of cued fear conditioning in C57BL/6 mice. *Hippocampus* 17(6), 462-470. doi: 10.1002/hipo.20284.

Li, P., Stewart, R., Butler, A., Gonzalez-Cota, A.L., Harmon, S., and Salkoff, L. (2017). GABA-B Controls Persistent Na(+) Current and Coupled Na(+)-Activated K(+) Current. *eNeuro* 4(3). doi: 10.1523/eneuro.0114-17.2017.

Li, Y., Huang, X.F., Deng, C., Meyer, B., Wu, A., Yu, Y., et al. (2010). Alterations in 5-HT2A receptor binding in various brain regions among 6-hydroxydopamine-induced Parkinsonian rats. *Synapse* 64(3), 224-230. doi: 10.1002/syn.20722.

Liang, K.C., Hon, W., Tyan, Y.M., and Liao, W.L. (1994). Involvement of hippocampal NMDA and AMPA receptors in acquisition, formation and retrieval of spatial memory in the Morris water maze. *Chin J Physiol* 37(4), 201-212.

Licht, T., and Keshet, E. (2015). The vascular niche in adult neurogenesis. *Mech Dev* 138 Pt 1, 56-62. doi: 10.1016/j.mod.2015.06.001.

Limbird, L.E. (1988). Receptors linked to inhibition of adenylate cyclase: additional signaling mechanisms. *Faseb j* 2(11), 2686-2695. doi: 10.1096/fasebj.2.11.2840317.

Linster, C., and Hasselmo, M.E. (2001). Neuromodulation and the functional dynamics of piriform cortex. *Chem Senses* 26(5), 585-594. doi: 10.1093/chemse/26.5.585.

Linster, C., Nai, Q., and Ennis, M. (2011). Nonlinear effects of noradrenergic modulation of olfactory bulb function in adult rodents. *J Neurophysiol* 105(4), 1432-1443. doi: 10.1152/jn.00960.2010.

Lipton, P.A., Alvarez, P., and Eichenbaum, H. (1999). Crossmodal associative memory representations in rodent orbitofrontal cortex. *Neuron* 22(2), 349-359. doi: 10.1016/s0896-6273(00)81095-8.

Liu, L., Zhao, L., She, H., Chen, S., Wang, J.M., Wong, C., et al. (2010). Clinically relevant progestins regulate neurogenic and neuroprotective responses in vitro and in vivo. *Endocrinology* 151(12), 5782-5794. doi: 10.1210/en.2010-0005.

Liu, X., Wang, Q., Haydar, T.F., and Bordey, A. (2005). Nonsynaptic GABA signaling in postnatal subventricular zone controls proliferation of GFAP-expressing progenitors. *Nat Neurosci* 8(9), 1179-1187. doi: 10.1038/nn1522.

Lois, C., and Alvarez-Buylla, A. (1993). Proliferating subventricular zone cells in the adult mammalian forebrain can differentiate into neurons and glia. *Proc Natl Acad Sci U S A* 90(5), 2074-2077. doi: 10.1073/pnas.90.5.2074.

Lothmann, K., Amunts, K., and Herold, C. (2021). The Neurotransmitter Receptor Architecture of the Mouse Olfactory System. *Front Neuroanat* 15, 632549. doi: 10.3389/fnana.2021.632549.

Lothmann, K., Deitersen, J., Zilles, K., Amunts, K., and Herold, C. (2020). New boundaries and dissociation of the mouse hippocampus along the dorsal-ventral axis based on glutamatergic, GABAergic and catecholaminergic receptor densities. *Hippocampus* n/a(n/a). doi: 10.1002/hipo.23262.

Louissaint, A., Jr., Rao, S., Leventhal, C., and Goldman, S.A. (2002). Coordinated interaction of neurogenesis and angiogenesis in the adult songbird brain. *Neuron* 34(6), 945-960. doi: 10.1016/s0896-6273(02)00722-5.

Lowry, E.R., Kruyer, A., Norris, E.H., Cederroth, C.R., and Strickland, S. (2013). The GluK4 kainate receptor subunit regulates memory, mood, and excitotoxic neurodegeneration. *Neuroscience* 235, 215-225. doi: 10.1016/j.neuroscience.2013.01.029.

Lucantonio, F., Gardner, M.P., Mirenzi, A., Newman, L.E., Takahashi, Y.K., and Schoenbaum, G. (2015). Neural Estimates of Imagined Outcomes in Basolateral Amygdala Depend on Orbitofrontal Cortex. *J Neurosci* 35(50), 16521-16530. doi: 10.1523/jneurosci.3126-15.2015.

Luskin, M.B., and Price, J.L. (1983). The topographic organization of associational fibers of the olfactory system in the rat, including centrifugal fibers to the olfactory bulb. *J Comp Neurol* 216(3), 264-291. doi: 10.1002/cne.902160305.

Maejima, T., Masseck, O.A., Mark, M.D., and Herlitze, S. (2013). Modulation of firing and synaptic transmission of serotonergic neurons by intrinsic G protein-coupled receptors and ion channels. *Front Integr Neurosci* 7, 40. doi: 10.3389/fnint.2013.00040.

Mahmoud, R., Wainwright, S.R., and Galea, L.A. (2016). Sex hormones and adult hippocampal neurogenesis: Regulation, implications, and potential mechanisms. *Front Neuroendocrinol* 41, 129-152. doi: 10.1016/j.yfrne.2016.03.002.

Majak, K., and Moryś, J. (2007). Endopiriform nucleus connectivities: the implications for epileptogenesis and epilepsy. *Folia Morphol (Warsz)* 66(4), 267-271.

Mak, G.K., Enwere, E.K., Gregg, C., Pakarainen, T., Poutanen, M., Huhtaniemi, I., et al. (2007). Male pheromone-stimulated neurogenesis in the adult female brain: possible role in mating behavior. *Nat Neurosci* 10(8), 1003-1011. doi: 10.1038/nn1928.

Malberg, J.E., Eisch, A.J., Nestler, E.J., and Duman, R.S. (2000). Chronic antidepressant treatment increases neurogenesis in adult rat hippocampus. *J Neurosci* 20(24), 9104-9110. doi: 10.1523/jneurosci.20-24-09104.2000.

Mandairon, N., Peace, S., Karnow, A., Kim, J., Ennis, M., and Linster, C. (2008). Noradrenergic modulation in the olfactory bulb influences spontaneous and reward-motivated discrimination, but not the formation of habituation memory. *Eur J Neurosci* 27(5), 1210-1219. doi: 10.1111/j.1460-9568.2008.06101.x.

Mandyam, C.D., Crawford, E.F., Eisch, A.J., Rivier, C.L., and Richardson, H.N. (2008). Stress experienced in utero reduces sexual dichotomies in neurogenesis, microenvironment, and cell death in the adult rat hippocampus. *Dev Neurobiol* 68(5), 575-589. doi: 10.1002/dneu.20600.

Mann, E.O., Kohl, M.M., and Paulsen, O. (2009). Distinct roles of GABA(A) and GABA(B) receptors in balancing and terminating persistent cortical activity. *J Neurosci* 29(23), 7513-7518. doi: 10.1523/jneurosci.6162-08.2009.

Markakis, E.A., Palmer, T.D., Randolph-Moore, L., Rakic, P., and Gage, F.H. (2004). Novel neuronal phenotypes from neural progenitor cells. *J Neurosci* 24(12), 2886-2897. doi: 10.1523/jneurosci.4161-03.2004.

Marques, A.A., Bevilaqua, M.C., da Fonseca, A.M., Nardi, A.E., Thuret, S., and Dias, G.P. (2016). Gender Differences in the Neurobiology of Anxiety: Focus on Adult Hippocampal Neurogenesis. *Neural Plast* 2016, 5026713. doi: 10.1155/2016/5026713.

Martín-López, E., Corona, R., and López-Mascaraque, L. (2012). Postnatal characterization of cells in the accessory olfactory bulb of wild type and reeler mice. *Front Neuroanat* 6, 15. doi: 10.3389/fnana.2012.00015.

Marzolini, C., Decosterd, L.A., Shen, F., Gander, M., Leyvraz, S., Bauer, J., et al. (1998). Pharmacokinetics of temozolomide in association with fotemustine in malignant melanoma and malignant glioma patients: comparison of oral, intravenous, and hepatic intra-arterial administration. *Cancer Chemother Pharmacol* 42(6), 433-440. doi: 10.1007/s002800050842.

Mason, D.M., Nouraei, N., Pant, D.B., Miner, K.M., Hutchison, D.F., Luk, K.C., et al. (2016). Transmission of α-synucleinopathy from olfactory structures deep into the temporal lobe. *Mol Neurodegener* 11(1), 49. doi: 10.1186/s13024-016-0113-4.

Mateus-Pinheiro, A., Pinto, L., Bessa, J.M., Morais, M., Alves, N.D., Monteiro, S., et al. (2013). Sustained remission from depressive-like behavior depends on hippocampal neurogenesis. *Transl Psychiatry* 3(1), e210. doi: 10.1038/tp.2012.141.

Mazo, C., Lepousez, G., Nissant, A., Valley, M.T., and Lledo, P.M. (2016). GABAB Receptors Tune Cortical Feedback to the Olfactory Bulb. *J Neurosci* 36(32), 8289-8304. doi: 10.1523/jneurosci.3823-15.2016.

McDonald, A.J., Mascagni, F., and Guo, L. (1996). Projections of the medial and lateral prefrontal cortices to the amygdala: a Phaseolus vulgaris leucoagglutinin study in the rat. *Neuroscience* 71(1), 55-75. doi: 10.1016/0306-4522(95)00417-3.

McGann, J.P. (2017). Poor human olfaction is a 19th-century myth. *Science* 356(6338). doi: 10.1126/science.aam7263.

McGregor, I.S., Hargreaves, G.A., Apfelbach, R., and Hunt, G.E. (2004). Neural correlates of cat odor-induced anxiety in rats: region-specific effects of the benzodiazepine midazolam. *J Neurosci* 24(17), 4134-4144. doi: 10.1523/jneurosci.0187-04.2004.

McKay, R. (1997). Stem cells in the central nervous system. *Science* 276(5309), 66-71. doi: 10.1126/science.276.5309.66.

McNamara, A.M., Magidson, P.D., Linster, C., Wilson, D.A., and Cleland, T.A. (2008). Distinct neural mechanisms mediate olfactory memory formation at different timescales. *Learn Mem* 15(3), 117-125. doi: 10.1101/lm.785608.

McOmish, C.E., Demireva, E.Y., and Gingrich, J.A. (2016). Developmental expression of mGlu2 and mGlu3 in the mouse brain. *Gene Expr Patterns* 22(2), 46-53. doi: 10.1016/j.gep.2016.10.001.

Meisami, E., and Bhatnagar, K.P. (1998). Structure and diversity in mammalian accessory olfactory bulb. *Microsc Res Tech* 43(6), 476-499. doi: 10.1002/(sici)1097-0029(19981215)43:6<476::Aid-jemt2>3.0.Co;2-v.

Melchiorri, D., Cappuccio, I., Ciceroni, C., Spinsanti, P., Mosillo, P., Sarichelou, I., et al. (2007). Metabotropic glutamate receptors in stem/progenitor cells. *Neuropharmacology* 53(4), 473-480. doi: 10.1016/j.neuropharm.2007.05.031.

Meredith, M. (1998). Vomeronasal function. *Chem Senses* 23(4), 463-466. doi: 10.1093/chemse/23.4.463.

Meredith, M. (2001). Human vomeronasal organ function: a critical review of best and worst cases. *Chem Senses* 26(4), 433-445. doi: 10.1093/chemse/26.4.433.

Merker, B. (1983). Silver staining of cell bodies by means of physical development. *J Neurosci Methods* 9(3), 235-241. doi: 10.1016/0165-0270(83)90086-9.

Meyer, E.A., Illig, K.R., and Brunjes, P.C. (2006). Differences in chemo- and cytoarchitectural features within pars principalis of the rat anterior olfactory nucleus suggest functional specialization. *J Comp Neurol* 498(6), 786-795. doi: 10.1002/cne.21077.

Micheli, L., Ceccarelli, M., D'Andrea, G., and Tirone, F. (2018). Depression and adult neurogenesis: Positive effects of the antidepressant fluoxetine and of physical exercise. *Brain Res Bull* 143, 181-193. doi: 10.1016/j.brainresbull.2018.09.002.

Middleton, S., Jalics, J., Kispersky, T., Lebeau, F.E., Roopun, A.K., Kopell, N.J., et al. (2008). NMDA receptor-dependent switching between different gamma rhythm-generating microcircuits in entorhinal cortex. *Proc Natl Acad Sci U S A* 105(47), 18572-18577. doi: 10.1073/pnas.0809302105.

Ming, G.L., and Song, H. (2005). Adult neurogenesis in the mammalian central nervous system. *Annu Rev Neurosci* 28, 223-250. doi: 10.1146/annurev.neuro.28.051804.101459.

Mishra, A., Singh, S., Tiwari, V., Parul, and Shukla, S. (2019). Dopamine D1 receptor activation improves adult hippocampal neurogenesis and exerts anxiolytic and antidepressant-like effect via activation of Wnt/β-catenin pathways in rat model of Parkinson's disease. *Neurochem Int* 122**,** 170-186. doi: 10.1016/j.neuint.2018.11.020.

Missale, C., Nash, S.R., Robinson, S.W., Jaber, M., and Caron, M.G. (1998). Dopamine receptors: from structure to function. *Physiol Rev* 78(1)**,** 189-225. doi: 10.1152/physrev.1998.78.1.189.

Mohedano-Moriano, A., de la Rosa-Prieto, C., Saiz-Sanchez, D., Ubeda-Bañon, I., Pro-Sistiaga, P., de Moya-Pinilla, M., et al. (2012). Centrifugal telencephalic afferent connections to the main and accessory olfactory bulbs. *Front Neuroanat* 6**,** 19. doi: 10.3389/fnana.2012.00019.

Morrison, G.L., Fontaine, C.J., Harley, C.W., and Yuan, Q. (2013). A role for the anterior piriform cortex in early odor preference learning: evidence for multiple olfactory learning structures in the rat pup. *J Neurophysiol* 110(1)**,** 141-152. doi: 10.1152/jn.00072.2013.

Mucignat-Caretta, C. (2010). The rodent accessory olfactory system. *J Comp Physiol A Neuroethol Sens Neural Behav Physiol* 196(10)**,** 767-777. doi: 10.1007/s00359-010-0555-z.

Mukherjee, B., and Yuan, Q. (2016). NMDA receptors in mouse anterior piriform cortex initialize early odor preference learning and L-type calcium channels engage for long-term memory. *Sci Rep* 6**,** 35256. doi: 10.1038/srep35256.

Münster, A., Sommer, S., and Hauber, W. (2020). Dopamine D1 receptors in the medial orbitofrontal cortex support effort-related responding in rats. *Eur Neuropsychopharmacol* 32**,** 136-141. doi: 10.1016/j.euroneuro.2020.01.008.

Murata, K. (2020). Hypothetical Roles of the Olfactory Tubercle in Odor-Guided Eating Behavior. *Front Neural Circuits* 14**,** 577880. doi: 10.3389/fncir.2020.577880.

Murata, K., Kanno, M., Ieki, N., Mori, K., and Yamaguchi, M. (2015). Mapping of Learned Odor-Induced Motivated Behaviors in the Mouse Olfactory Tubercle. *J Neurosci* 35(29)**,** 10581-10599. doi: 10.1523/jneurosci.0073-15.2015.

Murata, K., Kinoshita, T., Fukazawa, Y., Kobayashi, K., Yamanaka, A., Hikida, T., et al. (2019). Opposing Roles of Dopamine Receptor D1- and D2-Expressing Neurons in the Anteromedial Olfactory Tubercle in Acquisition of Place Preference in Mice. *Front Behav Neurosci* 13**,** 50. doi: 10.3389/fnbeh.2019.00050.

Murphy, G.J., Darcy, D.P., and Isaacson, J.S. (2005). Intraglomerular inhibition: signaling mechanisms of an olfactory microcircuit. *Nat Neurosci* 8(3)**,** 354-364. doi: 10.1038/nn1403.

Nacher, J., and McEwen, B.S. (2006). The role of N-methyl-D-asparate receptors in neurogenesis. *Hippocampus* 16(3)**,** 267-270. doi: 10.1002/hipo.20160.

Nai, Q., Dong, H.W., Hayar, A., Linster, C., and Ennis, M. (2009). Noradrenergic regulation of GABAergic inhibition of main olfactory bulb mitral cells varies as a function of concentration and receptor subtype. *J Neurophysiol* 101(5)**,** 2472-2484. doi: 10.1152/jn.91187.2008.

Nai, Q., Dong, H.W., Linster, C., and Ennis, M. (2010). Activation of alpha1 and alpha2 noradrenergic receptors exert opposing effects on excitability of main olfactory bulb granule cells. *Neuroscience* 169(2)**,** 882-892. doi: 10.1016/j.neuroscience.2010.05.010.

Nguyen, L., Malgrange, B., Breuskin, I., Bettendorff, L., Moonen, G., Belachew, S., et al. (2003). Autocrine/paracrine activation of the GABA(A) receptor inhibits the proliferation of neurogenic polysialylated neural cell adhesion molecule-positive (PSA-NCAM+) precursor cells from postnatal striatum. *J Neurosci* 23(8), 3278-3294. doi: 10.1523/jneurosci.23-08-03278.2003.

Nibber, A., Mann, E.O., Pettingill, P., Waters, P., Irani, S.R., Kullmann, D.M., et al. (2017). Pathogenic potential of antibodies to the GABA(B) receptor. *Epilepsia Open* 2(3), 355-359. doi: 10.1002/epi4.12067.

Nicolle, M.M., Bizon, J.L., and Gallagher, M. (1996). In vitro autoradiography of ionotropic glutamate receptors in hippocampus and striatum of aged Long-Evans rats: relationship to spatial learning. *Neuroscience* 74(3), 741-756. doi: 10.1016/0306-4522(96)00147-9.

Nigri, A., Ferraro, S., D'Incerti, L., Critchley, H.D., Bruzzone, M.G., and Minati, L. (2013). Connectivity of the amygdala, piriform, and orbitofrontal cortex during olfactory stimulation: a functional MRI study. *Neuroreport* 24(4), 171-175. doi: 10.1097/WNR.0b013e32835d5d2b.

Niswender, C.M., and Conn, P.J. (2010). Metabotropic glutamate receptors: physiology, pharmacology, and disease. *Annu Rev Pharmacol Toxicol* 50, 295-322. doi: 10.1146/annurev.pharmtox.011008.145533.

Niswender, C.M., Johnson, K.A., Luo, Q., Ayala, J.E., Kim, C., Conn, P.J., et al. (2008). A novel assay of Gi/o-linked G protein-coupled receptor coupling to potassium channels provides new insights into the pharmacology of the group III metabotropic glutamate receptors. *Mol Pharmacol* 73(4), 1213-1224. doi: 10.1124/mol.107.041053.

O'Keeffe, G.C., Barker, R.A., and Caldwell, M.A. (2009). Dopaminergic modulation of neurogenesis in the subventricular zone of the adult brain. *Cell Cycle* 8(18), 2888-2894. doi: 10.4161/cc.8.18.9512.

Oboti, L., Russo, E., Tran, T., Durstewitz, D., and Corbin, J.G. (2018). Amygdala Corticofugal Input Shapes Mitral Cell Responses in the Accessory Olfactory Bulb. 5(3), ENEURO.0175-0118.2018. doi: 10.1523/ENEURO.0175-18.2018 %J eneuro.

Ohishi, H., Shigemoto, R., Nakanishi, S., and Mizuno, N. (1993). Distribution of the messenger RNA for a metabotropic glutamate receptor, mGluR2, in the central nervous system of the rat. *Neuroscience* 53(4), 1009-1018. doi: 10.1016/0306-4522(93)90485-x.

Ohm, T.G., and Braak, H. (1987). Olfactory bulb changes in Alzheimer's disease. *Acta Neuropathol* 73(4), 365-369. doi: 10.1007/bf00688261.

Olpe, H.R., Wörner, W., and Ferrat, T. (1993). Stimulation parameters determine role of GABAB receptors in long-term potentiation. *Experientia* 49(6-7), 542-546. doi: 10.1007/bf01955159.

Ongür, D., and Price, J.L. (2000). The organization of networks within the orbital and medial prefrontal cortex of rats, monkeys and humans. *Cereb Cortex* 10(3), 206-219. doi: 10.1093/cercor/10.3.206.

Ormerod, B.K., Lee, T.T., and Galea, L.A. (2004). Estradiol enhances neurogenesis in the dentate gyri of adult male meadow voles by increasing the survival of young granule neurons. *Neuroscience* 128(3), 645-654. doi: 10.1016/j.neuroscience.2004.06.039.

Orsini, C.A., Trotta, R.T., Bizon, J.L., and Setlow, B. (2015). Dissociable roles for the basolateral amygdala and orbitofrontal cortex in decision-making under risk of punishment. *J Neurosci* 35(4), 1368-1379. doi: 10.1523/jneurosci.3586-14.2015.

Ottersen, O.P. (1982). Connections of the amygdala of the rat. IV: Corticoamygdaloid and intraamygdaloid connections as studied with axonal transport of horseradish peroxidase. *J Comp Neurol* 205(1), 30-48. doi: 10.1002/cne.902050104.

Owens, N.C., and Verberne, A.J. (2001). Regional haemodynamic responses to activation of the medial prefrontal cortex depressor region. *Brain Res* 919(2), 221-231. doi: 10.1016/s0006-8993(01)03017-7.

Ozawa, S., Kamiya, H., and Tsuzuki, K. (1998). Glutamate receptors in the mammalian central nervous system. *Prog Neurobiol* 54(5), 581-618. doi: 10.1016/s0301-0082(97)00085-3.

Pallotto, M., and Deprez, F. (2014). Regulation of adult neurogenesis by GABAergic transmission: signaling beyond GABAA-receptors. *Front Cell Neurosci* 8, 166. doi: 10.3389/fncel.2014.00166.

Palomero-Gallagher, N., Bidmon, H.J., Cremer, M., Schleicher, A., Kircheis, G., Reifenberger, G., et al. (2009). Neurotransmitter receptor imbalances in motor cortex and basal ganglia in hepatic encephalopathy. *Cell Physiol Biochem* 24(3-4), 291-306. doi: 10.1159/000233254.

Palomero-Gallagher, N., Bidmon, H.J., and Zilles, K. (2003). AMPA, kainate, and NMDA receptor densities in the hippocampus of untreated male rats and females in estrus and diestrus. *J Comp Neurol* 459(4), 468-474. doi: 10.1002/cne.10638.

Palomero-Gallagher, N., and Zilles, K. (2018). Cyto- and receptor architectonic mapping of the human brain. *Handb Clin Neurol* 150, 355-387. doi: 10.1016/b978-0-444-63639-3.00024-4.

Pałucha-Poniewiera, A., Podkowa, K., and Rafało-Ulińska, A. (2021). The group II mGlu receptor antagonist LY341495 induces a rapid antidepressant-like effect and enhances the effect of ketamine in the chronic unpredictable mild stress model of depression in C57BL/6J mice. *Prog Neuropsychopharmacol Biol Psychiatry* 109, 110239. doi: 10.1016/j.pnpbp.2020.110239.

Panzanelli, P., Perazzini, A., Fritschy, J.-M., and Sassoè-Pognetto, M. (2005). Heterogeneity of GABAA receptor subtypes in mitral and tufted cells of the rat main olfactory bulb. *The Journal of comparative neurology* 484, 121-131. doi: 10.1002/cne.20440.

Papay, R., Gaivin, R., Jha, A., McCune, D.F., McGrath, J.C., Rodrigo, M.C., et al. (2006). Localization of the mouse alpha1A-adrenergic receptor (AR) in the brain: alpha1AAR is expressed in neurons, GABAergic interneurons, and NG2 oligodendrocyte progenitors. *J Comp Neurol* 497(2), 209-222. doi: 10.1002/cne.20992.

Parent, J.M., Jessberger, S., Gage, F.H., and Gong, C. (2007). Is neurogenesis reparative after status epilepticus? *Epilepsia* 48 Suppl 8, 69-71. doi: 10.1111/j.1528-1167.2007.01355.x.

Pasquini, J., and Pavese, N. (2021). Striatal dopaminergic denervation and hypomimia in Parkinson's disease. *Eur J Neurol* 28(1), e2-e3. doi: 10.1111/ene.14483.

Paxinos, G., Watson, C.R., and Emson, P.C. (1980). AChE-stained horizontal sections of the rat brain in stereotaxic coordinates. *Journal of neuroscience methods* 3(2), 129-149.

Perez-Lloret, S., and Barrantes, F.J. (2016). Deficits in cholinergic neurotransmission and their clinical correlates in Parkinson's disease. *NPJ Parkinsons Dis* 2, 16001. doi: 10.1038/npjparkd.2016.1.

Pérez-Martín, M., Cifuentes, M., Grondona, J.M., López-Avalos, M.D., Gómez-Pinedo, U., García-Verdugo, J.M., et al. (2010). IGF-I stimulates neurogenesis in the hypothalamus of adult rats. *Eur J Neurosci* 31(9), 1533-1548. doi: 10.1111/j.1460-9568.2010.07220.x.

Peters, J., Kalivas, P.W., and Quirk, G.J. (2009). Extinction circuits for fear and addiction overlap in prefrontal cortex. *Learn Mem* 16(5), 279-288. doi: 10.1101/lm.1041309.

Petralia, R.S., and Wenthold, R.J. (1992). Light and electron immunocytochemical localization of AMPA-selective glutamate receptors in the rat brain. *J Comp Neurol* 318(3), 329-354. doi: 10.1002/cne.903180309.

Petralia, R.S., Yokotani, N., and Wenthold, R.J. (1994). Light and electron microscope distribution of the NMDA receptor subunit NMDAR1 in the rat nervous system using a selective anti-peptide antibody. *J Neurosci* 14(2), 667-696. doi: 10.1523/jneurosci.14-02-00667.1994.

Peyron, C., Petit, J.-M., Rampon, C., Jouvet, M., and Luppi, P.-H. (1997). Forebrain afferents to the rat dorsal raphe nucleus demonstrated by retrograde and anterograde tracing methods. *Neuroscience* 82(2), 443-468.

Pigache, R.M. (1970). The anatomy of "paleocortex". A critical review. *Ergeb Anat Entwicklungsgesch* 43(6), 3-62.

Pilc, A., Chaki, S., Nowak, G., and Witkin, J.M. (2008). Mood disorders: regulation by metabotropic glutamate receptors. *Biochem Pharmacol* 75(5), 997-1006. doi: 10.1016/j.bcp.2007.09.021.

Pin, J.P., and Duvoisin, R. (1995). The metabotropic glutamate receptors: structure and functions. *Neuropharmacology* 34(1), 1-26. doi: 10.1016/0028-3908(94)00129-g.

Pinching, A.J., and Powell, T.P. (1971a). The neuron types of the glomerular layer of the olfactory bulb. *J Cell Sci* 9(2), 305-345.

Pinching, A.J., and Powell, T.P. (1971b). The neuropil of the glomeruli of the olfactory bulb. *J Cell Sci* 9(2), 347-377.

Pinching, A.J., and Powell, T.P. (1972). A study of terminal degeneration in the olfactory bulb of the rat. *J Cell Sci* 10(3), 585-619.

Pinheiro, P.S., and Mulle, C. (2008). Presynaptic glutamate receptors: physiological functions and mechanisms of action. *Nat Rev Neurosci* 9(6), 423-436. doi: 10.1038/nrn2379.

Piredda, S., and Gale, K. (1986). Role of excitatory amino acid transmission in the genesis of seizures elicited from the deep prepiriform cortex. *Brain Res* 377(2), 205-210. doi: 10.1016/0006-8993(86)90859-0.

Platel, J.C., and Bordey, A. (2016). The multifaceted subventricular zone astrocyte: From a metabolic and pro-neurogenic role to acting as a neural stem cell. *Neuroscience* 323, 20-28. doi: 10.1016/j.neuroscience.2015.10.053.

Platel, J.C., Dave, K.A., Gordon, V., Lacar, B., Rubio, M.E., and Bordey, A. (2010). NMDA receptors activated by subventricular zone astrocytic glutamate are critical for neuroblast survival prior to entering a synaptic network. *Neuron* 65(6), 859-872. doi: 10.1016/j.neuron.2010.03.009.

Platel, J.C., Heintz, T., Young, S., Gordon, V., and Bordey, A. (2008). Tonic activation of GLUK5 kainate receptors decreases neuroblast migration in whole-mounts of the subventricular zone. *J Physiol* 586(16), 3783-3793. doi: 10.1113/jphysiol.2008.155879.

Platel, J.C., and Kelsch, W. (2013). Role of NMDA receptors in adult neurogenesis: an ontogenetic (re)view on activity-dependent development. *Cell Mol Life Sci* 70(19), 3591-3601. doi: 10.1007/s00018-013-1262-z.

Platel, J.C., Lacar, B., and Bordey, A. (2007). GABA and glutamate signaling: homeostatic control of adult forebrain neurogenesis. *J Mol Histol* 38(4), 303-311. doi: 10.1007/s10735-007-9103-8.

Plested, A.J., and Mayer, M.L. (2007). Structure and mechanism of kainate receptor modulation by anions. *Neuron* 53(6), 829-841. doi: 10.1016/j.neuron.2007.02.025.

Pontes, A., Zhang, Y., and Hu, W. (2013). Novel functions of GABA signaling in adult neurogenesis. *Front Biol (Beijing)* 8(5). doi: 10.1007/s11515-013-1270-2.

Pralong, E., and Magistretti, P.J. (1995). Noradrenaline increases K-conductance and reduces glutamatergic transmission in the mouse entorhinal cortex by activation of alpha 2-adrenoreceptors. *Eur J Neurosci* 7(12), 2370-2378. doi: 10.1111/j.1460-9568.1995.tb01034.x.

Priest, C.A., and Puche, A.C. (2004). GABAB receptor expression and function in olfactory receptor neuron axon growth. *J Neurobiol* 60(2), 154-165. doi: 10.1002/neu.20011.

Raisman, G. (1972). An experimental study of the projection of the amygdala to the accessory olfactory bulb and its relationship to the concept of a dual olfactory system. *Exp Brain Res* 14(4), 395-408. doi: 10.1007/bf00235035.

Ramon y Cajal, S. (1913a). Degeneration and regeneration of the nervous system. *Oxford Univ Press, London*.

Ramon y Cajal, S. (1913b). Degeneration and regeneration of the nervous system. *Oxford Univ Press, London*.

Recabal, A., Caprile, T., and García-Robles, M.L.A. (2017). Hypothalamic Neurogenesis as an Adaptive Metabolic Mechanism. *Front Neurosci* 11, 190. doi: 10.3389/fnins.2017.00190.

Reiner, D.J., Lofaro, O.M., Applebey, S.V., Korah, H., Venniro, M., Cifani, C., et al. (2020). Role of Projections between Piriform Cortex and Orbitofrontal Cortex in Relapse to Fentanyl Seeking after Palatable Food Choice-Induced Voluntary Abstinence. *J Neurosci* 40(12), 2485-2497. doi: 10.1523/jneurosci.2693-19.2020.

Richards, J.G., Schoch, P., Häring, P., Takacs, B., and Möhler, H. (1987). Resolving GABAA/benzodiazepine receptors: cellular and subcellular localization in the CNS with monoclonal antibodies. *J Neurosci* 7(6), 1866-1886. doi: 10.1523/jneurosci.07-06-01866.1987.

Rolls, E.T. (2004). The functions of the orbitofrontal cortex. *Brain Cogn* 55(1), 11-29. doi: 10.1016/s0278-2626(03)00277-x.

Rolls, E.T., and Baylis, L.L. (1994). Gustatory, olfactory, and visual convergence within the primate orbitofrontal cortex. *J Neurosci* 14(9), 5437-5452. doi: 10.1523/jneurosci.14-09-05437.1994.

Rosenkranz, J.A., and Johnston, D. (2006). Dopaminergic regulation of neuronal excitability through modulation of Ih in layer V entorhinal cortex. *J Neurosci* 26(12), 3229-3244. doi: 10.1523/jneurosci.4333-05.2006.

Rothermel, M., and Wachowiak, M. (2014). Functional imaging of cortical feedback projections to the olfactory bulb. *Front Neural Circuits* 8, 73. doi: 10.3389/fncir.2014.00073.

Rudolph, U., and Knoflach, F. (2011). Beyond classical benzodiazepines: novel therapeutic potential of GABAA receptor subtypes. *Nat Rev Drug Discov* 10(9), 685-697. doi: 10.1038/nrd3502.

Rudolph, U., and Möhler, H. (2004). Analysis of GABAA receptor function and dissection of the pharmacology of benzodiazepines and general anesthetics through mouse genetics. *Annu Rev Pharmacol Toxicol* 44**,** 475-498. doi: 10.1146/annurev.pharmtox.44.101802.121429.

Ruffolo, R.R., Jr., Nichols, A.J., Stadel, J.M., and Hieble, J.P. (1993). Pharmacologic and therapeutic applications of alpha 2-adrenoceptor subtypes. *Annu Rev Pharmacol Toxicol* 33**,** 243-279. doi: 10.1146/annurev.pa.33.040193.001331.

Sahay, A., and Hen, R. (2007). Adult hippocampal neurogenesis in depression. *Nat Neurosci* 10(9)**,** 1110-1115. doi: 10.1038/nn1969.

Sahraei, H., Askaripour, M., Esmaeilpour, K., Shahsavari, F., Rajabi, S., and Moradi-Kor, N. (2019). GABA(B) receptor activation ameliorates spatial memory impairments in stress-exposed rats. *Neuropsychiatr Dis Treat* 15**,** 1497-1506. doi: 10.2147/ndt.S205951.

Salazar, I., and Brennan, P.A. (2001). Retrograde labelling of mitral/tufted cells in the mouse accessory olfactory bulb following local injections of the lipophilic tracer DiI into the vomeronasal amygdala. *Brain Res* 896(1-2)**,** 198-203. doi: 10.1016/s0006-8993(01)02225-9.

Salin, P.A., Lledo, P.M., Vincent, J.D., and Charpak, S. (2001). Dendritic glutamate autoreceptors modulate signal processing in rat mitral cells. *J Neurophysiol* 85(3)**,** 1275-1282. doi: 10.1152/jn.2001.85.3.1275.

Santana, N., Mengod, G., and Artigas, F. (2009). Quantitative analysis of the expression of dopamine D1 and D2 receptors in pyramidal and GABAergic neurons of the rat prefrontal cortex. *Cereb Cortex* 19(4)**,** 849-860. doi: 10.1093/cercor/bhn134.

Santiago, A.C., and Shammah-Lagnado, S.J. (2005). Afferent connections of the amygdalopiriform transition area in the rat. *J Comp Neurol* 489(3)**,** 349-371. doi: 10.1002/cne.20637.

Scalia, F., and Winans, S.S. (1975). The differential projections of the olfactory bulb and accessory olfactory bulb in mammals. *J Comp Neurol* 161(1)**,** 31-55. doi: 10.1002/cne.901610105.

Scheinin, M., Lomasney, J.W., Hayden-Hixson, D.M., Schambra, U.B., Caron, M.G., Lefkowitz, R.J., et al. (1994). Distribution of alpha 2-adrenergic receptor subtype gene expression in rat brain. *Brain Res Mol Brain Res* 21(1-2)**,** 133-149. doi: 10.1016/0169-328x(94)90386-7.

Scheperjans, F., Grefkes, C., Palomero-Gallagher, N., Schleicher, A., and Zilles, K. (2005). Subdivisions of human parietal area 5 revealed by quantitative receptor autoradiography: a parietal region between motor, somatosensory, and cingulate cortical areas. *Neuroimage* 25(3)**,** 975-992. doi: 10.1016/j.neuroimage.2004.12.017.

Schlegel, J.R., and Kriegstein, A.R. (1987). Quantitative autoradiography of muscarinic and benzodiazepine receptors in the forebrain of the turtle, Pseudemys scripta. *J Comp Neurol* 265(4)**,** 521-529. doi: 10.1002/cne.902650406.

Schleicher, A., Palomero-Gallagher, N., Morosan, P., Eickhoff, S.B., Kowalski, T., de Vos, K., et al. (2005). Quantitative architectural analysis: a new approach to cortical mapping. *Anat Embryol (Berl)* 210(5-6)**,** 373-386. doi: 10.1007/s00429-005-0028-2.

Schleicher, A., and Zilles, K. (1988). "The use of automated image analysis for quantitative receptor autoradiography," in *Molecular neuroanatomy*. Elsevier Amsterdam), 147-157.

Schlösser, B., Klausa, G., Prime, G., and Ten Bruggencate, G. (1999). Postnatal development of calretinin- and parvalbumin-positive interneurons in the rat neostriatum: an immunohistochemical study. *J Comp Neurol* 405(2), 185-198. doi: 10.1002/(sici)1096-9861(19990308)405:2<185::aid-cne4>3.0.co;2-b.

Schmidt, P.J., Nieman, L.K., Danaceau, M.A., Adams, L.F., and Rubinow, D.R. (1998). Differential behavioral effects of gonadal steroids in women with and in those without premenstrual syndrome. *N Engl J Med* 338(4), 209-216. doi: 10.1056/nejm199801223380401.

Schoenbaum, G., Chiba, A.A., and Gallagher, M. (1999). Neural encoding in orbitofrontal cortex and basolateral amygdala during olfactory discrimination learning. *J Neurosci* 19(5), 1876-1884. doi: 10.1523/jneurosci.19-05-01876.1999.

Schoenbaum, G., and Roesch, M. (2005). Orbitofrontal cortex, associative learning, and expectancies. *Neuron* 47(5), 633-636. doi: 10.1016/j.neuron.2005.07.018.

Schoenfeld, T.A., and Macrides, F. (1984). Topographic organization of connections between the main olfactory bulb and pars externa of the anterior olfactory nucleus in the hamster. *J Comp Neurol* 227(1), 121-135. doi: 10.1002/cne.902270113.

Schreck, K.C., and Grossman, S.A. (2018). Role of Temozolomide in the Treatment of Cancers Involving the Central Nervous System. *Oncology (Williston Park)* 32(11), 555-560, 569.

Schultz, E.W. (1960). Repair of the olfactory mucosa with special reference to regeneration of olfactory cells (sensory neurons). *Am J Pathol* 37(1), 1-19.

Schwob, J.E., and Price, J.L. (1984). The development of lamination of afferent fibers to the olfactory cortex in rats, with additional observations in the adult. *J Comp Neurol* 223(2), 203-222. doi: 10.1002/cne.902230205.

Scott, J.W., McBride, R.L., and Schneider, S.P. (1980). The organization of projections from the olfactory bulb to the piriform cortex and olfactory tubercle in the rat. *J Comp Neurol* 194(3), 519-534. doi: 10.1002/cne.901940304.

Seeman, P., Chau-Wong, M., Tedesco, J., and Wong, K. (1975). Brain receptors for antipsychotic drugs and dopamine: direct binding assays. *Proc Natl Acad Sci U S A* 72(11), 4376-4380. doi: 10.1073/pnas.72.11.4376.

Sharpe, M.J., and Schoenbaum, G. (2016). Back to basics: Making predictions in the orbitofrontal-amygdala circuit. *Neurobiol Learn Mem* 131, 201-206. doi: 10.1016/j.nlm.2016.04.009.

Shepherd, G.M. (1972). Synaptic organization of the mammalian olfactory bulb. *Physiol Rev* 52(4), 864-917. doi: 10.1152/physrev.1972.52.4.864.

Shepherd, G.M. (2004). *The synaptic organization of the brain.* Oxford; New York: Oxford University Press.

Shiotani, K., Tanisumi, Y., Murata, K., Hirokawa, J., Sakurai, Y., and Manabe, H. (2020). Tuning of olfactory cortex ventral tenia tecta neurons to distinct task elements of goal-directed behavior. *Elife* 9. doi: 10.7554/eLife.57268.

Shipley, M.T., and Ennis, M. (1996). Functional organization of olfactory system. *J Neurobiol* 30(1), 123-176. doi: 10.1002/(sici)1097-4695(199605)30:1<123::Aid-neu11>3.0.Co;2-n.

Shohayeb, B., Diab, M., Ahmed, M., and Ng, D.C.H. (2018). Factors that influence adult neurogenesis as potential therapy. *Transl Neurodegener* 7, 4. doi: 10.1186/s40035-018-0109-9.

Sibley, D.R. (1999). New insights into dopaminergic receptor function using antisense and genetically altered animals. *Annu Rev Pharmacol Toxicol* 39**,** 313-341. doi: 10.1146/annurev.pharmtox.39.1.313.

Sibley, D.R., and Monsma, F.J., Jr. (1992). Molecular biology of dopamine receptors. *Trends Pharmacol Sci* 13(2)**,** 61-69. doi: 10.1016/0165-6147(92)90025-2.

Sieghart, W. (1995). Structure and pharmacology of gamma-aminobutyric acidA receptor subtypes. *Pharmacol Rev* 47(2)**,** 181-234.

Simon, J., Wakimoto, H., Fujita, N., Lalande, M., and Barnard, E.A. (2004). Analysis of the set of GABA(A) receptor genes in the human genome. *J Biol Chem* 279(40)**,** 41422-41435. doi: 10.1074/jbc.M401354200.

Simmons, D. (2008). The Use of Animal Models in Studying Genetic Disease: Transgenesis and Induced Mutation. *Nature Education* 1(1):70.

Sirviö, J., and MacDonald, E. (1999). Central alpha1-adrenoceptors: their role in the modulation of attention and memory formation. *Pharmacol Ther* 83(1)**,** 49-65. doi: 10.1016/s0163-7258(99)00017-0.

Slattery, D.A., Desrayaud, S., and Cryan, J.F. (2005). GABAB receptor antagonist-mediated antidepressant-like behavior is serotonin-dependent. *J Pharmacol Exp Ther* 312(1)**,** 290-296. doi: 10.1124/jpet.104.073536.

Smith, S.S., and Woolley, C.S. (2004). Cellular and molecular effects of steroid hormones on CNS excitability. *Cleve Clin J Med* 71 Suppl 2**,** S4-10. doi: 10.3949/ccjm.71.suppl_2.s4.

Smith, T.C., and Jahr, C.E. (2002). Self-inhibition of olfactory bulb neurons. *Nat Neurosci* 5(8)**,** 760-766. doi: 10.1038/nn882.

Smith, T.D., and Bhatnagar, K.P. (2000). The human vomeronasal organ. Part II: prenatal development. *J Anat* 197 Pt 3(Pt 3)**,** 421-436. doi: 10.1046/j.1469-7580.2000.19730421.x.

Snyder, S.H., Taylor, K.M., Coyle, J.T., and Meyerhoff, J.L. (1970). The role of brain dopamine in behavioral regulation and the actions of psychotropic drugs. *Am J Psychiatry* 127(2)**,** 199-207. doi: 10.1176/ajp.127.2.199.

Sokolic, L., and McGregor, I.S. (2007). Benzodiazepines impair the acquisition and reversal of olfactory go/no-go discriminations in rats. *Behav Neurosci* 121(3)**,** 527-534. doi: 10.1037/0735-7044.121.3.527.

Sommer, B., and Seeburg, P.H. (1992). Glutamate receptor channels: novel properties and new clones. *Trends Pharmacol Sci* 13(7)**,** 291-296. doi: 10.1016/0165-6147(92)90088-n.

Song, D., Chen, Y., Chen, C., Chen, L., and Cheng, O. (2021). GABA(B) receptor antagonist promotes hippocampal neurogenesis and facilitates cognitive function recovery following acute cerebral ischemia in mice. *Stem Cell Res Ther* 12(1)**,** 22. doi: 10.1186/s13287-020-02059-x.

Spano, P.F., Govoni, S., and Trabucchi, M. (1978). Studies on the pharmacological properties of dopamine receptors in various areas of the central nervous system. *Adv Biochem Psychopharmacol* 19**,** 155-165.

Stanton, P.K., Jones, R.S., Mody, I., and Heinemann, U. (1987). Epileptiform activity induced by lowering extracellular [Mg2+] in combined hippocampal-entorhinal cortex slices: modulation by receptors for norepinephrine and N-methyl-D-aspartate. *Epilepsy Res* 1(1)**,** 53-62. doi: 10.1016/0920-1211(87)90051-9.

Starke, K., Göthert, M., and Kilbinger, H. (1989). Modulation of neurotransmitter release by presynaptic autoreceptors. *Physiol Rev* 69(3), 864-989. doi: 10.1152/physrev.1989.69.3.864.

Stäubli, U., Ivy, G., and Lynch, G. (1984). Hippocampal denervation causes rapid forgetting of olfactory information in rats. *Proc Natl Acad Sci U S A* 81(18), 5885-5887. doi: 10.1073/pnas.81.18.5885.

Staubli, U., Schottler, F., and Nejat-Bina, D. (1987). Role of dorsomedial thalamic nucleus and piriform cortex in processing olfactory information. *Behav Brain Res* 25(2), 117-129. doi: 10.1016/0166-4328(87)90005-2.

Stecher, J., Müller, W.E., and Hoyer, S. (1997). Learning abilities depend on NMDA-receptor density in hippocampus in adult rats. *J Neural Transm (Vienna)* 104(2-3), 281-289. doi: 10.1007/bf01273188.

Stefanits, H., Milenkovic, I., Mahr, N., Pataraia, E., Baumgartner, C., Hainfellner, J.A., et al. (2019). Alterations in GABAA Receptor Subunit Expression in the Amygdala and Entorhinal Cortex in Human Temporal Lobe Epilepsy. *J Neuropathol Exp Neurol* 78(11), 1022-1048. doi: 10.1093/jnen/nlz085.

Stevens, M.F., Hickman, J.A., Langdon, S.P., Chubb, D., Vickers, L., Stone, R., et al. (1987). Antitumor activity and pharmacokinetics in mice of 8-carbamoyl-3-methyl-imidazo[5,1-d]-1,2,3,5-tetrazin-4(3H)-one (CCRG 81045; M & B 39831), a novel drug with potential as an alternative to dacarbazine. *Cancer Res* 47(22), 5846-5852.

Stoop, R., Epiney, S., Meier, E., and Pralong, E. (2000). Modulation of epileptiform discharges in the rat limbic system in vitro by noradrenergic agents. *Neurosci Lett* 287(1), 5-8. doi: 10.1016/s0304-3940(00)01154-x.

Struikmans, H., Rutgers, D.H., Jansen, G.H., Tulleken, C.A., van der Tweel, I., and Battermann, J.J. (1997). S-phase fraction, 5-bromo-2'-deoxy-uridine labelling index, duration of S-phase, potential doubling time, and DNA index in benign and malignant brain tumors. *Radiat Oncol Investig* 5(4), 170-179. doi: 10.1002/(sici)1520-6823(1997)5:4<170::Aid-roi2>3.0.Co;2-v.

Stumpf, W.E., and Roth, L.J. (1964). VACUUM FREEZE DRYING OF FROZEN SECTIONS FOR DRY-MOUNTING, HIGH-RESOLUTION AUTORADIOGRAPHY. *Stain Technol* 39, 219-223. doi: 10.3109/10520296409061233.

Sugai, T., Yamamoto, R., Yoshimura, H., and Kato, N. (2012). Multimodal cross-talk of olfactory and gustatory information in the endopiriform nucleus in rats. *Chem Senses* 37(8), 681-688. doi: 10.1093/chemse/bjs046.

Suh, Y.H., Chang, K., and Roche, K.W. (2018). Metabotropic glutamate receptor trafficking. *Mol Cell Neurosci* 91, 10-24. doi: 10.1016/j.mcn.2018.03.014.

Sulzer, D., Cragg, S.J., and Rice, M.E. (2016). Striatal dopamine neurotransmission: regulation of release and uptake. *Basal Ganglia* 6(3), 123-148. doi: 10.1016/j.baga.2016.02.001.

Swanson, A.M., Allen, A.G., Shapiro, L.P., and Gourley, S.L. (2015). GABAAα1-mediated plasticity in the orbitofrontal cortex regulates context-dependent action selection. *Neuropsychopharmacology* 40(4), 1027-1036. doi: 10.1038/npp.2014.292.

Tahvildari, B., and Alonso, A. (2005). Morphological and electrophysiological properties of lateral entorhinal cortex layers II and III principal neurons. *J Comp Neurol* 491(2), 123-140. doi: 10.1002/cne.20706.

Takahashi, Y.K., Roesch, M.R., Stalnaker, T.A., Haney, R.Z., Calu, D.J., Taylor, A.R., et al. (2009). The orbitofrontal cortex and ventral tegmental area are necessary for

learning from unexpected outcomes. *Neuron* 62(2), 269-280. doi: 10.1016/j.neuron.2009.03.005.

Takamura, N., Nakagawa, S., Masuda, T., Boku, S., Kato, A., Song, N., et al. (2014). The effect of dopamine on adult hippocampal neurogenesis. *Prog Neuropsychopharmacol Biol Psychiatry* 50, 116-124. doi: 10.1016/j.pnpbp.2013.12.011.

Tanabe, T., Yarita, H., Iino, M., Ooshima, Y., and Takagi, S.F. (1975). An olfactory projection area in orbitofrontal cortex of the monkey. *J Neurophysiol* 38(5), 1269-1283. doi: 10.1152/jn.1975.38.5.1269.

Tanapat, P., Hastings, N.B., and Gould, E. (2005). Ovarian steroids influence cell proliferation in the dentate gyrus of the adult female rat in a dose- and time-dependent manner. *J Comp Neurol* 481(3), 252-265. doi: 10.1002/cne.20385.

Tapiero, H., Mathé, G., Couvreur, P., and Tew, K.D. (2002). II. Glutamine and glutamate. *Biomed Pharmacother* 56(9), 446-457. doi: 10.1016/s0753-3322(02)00285-8.

Thompson, S.E., Ayman, G., Woodhall, G.L., and Jones, R.S. (2006). Depression of glutamate and GABA release by presynaptic GABAB receptors in the entorhinal cortex in normal and chronically epileptic rats. *Neurosignals* 15(4), 202-215. doi: 10.1159/000098515.

Tisdale, M.J. (1987). Antitumor imidazotetrazines--XV. Role of guanine O6 alkylation in the mechanism of cytotoxicity of imidazotetrazinones. *Biochem Pharmacol* 36(4), 457-462. doi: 10.1016/0006-2952(87)90351-0.

Torigoe, M., Yamauchi, K., Zhu, Y., Kobayashi, H., and Murakami, F. (2015). Association of astrocytes with neurons and astrocytes derived from distinct progenitor domains in the subpallium. *Sci Rep* 5, 12258. doi: 10.1038/srep12258.

Tortorella, A., Halonen, T., Sahibzada, N., and Gale, K. (1997). A crucial role of the alpha-amino-3-hydroxy-5-methylisoxazole-4-propionic acid subtype of glutamate receptors in piriform and perirhinal cortex for the initiation and propagation of limbic motor seizures. *J Pharmacol Exp Ther* 280(3), 1401-1405.

Trotier, D., Eloit, C., Wassef, M., Talmain, G., Bensimon, J.L., Døving, K.B., et al. (2000). The vomeronasal cavity in adult humans. *Chem Senses* 25(4), 369-380. doi: 10.1093/chemse/25.4.369.

Truong, B.G., Magrum, L.J., and Gietzen, D.W. (2002). GABA(A) and GABA(B) receptors in the anterior piriform cortex modulate feeding in rats. *Brain Res* 924(1), 1-9. doi: 10.1016/s0006-8993(01)03213-9.

Ubeda-Bañon, I., Saiz-Sanchez, D., Flores-Cuadrado, A., Rioja-Corroto, E., Gonzalez-Rodriguez, M., Villar-Conde, S., et al. (2020). The human olfactory system in two proteinopathies: Alzheimer's and Parkinson's diseases. *Transl Neurodegener* 9(1), 22. doi: 10.1186/s40035-020-00200-7.

Ucha, M., Roura-Martínez, D., Contreras, A., Pinto-Rivero, S., Orihuel, J., Ambrosio, E., et al. (2019). Impulsive Action and Impulsive Choice Are Differentially Associated With Gene Expression Variations of the GABA(A) Receptor Alfa 1 Subunit and the CB(1) Receptor in the Lateral and Medial Orbitofrontal Cortices. *Front Behav Neurosci* 13, 22. doi: 10.3389/fnbeh.2019.00022.

Unnerstall, J.R., Kopajtic, T.A., and Kuhar, M.J. (1984). Distribution of alpha 2 agonist binding sites in the rat and human central nervous system: analysis of some functional, anatomic correlates of the pharmacologic effects of clonidine and related adrenergic agents. *Brain Res* 319(1), 69-101. doi: 10.1016/0165-0173(84)90030-4.

Urban, N.N., and Sakmann, B. (2002). Reciprocal intraglomerular excitation and intra- and interglomerular lateral inhibition between mouse olfactory bulb mitral cells. *J Physiol* 542(Pt 2), 355-367. doi: 10.1113/jphysiol.2001.013491.

Usrey, W.M. (2002). AMPA autoreceptors fill the gap in olfactory temporal coding. *Nat Neurosci* 5(11), 1108-1109. doi: 10.1038/nn1102-1108.

Uylings, H.B., Zilles, K., and Rajkowska, G. (1999). Optimal staining methods for delineation of cortical areas and neuron counts in human brains. *Neuroimage* 9(4), 439-445. doi: 10.1006/nimg.1999.0417.

Vallone, D., Picetti, R., and Borrelli, E. (2000). Structure and function of dopamine receptors. *Neurosci Biobehav Rev* 24(1), 125-132. doi: 10.1016/s0149-7634(99)00063-9.

van der Kooy, D., and Weiss, S. (2000). Why stem cells? *Science* 287(5457), 1439-1441. doi: 10.1126/science.287.5457.1439.

Van Hoesen, G.W., Hyman, B.T., and Damasio, A.R. (1986). Cell-specific pathology in neural systems of the temporal lobe in Alzheimer's disease. *Prog Brain Res* 70, 321-335. doi: 10.1016/s0079-6123(08)64313-7.

van Praag, H., Christie, B.R., Sejnowski, T.J., and Gage, F.H. (1999a). Running enhances neurogenesis, learning, and long-term potentiation in mice. *Proc Natl Acad Sci U S A* 96(23), 13427-13431. doi: 10.1073/pnas.96.23.13427.

van Praag, H., Kempermann, G., and Gage, F.H. (1999b). Running increases cell proliferation and neurogenesis in the adult mouse dentate gyrus. *Nat Neurosci* 2(3), 266-270. doi: 10.1038/6368.

van Praag, H., Kempermann, G., and Gage, F.H. (2000). Neural consequences of environmental enrichment. *Nat Rev Neurosci* 1(3), 191-198. doi: 10.1038/35044558.

van Wingen, G.A., van Broekhoven, F., Verkes, R.J., Petersson, K.M., Bäckström, T., Buitelaar, J.K., et al. (2008). Progesterone selectively increases amygdala reactivity in women. *Mol Psychiatry* 13(3), 325-333. doi: 10.1038/sj.mp.4002030.

Vaughan, D.N., and Jackson, G.D. (2014). The piriform cortex and human focal epilepsy. *Front Neurol* 5, 259. doi: 10.3389/fneur.2014.00259.

Veldhuizen, M.G., and Small, D.M. (2011). Modality-specific neural effects of selective attention to taste and odor. *Chem Senses* 36(8), 747-760. doi: 10.1093/chemse/bjr043.

Venault, P., Chapouthier, G., de Carvalho, L.P., Simiand, J., Morre, M., Dodd, R.H., et al. (1986). Benzodiazepine impairs and beta-carboline enhances performance in learning and memory tasks. *Nature* 321(6073), 864-866. doi: 10.1038/321864a0.

Vidal-Gonzalez, I., Vidal-Gonzalez, B., Rauch, S.L., and Quirk, G.J. (2006). Microstimulation reveals opposing influences of prelimbic and infralimbic cortex on the expression of conditioned fear. *Learn Mem* 13(6), 728-733. doi: 10.1101/lm.306106.

von Campenhausen, H., and Mori, K. (2000). Convergence of segregated pheromonal pathways from the accessory olfactory bulb to the cortex in the mouse. *Eur J Neurosci* 12(1), 33-46. doi: 10.1046/j.1460-9568.2000.00879.x.

Vorhees, C.V., and Williams, M.T. (2006). Morris water maze: procedures for assessing spatial and related forms of learning and memory. *Nat Protoc* 1(2), 848-858. doi: 10.1038/nprot.2006.116.

Wachowiak, M., McGann, J.P., Heyward, P.M., Shao, Z., Puche, A.C., and Shipley, M.T. (2005). Inhibition [corrected] of olfactory receptor neuron input to olfactory bulb

glomeruli mediated by suppression of presynaptic calcium influx. *J Neurophysiol* 94(4), 2700-2712. doi: 10.1152/jn.00286.2005.

Wada, E., Shigemoto, R., Kinoshita, A., Ohishi, H., and Mizuno, N. (1998). Metabotropic glutamate receptor subtypes in axon terminals of projection fibers from the main and accessory olfactory bulbs: a light and electron microscopic immunohistochemical study in the rat. *J Comp Neurol* 393(4), 493-504.

Wamsley, J.K., Hunt, M.E., McQuade, R.D., and Alburges, M.E. (1991). [3H]SCH39166, a D1 dopamine receptor antagonist: binding characteristics and localization. *Exp Neurol* 111(2), 145-151. doi: 10.1016/0014-4886(91)90001-s.

Wang, L.P., Kempermann, G., and Kettenmann, H. (2005). A subpopulation of precursor cells in the mouse dentate gyrus receives synaptic GABAergic input. *Mol Cell Neurosci* 29(2), 181-189. doi: 10.1016/j.mcn.2005.02.002.

Watson, C., and Puelles, L. (2017). Developmental gene expression in the mouse clarifies the organization of the claustrum and related endopiriform nuclei. *J Comp Neurol* 525(6), 1499-1508. doi: 10.1002/cne.24034.

Weiss, S., Dunne, C., Hewson, J., Wohl, C., Wheatley, M., Peterson, A.C., et al. (1996). Multipotent CNS stem cells are present in the adult mammalian spinal cord and ventricular neuroaxis. *J Neurosci* 16(23), 7599-7609. doi: 10.1523/jneurosci.16-23-07599.1996.

Weldon, D.A., Travis, M.L., and Kennedy, D.A. (1991). Posttraining D1 receptor blockade impairs odor conditioning in neonatal rats. *Behav Neurosci* 105(3), 450-458. doi: 10.1037//0735-7044.105.3.450.

Wesson, D.W., and Wilson, D.A. (2010). Smelling sounds: olfactory-auditory sensory convergence in the olfactory tubercle. *J Neurosci* 30(8), 3013-3021. doi: 10.1523/jneurosci.6003-09.2010.

Wesson, D.W., and Wilson, D.A. (2011). Sniffing out the contributions of the olfactory tubercle to the sense of smell: hedonics, sensory integration, and more? *Neurosci Biobehav Rev* 35(3), 655-668. doi: 10.1016/j.neubiorev.2010.08.004.

Westenbroek, C., Den Boer, J.A., Veenhuis, M., and Ter Horst, G.J. (2004). Chronic stress and social housing differentially affect neurogenesis in male and female rats. *Brain Res Bull* 64(4), 303-308. doi: 10.1016/j.brainresbull.2004.08.006.

Willard, S.S., and Koochekpour, S. (2013). Glutamate, glutamate receptors, and downstream signaling pathways. *Int J Biol Sci* 9(9), 948-959. doi: 10.7150/ijbs.6426.

Wilman, D.E. (1986). Prodrugs in cancer chemotherapy. *Biochem Soc Trans* 14(2), 375-382. doi: 10.1042/bst0140375.

Wilson, R.I., and Laurent, G. (2005). Role of GABAergic inhibition in shaping odor-evoked spatiotemporal patterns in the Drosophila antennal lobe. *J Neurosci* 25(40), 9069-9079. doi: 10.1523/jneurosci.2070-05.2005.

Winans, S.S., and Scalia, F. (1970). Amygdaloid nucleus: new afferent input from the vomeronasal organ. *Science* 170(3955), 330-332. doi: 10.1126/science.170.3955.330.

Wisden, W., and Seeburg, P.H. (1993). A complex mosaic of high-affinity kainate receptors in rat brain. *J Neurosci* 13(8), 3582-3598. doi: 10.1523/jneurosci.13-08-03582.1993.

Witter, M.P., Doan, T.P., Jacobsen, B., Nilssen, E.S., and Ohara, S. (2017). Architecture of the Entorhinal Cortex A Review of Entorhinal Anatomy in Rodents with Some Comparative Notes. *Front Syst Neurosci* 11, 46. doi: 10.3389/fnsys.2017.00046.

Wolfer, D.P., Litvin, O., Morf, S., Nitsch, R.M., Lipp, H.P., and Würbel, H. (2004). Laboratory animal welfare: cage enrichment and mouse behaviour. *Nature* 432(7019), 821-822. doi: 10.1038/432821a.

Woolley, C.S., Weiland, N.G., McEwen, B.S., and Schwartzkroin, P.A. (1997). Estradiol increases the sensitivity of hippocampal CA1 pyramidal cells to NMDA receptor-mediated synaptic input: correlation with dendritic spine density. *J Neurosci* 17(5), 1848-1859. doi: 10.1523/jneurosci.17-05-01848.1997.

Wright, R.A., Johnson, B.G., Zhang, C., Salhoff, C., Kingston, A.E., Calligaro, D.O., et al. (2013). CNS distribution of metabotropic glutamate 2 and 3 receptors: transgenic mice and [^{3}H]LY459477 autoradiography. *Neuropharmacology* 66, 89-98. doi: 10.1016/j.neuropharm.2012.01.019.

Würbel, H. (2001). Ideal homes? Housing effects on rodent brain and behaviour. *Trends Neurosci* 24(4), 207-211. doi: 10.1016/s0166-2236(00)01718-5.

Wyss, J.M., and Sripanidkulchai, K. (1983). The indusium griseum and anterior hippocampal continuation in the rat. *J Comp Neurol* 219(3), 251-272. doi: 10.1002/cne.902190302.

Xia, S., Miyashita, T., Fu, T.F., Lin, W.Y., Wu, C.L., Pyzocha, L., et al. (2005). NMDA receptors mediate olfactory learning and memory in Drosophila. *Curr Biol* 15(7), 603-615. doi: 10.1016/j.cub.2005.02.059.

Xiong, A., and Wesson, D.W. (2016). Illustrated Review of the Ventral Striatum's Olfactory Tubercle. *Chem Senses* 41(7), 549-555. doi: 10.1093/chemse/bjw069.

Xu, Y., Yan, J., Zhou, P., Li, J., Gao, H., Xia, Y., et al. (2012). Neurotransmitter receptors and cognitive dysfunction in Alzheimer's disease and Parkinson's disease. *Prog Neurobiol* 97(1), 1-13. doi: 10.1016/j.pneurobio.2012.02.002.

Xu, Z., Wang, Y., Chen, B., Xu, C., Wu, X., Wang, Y., et al. (2016). Entorhinal Principal Neurons Mediate Brain-stimulation Treatments for Epilepsy. *EBioMedicine* 14, 148-160. doi: 10.1016/j.ebiom.2016.11.027.

Yagi, S., and Galea, L.A.M. (2019). Sex differences in hippocampal cognition and neurogenesis. *Neuropsychopharmacology* 44(1), 200-213. doi: 10.1038/s41386-018-0208-4.

Yankova, M., Hart, S.A., and Woolley, C.S. (2001). Estrogen increases synaptic connectivity between single presynaptic inputs and multiple postsynaptic CA1 pyramidal cells: a serial electron-microscopic study. *Proc Natl Acad Sci U S A* 98(6), 3525-3530. doi: 10.1073/pnas.051624598.

Yanpallewar, S.U., Fernandes, K., Marathe, S.V., Vadodaria, K.C., Jhaveri, D., Rommelfanger, K., et al. (2010). Alpha2-adrenoceptor blockade accelerates the neurogenic, neurotrophic, and behavioral effects of chronic antidepressant treatment. *J Neurosci* 30(3), 1096-1109. doi: 10.1523/jneurosci.2309-09.2010.

Yokomaku, D., Numakawa, T., Numakawa, Y., Suzuki, S., Matsumoto, T., Adachi, N., et al. (2003). Estrogen enhances depolarization-induced glutamate release through activation of phosphatidylinositol 3-kinase and mitogen-activated protein kinase in cultured hippocampal neurons. *Mol Endocrinol* 17(5), 831-844. doi: 10.1210/me.2002-0314.

Yoshida, M., Fransén, E., and Hasselmo, M.E. (2008). mGluR-dependent persistent firing in entorhinal cortex layer III neurons. *Eur J Neurosci* 28(6), 1116-1126. doi: 10.1111/j.1460-9568.2008.06409.x.

Young, S.Z., Taylor, M.M., and Bordey, A. (2011). Neurotransmitters couple brain activity to subventricular zone neurogenesis. *Eur J Neurosci* 33(6), 1123-1132. doi: 10.1111/j.1460-9568.2011.07611.x.

Yu, H.H., Hseu, S.S., Chan, K.H., Chen, C.F., and Lee, T.Y. (1990). Flumazenil as an antagonist for midazolam anesthesia in outpatient surgery. *Ma Zui Xue Za Zhi* 28(4), 401-409.

Yuan, T.F., and Slotnick, B.M. (2014). Roles of olfactory system dysfunction in depression. *Prog Neuropsychopharmacol Biol Psychiatry* 54, 26-30. doi: 10.1016/j.pnpbp.2014.05.013.

Zatorre, R.J., and Jones-Gotman, M. (1991). Human olfactory discrimination after unilateral frontal or temporal lobectomy. *Brain* 114 (Pt 1A), 71-84.

Zatorre, R.J., Jones-Gotman, M., Evans, A.C., and Meyer, E. (1992). Functional localization and lateralization of human olfactory cortex. *Nature* 360(6402), 339-340. doi: 10.1038/360339a0.

Zelano, C., Bensafi, M., Porter, J., Mainland, J., Johnson, B., Bremner, E., et al. (2005). Attentional modulation in human primary olfactory cortex. *Nat Neurosci* 8(1), 114-120. doi: 10.1038/nn1368.

Zelano, C., Montag, J., Johnson, B., Khan, R., and Sobel, N. (2007). Dissociated representations of irritation and valence in human primary olfactory cortex. *J Neurophysiol* 97(3), 1969-1976. doi: 10.1152/jn.01122.2006.

Zelano, C., Montag, J., Khan, R., and Sobel, N. (2009). A specialized odor memory buffer in primary olfactory cortex. *PLoS One* 4(3), e4965. doi: 10.1371/journal.pone.0004965.

Zhang, J.H., Araki, T., Sato, M., and Tohyama, M. (1991). Distribution of GABAA-receptor alpha 1 subunit gene expression in the rat forebrain. *Brain Res Mol Brain Res* 11(3-4), 239-247. doi: 10.1016/0169-328x(91)90032-s.

Zhang, L., and Goldman, J.E. (1996). Generation of cerebellar interneurons from dividing progenitors in white matter. *Neuron* 16(1), 47-54. doi: 10.1016/s0896-6273(00)80022-7.

Zhang, S., and Manahan-Vaughan, D. (2015). Spatial olfactory learning contributes to place field formation in the hippocampus. *Cereb Cortex* 25(2), 423-432. doi: 10.1093/cercor/bht239.

Zhang, S., Xiao, Q., and Le, W. (2015). Olfactory dysfunction and neurotransmitter disturbance in olfactory bulb of transgenic mice expressing human A53T mutant α-synuclein. *PloS one* 10(3), e0119928-e0119928. doi: 10.1371/journal.pone.0119928.

Zhang, Z., Liu, Q., Wen, P., Zhang, J., Rao, X., Zhou, Z., et al. (2017). Activation of the dopaminergic pathway from VTA to the medial olfactory tubercle generates odor-preference and reward. *Elife* 6. doi: 10.7554/eLife.25423.

Zhao, F., Wang, X., Zariwala, H.A., Uslaner, J.M., Houghton, A.K., Evelhoch, J.L., et al. (2017). fMRI study of the role of glutamate NMDA receptor in the olfactory adaptation in rats: Insights into cellular and molecular mechanisms of olfactory adaptation. *Neuroimage* 149, 348-360. doi: 10.1016/j.neuroimage.2017.01.068.

Zhu, Y., Armstrong, J.N., and Contractor, A. (2021). Kainate receptors regulate the functional properties of young adult-born dentate granule cells. *Cell Rep* 36(12), 109751. doi: 10.1016/j.celrep.2021.109751.

Zilles, K. (2012). *The cortex of the rat: a stereotaxic atlas.* Springer Science & Business Media.

Zilles, K., Bacha-Trams, M., Palomero-Gallagher, N., Amunts, K., and Friederici, A.D. (2015). Common molecular basis of the sentence comprehension network revealed by neurotransmitter receptor fingerprints. *Cortex* 63**,** 79-89. doi: 10.1016/j.cortex.2014.07.007.

Zilles, K., and Palomero-Gallagher, N. (2001). Cyto-, myelo-, and receptor architectonics of the human parietal cortex. *Neuroimage* 14(1 Pt 2)**,** S8-20. doi: 10.1006/nimg.2001.0823.

Zilles, K., and Palomero-Gallagher, N. (2017). Multiple Transmitter Receptors in Regions and Layers of the Human Cerebral Cortex. *Front Neuroanat* 11**,** 78. doi: 10.3389/fnana.2017.00078.

Zilles, K., Palomero-Gallagher, N., Grefkes, C., Scheperjans, F., Boy, C., Amunts, K., et al. (2002a). Architectonics of the human cerebral cortex and transmitter receptor fingerprints: reconciling functional neuroanatomy and neurochemistry. *Eur Neuropsychopharmacol* 12(6)**,** 587-599. doi: 10.1016/s0924-977x(02)00108-6.

Zilles, K., Palomero-Gallagher, N., and Schleicher, A. (2004). Transmitter receptors and functional anatomy of the cerebral cortex. *J Anat* 205(6)**,** 417-432. doi: 10.1111/j.0021-8782.2004.00357.x.

Zilles, K., Qü, M.S., Schröder, H., and Schleicher, A. (1991). Neurotransmitter receptors and cortical architecture. *J Hirnforsch* 32(3)**,** 343-356.

Zilles, K., and Schleicher, A. (1991). Quantitative receptor autoradiography and image analysis. *Bull Assoc Anat (Nancy)* 75(229)**,** 117-121.

Zilles, K., Schleicher, A., Palomero-Gallagher, N., and Amunts, K. (2002b). "Quantitative Analysis of Cyto- and Receptor Architecture of the Human Brain."), 573-602.

Zilles, K., Schleicher, A., Rath, M., Glaser, T., and Traber, J.J.J.o.n.m. (1986). Quantitative autoradiography of transmitter binding sites with an image analyzer. 18(1-2)**,** 207-220.

Zilles, K., Wu, J., Crusio, W.E., and Schwegler, H. (2000). Water maze and radial maze learning and the density of binding sites of glutamate, GABA, and serotonin receptors in the hippocampus of inbred mouse strains. *Hippocampus* 10(3)**,** 213-225. doi: 10.1002/1098-1063(2000)10:3<213::Aid-hipo2>3.0.Co;2-q.

Zimmermann, K.S., Yamin, J.A., Rainnie, D.G., Ressler, K.J., and Gourley, S.L. (2018). Connections of the Mouse Orbitofrontal Cortex and Regulation of Goal-Directed Action Selection by Brain-Derived Neurotrophic Factor. *Biol Psychiatry* 81(4)**,** 366-377. doi: 10.1016/j.biopsych.2015.10.026.

Zucchetti, M., Catapano, C.V., Filippeschi, S., Erba, E., and D'Incalci, M. (1989). Temozolomide induced differentiation of K562 leukemia cells is not mediated by gene hypomethylation. *Biochem Pharmacol* 38(13)**,** 2069-2075. doi: 10.1016/0006-2952(89)90059-2.

Eidesstattliche Versicherung

Ich versichere an Eides Statt, dass die Dissertation von mir selbständig und ohne unzulässige fremde Hilfe unter Beachtung der Grundsätze zur Sicherung guter wissenschaftlicher Praxis an der Heinrich-Heine-Universität Düsseldorf sowie der Richtlinien der Medizinischen Fakultät zur Sicherung guter wissenschaftlicher Praxis erstellt worden ist. Die aus fremden Quellen direkt oder indirekt übernommenen Inhalte wurden als solche kenntlich gemacht.

Ich bin mir darüber klar, dass der Bruch der obigen eidesstattlichen Versicherung in jedem Fall zum Nichtbestehen der betreffenden Promotionsleistung führt und die weitere Folge hat, dass die Fakultät über die Entziehung des Doktorgrades entscheidet (§ 16 Promotionsordnung). Die strafrechtlichen Konsequenzen einer falschen eidesstattlichen Versicherung sind mir bekannt (§156 StGB). Des Weiteren kann gemäß § 63 Absatz 5 HG eine Zuwiderhandlung mit einer Geldbuße von bis zu 50.000 € geahndet werden. Der/Die Antragsteller/in erklärt sich mit einer Überprüfung der Dissertationsschrift mittels einer Plagiatssoftware einverstanden.

Ich versichere weiterhin, dass alle von mir gemachten Angaben wahrheitsgemäß und vollständig sind.

Ort, Datum

Danksagung

An dieser Stelle möchte ich Prof. Dr. med. Katrin Amunts meinen großen Dank aussprechen. Danke, dass mir ermöglicht wurde meine Arbeit unter deinem Namen im Cécile & Oskar-Vogt-Institut für Hirnforschung anzufertigen. Ohne deine Unterstützung und dein Verständnis wäre diese Arbeit nicht zustande gekommen. Ich hätte mir keine bessere Doktormutter vorstellen können, die so herzlich und konstruktiv mit ihren Schützlingen umgeht. Ich werde mir für den weiteren beruflichen Weg dein offenes Ohr und deine professionelle und gleichzeitig herzliche Art zum Vorbild nehmen!

Mein weiterer Dank gilt Prof. Dr. rer. nat. Dieter Willbold. Nachdem ich dir bereits für die Ausführung meiner Masterarbeit in deinem Institut danken durfte, danke ich dir jetzt dafür, dass du mir mit als Zweitprüfer die Möglichkeit gegeben hast an der medizinischen Fakultät promovieren zu können. Ich bewundere deine Arbeit und denke immer mit Freuden an die gemeinsamen Institutsfeiern zurück!

PD Dr. rer. Nat. Christina Herold möchte ich ebenfalls danken! Danke, dass du in mir das Potential gesehen hast zu promovieren und dass mir durch dein riesiges Projekt so ein interessantes Thema zur Verfügung stand!

Mein besonderer Dank gilt meinen Kollegen und Kolleginnen: Ariane, nach wenigen Worten mit dir wusste ich, dass ich mit dir noch viel Spaß haben werde. Deine Kinder haben sich in unserer Doktorandenzahl verdoppelt und ich liebe beide über alle Maßen! Danke für jeden Cocktail, jeden Rat und jedes Lachen! Und auch danke an Raphael, der nie zu müde war, um sich um meine Wehwehchen zu kümmern! Kai, dir danke ich dafür, dass du mit deiner ruhigen Art dafür gesorgt hast, dass ab und zu auch mal Ruhe im Büro herrschte. Auch wenn du oft mitgemacht hast! Ohne dich hätte ich weder eine Ahnung von Statistik noch einen Tisch. Du hast mich so gesehen aus dem Keller geholt! Ich bin froh Ariane und dich als Freunde zu wissen und freue mich auf weitere Projekte mit euch, sowohl privat als auch beruflich! Cheers!

Evelyn, dein Lachen und deine Persönlichkeit sind mir sehr ans Herz gewachsen! Von der ganzen Zeit, die ich in diesem Institut bisher verbracht habe, war ein Großteil mit dir vor der Kaffeemaschine. Ich möchte davon keine Minute missen – danke für dein stets offenes Ohr! Dasselbe gilt für Manuel! Ich kann nicht sagen, wie oft ich mich mit dir oder Evelyn verquatscht habe. Bei jeder Nachtschicht wusste ich, dass du auch noch nebenan sitzt und bereit für einen Kaffee oder „frische Luft“ wärst!

Generell möchte ich so vielen KollegInnen danken, jedoch ist die Arbeit bereits sehr lang. Also danke an Daisy, Manuel, Erhan, Andrea, Nicole, Lilia, Anna, Melanie, Herr Bidmon, René, Uli (mit nur einem l!), Philipp, Nina, Magdalena, Nicola, Sabrina und Dominique.

Tief verbunden und dankbar bin ich meinem Freund Dominik und meinen Freundinnen Laura, Sara, Jessi und Rachel. Den Dank an euch kann keine Arbeit dieser Welt in Worte fassen. Es wäre eine weitere Dissertation. Ich liebe euch! Danke, danke, danke!

Mein größter Dank gilt meiner Familie, insbesondere Gudrun Lothmann, Rainer Lothmann und Caroline Lothmann. Eure Unterstützung und liebevoller Zuspruch gaben mir jedes Mal die Kraft an mich zu glauben. Wenn mir der Horizont fehlte, wart ihr immer da und habt mich wieder geerdet. Ich bin überaus glücklich euch in dieser Arbeit abermals danken zu können. Eure Liebe und Unterstützung sind mir das Wichtigste auf dieser Welt. Ihr seid mein Rückhalt und mein Mut. Danke für Alles, ich liebe euch!

Appendix

Supp. Tab. 1: Sectioning protocol of mouse brains for autoradiography and staining methods including cell body staining and myelin staining.

The section thickness was 16 µm, start coordinate was bregma 3.8 mm and end coordinate was bregma -3.8 mm. Series 6, 11, 16 and 21 were distinguished by the fact that they included sections with non-specific binding of the respective receptor, in which the binding of a displacer was observed to reveal actual specific binding in the remaining sections, thus revealing the quality of the autoradiography.

Serien 1 - 5, 7 - 19, 12 - 15, 17 - 20, 22 - Ende		Serie 6, 11, 16, 21	
1	AMPA	1	AMPA
		1b	AMPA_UB
2	Kainate	2	Kainate
		2b	Kainate_UB
3	MK801	3	MK801
		3b	MK801_UB
4	LY341495	4	LY341495
		4b	LY341495_UB
5	Muscimol	5	Muscimol
		5b	Muscimol_UB
6	CGP54262	6	CGP54262
		6b	CGP54262_UB
7	Flumazenil	7	Flumazenil
		7b	Flumazenil_UB
8	SCH23390	8	SCH23390
		8b	SCH23390_UB
9	Raclopride/Fallypride	9	Raclopride/Fallypride
		9b	Raclopride/Fallypride_UB
10	Cell body staining	10	Cell body staining
11	Myelin staining	11	Myelin staining
12	Prazosin	12	Prazosin
		12b	Prazosin_UB
13	RX812002	13	RX812002
		13b	RX812002_UB
14	Reserve	14	Reserve
		14b	Reserve_UB

Supp. Tab. 2: Chemical composition of cell body staining

1. Fixation		120 min
	Neutral buffered formalin	
	H_2O dest.	900 ml
	$NaH_2PO_4 \cdot H_2O$	4 g
	$Na_2HPO_4 \cdot H_2O$	6.5 g
	Formaldehyde 37 – 40 %	100 ml
2. H_2O dest. (flowing)		2 x 5 min
3. Pyridine acetic anhydride solution		60 min
	Pyridine	200 ml
	Acetic anhydride	100 ml
4. H_2O dest. (flowing)		3 x 5 min
5. Ammonium silver nitrate		30 min
Ammonium nitrate		0.3 g
Silver nitrate		0.3 g
Sodium hydroxide (4%)		0.9 g
6. Acetic acid (1%)		3 x 3 min
7. Developer solution		30 min
	Stock A	**100 ml**
	H_2O dest.	1000 ml
	Sodium carbonate anhydrous	50 g
	Stock B	**30 ml**
	H_2O dest.	1000 ml
	Ammonium nitrate	2 g
	Silver nitrate	2 g
	Tungstosilicic acid	10 g
	Stock C	**70 ml**
	H_2O dest.	1000 ml
	Ammonium nitrate	2 g
	Silver nitrate	2 g

	Tungstosilicic acid	10 g
	Formalin (37%)	7.3 ml
8. H_2O dest. (flowing)		5 min
9. Acetic Acid (1%)		5 min
10. Fixative solution		10 min
11. H_2O dest.		5 min
12. Ascending alcohol series		

Supp. Tab. 3: Chemical composition of myelin staining

1. Fixation		120 min
	A. Neutral buffered formalin	
	H_2O dest.	900 ml
	$NaH_2PO_4 \cdot H_2O$	4 g
	$Na_2HPO_4 \cdot H_2O$	6.5 g
	Formaldehyde 37 – 40 %	100 ml
	B. Bodian's fixation mixture	
	EtOH (80%)	180 ml
	Formalin (37%)	10 ml
	Acetic acid (100%)	10 ml
2. H_2O dest.		2 x 5 min
3. Formic acid (4%)		180 min
	Formic acid	40 ml
	H_2O dest.	1000 ml
4. Formic acid/H_2O_2		Over night
	Formic acid	100 ml
	H_2O_2 (30%)	300 ml
	H_2O dest.	600 ml
5. H_2O dest. (flowing)		15 min
6. Acetic acid (1%)		2 x 5 min
7. Developer solution		30 min
	Stock A	**100 ml**
	H_2O dest.	1000 ml
	Sodium carbonate anhydrous	50 g
	Stock B	**30 ml**
	H_2O dest.	1000 ml
	Ammonium nitrate	2 g
	Silver nitrate	2 g
	Tungstosilicic acid	10 g

	Stock C	**70 ml**
	H_2O dest.	1000 ml
	Ammonium nitrate	2 g
	Silver nitrate	2 g
	Tungstosilicic acid	10 g
	Formalin (37%)	7.3 ml
8. Acetic Acid (1%)		5 min
9. H_2O dest. (flowing)		5 min
10. Fixative solution		10 min
11. H_2O dest.		5 min
12. Ascending alcohol series		

Supp. Tab. 4: Monitoring of adult neurogenesis by immunofluorescence

Used primary and secondary antibodies with appropriate concentration. The performance of these experiments is the content of a non-published work of the institute.

	primary antibodies	concentration	primary antibodies	concentration
GFAP	Anti GFAP Polyclonal, rabbit (Sigma-Aldrich)	1 : 500	Biotin. Goat. Anti rabbit (Dianova)	1 : 200
BrdU	Anti BrdU monoclonal, rat (AbD Serotec)	1 : 100	Biotin. Rabbit anti rat (Vector Lab)	1 : 200
NeuN	Anti NeuN Monoclonal, mouse (Millipore)	1 : 1000	Biotin. Horse anti mouse (Vector Lab)	1 : 200

Supp. Tab. 5: Incubation conditions of receptor autoradiography

Including the ^{3}H-ligand and displacer for glutamatergic (AMPA, kainite, NMDA, $mGlu_{2/3}$), GABAergic ($GABA_A$, $GABA_{A(BZ)}$, $GABA_B$), and catecholaminergic (α_1, α_2, $D_{1/5}$) receptors (see Lothmann et. al, 2021)

Receptor	[^{3}H] ligand (incubation concentration)	Displacer (incubation concentration)	Incubation buffer	Preincubation step	Main incubation step	Rinsing step	Exposure times
AMPA	[^{3}H] AMPA (10 nM)	Quisqualate (10 µM)	50 nM Tris-acetate (pH 7.2)	3 x 10 min at 4°C in incubation buffer	45 min at 4°C in incubation buffer + 100 mM KSCN	4 x 4 sec at 4 °C in incubation buffer + 2 x 2 sec at 25°C in acetone/glutaraldehyde	15 weeks
Kainate	[^{3}H] kainate (9.4 nM)	SYM-2081 (100 µM)	50 nM Tris-citrate (pH 7.1)	3 x 10 min at 4°C in incubation buffer	45 min at 4°C in incubation buffer + 10 nM Ca-acetate	3 x 4 sec at 4 °C in incubation buffer + 2 x 2 sec at 25°C in acetone/glutaraldehyde	12 weeks
NMDA	[^{3}H] MK-801 (3.3 nM)	MK-801 (100 µM)	50 nM Tris-HCl (pH 7.2)	15 min at 4°C in incubation buffer	60 min at 25°C in incubation buffer + 50 µM glutamate + 30 µM glycine + 50 µM spermidine	2 x 5 min at 4°C in incubation buffer + 50 µM glutamate + 1 dip at 25°C in H_2O dest.	12 weeks
$mGluR_{2/3}$	[^{3}H] LY-341495 (1 nM)	L-glutamate (1 mM)	10 nM phosphate buffer (pH 7.6)	2 x 5 min at 4°C in incubation buffer	60 min at 4°C in incubation buffer + 100 mM KBr	2 x 5 min at 4°C in incubation buffer + 1 dip at 25°C in H_2O dest	12 weeks
$GABA_A$	[^{3}H] muscimol (7.7 nM)	GABA (10 µM)	50 nM Tris-citrate (pH 7.0)	3 x 5 min at 4°C in incubation buffer	40 min at 4°C in incubation buffer	3 x 3 min at 4°C in incubation buffer + 1 dip at 25°C in H_2O dest	12 weeks

$GABA_B$	[^{3}H] CGP-54626 (2 nM)	CGP-55845 (100 µM)	50 nM Tris-HCl (pH 7.2)	3 x 5 min at 4°C in incubation buffer	60 min at 4°C in incubation buffer + 2,5 mM $CaCl_2$	3 x 2 min at 4°C in incubation buffer + 1 dip at 25°C in H_2O dest	12 weeks
$GABA_{A(BZ)}$	[^{3}H] Flumazenil (1 nM)	Clonazepam (2 µM)	170 nM Tris-HCl (pH 7.4)	15 min at 4°C in incubation buffer	60 min at 4°C in incubation buffer	2 x 1 min at 4 °C in incubation buffer + 1 dip in H_2O dest	10 weeks
α_1	[^{3}H] Prazosin (0.09 nM)	Phentolamine (10 µm)	50 mM Na/K phosphate buffer (pH 7.4)	15 min at 25°C in incubation buffer	60 min at 25°C in incubation buffer	2 x 5 min at 4°C in incubation buffer + 1 dip at 25°C in H_2O dest	12 weeks
α_2	[^{3}H] RX 821002 (1.4 nM)	Phentolamine (10 µm)	50 nM Tris-HCl (pH 7.7)	15 min at 25°C in incubation buffer	90 min at 25°C in incubation buffer	5 min at 4°C in incubation buffer + 1 dip at 25°C in H_2O dest	12 weeks
$D_{1/5}$	[^{3}H] SCH-23390 (1.67 nM)	SKF-83566 (1 µM)	50 nM Tris-HCl (pH 7.4)	20 min at 25°C in incubation buffer + 120 mM NaCl + 5 mM KCl + 2 mM $CaCl_2$ + 1 mM $MgCl_2$	90 min at 25°C in incubation buffer + 120 mM NaCl + 5 mM KCl + 2 mM $CaCl_2$ + 1 mM $MgCl_2$ + 1 µM Mianserine	6 x 1 min at 4°C in incubation buffer + 0,1 % Ascorbic acid + 150 nM NaCl + 1 dip in H_2O dest.	15 weeks

Supp. Tab. 6: Region-specific receptor concentrations of CG

Neurotransmitter receptor densities (fmol/mg protein) in different regions of the mouse olfactory system (Mean ± SEM). The Friedman ANOVAs display regional differences for each receptor type (all N = 10, df = 13). For pairwise comparisons between regions see further Supp. Tab. 7. (see Lothmann et. al, 2021)

	Receptor (fmol/mg protein)									
	AMPA	kainate	NMDA	$mGlu_{2/3}$	$GABA_A$	$GABA_{A(BZ)}$	$GABA_B$	α_1	α_2	$D_{1/5}$
Main olfactory bulb	727 ± 54	1281 ± 95	954 ± 158	2180 ± 121	803 ± 93	3867 ± 577	2144 ± 119	547 ± 33	497 ± 32	61 ± 6
Accessory olfactory bulb	909 ± 88	1328 ± 94	1203 ± 156	3948 ± 376	950 ± 212	6409 ± 664	3617 ± 288	675 ± 50	547 ± 69	100 ± 15
Anterior olfactory cortex	1044 ± 87	1432 ± 69	1445 ± 189	2365 ± 165	566 ± 73	2038 ± 181	4223 ± 345	338 ± 19	1809 ± 160	171 ± 29
taenia tecta, dorsal	1151 ± 58	1356 ± 124	1878 ± 213	2977 ± 212	906 ± 64	3662 ± 331	4736 ± 428	308 ± 36	1589 ± 141	357 ± 49
taenia tecta, ventral	1361 ± 86	1022 ± 114	1716 ± 125	2825 ± 222	788 ± 85	3214 ± 272	4316 ± 442	321 ± 45	1377 ± 177	315 ± 90
Dorsal peduncular cortex	1069 ± 62	1624 ± 95	1909 ± 255	3442 ± 155	1048 ± 78	4125 ± 340	5048 ± 674	317 ± 52	1031 ± 94	360 ± 44
Endopiriform nucleus (dorsal)	789 ± 51	1480 ± 75	1239 ± 129	1836 ± 224	695 ± 61	2791 ± 257	4059 ± 211	238 ± 23	1032 ± 49	888 ± 95
Piriform cortex	1060 ± 41	785 ± 48	1821 ± 162	3328 ± 207	1034 ± 68	3961 ± 243	4853 ± 158	448 ± 40	1027 ± 80	242 ± 28
Entorhinal Cortex, lateral	1664 ± 59	1054 ± 32	3037 ± 224	3070 ± 198	1297 ± 84	3627 ± 221	5894 ± 254	314 ± 19	1771 ± 137	345 ± 26
Entorhinal Cortex, medial	1580 ± 102	1040 ± 71	2091 ± 301	3081 ± 268	1190 ± 98	3553 ± 487	6201 ± 200	304 ± 26	1770 ± 136	330 ± 17
Orbitofrontal Cortex, medial	1089 ± 83	1095 ± 164	2292 ± 278	3867 ± 360	1553 ± 105	4894 ± 323	5925 ± 392	502 ± 38	650 ± 22	175 ± 43
Orbitofrontal Cortex, ventrolateral	1034 ± 79	995 ± 140	2101 ± 236	4024 ± 511	1520 ± 162	4762 ± 406	5909 ± 461	495 ± 48	570 ± 24	131 ± 28
Orbitofrontal Cortex, lateral	1100 ± 75	1039 ± 175	2168 ± 209	3983 ± 524	1393 ± 172	4269 ± 529	5003 ± 404	513 ± 67	564 ± 22	211 ± 33
Olfactory Tubercle	1079 ± 88	964 ± 70	1638 ± 131	3964 ± 346	853 ± 77	3048 ± 403	2995 ± 277	204 ± 25	770 ± 107	5340 ± 439
Friedman ANOVA (χ^2), ***p < 0.001	85.531***	78.060***	82.983***	79.952***	93.630***	70.971***	94.811***	102.142***	105.714***	106.140***
n = 10, df = 13										

Supp. Tab. 7: Statistical analysis of region-specific receptor concentrations of CG

Significant differences between receptor densities between the olfactory regions. Each receptor type was tested with pairwise Dunn-Bonferroni post hoc test if the Friedman ANOVA showed regional differences in-between the regions. Significance (Sig., p-value) and adjusted significance (Adj. Sig., p-value multiplied by the number of tests carried out) labelled $p < 0.05$ (see Lothmann et. al, 2021)

	AMPA		Kainate		NMDA		$mGlu_{2/3}$		$GABA_A$		$GABA_{A(BZ)}$		$GABA_B$		α_1		α_2		$D_{1/5}$	
	Sig	Adj. Sig	Sig	Adj. Sig	Sig	Adj. Sig	Sig	Adj. Sig	Sig	Adj. Sig	Sig	Adj. Sig	Sig	Adj. Sig	Sig	Adj. Sig	Sig	Adj. Sig	Sig	Adj. Sig
MOB-Epd	.748	1.000	.098	1.000	.392	1.000	.748	1.000	.708	1.000	.121	1.000	**.022**	1.000	**.000**	**.000**	**.001**	.122	**.000**	**.000**
MOB-AOB	.149	1.000	.612	1.000	.310	1.000	**.000**	**.001**	.378	1.000	**.001**	.069	.121	1.000	.630	1.000	.423	1.000	.219	1.000
MOB-ORBvl	**.037**	1.000	.054	1.000	**.000**	**.002**	**.000**	**.000**	**.000**	**.000**	**.022**	1.000	**.000**	**.000**	.575	1.000	.487	1.000	.219	1.000
MOB-AON	**.033**	1.000	.121	1.000	**.042**	1.000	.454	1.000	.285	1.000	**.012**	1.000	**.016**	1.000	**.001**	.092	**.000**	**.000**	.054	1.000
MOB-OT	**.010**	.937	**.016**	1.000	**.016**	1.000	**.000**	**.000**	.557	1.000	.219	1.000	.392	1.000	**.000**	**.000**	.061	1.000	**.000**	**.000**
MOB-ORBl	**.009**	.802	.364	1.000	**.000**	**.000**	**.000**	**.002**	**.000**	**.000**	**.008**	.685	**.000**	**.000**	.688	1.000	.134	1.000	**.025**	1.000
MOB-PIR	**.008**	.685	**.000**	**.021**	**.002**	.176	**.000**	**.038**	.054	1.000	.364	1.000	**.000**	**.031**	.181	1.000	**.001**	.122	**.001**	.101
MOB-DP	**.005**	.420	**.042**	1.000	**.000**	**.017**	**.000**	**.017**	**.028**	1.000	.262	1.000	**.000**	**.007**	**.000**	**.015**	**.002**	.147	**.000**	**.000**
MOB-ORBm	**.002**	.210	.240	1.000	**.000**	**.001**	**.000**	**.001**	**.000**	**.021**	.134	1.000	**.000**	**.017**	.708	1.000	.593	1.000	**.002**	.161
MOB-TTd	**.000**	**.025**	.487	1.000	**.000**	**.031**	**.048**	1.000	.262	1.000	.748	1.000	**.000**	**.031**	**.000**	**.007**	**.000**	**.000**	**.000**	**.001**
MOB-TTv	**.000**	**.000**	.054	1.000	**.004**	.355	.061	1.000	.979	1.000	.630	1.000	**.005**	.420	**.000**	**.013**	**.000**	**.013**	**.001**	.057
MOB-ENTm	**.000**	**.000**	.082	1.000	**.000**	**.007**	**.011**	1.000	**.008**	.685	.200	1.000	**.000**	**.000**	**.000**	**.013**	**.000**	**.000**	**.000**	**.000**
MOB-ENTl	**.000**	**.000**	.098	1.000	**.000**	**.000**	**.003**	.299	**.000**	**.023**	.134	1.000	**.000**	**.000**	**.000**	**.031**	**.000**	**.000**	**.000**	**.000**
Epd-AOB	.262	1.000	.250	1.000	.873	1.000	**.000**	**.000**	.209	1.000	**.000**	**.000**	.454	1.000	**.000**	**.000**	**.016**	1.000	**.000**	**.000**
Epd-ORBvl	.078	1.000	.915	1.000	**.001**	.057	**.000**	**.000**	**.000**	**.000**	**.000**	**.011**	**.002**	.210	**.000**	**.004**	**.012**	1.000	**.000**	**.000**
Epd-AON	.069	1.000	.915	1.000	.240	1.000	.285	1.000	.487	1.000	.336	1.000	.915	1.000	.173	1.000	**.016**	1.000	**.000**	**.001**
Epd-OT	**.025**	1.000	**.000**	**.004**	.121	1.000	**.000**	**.000**	.336	1.000	.748	1.000	.149	1.000	.454	1.000	.181	1.000	**.000**	**.000**
Epd-ORBl	**.022**	1.000	**.010**	.932	**.000**	**.001**	**.000**	**.000**	**.000**	**.000**	**.000**	**.002**	**.001**	**.047**	**.000**	**.002**	.087	1.000	**.000**	**.004**
Epd-PIR	**.019**	1.000	**.000**	**.000**	**.025**	1.000	**.000**	**.011**	**.022**	1.000	**.014**	1.000	.200	1.000	**.001**	.084	**1.000**	1.000	**.002**	.210
Epd-DP	**.012**	1.000	.708	1.000	**.004**	.355	**.000**	**.004**	**.010**	.937	**.008**	.685	.098	1.000	.378	1.000	.957	1.000	.957	1.000
Epd-ORBm	**.006**	.583	**.005**	.420	**.000**	**.021**	**.000**	**.000**	**.000**	**.004**	**.002**	.210	.149	1.000	**.000**	**.002**	**.008**	.685	**.001**	.134
Epd-TTd	**.001**	.084	.336	1.000	**.006**	.583	**.022**	1.00	.134	1.000	.061	1.000	.200	1.000	.487	1.000	.078	1.000	.051	1.000

Epd-TTv	**.000**	**.000**	**.000**	**.031**	**.042**	1.000	**.028**	1.000	.688	1.000	.285	1.000	.593	1.000	.392	1.000	.557	1.000	**.004**	.355
Epd-ENTm	**.000**	**.000**	**.001**	.063	**.002**	.176	**.004**	.386	**.002**	.210	.109	1.000	**.000**	**.007**	.392	1.000	**.022**	1.000	.098	1.000
Epd-ENTl	**.000**	**.000**	**.001**	.084	**.000**	**.000**	**.001**	.101	**.000**	**.005**	.069	1.000	**.001**	.057	.285	1.000	**.019**	1.000	.121	1.000
AOB-ORBvl	.521	1.000	**.015**	1.000	**.001**	.101	.669	1.000	**.000**	**.021**	.285	1.000	**.000**	**.013**	.297	1.000	.915	1.000	.748	1.000
AOB-AON	.487	1.000	.297	1.000	.310	1.000	**.000**	**.025**	.051	1.000	**.000**	**.000**	.392	1.000	**.000**	**.015**	**.000**	**.000**	.310	1.000
AOB-OT	.262	1.000	**.004**	.326	.165	1.000	**.000**	**.006**	.769	1.000	**.000**	**.000**	.487	1.000	**.000**	**.000**	.285	1.000	**.000**	**.000**
AOB-ORBl	.240	1.000	.157	1.000	**.000**	**.001**	.915	1.000	**.000**	**.008**	.487	1.000	**.000**	**.002**	.378	1.000	.487	1.000	.181	1.000
AOB-PIR	.219	1.000	**.000**	**.002**	.285	1.000	.392	1.000	.297	1.000	**.014**	1.000	**.042**	1.000	.069	1.000	**.016**	1.000	**.019**	1.000
AOB-DP	.165	1.000	.128	1.000	**.006**	.583	.521	1.000	.190	1.000	**.025**	1.000	**.016**	1.000	**.000**	**.002**	**.019**	1.000	**.000**	**.009**
AOB-ORBm	.109	1.000	.092	1.000	**.000**	**.038**	.979	1.000	**.005**	.456	.061	1.000	**.028**	1.000	.392	1.000	.789	1.000	**.027**	1.000
AOB-TTd	**.028**	1.000	.852	1.000	**.010**	.937	**.016**	1.000	.810	1.000	**.002**	.210	**.042**	1.000	**.000**	**.001**	**.000**	**.003**	**.001**	.051
AOB-TTv	**.000**	**.011**	**.015**	1.000	.061	1.000	**.012**	1.000	.392	1.000	**.000**	**.011**	.200	1.000	**.000**	**.002**	**.003**	.251	**.012**	1.000
AOB-ENTm	**.000**	**.002**	**.025**	1.000	**.003**	.299	.065	1.000	.073	1.000	**.001**	.084	**.000**	**.000**	**.000**	**.002**	**.000**	**.000**	**.000**	**.017**
AOB-ENTl	**.000**	**.000**	**.030**	1.000	**.000**	**.000**	.149	1.000	**.005**	.495	**.002**	.176	**.000**	**.003**	**.000**	**.004**	**.000**	**.000**	**.000**	**.011**
ORBvl-AON	.957	1.000	**.001**	**.047**	**.025**	1.000	**.000**	**.004**	**.000**	**.000**	**.000**	**.000**	**.003**	.299	**.006**	.583	**.000**	**.000**	.487	1.000
ORBvl-OT	.630	1.000	.630	1.000	0.61	1.000	.957	1.000	**.002**	.183	**.000**	**.038**	**.000**	**.001**	**.000**	**.000**	.240	1.000	**.000**	**.000**
ORBvl-ORBl	.593	1.000	.310	1.000	.285	1.000	.593	1.000	.810	1.000	.708	1.000	.669	1.000	.873	1.000	.423	1.000	.310	1.000
ORBvl-PIR	.557	1.000	.078	1.000	.240	1.000	.200	1.000	**.008**	.741	.165	1.000	.078	1.000	.438	1.000	**.012**	1.000	**.042**	1.000
ORBvl-DP	.454	1.000	**.000**	**.007**	.593	1.000	.285	1.000	**.017**	1.000	.240	1.000	.165	1.000	**.001**	.122	**.014**	1.000	**.000**	**.031**
ORBvl-ORBm	.336	1.000	.454	1.000	.789	1.000	**.023**	1.000	.378	1.000	.423	1.000	.109	1.000	.852	1.000	.873	1.000	.058	1.000
ORBvl-TTd	.121	1.000	**.009**	.802	.487	1.000	**.005**	.420	**.001**	.051	**.048**	1.000	.078	1.000	**.001**	.063	**.000**	**.002**	**.002**	.161
ORBvl-TTv	**.001**	.122	1.000	1.000	.165	1.000	**.003**	.299	**.000**	**.001**	**.005**	.495	**.012**	1.000	**.001**	.111	**.002**	.176	**.028**	1.000
ORBvl-ENTm	**.000**	**.025**	.852	1.000	.748	1.000	.688	1.000	.058	1.000	**.025**	1.000	.364	1.000	**.001**	.111	**.000**	**.000**	**.001**	.057
ORBvl-ENTl	**.000**	**.007**	.789	1.000	**.033**	1.000	.061	1.000	.364	1.000	**.042**	1.000	.708	1.000	**.003**	.230	**.000**	**.000**	**.000**	**.038**
AON-OT	.669	1.000	**.000**	**.007**	.708	1.000	**.000**	**.006**	.098	1.000	.200	1.000	.121	1.000	**.035**	1.000	**.000**	**.017**	**.000**	**.000**
AON-ORBl	.630	1.000	**.014**	1.000	**.001**	0.84	**.000**	**.038**	**.000**	**.000**	**.000**	**.000**	**.001**	.069	**.004**	.355	**.000**	**.004**	.748	1.000
AON-PIR	.593	1.000	**.000**	**.000**	.285	1.000	**.005**	.495	**.003**	.251	**.001**	.057	.240	1.000	.051	1.000	**.016**	1.000	.181	1.000
AON-DP	.487	1.000	.128	1.000	.087	1.000	**.003**	.251	**.001**	.101	**.000**	**.025**	.121	1.000	.630	1.000	**.014**	1.000	**.004**	.355
AON-ORBm	.364	1.000	**.006**	.583	**.012**	1.000	**.000**	**.023**	**.000**	**.000**	**.000**	**.006**	.181	1.000	**.004**	.326	**.000**	**.000**	.229	1.000
AON-TTd	.134	1.000	.392	1.000	.121	1.000	.219	1.000	**.028**	1.000	**.005**	.420	.240	1.000	.504	1.000	.521	1.000	**.015**	1.000
AON-TTv	**.002**	.147	**.001**	**.047**	.392	1.000	.262	1.000	.273	1.000	**.042**	1.000	.669	1.000	.612	1.000	.069	1.000	.134	1.000

AON-ENTm	**.000**	**.031**	**.001**	.092	.054	1.000	.073	1.000	**.000**	**.017**	**.010**	.937	**.000**	**.011**	.612	1.000	.915	1.000	**.006**	.583
AON-ENTl	**.000**	**.009**	**.001**	.122	**.000**	**.001**	**.028**	1.000	**.000**	**.000**	**.005**	.495	**.001**	.084	.769	1.000	.957	1.000	**.005**	.420
OT-ORBl	.957	1.000	.134	1.000	**.003**	.299	.630	1.000	**.000**	**.002**	**.000**	**.009**	**.000**	**.000**	**.000**	**.000**	.708	1.000	**.000**	**.000**
OT-PIR	.915	1.000	.200	1.000	.487	1.000	.219	1.000	.181	1.000	**.033**	1.000	**.006**	.583	**.000**	**.004**	.181	1.000	**.000**	.025
OT-DP	.789	1.000	**.000**	**.001**	.181	1.000	.310	1.000	.109	1.000	**.019**	1.000	**.002**	.176	.103	1.000	.200	1.000	**.037**	1.000
OT-ORBm	.630	1.000	.219	1.000	**.033**	1.000	.728	1.000	**.002**	.176	**.006**	.583	**.004**	.355	**.000**	**.000**	.181	1.000	**.000**	**.015**
OT-TTd	.285	1.000	**.002**	.176	.240	1.000	**.005**	.495	.593	1.000	.121	1.000	**.006**	.583	.149	1.000	**.002**	.176	**.011**	1.000
OT-TTv	**.006**	.583	.630	1.000	.630	1.000	**.004**	.355	.575	1.000	.454	1.000	**.048**	1.000	.109	1.000	.054	1.000	**.001**	**.047**
OT-ENTm	**.002**	.147	.504	1.000	.121	1.000	**.027**	1.000	**.037**	1.000	.200	1.000	**.000**	**.000**	.109	1.000	**.000**	**.025**	**.025**	1.000
OT-ENTl	**.001**	**.047**	.454	1.000	**.000**	**.006**	.069	1.000	**.002**	.176	.134	1.000	**.000**	**.000**	.069	1.000	**.000**	**.021**	**.033**	1.000
ORBl-PIR	.957	1.000	**.005**	.495	**.025**	1.000	.454	1.000	**.004**	.355	.078	1.000	**.028**	1.000	.350	1.000	.087	1.000	.310	1.000
ORBl-DP	.831	1.000	**.003**	.299	.109	1.000	.593	1.000	**.009**	.802	.121	1.000	.069	1.000	**.001**	.069	.098	1.000	**.010**	.937
ORBl-ORBm	.669	1.000	.789	1.000	.423	1.000	.894	1.000	.262	1.000	.240	1.000	**.042**	1.000	.979	1.000	.336	1.000	.378	1.000
ORBl-TTd	.310	1.000	.109	1.000	.078	1.000	**.022**	1.000	**.000**	**.021**	**.019**	1.000	**.028**	1.000	**.000**	**.034**	**.001**	**.047**	**.035**	1.000
ORBl-TTv	**.008**	.685	.310	1.000	**.014**	1.000	**.016**	1.000	**.000**	**.000**	**.002**	.147	**.003**	.299	**.001**	.063	**.022**	1.000	.240	1.000
ORBl-ENTm	**.002**	.176	.407	1.000	.165	1.000	.082	1.000	**.033**	1.000	**.009**	.802	.630	1.000	**.001**	.063	**.000**	**.006**	**.016**	1.000
ORBl-ENTl	**.001**	.057	.454	1.000	.165	1.000	.181	1.000	.250	1.000	**.016**	1.000	.957	1.000	**.001**	.134	**.000**	**.004**	**.012**	1.000
PIR-DP	.873	1.000	**.000**	**.000**	.521	1.000	.831	1.000	.789	1.000	.831	1.000	.708	1.000	**.015**	1.000	.957	1.000	.121	1.000
PIR-ORBm	.708	1.000	**.012**	1.000	.149	1.000	.378	1.000	.078	1.000	.557	1.000	.873	1.000	.336	1.000	**.008**	.685	.894	1.000
PIR-TTd	.336	1.000	**.000**	**.001**	.630	1.000	.121	1.000	.423	1.000	.557	1.000	**1.000**	1.000	**.009**	.802	.078	1.000	.273	1.000
PIR-TTv	**.009**	.802	.078	1.000	.831	1.000	.098	1.000	.058	1.000	.165	1.000	.454	1.000	**.014**	1.000	.557	1.000	.873	1.000
PIR-ENTm	**.002**	.210	.051	1.000	.392	1.000	.323	1.000	.454	1.000	.392	1.000	**.008**	.685	**.014**	1.000	**.022**	1.000	.165	1.000
PIR-ENTl	**.001**	.069	**.042**	1.000	**.001**	.084	.557	1.000	.082	1.000	.521	1.000	**.033**	1.000	**.025**	1.000	**.019**	1.000	.134	1.000
DP-ORBm	.831	1.000	**.001**	.122	.423	1.000	.504	1.000	.134	1.000	.708	1.000	.831	1.000	**.001**	.063	**.009**	.802	.092	1.000
DP-TTd	.423	1.000	.181	1.000	.873	1.000	.078	1.000	.285	1.000	.423	1.000	.708	1.000	.852	1.000	.069	1.000	.650	1.000
DP-TTv	**.014**	1.000	**.000**	**.007**	.392	1.000	.061	1.000	**.030**	1.000	.109	1.000	.262	1.000	.979	1.000	.521	1.000	.165	1.000
DP-ENTm	**.004**	.355	**.000**	**.015**	.831	1.000	.229	1.000	.121	1.000	.285	1.000	**.022**	1.000	.979	1.000	**.019**	1.000	.873	1.000
DP-ENTl	**.001**	.122	**.000**	**.021**	**.008**	.685	.423	1.000	.142	1.000	.392	1.000	.078	1.000	.852	1.000	**.016**	1.000	.957	1.000
ORBm-TTd	.557	1.000	.061	1.000	.336	1.000	**.015**	1.000	**.010**	.937	.240	1.000	.873	1.000	**.000**	**.031**	**.000**	**.001**	.219	1.000
ORBm-TTv	**.025**	1.000	.454	1.000	.098	1.000	**.011**	1.000	**.000**	**.023**	**.048**	1.000	.364	1.000	**.001**	.057	**.001**	.101	.769	1.000
ORBm-ENTm	**.008**	.685	.575	1.000	.557	1.000	.061	1.000	.310	1.000	.149	1.000	**.012**	1.000	**.001**	.057	**.000**	**.000**	.128	1.000

ORBm-ENTl	**.003**	.251	.630	1.000	.285	1.000	.142	1.000	.979	1.000	.219	1.000	**.048**	1.000	**.001**	.122	**.000**	**.000**	.103	1.000
TTd-TTv	.098	1.000	**.015**	1.000	.487	1.000	.915	1.000	.273	1.000	.423	1.000	.454	1.000	.873	1.000	.240	1.000	.350	1.000
TTd-ENTm	**.037**	1.000	**.015**	1.000	.708	1.000	.575	1.000	.121	1.000	.789	1.000	**.008**	.685	.873	1.000	.593	1.000	.769	1.000
TTd-ENTl	**.016**	1.000	**.019**	1.000	**.005**	.420	.336	1.000	**.011**	1.000	.957	1.000	**.033**	1.000	.708	1.000	.557	1.000	.688	1.000
TTv-ENTm	.669	1.000	.852	1.000	.285	1.000	.504	1.000	**.008**	.741	.593	1.000	**.001**	.057	**1.000**	1.000	.087	1.000	.219	1.000
TTv-ENTl	.454	1.000	.789	1.000	**.000**	**.038**	.285	1.000	**.000**	**.025**	.454	1.000	**.004**	.355	.831	1.000	.078	1.000	.181	1.000
ENTm-ENTl	.748	1.000	.936	1.000	0.14	1.000	.688	1.000	.323	1.000	.831	1.000	.593	1.000	.831	1.000	.957	1.000	.915	1.000

Supp. Tab. 8: Layer-specific receptor concentrations of CG

Layer-specific absolute receptor densities of the subregions of the olfactory system (mean ± SEM) in control mice (CG).

CG	Receptor (fmol/mg protein)									
	AMPA	kainate	NMDA	$mGlu_{2/3}$	$GABA_A$	$GABA_{A(BZ)}$	$GABA_B$	α_1	α_2	$D_{1/5}$
Main olfactory bulb										
ipl	764 ± 55	911 ± 72	823 ± 111	1697 ± 32	260 ± 42	976 ± 67	2062 ± 119	447 ± 22	1027 ± 31	49 ± 4
mi	719 ± 40	1311 ± 114	796 ± 132	1876 ± 64	375 ± 58	1025 ± 96	1920 ± 77	406 ± 23	442 ± 26	57 ± 6
opl	678 ± 35	1087 ± 88	886 ± 168	1686 ± 33	303 ± 42	950 ± 73	1971 ± 75	404 ± 20	588 ± 44	49 ± 7
gl	665 ± 31	1567 ± 136	975 ± 161	2369 ± 159	670 ± 86	2578 ± 255	1930 ± 31	572 ± 28	337 ± 29	68 ± 5
onl	622 ± 45	1943 ± 155	1684 ± 211	3064 ± 215	2367 ± 336	9695 ± 533	3391 ± 296	1032 ± 92	351 ± 18	79 ± 9
onl	694 ± 97	1025 ± 101	672 ± 101	1986 ± 171	831 ± 96	4308 ± 227	2173 ± 254	381 ± 22	304 ± 29	73 ± 7
Accessory olfactory bulb										
mi	942 ± 84	1189 ± 88	1183 ± 183	3320 ± 257	744 ± 214	6982 ± 579	2955 ± 340	621 ± 68	607 ± 95	106 ± 19
gl	946 ± 98	1930 ± 45	1553 ± 25	4907 ± 617	1693 ± 312	7090 ± 868	2880 ± 100	1016 ± 67	469 ± 98	107 ± 21
gl	661 ± 283	785 ± 17	1226 ± 167	1298 ± 175	462 ± 150	2910 ± 528	5087 ± 810	400 ± 81	531 ± 127	67 ± 10
Anterior olfactory cortex										
m	940 ± 124	1298 ± 29	1124 ± 98	3081 ± 321	825 ± 147	2597 ± 250	3551 ± 505	449 ± 37	1340 ± 219	161 ± 37
d	1226 ± 81	1327 ± 141	1416 ± 50	2266 ± 208	545 ± 100	2073 ± 224	4608 ± 423	315 ± 10	2169 ± 176	189 ± 34
pv	1040 ± 112	1454 ± 137	1668 ± 114	2420 ± 194	397 ± 99	1414 ± 146	4389 ± 374	318 ± 24	2296 ± 165	234 ± 69
l	1078 ± 111	1783 ± 138	996 ± 62	1846 ± 115	565 ± 21	1972 ± 294	3629 ± 328	308 ± 22	1925 ± 221	137 ± 36
e	1177 ± 120	1433 ± 85	2469 ± 259	3001 ± 484	311 ± 66	2134 ± 186	4602 ± 570	327 ± 20	1925 ± 214	107 ± 4
e	910 ± 48	1246 ± 227	799 ± 23	3054 ± 653	991 ± 351	1923 ± 467	3197 ± 584	366 ± 75	1271 ± 240	42 ± 26
taenia tecta, dorsal										
II	1161 ± 94	994 ± 162	2319 ± 250	3559 ± 357	1003 ± 119	3316 ± 425	4995 ± 333	300 ± 62	1362 ± 186	216 ± 44
III	1404 ± 120	1120 ± 98	2210 ± 158	3019 ± 209	888 ± 79	3731 ± 350	4999 ± 570	283 ± 38	1798 ± 135	267 ± 46
IV	1100 ± 65	1293 ± 97	2140 ± 219	2554 ± 154	914 ± 83	3967 ± 358	4922 ± 591	302 ± 25	1649 ± 181	372 ± 58
IV	924 ± 64	1843 ± 185	1506 ± 148	2491 ± 199	730 ± 36	3633 ± 310	3377 ± 318	341 ± 43	2000 ± 180	594 ± 92
taenia tecta, ventral										
II	1014 ± 91	699 ± 104	1665 ± 179	2767 ± 327	796 ± 142	2949 ± 375	796 ± 281	288 ± 51	1028 ± 165	201 ± 55

III	1477 ± 105	1067 ± 142	1814 ± 164	2948 ± 282	876 ± 118	3315 ± 334	876 ± 512	318 ± 60	1463 ± 220	251 ± 72
III	1442 ± 93	1299 ± 163	1721 ± 116	2667 ± 174	693 ± 44	3222 ± 257	693 ± 399	338 ± 40	1638 ± 225	492 ± 151
Dorsal peduncular cortex										
II/III	1092 ± 36	1154 ± 46	2067 ± 173	4126 ± 334	952 ± 93	4188 ± 588	5035 ± 648	265 ± 54	1121 ± 137	253 ± 39
V	1358 ± 108	1587 ± 135	2677 ± 280	3665 ± 215	1085 ± 90	4273 ± 406	5683 ± 837	343 ± 69	951 ± 65	330 ± 55
VI	992 ± 54	1611 ± 119	2245 ± 210	3126 ± 183	1154 ± 82	4364 ± 293	5251 ± 801	374 ± 74	1032 ± 85	348 ± 40
VI	909 ± 90	1860 ± 129	1631 ± 233	2860 ± 122	963 ± 91	3715 ± 328	4224 ± 506	260 ± 34	950 ± 101	509 ± 61
Piriform cortex										
II	780 ± 32	580 ± 66	2103 ± 165	4400 ± 283	1169 ± 77	4193 ± 205	4727 ± 141	497 ± 42	832 ± 52	149 ± 18
III	1607 ± 53	764 ± 49	1877 ± 190	3380 ± 214	1153 ± 42	3993 ± 259	5382 ± 210	467 ± 52	1116 ± 101	208 ± 21
III	877 ± 38	977 ± 48	1627 ± 151	2613 ± 154	888 ± 66	3603 ± 143	4518 ± 115	381 ± 37	1159 ± 99	368 ± 51
Entorhinal cortex, lateral										
II	1066 ± 120	407 ± 61	2302 ± 316	3264 ± 325	1150 ± 88	3197 ± 448	5416 ± 419	271 ± 16	943 ± 84	230 ± 33
III	2009 ± 116	722 ± 48	3401 ± 274	3431 ± 194	1623 ± 66	3868 ± 348	6602 ± 331	292 ± 22	1592 ± 156	344 ± 43
IV	2106 ± 80	823 ± 42	3628 ± 281	3380 ± 154	1595 ± 95	3637 ± 250	6719 ± 374	279 ± 18	1815 ± 175	356 ± 36
V	1966 ± 101	945 ± 12	3417 ± 215	3242 ± 269	1539 ± 100	3423 ± 151	6514 ± 323	267 ± 23	2012 ± 168	312 ± 24
VIa	1746 ± 101	1206 ± 74	3330 ± 192	3064 ± 261	1282 ± 95	3371 ± 136	6106 ± 337	293 ± 27	2061 ± 168	311 ± 33
VIb	1520 ± 88	1710 ± 112	2781 ± 179	2612 ± 131	1199 ± 82	3928 ± 148	5705 ± 222	381 ± 21	2020 ± 135	406 ± 45
VIb	1187 ± 62	1616 ± 100	2123 ± 187	1964 ± 70	995 ± 85	3572 ± 207	4258 ± 155	430 ± 34	1952 ± 127	453 ± 67
Entorhinal cortex, medial										
II	1452 ± 82	648 ± 70	1679 ± 253	3201 ± 373	1116 ± 58	3679 ± 602	5815 ± 301	271 ± 39	941 ± 107	212 ± 30
III	1538 ± 188	869 ± 58	2698 ± 163	3512 ± 432	1504 ± 53	3833 ± 691	7038 ± 286	302 ± 38	1659 ± 186	333 ± 40
IV	1542 ± 194	1065 ± 61	2602 ± 137	3274 ± 349	1599 ± 72	3602 ± 464	6677 ± 272	286 ± 26	1938 ± 152	385 ± 36
V	1564 ± 93	1207 ± 111	1681 ± 300	3117 ± 292	1458 ± 42	3495 ± 486	6478 ± 210	259 ± 28	2109 ± 207	349 ± 30
VI	1497 ± 106	1276 ± 96	2383 ± 304	3000 ± 263	1246 ± 88	3544 ± 611	5921 ± 280	323 ± 32	2127 ± 146	345 ± 23
VI	1501 ± 134	1309 ± 107	1360 ± 155	2375 ± 213	905 ± 86	3168 ± 394	5276 ± 471	377 ± 31	1651 ± 89	375 ± 10
Orbitofrontal cortex, medial										
II	1253 ± 75	595 ± 114	2741 ± 237	4846 ± 598	1371 ± 201	4362 ± 282	5681 ± 365	445 ± 57	700 ± 54	127 ± 23
II/III	1132 ± 87	945 ± 220	2365 ± 270	4004 ± 532	1537 ± 231	4519 ± 659	5465 ± 669	536 ± 91	660 ± 26	166 ± 30
V	1076 ± 44	1063 ± 177	2041 ± 249	4060 ± 755	1362 ± 231	4362 ± 714	5046 ± 429	575 ± 84	573 ± 34	216 ± 52
VI	995 ± 109	1300 ± 66	1661 ± 160	3387 ± 605	1330 ± 193	4088 ± 679	4725 ± 359	521 ± 62	454 ± 21	272 ± 46

VI	948 ± 103	1518 ± 43	2070 ± 207	3475 ± 597	1364 ± 137	4140 ± 649	4359 ± 327	491 ± 61	435 ± 20	276 ± 44
Orbitofrontal cortex, ventrolateral										
II/III	1174 ± 72	769 ± 114	2459 ± 317	4515 ± 528	1578 ± 136	4676 ± 317	6181 ± 481	505 ± 52	767 ± 54	77 ± 23
V	991 ± 77	885 ± 78	2266 ± 248	4088 ± 532	1559 ± 233	5096 ± 481	6482 ± 530	475 ± 58	580 ± 24	108 ± 34
VI	1013 ± 104	1253 ± 115	2200 ± 254	3963 ± 541	1494 ± 178	5192 ± 539	5653 ± 437	499 ± 52	535 ± 40	127 ± 29
VI	959 ± 108	1470 ± 81	2013 ± 194	3531 ± 496	1449 ± 162	4083 ± 619	5320 ± 475	500 ± 42	409 ± 19	212 ± 35
Orbitofrontal cortex, lateral										
II/III	1248 ± 100	702 ± 102	2482 ± 281	5193 ± 110	1566 ± 98	4732 ± 324	6500 ± 276	384 ± 29	802 ± 35	119 ± 46
V	1035 ± 81	973 ± 173	2610 ± 323	4458 ± 88	1667 ± 69	5491 ± 443	6190 ± 220	505 ± 50	685 ± 23	164 ± 56
VI	1092 ± 83	1468 ± 131	2242 ± 253	4083 ± 288	1473 ± 120	4947 ± 434	5829 ± 459	544 ± 34	562 ± 43	169 ± 45
VI	982 ± 96	1609 ± 126	2240 ± 243	2983 ± 300	1449 ± 164	4405 ± 348	5744 ± 561	537 ± 44	534 ± 31	248 ± 34
Olfactory tubercle										
II	757 ± 44	711 ± 62	1445 ± 166	4837 ± 283	773 ± 87	2656 ± 449	2131 ± 286	185 ± 28	589 ± 100	4529 ± 404
III	1381 ± 98	1100 ± 101	1768 ± 116	4090 ± 409	973 ± 91	3195 ± 408	3344 ± 316	201 ± 25	813 ± 113	6451 ± 563
III	1092 ± 80	1147 ± 80	1700 ± 129	3487 ± 248	812 ± 67	3293 ± 399	3508 ± 286	227 ± 23	909 ± 116	5041 ± 503

Supp. Tab. 9: Statistical analysis of layer-specific receptor concentrations of the main olfactory bulb in CG

Statistical data of differences between receptor densities across layers within the main olfactory bulb of control mice (CG). Each receptor type was tested separately with pair-wise Wilcoxon-rank test if the Friedman ANOVA showed differences within the region. Wilcoxon-rank: Z-score (Z), minimum of sum of the ranks of positive or negative changes (T), red labelling if $p < 0.05$ (N = 10, df = 13) (see Lothmann et al., 2021).

CG	AMPA			Kainate			NMDA			$mGlu_{2/3}$			$GABA_A$		
	T	*Z*	*p-value*	*T*	*Z*	*p-value*	*T*	*Z*	*p-value*	*T*	*Z*	*p-value*	*T*	*Z*	*p-value*
MOBgr & MOB ipl	7,000	2,090	0,037	0,000	2,803	0,005	18,000	0,968	0,333	0,000	2,803	0,005	0,000	2,803	0,005
MOBgr & MOB mi	9,000	1,886	0,059	1,000	2,701	0,007	25,000	0,255	0,799	23,000	0,459	0,646	0,000	2,803	0,005
MOBgr & MOB opl	4,000	2,395	0,017	0,000	2,803	0,005	0,000	2,803	0,005	0,000	2,803	0,005	0,000	2,803	0,005
MOBgr & MOB gl	4,000	2,395	0,017	0,000	2,803	0,005	0,000	2,803	0,005	0,000	2,803	0,005	0,000	2,803	0,005
MOBgr & MOB onl	21,000	0,663	0,508	9,000	1,886	0,059	10,000	1,784	0,074	9,000	1,886	0,059	0,000	2,803	0,005
MOB ipl & MOBgr	7,000	2,090	0,037	0,000	2,803	0,005	18,000	0,968	0,333	0,000	2,803	0,005	0,000	2,803	0,005
MOB ipl & MOB mi	13,000	1,478	0,139	0,000	2,803	0,005	2,000	2,599	0,009	0,000	2,803	0,005	0,000	2,803	0,005
MOB ipl & MOB opl	16,000	1,172	0,241	13,000	1,478	0,139	0,000	2,803	0,005	0,000	2,803	0,005	0,000	2,803	0,005
MOB ipl & MOB gl	6,000	2,191	0,028	0,000	2,803	0,005	0,000	2,803	0,005	0,000	2,803	0,005	0,000	2,803	0,005
MOB ipl & MOB onl	23,000	0,459	0,646	0,000	2,803	0,005	13,000	1,478	0,139	23,000	0,459	0,646	0,000	2,803	0,005
MOB mi & MOBgr	9,000	1,886	0,059	1,000	2,701	0,007	25,000	0,255	0,799	23,000	0,459	0,646	0,000	2,803	0,005
MOB mi & MOB ipl	13,000	1,478	0,139	0,000	2,803	0,005	2,000	2,599	0,009	0,000	2,803	0,005	0,000	2,803	0,005
MOB mi & MOB opl	24,000	0,357	0,721	3,000	2,497	0,013	6,000	2,191	0,028	0,000	2,803	0,005	0,000	2,803	0,005
MOB mi & MOB gl	12,000	1,580	0,114	0,000	2,803	0,005	0,000	2,803	0,005	0,000	2,803	0,005	0,000	2,803	0,005
MOB mi & MOB onl	26,000	0,153	0,878	11,000	1,682	0,093	12,000	1,580	0,114	7,000	2,090	0,037	0,000	2,803	0,005
MOB opl & MOBgr	4,000	2,395	0,017	0,000	2,803	0,005	0,000	2,803	0,005	0,000	2,803	0,005	0,000	2,803	0,005
MOB opl & MOB ipl	16,000	1,172	0,241	13,000	1,478	0,139	0,000	2,803	0,005	0,000	2,803	0,005	0,000	2,803	0,005
MOB opl & MOB mi	24,000	0,357	0,721	3,000	2,497	0,013	6,000	2,191	0,028	0,000	2,803	0,005	0,000	2,803	0,005

MOB opl & MOB gl	6,000	2,191	0,028	1,000	2,701	0,007	0,000	2,803	0,005	0,000	2,803	0,005	0,000	2,803	0,005
MOB opl & MOB onl	27,000	0,051	0,959	3,000	2,497	0,013	5,000	2,293	0,022	3,000	2,497	0,013	6,000	2,191	0,028
MOB gl & MOBgr	4,000	2,395	0,017	0,000	2,803	0,005	0,000	2,803	0,005	0,000	2,803	0,005	0,000	2,803	0,005
MOB gl & MOB ipl	6,000	2,191	0,028	0,000	2,803	0,005	0,000	2,803	0,005	0,000	2,803	0,005	0,000	2,803	0,005
MOB gl & MOB mi	12,000	1,580	0,114	0,000	2,803	0,005	0,000	2,803	0,005	0,000	2,803	0,005	0,000	2,803	0,005
MOB gl & MOB opl	6,000	2,191	0,028	1,000	2,701	0,007	0,000	2,803	0,005	0,000	2,803	0,005	0,000	2,803	0,005
MOB gl & MOB onl	19,000	0,866	0,386	0,000	2,803	0,005	0,000	2,803	0,005	0,000	2,803	0,005	0,000	2,803	0,005
MOB onl & MOBgr	21,000	0,663	0,508	9,000	1,886	0,059	10,000	1,784	0,074	9,000	1,886	0,059	0,000	2,803	0,005
MOB onl & MOB ipl	23,000	0,459	0,646	0,000	2,803	0,005	13,000	1,478	0,139	23,000	0,459	0,646	0,000	2,803	0,005
MOB onl & MOB mi	26,000	0,153	0,878	11,000	1,682	0,093	12,000	1,580	0,114	7,000	2,090	0,037	0,000	2,803	0,005
MOB onl & MOB opl	27,000	0,051	0,959	3,000	2,497	0,013	5,000	2,293	0,022	3,000	2,497	0,013	6,000	2,191	0,028
MOB onl & MOB gl	19,000	0,866	0,386	0,000	2,803	0,005	0,000	2,803	0,005	0,000	2,803	0,005	0,000	2,803	0,005

CG	$GABA_{A(BZ)}$			$GABA_B$			α_1			α_2			$D_{1/5}$		
	T	*Z*	*p-value*	*T*	*Z*	*p-value*	*T*	*Z*	*p-value*	*T*	*Z*	*p-value*	*T*	*Z*	*p-value*
MOBgr & MOB ipl	20,000	0,764	0,445	13,000	1,478	0,139	10,000	1,784	0,074	0,000	2,803	0,005	7,000	2,090	0,037
MOBgr & MOB mi	20,000	0,764	0,445	15,000	1,274	0,203	10,000	1,784	0,074	0,000	2,803	0,005	17,000	1,070	0,285
MOBgr & MOB opl	0,000	2,803	0,005	17,000	1,070	0,285	0,000	2,803	0,005	0,000	2,803	0,005	0,000	2,803	0,005
MOBgr & MOB gl	0,000	2,803	0,005	1,000	2,701	0,007	0,000	2,803	0,005	0,000	2,803	0,005	3,000	2,497	0,013
MOBgr & MOB onl	0,000	2,803	0,005	26,000	0,153	0,878	5,000	2,293	0,022	0,000	2,803	0,005	2,000	2,599	0,009
MOB ipl & MOBgr	20,000	0,764	0,445	13,000	1,478	0,139	10,000	1,784	0,074	0,000	2,803	0,005	7,000	2,090	0,037
MOB ipl & MOB mi	7,000	2,090	0,037	6,000	2,191	0,028	21,000	0,663	0,508	2,000	2,599	0,009	10,000	1,784	0,074
MOB ipl & MOB opl	0,000	2,803	0,005	22,000	0,561	0,575	0,000	2,803	0,005	1,000	2,701	0,007	3,000	2,497	0,013
MOB ipl & MOB gl	0,000	2,803	0,005	0,000	2,803	0,005	0,000	2,803	0,005	5,000	2,293	0,022	7,000	2,090	0,037
MOB ipl & MOB onl	0,000	2,803	0,005	18,000	0,968	0,333	16,000	1,172	0,241	1,000	2,701	0,007	10,000	1,784	0,074
MOB mi & MOBgr	20,000	0,764	0,445	15,000	1,274	0,203	10,000	1,784	0,074	0,000	2,803	0,005	17,000	1,070	0,285
MOB mi & MOB ipl	7,000	2,090	0,037	6,000	2,191	0,028	21,000	0,663	0,508	2,000	2,599	0,009	10,000	1,784	0,074

MOB mi & MOB opl	0,000	2,803	0,005	16,000	1,172	0,241	0,000	2,803	0,005	0,000	2,803	0,005	1,000	2,701	0,007
MOB mi & MOB gl	0,000	2,803	0,005	0,000	2,803	0,005	0,000	2,803	0,005	0,000	2,803	0,005	0,000	2,803	0,005
MOB mi & MOB onl	0,000	2,803	0,005	18,000	0,968	0,333	13,000	1,478	0,139	0,000	2,803	0,005	2,000	2,599	0,009
MOB opl & MOBgr	0,000	2,803	0,005	17,000	1,070	0,285	0,000	2,803	0,005	0,000	2,803	0,005	0,000	2,803	0,005
MOB opl & MOB ipl	0,000	2,803	0,005	22,000	0,561	0,575	0,000	2,803	0,005	1,000	2,701	0,007	3,000	2,497	0,013
MOB opl & MOB mi	0,000	2,803	0,005	16,000	1,172	0,241	0,000	2,803	0,005	0,000	2,803	0,005	1,000	2,701	0,007
MOB opl & MOB gl	0,000	2,803	0,005	0,000	2,803	0,005	1,000	2,701	0,007	25,000	0,255	0,799	11,000	1,682	0,093
MOB opl & MOB onl	0,000	2,803	0,005	11,000	1,682	0,093	0,000	2,803	0,005	12,000	1,580	0,114	21,000	0,663	0,508
MOB gl & MOBgr	0,000	2,803	0,005	1,000	2,701	0,007	0,000	2,803	0,005	0,000	2,803	0,005	3,000	2,497	0,013
MOB gl & MOB ipl	0,000	2,803	0,005	0,000	2,803	0,005	0,000	2,803	0,005	5,000	2,293	0,022	7,000	2,090	0,037
MOB gl & MOB mi	0,000	2,803	0,005	0,000	2,803	0,005	0,000	2,803	0,005	0,000	2,803	0,005	0,000	2,803	0,005
MOB gl & MOB opl	0,000	2,803	0,005	0,000	2,803	0,005	1,000	2,701	0,007	25,000	0,255	0,799	11,000	1,682	0,093
MOB gl & MOB gl															
MOB gl & MOB onl	0,000	2,803	0,005	0,000	2,803	0,005	0,000	2,803	0,005	10,000	1,784	0,074	14,000	1,376	0,169
MOB onl & MOBgr	0,000	2,803	0,005	26,000	0,153	0,878	5,000	2,293	0,022	0,000	2,803	0,005	2,000	2,599	0,009
MOB onl & MOB ipl	0,000	2,803	0,005	18,000	0,968	0,333	16,000	1,172	0,241	1,000	2,701	0,007	10,000	1,784	0,074
MOB onl & MOB mi	0,000	2,803	0,005	18,000	0,968	0,333	13,000	1,478	0,139	0,000	2,803	0,005	2,000	2,599	0,009
MOB onl & MOB opl	0,000	2,803	0,005	11,000	1,682	0,093	0,000	2,803	0,005	12,000	1,580	0,114	21,000	0,663	0,508
MOB onl & MOB gl	0,000	2,803	0,005	0,000	2,803	0,005	0,000	2,803	0,005	10,000	1,784	0,074	14,000	1,376	0,169

Supp. Tab. 10: Statistical analysis of layer-specific receptor concentrations of the accessory olfactory bulb in CG

Statistical data of differences between receptor densities across layers within the accessory olfactory bulb of control mice (CG). Each receptor type was tested separately with pair-wise Wilcoxon-rank test if the Friedman ANOVA showed differences within the region. Wilcoxon-rank: Z-score (Z), minimum of sum of the ranks of positive or negative changes (T), red labelling if $p < 0.05$ (N = 10, df = 13) (see Lothmann et al., 2021).

CG	AMPA			Kainate			NMDA			$mGlu_{2/3}$			$GABA_A$		
	T	*Z*	*p-value*	*T*	*Z*	*p-value*	*T*	*Z*	*p-value*	*T*	*Z*	*p-value*	*T*	*Z*	*p-value*
AOB gr & AOB mi	25,000	0,255	0,799	0,000	2,803	0,005	0,000	2,803	0,005	4,000	2,395	0,017	2,000	2,599	0,009
AOB gr & AOB gl	14,000	1,376	0,169	1,000	2,701	0,007	24,000	0,357	0,721	0,000	2,803	0,005	16,000	1,172	0,241
AOB mi & AOB gr	25,000	0,255	0,799	0,000	2,803	0,005	0,000	2,803	0,005	4,000	2,395	0,017	2,000	2,599	0,009
AOB mi & AOB gl	11,000	1,682	0,093	0,000	2,803	0,005	3,000	2,497	0,013	0,000	2,803	0,005	0,000	2,803	0,005
AOB gl & AOB gr	14,000	1,376	0,169	1,000	2,701	0,007	24,000	0,357	0,721	0,000	2,803	0,005	16,000	1,172	0,241
AOB gl & AOB mi	11,000	1,682	0,093	0,000	2,803	0,005	3,000	2,497	0,013	0,000	2,803	0,005	0,000	2,803	0,005

CG	$GABA_{A(BZ)}$			$GABA_B$			α_1			α_2			$D_{1/5}$		
	T	*Z*	*p-value*	*T*	*Z*	*p-value*	*T*	*Z*	*p-value*	*T*	*Z*	*p-value*	*T*	*Z*	*p-value*
AOB gr & AOB mi	27,000	0,051	0,959	18,000	0,968	0,333	2,000	2,599	0,009	25,000	0,255	0,799	26,000	0,153	0,878
AOB gr & AOB gl	0,000	2,803	0,005	0,000	2,803	0,005	8,000	1,988	0,047	23,000	0,459	0,646	11,000	1,682	0,093
AOB mi & AOB gr	27,000	0,051	0,959	18,000	0,968	0,333	2,000	2,599	0,009	25,000	0,255	0,799	26,000	0,153	0,878
AOB mi & AOB gl	0,000	2,803	0,005	0,000	2,803	0,005	1,000	2,701	0,007	5,000	2,293	0,022	7,000	2,090	0,037
AOB gl & AOB gr	0,000	2,803	0,005	0,000	2,803	0,005	8,000	1,988	0,047	23,000	0,459	0,646	11,000	1,682	0,093
AOB gl & AOB mi	0,000	2,803	0,005	0,000	2,803	0,005	1,000	2,701	0,007	5,000	2,293	0,022	7,000	2,090	0,037

Supp. Tab. 11: Statistical analysis of layer-specific receptor concentrations of the anterior olfactory cortex in CG

Statistical data of differences between receptor densities across layers within the anterior olfactory cortex of control mice (CG). Each receptor type was tested separately with pair-wise Wilcoxon-rank test if the Friedman ANOVA showed differences within the region. Wilcoxon-rank: Z-score (Z), minimum of sum of the ranks of positive or negative changes (T), red labelling if $p < 0.05$ (N = 10, df = 13) (see Lothmann et al., 2021).

CG	AMPA			Kainate			NMDA			$mGlu_{2/3}$			$GABA_A$		
	T	*Z*	*p-value*	*T*	*Z*	*p-value*	*T*	*Z*	*p-value*	*T*	*Z*	*p-value*	*T*	*Z*	*p-value*
AOC 1 & AOC m	4,000	2,395	0,017	26,000	0,153	0,878	6,000	2,191	0,028	0,000	2,803	0,005	14,000	1,376	0,169
AOC 1 & AOC d	19,000	0,866	0,386	10,000	1,784	0,074	0,000	2,803	0,005	1,000	2,701	0,007	1,000	2,701	0,007
AOC 1 & AOC pv	17,000	1,070	0,285	1,000	2,701	0,007	16,000	1,172	0,241	0,000	2,803	0,005	5,000	2,293	0,022
AOC 1 & AOC l	8,000	1,988	0,047	6,000	2,191	0,028	0,000	2,803	0,005	22,000	0,561	0,575	0,000	2,803	0,005
AOC m & AOC 1	4,000	2,395	0,017	26,000	0,153	0,878	6,000	2,191	0,028	0,000	2,803	0,005	14,000	1,376	0,169
AOC m & AOC d	6,000	2,191	0,028	16,000	1,172	0,241	2,000	2,599	0,009	16,000	1,172	0,241	14,000	1,376	0,169
AOC m & AOC pv	10,000	1,784	0,074	6,000	2,191	0,028	0,000	2,803	0,005	3,000	2,497	0,013	26,000	0,153	0,878
AOC m & AOC l	11,000	1,682	0,093	17,000	1,070	0,285	0,000	2,803	0,005	6,000	2,191	0,028	7,000	2,090	0,037
AOC d & AOC 1	19,000	0,866	0,386	10,000	1,784	0,074	0,000	2,803	0,005	1,000	2,701	0,007	1,000	2,701	0,007
AOC d & AOC m	6,000	2,191	0,028	16,000	1,172	0,241	2,000	2,599	0,009	16,000	1,172	0,241	14,000	1,376	0,169
AOC d & AOC pv	25,000	0,255	0,799	4,000	2,395	0,017	0,000	2,803	0,005	1,000	2,701	0,007	7,000	2,090	0,037
AOC d & AOC l	16,000	1,172	0,241	19,000	0,866	0,386	0,000	2,803	0,005	8,000	1,988	0,047	16,000	1,172	0,241
AOC pv & AOC 1	17,000	1,070	0,285	1,000	2,701	0,007	16,000	1,172	0,241	0,000	2,803	0,005	5,000	2,293	0,022
AOC pv & AOC m	10,000	1,784	0,074	6,000	2,191	0,028	0,000	2,803	0,005	3,000	2,497	0,013	26,000	0,153	0,878
AOC pv & AOC d	25,000	0,255	0,799	4,000	2,395	0,017	0,000	2,803	0,005	1,000	2,701	0,007	7,000	2,090	0,037
AOC pv & AOC l	10,000	1,784	0,074	2,000	2,599	0,009	0,000	2,803	0,005	0,000	2,803	0,005	1,000	2,701	0,007
AOC l & AOC 1	8,000	1,988	0,047	6,000	2,191	0,028	0,000	2,803	0,005	22,000	0,561	0,575	0,000	2,803	0,005
AOC l & AOC m	11,000	1,682	0,093	17,000	1,070	0,285	0,000	2,803	0,005	6,000	2,191	0,028	7,000	2,090	0,037
AOC l & AOC d	16,000	1,172	0,241	19,000	0,866	0,386	0,000	2,803	0,005	8,000	1,988	0,047	16,000	1,172	0,241

AOC l & AOC pv	10,000	1,784	0,074	2,000	2,599	0,009	0,000	2,803	0,005	0,000	2,803	0,005	1,000	2,701	0,007
CG	$GABA_{A(BZ)}$			$GABA_B$			α_1			α_2			$D_{1/5}$		
	T	*Z*	*p-value*	*T*	*Z*	*p-value*	*T*	*Z*	*p-value*	*T*	*Z*	*p-value*	*T*	*Z*	*p-value*
AOC 1 & AOC m	10,000	1,784	0,074	6,000	2,191	0,028	1,000	2,701	0,007	3,000	2,497	0,013	19,000	0,866	0,386
AOC 1 & AOC d	1,000	2,701	0,007	6,000	2,191	0,028	1,000	2,701	0,007	0,000	2,803	0,005	7,000	2,090	0,037
AOC 1 & AOC pv	13,000	1,478	0,139	21,000	0,663	0,508	1,000	2,701	0,007	10,000	1,784	0,074	12,000	1,580	0,114
AOC 1 & AOC l	9,000	1,886	0,059	5,000	2,293	0,022	3,000	2,497	0,013	3,000	2,497	0,013	5,000	2,293	0,022
AOC m & AOC 1	10,000	1,784	0,074	6,000	2,191	0,028	1,000	2,701	0,007	3,000	2,497	0,013	19,000	0,866	0,386
AOC m & AOC d	3,000	2,497	0,013	23,000	0,459	0,646	25,000	0,255	0,799	19,000	0,866	0,386	11,000	1,682	0,093
AOC m & AOC pv	26,000	0,153	0,878	0,000	2,803	0,005	25,000	0,255	0,799	16,000	1,172	0,241	9,000	1,886	0,059
AOC m & AOC l	24,000	0,357	0,721	24,000	0,357	0,721	17,000	1,070	0,285	11,000	1,682	0,093	6,000	2,191	0,028
AOC d & AOC 1	1,000	2,701	0,007	6,000	2,191	0,028	1,000	2,701	0,007	0,000	2,803	0,005	7,000	2,090	0,037
AOC d & AOC m	3,000	2,497	0,013	23,000	0,459	0,646	25,000	0,255	0,799	19,000	0,866	0,386	11,000	1,682	0,093
AOC d & AOC pv	13,000	1,478	0,139	1,000	2,701	0,007	23,000	0,459	0,646	13,000	1,478	0,139	3,000	2,497	0,013
AOC d & AOC l	0,000	2,803	0,005	17,000	1,070	0,285	25,000	0,255	0,799	7,000	2,090	0,037	4,000	2,395	0,017
AOC pv & AOC 1	13,000	1,478	0,139	21,000	0,663	0,508	1,000	2,701	0,007	10,000	1,784	0,074	12,000	1,580	0,114
AOC pv & AOC m	26,000	0,153	0,878	0,000	2,803	0,005	25,000	0,255	0,799	16,000	1,172	0,241	9,000	1,886	0,059
AOC pv & AOC d	13,000	1,478	0,139	1,000	2,701	0,007	23,000	0,459	0,646	13,000	1,478	0,139	3,000	2,497	0,013
AOC pv & AOC l	23,000	0,459	0,646	3,000	2,497	0,013	21,000	0,663	0,508	15,000	1,274	0,203	20,000	0,764	0,445
AOC l & AOC 1	9,000	1,886	0,059	5,000	2,293	0,022	3,000	2,497	0,013	3,000	2,497	0,013	5,000	2,293	0,022
AOC l & AOC m	24,000	0,357	0,721	24,000	0,357	0,721	17,000	1,070	0,285	11,000	1,682	0,093	6,000	2,191	0,028
AOC l & AOC d	0,000	2,803	0,005	17,000	1,070	0,285	25,000	0,255	0,799	7,000	2,090	0,037	4,000	2,395	0,017
AOC l & AOC pv	23,000	0,459	0,646	3,000	2,497	0,013	21,000	0,663	0,508	15,000	1,274	0,203	20,000	0,764	0,445

Supp. Tab. 12: Statistical analysis of layer-specific receptor concentrations of the dorsal taenia tecta in CG

Statistical data of differences between receptor densities across layers within the dorsal taenia tecta of control mice (CG). Each receptor type was tested separately with pair-wise Wilcoxon-rank test if the Friedman ANOVA showed differences within the region. Wilcoxon-rank: Z-score (Z), minimum of sum of the ranks of positive or negative changes (T), red labelling if $p < 0.05$ (N = 10, df = 13) (see Lothmann et al., 2021).

CG	AMPA			Kainate			NMDA			$mGlu_{2/3}$			$GABA_A$		
	T	*Z*	*p-value*	*T*	*Z*	*p-value*	*T*	*Z*	*p-value*	*T*	*Z*	*p-value*	*T*	*Z*	*p-value*
TTd 1 & TTd 2	1,000	2,701	0,007	10,000	1,784	0,074	22,000	0,561	0,575	10,000	1,784	0,074	26,000	0,153	0,878
TTd 1 & TTd 3	23,000	0,459	0,646	10,000	1,784	0,074	15,000	1,274	0,203	4,000	2,395	0,017	20,000	0,764	0,445
TTd 1 & TTd 4	7,000	2,090	0,037	1,000	2,701	0,007	3,000	2,497	0,013	5,000	2,293	0,022	7,000	2,090	0,037
TTd 2 & TTd 1	1,000	2,701	0,007	10,000	1,784	0,074	22,000	0,561	0,575	10,000	1,784	0,074	26,000	0,153	0,878
TTd 2 & TTd 3	2,000	2,599	0,009	7,000	2,090	0,037	19,000	0,866	0,386	5,000	2,293	0,022	22,000	0,561	0,575
TTd 2 & TTd 4	1,000	2,701	0,007	0,000	2,803	0,005	2,000	2,599	0,009	9,000	1,886	0,059	10,000	1,784	0,074
TTd 3 & TTd 1	23,000	0,459	0,646	10,000	1,784	0,074	15,000	1,274	0,203	4,000	2,395	0,017	20,000	0,764	0,445
TTd 3 & TTd 2	2,000	2,599	0,009	7,000	2,090	0,037	19,000	0,866	0,386	5,000	2,293	0,022	22,000	0,561	0,575
TTd 3 & TTd 4	7,000	2,090	0,037	1,000	2,701	0,007	3,000	2,497	0,013	20,000	0,764	0,445	6,000	2,191	0,028
TTd 4 & TTd 1	7,000	2,090	0,037	1,000	2,701	0,007	3,000	2,497	0,013	5,000	2,293	0,022	7,000	2,090	0,037
TTd 4 & TTd 2	1,000	2,701	0,007	0,000	2,803	0,005	2,000	2,599	0,009	9,000	1,886	0,059	10,000	1,784	0,074
TTd 4 & TTd 3	7,000	2,090	0,037	1,000	2,701	0,007	3,000	2,497	0,013	20,000	0,764	0,445	6,000	2,191	0,028
CG	$GABA_{A(BZ)}$			$GABA_B$			α_1			α_2			$D_{1/5}$		
	T	*Z*	*p-value*	*T*	*Z*	*p-value*	*T*	*Z*	*p-value*	*T*	*Z*	*p-value*	*T*	*Z*	*p-value*
TTd 1 & TTd 2	8,000	1,988	0,047	25,000	0,255	0,799	23,000	0,459	0,646	8,000	1,988	0,047	12,000	1,580	0,114
TTd 1 & TTd 3	6,000	2,191	0,028	22,000	0,561	0,575	22,000	0,561	0,575	15,000	1,274	0,203	0,000	2,803	0,005
TTd 1 & TTd 4	18,000	0,968	0,333	0,000	2,803	0,005	13,000	1,478	0,139	3,000	2,497	0,013	0,000	2,803	0,005
TTd 2 & TTd 1	8,000	1,988	0,047	25,000	0,255	0,799	23,000	0,459	0,646	8,000	1,988	0,047	12,000	1,580	0,114
TTd 2 & TTd 3	13,000	1,478	0,139	18,000	0,968	0,333	16,000	1,172	0,241	16,000	1,172	0,241	0,000	2,803	0,005

TTd 2 & TTd 4	27,000	0,051	0,959	1,000	2,701	0,007	12,000	1,580	0,114	20,000	0,764	0,445	0,000	2,803	0,005
TTd 3 & TTd 1	6,000	2,191	0,028	22,000	0,561	0,575	22,000	0,561	0,575	15,000	1,274	0,203	0,000	2,803	0,005
TTd 3 & TTd 2	13,000	1,478	0,139	18,000	0,968	0,333	16,000	1,172	0,241	16,000	1,172	0,241	0,000	2,803	0,005
TTd 3 & TTd 4	19,000	0,866	0,386	3,000	2,497	0,013	9,000	1,886	0,059	12,000	1,580	0,114	0,000	2,803	0,005
TTd 4 & TTd 1	18,000	0,968	0,333	0,000	2,803	0,005	13,000	1,478	0,139	3,000	2,497	0,013	0,000	2,803	0,005
TTd 4 & TTd 2	27,000	0,051	0,959	1,000	2,701	0,007	12,000	1,580	0,114	20,000	0,764	0,445	0,000	2,803	0,005
TTd 4 & TTd 3	19,000	0,866	0,386	3,000	2,497	0,013	9,000	1,886	0,059	12,000	1,580	0,114	0,000	2,803	0,005

Supp. Tab. 13: Statistical analysis of layer-specific receptor concentrations of the ventral taenia tecta in CG

Statistical data of differences between receptor densities across layers within the ventral taenia tecta of control mice (CG). Each receptor type was tested separately with pair-wise Wilcoxon-rank test if the Friedman ANOVA showed differences within the region. Wilcoxon-rank: Z-score (Z), minimum of sum of the ranks of positive or negative changes (T), red labelling if $p < 0.05$ ($N = 10$, $df = 13$) (see Lothmann et al., 2021).

CG	AMPA			Kainate			NMDA			$mGlu_{2/3}$			$GABA_A$		
	T	*Z*	*p-value*	*T*	*Z*	*p-value*	*T*	*Z*	*p-value*	*T*	*Z*	*p-value*	*T*	*Z*	*p-value*
TTv 1 & TTv 2	0,000	2,803	0,005	1,000	2,701	0,007	8,000	1,988	0,047	22,000	0,561	0,575	18,000	0,968	0,333
TTv 1 & TTv 3	0,000	2,803	0,005	2,000	2,599	0,009	25,000	0,255	0,799	22,000	0,561	0,575	23,000	0,459	0,646
TTv 2 & TTv 1	0,000	2,803	0,005	1,000	2,701	0,007	8,000	1,988	0,047	22,000	0,561	0,575	18,000	0,968	0,333
TTv 2 & TTv 3	20,000	0,764	0,445	9,000	1,886	0,059	18,000	0,968	0,333	13,000	1,478	0,139	9,000	1,886	0,059
TTv 3 & TTv 1	0,000	2,803	0,005	2,000	2,599	0,009	25,000	0,255	0,799	22,000	0,561	0,575	23,000	0,459	0,646
TTv 3 & TTv 2	20,000	0,764	0,445	9,000	1,886	0,059	18,000	0,968	0,333	13,000	1,478	0,139	9,000	1,886	0,059
CG	$GABA_{A(BZ)}$			$GABA_B$			α_1			α_2			$D_{1/5}$		
	T	*Z*	*p-value*	*T*	*Z*	*p-value*	*T*	*Z*	*p-value*	*T*	*Z*	*p-value*	*T*	*Z*	*p-value*
TTv 1 & TTv 2	14,000	1,376	0,169	10,000	1,784	0,074	21,000	0,663	0,508	4,000	2,395	0,017	13,000	1,478	0,139
TTv 1 & TTv 3	14,000	1,376	0,169	2,000	2,599	0,009	12,000	1,580	0,114	5,000	2,293	0,022	3,000	2,497	0,013
TTv 2 & TTv 1	14,000	1,376	0,169	10,000	1,784	0,074	21,000	0,663	0,508	4,000	2,395	0,017	13,000	1,478	0,139
TTv 2 & TTv 3	22,000	0,561	0,575	27,000	0,051	0,959	20,000	0,764	0,445	18,000	0,968	0,333	0,000	2,803	0,005
TTv 3 & TTv 1	14,000	1,376	0,169	2,000	2,599	0,009	12,000	1,580	0,114	5,000	2,293	0,022	3,000	2,497	0,013
TTv 3 & TTv 2	22,000	0,561	0,575	27,000	0,051	0,959	20,000	0,764	0,445	18,000	0,968	0,333	0,000	2,803	0,005

Supp. Tab. 14: Statistical analysis of layer-specific receptor concentrations of the olfactory tubercle in CG

Statistical data of differences between receptor densities across layers within the olfactory tubercle of control mice (CG). Each receptor type was tested separately with pair-wise Wilcoxon-rank test if the Friedman ANOVA showed differences within the region. Wilcoxon-rank: Z-score (Z), minimum of sum of the ranks of positive or negative changes (T), red labelling if $p < 0.05$ ($N = 10$, $df = 13$) (see Lothmann et al., 2021).

CG	AMPA			Kainate			NMDA			$mGlu_{2/3}$			$GABA_A$		
	T	*Z*	*p-value*	*T*	*Z*	*p-value*	*T*	*Z*	*p-value*	*T*	*Z*	*p-value*	*T*	*Z*	*p-value*
OT 1 & OT 2	0,000	2,803	0,005	1,000	2,701	0,007	0,000	2,803	0,005	10,000	1,784	0,074	0,000	2,803	0,005
OT 1 & OT 3	0,000	2,803	0,005	0,000	2,803	0,005	1,000	2,701	0,007	0,000	2,803	0,005	18,000	0,968	0,333
OT 2 & OT 1	0,000	2,803	0,005	1,000	2,701	0,007	0,000	2,803	0,005	10,000	1,784	0,074	0,000	2,803	0,005
OT 2 & OT 3	0,000	2,803	0,005	24,000	0,357	0,721	10,000	1,784	0,074	6,000	2,191	0,028	1,000	2,701	0,007
OT 3 & OT 1	0,000	2,803	0,005	0,000	2,803	0,005	1,000	2,701	0,007	0,000	2,803	0,005	18,000	0,968	0,333
OT 3 & OT 2	0,000	2,803	0,005	24,000	0,357	0,721	10,000	1,784	0,074	6,000	2,191	0,028	1,000	2,701	0,007
CG	$GABA_{A(BZ)}$			$GABA_B$			α_1			α_2			$D_{1/5}$		
	T	*Z*	*p-value*	*T*	*Z*	*p-value*	*T*	*Z*	*p-value*	*T*	*Z*	*p-value*	*T*	*Z*	*p-value*
OT 1 & OT 2	7,000	2,090	0,037	0,000	2,803	0,005	9,000	1,886	0,059	0,000	2,803	0,005	1,000	2,701	0,007
OT 1 & OT 3	10,000	1,784	0,074	0,000	2,803	0,005	3,000	2,497	0,013	0,000	2,803	0,005	15,000	1,274	0,203
OT 2 & OT 1	7,000	2,090	0,037	0,000	2,803	0,005	9,000	1,886	0,059	0,000	2,803	0,005	1,000	2,701	0,007
OT 2 & OT 3	20,000	0,764	0,445	10,000	1,784	0,074	1,000	2,701	0,007	2,000	2,599	0,009	1,000	2,701	0,007
OT 3 & OT 1	10,000	1,784	0,074	0,000	2,803	0,005	3,000	2,497	0,013	0,000	2,803	0,005	15,000	1,274	0,203
OT 3 & OT 2	20,000	0,764	0,445	10,000	1,784	0,074	1,000	2,701	0,007	2,000	2,599	0,009	1,000	2,701	0,007

Supp. Tab. 15: Statistical analysis of layer-specific receptor concentrations of the dorsal peduncular cortex in CG

Statistical data of differences between receptor densities across layers within the dorsal peduncular cortex of control mice (CG). Each receptor type was tested separately with pair-wise Wilcoxon-rank test if the Friedman ANOVA showed differences within the region. Wilcoxon-rank: Z-score (Z), minimum of sum of the ranks of positive or negative changes (T), red labelling if $p < 0.05$ (N = 10, df = 13) (see Lothmann et al., 2021).

CG	AMPA			Kainate			NMDA			$mGlu_{2/3}$			$GABA_A$		
	T	*Z*	*p-value*	*T*	*Z*	*p-value*	*T*	*Z*	*p-value*	*T*	*Z*	*p-value*	*T*	*Z*	*p-value*
DP 1 & DP 2/3	0,000	2,803	0,005	1,000	2,701	0,007	2,000	2,599	0,009	0,000	2,803	0,005	11,000	1,682	0,093
DP 1 & DP 5	6,000	2,191	0,028	0,000	2,803	0,005	10,000	1,784	0,074	1,000	2,701	0,007	6,000	2,191	0,028
DP 1 & DP 6	8,000	1,988	0,047	0,000	2,803	0,005	9,000	1,886	0,059	0,000	2,803	0,005	23,000	0,459	0,646
DP 2/3 & DP 1	0,000	2,803	0,005	1,000	2,701	0,007	2,000	2,599	0,009	5,000	2,293	0,022	11,000	1,682	0,093
DP 2/3 & DP 5	0,000	2,803	0,005	20,000	0,764	0,445	0,000	2,803	0,005	6,000	2,191	0,028	20,000	0,764	0,445
DP 2/3 & DP 6	0,000	2,803	0,005	6,000	2,191	0,028	0,000	2,803	0,005	12,000	1,580	0,114	18,000	0,968	0,333
DP 5 & DP 1	6,000	2,191	0,028	0,000	2,803	0,005	10,000	1,784	0,074	0,000	2,803	0,005	6,000	2,191	0,028
DP 5 & DP 2/3	0,000	2,803	0,005	20,000	0,764	0,445	0,000	2,803	0,005	1,000	2,701	0,007	20,000	0,764	0,445
DP 5 & DP 6	19,000	0,866	0,386	2,000	2,599	0,009	3,000	2,497	0,013	12,000	1,580	0,114	6,000	2,191	0,028
DP 6 & DP 1	8,000	1,988	0,047	0,000	2,803	0,005	9,000	1,886	0,059	0,000	2,803	0,005	23,000	0,459	0,646
DP 6 & DP 2/3	0,000	2,803	0,005	6,000	2,191	0,028	0,000	2,803	0,005	6,000	2,191	0,028	18,000	0,968	0,333
DP 6 & DP 5	19,000	0,866	0,386	2,000	2,599	0,009	3,000	2,497	0,013	6,000	2,191	0,028	6,000	2,191	0,028
CG	$GABA_{A(BZ)}$			$GABA_B$			α_1			α_2			$D_{1/5}$		
	T	*Z*	*p-value*	*T*	*Z*	*p-value*	*T*	*Z*	*p-value*	*T*	*Z*	*p-value*	T	*Z*	*p-value*
DP 1 & DP 2/3	24,000	0,357	0,721	13,000	1,478	0,139	7,000	2,090	0,037	14,000	1,376	0,169	3,000	2,497	0,013
DP 1 & DP 5	19,000	0,866	0,386	21,000	0,663	0,508	8,000	1,988	0,047	18,000	0,968	0,333	0,000	2,803	0,005
DP 1 & DP 6	20,000	0,764	0,445	5,000	2,293	0,022	26,000	0,153	0,878	16,000	1,172	0,241	0,000	2,803	0,005
DP 2/3 & DP 1	24,000	0,357	0,721	13,000	1,478	0,139	7,000	2,090	0,037	14,000	1,376	0,169	3,000	2,497	0,013
DP 2/3 & DP 5	23,000	0,459	0,646	6,000	2,191	0,028	18,000	0,968	0,333	17,000	1,070	0,285	25,000	0,255	0,799

DP 2/3 & DP 6	11,000	1,682	0,093	0,000	2,803	0,005	16,000	1,172	0,241	25,000	0,255	0,799	0,000	2,803	0,005
DP 5 & DP 1	19,000	0,866	0,386	21,000	0,663	0,508	8,000	1,988	0,047	18,000	0,968	0,333	0,000	2,803	0,005
DP 5 & DP 2/3	23,000	0,459	0,646	6,000	2,191	0,028	18,000	0,968	0,333	17,000	1,070	0,285	25,000	0,255	0,799
DP 5 & DP 6	9,000	1,886	0,059	4,000	2,395	0,017	10,000	1,784	0,074	13,000	1,478	0,139	1,000	2,701	0,007
DP 6 & DP 1	20,000	0,764	0,445	5,000	2,293	0,022	26,000	0,153	0,878	16,000	1,172	0,241	0,000	2,803	0,005
DP 6 & DP 2/3	11,000	1,682	0,093	0,000	2,803	0,005	16,000	1,172	0,241	25,000	0,255	0,799	0,000	2,803	0,005
DP 6 & DP 5	9,000	1,886	0,059	4,000	2,395	0,017	10,000	1,784	0,074	13,000	1,478	0,139	1,000	2,701	0,007

Supp. Tab. 16: Statistical analysis of layer-specific receptor concentrations of the piriform cortex in CG

Statistical data of differences between receptor densities across layers within the piriform cortex of control mice (CG). Each receptor type was tested separately with pair-wise Wilcoxon-rank test if the Friedman ANOVA showed differences within the region. Wilcoxon-rank: Z-score (Z), minimum of sum of the ranks of positive or negative changes (T), red labelling if $p < 0.05$ (N = 10, df = 13) (see Lothmann et al., 2021).

CG	AMPA			Kainate			NMDA			$mGlu_{2/3}$			$GABA_A$		
	T	*Z*	*p-value*	*T*	*Z*	*p-value*	*T*	*Z*	*p-value*	*T*	*Z*	*p-value*	*T*	*Z*	*p-value*
PIR 1 & PIR 2	0,000	2,803	0,005	9,000	1,886	0,059	11,000	1,682	0,093	0,000	2,803	0,005	26,000	0,153	0,878
PIR 1 & PIR 3	3,000	2,497	0,013	1,000	2,701	0,007	3,000	2,497	0,013	0,000	2,803	0,005	2,000	2,599	0,009
PIR 2 & PIR 1	0,000	2,803	0,005	9,000	1,886	0,059	11,000	1,682	0,093	0,000	2,803	0,005	26,000	0,153	0,878
PIR 2 & PIR 3	0,000	2,803	0,005	0,000	2,803	0,005	6,000	2,191	0,028	0,000	2,803	0,005	0,000	2,803	0,005
PIR 3 & PIR 1	3,000	2,497	0,013	1,000	2,701	0,007	3,000	2,497	0,013	0,000	2,803	0,005	2,000	2,599	0,009
PIR 3 & PIR 2	0,000	2,803	0,005	0,000	2,803	0,005	6,000	2,191	0,028	0,000	2,803	0,005	0,000	2,803	0,005
CG	$GABA_{A(BZ)}$			$GABA_B$			α_1			α_2			$D_{1/5}$		
	T	*Z*	*p-value*	*T*	*Z*	*p-value*	*T*	*Z*	*p-value*	*T*	*Z*	*p-value*	*T*	*Z*	*p-value*
PIR 1 & PIR 2	17,000	1,070	0,285	4,000	2,395	0,017	15,000	1,274	0,203	5,000	2,293	0,022	0,000	2,803	0,005
PIR 1 & PIR 3	3,000	2,497	0,013	10,000	1,784	0,074	3,000	2,497	0,013	3,000	2,497	0,013	0,000	2,803	0,005
PIR 2 & PIR 1	17,000	1,070	0,285	4,000	2,395	0,017	15,000	1,274	0,203	5,000	2,293	0,022	0,000	2,803	0,005
PIR 2 & PIR 3	13,000	1,478	0,139	0,000	2,803	0,005	2,000	2,599	0,009	16,000	1,172	0,241	0,000	2,803	0,005
PIR 3 & PIR 1	3,000	2,497	0,013	10,000	1,784	0,074	3,000	2,497	0,013	3,000	2,497	0,013	0,000	2,803	0,005
PIR 3 & PIR 2	13,000	1,478	0,139	0,000	2,803	0,005	2,000	2,599	0,009	16,000	1,172	0,241	0,000	2,803	0,005

Supp. Tab. 17: Statistical analysis of layer-specific receptor concentrations of the lateral entorhinal cortex in CG

Statistical data of differences between receptor densities across layers within the lateral entorhinal cortex of control mice (CG). Each receptor type was tested separately with pair-wise Wilcoxon-rank test if the Friedman ANOVA showed differences within the region. Wilcoxon-rank: Z-score (Z), minimum of sum of the ranks of positive or negative changes (T), red labelling if $p < 0.05$ (N = 10, df = 13) (see Lothmann et al., 2021).

CG	AMPA			Kainate			NMDA			$mGlu_{2/3}$			$GABA_A$		
	T	*Z*	*p-value*	*T*	*Z*	*p-value*	*T*	*Z*	*p-value*	*T*	*Z*	*p-value*	*T*	*Z*	*p-value*
ENT I 1 & ENT I 2	0,00	2,80	0,01	0,00	2,80	0,01	0,00	2,80	0,01	18,00	0,97	0,33	0,00	2,80	0,01
ENT I 1 & ENT I 3	0,00	2,80	0,01	0,00	2,80	0,01	0,00	2,80	0,01	26,00	0,15	0,88	1,00	2,70	0,01
ENT I 1 & ENT I 4	0,00	2,80	0,01	0,00	2,80	0,01	0,00	2,80	0,01	27,00	0,05	0,96	0,00	2,80	0,01
ENT I 1 & ENT I 5	0,00	2,80	0,01	0,00	2,80	0,01	0,00	2,80	0,01	25,00	0,25	0,80	15,00	1,27	0,20
ENT I 1 & ENT I 6a	3,00	2,50	0,01	0,00	2,80	0,01	5,00	2,29	0,02	12,00	1,58	0,11	23,00	0,46	0,65
ENT I 1 & ENT I 6b	18,00	0,97	0,33	0,00	2,80	0,01	13,00	1,48	0,14	0,00	2,80	0,01	9,00	1,89	0,06
ENT I 2 & ENT I 1	0,00	2,80	0,01	0,00	2,80	0,01	0,00	2,80	0,01	18,00	0,97	0,33	0,00	2,80	0,01
ENT I 2 & ENT I 3	21,00	0,66	0,51	0,00	2,80	0,01	4,00	2,40	0,02	21,00	0,66	0,51	24,00	0,36	0,72
ENT I 2 & ENT I 4	22,00	0,56	0,58	0,00	2,80	0,01	22,00	0,56	0,58	22,00	0,56	0,58	18,00	0,97	0,33
ENT I 2 & ENT I 5	3,00	2,50	0,01	0,00	2,80	0,01	20,00	0,76	0,44	17,00	1,07	0,28	1,00	2,70	0,01
ENT I 2 & ENT I 6a	0,00	2,80	0,01	0,00	2,80	0,01	0,00	2,80	0,01	2,00	2,60	0,01	0,00	2,80	0,01
ENT I 2 & ENT I 6b	0,00	2,80	0,01	0,00	2,80	0,01	0,00	2,80	0,01	0,00	2,80	0,01	0,00	2,80	0,01
ENT I 3 & ENT I 1	0,00	2,80	0,01	0,00	2,80	0,01	0,00	2,80	0,01	26,00	0,15	0,88	1,00	2,70	0,01
ENT I 3 & ENT I 2	21,00	0,66	0,51	0,00	2,80	0,01	4,00	2,40	0,02	21,00	0,66	0,51	24,00	0,36	0,72
ENT I 3 & ENT I 4	9,00	1,89	0,06	3,00	2,50	0,01	4,00	2,40	0,02	19,00	0,87	0,39	11,00	1,68	0,09
ENT I 3 & ENT I 5	4,00	2,40	0,02	0,00	2,80	0,01	4,00	2,40	0,02	17,00	1,07	0,28	3,00	2,50	0,01
ENT I 3 & ENT I 6a	0,00	2,80	0,01	0,00	2,80	0,01	0,00	2,80	0,01	1,00	2,70	0,01	1,00	2,70	0,01
ENT I 3 & ENT I 6b	0,00	2,80	0,01	0,00	2,80	0,01	0,00	2,80	0,01	0,00	2,80	0,01	0,00	2,80	0,01
ENT I 4 & ENT I 1	0,00	2,80	0,01	0,00	2,80	0,01	0,00	2,80	0,01	27,00	0,05	0,96	0,00	2,80	0,01
ENT I 4 & ENT I 2	22,00	0,56	0,58	0,00	2,80	0,01	22,00	0,56	0,58	22,00	0,56	0,58	18,00	0,97	0,33

ENT I 4 & ENT I 3	9,00	1,89	0,06	3,00	2,50	0,01	4,00	2,40	0,02	19,00	0,87	0,39	11,00	1,68	0,09
ENT I 4 & ENT I 5	8,00	1,99	0,05	1,00	2,70	0,01	4,00	2,40	0,02	8,00	1,99	0,05	1,00	2,70	0,01
ENT I 4 & ENT I 6a	1,00	2,70	0,01	0,00	2,80	0,01	0,00	2,80	0,01	0,00	2,80	0,01	0,00	2,80	0,01
ENT I 4 & ENT I 6b	0,00	2,80	0,01	0,00	2,80	0,01	0,00	2,80	0,01	0,00	2,80	0,01	0,00	2,80	0,01
ENT I 5 & ENT I 1	0,00	2,80	0,01	0,00	2,80	0,01	0,00	2,80	0,01	25,00	0,25	0,80	15,00	1,27	0,20
ENT I 5 & ENT I 2	3,00	2,50	0,01	0,00	2,80	0,01	20,00	0,76	0,44	17,00	1,07	0,28	1,00	2,70	0,01
ENT I 5 & ENT I 3	4,00	2,40	0,02	0,00	2,80	0,01	4,00	2,40	0,02	17,00	1,07	0,28	3,00	2,50	0,01
ENT I 5 & ENT I 4	8,00	1,99	0,05	1,00	2,70	0,01	4,00	2,40	0,02	8,00	1,99	0,05	1,00	2,70	0,01
ENT I 5 & ENT I 6a	0,00	2,80	0,01	0,00	2,80	0,01	0,00	2,80	0,01	10,00	1,78	0,07	8,00	1,99	0,05
ENT I 5 & ENT I 6b	0,00	2,80	0,01	0,00	2,80	0,01	0,00	2,80	0,01	0,00	2,80	0,01	0,00	2,80	0,01
ENT I 6a & ENT I 1	3,00	2,50	0,01	0,00	2,80	0,01	5,00	2,29	0,02	12,00	1,58	0,11	23,00	0,46	0,65
ENT I 6a & ENT I 2	0,00	2,80	0,01	0,00	2,80	0,01	0,00	2,80	0,01	2,00	2,60	0,01	0,00	2,80	0,01
ENT I 6a & ENT I 3	0,00	2,80	0,01	0,00	2,80	0,01	0,00	2,80	0,01	1,00	2,70	0,01	1,00	2,70	0,01
ENT I 6a & ENT I 4	1,00	2,70	0,01	0,00	2,80	0,01	0,00	2,80	0,01	0,00	2,80	0,01	0,00	2,80	0,01
ENT I 6a & ENT I 5	0,00	2,80	0,01	0,00	2,80	0,01	0,00	2,80	0,01	10,00	1,78	0,07	8,00	1,99	0,05
ENT I 6a & ENT I 6b	2,00	2,60	0,01	21,00	0,66	0,51	0,00	2,80	0,01	0,00	2,80	0,01	0,00	2,80	0,01
ENT I 6b & ENT I 1	18,00	0,97	0,33	0,00	2,80	0,01	13,00	1,48	0,14	0,00	2,80	0,01	9,00	1,89	0,06
ENT I 6b & ENT I 2	0,00	2,80	0,01	0,00	2,80	0,01	0,00	2,80	0,01	0,00	2,80	0,01	0,00	2,80	0,01
ENT I 6b & ENT I 3	0,00	2,80	0,01	0,00	2,80	0,01	0,00	2,80	0,01	0,00	2,80	0,01	0,00	2,80	0,01
ENT I 6b & ENT I 4	0,00	2,80	0,01	0,00	2,80	0,01	0,00	2,80	0,01	0,00	2,80	0,01	0,00	2,80	0,01
ENT I 6b & ENT I 5	0,00	2,80	0,01	0,00	2,80	0,01	0,00	2,80	0,01	0,00	2,80	0,01	0,00	2,80	0,01
ENT I 6b & ENT I 6a	2,00	2,60	0,01	21,00	0,66	0,51	0,00	2,80	0,01	0,00	2,80	0,01	0,00	2,80	0,01
CG	$GABA_{A(BZ)}$			$GABA_B$			α_1			α_2			$D_{1/5}$		
	T	*Z*	*p-value*	*T*	*Z*	*p-value*	*T*	*Z*	*p-value*	*T*	*Z*	*p-value*	*T*	*Z*	*p-value*
ENT I 1 & ENT I 2	1,00	2,70	0,01	4,00	2,40	0,02	13,00	1,48	0,14	0,00	2,80	0,01	0,00	2,80	0,01
ENT I 1 & ENT I 3	15,00	1,27	0,20	1,00	2,70	0,01	23,00	0,46	0,65	0,00	2,80	0,01	0,00	2,80	0,01
ENT I 1 & ENT I 4	21,00	0,66	0,51	3,00	2,50	0,01	23,00	0,46	0,65	0,00	2,80	0,01	7,00	2,09	0,04
ENT I 1 & ENT I 5	24,00	0,36	0,72	11,00	1,68	0,09	21,00	0,66	0,51	0,00	2,80	0,01	11,00	1,68	0,09

ENT I 1 & ENT I 6a	12,00	1,58	0,11	21,00	0,66	0,51	0,00	2,80	0,01	0,00	2,80	0,01	5,00	2,29	0,02
ENT I 1 & ENT I 6b	19,00	0,87	0,39	0,00	2,80	0,01	0,00	2,80	0,01	0,00	2,80	0,01	5,00	2,29	0,02
ENT I 2 & ENT I 1	1,00	2,70	0,01	4,00	2,40	0,02	13,00	1,48	0,14	0,00	2,80	0,01	0,00	2,80	0,01
ENT I 2 & ENT I 3	16,00	1,17	0,24	26,00	0,15	0,88	17,00	1,07	0,28	2,00	2,60	0,01	22,00	0,56	0,58
ENT I 2 & ENT I 4	12,00	1,58	0,11	24,00	0,36	0,72	14,00	1,38	0,17	0,00	2,80	0,01	18,00	0,97	0,33
ENT I 2 & ENT I 5	14,00	1,38	0,17	15,00	1,27	0,20	24,00	0,36	0,72	0,00	2,80	0,01	21,00	0,66	0,51
ENT I 2 & ENT I 6a	25,00	0,25	0,80	4,00	2,40	0,02	3,00	2,50	0,01	0,00	2,80	0,01	19,00	0,87	0,39
ENT I 2 & ENT I 6b	14,00	1,38	0,17	0,00	2,80	0,01	0,00	2,80	0,01	0,00	2,80	0,01	15,00	1,27	0,20
ENT I 3 & ENT I 1	15,00	1,27	0,20	1,00	2,70	0,01	23,00	0,46	0,65	0,00	2,80	0,01	0,00	2,80	0,01
ENT I 3 & ENT I 2	16,00	1,17	0,24	26,00	0,15	0,88	17,00	1,07	0,28	2,00	2,60	0,01	22,00	0,56	0,58
ENT I 3 & ENT I 4	12,00	1,58	0,11	13,00	1,48	0,14	20,00	0,76	0,44	3,00	2,50	0,01	12,00	1,58	0,11
ENT I 3 & ENT I 5	17,00	1,07	0,28	4,00	2,40	0,02	18,00	0,97	0,33	1,00	2,70	0,01	19,00	0,87	0,39
ENT I 3 & ENT I 6a	11,00	1,68	0,09	5,00	2,29	0,02	0,00	2,80	0,01	8,00	1,99	0,05	19,00	0,87	0,39
ENT I 3 & ENT I 6b	18,00	0,97	0,33	0,00	2,80	0,01	0,00	2,80	0,01	18,00	0,97	0,33	14,00	1,38	0,17
ENT I 4 & ENT I 1	21,00	0,66	0,51	3,00	2,50	0,01	23,00	0,46	0,65	0,00	2,80	0,01	7,00	2,09	0,04
ENT I 4 & ENT I 2	12,00	1,58	0,11	24,00	0,36	0,72	14,00	1,38	0,17	0,00	2,80	0,01	18,00	0,97	0,33
ENT I 4 & ENT I 3	12,00	1,58	0,11	13,00	1,48	0,14	20,00	0,76	0,44	3,00	2,50	0,01	12,00	1,58	0,11
ENT I 4 & ENT I 5	24,00	0,36	0,72	2,00	2,60	0,01	14,00	1,38	0,17	16,00	1,17	0,24	24,00	0,36	0,72
ENT I 4 & ENT I 6a	0,00	2,80	0,01	4,00	2,40	0,02	0,00	2,80	0,01	27,00	0,05	0,96	7,00	2,09	0,04
ENT I 4 & ENT I 6b	24,00	0,36	0,72	0,00	2,80	0,01	0,00	2,80	0,01	23,00	0,46	0,65	4,00	2,40	0,02
ENT I 5 & ENT I 1	24,00	0,36	0,72	11,00	1,68	0,09	21,00	0,66	0,51	0,00	2,80	0,01	11,00	1,68	0,09
ENT I 5 & ENT I 2	14,00	1,38	0,17	15,00	1,27	0,20	24,00	0,36	0,72	0,00	2,80	0,01	21,00	0,66	0,51
ENT I 5 & ENT I 3	17,00	1,07	0,28	4,00	2,40	0,02	18,00	0,97	0,33	1,00	2,70	0,01	19,00	0,87	0,39
ENT I 5 & ENT I 4	24,00	0,36	0,72	2,00	2,60	0,01	14,00	1,38	0,17	16,00	1,17	0,24	24,00	0,36	0,72
ENT I 5 & ENT I 6a	0,00	2,80	0,01	11,00	1,68	0,09	0,00	2,80	0,01	19,00	0,87	0,39	3,00	2,50	0,01
ENT I 5 & ENT I 6b	13,00	1,48	0,14	0,00	2,80	0,01	0,00	2,80	0,01	15,00	1,27	0,20	4,00	2,40	0,02
ENT I 6a & ENT I 1	12,00	1,58	0,11	21,00	0,66	0,51	0,00	2,80	0,01	0,00	2,80	0,01	5,00	2,29	0,02

ENT I 6a & ENT I 2	25,00	0,25	0,80	4,00	2,40	0,02	3,00	2,50	0,01	0,00	2,80	0,01	19,00	0,87	0,39
ENT I 6a & ENT I 3	11,00	1,68	0,09	5,00	2,29	0,02	0,00	2,80	0,01	8,00	1,99	0,05	19,00	0,87	0,39
ENT I 6a & ENT I 4	0,00	2,80	0,01	4,00	2,40	0,02	0,00	2,80	0,01	27,00	0,05	0,96	7,00	2,09	0,04
ENT I 6a & ENT I 5	0,00	2,80	0,01	11,00	1,68	0,09	0,00	2,80	0,01	19,00	0,87	0,39	3,00	2,50	0,01
ENT I 6a & ENT I 6b	8,00	1,99	0,05	0,00	2,80	0,01	8,00	1,99	0,05	18,00	0,97	0,33	19,00	0,87	0,39
ENT I 6b & ENT I 1	19,00	0,87	0,39	0,00	2,80	0,01	0,00	2,80	0,01	0,00	2,80	0,01	5,00	2,29	0,02
ENT I 6b & ENT I 2	14,00	1,38	0,17	0,00	2,80	0,01	0,00	2,80	0,01	0,00	2,80	0,01	15,00	1,27	0,20
ENT I 6b & ENT I 3	18,00	0,97	0,33	0,00	2,80	0,01	0,00	2,80	0,01	18,00	0,97	0,33	14,00	1,38	0,17
ENT I 6b & ENT I 4	24,00	0,36	0,72	0,00	2,80	0,01	0,00	2,80	0,01	23,00	0,46	0,65	4,00	2,40	0,02
ENT I 6b & ENT I 5	13,00	1,48	0,14	0,00	2,80	0,01	0,00	2,80	0,01	15,00	1,27	0,20	4,00	2,40	0,02
ENT I 6b & ENT I 6a	8,00	1,99	0,05	0,00	2,80	0,01	8,00	1,99	0,05	18,00	0,97	0,33	19,00	0,87	0,39

Supp. Tab. 18: Statistical analysis of layer-specific receptor concentrations of the medial entorhinal cortex in CG

Statistical data of differences between receptor densities across layers within the medial entorhinal cortex of control mice (CG). Each receptor type was tested separately with pair-wise Wilcoxon-rank test if the Friedman ANOVA showed differences within the region. Wilcoxon-rank: Z-score (Z), minimum of sum of the ranks of positive or negative changes (T), red labelling if $p < 0.05$ (N = 10, df = 13) (see Lothmann et al., 2021).

CG	AMPA			Kainate			NMDA			$mGlu_{2/3}$			$GABA_A$		
	T	*Z*	*p-value*	*T*	*Z*	*p-value*	*T*	*Z*	*p-value*	*T*	*Z*	*p-value*	*T*	*Z*	*p-value*
ENT m 1 & ENT m 2	16,00	1,17	0,24	0,00	2,80	0,01	0,00	2,80	0,01	18,00	0,97	0,33	0,00	2,80	0,01
ENT m 1 & ENT m 3	17,00	1,07	0,28	0,00	2,80	0,01	0,00	2,80	0,01	25,00	0,25	0,80	0,00	2,80	0,01
ENT m 1 & ENT m 4	16,00	1,17	0,24	1,00	2,70	0,01	26,00	0,15	0,88	21,00	0,66	0,51	2,00	2,60	0,01
ENT m 1 & ENT m 5	22,00	0,56	0,58	1,00	2,70	0,01	1,00	2,70	0,01	19,00	0,87	0,39	6,00	2,19	0,03
ENT m 1 & ENT m 6	26,00	0,15	0,88	0,00	2,80	0,01	11,00	1,68	0,09	7,00	2,09	0,04	13,00	1,48	0,14
ENT m 2 & ENT m 1	16,00	1,17	0,24	0,00	2,80	0,01	0,00	2,80	0,01	18,00	0,97	0,33	0,00	2,80	0,01
ENT m 2 & ENT m 3	21,00	0,66	0,51	4,00	2,40	0,02	18,00	0,97	0,33	16,00	1,17	0,24	9,00	1,89	0,06
ENT m 2 & ENT m 4	21,00	0,66	0,51	4,00	2,40	0,02	2,00	2,60	0,01	12,00	1,58	0,11	15,00	1,27	0,20
ENT m 2 & ENT m 5	27,00	0,05	0,96	1,00	2,70	0,01	11,00	1,68	0,09	13,00	1,48	0,14	2,00	2,60	0,01
ENT m 2 & ENT m 6	25,00	0,25	0,80	0,00	2,80	0,01	0,00	2,80	0,01	6,00	2,19	0,03	0,00	2,80	0,01
ENT m 3 & ENT m 1	17,00	1,07	0,28	0,00	2,80	0,01	0,00	2,80	0,01	25,00	0,25	0,80	0,00	2,80	0,01
ENT m 3 & ENT m 2	21,00	0,66	0,51	4,00	2,40	0,02	18,00	0,97	0,33	16,00	1,17	0,24	9,00	1,89	0,06
ENT m 3 & ENT m 4	24,00	0,36	0,72	11,00	1,68	0,09	1,00	2,70	0,01	19,00	0,87	0,39	1,00	2,70	0,01
ENT m 3 & ENT m 5	26,00	0,15	0,88	8,00	1,99	0,05	19,00	0,87	0,39	12,00	1,58	0,11	0,00	2,80	0,01
ENT m 3 & ENT m 6	25,00	0,25	0,80	4,00	2,40	0,02	0,00	2,80	0,01	7,00	2,09	0,04	0,00	2,80	0,01
ENT m 4 & ENT m 1	16,00	1,17	0,24	1,00	2,70	0,01	26,00	0,15	0,88	21,00	0,66	0,51	2,00	2,60	0,01
ENT m 4 & ENT m 2	21,00	0,66	0,51	4,00	2,40	0,02	2,00	2,60	0,01	12,00	1,58	0,11	15,00	1,27	0,20
ENT m 4 & ENT m 3	24,00	0,36	0,72	11,00	1,68	0,09	1,00	2,70	0,01	19,00	0,87	0,39	1,00	2,70	0,01
ENT m 4 & ENT m 5	22,00	0,56	0,58	15,00	1,27	0,20	8,00	1,99	0,05	18,00	0,97	0,33	9,00	1,89	0,06

ENT m 4 & ENT m 6	20,00	0,76	0,44	20,00	0,76	0,44	9,00	1,89	0,06	6,00	2,19	0,03	1,00	2,70	0,01
ENT m 5 & ENT m 1	22,00	0,56	0,58	1,00	2,70	0,01	1,00	2,70	0,01	19,00	0,87	0,39	6,00	2,19	0,03
ENT m 5 & ENT m 2	27,00	0,05	0,96	1,00	2,70	0,01	11,00	1,68	0,09	13,00	1,48	0,14	2,00	2,60	0,01
ENT m 5 & ENT m 3	26,00	0,15	0,88	8,00	1,99	0,05	19,00	0,87	0,39	12,00	1,58	0,11	0,00	2,80	0,01
ENT m 5 & ENT m 4	22,00	0,56	0,58	15,00	1,27	0,20	8,00	1,99	0,05	18,00	0,97	0,33	9,00	1,89	0,06
ENT m 5 & ENT m 6	25,00	0,25	0,80	24,00	0,36	0,72	0,00	2,80	0,01	2,00	2,60	0,01	7,00	2,09	0,04
ENT m 6 & ENT m 1	26,00	0,15	0,88	0,00	2,80	0,01	11,00	1,68	0,09	7,00	2,09	0,04	13,00	1,48	0,14
ENT m 6 & ENT m 2	25,00	0,25	0,80	0,00	2,80	0,01	0,00	2,80	0,01	6,00	2,19	0,03	0,00	2,80	0,01
ENT m 6 & ENT m 3	25,00	0,25	0,80	4,00	2,40	0,02	0,00	2,80	0,01	7,00	2,09	0,04	0,00	2,80	0,01
ENT m 6 & ENT m 4	20,00	0,76	0,44	20,00	0,76	0,44	9,00	1,89	0,06	6,00	2,19	0,03	1,00	2,70	0,01
ENT m 6 & ENT m 5	25,00	0,25	0,80	24,00	0,36	0,72	0,00	2,80	0,01	2,00	2,60	0,01	7,00	2,09	0,04

CG	$GABA_{A(BZ)}$			$GABA_B$			α_1			α_2			$D_{1/5}$		
	T	*Z*	*p-value*	*T*	*Z*	*p-value*	*T*	*Z*	*p-value*	*T*	*Z*	*p-value*	*T*	*Z*	*p-value*
ENT m 1 & ENT m 2	17,00	1,07	0,28	1,00	2,70	0,01	11,00	1,68	0,09	0,00	2,80	0,01	0,00	2,80	0,01
ENT m 1 & ENT m 3	21,00	0,66	0,51	6,00	2,19	0,03	16,00	1,17	0,24	0,00	2,80	0,01	0,00	2,80	0,01
ENT m 1 & ENT m 4	22,00	0,56	0,58	5,00	2,29	0,02	27,00	0,05	0,96	0,00	2,80	0,01	7,00	2,09	0,04
ENT m 1 & ENT m 5	21,00	0,66	0,51	26,00	0,15	0,88	9,00	1,89	0,06	0,00	2,80	0,01	1,00	2,70	0,01
ENT m 1 & ENT m 6	19,00	0,87	0,39	18,00	0,97	0,33	5,00	2,29	0,02	1,00	2,70	0,01	0,00	2,80	0,01
ENT m 2 & ENT m 1	17,00	1,07	0,28	1,00	2,70	0,01	11,00	1,68	0,09	0,00	2,80	0,01	0,00	2,80	0,01
ENT m 2 & ENT m 3	17,00	1,07	0,28	4,00	2,40	0,02	15,00	1,27	0,20	10,00	1,78	0,07	9,00	1,89	0,06
ENT m 2 & ENT m 4	13,00	1,48	0,14	5,00	2,29	0,02	5,00	2,29	0,02	1,00	2,70	0,01	19,00	0,87	0,39
ENT m 2 & ENT m 5	20,00	0,76	0,44	1,00	2,70	0,01	17,00	1,07	0,28	1,00	2,70	0,01	23,00	0,46	0,65
ENT m 2 & ENT m 6	14,00	1,38	0,17	0,00	2,80	0,01	10,00	1,78	0,07	26,00	0,15	0,88	14,00	1,38	0,17
ENT m 3 & ENT m 1	21,00	0,66	0,51	6,00	2,19	0,03	16,00	1,17	0,24	0,00	2,80	0,01	0,00	2,80	0,01
ENT m 3 & ENT m 2	17,00	1,07	0,28	4,00	2,40	0,02	15,00	1,27	0,20	10,00	1,78	0,07	9,00	1,89	0,06
ENT m 3 & ENT m 4	18,00	0,97	0,33	15,00	1,27	0,20	14,00	1,38	0,17	11,00	1,68	0,09	26,00	0,15	0,88
ENT m 3 & ENT m 5	26,00	0,15	0,88	3,00	2,50	0,01	11,00	1,68	0,09	16,00	1,17	0,24	18,00	0,97	0,33
ENT m 3 & ENT m 6	17,00	1,07	0,28	0,00	2,80	0,01	4,00	2,40	0,02	8,00	1,99	0,05	25,00	0,25	0,80

ENT m 4 & ENT m 1	22,00	0,56	0,58	5,00	2,29	0,02	27,00	0,05	0,96	0,00	2,80	0,01	7,00	2,09	0,04
ENT m 4 & ENT m 2	13,00	1,48	0,14	5,00	2,29	0,02	5,00	2,29	0,02	1,00	2,70	0,01	19,00	0,87	0,39
ENT m 4 & ENT m 3	18,00	0,97	0,33	15,00	1,27	0,20	14,00	1,38	0,17	11,00	1,68	0,09	26,00	0,15	0,88
ENT m 4 & ENT m 5	22,00	0,56	0,58	5,00	2,29	0,02	0,00	2,80	0,01	18,00	0,97	0,33	25,00	0,25	0,80
ENT m 4 & ENT m 6	18,00	0,97	0,33	5,00	2,29	0,02	0,00	2,80	0,01	8,00	1,99	0,05	18,00	0,97	0,33
ENT m 5 & ENT m 1	21,00	0,66	0,51	26,00	0,15	0,88	9,00	1,89	0,06	0,00	2,80	0,01	1,00	2,70	0,01
ENT m 5 & ENT m 2	20,00	0,76	0,44	1,00	2,70	0,01	17,00	1,07	0,28	1,00	2,70	0,01	23,00	0,46	0,65
ENT m 5 & ENT m 3	26,00	0,15	0,88	3,00	2,50	0,01	11,00	1,68	0,09	16,00	1,17	0,24	18,00	0,97	0,33
ENT m 5 & ENT m 4	22,00	0,56	0,58	5,00	2,29	0,02	0,00	2,80	0,01	18,00	0,97	0,33	25,00	0,25	0,80
ENT m 5 & ENT m 6	14,00	1,38	0,17	14,00	1,38	0,17	6,00	2,19	0,03	5,00	2,29	0,02	13,00	1,48	0,14
ENT m 6 & ENT m 1	19,00	0,87	0,39	18,00	0,97	0,33	5,00	2,29	0,02	1,00	2,70	0,01	0,00	2,80	0,01
ENT m 6 & ENT m 2	14,00	1,38	0,17	0,00	2,80	0,01	10,00	1,78	0,07	26,00	0,15	0,88	14,00	1,38	0,17
ENT m 6 & ENT m 3	17,00	1,07	0,28	0,00	2,80	0,01	4,00	2,40	0,02	8,00	1,99	0,05	25,00	0,25	0,80
ENT m 6 & ENT m 4	18,00	0,97	0,33	5,00	2,29	0,02	0,00	2,80	0,01	8,00	1,99	0,05	18,00	0,97	0,33
ENT m 6 & ENT m 5	14,00	1,38	0,17	14,00	1,38	0,17	6,00	2,19	0,03	5,00	2,29	0,02	13,00	1,48	0,14

Supp. Tab. 19: Statistical analysis of layer-specific receptor concentrations of the medial orbitofrontal cortex in CG

Statistical data of differences between receptor densities across layers within the medial orbitofrontal cortex of control mice (CG). Each receptor type was tested separately with pair-wise Wilcoxon-rank test if the Friedman ANOVA showed differences within the region. Wilcoxon-rank: Z-score (Z), minimum of sum of the ranks of positive or negative changes (T), red labelling if $p < 0.05$ (N = 10, df = 13) (see Lothmann et al., 2021).

CG	AMPA			Kainate			NMDA			$mGlu_{2/3}$			$GABA_A$		
	T	*Z*	*p-value*	*T*	*Z*	*p-value*	*T*	*Z*	*p-value*	*T*	*Z*	*p-value*	*T*	*Z*	*p-value*
ORB m 1 & ORB m 2	7,00	2,09	0,04	2,00	2,60	0,01	6,00	2,19	0,03	2,00	2,60	0,01	10,00	1,78	0,07
ORB m 1 & ORB m 2/3	3,00	2,50	0,01	0,00	2,80	0,01	2,00	2,60	0,01	6,00	2,19	0,03	27,00	0,05	0,96
ORB m 1 & ORB m 5	4,00	2,40	0,02	0,00	2,80	0,01	0,00	2,80	0,01	0,00	2,80	0,01	21,00	0,66	0,51
ORB m 1 & ORB m 6a	4,00	2,40	0,02	0,00	2,80	0,01	2,00	2,60	0,01	1,00	2,70	0,01	22,00	0,56	0,58
ORB m 2 & ORB m 1	7,00	2,09	0,04	2,00	2,60	0,01	6,00	2,19	0,03	2,00	2,60	0,01	10,00	1,78	0,07
ORB m 2 & ORB m 2/3	9,00	1,89	0,06	13,00	1,48	0,14	2,00	2,60	0,01	10,00	1,78	0,07	13,00	1,48	0,14
ORB m 2 & ORB m 5	12,00	1,58	0,11	10,00	1,78	0,07	1,00	2,70	0,01	9,00	1,89	0,06	9,00	1,89	0,06
ORB m 2 & ORB m 6a	12,00	1,58	0,11	5,00	2,29	0,02	12,00	1,58	0,11	9,00	1,89	0,06	15,00	1,27	0,20
ORB m 2/3 & ORB m 1	3,00	2,50	0,01	0,00	2,80	0,01	2,00	2,60	0,01	6,00	2,19	0,03	27,00	0,05	0,96
ORB m 2/3 & ORB m 2	9,00	1,89	0,06	13,00	1,48	0,14	2,00	2,60	0,01	10,00	1,78	0,07	13,00	1,48	0,14
ORB m 2/3 & ORB m 5	17,00	1,07	0,28	18,00	0,97	0,33	0,00	2,80	0,01	3,00	2,50	0,01	11,00	1,68	0,09
ORB m 2/3 & ORB m 6a	15,00	1,27	0,20	1,00	2,70	0,01	24,00	0,36	0,72	3,00	2,50	0,01	26,00	0,15	0,88
ORB m 5 & ORB m 1	4,00	2,40	0,02	0,00	2,80	0,01	0,00	2,80	0,01	0,00	2,80	0,01	21,00	0,66	0,51
ORB m 5 & ORB m 2	12,00	1,58	0,11	10,00	1,78	0,07	1,00	2,70	0,01	9,00	1,89	0,06	9,00	1,89	0,06
ORB m 5 & ORB m 2/3	17,00	1,07	0,28	18,00	0,97	0,33	0,00	2,80	0,01	3,00	2,50	0,01	11,00	1,68	0,09
ORB m 5 & ORB m 6a	14,00	1,38	0,17	0,00	2,80	0,01	5,00	2,29	0,02	9,00	1,89	0,06	25,00	0,25	0,80
ORB m 6a & ORB m 1	4,00	2,40	0,02	0,00	2,80	0,01	2,00	2,60	0,01	1,00	2,70	0,01	22,00	0,56	0,58
ORB m 6a & ORB m 2	12,00	1,58	0,11	5,00	2,29	0,02	12,00	1,58	0,11	9,00	1,89	0,06	15,00	1,27	0,20
ORB m 6a & ORB m 2/3	15,00	1,27	0,20	1,00	2,70	0,01	24,00	0,36	0,72	3,00	2,50	0,01	26,00	0,15	0,88

ORB m 6a & ORB m 5	14,00	1,38	0,17	0,00	2,80	0,01	5,00	2,29	0,02	9,00	1,89	0,06	25,00	0,25	0,80
CG	$GABA_{A(BZ)}$			$GABA_B$			α_1			α_2			$D_{1/5}$		
	T	*Z*	*p-value*	*T*	*Z*	*p-value*	*T*	*Z*	*p-value*	*T*	*Z*	*p-value*	*T*	*Z*	*p-value*
ORB m 1 & ORB m 2	20,00	0,76	0,44	26,00	0,15	0,88	10,00	1,78	0,07	14,00	1,38	0,17	10,00	1,78	0,07
ORB m 1 & ORB m 2/3	20,00	0,76	0,44	1,00	2,70	0,01	6,00	2,19	0,03	3,00	2,50	0,01	4,00	2,40	0,02
ORB m 1 & ORB m 5	26,00	0,15	0,88	0,00	2,80	0,01	9,00	1,89	0,06	0,00	2,80	0,01	1,00	2,70	0,01
ORB m 1 & ORB m 6a	26,00	0,15	0,88	0,00	2,80	0,01	18,00	0,97	0,33	0,00	2,80	0,01	1,00	2,70	0,01
ORB m 2 & ORB m 1	20,00	0,76	0,44	26,00	0,15	0,88	10,00	1,78	0,07	14,00	1,38	0,17	10,00	1,78	0,07
ORB m 2 & ORB m 2/3	21,00	0,66	0,51	9,00	1,89	0,06	14,00	1,38	0,17	8,00	1,99	0,05	2,00	2,60	0,01
ORB m 2 & ORB m 5	15,00	1,27	0,20	9,00	1,89	0,06	22,00	0,56	0,58	0,00	2,80	0,01	0,00	2,80	0,01
ORB m 2 & ORB m 6a	14,00	1,38	0,17	0,00	2,80	0,01	23,00	0,46	0,65	0,00	2,80	0,01	0,00	2,80	0,01
ORB m 2/3 & ORB m 1	20,00	0,76	0,44	1,00	2,70	0,01	6,00	2,19	0,03	3,00	2,50	0,01	4,00	2,40	0,02
ORB m 2/3 & ORB m 2	21,00	0,66	0,51	9,00	1,89	0,06	14,00	1,38	0,17	8,00	1,99	0,05	2,00	2,60	0,01
ORB m 2/3 & ORB m 5	9,00	1,89	0,06	7,00	2,09	0,04	9,00	1,89	0,06	0,00	2,80	0,01	0,00	2,80	0,01
ORB m 2/3 & ORB m 6a	13,00	1,48	0,14	2,00	2,60	0,01	7,00	2,09	0,04	1,00	2,70	0,01	3,00	2,50	0,01
ORB m 5 & ORB m 1	26,00	0,15	0,88	0,00	2,80	0,01	9,00	1,89	0,06	0,00	2,80	0,01	1,00	2,70	0,01
ORB m 5 & ORB m 2	15,00	1,27	0,20	9,00	1,89	0,06	22,00	0,56	0,58	0,00	2,80	0,01	0,00	2,80	0,01
ORB m 5 & ORB m 2/3	9,00	1,89	0,06	7,00	2,09	0,04	9,00	1,89	0,06	0,00	2,80	0,01	0,00	2,80	0,01
ORB m 5 & ORB m 6a	26,00	0,15	0,88	7,00	2,09	0,04	16,00	1,17	0,24	14,00	1,38	0,17	17,00	1,07	0,28
ORB m 6a & ORB m 1	26,00	0,15	0,88	0,00	2,80	0,01	18,00	0,97	0,33	0,00	2,80	0,01	1,00	2,70	0,01
ORB m 6a & ORB m 2	14,00	1,38	0,17	0,00	2,80	0,01	23,00	0,46	0,65	0,00	2,80	0,01	0,00	2,80	0,01
ORB m 6a & ORB m 2/3	13,00	1,48	0,14	2,00	2,60	0,01	7,00	2,09	0,04	1,00	2,70	0,01	3,00	2,50	0,01
ORB m 6a & ORB m 5	26,00	0,15	0,88	7,00	2,09	0,04	16,00	1,17	0,24	14,00	1,38	0,17	17,00	1,07	0,28

Supp. Tab. 20: Statistical analysis of layer-specific receptor concentrations of the ventrolateral orbitofrontal cortex in CG

Statistical data of differences between receptor densities across layers within the ventrolateral orbitofrontal cortex of control mice (CG). Each receptor type was tested separately with pair-wise Wilcoxon-rank test if the Friedman ANOVA showed differences within the region. Wilcoxon-rank: Z-score (Z), minimum of sum of the ranks of positive or negative changes (T), red labelling if $p < 0.05$ (N = 10, df = 13) (see Lothmann et al., 2021).

CG	AMPA			Kainate			NMDA			$mGlu_{2/3}$			$GABA_A$		
	T	*Z*	*p-value*	*T*	*Z*	*p-value*	*T*	*Z*	*p-value*	*T*	*Z*	*p-value*	*T*	*Z*	*p-value*
ORB vl 1 & ORB vl 2/3	4,000	2,395	0,017	15,000	1,274	0,203	13,000	1,478	0,139	6,000	2,191	0,028	21,000	0,663	0,508
ORB vl 1 & ORB vl 5	7,000	2,090	0,037	0,000	2,803	0,005	8,000	1,988	0,047	6,000	2,191	0,028	16,000	1,172	0,241
ORB vl 1 & ORB vl 6a	7,000	2,090	0,037	0,000	2,803	0,005	6,000	2,191	0,028	0,000	2,803	0,005	17,000	1,070	0,285
ORB vl 2/3 & ORB vl 1	4,000	2,395	0,017	15,000	1,274	0,203	13,000	1,478	0,139	6,000	2,191	0,028	21,000	0,663	0,508
ORB vl 2/3 & ORB vl 5	20,000	0,764	0,445	0,000	2,803	0,005	13,000	1,478	0,139	9,000	1,886	0,059	15,000	1,274	0,203
ORB vl 2/3 & ORB vl 6a	26,000	0,153	0,878	0,000	2,803	0,005	2,000	2,599	0,009	0,000	2,803	0,005	17,000	1,070	0,285
ORB vl 5 & ORB vl 1	7,000	2,090	0,037	0,000	2,803	0,005	8,000	1,988	0,047	6,000	2,191	0,028	16,000	1,172	0,241
ORB vl 5 & ORB vl 2/3	20,000	0,764	0,445	0,000	2,803	0,005	13,000	1,478	0,139	9,000	1,886	0,059	15,000	1,274	0,203
ORB vl 5 & ORB vl 6a	14,000	1,376	0,169	0,000	2,803	0,005	10,000	1,784	0,074	1,000	2,701	0,007	16,000	1,172	0,241
ORB vl 6a & ORB vl 1	7,000	2,090	0,037	0,000	2,803	0,005	6,000	2,191	0,028	0,000	2,803	0,005	17,000	1,070	0,285
ORB vl 6a & ORB vl 2/3	26,000	0,153	0,878	0,000	2,803	0,005	2,000	2,599	0,009	0,000	2,803	0,005	17,000	1,070	0,285
ORB vl 6a & ORB vl 5	14,000	1,376	0,169	0,000	2,803	0,005	10,000	1,784	0,074	1,000	2,701	0,007	16,000	1,172	0,241
CG	$GABA_{A(BZ)}$			$GABA_B$			α_1			α_2			$D_{1/5}$		
	T	*Z*	*p-value*	*T*	*Z*	*p-value*	*T*	*Z*	*p-value*	*T*	*Z*	*p-value*	*T*	*Z*	*p-value*
ORB vl 1 & ORB vl 2/3	13,000	1,478	0,139	9,000	1,886	0,059	12,000	1,580	0,114	0,000	2,803	0,005	0,000	2,803	0,005
ORB vl 1 & ORB vl 5	6,000	2,191	0,028	1,000	2,701	0,007	20,000	0,764	0,445	0,000	2,803	0,005	2,000	2,599	0,009
ORB vl 1 & ORB vl 6a	12,000	1,580	0,114	1,000	2,701	0,007	23,000	0,459	0,646	0,000	2,803	0,005	0,000	2,803	0,005
ORB vl 2/3 & ORB vl 1	13,000	1,478	0,139	9,000	1,886	0,059	12,000	1,580	0,114	0,000	2,803	0,005	0,000	2,803	0,005
ORB vl 2/3 & ORB vl 5	27,000	0,051	0,959	0,000	2,803	0,005	11,000	1,682	0,093	13,000	1,478	0,139	9,000	1,886	0,059

ORB vl 2/3 & ORB vl 6a	13,000	1,478	0,139	0,000	2,803	0,005	17,000	1,070	0,285	0,000	2,803	0,005	1,000	2,701	0,007
ORB vl 5 & ORB vl 1	6,000	2,191	0,028	1,000	2,701	0,007	20,000	0,764	0,445	0,000	2,803	0,005	2,000	2,599	0,009
ORB vl 5 & ORB vl 2/3	27,000	0,051	0,959	0,000	2,803	0,005	11,000	1,682	0,093	13,000	1,478	0,139	9,000	1,886	0,059
ORB vl 5 & ORB vl 6a	1,000	2,701	0,007	8,000	1,988	0,047	22,000	0,561	0,575	3,000	2,497	0,013	0,000	2,803	0,005
ORB vl 6a & ORB vl 1	12,000	1,580	0,114	1,000	2,701	0,007	23,000	0,459	0,646	0,000	2,803	0,005	0,000	2,803	0,005
ORB vl 6a & ORB vl 2/3	13,000	1,478	0,139	0,000	2,803	0,005	17,000	1,070	0,285	0,000	2,803	0,005	1,000	2,701	0,007
ORB vl 6a & ORB vl 5	1,000	2,701	0,007	8,000	1,988	0,047	22,000	0,561	0,575	3,000	2,497	0,013	0,000	2,803	0,005

Supp. Tab. 21: Statistical analysis of layer-specific receptor concentrations of the lateral orbitofrontal cortex in CG

Statistical data of differences between receptor densities across layers within the lateral orbitofrontal cortex of control mice (CG). Each receptor type was tested separately with pair-wise Wilcoxon-rank test if the Friedman ANOVA showed differences within the region. Wilcoxon-rank: Z-score (Z), minimum of sum of the ranks of positive or negative changes (T), red labelling if $p < 0.05$ (N = 10, df = 13) (see Lothmann et al., 2021).

CG	AMPA			Kainate			NMDA			$mGlu_{2/3}$			$GABA_A$		
	T	*Z*	*p-value*	*T*	*Z*	*p-value*	*T*	*Z*	*p-value*	*T*	*Z*	*p-value*	*T*	*Z*	*p-value*
ORB l 1 & ORB l 2/3	0,000	2,803	0,005	3,000	2,497	0,013	19,000	0,866	0,386	0,000	2,803	0,005	21,000	0,663	0,508
ORB l 1 & ORB l 5	3,000	2,497	0,013	0,000	2,803	0,005	15,000	1,274	0,203	0,000	2,803	0,005	16,000	1,172	0,241
ORB l 1 & ORB l 6a	0,000	2,803	0,005	0,000	2,803	0,005	13,000	1,478	0,139	0,000	2,803	0,005	17,000	1,070	0,285
ORB l 2/3 & ORB l 1	0,000	2,803	0,005	3,000	2,497	0,013	19,000	0,866	0,386	0,000	2,803	0,005	21,000	0,663	0,508
ORB l 2/3 & ORB l 5	11,000	1,682	0,093	2,000	2,599	0,009	1,000	2,701	0,007	7,000	2,090	0,037	15,000	1,274	0,203
ORB l 2/3 & ORB l 6a	20,000	0,764	0,445	1,000	2,701	0,007	2,000	2,599	0,009	0,000	2,803	0,005	17,000	1,070	0,285
ORB l 5 & ORB l 1	3,000	2,497	0,013	0,000	2,803	0,005	15,000	1,274	0,203	0,000	2,803	0,005	16,000	1,172	0,241
ORB l 5 & ORB l 2/3	11,000	1,682	0,093	2,000	2,599	0,009	1,000	2,701	0,007	7,000	2,090	0,037	15,000	1,274	0,203
ORB l 5 & ORB l 6a	4,000	2,395	0,017	0,000	2,803	0,005	24,000	0,357	0,721	0,000	2,803	0,005	16,000	1,172	0,241
ORB l 6a & ORB l 1	0,000	2,803	0,005	0,000	2,803	0,005	13,000	1,478	0,139	0,000	2,803	0,005	17,000	1,070	0,285
ORB l 6a & ORB l 2/3	20,000	0,764	0,445	1,000	2,701	0,007	2,000	2,599	0,009	0,000	2,803	0,005	17,000	1,070	0,285
ORB l 6a & ORB l 5	4,000	2,395	0,017	0,000	2,803	0,005	24,000	0,357	0,721	0,000	2,803	0,005	16,000	1,172	0,241
CG	$GABA_{A(BZ)}$			$GABA_B$			α_1			α_2			$D_{1/5}$		
	T	*Z*	*p-value*	*T*	*Z*	*p-value*	*T*	*Z*	*p-value*	*T*	*Z*	*p-value*	*T*	*Z*	*p-value*
ORB l 1 & ORB l 2/3	0,000	2,803	0,005	8,000	1,988	0,047	3,000	2,497	0,013	0,000	2,803	0,005	1,000	2,701	0,007
ORB l 1 & ORB l 5	18,000	0,968	0,333	12,000	1,580	0,114	1,000	2,701	0,007	0,000	2,803	0,005	3,000	2,497	0,013
ORB l 1 & ORB l 6a	17,000	1,070	0,285	12,000	1,580	0,114	2,000	2,599	0,009	0,000	2,803	0,005	0,000	2,803	0,005
ORB l 2/3 & ORB l 1	0,000	2,803	0,005	8,000	1,988	0,047	3,000	2,497	0,013	0,000	2,803	0,005	1,000	2,701	0,007
ORB l 2/3 & ORB l 5	10,000	1,784	0,074	18,000	0,968	0,333	11,000	1,682	0,093	1,000	2,701	0,007	18,000	0,968	0,333

ORB I 2/3 & ORB I 6a	3,000	2,497	0,013	13,000	1,478	0,139	13,000	1,478	0,139	2,000	2,599	0,009	2,000	2,599	0,009
ORB I 5 & ORB I 1	18,000	0,968	0,333	12,000	1,580	0,114	1,000	2,701	0,007	0,000	2,803	0,005	3,000	2,497	0,013
ORB I 5 & ORB I 2/3	10,000	1,784	0,074	18,000	0,968	0,333	11,000	1,682	0,093	1,000	2,701	0,007	18,000	0,968	0,333
ORB I 5 & ORB I 6a	9,000	1,886	0,059	20,000	0,764	0,445	27,000	0,051	0,959	19,000	0,866	0,386	0,000	2,803	0,005
ORB I 6a & ORB I 1	17,000	1,070	0,285	12,000	1,580	0,114	2,000	2,599	0,009	0,000	2,803	0,005	0,000	2,803	0,005
ORB I 6a & ORB I 2/3	3,000	2,497	0,013	13,000	1,478	0,139	13,000	1,478	0,139	2,000	2,599	0,009	2,000	2,599	0,009
ORB I 6a & ORB I 5	9,000	1,886	0,059	20,000	0,764	0,445	27,000	0,051	0,959	19,000	0,866	0,386	0,000	2,803	0,005

Supp. Tab. 22: Immunohistochemical evidence for suppressed adult neurogenesis by TMZ

of control mice (CG) and trained mice (MWM). Mean values of collected cells per section ± SEM. Each group comparison (control vs. TMZ) was tested with non-parametric Mann-Whitney-U test; p-value (*p < .05).

		BrdU-NeuN				BrdU-GFAP				BrdU (total)			
		Mean	±	SEM	*p*	Mean	±	SEM	*p*	Mean	±	SEM	*p*
CG	control	301	±	43	.031*	27	±	5	.489	156	±	21	.004*
	TMZ	115	±	39		22	±	4		73	±	15	
MWM	control	511	±	104	.019*	21	±	5	.035*	237	±	45	.004*
	TMZ	140	±	30		27	±	4		74	±	12	

Supp. Tab. 23: Region-specific receptor concentrations of CG versus CG_{TMZ}

Neurotransmitter receptor densities (fmol/mg protein) in different regions of the mouse olfactory system (Mean ± SEM) of control mice (CG) and mice with suppressed adult neurogenesis (CG_{TMZ}). For pairwise comparisons between regions see further Supp. Tab. 23.

		AMPA	Kainate	NMDA	$mGlu_{2/3}$	$GABA_A$
MOB	CG	727 ± 54	1281 ± 95	954 ± 158	2180 ± 121	803 ± 93
	CG_{TMZ}	578 ± 42	1291 ± 56	656 ± 25	2001 ± 119	975 ± 53
AOB	CG	909 ± 88	1328 ± 94	1203 ± 156	3948 ± 376	950 ± 212
	CG_{TMZ}	808 ± 79	1975 ± 143	696 ± 40	3869 ± 244	1026 ± 97
AON	CG	1044 ± 87	1432 ± 69	1445 ± 189	2365 ± 165	566 ± 73
	CG_{TMZ}	944 ± 51	1570 ± 69	1586 ± 99	2543 ± 177	553 ± 66
TTd	CG	1151 ± 58	1356 ± 124	1878 ± 213	2977 ± 212	906 ± 64
	CG_{TMZ}	1076 ± 44	1361 ± 75	1733 ± 99	3040 ± 161	1334 ± 114
TTv	CG	1361 ± 86	1022 ± 114	1716 ± 125	2825 ± 222	788 ± 85
	CG_{TMZ}	1175 ± 74	1376 ± 92	1546 ± 64	3184 ± 214	1078 ± 113
EPd	CG	789 ± 51	1480 ± 75	1239 ± 129	1836 ± 224	695 ± 61
	CG_{TMZ}	733 ± 123	1484 ± 87	1055 ± 80	1881 ± 137	865 ± 67
OT	CG	1079 ± 88	964 ± 70	1638 ± 131	3964 ± 346	853 ± 77
	CG_{TMZ}	1012 ± 81	1224 ± 87	1311 ± 76	3752 ± 288	1120 ± 70
DP	CG	1069 ± 62	1624 ± 95	1909 ± 255	3442 ± 155	1048 ± 78
	CG_{TMZ}	1017 ± 89	1568 ± 106	1831 ± 101	3227 ± 195	1490 ± 124
PIR	CG	1060 ± 41	785 ± 48	1821 ± 162	3328 ± 207	1034 ± 68
	CG_{TMZ}	961 ± 48	796 ± 47	1388 ± 80	3126 ± 220	1198 ± 109
ENTl	CG	1664 ± 59	1054 ± 32	3037 ± 224	3070 ± 198	1297 ± 84
	CG_{TMZ}	1702 ± 98	1068 ± 80	1986 ± 109	2868 ± 239	1217 ± 109
ENTm	CG	1580 ± 102	1040 ± 71	2091 ± 301	3081 ± 268	1190 ± 98
	CG_{TMZ}	1327 ± 65	1011 ± 163	1607 ± 82	2766 ± 310	1308 ± 164
ORBl	CG	1089 ± 83	1095 ± 164	2292 ± 278	3867 ± 360	1553 ± 105
	CG_{TMZ}	1016 ± 88	1024 ± 130	1765 ± 57	3716 ± 225	1661 ± 137
ORBvl	CG	1034 ± 79	995 ± 140	2101 ± 236	4024 ± 511	1520 ± 162
	CG_{TMZ}	1023 ± 67	1078 ± 116	1723 ± 84	4154 ± 419	1728 ± 143

ORBm	CG	1100 ± 75	1039 ± 175	2168 ± 209	3983 ± 524	1393 ± 172
	CG_{TMZ}	1111 ± 75	1224 ± 171	1692 ± 47	4288 ± 445	1823 ± 161
		$GABA_{A(BZ)}$	$GABA_B$	α_1	α_2	$D_{1/5}$
MOB	CG	3867 ± 577	2246 ± 71	547 ± 33	497 ± 32	61 ± 6
	CG_{TMZ}	3591 ± 166	2459 ± 144	556 ± 17	493 ± 30	62 ± 10
AOB	CG	6409 ± 664	3617 ± 288	675 ± 50	547 ± 69	100 ± 15
	CG_{TMZ}	7144 ± 412	3802 ± 384	584 ± 23	533 ± 31	67 ± 12
AON	CG	2038 ± 181	4223 ± 345	338 ± 19	1809 ± 160	171 ± 29
	CG_{TMZ}	2272 ± 164	5315 ± 306	381 ± 15	1924 ± 138	200 ± 26
TTd	CG	3662 ± 331	4736 ± 428	308 ± 36	1589 ± 141	357 ± 49
	CG_{TMZ}	4164 ± 247	5486 ± 359	359 ± 18	1652 ± 122	344 ± 48
TTv	CG	3214 ± 272	4316 ± 442	321 ± 45	1377 ± 177	315 ± 90
	CG_{TMZ}	3280 ± 239	6459 ± 366	336 ± 23	1394 ± 143	320 ± 45
Epd	CG	2791 ± 257	4059 ± 211	238 ± 23	1032 ± 49	888 ± 95
	CG_{TMZ}	3094 ± 210	4630 ± 333	323 ± 17	1171 ± 126	323 ± 76
OT	CG	3048 ± 403	2995 ± 277	204 ± 25	770 ± 107	5340 ± 439
	CG_{TMZ}	3137 ± 217	4721 ± 534	278 ± 34	1231 ± 135	4726 ± 657
DP	CG	4125 ± 340	5048 ± 674	317 ± 52	1031 ± 94	360 ± 44
	CG_{TMZ}	4512 ± 259	5996 ± 483	447 ± 38	1151 ± 127	368 ± 33
PIR	CG	3961 ± 243	4853 ± 158	448 ± 40	1027 ± 80	242 ± 28
	CG_{TMZ}	4102 ± 151	5334 ± 341	515 ± 28	1069 ± 92	234 ± 29
ENTl	CG	3627 ± 221	5894 ± 254	314 ± 19	1771 ± 137	345 ± 26
	CG_{TMZ}	4134 ± 250	7621 ± 384	343 ± 20	1843 ± 125	404 ± 33
ENTm	CG	3553 ± 487	6201 ± 200	304 ± 26	1770 ± 136	330 ± 17
	CG_{TMZ}	4882 ± 407	6880 ± 629	462 ± 39	2058 ± 156	352 ± 39
ORBl	CG	4894 ± 323	5925 ± 392	502 ± 38	650 ± 22	175 ± 43
	CG_{TMZ}	5355 ± 331	6620 ± 420	538 ± 32	570 ± 32	226 ± 31
ORBvl	CG	4762 ± 406	5909 ± 461	495 ± 48	570 ± 24	131 ± 28
	CG_{TMZ}	5373 ± 304	6688 ± 521	526 ± 28	540 ± 29	194 ± 27
ORBm	CG	4269 ± 529	5003 ± 404	513 ± 67	564 ± 22	211 ± 33
	CG_{TMZ}	5270 ± 354	7078 ± 405	530 ± 32	586 ± 32	228 ± 39

Supp. Tab. 24: Statistical analysis of the comparison of region-specific receptor concentrations of CG versus CG_{TMZ}

Significant differences between receptor densities between the olfactory regions of control mice (CG) and mice with suppressed adult neurogenesis (CG_{TMZ}). Each receptor type was tested with non-parametric Mann-Whitney-U test. The percentage difference in absolute receptor concentrations (first column), p-value (middle column), and correlation coefficient r (limits: weak (0.1-0.3), medium (0.3-0.5), and strong (> 0.5) to evaluate the effect size (right column).

CG | CG_{TMZ}	AMPAR			kainateR			NMDAR			$mGlu_{2/3}R$			$GABA_AR$		
	[%]	*p*	[r]	[%]	*p*	[r]	[%]	*p*	[r]	[%]	*p*	[r]	[%]	*p*	[r]
MOB | MOB	-20,53	**0.035**	0.473	0,76	0.529	-	-31,22	0.393	-	-8,21	0.393	-	21,44	0.143	-
AOB | AOB	-11,05	0.218	-	48,68	**0.001**	0.693	-42,17	**0.005**	0.609	-2,00	0.631	-	8,00	0.529	-
AOC | AOC	-9,51	0.436	-	9,65	0.165	-	9,74	0.280	-	7,52	0.353	-	-2,31	0.796	-
TTd | TTd	-6,58	0.353	-	0,36	0.912	-	-7,68	0.481	-	2,13	0.739	-	47,34	**0.005**	0.608
TTv | TTv	-13,65	0.063	-	34,6	**0.011**	0.557	-9,89	0.165	-	12,73	0.28	-	36,75	0.105	-
EPd | EPd	-7,17	0.529	-	0,23	0.912	-	-14,83	0.280	-	2,44	0.165	-	24,41	**0.035**	0.473
OT | OT	-6,18	0.579	-	26,99	**0.019**	0.523	-19,94	**0.009**	0.577	-5,37	0.436	-	31,37	**0.019**	0.523
DP | DP	-4,80	0.393	-	-3,48	0.796	-	-4,09	0.631	-	-6,24	0.436	-	42,23	**0.005**	0.600
PIR | PIR	-9,39	0.123	-	1,36	0.739	-	-23,76	0.123	-	-6,07	0.353	-	15,82	0.247	-
ENTl | ENTl	2,27	0.853	-	1,35	0.912	-	-34,61	**0.000**	0.795	-6,58	0.853	-	-6,17	0.684	-
ENTm | ENTm	-15,98	**0.005**	0.609	-2,75	0.739	-	-23,15	**0.043**	0.457	-10,24	0.529	-	9,88	0.280	-
ORBl | ORBl	-6,71	0.684	-	-6,51	0.436	-	-22,99	**0.004**	0.626	-3,90	0.631	-	6,95	**0.023**	0.507
ORBvl | ORBvl	-1,12	1.00	-	8,38	1.000	-	-17,99	0.089	-	3,23	0.912	-	13,69	0.393	-
ORBm | ORBm	1,03	0.436	-	17,77	0.436	-	-21,95	**0.029**	0.490	7,66	0.247	-	30,88	0.529	-
CG | CG_{TMZ}	$GABA_{A(BZ)}R$			$GABA_BR$			α_1R			α_2R			$D_{1/5}R$		
	[%]	*p*	[r]	[%]	*p*	[r]	[%]	*p*	[r]	[%]	*p*	[r]	[%]	*p*	[r]
MOB | MOB	-7,14	0.796	-	9,45	0.218	-	1,54	0.796	-	-0,72	0.912	-	2,04	0.529	-
AOB | AOB	11,46	0.353	-	5,11	0.579	-	-13,56	**0.029**	0.490	-2,44	0.853	-	-32,72	**0.043**	0.458
AOC | AOC	11,52	0.353	-	25,86	**0.029**	0.490	12,77	0.123	-	6,37	0.912	-	17,37	0.28	-
TTd | TTd	13,73	0.315	-	15,82	0.436	-	16,51	0.247	-	3,99	0.684	-	-3,77	0.971	-
TTv | TTv	2,04	0.796	-	49,66	**0**	0.727	4,74	0.853	-	1,26	0.971	-	1,63	0.247	-
EPd | EPd	10,86	0.315	-	14,09	0.105	-	35,61	**0.001**	0.711	13,45	0.143	-	-63,60	**0**	0.812

OT | OT	2,93	0.631	-	57,67	**0.002**	0.676	35,79	0.143	-	59,81	**0.009**	0.574	-11,50	0.105	-
DP | DP	9,37	0.393	-	18,77	0.481	-	40,94	0.075	-	11,65	0.529	-	2,30	0.529	-
PIR | PIR	3,56	0.529	-	9,90	0.19	-	14,89	0.123	-	4,16	0.971	-	-3,39	0.796	-
ENTl | ENTl	13,98	0.143	-	29,30	**0.002**	0.676	9,19	0.218	-	4,07	0.853	-	17,33	0.123	-
ENTm | ENTm	37,38	**0.019**	0.524	10,95	**0.043**	0.456	52,25	**0.003**	0.642	16,25	0.105	-	6,73	0.481	-
ORBl | ORBl	9,43	0.089	-	11,73	**0.001**	0.712	6,97	0.579	-	-12,25	0.529	-	28,81	0.853	-
ORBvl | ORBvl	12,83	0.28	-	13,19	0.315	-	6,33	0.684	-	-5,38	0.143	-	47,86	**0.029**	0.492
ORBm | ORBm	23,43	0.28	-	41,45	0.123	-	3,27	0.393	-	3,81	0.123	-	7,67	0.143	-

Supp. Tab. 25: Mean receptor densities of olfactory layers (CG versus CG_{TMZ})

Layer-specific absolute receptor densities of the subregions of the olfactory system (mean ± SEM) of control mice (CG) and mice with suppressed adult neurogenesis (CG_{TMZ}). For pairwise comparisons between layers see further Supp. Tab. 26.

		CG | CG_{TMZ}	Receptor (fmol/mg protein)									
			AMPA	kainate	NMDA	$mGlu_{2/3}$	$GABA_A$	$GABA_{A(BZ)}$	$GABA_B$	α_1	α_2	$D_{1/5}$
Main olfactory bulb												
	gr	CG	764 ± 55	911 ± 72	823 ± 111	1697 ± 32	260 ± 42	976 ± 67	2062 ± 119	447 ± 22	1027 ± 31	49 ± 4
		CG_{TMZ}	678 ± 46	916 ± 20	587 ± 41	1553 ± 97	587 ± 41	1027 ± 41	2280 ± 104	426 ± 14	895 ± 56	53 ± 12
	ipl	CG	719 ± 40	1311 ± 114	796 ± 132	1876 ± 64	375 ± 58	1025 ± 96	1920 ± 77	406 ± 23	442 ± 26	57 ± 6
		CG_{TMZ}	523 ± 30	1367 ± 56	522 ± 22	1776 ± 142	522 ± 22	1290 ± 48	2104 ± 87	382 ± 8	438 ± 18	41 ± 7
	mi	CG	678 ± 35	1087 ± 88	886 ± 168	1686 ± 33	303 ± 42	950 ± 73	1971 ± 75	404 ± 20	588 ± 44	49 ± 7
		CG_{TMZ}	547 ± 41	993 ± 46	488 ± 22	1597 ± 130	488 ± 22	1012 ± 47	2048 ± 87	356 ± 13	626 ± 59	39 ± 7
	opl	CG	665 ± 31	1567 ± 136	975 ± 161	2369 ± 159	670 ± 86	2578 ± 255	1930 ± 31	572 ± 28	337 ± 29	68 ± 5
		CG_{TMZ}	589 ± 38	1677 ± 83	755 ± 55	2268 ± 152	755 ± 55	2716 ± 122	1901 ± 42	584 ± 15	376 ± 21	48 ± 3
	gl	CG	622 ± 45	1943 ± 155	1684 ± 211	3064 ± 215	2367 ± 336	9695 ± 533	3391 ± 296	1032 ± 92	351 ± 18	79 ± 9
		CG_{TMZ}	558 ± 36	2165 ± 70	987 ± 66	2899 ± 198	987 ± 66	10296 ± 406	3100 ± 460	1116 ± 37	363 ± 19	77 ± 5
	onl	CG	694 ± 97	1025 ± 101	672 ± 101	1986 ± 171	831 ± 96	4308 ± 227	2173 ± 254	381 ± 22	304 ± 29	73 ± 7
		CG_{TMZ}	455 ± 57	887 ± 81	554 ± 62	1797 ± 84	554 ± 62	3980 ± 314	3013 ± 534	383 ± 20	274 ± 14	66 ± 6
Accessory olfactory bulb												
	gr	CG	942 ± 84	1189 ± 88	1183 ± 183	3320 ± 257	744 ± 214	6982 ± 579	2955 ± 340	621 ± 68	607 ± 95	106 ± 19
		CG_{TMZ}	792 ± 99	1177 ± 57	642 ± 27	2975 ± 139	642 ± 27	6258 ± 178	3200 ± 323	527 ± 17	692 ± 96	61 ± 9
	mi	CG	946 ± 98	1930 ± 45	1553 ± 25	4907 ± 617	1693 ± 312	7090 ± 868	2880 ± 100	1016 ± 67	469 ± 98	107 ± 21
		CG_{TMZ}	885 ± 68	2514 ± 118	819 ± 63	5185 ± 422	819 ± 63	9636 ± 714	2908 ± 296	834 ± 29	429 ± 30	72 ± 19
	gl	CG	661 ± 283	785 ± 17	1226 ± 167	1298 ± 175	462 ± 150	2910 ± 528	5087 ± 810	400 ± 81	531 ± 127	67 ± 10
		CG_{TMZ}	895 ± 63	2481 ± 178	604 ± 81	1263 ± 179	604 ± 81	3726 ± 490	4159 ± 1095	395 ± 96	474 ± 14	71 ± 25
Anterior olfactory cortex												
	pe	CG	940 ± 124	1298 ± 29	1124 ± 98	3081 ± 321	825 ± 147	2597 ± 250	3551 ± 505	449 ± 37	1340 ± 219	161 ± 37
		CG_{TMZ}	643 ± 65	1096 ± 104	1381 ± 130	3405 ± 322	1381 ± 130	2639 ± 237	4653 ± 286	485 ± 31	1157 ± 121	141 ± 22

m	CG	1226 ± 81	1327 ± 141	1416 ± 50	2266 ± 208	545 ± 100	2073 ± 224	4608 ± 423	315 ± 10	2169 ± 176	189 ± 34
	CG_{TMZ}	1135 ± 76	1651 ± 108	1615 ± 110	2371 ± 144	1615 ± 110	2517 ± 302	5661 ± 256	348 ± 19	2211 ± 147	228 ± 46
d	CG	1040 ± 112	1454 ± 137	1668 ± 114	2420 ± 194	397 ± 99	1414 ± 146	4389 ± 374	318 ± 24	2296 ± 165	234 ± 69
	CG_{TMZ}	1001 ± 73	1622 ± 118	1800 ± 151	1937 ± 117	1800 ± 151	1929 ± 271	5118 ± 305	440 ± 37	2366 ± 172	182 ± 57
pv	CG	1078 ± 111	1783 ± 138	996 ± 62	1846 ± 115	565 ± 21	1972 ± 294	3629 ± 328	308 ± 22	1925 ± 221	137 ± 36
	CG_{TMZ}	992 ± 67	1978 ± 87	1810 ± 90	2281 ± 248	1810 ± 90	2394 ± 270	5413 ± 291	308 ± 20	2121 ± 182	191 ± 38
l	CG	1177 ± 120	1433 ± 85	2469 ± 259	3001 ± 484	311 ± 66	2134 ± 186	4602 ± 570	327 ± 20	1925 ± 214	107 ± 4
	CG_{TMZ}	1096 ± 31	1538 ± 56	1726 ± 57	2511 ± 217	1726 ± 57	1859 ± 44	6015 ± 343	370 ± 30	2328 ± 177	115 ± 8
e	CG	910 ± 48	1246 ± 227	799 ± 23	3054 ± 653	991 ± 351	1923 ± 467	3197 ± 584	366 ± 75	1271 ± 240	42 ± 26
	CG_{TMZ}	571 ± 58	1401 ± 245	596 ± 110	2259 ± 406	596 ± 110	1433 ± 297	1920 ± 268	306 ± 22	1003 ± 146	424 ± 251
taenia tecta, dorsal											
I	CG	1161 ± 94	994 ± 162	2319 ± 250	3559 ± 357	1003 ± 119	3316 ± 425	4995 ± 333	300 ± 62	1362 ± 186	216 ± 44
	CG_{TMZ}	1010 ± 82	1112 ± 124	1940 ± 89	3977 ± 269	1940 ± 89	4117 ± 284	6259 ± 498	329 ± 21	1446 ± 121	240 ± 32
II	CG	1404 ± 120	1120 ± 98	2210 ± 158	3019 ± 209	888 ± 79	3731 ± 350	4999 ± 570	283 ± 38	1798 ± 135	267 ± 46
	CG_{TMZ}	1298 ± 97	1323 ± 72	1938 ± 144	3096 ± 243	1938 ± 144	4273 ± 276	6372 ± 487	397 ± 36	1861 ± 153	257 ± 25
III	CG	1100 ± 65	1293 ± 97	2140 ± 219	2554 ± 154	914 ± 83	3967 ± 358	4922 ± 591	302 ± 25	1649 ± 181	372 ± 58
	CG_{TMZ}	1070 ± 68	1515 ± 109	1592 ± 148	2637 ± 149	1592 ± 148	4027 ± 257	4570 ± 308	343 ± 17	1842 ± 146	352 ± 54
IV	CG	924 ± 64	1843 ± 185	1506 ± 148	2491 ± 199	730 ± 36	3633 ± 310	3377 ± 318	341 ± 43	2000 ± 180	594 ± 92
	CG_{TMZ}	869 ± 65	1629 ± 93	1464 ± 130	2204 ± 43	1464 ± 130	4265 ± 340	4569 ± 303	358 ± 28	1461 ± 129	520 ± 102
taenia tecta, ventral											
I	CG	1014 ± 91	699 ± 104	1665 ± 179	2767 ± 327	796 ± 142	2949 ± 375	796 ± 281	288 ± 51	1028 ± 165	201 ± 55
	CG_{TMZ}	911 ± 72	895 ± 86	1344 ± 80	4467 ± 244	1344 ± 80	2651 ± 315	6194 ± 485	336 ± 39	804 ± 86	207 ± 38
II	CG	1477 ± 105	1067 ± 142	1814 ± 164	2948 ± 282	876 ± 118	3315 ± 334	876 ± 512	318 ± 60	1463 ± 220	251 ± 72
	CG_{TMZ}	1309 ± 95	1459 ± 97	1622 ± 112	3015 ± 212	1622 ± 112	3628 ± 191	6484 ± 440	347 ± 29	1458 ± 158	297 ± 30
III	CG	1442 ± 93	1299 ± 163	1721 ± 116	2667 ± 174	693 ± 44	3222 ± 257	693 ± 399	338 ± 40	1638 ± 225	492 ± 151
	CG_{TMZ}	1317 ± 158	1613 ± 113	1761 ± 72	2542 ± 108	1761 ± 72	3102 ± 268	6700 ± 317	299 ± 15	1770 ± 142	456 ± 80
Dorsal peduncular cortex											
I	CG	1092 ± 36	1154 ± 46	2067 ± 173	4126 ± 334	952 ± 93	4188 ± 588	5035 ± 648	265 ± 54	1121 ± 137	253 ± 39
	CG_{TMZ}	938 ± 86	1149 ± 99	1834 ± 91	4355 ± 297	1834 ± 91	4032 ± 367	6697 ± 801	377 ± 42	1196 ± 151	254 ± 24
II/III	CG	1358 ± 108	1587 ± 135	2677 ± 280	3665 ± 215	1085 ± 90	4273 ± 406	5683 ± 837	343 ± 69	951 ± 65	330 ± 55
	CG_{TMZ}	1282 ± 132	1534 ± 127	2051 ± 130	3306 ± 270	2051 ± 130	4774 ± 246	6946 ± 484	448 ± 42	1278 ± 161	334 ± 32

	V	CG	992 ± 54	1611 ± 119	2245 ± 210	3126 ± 183	1154 ± 82	4364 ± 293	5251 ± 801	374 ± 74	1032 ± 85	348 ± 40
		CG_{TMZ}	984 ± 33	1561 ± 123	1789 ± 164	2706 ± 154	1789 ± 164	4865 ± 313	5520 ± 352	480 ± 48	1056 ± 103	397 ± 53
	VI	CG	909 ± 90	1860 ± 129	1631 ± 233	2860 ± 122	963 ± 91	3715 ± 328	4224 ± 506	260 ± 34	950 ± 101	509 ± 61
		CG_{TMZ}	663 ± 105	2172 ± 194	1651 ± 122	2379 ± 206	1651 ± 122	4377 ± 271	4257 ± 309	483 ± 56	872 ± 76	444 ± 62
Piriform cortex												
	I	CG	780 ± 32	580 ± 66	2103 ± 165	4400 ± 283	1169 ± 77	4193 ± 205	4727 ± 141	497 ± 42	832 ± 52	149 ± 18
		CG_{TMZ}	716 ± 28	541 ± 41	1352 ± 76	4238 ± 298	1352 ± 76	4359 ± 220	5448 ± 451	575 ± 29	827 ± 87	140 ± 24
	II	CG	1607 ± 53	764 ± 49	1877 ± 190	3380 ± 214	1153 ± 42	3993 ± 259	5382 ± 210	467 ± 52	1116 ± 101	208 ± 21
		CG_{TMZ}	1597 ± 16	828 ± 43	1510 ± 86	3122 ± 261	1510 ± 86	4128 ± 117	5813 ± 403	553 ± 27	1219 ± 115	209 ± 19
	III	CG	877 ± 38	977 ± 48	1627 ± 151	2613 ± 154	888 ± 66	3603 ± 143	4518 ± 115	381 ± 37	1159 ± 99	368 ± 51
		CG_{TMZ}	836 ± 31	1018 ± 63	1303 ± 96	2355 ± 191	1303 ± 96	3776 ± 167	4740 ± 213	406 ± 13	1162 ± 92	352 ± 47
Entorhinal cortex, lateral												
	I	CG	1066 ± 120	407 ± 61	2302 ± 316	3264 ± 325	1150 ± 88	3197 ± 448	5416 ± 419	271 ± 16	943 ± 84	230 ± 33
		CG_{TMZ}	833 ± 69	420 ± 18	1590 ± 113	3497 ± 231	1590 ± 113	3663 ± 342	7298 ± 257	288 ± 31	955 ± 46	321 ± 34
	II	CG	2009 ± 116	722 ± 48	3401 ± 274	3431 ± 194	1623 ± 66	3868 ± 348	6602 ± 331	292 ± 22	1592 ± 156	344 ± 43
		CG_{TMZ}	1724 ± 108	743 ± 47	2182 ± 127	3732 ± 285	2182 ± 127	4989 ± 274	9171 ± 413	347 ± 13	1502 ± 126	450 ± 39
	III	CG	2106 ± 80	823 ± 42	3628 ± 281	3380 ± 154	1595 ± 95	3637 ± 250	6719 ± 374	279 ± 18	1815 ± 175	356 ± 36
		CG_{TMZ}	2077 ± 180	838 ± 75	2283 ± 121	3163 ± 314	2283 ± 121	4608 ± 347	8659 ± 580	301 ± 8	1833 ± 148	485 ± 27
	IV	CG	1966 ± 101	945 ± 12	3417 ± 215	3242 ± 269	1539 ± 100	3423 ± 151	6514 ± 323	267 ± 23	2012 ± 168	312 ± 24
		CG_{TMZ}	2057 ± 145	1051 ± 87	2246 ± 139	2801 ± 255	2246 ± 139	4172 ± 257	8201 ± 454	299 ± 19	2057 ± 165	367 ± 28
	V	CG	1746 ± 101	1206 ± 74	3330 ± 192	3064 ± 261	1282 ± 95	3371 ± 136	6106 ± 337	293 ± 27	2061 ± 168	311 ± 33
		CG_{TMZ}	1991 ± 139	1204 ± 98	2102 ± 115	2753 ± 225	2102 ± 115	3887 ± 243	7713 ± 370	330 ± 19	2128 ± 160	343 ± 28
	VIa	CG	1520 ± 88	1710 ± 112	2781 ± 179	2612 ± 131	1199 ± 82	3928 ± 148	5705 ± 222	381 ± 21	2020 ± 135	406 ± 45
		CG_{TMZ}	1787 ± 104	1809 ± 203	1953 ± 104	2618 ± 225	1953 ± 104	4149 ± 285	7308 ± 379	403 ± 20	2273 ± 157	423 ± 50
	VIb	CG	1187 ± 62	1616 ± 100	2123 ± 187	1964 ± 70	995 ± 85	3572 ± 207	4258 ± 155	430 ± 34	1952 ± 127	453 ± 67
		CG_{TMZ}	1400 ± 94	1626 ± 162	1545 ± 85	1939 ± 152	1545 ± 85	3544 ± 236	5483 ± 299	479 ± 14	2115 ± 144	468 ± 57
Entorhinal cortex, medial												
	I	CG	1452 ± 82	648 ± 70	1679 ± 253	3201 ± 373	1116 ± 58	3679 ± 602	5815 ± 301	271 ± 39	941 ± 107	212 ± 30
		CG_{TMZ}	734 ± 31	546 ± 94	1207 ± 98	3902 ± 94	1207 ± 98	4343 ± 428	6908 ± 485	382 ± 45	1235 ± 134	277 ± 46
	II	CG	1538 ± 188	869 ± 58	2698 ± 163	3512 ± 432	1504 ± 53	3833 ± 691	7038 ± 286	302 ± 38	1659 ± 186	333 ± 40
		CG_{TMZ}	1083 ± 86	800 ± 129	1730 ± 90	3679 ± 326	1730 ± 90	5301 ± 564	8155 ± 542	443 ± 46	1723 ± 191	345 ± 46

III	CG	1542 ± 194	1065 ± 61	2602 ± 137	3274 ± 349	1599 ± 72	3602 ± 464	6677 ± 272	286 ± 26	1938 ± 152	385 ± 36
	CG_{TMZ}	1481 ± 101	1124 ± 70	1857 ± 98	2841 ± 379	1857 ± 98	6209 ± 355	8025 ± 514	468 ± 49	1891 ± 170	375 ± 47
IV	CG	1564 ± 93	1207 ± 111	1681 ± 300	3117 ± 292	1458 ± 42	3495 ± 486	6478 ± 210	259 ± 28	2109 ± 207	349 ± 30
	CG_{TMZ}	1569 ± 125	1180 ± 127	1862 ± 133	2574 ± 329	1862 ± 133	6160 ± 319	7842 ± 642	499 ± 54	2576 ± 141	363 ± 32
V	CG	1497 ± 106	1276 ± 96	2383 ± 304	3000 ± 263	1246 ± 88	3544 ± 611	5921 ± 280	323 ± 32	2127 ± 146	345 ± 23
	CG_{TMZ}	1808 ± 125	1484 ± 186	1744 ± 93	2484 ± 291	1744 ± 93	4559 ± 453	6693 ± 703	525 ± 55	2855 ± 160	333 ± 29
VI	CG	1501 ± 134	1309 ± 107	1360 ± 155	2375 ± 213	905 ± 86	3168 ± 394	5276 ± 471	377 ± 31	1651 ± 89	375 ± 10
	CG_{TMZ}	1288 ± 111	1593 ± 188	1344 ± 83	2049 ± 190	1344 ± 83	3875 ± 338	5678 ± 477	446 ± 43	2354 ± 210	403 ± 62
Orbitofrontal cortex, medial											
I	CG	1253 ± 75	595 ± 114	2741 ± 237	4846 ± 598	1371 ± 201	4362 ± 282	5681 ± 365	445 ± 57	700 ± 54	127 ± 23
	CG_{TMZ}	1224 ± 63	780 ± 70	1700 ± 60	5666 ± 538	1575 ± 148	4572 ± 359	7686 ± 394	481 ± 32	654 ± 56	91 ± 12
II	CG	1132 ± 87	945 ± 220	2365 ± 270	4004 ± 532	1537 ± 231	4519 ± 659	5465 ± 669	536 ± 91	660 ± 26	166 ± 30
	CG_{TMZ}	1243 ± 121	865 ± 103	1804 ± 51	4886 ± 433	2126 ± 153	5588 ± 252	7979 ± 587	578 ± 45	639 ± 33	194 ± 41
II/III	CG	1076 ± 44	1063 ± 177	2041 ± 249	4060 ± 755	1362 ± 231	4362 ± 714	5046 ± 429	575 ± 84	573 ± 34	216 ± 52
	CG_{TMZ}	1046 ± 58	1300 ± 220	1720 ± 79	3926 ± 445	2027 ± 192	5587 ± 480	7063 ± 480	586 ± 37	595 ± 40	260 ± 51
V	CG	995 ± 109	1300 ± 66	1661 ± 160	3387 ± 605	1330 ± 193	4088 ± 679	4725 ± 359	521 ± 62	454 ± 21	272 ± 46
	CG_{TMZ}	1043 ± 85	1465 ± 235	1678 ± 83	3303 ± 320	1840 ± 206	5614 ± 549	6365 ± 473	487 ± 31	533 ± 33	280 ± 40
VI	CG	948 ± 103	1518 ± 43	2070 ± 207	3475 ± 597	1364 ± 137	4140 ± 649	4359 ± 327	491 ± 61	435 ± 20	276 ± 44
	CG_{TMZ}	999 ± 95	1617 ± 262	1574 ± 70	2922 ± 226	1672 ± 188	5250 ± 589	6295 ± 502	500 ± 53	504 ± 32	245 ± 25
Orbitofrontal cortex, ventrolateral											
I	CG	1174 ± 72	769 ± 114	2459 ± 317	4515 ± 528	1578 ± 136	4676 ± 317	6181 ± 481	505 ± 52	767 ± 54	77 ± 23
	CG_{TMZ}	1137 ± 112	757 ± 28	1892 ± 46	4288 ± 414	1892 ± 46	5273 ± 331	6877 ± 632	549 ± 38	693 ± 58	154 ± 24
II/III	CG	991 ± 77	885 ± 78	2266 ± 248	4088 ± 532	1559 ± 233	5096 ± 481	6482 ± 530	475 ± 58	580 ± 24	108 ± 34
	CG_{TMZ}	1015 ± 42	789 ± 59	1853 ± 78	4557 ± 426	1853 ± 78	5052 ± 220	7041 ± 638	523 ± 25	554 ± 22	147 ± 38
V	CG	1013 ± 104	1253 ± 115	2200 ± 254	3963 ± 541	1494 ± 178	5192 ± 539	5653 ± 437	499 ± 52	535 ± 40	127 ± 29
	CG_{TMZ}	967 ± 76	1152 ± 167	1660 ± 115	3955 ± 390	1660 ± 115	5834 ± 345	6804 ± 550	520 ± 38	475 ± 26	205 ± 34
VI	CG	959 ± 108	1470 ± 81	2013 ± 194	3531 ± 496	1449 ± 162	4083 ± 619	5320 ± 475	500 ± 42	409 ± 19	212 ± 35
	CG_{TMZ}	941 ± 68	1395 ± 173	1552 ± 102	3188 ± 307	1552 ± 102	5199 ± 502	6032 ± 453	512 ± 42	433 ± 17	270 ± 18
Orbitofrontal cortex, lateral											
I	CG	1248 ± 100	702 ± 102	2482 ± 281	5193 ± 110	1566 ± 98	4732 ± 324	6500 ± 276	384 ± 29	802 ± 35	119 ± 46
	CG_{TMZ}	1077 ± 102	695 ± 34	1797 ± 42	4781 ± 312	1797 ± 42	4802 ± 364	6584 ± 420	461 ± 27	731 ± 18	148 ± 32

	II/III	CG	1035 ± 81	973 ± 173	2610 ± 323	4458 ± 88	1667 ± 69	5491 ± 443	6190 ± 220	505 ± 50	685 ± 23	164 ± 56
		CG_{TMZ}	1018 ± 108	708 ± 51	1808 ± 87	3899 ± 284	1808 ± 87	5876 ± 456	7363 ± 535	542 ± 47	608 ± 52	182 ± 25
	V	CG	1092 ± 83	1468 ± 131	2242 ± 253	4083 ± 288	1473 ± 120	4947 ± 434	5829 ± 459	544 ± 34	562 ± 43	169 ± 45
		CG_{TMZ}	1013 ± 100	1123 ± 179	1774 ± 70	3339 ± 272	1774 ± 70	5949 ± 484	6262 ± 459	593 ± 52	541 ± 37	260 ± 40
	VI	CG	982 ± 96	1609 ± 126	2240 ± 243	2983 ± 300	1449 ± 164	4405 ± 348	5744 ± 561	537 ± 44	534 ± 31	248 ± 34
		CG_{TMZ}	915 ± 88	1329 ± 157	1682 ± 83	2845 ± 241	1682 ± 83	5007 ± 441	6031 ± 491	575 ± 31	444 ± 20	287 ± 27
Olfactory tubercle													
	I	CG	757 ± 44	711 ± 62	1445 ± 166	4837 ± 283	773 ± 87	2656 ± 449	2131 ± 286	185 ± 28	589 ± 100	4529 ± 404
		CG_{TMZ}	681 ± 47	890 ± 74	938 ± 62	4681 ± 274	938 ± 62	2382 ± 183	3595 ± 449	241 ± 44	850 ± 95	4979 ± 564
	II	CG	1381 ± 98	1100 ± 101	1768 ± 116	4090 ± 409	973 ± 91	3195 ± 408	3344 ± 316	201 ± 25	813 ± 113	6451 ± 563
		CG_{TMZ}	1176 ± 94	1287 ± 84	1361 ± 97	3884 ± 323	1361 ± 97	3533 ± 249	5163 ± 579	284 ± 34	1246 ± 138	5997 ± 879
	III	CG	1092 ± 80	1147 ± 80	1700 ± 129	3487 ± 248	812 ± 67	3293 ± 399	3508 ± 286	227 ± 23	909 ± 116	5041 ± 503
		CG_{TMZ}	1072 ± 70	1481 ± 115	1450 ± 81	2914 ± 201	1450 ± 81	3342 ± 196	4853 ± 546	271 ± 13	1436 ± 172	4190 ± 566

Supp. Tab. 26: Statistical analysis of the comparison of layer-specific receptor concentrations of CG versus CG_{TMZ}

Significant differences between receptor densities between the olfactory layers of control mice (CG) and mice with suppressed adult neurogenesis (CG_{TMZ}). Each receptor type was tested with non-parametric Mann-Whitney-U test. The percentage difference in absolute receptor concentrations (first column), sum of the ranks (W, middle column), p-value (right column).

CG | CG_{TMZ}	AMPA			Kainate			NMDA			$mGlu_{2/3}$			$GABA_A$		
	%	*W*	*p-value*	%	*W*	*p-value*	%	*W*	*p-value*	%	*W*	*p-value*	%	*W*	*p-value*
MOB gr	-11,23	86,000	0,165	0,53	104,000	0,971	-28,62	92,000	0,353	-8,50	94,000	0,436	125,86	97,000	0,579
MOB ipl	-27,33	61,000	0,000	4,27	98,000	0,631	-34,46	92,000	0,353	-5,29	84,500	0,123	39,15	97,000	0,579
MOB mi	-19,35	73,000	0,015	-8,67	95,000	0,481	-44,98	87,000	0,19	-5,29	85,000	0,143	60,69	99,000	0,684
MOB opl	-11,42	84,000	0,123	7,00	91,000	0,315	-22,65	92,000	0,353	-4,26	100,000	0,739	12,54	104,000	0,971
MOB gl	-10,29	90,000	0,28	11,43	76,000	0,029	-41,38	67,000	0,003	-5,41	95,000	0,481	-58,31	83,000	0,105
MOB onl	-34,48	74,000	0,019	-13,43	92,000	0,353	-17,61	91,000	0,315	-9,48	87,000	0,19	-33,33	103,000	0,912
AOB gr	-15,91	90,000	0,28	-1,06	99,000	0,684	-45,72	67,000	0,003	-10,39	88,000	0,218	-13,72	79,500	0,052
AOB mi	-6,45	88,000	0,218	30,29	57,000	0,000	-47,28	55,000	0,000	5,66	94,000	0,436	-51,64	86,000	0,165
AOB gl	35,49	98,000	0,631	216,13	55,000	0,000	-50,74	57,000	0,001	-2,73	7,000	1,000	30,79	89,000	0,247
AON pe	-31,64	73,000	0,015	-15,58	75,500	0,023	22,86	71,000	0,133	10,51	95,000	0,481	67,48	89,000	0,247
AON m	-7,38	99,000	0,684	24,43	76,000	0,029	14,06	82,000	0,089	4,64	95,000	0,481	196,40	96,000	0,529
AON d	-3,77	103,000	0,912	11,54	91,000	0,315	7,91	92,000	0,353	-19,95	64,000	0,001	352,98	95,000	0,481
AON pv	-7,98	95,000	0,481	10,94	93,000	0,393	81,75	55,000	0,000	23,57	82,000	0,089	220,32	100,500	0,739
AON l	-6,95	89,000	0,247	7,32	85,000	0,143	-30,10	71,000	0,147	-16,33	57,500	0,755	454,86	92,000	0,353
TTd I	-12,95	85,000	0,143	11,93	95,000	0,481	-16,32	84,000	0,123	11,75	96,000	0,529	93,40	83,000	0,105
TTd II	-7,52	97,000	0,579	18,05	80,000	0,063	-12,33	89,000	0,247	2,55	102,000	0,853	118,33	69,000	0,005
TTd III	-2,70	101,000	0,796	17,18	83,000	0,105	-25,63	77,000	0,035	3,25	97,000	0,579	74,21	74,000	0,019
TTd IV	-5,95	95,000	0,481	-11,58	95,000	0,481	-2,80	104,000	0,971	-11,53	93,000	0,393	100,51	67,000	0,003

TTv I	-10,19	84,000	0,123	27,99	85,000	0,143	-19,29	74,000	0,019	61,44	57,000	0,000	68,72	79,000	0,052
TTv II	-11,36	82,000	0,089	36,82	76,000	0,029	-10,59	88,000	0,218	2,26	103,000	0,912	85,23	86,000	0,165
TTv III	-8,68	90,000	0,28	24,15	81,000	0,075	2,35	94,000	0,436	-4,66	103,000	0,912	154,12	70,000	0,007
OT I	-10,11	86,000	0,165	25,23	85,000	0,143	-35,11	63,000	0,001	-3,23	92,000	0,353	21,29	65,000	0,002
OT II	-14,82	85,000	0,143	17,01	85,000	0,143	-23,02	68,000	0,004	-5,05	98,000	0,631	39,93	84,000	0,123
OT III	-1,78	100,000	0,739	29,13	72,000	0,011	-14,73	74,000	0,019	-16,44	84,000	0,123	78,53	81,000	0,075
DP I	-14,09	85,000	0,143	-0,43	103,000	0,912	-11,29	89,000	0,247	5,56	101,000	0,796	92,54	73,000	0,015
DP II/III	-5,63	99,000	0,684	-3,37	99,000	0,684	-23,40	73,000	0,015	-9,79	93,500	0,393	88,97	72,000	0,011
DP V	-0,84	100,000	0,739	-3,09	93,000	0,393	-20,31	79,000	0,052	-13,44	78,500	0,043	55,03	76,000	0,029
DP VI	-27,07	82,000	0,089	16,77	82,000	0,089	1,20	101,000	0,796	-16,83	81,000	0,075	71,37	57,000	0,000
PIR I	-8,13	86,000	0,165	-6,66	100,000	0,739	-35,73	65,000	0,002	-3,69	88,000	0,218	15,61	94,000	0,436
PIR II	-0,63	95,000	0,481	8,31	86,000	0,165	-19,54	87,000	0,19	-7,64	91,000	0,315	31,02	92,000	0,353
PIR III	-4,69	91,000	0,315	4,22	98,000	0,631	-19,90	83,000	0,105	-9,86	91,000	0,315	46,73	89,000	0,247
ENT I I	-21,86	85,000	0,143	3,17	100,000	0,739	-30,94	80,000	0,063	7,15	103,000	0,912	38,19	96,000	0,529
ENT I II	-14,17	81,000	0,075	2,88	103,000	0,912	-35,83	59,000	0,000	8,76	94,000	0,436	34,43	91,000	0,315
ENT I III	-1,37	102,000	0,853	1,71	103,000	0,912	-37,07	58,000	0,000	-6,42	102,000	0,853	43,14	95,500	0,481
ENT I IV	4,64	94,000	0,436	11,21	87,000	0,19	-34,26	58,000	0,000	-13,60	93,000	0,393	45,96	84,000	0,123
ENT I V	14,02	83,000	0,105	-0,15	104,000	0,971	-36,87	58,000	0,000	-10,16	97,000	0,579	64,01	99,000	0,684
ENT I VIa	17,55	78,000	0,043	5,74	103,000	0,912	-29,77	62,000	0,000	0,20	104,000	0,971	62,92	104,000	0,971
ENT I VIb	17,91	80,000	0,063	0,62	101,000	0,796	-27,24	71,000	0,009	-1,30	100,000	0,739	55,34	97,000	0,579
ENT m I	-49,46	55,000	0	-15,65	83,000	0,105	-28,11	77,000	0,035	21,88	82,000	0,089	8,21	95,000	0,481
ENT m II	-29,62	67,000	0,003	-8,00	87,000	0,19	-35,90	57,000	0,000	4,74	101,000	0,796	15,03	101,000	0,796
ENT m III	-3,99	98,000	0,631	5,50	98,000	0,631	-28,62	58,000	0,000	-13,22	95,000	0,481	16,14	87,000	0,19
ENT m IV	0,30	91,000	0,315	-2,24	97,000	0,579	10,76	89,000	0,247	-17,42	89,000	0,247	27,66	86,000	0,165
ENT m V	20,77	76,000	0,029	16,29	90,000	0,28	-26,80	74,000	0,019	-17,21	86,000	0,165	40,01	104,000	0,971
ENT m VI	-14,19	95,000	0,481	21,73	84,000	0,123	-1,14	100,000	0,739	-13,73	90,000	0,28	48,53	93,000	0,393

ORB m I	-2,33	97,000	0,579	31,03	96,000	0,529	-37,98	65,000	0,002	16,92	98,000	0,631	14,86	85,000	0,143
ORB m II	9,81	101,500	0,796	-8,54	89,000	0,247	-23,75	76,000	0,029	22,01	81,000	0,075	38,30	71,000	0,009
ORB m II/III	-2,75	103,000	0,912	22,31	98,000	0,631	-15,74	75,000	0,023	-3,28	101,000	0,796	48,85	73,000	0,015
ORB m V	4,80	98,000	0,631	12,64	96,000	0,529	1,03	96,000	0,529	-2,49	98,000	0,631	38,38	79,000	0,052
ORB m VIa	5,39	101,000	0,796	6,52	96,000	0,529	-23,93	69,000	0,005	-15,93	101,000	0,796	22,58	91,000	0,315
ORB vl I	-3,18	96,000	0,529	-1,59	94,000	0,436	-23,03	85,000	0,143	-5,05	102,000	0,853	19,92	103,000	0,912
ORB vl II/III	2,44	100,000	0,739	-10,86	86,000	0,165	-18,23	81,000	0,075	11,47	90,000	0,28	18,83	88,500	0,218
ORB vl V	-4,53	101,000	0,796	-8,02	101,000	0,796	-24,54	79,000	0,052	-0,19	103,000	0,912	11,09	94,000	0,436
ORB vl VIa	-1,88	101,000	0,796	-5,11	95,000	0,481	-22,92	73,000	0,015	-9,71	97,000	0,579	7,11	88,000	0,218
ORB l I	-13,67	88,000	0,218	-0,99	99,000	0,684	-27,58	76,000	0,029	-7,93	73,000	0,015	14,75	94,000	0,436
ORB l II/III	-1,65	100,000	0,739	-27,31	76,000	0,029	-30,74	76,000	0,029	-12,55	73,000	0,015	8,42	104,000	0,971
ORB l V	-7,19	96,000	0,529	-23,48	89,000	0,247	-20,85	81,000	0,075	-18,22	75,000	0,023	20,47	98,000	0,631
ORB l VIa	-6,79	97,000	0,579	-17,43	87,000	0,19	-24,93	75,000	0,023	-4,66	95,000	0,481	16,07	98,000	0,631
CG | CG_{TMZ}	$GABA_{A(BZ)}$			$GABA_B$			α_1			α_2			$D_{1/5}$		
	%	*W*	*p-value*	%	*W*	*p-value*	%	*W*	*p-value*	%	*W*	*p-value*	%	*W*	*p-value*
MOB gr	5,18	98,000	0,631	10,60	87,000	0,19	-4,68	92,500	0,353	-12,81	79,000	0,052	7,36	97,500	0,579
MOB ipl	25,83	65,000	0,002	9,58	80,000	0,063	-5,87	86,500	0,165	-1,00	98,500	0,631	-28,19	73,000	0,015
MOB mi	6,49	92,000	0,353	3,96	90,000	0,28	-11,83	77,000	0,035	6,48	96,000	0,529	-20,22	81,500	0,075
MOB opl	5,33	103,000	0,912	-1,49	92,000	0,353	2,18	100,000	0,739	11,54	89,000	0,247	-28,76	64,000	0,001
MOB gl	6,20	92,000	0,353	-8,57	92,000	0,353	8,09	100,000	0,739	3,58	103,000	0,912	-2,59	101,000	0,796
MOB onl	-7,63	87,000	0,19	38,67	89,000	0,247	0,56	103,500	0,912	-9,68	93,000	0,393	-9,27	94,500	0,436
AOB gr	-10,36	85,000	0,143	8,32	94,000	0,436	-15,16	93,000	0,393	13,91	90,500	0,28	-42,45	67,000	0,003
AOB mi	35,92	78,000	0,043	0,99	96,000	0,529	-17,94	73,000	0,015	-8,49	90,000	0,28	-33,17	78,000	0,043
AOB gl	28,03	73,000	0,015	-18,24	88,000	0,218	-1,12	96,000	0,529	-10,82	83,000	0,105	7,21	100,500	0,739
AON pe	1,61	101,000	0,796	31,03	74,000	0,019	7,98	101,000	0,796	-13,67	102,000	0,853	-12,73	94,500	0,436
AON m	21,41	88,000	0,218	22,85	78,000	0,043	10,50	92,000	0,353	1,92	104,000	0,971	20,89	92,000	0,353

AON d	36,40	82,000	0,089	16,62	82,000	0,089	38,47	74,000	0,019	3,06	100,000	0,739	-22,08	91,000	0,315
AON pv	21,36	91,500	0,315	49,16	59,000	0	0,14	104,500	0,971	10,21	100,000	0,739	39,56	88,000	0,218
AON l	-12,91	75,000	0,023	30,70	73,000	0,015	13,12	90,000	0,28	20,95	86,000	0,165	7,47	75,000	0,023
TTd I	24,15	87,000	0,19	25,29	81,000	0,075	9,78	99,000	0,684	6,13	97,000	0,579	11,00	92,000	0,353
TTd II	14,51	96,000	0,529	27,46	81,000	0,075	40,10	75,500	0,023	3,47	96,000	0,529	-3,76	100,000	0,739
TTd III	1,52	103,000	0,912	-7,14	97,000	0,579	13,68	84,000	0,123	11,71	94,000	0,436	-5,31	103,000	0,912
TTd IV	17,40	87,000	0,19	35,30	69,000	0,005	4,85	105,000	1	-26,95	73,000	0,015	-12,45	96,000	0,529
TTv I	-10,12	92,000	0,353	677,78	55,000	0	16,55	90,000	0,28	-21,82	92,000	0,353	2,93	96,000	0,529
TTv II	9,42	91,000	0,315	640,52	70,000	0,007	8,96	97,000	0,579	-0,37	101,000	0,796	18,14	81,000	0,075
TTv III	-3,72	100,000	0,739	866,92	61,000	0	-11,49	96,000	0,529	8,04	97,000	0,579	-7,35	96,000	0,529
OT I	-10,32	98,000	0,631	68,71	74,000	0,019	30,36	98,500	0,631	44,34	81,000	0,075	9,95	100,000	0,739
OT II	10,57	95,000	0,481	54,39	70,000	0,007	40,87	83,000	0,105	53,24	79,000	0,052	-7,03	95,000	0,481
OT III	1,49	99,000	0,684	38,33	83,000	0,105	19,55	77,000	0,035	58,04	75,000	0,023	-16,89	84,000	0,123
DP I	-3,72	101,000	0,796	33,00	80,000	0,063	41,99	83,000	0,105	6,65	101,000	0,796	0,42	97,000	0,579
DP II/III	11,73	94,000	0,436	22,23	88,000	0,218	30,61	87,000	0,19	34,30	78,000	0,043	1,09	93,000	0,393
DP V	11,50	89,000	0,247	5,13	104,000	0,971	28,41	92,000	0,353	2,37	101,000	0,796	13,94	94,000	0,436
DP VI	17,82	81,000	0,075	0,78	103,000	0,912	85,80	62,000	0	-8,19	101,000	0,796	-12,89	97,500	0,579
PIR I	3,95	95,000	0,481	15,25	88,000	0,218	15,74	84,000	0,123	-0,59	99,000	0,684	-6,35	93,000	0,393
PIR II	3,38	96,000	0,529	8,01	89,000	0,247	18,24	81,000	0,075	9,25	98,500	0,631	0,65	104,000	0,971
PIR III	4,79	92,000	0,353	4,91	87,000	0,19	6,55	91,000	0,315	0,24	103,500	0,912	-4,48	101,000	0,796
ENT I I	14,59	97,000	0,579	34,75	65,000	0,002	6,28	97,000	0,579	1,30	97,000	0,579	39,89	81,000	0,075
ENT I II	28,98	76,000	0,029	38,92	59,000	0	18,67	79,000	0,052	-5,61	97,500	0,579	30,88	81,000	0,075
ENT I III	26,67	77,000	0,035	28,87	73,000	0,015	8,05	93,000	0,393	0,99	102,000	0,853	36,28	68,500	0,004
ENT I IV	21,86	77,000	0,035	25,90	71,000	0,009	11,82	90,000	0,28	2,22	103,000	0,912	17,71	86,000	0,165
ENT I V	15,31	86,000	0,165	26,32	68,000	0,004	12,82	92,000	0,353	3,25	101,000	0,796	10,22	94,000	0,436

ENT l VIa	5,63	96,000	0,529	28,09	63,000	0,001	5,97	90,500	0,28	12,52	88,000	0,218	4,20	102,000	0,853
ENT l VIb	-0,80	102,000	0,853	28,79	61,000	0	11,60	95,500	0,481	8,36	94,000	0,436	3,49	99,000	0,684
ENT m I	18,06	85,000	0,143	18,80	74,000	0,019	41,09	78,000	0,043	31,24	85,000	0,143	31,08	93,000	0,393
ENT m II	38,32	81,000	0,075	15,87	77,000	0,035	46,65	74,000	0,019	3,85	101,000	0,796	3,62	101,000	0,796
ENT m III	72,38	60,000	0	20,19	70,000	0,007	64,03	69,000	0,005	-2,47	104,000	0,971	-2,73	101,000	0,796
ENT m IV	76,28	57,000	0	21,06	68,000	0,004	92,98	65,000	0,002	22,14	78,000	0,043	4,20	99,000	0,684
ENT m V	28,62	83,000	0,105	13,04	91,000	0,315	62,59	69,000	0,005	34,22	64,500	0,001	-3,46	103,000	0,912
ENT m VI	22,32	85,000	0,143	7,62	93,000	0,393	18,56	82,000	0,089	42,54	65,000	0,002	7,26	104,000	0,971
ORB m I	4,83	100,000	0,739	35,30	66,000	0,002	7,94	96,500	0,529	-6,57	90,000	0,28	-28,59	79,500	0,052
ORB m II	23,66	77,000	0,035	46,01	73,000	0,015	7,83	97,000	0,579	-3,10	105,000	1	16,70	100,000	0,739
ORB m II/III	28,08	86,000	0,165	39,96	72,000	0,011	1,91	98,000	0,631	3,89	92,000	0,353	20,25	96,000	0,529
ORB m V	37,32	77,000	0,035	34,70	75,000	0,023	-6,48	98,000	0,631	17,37	80,000	0,063	3,11	100,500	0,739
ORB m VIa	26,81	88,000	0,218	44,42	69,000	0,005	1,88	102,500	0,853	15,90	92,000	0,353	-11,31	91,000	0,315
ORB vl I	12,77	83,000	0,105	11,26	100,000	0,739	8,70	93,000	0,393	-9,68	88,000	0,218	98,90	66,000	0,002
ORB vl II/III	-0,87	97,000	0,579	8,63	97,000	0,579	10,13	94,000	0,436	-4,48	89,000	0,247	35,41	92,000	0,353
ORB vl V	12,35	91,000	0,315	20,36	81,000	0,075	4,33	102,000	0,853	-11,26	83,000	0,105	62,17	75,500	0,023
ORB vl VIa	27,33	87,000	0,19	13,38	91,000	0,315	2,33	105,000	1	5,78	91,000	0,315	27,07	78,000	0,043
ORB l I	1,46	100,000	0,739	1,29	103,000	0,912	20,20	75,000	0,023	-8,90	78,000	0,043	23,74	90,000	0,28
ORB l II/III	7,01	89,000	0,247	18,94	78,000	0,043	7,27	99,000	0,684	-11,25	88,000	0,218	10,92	86,000	0,165
ORB l V	20,24	82,000	0,089	7,42	90,000	0,28	8,91	100,000	0,739	-3,72	104,000	0,971	54,35	77,000	0,035
ORB l VIa	13,65	87,000	0,19	4,99	104,000	0,971	7,14	96,000	0,529	-16,77	66,000	0,002	15,46	83,000	0,105

Supp. Tab. 27: Region-specific receptor concentrations of CG versus MWM_{CG}

Neurotransmitter receptor densities (fmol/mg protein) in different regions of the mouse olfactory system (Mean ± SEM) of control mice (CG) and trained mice with intact adult neurogenesis (MWM_{CG}). For pairwise comparisons between regions see further Supp. Tab. 28.

CG | MWM_{CG}		AMPA			Kainate			NMDA			$mGlu_{2/3}$			$GABA_A$		
MOB	CG	727	±	54	1281	±	95	954	±	158	2180	±	121	803	±	93
	MWM_{CG}	642	±	42	1357	±	77	425	±	18	3258	±	146	1642	±	110
AOB	CG	909	±	88	1328	±	94	1203	±	156	3948	±	376	950	±	212
	MWM_{CG}	1017	±	53	1534	±	100	631	±	90	6108	±	301	2225	±	289
AON	CG	1044	±	87	1432	±	69	1445	±	189	2365	±	165	566	±	73
	MWM_{CG}	1356	±	56	1255	±	41	1174	±	70	5592	±	426	503	±	28
TTd	CG	1151	±	58	1356	±	124	1878	±	213	2977	±	212	906	±	64
	MWM_{CG}	1262	±	74	1355	±	94	1268	±	131	6068	±	663	1582	±	145
TTv	CG	1361	±	86	1022	±	114	1716	±	125	2825	±	222	788	±	85
	MWM_{CG}	1186	±	49	1182	±	51	1013	±	117	5411	±	490	1337	±	93
Epd	CG	789	±	51	1480	±	75	1239	±	129	1836	±	224	695	±	61
	MWM_{CG}	749	±	61	1282	±	34	808	±	101	4928	±	552	636	±	48
OT	CG	1079	±	88	964	±	70	1638	±	131	3964	±	346	853	±	77
	MWM_{CG}	669	±	51	833	±	39	492	±	53	7490	±	273	1434	±	198
DP	CG	1069	±	62	1624	±	95	1909	±	255	3442	±	155	1048	±	78
	MWM_{CG}	1064	±	59	1437	±	69	1242	±	150	7905	±	471	2376	±	164
PIR	CG	1060	±	41	785	±	48	1821	±	162	3328	±	207	1034	±	68
	MWM_{CG}	989	±	48	772	±	44	1027	±	67	7802	±	237	1531	±	105
ENTl	CG	1664	±	59	1054	±	32	3037	±	224	3070	±	198	1297	±	84
	MWM_{CG}	1168	±	67	1271	±	80	1680	±	93	6726	±	245	1601	±	99
ENTm	CG	1580	±	102	1040	±	71	2091	±	301	3081	±	268	1190	±	98
	MWM_{CG}	1065	±	77	1066	±	74	1495	±	165	6663	±	423	1574	±	69
ORBl	CG	1089	±	83	1095	±	164	2292	±	278	3867	±	360	1553	±	105
	MWM_{CG}	1165	±	80	965	±	70	1214	±	76	9498	±	755	2605	±	170
ORBvl	CG	1034	±	79	995	±	140	2101	±	236	4024	±	511	1520	±	162
	MWM_{CG}	1052	±	89	909	±	46	1124	±	79	9713	±	708	2840	±	205
ORBm	CG	1100	±	75	1039	±	175	2168	±	209	3983	±	524	1393	±	172

	MWM_{CG}	995	±	105	1119	±	89	1290	±	61	9503	±	793	2415	±	159
		$GABA_{A(BZ)}$			$GABA_B$			α_1			α_2			$D_{1/5}$		
MOB	CG	3867	±	577	2246	±	71	547	±	33	497	±	32	61	±	6
	MWM_{CG}	4887	±	258	2538	±	83	475	±	24	265	±	26	89	±	3
AOB	CG	6409	±	664	3617	±	288	675	±	50	547	±	69	100	±	15
	MWM_{CG}	6875	±	718	3898	±	210	656	±	50	359	±	36	108	±	8
AON	CG	2038	±	181	4223	±	345	338	±	19	1809	±	160	171	±	29
	MWM_{CG}	3403	±	143	5665	±	147	309	±	32	1630	±	82	142	±	10
TTd	CG	3662	±	331	4736	±	428	308	±	36	1589	±	141	357	±	49
	MWM_{CG}	5803	±	288	7499	±	95	270	±	13	1694	±	33	212	±	19
TTv	CG	3214	±	272	4316	±	442	321	±	45	1377	±	177	315	±	90
	MWM_{CG}	5286	±	131	7372	±	153	238	±	15	1037	±	116	192	±	23
Epd	CG	2791	±	257	4059	±	211	238	±	23	1032	±	49	888	±	95
	MWM_{CG}	4431	±	347	4009	±	159	299	±	15	972	±	61	257	±	38
OT	CG	3048	±	403	2995	±	277	204	±	25	770	±	107	5340	±	439
	MWM_{CG}	4493	±	308	5000	±	415	210	±	15	586	±	54	6389	±	155
DP	CG	4125	±	340	5048	±	674	317	±	52	1031	±	94	360	±	44
	MWM_{CG}	7175	±	299	6193	±	304	324	±	15	1194	±	91	254	±	20
PIR	CG	3961	±	243	4853	±	158	448	±	40	1027	±	80	242	±	28
	MWM_{CG}	6358	±	185	5410	±	159	418	±	26	732	±	42	137	±	11
ENTl	CG	3627	±	221	5894	±	254	314	±	19	1771	±	137	345	±	26
	MWM_{CG}	6789	±	95	8572	±	438	406	±	23	1571	±	78	505	±	33
ENTm	CG	3553	±	487	6201	±	200	304	±	26	1770	±	136	330	±	17
	MWM_{CG}	6687	±	163	9548	±	526	391	±	26	1768	±	98	522	±	90
ORBl	CG	4894	±	323	5925	±	392	502	±	38	650	±	22	175	±	43
	MWM_{CG}	9173	±	219	6946	±	438	448	±	21	396	±	20	172	±	10
ORBvl	CG	4762	±	406	5909	±	461	495	±	48	570	±	24	131	±	28
	MWM_{CG}	9129	±	183	7806	±	427	513	±	33	386	±	25	164	±	9
ORBm	CG	4269	±	529	5003	±	404	513	±	67	564	±	22	211	±	33
	MWM_{CG}	8304	±	256	8368	±	406	550	±	29	400	±	21	228	±	29

Supp. Tab. 28: Statistical analysis of the comparison of region-specific receptor concentrations of CG versus MWM_{CG}

Significant differences between receptor densities between the olfactory regions of control mice (CG) and trained mice with intact adult neurogenesis (MWM_{CG}). Each receptor type was tested with non-parametric Mann-Whitney-U test. The percentage difference in absolute receptor concentrations (first column), p-value (middle column), and correlation coefficient r (limits: weak (0.1-0.3), medium (0.3-0.5), and strong (> 0.5) to evaluate the effect size (right column).

CG | MWM_{CG}	AMPAR			kainateR			NMDAR			$mGlu_{2/3}R$			$GABA_AR$		
	[%]	*p*	[r]	[%]	*p*	[r]	[%]	*p*	[r]	[%]	*p*	[r]	[%]	*p*	[r]
MOB | MOB	-11,75	0.315	-	5,93	0.529	-	-55,42	**0.005**	0.642	49,47	**< .001**	0.828	104,55	**< .001**	0.811
AOB | AOB	11,89	0.186	-	15,48	**0.031**	0.490	-47,53	**0.004**	0.660	54,74	**< .001**	0.777	134,15	**0.005**	0.642
AOC | AOC	29,91	**0.010**	0,583	-12,36	**0.041**	0.465	-18,79	0.307	-	136,48	**< .001**	0.845	-11,23	0.112	-
TTd | TTd	9,57	0.218	-	-0,13	0.912	-	-32,45	**0.023**	0.507	103,86	**< .001**	0.709	74,71	**< .001**	0.760
TTv | TTv	-12,87	**0.045**	0,456	15,66	0.307	-	-40,99	**< .001**	0.777	91,56	**< .001**	0.709	69,59	**0.002**	0.684
EPd | EPd	-5,11	0.384	-	-13,35	0.063	-	-34,75	**0.011**	0.557	168,42	**< .001**	0.828	-8,49	0.344	-
OT | OT	-37,97	**0.004**	0,659	-13,55	0.052	-	-69,98	**< .001**	0.848	88,94	**< .001**	0.845	68,22	**0.035**	0.473
DP | DP	-0,43	0.912	-	-11,52	0.105	-	-34,97	**0.035**	0.473	129,64	**< .001**	0.845	126,72	**< .001**	0.845
PIR | PIR	-6,77	0.218	-	-1,65	0.684	-	-43,58	**0.001**	0.727	134,43	**< .001**	0.845	47,98	**0.002**	0.659
ENTl | ENTl	-29,79	**0.000**	0,811	20,56	**0.017**	0.541	-44,69	**< .001**	0.812	119,13	**< .001**	0.845	23,49	**0.035**	0.473
ENTm | ENTm	-32,59	**0.000**	0,744	2,53	0.971	-	-28,52	**0.031**	0.490	116,24	**< .001**	0.811	32,22	**0.004**	0.659
ORBl | ORBl	6,90	0.307	-	-11,92	1.000	-	-47,05	**< .001**	0.795	145,65	**< .001**	0.848	67,73	**< .001**	0.794
ORBvl | ORBvl	1,71	0.910	-	-8,56	0.226	-	-46,48	**< .001**	0.812	141,36	**< .001**	0.851	86,85	**< .001**	0.811
ORBm | ORBm	-9,56	0.880	-	7,67	0.161	-	-40,51	**< .001**	0.744	138,57	**< .001**	0.856	73,40	**< .001**	0.829
CG | MWM_{CG}	$GABA_{A(BZ)}R$			$GABA_BR$			α_1R			α_2R			$D_{1/5}R$		
	[%]	*p*	[r]	[%]	*p*	[r]	[%]	*p*	[r]	[%]	*p*	[r]	[%]	*p*	[r]
MOB | MOB	26,37	**0.029**	0.490	18,37	**0.009**	0.676	-13,16	0.140	-	-46,68	**< .001**	0.744	46,80	**< .001**	0,761
AOB | AOB	7,26	0.579	-	7,77	0.343	-	-2,88	0.791	-	-34,39	0.064	-	8,07	0.762	-
AOC | AOC	67,02	**< .001**	0.811	34,14	**< .001**	0.760	-8,61	0.257	-	-9,90	0.105	-	-16,89	0.186	-
TTd | TTd	58,46	**< .001**	0.726	58,33	**< .001**	0.845	-12,22	0.405	-	6,62	0.623	-	-40,71	**0.023**	0,507
TTv | TTv	64,47	**< .001**	0.845	70,80	**< .001**	0.845	-25,88	0.315	-	-24,69	0.143	-	-38,91	0.393	-
EPd | EPd	58,76	**< .001**	0.760	-1,23	0.842	-	25,36	**0.038**	0.473	-5,78	0.912	-	-71,10	**< .001**	0,845

OT | OT	47,41	**0.019**	0.523	66,98	**< .001**	0.693	2,66	0.850	-	-23,85	0.054	-	19,65	**0.037**	0,473
DP | DP	73,92	**< .001**	0.828	22,68	0.107	-	2,20	0.910	-	15,90	0.247	-	-29,46	**0.021**	0,524
PIR | PIR	60,53	**< .001**	0.828	11,47	**0.018**	0.540	-6,75	0.684	-	-28,66	**0.005**	0.608	-43,46	**< .001**	0,769
ENTl | ENTl	87,17	**< .001**	0.845	45,43	**< .001**	0.760	29,02	**0.014**	0.558	-11,27	0.105	-	46,67	**0.003**	0,667
ENTm | ENTm	88,18	**< .001**	0.828	53,99	**< .001**	0.845	28,68	**0.043**	0.456	-0,15	0.684	-	58,30	**0.017**	0,541
ORBl | ORBl	87,44	**< .001**	0.846	17,23	**< .001**	0.848	-10,80	0.307	-	-39,10	**< .001**	0.847	-1,57	0.761	-
ORBvl | ORBvl	91,71	**< .001**	0.846	32,10	**0.002**	0.660	3,62	0.791	-	-32,39	**< .001**	0.795	25,23	0.074	-
ORBm | ORBm	94,49	**< .001**	0.846	67,24	0.062	-	7,13	0.162	-	-29,04	**< .001**	0.846	7,68	0.676	-

Supp. Tab. 29: Mean receptor densities of olfactory layers (CG versus MWM_{CG})

Layer-specific absolute receptor densities of the subregions of the olfactory system (mean ± SEM) for control mice (CG) versus trained mice (MWM_{CG}). For pairwise comparisons between regions see further Supp. Tab. 30.

CG | MWM_{CG}			Receptor (fmol/mg protein)									
			AMPA	kainate	NMDA	$mGlu_{2/3}$	$GABA_A$	$GABA_{A(BZ)}$	$GABA_B$	α_1	α_2	$D_{1/5}$
Main olfactory bulb												
	gr	CG	764 ± 55	911 ± 72	823 ± 111	1697 ± 32	260 ± 42	976 ± 67	2062 ± 119	447 ± 22	1027 ± 31	49 ± 4
		MWM_{CG}	711 ± 40	1118 ± 101	366 ± 19	2725 ± 144	351 ± 31	1525 ± 49	1873 ± 43	424 ± 28	562 ± 74	81 ± 5
	ipl	CG	719 ± 40	1311 ± 114	796 ± 132	1876 ± 64	375 ± 58	1025 ± 96	1920 ± 77	406 ± 23	442 ± 26	57 ± 6
		MWM_{CG}	729 ± 58	1596 ± 82	381 ± 18	3735 ± 185	478 ± 38	2563 ± 64	1544 ± 76	432 ± 31	191 ± 18	85 ± 4
	mi	CG	678 ± 35	1087 ± 88	886 ± 168	1686 ± 33	303 ± 42	950 ± 73	1971 ± 75	404 ± 20	588 ± 44	49 ± 7
		MWM_{CG}	699 ± 61	1527 ± 79	364 ± 18	3303 ± 167	564 ± 44	2190 ± 60	1711 ± 80	422 ± 29	251 ± 38	85 ± 3
	opl	CG	665 ± 31	1567 ± 136	975 ± 161	2369 ± 159	670 ± 86	2578 ± 255	1930 ± 31	572 ± 28	337 ± 29	68 ± 5
		MWM_{CG}	697 ± 48	1643 ± 100	479 ± 30	4133 ± 266	981 ± 75	3872 ± 185	1256 ± 51	471 ± 31	212 ± 26	97 ± 3
	gl	CG	622 ± 45	1943 ± 155	1684 ± 211	3064 ± 215	2367 ± 336	9695 ± 533	3391 ± 296	1032 ± 92	351 ± 18	79 ± 9
		MWM_{CG}	642 ± 55	1674 ± 158	604 ± 33	3811 ± 164	6246 ± 505	14511 ± 201	6603 ± 145	940 ± 42	189 ± 14	100 ± 5
	onl	CG	694 ± 97	1025 ± 101	672 ± 101	1986 ± 171	831 ± 96	4308 ± 227	2173 ± 254	381 ± 22	304 ± 29	73 ± 7
		MWM_{CG}	374 ± 44	587 ± 31	268 ± 22	1855 ± 155	1320 ± 109	4862 ± 241	1999 ± 189	207 ± 8	158 ± 15	85 ± 4
Accessory olfactory bulb												
	gr	CG	942 ± 84	1189 ± 88	1183 ± 183	3320 ± 257	744 ± 214	6982 ± 579	2955 ± 340	621 ± 68	607 ± 95	106 ± 19
		MWM_{CG}	821 ± 59	969 ± 48	529 ± 53	4930 ± 228	1471 ± 462	1293 ± 272	2798 ± 122	548 ± 26	512 ± 94	82 ± 6
	mi	CG	946 ± 98	1930 ± 45	1553 ± 25	4907 ± 617	1693 ± 312	7090 ± 868	2880 ± 100	1016 ± 67	469 ± 98	107 ± 21
		MWM_{CG}	1196 ± 82	2051 ± 177	650 ± 96	9180 ± 355	2078 ± 298	12455 ± 778	3033 ± 128	921 ± 79	259 ± 36	121 ± 13
	gl	CG	661 ± 283	785 ± 17	1226 ± 167	1298 ± 175	462 ± 150	2910 ± 528	5087 ± 810	400 ± 81	531 ± 127	67 ± 10
		MWM_{CG}	1033 ± 73	1582 ± 226	568 ± 33	4215 ± 414	2949 ± 716	6672 ± 388	6037 ± 147	499 ± 80	283 ± 30	118 ± 9
Anterior olfactory cortex												
	pe	CG	940 ± 124	1298 ± 29	1124 ± 98	3081 ± 321	825 ± 147	2597 ± 250	3551 ± 505	449 ± 37	1340 ± 219	161 ± 37

	m	MWM_{CG}	1050	±	66	1026	±	37	1019	±	90	5878	±	465	639	±	40	4215	±	189	5957	±	279	338	±	36	969	±	75	146	±	13
		CG	1226	±	81	1327	±	141	1416	±	50	2266	±	208	545	±	100	2073	±	224	4608	±	423	315	±	10	2169	±	176	189	±	34
	d	MWM_{CG}	1400	±	109	1280	±	77	1251	±	133	4763	±	664	483	±	45	3500	±	193	5875	±	274	325	±	37	1984	±	111	161	±	17
		CG	1040	±	112	1454	±	137	1668	±	114	2420	±	194	397	±	99	1414	±	146	4389	±	374	318	±	24	2296	±	165	234	±	69
	pv	MWM_{CG}	1516	±	101	1606	±	125	1324	±	84	6361	±	535	497	±	33	3121	±	195	5624	±	251	244	±	23	1803	±	116	143	±	14
		CG	1078	±	111	1783	±	138	996	±	62	1846	±	115	565	±	21	1972	±	294	3629	±	328	308	±	22	1925	±	221	137	±	36
	l	MWM_{CG}	1406	±	54	1477	±	73	1212	±	124	4960	±	409	402	±	53	3605	±	370	5447	±	269	239	±	18	1813	±	80	136	±	14
		CG	1177	±	120	1433	±	85	2469	±	259	3001	±	484	311	±	66	2134	±	186	4602	±	570	327	±	20	1925	±	214	107	±	4
	e	MWM_{CG}	1476	±	37	1281	±	64	1230	±	97	6834	±	572	496	±	32	3057	±	138	6097	±	141	320	±	48	1926	±	102	125	±	9
		CG	910	±	48	1246	±	227	799	±	23	3054	±	653	991	±	351	1923	±	467	3197	±	584	366	±	75	1271	±	240	42	±	26
		MWM_{CG}	1215	±	79	809	±	78	1007	±	148	4822	±	685	491	±	83	2758	±	221	5259	±	262	309	±	30	1527	±	244	141	±	28
taenia tecta, dorsal																															
	I	CG	1161	±	94	994	±	162	2319	±	250	3559	±	357	1003	±	119	3316	±	425	4995	±	333	300	±	62	1362	±	186	216	±	44
		MWM_{CG}	1161	±	80	900	±	72	1264	±	170	7133	±	834	1690	±	153	5342	±	87	8146	±	131	262	±	19	1270	±	50	184	±	19
	II	CG	1404	±	120	1120	±	98	2210	±	158	3019	±	209	888	±	79	3731	±	350	4999	±	570	283	±	38	1798	±	135	267	±	46
		MWM_{CG}	1458	±	78	1263	±	95	1532	±	61	6537	±	693	1702	±	156	6488	±	198	7508	±	114	276	±	18	1730	±	84	190	±	19
	III	CG	1100	±	65	1293	±	97	2140	±	219	2554	±	154	914	±	83	3967	±	358	4922	±	591	302	±	25	1649	±	181	372	±	58
		MWM_{CG}	1254	±	89	1519	±	150	1288	±	119	5665	±	690	1479	±	151	6364	±	317	7846	±	131	284	±	18	1875	±	62	210	±	27
	IV	CG	924	±	64	1843	±	185	1506	±	148	2491	±	199	730	±	36	3633	±	310	3377	±	318	341	±	43	2000	±	180	594	±	92
		MWM_{CG}	1173	±	124	1737	±	134	1178	±	136	4938	±	661	1458	±	176	5658	±	352	6497	±	190	259	±	11	1901	±	85	264	±	27
taenia tecta, ventral																															
	I	CG	1014	±	91	699	±	104	1665	±	179	2767	±	327	796	±	142	2949	±	375	796	±	281	288	±	51	1028	±	165	201	±	55
		MWM_{CG}	1013	±	67	559	±	65	721	±	128	5706	±	538	1354	±	129	4287	±	226	6683	±	183	215	±	8	724	±	91	150	±	23
	II	CG	1477	±	105	1067	±	142	1814	±	164	2948	±	282	876	±	118	3315	±	334	876	±	512	318	±	60	1463	±	220	251	±	72
		MWM_{CG}	1331	±	89	1151	±	60	1125	±	113	6009	±	553	1492	±	88	5851	±	163	7668	±	307	248	±	22	1151	±	101	189	±	28
	III	CG	1442	±	93	1299	±	163	1721	±	116	2667	±	174	693	±	44	3222	±	257	693	±	399	338	±	40	1638	±	225	492	±	151
		MWM_{CG}	1214	±	33	1836	±	61	1397	±	55	4824	±	432	1164	±	68	5721	±	197	7764	±	207	246	±	18	1439	±	79	238	±	26
Dorsal peduncular cortex																															
	I	CG	1092	±	36	1154	±	46	2067	±	173	4126	±	334	952	±	93	4188	±	588	5035	±	648	265	±	54	1121	±	137	253	±	39

	II/III	MWM_{CG}	1085	±	72	997	±	75	1153	±	189	8934	±	491	2292	±	298	5949	±	524	8057	±	411	313	±	25	1140	±	79	210	±	15
		CG	1358	±	108	1587	±	135	2677	±	280	3665	±	215	1085	±	90	4273	±	406	5683	±	837	343	±	69	951	±	65	330	±	55
	V	MWM_{CG}	1210	±	93	1571	±	131	1378	±	171	8101	±	645	2484	±	150	7469	±	339	7232	±	442	339	±	21	1230	±	118	262	±	26
		CG	992	±	54	1611	±	119	2245	±	210	3126	±	183	1154	±	82	4364	±	293	5251	±	801	374	±	74	1032	±	85	348	±	40
		MWM_{CG}	1073	±	76	1621	±	135	1183	±	122	7330	±	536	2420	±	163	7861	±	315	5360	±	493	319	±	22	1332	±	89	274	±	33
	VI	CG	909	±	90	1860	±	129	1631	±	233	2860	±	122	963	±	91	3715	±	328	4224	±	506	260	±	34	950	±	101	509	±	61
		MWM_{CG}	888	±	56	1560	±	168	1252	±	163	7513	±	512	2307	±	178	7357	±	313	4996	±	232	316	±	22	1296	±	98	271	±	20
Piriform cortex																														
	I	CG	780	±	32	580	±	66	2103	±	165	4400	±	283	1169	±	77	4193	±	205	4727	±	141	497	±	42	832	±	52	149	±	18
		MWM_{CG}	768	±	82	537	±	55	940	±	55	8867	±	512	1712	±	127	6757	±	124	5577	±	88	419	±	30	533	±	53	119	±	10
	II	CG	1607	±	53	764	±	49	1877	±	190	3380	±	214	1153	±	42	3993	±	259	5382	±	210	467	±	52	1116	±	101	208	±	21
		MWM_{CG}	1154	±	32	804	±	53	1142	±	82	7459	±	385	1633	±	117	6792	±	65	5852	±	210	433	±	33	846	±	43	135	±	11
	III	CG	877	±	38	977	±	48	1627	±	151	2613	±	154	888	±	66	3603	±	143	4518	±	115	381	±	37	1159	±	99	368	±	51
		MWM_{CG}	1044	±	73	976	±	54	999	±	80	7131	±	247	1246	±	79	5914	±	168	4731	±	219	403	±	26	883	±	22	156	±	15
Entorhinal cortex, lateral																														
	I	CG	1066	±	120	407	±	61	2302	±	316	3264	±	325	1150	±	88	3197	±	448	5416	±	419	271	±	16	943	±	84	230	±	33
		MWM_{CG}	604	±	65	260	±	45	1309	±	80	8535	±	236	1414	±	149	4982	±	250	8916	±	414	433	±	38	998	±	75	391	±	42
	II	CG	2009	±	116	722	±	48	3401	±	274	3431	±	194	1623	±	66	3868	±	348	6602	±	331	292	±	22	1592	±	156	344	±	43
		MWM_{CG}	1154	±	98	545	±	35	1738	±	157	7978	±	289	1888	±	135	6952	±	205	8773	±	502	455	±	33	1584	±	68	505	±	47
	III	CG	2106	±	80	823	±	42	3628	±	281	3380	±	154	1595	±	95	3637	±	250	6719	±	374	279	±	18	1815	±	175	356	±	36
		MWM_{CG}	1360	±	95	737	±	51	1921	±	143	7101	±	212	2024	±	136	7190	±	147	10159	±	613	329	±	28	1652	±	60	468	±	39
	IV	CG	1966	±	101	945	±	12	3417	±	215	3242	±	269	1539	±	100	3423	±	151	6514	±	323	267	±	23	2012	±	168	312	±	24
		MWM_{CG}	1329	±	95	1021	±	94	1950	±	115	6810	±	400	1836	±	130	7111	±	142	9551	±	572	326	±	18	1821	±	101	447	±	36
	V	CG	1746	±	101	1206	±	74	3330	±	192	3064	±	261	1282	±	95	3371	±	136	6106	±	337	293	±	27	2061	±	168	311	±	33
		MWM_{CG}	1354	±	69	1407	±	126	1770	±	106	6290	±	290	1512	±	102	7256	±	147	9200	±	600	341	±	20	1753	±	115	440	±	22
	VIa	CG	1520	±	88	1710	±	112	2781	±	179	2612	±	131	1199	±	82	3928	±	148	5705	±	222	381	±	21	2020	±	135	406	±	45
		MWM_{CG}	1269	±	88	2300	±	236	1516	±	58	5977	±	393	1361	±	89	7666	±	159	8052	±	396	439	±	13	1730	±	118	641	±	80
	VIb	CG	1187	±	62	1616	±	100	2123	±	187	1964	±	70	995	±	85	3572	±	207	4258	±	155	430	±	34	1952	±	127	453	±	67
		MWM_{CG}	1109	±	113	2625	±	159	1442	±	69	4394	±	395	1173	±	87	6256	±	298	5517	±	220	509	±	32	1457	±	73	645	±	61

Entorhinal cortex, medial																								
	I	CG	1452	±	82	648	±	70	1679	±	253	3201	±	373	1116	±	58	3679	±	602	5815	±	301	271	±	39	941	±	107	212	±	30
		MWM_{CG}	576	±	78	293	±	33	1193	±	174	6915	±	751	1329	±	139	5613	±	221	7819	±	646	293	±	20	1071	±	85	388	±	74
	II	CG	1538	±	188	869	±	58	2698	±	163	3512	±	432	1504	±	53	3833	±	691	7038	±	286	302	±	38	1659	±	186	333	±	40
		MWM_{CG}	819	±	138	737	±	41	1590	±	265	7595	±	395	1691	±	92	7013	±	146	11511	±	404	384	±	35	1952	±	162	578	±	112
	III	CG	1542	±	194	1065	±	61	2602	±	137	3274	±	349	1599	±	72	3602	±	464	6677	±	272	286	±	26	1938	±	152	385	±	36
		MWM_{CG}	1103	±	116	902	±	76	1784	±	205	7172	±	397	1778	±	78	7292	±	227	10520	±	483	409	±	27	1693	±	117	593	±	125
	IV	CG	1564	±	93	1207	±	111	1681	±	300	3117	±	292	1458	±	42	3495	±	486	6478	±	210	259	±	28	2109	±	207	349	±	30
		MWM_{CG}	1293	±	50	1273	±	140	1698	±	150	6708	±	474	1754	±	96	7046	±	229	9765	±	560	381	±	30	2014	±	141	579	±	106
	V	CG	1497	±	106	1276	±	96	2383	±	304	3000	±	263	1246	±	88	3544	±	611	5921	±	280	323	±	32	2127	±	146	345	±	23
		MWM_{CG}	1385	±	80	1728	±	151	1512	±	192	6369	±	392	1671	±	58	6676	±	215	9119	±	548	419	±	33	1886	±	167	507	±	84
	VI	CG	1501	±	134	1309	±	107	1360	±	155	2375	±	213	905	±	86	3168	±	394	5276	±	471	377	±	31	1651	±	89	375	±	10
		MWM_{CG}	1214	±	91	1465	±	172	1225	±	157	5219	±	485	1218	±	74	6650	±	339	6626	±	208	459	±	32	1933	±	89	485	±	74
Orbitofrontal cortex, medial																								
	I	CG	1253	±	75	595	±	114	2741	±	237	4846	±	598	1371	±	201	4362	±	282	5681	±	365	445	±	57	700	±	54	127	±	23
		MWM_{CG}	1109	±	115	827	±	70	1251	±	121	11006	±	960	2448	±	126	6365	±	195	10866	±	610	506	±	35	532	±	27	189	±	23
	II	CG	1132	±	87	945	±	220	2365	±	270	4004	±	532	1537	±	231	4519	±	659	5465	±	669	536	±	91	660	±	26	166	±	30
		MWM_{CG}	1332	±	191	1005	±	68	1532	±	52	10459	±	904	2650	±	160	8216	±	372	10009	±	587	605	±	31	451	±	34	195	±	23
	II/III	CG	1076	±	44	1063	±	177	2041	±	249	4060	±	755	1362	±	231	4362	±	714	5046	±	429	575	±	84	573	±	34	216	±	52
		MWM_{CG}	1323	±	137	1213	±	143	1339	±	72	9293	±	865	2622	±	200	8718	±	353	8164	±	479	613	±	32	378	±	23	235	±	30
	V	CG	995	±	109	1300	±	66	1661	±	160	3387	±	605	1330	±	193	4088	±	679	4725	±	359	521	±	62	454	±	21	272	±	46
		MWM_{CG}	1092	±	76	1175	±	119	1144	±	125	8938	±	833	2451	±	225	8945	±	334	6551	±	325	555	±	39	354	±	9	254	±	46
	VI	CG	948	±	103	1518	±	43	2070	±	207	3475	±	597	1364	±	137	4140	±	649	4359	±	327	491	±	61	435	±	20	276	±	44
		MWM_{CG}	966	±	61	1374	±	121	1160	±	60	7819	±	746	1904	±	158	9273	±	442	6249	±	415	452	±	31	310	±	16	264	±	40
Orbitofrontal cortex, ventrolateral																								
	I	CG	1174	±	72	769	±	114	2459	±	317	4515	±	528	1578	±	136	4676	±	317	6181	±	481	505	±	52	767	±	54	77	±	23
		MWM_{CG}	1022	±	129	755	±	44	1095	±	111	10354	±	725	3047	±	184	8272	±	317	9802	±	567	513	±	45	551	±	40	169	±	15
	II/III	CG	991	±	77	885	±	78	2266	±	248	4088	±	532	1559	±	233	5096	±	481	6482	±	530	475	±	58	580	±	24	108	±	34
		MWM_{CG}	1182	±	133	814	±	38	1279	±	45	10528	±	831	3090	±	200	8581	±	218	8711	±	509	542	±	46	346	±	24	141	±	11

	V	CG	1013	±	104	1253	±	115	2200	±	254	3963	±	541	1494	±	178	5192	±	539	5653	±	437	499	±	52	535	±	40	127	±	29
		MWM_{CG}	1053	±	69	819	±	52	1108	±	106	9797	±	764	2886	±	338	9822	±	341	6977	±	539	558	±	39	291	±	16	151	±	15
	VI	CG	959	±	108	1470	±	81	2013	±	194	3531	±	496	1449	±	162	4083	±	619	5320	±	475	500	±	42	409	±	19	212	±	35
		MWM_{CG}	951	±	67	1249	±	126	1094	±	94	8172	±	677	2338	±	262	9934	±	327	5732	±	294	448	±	39	328	±	25	196	±	19
Orbitofrontal cortex, lateral																															
	I	CG	1248	±	100	702	±	102	2482	±	281	5193	±	110	1566	±	98	4732	±	324	6500	±	276	384	±	29	802	±	35	119	±	46
		MWM_{CG}	1096	±	105	597	±	38	1178	±	122	13218	±	971	3134	±	156	8028	±	323	8541	±	185	426	±	39	534	±	40	168	±	7
	II/III	CG	1035	±	81	973	±	173	2610	±	323	4458	±	88	1667	±	69	5491	±	443	6190	±	220	505	±	50	685	±	23	164	±	56
		MWM_{CG}	943	±	80	805	±	55	1253	±	54	10073	±	773	2891	±	252	9655	±	356	7283	±	524	428	±	17	394	±	19	145	±	15
	V	CG	1092	±	83	1468	±	131	2242	±	253	4083	±	288	1473	±	120	4947	±	434	5829	±	459	544	±	34	562	±	43	169	±	45
		MWM_{CG}	987	±	94	1105	±	105	1277	±	79	8693	±	713	2450	±	246	9707	±	332	6497	±	478	451	±	28	304	±	10	171	±	16
	VI	CG	982	±	96	1609	±	126	2240	±	243	2983	±	300	1449	±	164	4405	±	348	5744	±	561	537	±	44	534	±	31	248	±	34
		MWM_{CG}	953	±	69	1352	±	120	1117	±	115	7854	±	586	1947	±	155	9303	±	492	6191	±	400	488	±	40	324	±	24	206	±	20
Olfactoryt tubercle																															
	I	CG	757	±	44	711	±	62	1445	±	166	4837	±	283	773	±	87	2656	±	449	2131	±	286	185	±	28	589	±	100	4529	±	404
		MWM_{CG}	416	±	58	275	±	18	205	±	76	7981	±	204	1359	±	188	2779	±	185	3790	±	327	181	±	17	460	±	49	5767	±	235
	II	CG	1381	±	98	1100	±	101	1768	±	116	4090	±	409	973	±	91	3195	±	408	3344	±	316	201	±	25	813	±	113	6451	±	563
		MWM_{CG}	733	±	56	956	±	65	569	±	65	8318	±	383	1655	±	215	4740	±	394	6038	±	440	213	±	14	596	±	66	7237	±	168
	III	CG	1092	±	80	1147	±	80	1700	±	129	3487	±	248	812	±	67	3293	±	399	3508	±	286	227	±	23	909	±	116	5041	±	503
		MWM_{CG}	859	±	66	1268	±	61	764	±	40	6513	±	408	1290	±	204	5572	±	356	4529	±	338	236	±	22	703	±	58	6254	±	253

Supp. Tab. 30: Statistical analysis of the comparison of layer-specific receptor concentrations of CG versus MWM_{CG}

Significant differences between receptor densities between the olfactory layers of control mice (CG) and trained mice with intact adult neurogenesis (MWM_{CG}). Each receptor type was tested with non-parametric Mann-Whitney-U test. The percentage difference in absolute receptor concentrations (first column), Z-value (negative: group MWM_{CG} is significantly higher; positive: group CG is significantly higher; middle column), p-value (right column).

CG | MWM_{CG}	AMPA			Kainate			NMDA			$mGlu_{2/3}$			$GABA_A$		
	%	*Z*	*p-value*	%	*Z*	*p-value*	%	*Z*	*p-value*	%	*Z*	*p-value*	%	*Z*	*p-value*
MOB gr	-6,99	0,42	0,684	22,69	-1,474	0,143	-55,56	3,288	0,000	60,54	-3,742	0,000	34,87	-1,776	0,075
MOB ipl	1,32	0,04	0,971	21,75	-2,154	0,029	-52,15	2,457	0,011	99,12	-3,742	0,000	27,50	-1,928	0,052
MOB mi	3,05	-0,04	1,000	40,46	-3,213	0,000	-58,87	2,835	0,003	95,87	-3,742	0,000	85,78	-3,439	0,000
MOB opl	4,84	-0,64	0,529	4,81	-0,718	0,481	-50,86	2,306	0,019	74,45	-3,668	0,000	46,26	-2,306	0,019
MOB gl	3,26	0,04	1,000	-13,86	1,021	0,315	-64,11	3,743	0,000	24,34	-2,836	0,003	163,85	-3,742	0,000
MOB onl	-46,19	3,21	0,000	-42,70	3,518	0,000	-60,08	3,743	0,000	-6,56	0,416	0,684	58,87	-2,986	0,002
AOB gr	-12,86	1,17	0,247	-18,57	2,079	0,035	-55,30	3,378	0,000	48,47	-3,364	0,000	97,63	-1,021	0,315
AOB mi	26,52	-1,93	0,052	6,27	-1,324	0,190	-58,11	3,749	0,000	87,08	-3,742	0,000	22,74	-2,012	0,043
AOB gl	56,42	-2,24	0,023	101,62	-2,007	0,043	-53,69	3,750	0,000	224,63	-3,752	0,000	538,68	-3,596	0,000
AON pe	11,74	-1,10	0,280	-21,00	3,668	0,000	-9,36	1,021	0,315	90,78	-3,596	0,000	-22,49	1,400	0,165
AON m	14,24	-1,02	0,315	-3,53	-0,265	0,796	-11,65	1,022	0,315	110,23	-2,835	0,003	-11,32	0,718	0,481
AON d	45,72	-3,14	0,001	10,41	-0,718	0,481	-20,65	2,230	0,023	162,88	-3,756	0,000	25,06	-1,399	0,165
AON pv	30,42	-2,46	0,011	-17,17	2,306	0,019	21,76	-1,625	0,105	168,73	-3,742	0,000	-28,81	2,760	0,004
AON l	25,34	-3,00	0,002	-10,61	1,248	0,218	-50,19	3,747	0,000	127,76	-3,597	0,000	59,45	-2,839	0,003
TTd I	0,00	-0,19	0,853	-9,42	0,567	0,579	-45,49	3,063	0,001	100,42	-2,532	0,009	68,44	-2,835	0,003
TTd II	3,90	-0,57	0,579	12,75	-0,718	0,481	-30,70	3,668	0,000	116,52	-3,290	0,000	91,82	-3,439	0,000
TTd III	14,00	-1,10	0,280	17,43	-1,021	0,315	-39,82	3,293	0,000	121,82	-3,063	0,001	61,86	-3,062	0,001
TTd IV	26,91	-1,55	0,123	-5,72	0,265	0,796	-21,81	1,701	0,089	98,19	-2,608	0,007	99,64	-3,439	0,000

TTv I	-0,08	0,26	0,796	-20,03	1,323	0,190	-56,66	3,214	0,000	106,19	-3,138	0,001	70,05	-2,457	0,011
TTv II	-9,89	2,31	0,019	7,87	-0,340	0,739	-38,00	3,137	0,001	103,82	-3,364	0,000	70,43	-2,986	0,002
TTv III	-15,82	2,46	0,011	41,35	-2,986	0,002	-18,79	2,835	0,003	80,92	-3,213	0,000	68,01	-3,591	0,000
OT I	-45,02	3,29	0,000	-61,24	3,666	0,000	-85,79	3,756	0,000	64,99	-3,743	0,000	75,70	-2,306	0,019
OT II	-46,92	3,74	0,000	-13,05	1,550	0,123	-67,82	3,745	0,000	103,35	-3,742	0,000	70,17	-2,154	0,029
OT III	-21,34	1,85	0,063	10,51	-1,625	0,105	-55,06	3,747	0,000	86,79	-3,742	0,000	58,77	-2,003	0,043
DP I	-0,66	0,87	0,393	-13,64	1,550	0,123	-44,21	3,441	0,000	116,55	-3,742	0,000	140,69	-3,515	0,000
DP II/III	-10,94	1,17	0,247	-1,03	0,113	0,912	-48,54	3,369	0,000	121,06	-3,742	0,000	128,83	-3,742	0,000
DP V	8,18	-0,79	0,436	0,63	0,340	0,739	-47,31	3,592	0,000	134,49	-3,742	0,000	109,66	-3,742	0,000
DP VI	-2,31	0,26	0,796	-16,15	1,248	0,218	-23,22	0,643	0,529	162,64	-3,742	0,000	139,50	-3,742	0,000
PIR I	-1,43	0,19	0,853	-7,36	0,340	0,739	-55,29	3,742	0,000	101,51	-3,743	0,000	46,44	-2,986	0,002
PIR II	-28,21	3,67	0,000	5,12	-0,340	0,739	-39,13	3,138	0,001	120,68	-3,742	0,000	41,71	-2,835	0,003
PIR III	19,04	-1,85	0,063	-0,15	-0,113	0,912	-38,57	3,062	0,001	172,96	-3,747	0,000	40,34	-2,835	0,003
ENT I I	-43,40	2,99	0,002	-36,22	2,003	0,043	-43,12	3,063	0,001	161,52	-3,742	0,000	22,94	-1,172	0,247
ENT I II	-42,56	3,44	0,000	-24,53	2,836	0,003	-48,91	3,743	0,000	132,52	-3,742	0,000	16,32	-1,474	0,143
ENT I III	-35,43	3,67	0,000	-10,50	1,248	0,218	-47,04	3,668	0,000	110,10	-3,742	0,000	26,95	-2,154	0,029
ENT I IV	-32,40	3,44	0,000	8,11	-0,038	1,000	-42,95	3,672	0,000	110,07	-3,742	0,000	19,27	-1,474	0,143
ENT I V	-22,46	2,76	0,004	16,65	-1,172	0,247	-46,84	3,747	0,000	105,25	-3,742	0,000	17,95	-1,701	0,089
ENT I VIa	-16,50	1,47	0,143	34,50	-1,852	0,063	-45,49	3,747	0,000	128,80	-3,742	0,000	13,55	-1,247	0,218
ENT I VIb	-6,58	0,57	0,579	62,46	-3,213	0,000	-32,10	2,911	0,002	123,71	-3,742	0,000	17,92	-1,247	0,218
ENT m I	-60,36	3,74	0,000	-54,71	3,213	0,000	-28,97	2,003	0,043	116,02	-3,062	0,001	19,11	-1,323	0,190
ENT m II	-46,75	2,91	0,002	-15,29	2,230	0,023	-41,08	2,986	0,002	116,23	-3,666	0,000	12,49	-1,399	0,165
ENT m III	-28,51	2,23	0,023	-15,30	1,474	0,143	-31,44	2,986	0,002	119,04	-3,666	0,000	11,19	-2,080	0,035
ENT m IV	-17,33	2,76	0,004	5,49	-0,340	0,739	1,00	-0,492	0,631	115,19	-3,666	0,000	20,28	-2,532	0,009
ENT m V	-7,46	1,17	0,247	35,41	-2,382	0,015	-36,57	2,460	0,011	112,29	-3,742	0,000	34,14	-3,366	0,000
ENT m VI	-19,15	1,47	0,143	11,94	-0,491	0,631	-9,89	0,870	0,393	119,74	-3,591	0,000	34,59	-2,382	0,015

ORB m I	-11,49	1,70	0,089	38,87	-1,172	0,247	-54,35	3,516	0,000	127,10	-3,752	0,000	78,49	-3,516	0,000
ORB m II	17,63	-0,34	0,739	6,27	0,340	0,739	-35,22	3,064	0,001	161,20	-3,750	0,000	72,40	-3,365	0,000
ORB m II/III	23,01	-2,16	0,029	14,09	-0,038	1,000	-34,40	3,138	0,001	128,89	-3,523	0,000	92,59	-3,592	0,000
ORB m V	9,79	-1,17	0,247	-9,68	1,324	0,190	-31,15	2,836	0,003	163,87	-3,675	0,000	84,29	-3,441	0,000
ORB m VIa	1,91	-0,49	0,631	-9,48	0,567	0,579	-43,93	3,743	0,000	124,99	-3,447	0,000	39,61	-2,306	0,019
ORB vl I	-12,96	1,17	0,247	-1,78	0,492	0,631	-55,48	3,515	0,000	129,30	-3,750	0,000	93,10	-3,668	0,000
ORB vl II/III	19,27	-1,02	0,315	-8,03	0,492	0,631	-43,55	3,214	0,000	157,56	-3,750	0,000	98,21	-3,668	0,000
ORB vl V	3,92	-0,42	0,684	-34,60	3,291	0,000	-49,64	3,364	0,000	147,22	-3,750	0,000	93,13	-2,839	0,003
ORB vl VIa	-0,83	0,11	0,912	-15,04	0,794	0,436	-45,67	3,439	0,000	131,45	-3,675	0,000	61,36	-2,158	0,029
ORB l I	-12,21	1,32	0,190	-14,93	1,476	0,143	-52,53	3,516	0,000	154,53	-3,762	0,000	100,09	-3,743	0,000
ORB l II/III	-8,95	1,10	0,280	-17,30	1,776	0,075	-51,97	3,214	0,000	125,95	-3,760	0,000	73,40	-3,745	0,000
ORB l V	-9,60	0,95	0,353	-24,71	2,080	0,035	-43,02	2,987	0,002	112,93	-3,760	0,000	66,33	-3,441	0,000
ORB l VIa	-2,98	0,42	0,684	-16,01	1,702	0,089	-50,14	3,137	0,001	163,26	-3,752	0,000	34,36	-2,004	0,043
CG | MWM_{CG}	$GABA_{A(BZ)}$			$GABA_B$			α_1			α_2			$D_{1/5}$		
	%	*Z*	*p-value*	%	*Z*	*p-value*	%	*Z*	*p-value*	%	*Z*	*p-value*	%	*Z*	*p-value*
MOB gr	56,17	-3,67	0,000	-9,16	1,323	0,190	-5,25	0,384	0,393	-45,28	3,742	0,000	65,58	-3,592	0,000
MOB ipl	150,01	-3,74	0,000	-19,57	2,990	0,002	6,29	0,427	0,436	-56,74	3,666	0,000	49,89	-3,063	0,001
MOB mi	130,48	-3,74	0,000	-13,19	2,004	0,043	4,53	0,791	0,796	-57,32	3,591	0,000	73,52	-3,515	0,000
MOB opl	50,17	-3,36	0,000	-34,92	3,743	0,000	-17,65	0,031	0,029	-37,24	2,684	0,005	43,17	-3,591	0,000
MOB gl	49,66	-3,74	0,000	94,72	-3,743	0,000	-8,92	0,345	0,353	-46,12	3,742	0,000	26,28	-1,172	0,247
MOB onl	12,84	-1,70	0,089	-8,01	1,021	0,315	-45,56	0,000	0,000	-47,83	3,288	0,000	16,13	-0,794	0,436
AOB gr	-81,48	3,74	0,000	-5,29	0,567	0,579	-11,80	0,571	0,579	-15,62	0,491	0,631	-23,20	1,855	0,063
AOB mi	75,68	-3,67	0,000	5,32	1,551	0,123	-9,30	0,473	0,481	-44,75	2,542	0,009	12,76	-0,038	1,000
AOB gl	129,26	-3,77	0,000	18,66	-2,917	0,002	24,73	0,791	0,796	-46,67	2,770	0,004	76,79	-2,845	0,003
AON pe	62,29	-3,59	0,000	67,74	-3,442	0,000	-24,64	0,064	0,063	-27,68	0,869	0,393	-9,70	0,718	0,481
AON m	68,82	-3,21	0,000	27,50	-2,457	0,011	3,07	0,970	0,971	-8,53	1,398	0,165	-14,70	0,718	0,481

AON d	120,68	-3,74	0,000	28,15	-2,910	0,002	-23,32	0,021	0,019	-21,48	2,457	0,011	-38,95	1,398	0,165
AON pv	82,77	-2,76	0,004	50,10	-3,290	0,000	-22,30	0,026	0,023	-5,80	0,643	0,529	-1,04	-0,265	0,796
AON l	43,24	-3,44	0,000	32,49	-2,760	0,004	-2,24	0,677	0,684	0,05	0,189	0,853	17,59	-2,087	0,035
TTd I	61,10	-3,74	0,000	63,07	-3,743	0,000	-12,48	0,850	0,853	-6,77	-0,038	0,971	-14,87	0,491	0,631
TTd II	73,88	-3,74	0,000	50,19	-3,596	0,000	-2,60	0,791	0,796	-3,79	0,946	0,353	-28,83	1,247	0,218
TTd III	60,42	-3,52	0,000	59,43	-3,441	0,000	-6,05	0,473	0,481	13,73	-0,794	0,436	-43,53	2,457	0,011
TTd IV	55,76	-3,14	0,001	92,38	-3,745	0,000	-24,00	0,009	0,007	-4,95	-0,416	0,684	-55,57	3,288	0,000
TTv I	45,35	-3,21	0,000	91,87	-3,745	0,000	-25,33	0,678	0,684	-29,58	1,247	0,218	-25,48	0,643	0,529
TTv II	76,48	-3,74	0,000	66,36	-3,516	0,000	-22,05	0,571	0,579	-21,35	1,021	0,315	-24,71	0,113	0,912
TTv III	77,55	-3,75	0,000	74,15	-3,747	0,000	-27,30	0,121	0,123	-12,16	0,340	0,739	-51,66	1,247	0,218
OT I	4,64	-0,19	0,853	77,83	-3,291	0,000	-2,10	0,733	0,739	-21,93	1,701	0,089	27,35	-2,685	0,005
OT II	48,34	-2,15	0,029	80,55	-3,668	0,000	5,52	0,570	0,579	-26,63	1,777	0,075	12,20	-0,718	0,481
OT III	69,24	-3,06	0,001	29,08	-2,609	0,007	4,00	0,427	0,436	-22,60	1,626	0,105	24,05	-2,006	0,043
DP I	42,06	-2,31	0,019	60,00	-3,063	0,001	17,93	0,345	0,353	1,74	-0,265	0,796	-16,93	0,945	0,353
DP II/III	74,80	-3,67	0,000	27,26	-1,247	0,218	-1,13	0,734	0,739	29,32	-2,087	0,035	-20,70	0,718	0,481
DP V	80,14	-3,74	0,000	2,08	0,038	1,000	-14,75	0,623	0,631	29,14	-2,381	0,015	-21,35	1,398	0,165
DP VI	98,05	-3,74	0,000	18,28	-1,247	0,218	21,56	0,089	0,089	36,49	-2,532	0,009	-46,71	3,591	0,000
PIR I	61,15	-3,74	0,000	17,97	-3,743	0,000	-15,60	0,121	0,123	-35,88	3,137	0,001	-20,43	1,398	0,165
PIR II	70,07	-3,74	0,000	8,74	-1,474	0,143	-7,47	0,734	0,739	-24,17	2,230	0,023	-35,05	2,457	0,011
PIR III	64,12	-3,74	0,000	4,71	-1,550	0,123	5,66	0,734	0,739	-23,83	2,835	0,003	-57,54	3,439	0,000
ENT I I	55,86	-2,61	0,007	64,63	-3,668	0,000	59,92	0,004	0,002	5,80	-0,416	0,684	70,36	-2,835	0,003
ENT I II	79,72	-3,74	0,000	32,90	-3,365	0,000	55,72	0,002	0,001	-0,47	0,491	0,631	46,66	-2,306	0,019
ENT I III	97,67	-3,74	0,000	51,20	-3,364	0,000	17,95	0,140	0,143	-8,96	1,096	0,280	31,36	-2,155	0,029
ENT I IV	107,73	-3,74	0,000	46,62	-3,137	0,001	21,92	0,089	0,089	-9,48	1,474	0,143	43,40	-2,839	0,003
ENT I V	115,27	-3,74	0,000	50,66	-3,062	0,001	16,72	0,162	0,165	-14,98	1,474	0,143	41,20	-2,763	0,004

ENT l VIa	95,18	-3,74	0,000	41,13	-3,439	0,000	15,40	0,021	0,019	-14,37	1,550	0,123	57,95	-2,154	0,029
ENT l VIb	75,14	-3,67	0,000	29,57	-3,515	0,000	18,41	0,273	0,280	-25,38	2,835	0,003	42,60	-2,154	0,029
ENT m I	52,58	-2,76	0,004	34,47	-2,608	0,007	8,46	0,384	0,393	13,80	-1,172	0,247	83,31	-2,004	0,043
ENT m II	82,98	-3,21	0,000	63,56	-3,743	0,000	27,14	0,104	0,105	17,63	-0,794	0,436	73,63	-1,550	0,123
ENT m III	102,46	-3,74	0,000	57,57	-3,668	0,000	43,40	0,006	0,004	-12,68	1,853	0,063	54,03	-1,398	0,165
ENT m IV	101,63	-3,74	0,000	50,74	-3,139	0,001	47,20	0,009	0,007	-4,50	0,643	0,529	66,01	-1,928	0,052
ENT m V	88,36	-3,44	0,000	54,01	-3,666	0,000	29,84	0,064	0,063	-11,31	1,323	0,190	47,25	-2,080	0,035
ENT m VI	109,89	-3,67	0,000	25,59	-2,761	0,004	21,86	0,054	0,052	17,08	-2,913	0,002	29,32	-1,247	0,218
ORB m I	45,94	-3,74	0,000	91,27	-3,742	0,000	13,69	0,427	0,436	-24,04	2,836	0,003	49,21	-2,005	0,043
ORB m II	81,80	-3,52	0,000	83,14	-3,745	0,000	12,98	0,345	0,353	-31,58	3,596	0,000	17,59	-1,404	0,165
ORB m II/III	99,84	-3,67	0,000	61,78	-3,592	0,000	6,58	0,307	0,315	-34,02	3,747	0,000	8,90	-0,341	0,739
ORB m V	118,81	-3,75	0,000	38,64	-3,215	0,000	6,70	0,520	0,529	-21,93	3,743	0,000	-6,59	1,176	0,247
ORB m VIa	123,97	-3,74	0,000	43,37	-3,064	0,001	-7,97	0,678	0,684	-28,69	3,596	0,000	-4,29	0,948	0,353
ORB vl I	76,91	-3,74	0,000	58,58	-3,592	0,000	1,61	0,970	0,971	-28,18	3,063	0,001	117,95	-3,377	0,000
ORB vl II/III	68,39	-3,75	0,000	34,40	-2,915	0,002	14,03	0,427	0,436	-40,41	3,743	0,000	30,42	-1,401	0,165
ORB vl V	89,16	-3,75	0,000	23,43	-1,777	0,075	11,92	0,186	0,190	-45,65	3,743	0,000	19,64	-1,324	0,190
ORB vl VIa	143,33	-3,74	0,000	7,73	-0,945	0,353	-10,53	0,186	0,190	-19,86	2,609	0,007	-7,91	0,645	0,529
ORB l I	69,65	-3,74	0,000	31,39	-3,746	0,000	10,99	0,521	0,529	-33,39	3,747	0,000	40,87	-2,233	0,023
ORB l II/III	75,83	-3,74	0,000	17,65	-0,870	0,393	-15,32	0,140	0,143	-42,41	3,747	0,000	-11,85	0,114	0,912
ORB l V	96,21	-3,74	0,000	11,45	-1,021	0,315	-17,16	0,054	0,052	-45,85	3,747	0,000	1,20	-0,416	0,684
ORB l VIa	111,18	-3,74	0,000	7,77	-1,097	0,280	-9,05	0,384	0,393	-39,40	3,743	0,000	-17,07	1,855	0,063

Supp. Tab. 31: Region-specific receptor concentrations of MWM_{CG} versus MWM_{TMZ}

Neurotransmitter receptor densities (fmol/mg protein) in different regions of the mouse olfactory system (Mean ± SEM) of trained mice with intact adult neurogenesis (MWM_{CG}) and trained mice with suppressed adult neurogenesis (MWM_{TMZ}). For pairwise comparisons between regions see further Supp. Tab. 32.

MWM_{CG} | MWM_{TMZ}		AMPA			Kainate			NMDA			$mGlu_{2/3}$			$GABA_A$		
MOB	MWM_{CG}	642	±	42	1357	±	77	425	±	18	3258	±	146	1642	±	110
	MWM_{TMZ}	742	±	77	1357	±	55	442	±	19	2961	±	117	1475	±	214
AOB	MWM_{CG}	1017	±	53	1534	±	100	631	±	90	6108	±	301	2225	±	289
	MWM_{TMZ}	892	±	92	1327	±	75	596	±	32	4746	±	426	2036	±	221
AON	MWM_{CG}	1356	±	56	1255	±	41	1174	±	70	5592	±	426	503	±	28
	MWM_{TMZ}	1449	±	118	1329	±	61	1264	±	50	4867	±	383	430	±	28
TTd	MWM_{CG}	1262	±	74	1355	±	94	1268	±	131	6068	±	663	1582	±	145
	MWM_{TMZ}	1216	±	93	1553	±	117	1471	±	87	5283	±	339	1171	±	122
TTv	MWM_{CG}	1186	±	49	1182	±	51	1013	±	117	5411	±	490	1337	±	93
	MWM_{TMZ}	1123	±	48	1266	±	135	910	±	83	5723	±	713	1222	±	156
Epd	MWM_{CG}	749	±	61	1282	±	34	808	±	101	4928	±	552	636	±	48
	MWM_{TMZ}	852	±	100	1150	±	82	793	±	91	3797	±	260	886	±	102
OT	MWM_{CG}	669	±	51	833	±	39	492	±	53	7490	±	273	1434	±	198
	MWM_{TMZ}	668	±	70	856	±	104	529	±	44	7551	±	324	1213	±	102
DP	MWM_{CG}	1064	±	59	1437	±	69	1242	±	150	7905	±	471	2376	±	164
	MWM_{TMZ}	1259	±	59	1322	±	111	1386	±	111	6622	±	356	2054	±	149
PIR	MWM_{CG}	989	±	48	772	±	44	1027	±	67	7802	±	237	1531	±	105
	MWM_{TMZ}	890	±	37	698	±	37	1023	±	77	6765	±	301	1368	±	64
ENTl	MWM_{CG}	1168	±	67	1271	±	80	1680	±	93	6726	±	245	1601	±	99

ENTm	MWM_{TMZ}	1127	±	66	1356	±	72	1791	±	65	6699	±	308	1632	±	83
	MWM_{CG}	1065	±	77	1066	±	74	1495	±	165	6663	±	423	1574	±	69
ORBl	MWM_{TMZ}	1195	±	109	1072	±	86	1702	±	105	6947	±	328	1590	±	83
	MWM_{CG}	1165	±	80	965	±	70	1214	±	76	9498	±	755	2605	±	170
ORBvl	MWM_{TMZ}	1047	±	111	862	±	78	1340	±	47	7537	±	274	2379	±	99
	MWM_{CG}	1052	±	89	909	±	46	1124	±	79	9713	±	708	2840	±	205
ORBm	MWM_{TMZ}	1111	±	110	843	±	59	1487	±	71	8182	±	284	2539	±	124
	MWM_{CG}	995	±	105	1119	±	89	1290	±	61	9503	±	793	2415	±	159
	MWM_{TMZ}	1272	±	102	890	±	53	1481	±	77	7972	±	266	2235	±	131
		$GABA_{A(BZ)}$			$GABA_B$			α_1			α_2			$D_{1/5}$		
MOB	MWM_{CG}	4887	±	258	2538	±	83	475	±	24	265	±	26	89	±	3
	MWM_{TMZ}	4739	±	349	2078	±	48	584	±	25	351	±	20	89	±	10
AOB	MWM_{CG}	6875	±	718	3898	±	210	656	±	50	359	±	36	108	±	8
	MWM_{TMZ}	6346	±	867	5285	±	274	703	±	41	318	±	27	98	±	13
AON	MWM_{CG}	3403	±	143	5665	±	147	309	±	32	1630	±	82	142	±	10
	MWM_{TMZ}	3238	±	176	6017	±	92	339	±	13	2252	±	103	112	±	11
TTd	MWM_{CG}	5803	±	288	7499	±	95	270	±	13	1694	±	33	212	±	19
	MWM_{TMZ}	5718	±	287	7295	±	112	334	±	13	1854	±	82	230	±	14
TTv	MWM_{CG}	5286	±	131	7372	±	153	238	±	15	1037	±	116	192	±	23
	MWM_{TMZ}	5083	±	198	5321	±	156	252	±	9	1251	±	123	198	±	20
Epd	MWM_{CG}	4431	±	347	4009	±	159	299	±	15	972	±	61	257	±	38
	MWM_{TMZ}	4747	±	377	3902	±	95	324	±	17	1043	±	44	226	±	24
OT	MWM_{CG}	4493	±	308	5000	±	415	210	±	15	586	±	54	6389	±	155
	MWM_{TMZ}	4286	±	297	3143	±	98	203	±	16	692	±	52	5533	±	164

DP	MWM_{CG}	7175	±	299	6193	±	304	324	±	15	1194	±	91	254	±	20
	MWM_{TMZ}	7465	±	269	6019	±	304	423	±	31	1445	±	92	234	±	22
PIR	MWM_{CG}	6358	±	185	5410	±	159	418	±	26	732	±	42	137	±	11
	MWM_{TMZ}	6541	±	248	5170	±	199	536	±	24	855	±	40	137	±	6
ENTl	MWM_{CG}	6789	±	95	8572	±	438	406	±	23	1571	±	78	505	±	33
	MWM_{TMZ}	7149	±	421	9753	±	292	409	±	12	1864	±	39	406	±	20
ENTm	MWM_{CG}	6687	±	163	9548	±	526	391	±	26	1768	±	98	522	±	90
	MWM_{TMZ}	6113	±	792	8701	±	187	419	±	26	1887	±	125	474	±	39
ORBl	MWM_{CG}	9173	±	219	6946	±	438	448	±	21	396	±	20	172	±	10
	MWM_{TMZ}	8720	±	277	6572	±	327	538	±	10	531	±	35	186	±	12
ORBvl	MWM_{CG}	9129	±	183	7806	±	427	513	±	33	386	±	25	164	±	9
	MWM_{TMZ}	8803	±	317	7680	±	530	610	±	15	572	±	40	154	±	10
ORBm	MWM_{CG}	8304	±	256	8368	±	406	550	±	29	400	±	21	228	±	29
	MWM_{TMZ}	8351	±	352	7846	±	509	614	±	16	531	±	35	227	±	24

Supp. Tab. 32: Statistical analysis of the comparison of region-specific receptor concentrations of MWM_{CG} versus MWM_{TMZ}

Significant differences between receptor densities between the olfactory regions of trained mice with intact adult neurogenesis (MWM_{CG}) and trained mice with suppressed adult neurogenesis (MWM_{TMZ}). Each receptor type was tested with non-parametric Mann-Whitney-U test. The percentage difference in absolute receptor concentrations (first column), p-value (middle column), and correlation coefficient r (limits: weak (0.1-0.3), medium (0.3-0.5), and strong (> 0.5) to evaluate the effect size (right column).

MWM_{CG} | MWM_{TMZ}	AMPAR			kainateR			NMDAR			$mGlu_{2/3}R$			$GABA_AR$		
	[%]	*p*	[r]	[%]	*p*	[r]	[%]	*p*	[r]	[%]	*p*	[r]	[%]	*p*	[r]
MOB | MOB	15,63	0.353	-	-0,01	0.971	-	3,95	0.481	-	-9,11	0.123	-	-10,16	0.218	-
AOB | AOB	-12,22	0.28	-	-13,52	**0.043**	**0.456**	-5,63	0.796	-	-22,30	**0.023**	**0.507**	-8,50	0.529	-
AOC | AOC	6,87	0.393	-	5,91	0.247	-	7,70	0.393	-	-12,96	0.315	-	-14,41	0.075	-
TTd | TTd	-3,65	0.631	-	14,62	0.105	-	15,99	0.353	-	-12,94	0.315	-	-25,97	0.075	-
TTv | TTv	-5,34	0.353	-	7,13	0.796	-	-10,14	0.529	-	5,76	0.971	-	-8,63	0.393	-
EPd | EPd	13,72	0.353	-	-10,30	0.089	-	-1,91	0.796	-	-22,95	0.105	-	39,32	0.052	-
OT | OT	-0,20	0.796	-	2,77	0.684	-	7,52	0.684	-	0,81	0.912	-	-15,40	0.315	-
DP | DP	18,36	0.052	-	-8,00	0.481	-	11,61	0.393	-	-16,22	0.063	-	-13,53	0.28	-
PIR | PIR	-9,94	0.28	-	-9,60	0.218	-	-0,47	0.853	-	-13,30	**0.007**	**0.584**	-10,61	0.28	-
ENTl | ENTl	-3,56	0.739	-	6,72	0.353	-	6,65	0.315	-	-0,41	0.796	-	1,92	0.853	-
ENTm | ENTm	12,18	0.436	-	0,50	0.853	-	13,88	0.393	-	4,26	0.739	-	1,01	0.912	-
ORBl | ORBl	-10,13	0.529	-	-10,69	0.052	-	10,44	0.089	-	-20,65	0.123	-	-8,69	0.393	-
ORBvl | ORBvl	5,62	0.912	-	-7,28	0.353	-	32,27	**0.000**	**0.727**	-15,76	0.089	-	-10,61	0.393	-
ORBm | ORBm	27,86	0.912	-	-20,47	0.247	-	14,84	0.123	-	-16,11	0.063	-	-7,47	0.579	-
MWM_{CG} | MWM_{TMZ}	$GABA_{A(BZ)}R$			$GABA_BR$			α_1R			α_2R			$D_{1/5}R$		
	[%]	*p*	[r]	[%]	*p*	[r]	[%]	*p*	[r]	[%]	*p*	[r]	[%]	*p*	[r]
MOB | MOB	-3,02	0.912	-	-18,15	**0.000**	**0.845**	22,80	**0.007**	**0.592**	32,48	**0.019**	**0.525**	-0,08	0.579	-
AOB | AOB	-7,69	0.796	-	35,59	**0.002**	**0.676**	7,10	0.579	-	-11,45	0.481	-	-9,27	0.165	-
AOC | AOC	-4,87	0.971	-	6,22	0.075	-	9,80	0.123	-	38,20	**0.001**	**0.719**	-20,73	0.063	-
TTd | TTd	-1,46	0.529	-	-2,72	0.143	-	23,42	**0.005**	**0.609**	9,47	0.165	-	8,71	0.579	-
TTv | TTv	-3,85	0.105	-	-27,82	**0.000**	**0.845**	5,86	0.436	-	20,71	0.631	-	3,11	0.853	-
EPd | EPd	7,14	0.481	-	-2,66	0.684	-	8,39	0.353	-	7,29	0.393	-	-11,96	0.912	-

OT | OT	-4,59	0.631	-	-37,14	**0.002**	**0.659**	-3,06	1.000	-	18,01	0.19	-	-13,40	**0.004**	**0.626**
DP | DP	4,06	0.436	-	-2,81	0.796	-	30,59	**0.007**	**0.609**	21,00	**0.029**	**0.490**	-7,68	0.393	-
PIR | PIR	2,88	0.393	-	-4,44	0.393	-	28,10	**0.005**	**0.609**	16,70	0.123	-	0,49	0.529	-
ENTl | ENTl	5,31	0.631	-	13,77	0.052	-	0,91	0.853	-	18,64	**0.004**	**0.625**	-19,59	0.063	-
ENTm | ENTm	-8,58	0.353	-	-8,87	0.123	-	7,22	0.631	-	6,76	0.218	-	-9,18	1.000	-
ORBl | ORBl	-4,95	0.853	-	-5,38	0.393	-	20,14	0.089	-	34,16	**0.011**	**0.558**	7,78	0.684	-
ORBvl | ORBvl	-3,57	0.393	-	-1,61	0.796	-	19,03	**0.035**	**0.474**	48,35	**0.000**	**0.761**	-6,05	0.393	-
ORBm | ORBm	0,57	0.247	-	-6,23	0.436	-	11,70	**0.005**	**0.609**	32,66	**0.000**	**0.761**	-0,43	0.436	-

Supp. Tab. 33: Mean receptor densities of olfactory layers (MWM_{CG} versus MWM_{TMZ}).

Layer-specific absolute receptor densities of the subregions of the olfactory system (mean ± SEM) for trained mice (MWM_{CG}) with intact adult neurogenesis versus trained mice with suppressed adult neurogenesis (MWM_{TMZ}). For pairwise comparisons between regions see further Supp. Tab. 34.

		MWM_{CG} | MWM_{TMZ}	Receptor (fmol/mg protein)									
			AMPA	kainate	NMDA	$mGlu_{2/3}$	$GABA_A$	$GABA_{A(BZ)}$	$GABA_B$	α_1	α_2	$D_{1/5}$
Main olfactory bulb												
	gr	MWM_{CG}	711 ± 40	1118 ± 101	366 ± 19	2725 ± 144	351 ± 31	1525 ± 49	1873 ± 43	424 ± 28	562 ± 74	81 ± 5
		MWM_{TMZ}	792 ± 98	1159 ± 95	400 ± 28	2585 ± 115	319 ± 35	1675 ± 143	1667 ± 67	450 ± 25	749 ± 53	70 ± 6
	ipl	MWM_{CG}	729 ± 58	1596 ± 82	381 ± 18	3735 ± 185	478 ± 38	2563 ± 64	1544 ± 76	432 ± 31	191 ± 18	85 ± 4
		MWM_{TMZ}	832 ± 96	1547 ± 38	508 ± 19	3134 ± 100	379 ± 29	2704 ± 207	1291 ± 63	543 ± 29	288 ± 21	81 ± 6
	mi	MWM_{CG}	699 ± 61	1527 ± 79	364 ± 18	3303 ± 167	564 ± 44	2190 ± 60	1711 ± 80	422 ± 29	251 ± 38	85 ± 3
		MWM_{TMZ}	720 ± 73	1490 ± 80	400 ± 22	2929 ± 204	479 ± 26	2351 ± 195	1544 ± 75	497 ± 25	398 ± 28	86 ± 9
	opl	MWM_{CG}	697 ± 48	1643 ± 100	479 ± 30	4133 ± 266	981 ± 75	3872 ± 185	1256 ± 51	471 ± 31	212 ± 26	97 ± 3
		MWM_{TMZ}	765 ± 69	1742 ± 82	555 ± 50	3916 ± 221	857 ± 30	3987 ± 275	1155 ± 40	546 ± 35	270 ± 22	93 ± 8
	gl	MWM_{CG}	642 ± 55	1674 ± 158	604 ± 33	3811 ± 164	6246 ± 505	14511 ± 201	6603 ± 145	940 ± 42	189 ± 14	100 ± 5
		MWM_{TMZ}	741 ± 71	1729 ± 90	580 ± 49	3723 ± 224	4437 ± 396	14541 ± 787	5812 ± 188	1191 ± 53	249 ± 16	114 ± 17
	onl	MWM_{CG}	374 ± 44	587 ± 31	268 ± 22	1855 ± 155	1320 ± 109	4862 ± 241	1999 ± 189	207 ± 8	158 ± 15	85 ± 4
		MWM_{TMZ}	604 ± 98	477 ± 49	218 ± 22	1512 ± 128	968 ± 70	4809 ± 135	997 ± 80	236 ± 12	148 ± 15	89 ± 15
Accessory olfactory bulb												
	gr	MWM_{CG}	821 ± 59	969 ± 48	529 ± 53	4930 ± 228	1471 ± 462	1293 ± 272	2798 ± 122	548 ± 26	512 ± 94	82 ± 6
		MWM_{TMZ}	915 ± 167	1014 ± 26	763 ± 107	4042 ± 426	2449 ± 396	993 ± 74	2996 ± 70	489 ± 26	234 ± 25	101 ± 14
	mi	MWM_{CG}	1196 ± 82	2051 ± 177	650 ± 96	9180 ± 355	2078 ± 298	12455 ± 778	3033 ± 128	921 ± 79	259 ± 36	121 ± 13
		MWM_{TMZ}	861 ± 79	1921 ± 84	558 ± 35	8723 ± 595	1782 ± 361	15249 ± 467	2455 ± 64	1087 ± 82	356 ± 46	102 ± 14
	gl	MWM_{CG}	1033 ± 73	1582 ± 226	568 ± 33	4215 ± 414	2949 ± 716	6672 ± 388	6037 ± 147	499 ± 80	283 ± 30	118 ± 9

	MWM_{TMZ}	902 ± 92	1044 ± 207	481 ± 32	2554 ± 350	1894 ± 525	6549 ± 464	11246 ± 67	499 ± 91	326 ± 26	91 ± 14
Anterior olfactory cortex											
pe	MWM_{CG}	1050 ± 66	1026 ± 37	1019 ± 90	5878 ± 465	639 ± 40	4215 ± 189	5957 ± 279	338 ± 36	969 ± 75	146 ± 13
	MWM_{TMZ}	1272 ± 92	936 ± 73	973 ± 76	5944 ± 562	629 ± 34	4356 ± 217	5697 ± 219	462 ± 30	1166 ± 93	129 ± 21
m	MWM_{CG}	1400 ± 109	1280 ± 77	1251 ± 133	4763 ± 664	483 ± 45	3500 ± 193	5875 ± 274	325 ± 37	1984 ± 111	161 ± 17
	MWM_{TMZ}	1630 ± 192	1364 ± 75	1406 ± 88	4077 ± 300	473 ± 58	2715 ± 238	5873 ± 144	351 ± 22	2654 ± 209	123 ± 13
d	MWM_{CG}	1516 ± 101	1606 ± 125	1324 ± 84	6361 ± 535	497 ± 33	3121 ± 195	5624 ± 251	244 ± 23	1803 ± 116	143 ± 14
	MWM_{TMZ}	1405 ± 134	1701 ± 100	1606 ± 61	4660 ± 349	356 ± 17	3072 ± 110	6525 ± 132	286 ± 12	2785 ± 140	130 ± 15
pv	MWM_{CG}	1406 ± 54	1477 ± 73	1212 ± 124	4960 ± 409	402 ± 53	3605 ± 370	5447 ± 269	239 ± 18	1813 ± 80	136 ± 14
	MWM_{TMZ}	1672 ± 178	1774 ± 81	1242 ± 62	4698 ± 374	382 ± 51	2937 ± 231	6048 ± 124	283 ± 25	2555 ± 117	105 ± 10
l	MWM_{CG}	1476 ± 37	1281 ± 64	1230 ± 97	6834 ± 572	496 ± 32	3057 ± 138	6097 ± 141	320 ± 48	1926 ± 102	125 ± 9
	MWM_{TMZ}	1506 ± 147	1439 ± 72	1643 ± 68	5841 ± 660	432 ± 39	3326 ± 248	6214 ± 190	300 ± 21	2471 ± 97	97 ± 13
e	MWM_{CG}	1215 ± 79	809 ± 78	1007 ± 148	4822 ± 685	491 ± 83	2758 ± 221	5259 ± 262	309 ± 30	1527 ± 244	141 ± 28
	MWM_{TMZ}	1075 ± 85	790 ± 109	644 ± 129	3362 ± 363	279 ± 45	2915 ± 261	6053 ± 206	337 ± 33	1973 ± 208	90 ± 19
taenia tecta, dorsal											
I	MWM_{CG}	1161 ± 80	900 ± 72	1264 ± 170	7133 ± 834	1690 ± 153	5342 ± 87	8146 ± 131	262 ± 19	1270 ± 50	184 ± 19
	MWM_{TMZ}	1033 ± 105	950 ± 134	1167 ± 126	5937 ± 463	1301 ± 134	5185 ± 315	7745 ± 50	327 ± 26	1227 ± 107	183 ± 22
II	MWM_{CG}	1458 ± 78	1263 ± 95	1532 ± 61	6537 ± 693	1702 ± 156	6488 ± 198	7508 ± 114	276 ± 18	1730 ± 84	190 ± 19
	MWM_{TMZ}	1426 ± 106	1436 ± 125	1623 ± 106	6156 ± 371	1250 ± 145	5830 ± 392	8020 ± 177	353 ± 17	1893 ± 70	210 ± 18
III	MWM_{CG}	1254 ± 89	1519 ± 150	1288 ± 119	5665 ± 690	1479 ± 151	6364 ± 317	7846 ± 131	284 ± 18	1875 ± 62	210 ± 27
	MWM_{TMZ}	1298 ± 126	1831 ± 164	1746 ± 103	5167 ± 400	1092 ± 139	5547 ± 252	7444 ± 201	341 ± 13	2019 ± 96	252 ± 21
IV	MWM_{CG}	1173 ± 124	1737 ± 134	1178 ± 136	4938 ± 661	1458 ± 176	5658 ± 352	6497 ± 190	259 ± 11	1901 ± 85	264 ± 27
	MWM_{TMZ}	1105 ± 100	1994 ± 174	1349 ± 87	3871 ± 278	1042 ± 116	6111 ± 359	6100 ± 156	313 ± 18	2203 ± 99	277 ± 28
taenia tecta, ventral											
I	MWM_{CG}	1013 ± 67	559 ± 65	721 ± 128	5706 ± 538	1354 ± 129	4287 ± 226	6683 ± 183	215 ± 8	724 ± 91	150 ± 23

	II	MWM_{TMZ}	850	±	38	721	±	148	483	±	89	5826	±	943	1253	±	151	4457	±	253	4364	±	220	199	±	14	909	±	99	169	±	32
		MWM_{CG}	1331	±	89	1151	±	60	1125	±	113	6009	±	553	1492	±	88	5851	±	163	7668	±	307	248	±	22	1151	±	101	189	±	28
	III	MWM_{TMZ}	1340	±	71	1334	±	179	1083	±	89	5963	±	683	1304	±	179	5423	±	175	5764	±	162	280	±	9	1373	±	134	192	±	22
		MWM_{CG}	1214	±	33	1836	±	61	1397	±	55	4824	±	432	1164	±	68	5721	±	197	7764	±	207	246	±	18	1439	±	79	238	±	26
		MWM_{TMZ}	1177	±	91	1744	±	125	1164	±	79	5380	±	558	1108	±	150	5272	±	247	5835	±	235	290	±	13	1455	±	168	233	±	22
Dorsal peduncular cortex																															
	I	MWM_{CG}	1085	±	72	997	±	75	1153	±	189	8934	±	491	2292	±	298	5949	±	524	8057	±	411	313	±	25	1140	±	79	210	±	15
		MWM_{TMZ}	1345	±	77	1059	±	58	1389	±	171	7388	±	256	1940	±	184	6006	±	281	7399	±	490	406	±	50	1164	±	95	239	±	25
	II/III	MWM_{CG}	1210	±	93	1571	±	131	1378	±	171	8101	±	645	2484	±	150	7469	±	339	7232	±	442	339	±	21	1230	±	118	262	±	26
		MWM_{TMZ}	1244	±	81	1476	±	147	1655	±	145	7606	±	590	2138	±	147	7925	±	393	6647	±	409	377	±	19	1452	±	126	233	±	26
	V	MWM_{CG}	1073	±	76	1621	±	135	1183	±	122	7330	±	536	2420	±	163	7861	±	315	5360	±	493	319	±	22	1332	±	89	274	±	33
		MWM_{TMZ}	1561	±	98	1453	±	168	1463	±	110	6941	±	531	2145	±	148	8321	±	355	5612	±	252	435	±	30	1684	±	87	212	±	23
	VI	MWM_{CG}	888	±	56	1560	±	168	1252	±	163	7513	±	512	2307	±	178	7357	±	313	4996	±	232	316	±	22	1296	±	98	271	±	20
		MWM_{TMZ}	888	±	83	1301	±	129	1035	±	93	4672	±	231	1912	±	143	7571	±	94	4759	±	265	451	±	40	1629	±	111	254	±	31
Piriform cortex																															
	I	MWM_{CG}	768	±	82	537	±	55	940	±	55	8867	±	512	1712	±	127	6757	±	124	5577	±	88	419	±	30	533	±	53	119	±	10
		MWM_{TMZ}	602	±	50	377	±	29	945	±	67	9262	±	270	1526	±	72	6592	±	279	5118	±	239	566	±	21	553	±	34	118	±	8
	II	MWM_{CG}	1154	±	32	804	±	53	1142	±	82	7459	±	385	1633	±	117	6792	±	65	5852	±	210	433	±	33	846	±	43	135	±	11
		MWM_{TMZ}	921	±	52	766	±	38	1129	±	101	6303	±	231	1438	±	75	6616	±	253	5375	±	243	565	±	28	1027	±	71	131	±	7
	III	MWM_{CG}	1044	±	73	976	±	54	999	±	80	7131	±	247	1246	±	79	5914	±	168	4731	±	219	403	±	26	883	±	22	156	±	15
		MWM_{TMZ}	1149	±	53	951	±	53	993	±	84	5198	±	213	1140	±	53	6416	±	251	4997	±	222	457	±	25	981	±	49	163	±	10
Entorhinal cortex, lateral																															
	I	MWM_{CG}	604	±	65	260	±	45	1309	±	80	8535	±	236	1414	±	149	4982	±	250	8916	±	414	433	±	38	998	±	75	391	±	42
		MWM_{TMZ}	596	±	72	260	±	27	1440	±	88	8920	±	258	1328	±	141	4258	±	367	9783	±	557	363	±	30	1085	±	61	291	±	15
	II	MWM_{CG}	1154	±	98	545	±	35	1738	±	157	7978	±	289	1888	±	135	6952	±	205	8773	±	502	455	±	33	1584	±	68	505	±	47

	III	MWM_{TMZ}	1285	±	81	579	±	35	1997	±	78	8148	±	202	1810	±	145	6343	±	287	10861	±	365	438	±	15	1754	±	44	341	±	22
		MWM_{CG}	1360	±	95	737	±	51	1921	±	143	7101	±	212	2024	±	136	7190	±	147	10159	±	613	329	±	28	1652	±	60	468	±	39
	IV	MWM_{TMZ}	1346	±	63	794	±	55	2220	±	30	7387	±	342	1993	±	115	7152	±	335	11233	±	380	380	±	16	2051	±	73	382	±	28
		MWM_{CG}	1329	±	95	1021	±	94	1950	±	115	6810	±	400	1836	±	130	7111	±	142	9551	±	572	326	±	18	1821	±	101	447	±	36
	V	MWM_{TMZ}	1229	±	57	1135	±	78	2112	±	93	6744	±	375	1745	±	69	7882	±	651	11059	±	428	337	±	13	2218	±	43	389	±	26
		MWM_{CG}	1354	±	69	1407	±	126	1770	±	106	6290	±	290	1512	±	102	7256	±	147	9200	±	600	341	±	20	1753	±	115	440	±	22
	VIa	MWM_{TMZ}	1053	±	51	1494	±	98	1935	±	85	5826	±	687	1654	±	87	7894	±	439	10562	±	384	358	±	13	2035	±	61	379	±	23
		MWM_{CG}	1269	±	88	2300	±	236	1516	±	58	5977	±	393	1361	±	89	7666	±	159	8052	±	396	439	±	13	1730	±	118	641	±	80
	VIb	MWM_{TMZ}	1271	±	144	2525	±	192	1721	±	73	5379	±	440	1555	±	78	8249	±	422	9229	±	239	455	±	23	2094	±	61	479	±	32
		MWM_{CG}	1109	±	113	2625	±	159	1442	±	69	4394	±	395	1173	±	87	6256	±	298	5517	±	220	509	±	32	1457	±	73	645	±	61
		MWM_{TMZ}	1107	±	115	2706	±	112	1257	±	61	3780	±	273	1304	±	82	6978	±	174	5696	±	211	534	±	21	1884	±	131	582	±	57
Entorhinal cortex, medial																															
	I	MWM_{CG}	576	±	78	293	±	33	1193	±	174	6915	±	751	1329	±	139	5613	±	221	7819	±	646	293	±	20	1071	±	85	388	±	74
		MWM_{TMZ}	643	±	88	383	±	28	1285	±	121	7476	±	364	1348	±	93	4569	±	943	7722	±	370	308	±	23	1222	±	133	415	±	58
	II	MWM_{CG}	819	±	138	737	±	41	1590	±	265	7595	±	395	1691	±	92	7013	±	146	11511	±	404	384	±	35	1952	±	162	578	±	112
		MWM_{TMZ}	1138	±	126	792	±	46	1866	±	131	8203	±	401	1727	±	132	6394	±	311	9690	±	289	413	±	26	1841	±	186	532	±	70
	III	MWM_{CG}	1103	±	116	902	±	76	1784	±	205	7172	±	397	1778	±	78	7292	±	227	10520	±	483	409	±	27	1693	±	117	593	±	125
		MWM_{TMZ}	1313	±	144	871	±	46	2154	±	54	7349	±	522	1761	±	82	6705	±	303	9625	±	265	419	±	40	2083	±	141	489	±	50
	IV	MWM_{CG}	1293	±	50	1273	±	140	1698	±	150	6708	±	474	1754	±	96	7046	±	229	9765	±	560	381	±	30	2014	±	141	579	±	106
		MWM_{TMZ}	1493	±	168	1062	±	79	1955	±	116	6974	±	416	1799	±	95	6846	±	293	9446	±	190	385	±	42	2254	±	61	472	±	30
	V	MWM_{CG}	1385	±	80	1728	±	151	1512	±	192	6369	±	392	1671	±	58	6676	±	215	9119	±	548	419	±	33	1886	±	167	507	±	84
		MWM_{TMZ}	1405	±	133	1717	±	159	1685	±	128	6468	±	403	1608	±	79	7300	±	572	8579	±	327	461	±	37	2358	±	121	461	±	35
	VI	MWM_{CG}	1214	±	91	1465	±	172	1225	±	157	5219	±	485	1218	±	74	6650	±	339	6626	±	208	459	±	32	1933	±	89	485	±	74
		MWM_{TMZ}	1114	±	102	1820	±	188	1371	±	124	5065	±	285	1166	±	48	7216	±	467	7146	±	395	547	±	13	2086	±	171	474	±	61
Orbitofrontal cortex, medial																															

	I	MWM_{CG}	1109	±	115	827	±	70	1251	±	121	11006	±	960	2448	±	126	6365	±	195	10866	±	610	506	±	35	532	±	27	189	±	23
		MWM_{TMZ}	1296	±	100	668	±	41	1096	±	33	8633	±	453	2224	±	194	6718	±	360	8635	±	787	555	±	26	601	±	49	228	±	32
	II	MWM_{CG}	1332	±	191	1005	±	68	1532	±	52	10459	±	904	2650	±	160	8216	±	372	10009	±	587	605	±	31	451	±	34	195	±	23
		MWM_{TMZ}	1369	±	141	764	±	42	1514	±	88	8502	±	271	2382	±	168	8529	±	555	8813	±	658	650	±	28	588	±	45	213	±	28
	II/III	MWM_{CG}	1323	±	137	1213	±	143	1339	±	72	9293	±	865	2622	±	200	8718	±	353	8164	±	479	613	±	32	378	±	23	235	±	30
		MWM_{TMZ}	1383	±	141	898	±	62	1620	±	82	8712	±	384	2506	±	191	9214	±	487	8651	±	526	702	±	27	515	±	38	221	±	33
	V	MWM_{CG}	1092	±	76	1175	±	119	1144	±	125	8938	±	833	2451	±	225	8945	±	334	6551	±	325	555	±	39	354	±	9	254	±	46
		MWM_{TMZ}	1202	±	105	901	±	74	1634	±	73	7180	±	361	2237	±	145	8767	±	385	6937	±	438	629	±	16	473	±	40	216	±	32
	VI	MWM_{CG}	966	±	61	1374	±	121	1160	±	60	7819	±	746	1904	±	158	9273	±	442	6249	±	415	452	±	31	310	±	16	264	±	40
		MWM_{TMZ}	1109	±	157	1218	±	117	1401	±	114	6922	±	228	1823	±	114	8528	±	400	6195	±	438	526	±	21	450	±	35	255	±	21
Orbitofrontal cortex, ventrolateral																														
	I	MWM_{CG}	1022	±	129	755	±	44	1095	±	111	10354	±	725	3047	±	184	8272	±	317	9802	±	567	513	±	45	551	±	40	169	±	15
		MWM_{TMZ}	1171	±	179	744	±	19	1431	±	37	9174	±	364	3021	±	83	8180	±	370	9117	±	634	662	±	24	748	±	64	154	±	30
	II/III	MWM_{CG}	1182	±	133	814	±	38	1279	±	45	10528	±	831	3090	±	200	8581	±	218	8711	±	509	542	±	46	346	±	24	141	±	11
		MWM_{TMZ}	1188	±	113	729	±	63	1545	±	49	8968	±	292	2758	±	163	9503	±	514	8591	±	474	615	±	32	552	±	43	114	±	10
	V	MWM_{CG}	1053	±	69	819	±	52	1108	±	106	9797	±	764	2886	±	338	9822	±	341	6977	±	539	558	±	39	291	±	16	151	±	15
		MWM_{TMZ}	1082	±	89	718	±	64	1522	±	75	8106	±	324	2496	±	185	9160	±	395	7078	±	641	629	±	18	498	±	32	141	±	11
	VI	MWM_{CG}	951	±	67	1249	±	126	1094	±	94	8172	±	677	2338	±	262	9934	±	327	5732	±	294	448	±	39	328	±	25	196	±	19
		MWM_{TMZ}	1003	±	111	1168	±	124	1395	±	109	6705	±	267	2008	±	180	8368	±	354	5935	±	409	549	±	25	402	±	16	208	±	11
Orbitofrontal cortex, lateral																														
	I	MWM_{CG}	1096	±	105	597	±	38	1178	±	122	13218	±	971	3134	±	156	8028	±	323	8541	±	185	426	±	39	534	±	40	168	±	7
		MWM_{TMZ}	1037	±	110	630	±	42	1351	±	50	9594	±	268	2736	±	136	6955	±	378	7902	±	474	468	±	10	682	±	13	158	±	18
	II/III	MWM_{CG}	943	±	80	805	±	55	1253	±	54	10073	±	773	2891	±	252	9655	±	356	7283	±	524	428	±	17	394	±	19	145	±	15
		MWM_{TMZ}	1005	±	92	662	±	48	1328	±	61	8033	±	100	2596	±	148	9914	±	388	6799	±	374	564	±	13	542	±	28	161	±	11
	V	MWM_{CG}	987	±	94	1105	±	105	1277	±	79	8693	±	713	2450	±	246	9707	±	332	6497	±	478	451	±	28	304	±	10	171	±	16

	VI	MWM_{TMZ}	1048	±	142	938	±	111	1369	±	61	7000	±	190	2311	±	75	9391	±	321	5657	±	334	536	±	16	435	±	28	180	±	14
		MWM_{CG}	953	±	69	1352	±	120	1117	±	115	7854	±	586	1947	±	155	9303	±	492	6191	±	400	488	±	40	324	±	24	206	±	20
		MWM_{TMZ}	1096	±	152	1216	±	141	1285	±	66	6211	±	210	1886	±	133	8618	±	229	6055	±	266	585	±	14	402	±	32	244	±	22
Olfactory tubercle																																
	I	MWM_{CG}	416	±	58	275	±	18	205	±	76	7981	±	204	1359	±	188	2779	±	185	3790	±	327	181	±	17	460	±	49	5767	±	235
		MWM_{TMZ}	498	±	63	342	±	95	292	±	71	7882	±	286	1027	±	113	2459	±	254	2241	±	126	150	±	13	520	±	45	4524	±	86
	II	MWM_{CG}	733	±	56	956	±	65	569	±	65	8318	±	383	1655	±	215	4740	±	394	6038	±	440	213	±	14	596	±	66	7237	±	168
		MWM_{TMZ}	819	±	106	1057	±	147	633	±	47	7622	±	374	1401	±	120	4262	±	424	3669	±	198	217	±	19	751	±	57	6568	±	120
	III	MWM_{CG}	859	±	66	1268	±	61	764	±	40	6513	±	408	1290	±	204	5572	±	356	4529	±	338	236	±	22	703	±	58	6254	±	253
		MWM_{TMZ}	687	±	59	1170	±	117	690	±	34	6579	±	466	1212	±	106	5721	±	390	3520	±	151	244	±	20	806	±	60	5454	±	199

Supp. Tab. 34: Statistical analysis of the comparison of layer-specific receptor concentrations of MWM_{CG} versus MWM_{TMZ}

Significant differences between receptor densities between the olfactory layers for trained mice (MWM_{CG}) with intact adult neurogenesis versus trained mice with suppressed adult neurogenesis (MWM_{TMZ}). Each receptor type was tested with non-parametric Mann-Whitney-U test. The percentage difference in absolute receptor concentrations (first column), sum of the ranks (W, middle column), p-value (right column).

MWM_{CG} | MWM_{TMZ}	AMPA			Kainate			NMDA			$mGlu_{2/3}$			$GABA_A$		
	%	*W*	*p-value*	%	*W*	*p-value*	%	*W*	*p-value*	%	*W*	*p-value*	%	*W*	*p-value*
MOB gr	11,41	101,00	0,80	3,67	102,00	0,85	9,39	68,00	0,52	-5,12	92,00	0,35	-9,15	75,00	0,39
MOB ipl	14,20	95,00	0,48	-3,10	101,00	0,80	33,36	49,00	0,00	-16,09	42,00	0,04	-20,62	50,00	0,04
MOB mi	2,99	104,00	0,97	-2,39	100,00	0,74	9,89	62,00	0,37	-11,33	87,00	0,19	-15,09	44,00	0,11
MOB opl	9,74	95,00	0,48	6,06	98,00	0,63	15,72	65,00	0,08	-5,26	98,00	0,63	-12,57	49,00	0,19
MOB gl	15,31	90,00	0,28	3,31	104,00	0,97	-4,09	97,00	0,84	-2,30	98,00	0,91	-28,96	72,00	0,02
MOB onl	61,64	81,00	0,08	-18,81	79,00	0,05	-18,68	72,00	0,18	-18,50	85,00	0,14	-26,66	73,00	0,02
AOB gr	11,51	95,00	0,48	4,67	92,00	0,35	44,24	52,00	0,47	-18,01	85,00	0,14	66,46	66,00	0,17
AOB mi	-28,05	73,00	0,02	-6,30	95,00	0,48	-14,28	80,00	0,67	-4,98	64,00	0,32	-14,21	70,00	0,54
AOB gl	-12,74	94,00	0,44	-34,00	81,00	0,08	-15,28	68,00	0,07	-39,40	75,00	0,02	-35,77	87,00	0,19
AON pe	21,09	56,00	0,08	-8,75	87,50	0,19	-4,47	96,00	0,78	1,12	100,00	1,00	-1,56	98,50	0,91
AON m	16,41	94,00	0,44	6,62	96,50	0,53	12,44	78,00	0,36	-14,41	80,00	0,45	-2,18	99,00	0,68
AON d	-7,34	96,00	0,53	5,95	100,00	0,74	21,35	64,00	0,04	-26,74	59,00	0,01	-28,32	55,50	0,01
AON pv	18,95	83,00	0,11	20,12	68,00	0,01	2,46	89,00	0,97	-5,28	100,00	0,74	-4,91	94,00	0,44
AON l	2,06	91,00	0,32	12,33	82,00	0,09	33,62	54,00	0,00	-14,53	86,00	0,28	-12,97	95,00	0,48
TTd I	-10,95	92,50	0,35	5,58	104,50	0,97	-7,69	93,00	0,60	-16,76	87,00	0,19	-23,00	82,00	0,09
TTd II	-2,24	100,50	0,74	13,70	93,00	0,39	5,97	65,00	0,36	-5,83	101,00	0,80	-26,58	81,00	0,08
TTd III	3,51	102,50	0,85	20,56	87,00	0,19	35,53	60,00	0,01	-8,78	97,00	0,58	-26,15	85,00	0,14
TTd IV	-5,81	104,50	0,97	14,78	87,00	0,19	14,56	77,50	0,32	-21,60	90,00	0,28	-28,52	86,00	0,17

TTv I	-16,05	75,50	0,02	29,03	100,00	0,74	-33,00	83,00	0,18	2,10	100,00	1,00	-7,49	97,00	0,58
TTv II	0,67	92,50	0,35	15,91	100,00	0,74	-3,73	95,00	0,72	-0,76	101,00	0,80	-12,64	91,00	0,32
TTv III	-3,00	102,00	0,85	-5,03	91,00	0,32	-16,70	69,00	0,02	11,51	100,00	0,74	-4,82	101,00	0,80
OT I	19,56	94,50	0,44	24,00	97,00	0,58	42,25	81,00	0,50	-1,24	83,00	0,60	-24,40	74,00	0,02
OT II	11,73	101,00	0,80	10,56	96,00	0,53	11,19	81,00	0,50	-8,37	68,00	0,24	-15,35	79,00	0,05
OT III	-19,97	84,00	0,12	-7,71	96,00	0,53	-9,71	68,00	0,24	1,00	92,00	0,83	-6,00	99,00	0,68
DP I	24,01	72,00	0,01	6,31	97,00	0,58	20,50	81,00	0,50	-17,31	52,00	0,03	-15,37	89,00	0,25
DP II/III	2,80	97,00	0,58	-6,04	103,00	0,91	20,15	76,00	0,28	-6,11	94,00	0,44	-13,91	92,00	0,35
DP V	45,39	63,00	0,00	-10,41	97,00	0,58	23,65	70,00	0,11	-5,31	98,00	0,63	-11,38	100,00	0,74
DP VI	-0,01	98,50	0,63	-16,60	91,00	0,32	-17,34	89,00	0,40	-37,82	61,00	0,00	-17,14	95,00	0,48
PIR I	-21,71	85,00	0,14	-29,77	77,00	0,04	0,53	99,00	0,97	4,46	65,00	0,54	-10,85	87,50	0,19
PIR II	-20,20	71,00	0,01	-4,71	103,50	0,91	-1,17	86,00	0,78	-15,50	76,00	0,03	-11,96	92,00	0,35
PIR III	10,09	92,50	0,35	-2,52	104,50	0,97	-0,60	100,00	1,00	-27,11	57,00	0,00	-8,53	73,00	0,18
ENT I I	-1,18	102,00	0,85	0,10	97,50	0,58	9,97	53,00	0,36	4,51	94,00	0,44	-6,08	89,00	0,25
ENT I II	11,38	95,00	0,48	6,28	99,00	0,68	14,91	58,00	0,12	2,13	86,00	0,28	-4,12	89,00	0,25
ENT I III	-1,03	98,00	0,63	7,68	95,00	0,48	15,54	63,00	0,09	4,03	95,00	0,48	-1,56	87,00	0,19
ENT I IV	-7,50	87,00	0,19	11,16	90,00	0,28	8,33	82,00	0,55	-0,98	86,00	0,78	-4,93	102,00	0,85
ENT I V	-22,21	68,00	0,00	6,21	96,00	0,53	9,32	76,00	0,28	-7,37	83,00	0,60	9,42	99,00	0,68
ENT I VIa	0,11	103,00	0,91	9,74	92,00	0,35	13,53	41,00	0,03	-10,00	77,00	0,32	14,20	103,00	0,91
ENT I VIb	-0,22	104,00	0,97	3,08	104,00	0,97	-12,79	75,00	0,04	-13,98	78,00	0,36	11,18	82,50	0,55
ENT m I	11,75	95,50	0,48	30,63	80,00	0,06	7,75	73,00	0,83	8,11	94,00	0,66	1,44	90,00	0,28
ENT m II	38,94	85,00	0,14	7,57	94,50	0,44	17,36	87,00	0,84	8,01	94,00	0,44	2,09	85,00	0,14
ENT m III	19,06	89,00	0,40	-3,43	103,00	0,91	20,72	67,00	0,11	2,47	104,00	0,97	-0,95	92,00	0,35
ENT m IV	15,43	91,00	0,32	-16,57	90,00	0,28	15,14	77,00	0,32	3,97	101,00	0,80	2,54	89,00	0,97
ENT m V	1,41	100,00	0,74	-0,62	93,00	0,90	11,50	82,00	0,55	1,56	102,00	0,85	-3,78	103,00	0,91
ENT m VI	-8,23	96,50	0,53	24,23	83,00	0,11	11,94	79,00	0,40	-2,94	105,00	1,00	-4,27	101,00	0,80

ORB m I	16,87	91,00	0,32	-19,24	82,00	0,09	-12,42	59,00	0,24	-21,56	80,00	0,06	-9,12	104,00	0,97
ORB m II	2,75	95,00	0,48	-24,00	71,00	0,01	-1,22	98,00	0,91	-18,71	66,00	0,05	-10,10	93,00	0,39
ORB m II/III	4,50	101,00	0,80	-25,94	83,00	0,11	20,95	66,00	0,05	-6,25	81,00	0,50	-4,43	78,00	0,36
ORB m V	10,04	94,00	0,44	-23,29	80,00	0,06	42,87	57,00	0,01	-19,66	87,00	0,19	-8,72	96,00	0,53
ORB m VIa	14,77	99,00	0,68	-11,38	96,00	0,53	20,73	66,00	0,41	-11,47	81,00	0,50	-4,27	91,00	0,32
ORB vl I	14,58	99,00	0,68	-1,56	70,00	0,63	30,70	62,00	0,04	-11,39	90,00	0,28	-0,86	97,00	0,58
ORB vl II/III	0,53	104,00	0,97	-10,41	89,00	0,25	20,83	39,00	0,00	-14,82	73,00	0,18	-10,75	97,00	0,58
ORB vl V	2,76	100,00	0,74	-12,43	87,00	0,19	37,44	58,50	0,01	-17,27	82,00	0,09	-13,52	101,00	0,80
ORB vl VIa	5,47	104,00	0,97	-6,54	101,00	0,80	27,51	67,00	0,07	-17,95	87,00	0,19	-14,09	72,00	0,76
ORB l I	-5,34	97,00	0,58	5,63	97,00	0,58	14,66	79,00	0,40	-27,42	52,00	0,01	-12,71	90,00	0,28
ORB l II/III	6,56	95,00	0,48	-17,81	83,00	0,11	5,95	60,00	0,28	-20,25	66,00	0,05	-10,19	93,00	0,39
ORB l V	6,23	103,00	0,91	-15,17	88,00	0,22	7,22	82,00	0,55	-19,47	86,00	0,17	-5,65	90,00	0,28
ORB l VIa	15,05	103,00	0,91	-10,00	93,00	0,39	15,06	78,00	0,36	-20,93	80,00	0,06	-3,15	81,00	0,08
MWM_{CG} | MWM_{TMZ}	$GABA_{A(BZ)}$			$GABA_B$			α_1			α_2			$D_{1/5}$		
	%	*W*	*p-value*	%	*W*	*p-value*	%	*W*	*p-value*	%	*W*	*p-value*	%	*W*	*p-value*
MOB gr	9,84	97,00	0,58	-10,99	73,00	0,03	6,20	94,00	0,44	33,32	80,00	0,06	-14,36	87,50	0,19
MOB ipl	5,48	61,00	0,51	-16,40	74,00	0,02	25,75	74,00	0,02	50,74	56,50	0,00	-4,41	96,00	0,53
MOB mi	7,34	77,00	0,49	-9,77	90,00	0,28	17,69	79,00	0,05	58,56	62,00	0,02	0,81	102,00	0,85
MOB opl	2,97	100,00	0,74	-8,08	78,00	0,04	15,94	82,00	0,09	27,43	77,00	0,07	-3,69	102,50	0,85
MOB gl	0,21	71,00	0,96	-11,98	66,00	0,00	26,66	56,00	0,00	32,01	74,00	0,02	14,63	91,00	0,32
MOB onl	-1,08	60,00	0,81	-50,12	59,00	0,00	13,61	77,00	0,07	-6,37	99,50	0,68	5,25	102,00	0,85
AOB gr	-23,24	65,00	0,80	7,07	47,00	0,13	-10,74	70,00	0,11	-54,25	57,00	0,10	24,05	91,00	0,32
AOB mi	22,43	30,00	0,01	-19,07	62,00	0,00	17,94	87,00	0,19	37,26	81,00	0,13	-15,36	83,50	0,11
AOB gl	-1,84	68,00	1,00	86,30	28,00	0,00	-0,03	105,00	1,00	15,07	70,00	0,54	-22,91	92,00	0,35
AON pe	3,36	96,00	0,53	-4,37	68,00	0,41	36,46	78,00	0,04	20,34	83,00	0,18	-11,55	88,00	0,22
AON m	-22,41	75,00	0,02	-0,03	75,00	0,92	8,24	96,00	0,53	33,77	47,00	0,03	-23,43	84,00	0,12

AON d	-1,58	72,00	0,76	16,03	60,00	0,02	17,19	62,00	0,04	54,48	47,00	0,00	-9,08	94,50	0,44
AON pv	-18,52	88,00	0,22	11,05	67,00	0,11	18,29	74,00	0,21	40,92	49,00	0,00	-22,41	84,00	0,12
AON l	8,80	90,00	0,28	1,92	77,00	0,49	-6,17	99,00	0,68	28,32	50,00	0,00	-22,88	78,00	0,04
TTd I	-2,94	83,00	0,54	-4,93	63,00	0,03	24,85	76,50	0,03	-3,35	69,00	0,82	-0,84	99,00	0,68
TTd II	-10,14	79,00	0,10	6,83	79,00	0,05	27,85	70,00	0,01	9,41	58,00	0,33	10,55	95,50	0,48
TTd III	-12,84	64,00	0,06	-5,13	88,50	0,22	20,19	74,00	0,02	7,69	63,00	0,27	20,13	87,00	0,19
TTd IV	8,01	96,00	0,53	-6,11	83,00	0,11	20,89	55,00	0,07	15,88	53,00	0,04	4,98	103,00	0,91
TTv I	3,97	87,00	0,84	-34,70	55,00	0,00	-7,40	71,50	0,37	25,48	76,00	0,44	12,87	99,00	0,68
TTv II	-7,32	69,00	0,16	-24,83	58,00	0,00	13,09	77,00	0,12	19,30	79,00	0,40	1,53	100,00	0,74
TTv III	-7,84	83,00	0,18	-24,85	58,00	0,00	18,13	77,00	0,12	1,08	92,00	0,83	-1,78	103,50	0,91
OT I	-11,50	72,00	0,26	-40,86	61,00	0,00	-17,31	90,00	0,28	13,10	96,00	0,53	-21,56	58,00	0,00
OT II	-10,09	97,00	0,58	-39,23	57,00	0,00	2,07	104,00	0,97	25,88	86,00	0,17	-9,25	73,50	0,02
OT III	2,67	100,00	0,74	-22,28	65,00	0,01	3,24	103,00	0,91	14,54	90,00	0,28	-12,79	71,00	0,01
DP I	0,97	104,00	0,97	-8,17	59,00	0,38	29,76	87,50	0,19	2,06	87,00	0,84	13,91	89,00	0,25
DP II/III	6,10	83,00	0,60	-8,08	83,00	0,32	11,13	82,00	0,16	18,03	89,00	0,25	-11,02	93,00	0,39
DP V	5,86	89,00	0,25	4,71	102,00	0,85	36,30	70,00	0,01	26,43	44,00	0,01	-22,53	83,00	0,11
DP VI	2,91	63,00	1,00	-4,74	101,00	0,80	42,75	58,00	0,01	25,65	69,00	0,10	-6,52	97,00	0,58
PIR I	-2,45	100,00	1,00	-8,22	65,00	0,25	34,99	65,00	0,00	3,62	98,00	0,63	-0,30	103,50	0,91
PIR II	-2,59	100,00	1,00	-8,15	88,00	0,22	30,51	71,00	0,01	21,39	81,00	0,08	-3,02	104,00	0,97
PIR III	8,50	86,00	0,17	5,62	96,00	0,53	13,54	85,00	0,24	11,12	55,00	0,11	4,13	91,50	0,32
ENT I I	-14,54	69,00	0,16	9,73	56,00	0,23	-16,11	83,00	0,11	8,76	97,00	0,58	-25,54	74,00	0,02
ENT I II	-8,76	72,00	0,16	23,80	47,00	0,01	-3,80	103,50	0,91	10,74	81,00	0,08	-32,49	71,00	0,01
ENT I III	-0,53	90,00	1,00	10,58	87,00	0,19	15,56	85,00	0,14	24,15	67,00	0,00	-18,25	83,00	0,11
ENT I IV	10,84	103,00	0,91	15,79	79,00	0,05	3,52	97,00	0,58	21,76	59,00	0,00	-13,04	89,50	0,25
ENT I V	8,79	93,00	0,39	14,81	83,00	0,11	4,94	99,00	0,68	16,09	72,50	0,04	-13,78	87,00	0,19

ENT l VIa	7,60	79,00	0,40	14,62	72,00	0,01	3,64	87,50	0,84	21,04	72,00	0,02	-25,23	84,00	0,12
ENT l VIb	11,53	84,00	0,12	3,25	91,00	0,32	4,90	94,00	0,44	29,32	49,00	0,02	-9,75	102,00	0,85
ENT m l	-18,59	85,00	0,14	-1,25	92,00	0,83	4,80	82,00	0,55	14,16	94,00	0,66	6,90	99,00	0,68
ENT m II	-8,82	54,00	0,09	-15,82	63,00	0,00	7,47	97,00	0,58	-5,68	81,00	0,73	-8,01	102,00	0,85
ENT m III	-8,05	58,00	0,12	-8,51	79,00	0,05	2,22	99,50	0,97	23,05	49,00	0,05	-17,58	102,00	0,85
ENT m IV	-2,83	67,00	0,67	-3,26	86,00	0,28	1,09	104,00	0,97	11,92	71,00	0,37	-18,42	99,00	0,68
ENT m V	9,35	93,00	0,60	-5,92	95,00	0,48	10,09	96,00	0,53	24,98	60,00	0,05	-9,06	99,00	0,68
ENT m VI	8,51	92,00	0,55	7,84	71,00	0,13	19,23	63,00	0,05	7,92	50,50	0,81	-2,23	103,00	0,91
ORB m l	5,53	95,00	0,48	-20,53	79,00	0,05	9,53	90,50	0,45	13,07	74,00	0,21	20,20	91,00	0,32
ORB m II	3,81	100,00	0,74	-11,94	89,00	0,25	7,43	92,50	0,35	30,25	68,00	0,08	9,19	96,00	0,53
ORB m II/III	5,69	97,00	0,58	5,97	95,00	0,48	14,54	78,00	0,04	36,10	64,50	0,00	-5,92	99,00	0,68
ORB m V	-1,99	100,00	0,74	5,89	96,00	0,53	13,24	85,00	0,24	33,54	48,00	0,01	-15,04	102,00	0,85
ORB m VIa	-8,03	87,00	0,19	-0,86	104,00	0,97	16,45	62,00	0,04	45,26	68,00	0,00	-3,39	96,50	0,53
ORB vl l	-1,12	102,00	0,85	-6,99	97,00	0,58	29,07	68,00	0,01	35,73	76,00	0,03	-8,55	89,00	0,25
ORB vl II/III	10,75	59,00	0,15	-1,38	102,00	0,85	13,59	88,00	0,22	59,59	60,00	0,00	-19,19	82,50	0,09
ORB vl V	-6,74	82,00	0,16	1,45	103,00	0,91	12,63	76,00	0,28	71,34	65,00	0,00	-7,20	101,00	0,80
ORB vl VIa	-15,77	67,00	0,01	3,54	102,00	0,85	22,57	76,00	0,03	22,75	67,00	0,03	6,48	97,50	0,58
ORB l l	-13,37	79,00	0,05	-7,48	90,00	0,70	9,86	98,50	0,63	27,68	64,00	0,00	-5,94	90,00	0,28
ORB l II/III	2,68	98,00	0,63	-6,64	95,00	0,48	31,87	58,00	0,00	37,40	63,00	0,00	11,22	91,50	0,32
ORB l V	-3,25	93,00	0,39	-12,93	91,00	0,32	18,97	78,00	0,04	42,76	66,00	0,00	5,26	95,00	0,48
ORB l VIa	-7,36	90,00	0,28	-2,20	86,00	0,78	19,90	77,00	0,04	24,39	83,00	0,11	18,67	89,00	0,25

Supp. Tab. 35: Region-specific receptor concentrations of CG versus MWM_{TMZ}

Neurotransmitter receptor densities (fmol/mg protein) in different regions of the mouse olfactory system (Mean ± SEM) of control mice (CG) and trained mice with suppressed adult neurogenesis (MWM_{TMZ}). For pairwise comparisons between regions see further Supp. Tab. 36.

CG | MWM_{TMZ}		AMPA			Kainate			NMDA			$mGlu_{2/3}$			$GABA_A$		
MOB	CG	727	±	54	1281	±	95	954	±	158	2180	±	121	803	±	93
	MWM_{TMZ}	742	±	77	1357	±	55	442	±	19	2961	±	117	1475	±	214
AOB	CG	909	±	88	1328	±	94	1203	±	156	3948	±	376	950	±	212
	MWM_{TMZ}	892	±	92	1327	±	75	596	±	32	4746	±	426	2036	±	221
AON	CG	1044	±	87	1432	±	69	1445	±	189	2365	±	165	566	±	73
	MWM_{TMZ}	1449	±	118	1329	±	61	1264	±	50	4867	±	383	430	±	28
TTd	CG	1151	±	58	1356	±	124	1878	±	213	2977	±	212	906	±	64
	MWM_{TMZ}	1216	±	93	1553	±	117	1471	±	87	5283	±	339	1171	±	122
TTv	CG	1361	±	86	1022	±	114	1716	±	125	2825	±	222	788	±	85
	MWM_{TMZ}	1123	±	48	1266	±	135	910	±	83	5723	±	713	1222	±	156
Epd	CG	789	±	51	1480	±	75	1239	±	129	1836	±	224	695	±	61
	MWM_{TMZ}	852	±	100	1150	±	82	793	±	91	3797	±	260	886	±	102
OT	CG	1079	±	88	964	±	70	1638	±	131	3964	±	346	853	±	77
	MWM_{TMZ}	668	±	70	856	±	104	529	±	44	7551	±	324	1213	±	102
DP	CG	1069	±	62	1624	±	95	1909	±	255	3442	±	155	1048	±	78
	MWM_{TMZ}	1259	±	59	1322	±	111	1386	±	111	6622	±	356	2054	±	149
PIR	CG	1060	±	41	785	±	48	1821	±	162	3328	±	207	1034	±	68
	MWM_{TMZ}	890	±	37	698	±	37	1023	±	77	6765	±	301	1368	±	64
ENTl	CG	1664	±	59	1054	±	32	3037	±	224	3070	±	198	1297	±	84
	MWM_{TMZ}	1127	±	66	1356	±	72	1791	±	65	6699	±	308	1632	±	83
ENTm	CG	1580	±	102	1040	±	71	2091	±	301	3081	±	268	1190	±	98

ORBl	MWM_{TMZ}	1195	±	109	1072	±	86	1702	±	105	6947	±	328	1590	±	83
	CG	1089	±	83	1095	±	164	2292	±	278	3867	±	360	1553	±	105
ORBvl	MWM_{TMZ}	1047	±	111	862	±	78	1340	±	47	7537	±	274	2379	±	99
	CG	1034	±	79	995	±	140	2101	±	236	4024	±	511	1520	±	162
ORBm	MWM_{TMZ}	1111	±	110	843	±	59	1487	±	71	8182	±	284	2539	±	124
	CG	1100	±	75	1039	±	175	2168	±	209	3983	±	524	1393	±	172
	MWM_{TMZ}	1272	±	102	890	±	53	1481	±	77	7972	±	266	2235	±	131
CG | MWM_{TMZ}		$GABA_{A(BZ)}$			$GABA_B$			α_1			α_2			$D_{1/5}$		
MOB	CG	3867	±	577	2246	±	71	547	±	33	497	±	32	61	±	6
	MWM_{TMZ}	4739	±	349	2078	±	48	584	±	25	351	±	20	89	±	10
AOB	CG	6409	±	664	3617	±	288	675	±	50	547	±	69	100	±	15
	MWM_{TMZ}	6346	±	867	5285	±	274	703	±	41	318	±	27	98	±	13
AON	CG	2038	±	181	4223	±	345	338	±	19	1809	±	160	171	±	29
	MWM_{TMZ}	3238	±	176	6017	±	92	339	±	13	2252	±	103	112	±	11
TTd	CG	3662	±	331	4736	±	428	308	±	36	1589	±	141	357	±	49
	MWM_{TMZ}	5718	±	287	7295	±	112	334	±	13	1854	±	82	230	±	14
TTv	CG	3214	±	272	4316	±	442	321	±	45	1377	±	177	315	±	90
	MWM_{TMZ}	5083	±	198	5321	±	156	252	±	9	1251	±	123	198	±	20
Epd	CG	2791	±	257	4059	±	211	238	±	23	1032	±	49	888	±	95
	MWM_{TMZ}	4747	±	377	3902	±	95	324	±	17	1043	±	44	226	±	24
OT	CG	3048	±	403	2995	±	277	204	±	25	770	±	107	5340	±	439
	MWM_{TMZ}	4286	±	297	3143	±	98	203	±	16	692	±	52	5533	±	164
DP	CG	4125	±	340	5048	±	674	317	±	52	1031	±	94	360	±	44
	MWM_{TMZ}	7465	±	269	6019	±	304	423	±	31	1445	±	92	234	±	22
PIR	CG	3961	±	243	4853	±	158	448	±	40	1027	±	80	242	±	28
	MWM_{TMZ}	6541	±	248	5170	±	199	536	±	24	855	±	40	137	±	6

ENTl	CG	3627	±	221	5894	±	254	314	±	19	1771	±	137	345	±	26
	MWM_{TMZ}	7149	±	421	9753	±	292	409	±	12	1864	±	39	406	±	20
ENTm	CG	3553	±	487	6201	±	200	304	±	26	1770	±	136	330	±	17
	MWM_{TMZ}	6113	±	792	8701	±	187	419	±	26	1887	±	125	474	±	39
ORBl	CG	4894	±	323	5925	±	392	502	±	38	650	±	22	175	±	43
	MWM_{TMZ}	8720	±	277	6572	±	327	538	±	10	531	±	35	186	±	12
ORBvl	CG	4762	±	406	5909	±	461	495	±	48	570	±	24	131	±	28
	MWM_{TMZ}	8803	±	317	7680	±	530	610	±	15	572	±	40	154	±	10
ORBm	CG	4269	±	529	5003	±	404	513	±	67	564	±	22	211	±	33
	MWM_{TMZ}	8351	±	352	7846	±	509	614	±	16	531	±	35	227	±	24

Supp. Tab. 36: Statistical analysis of the comparison of region-specific receptor concentrations of CG versus MWM_{TMZ}

Significant differences between receptor densities between the olfactory regions of control mice (CG) and trained mice with suppressed adult neurogenesis (MWM_{TMZ}). Each receptor type was tested with non-parametric Mann-Whitney-U test. The percentage difference in absolute receptor concentrations (first column), p-value (middle column), and correlation coefficient r (limits: weak (0.1-0.3), medium (0.3-0.5), and strong (> 0.5) to evaluate the effect size (right column).

CG | MWM_{TMZ}	AMPAR			kainateR			NMDAR			$mGlu_{2/3}R$			$GABA_AR$		
	[%]	*p*	[r]	[%]	*p*	[r]	[%]	*p*	[r]	[%]	*p*	[r]	[%]	*p*	[r]
MOB | MOB	2,04	0.971	-	5,92	0.393	-	-53,66	**0.007**	0.608	35,85	**< .001**	0.811	83,77	**0.002**	0.659
AOB | AOB	-1,78	1.000	-	-0,13	0.791	-	-50,48	**0.002**	0.694	20,23	0.121	-	114,24	**0.006**	0.625
AOC | AOC	38,83	**0.011**	0.557	-7,19	0.631	-	-12,53	0.734	-	105,83	**< .001**	0.845	-24,02	**0.028**	0.499
TTd | TTd	5,57	0.579	-	14,47	0.315	-	-21,65	0.143	-	77,49	**< .001**	0.828	29,34	0.104	-
TTv | TTv	-17,53	**0.011**	0.574	23,91	0.481	-	-46,97	**< .001**	0.811	102,59	**< .001**	0.760	54,96	**0.029**	0.490
EPd | EPd	7,90	0.631	-	-22,27	**0.005**	0.608	-36,00	**0.007**	0.591	106,83	**< .001**	0.845	27,48	0.212	-
OT | OT	-38,09	**0.002**	0.676	-11,15	0.684	-	-67,72	**< .001**	0.848	90,47	**< .001**	0.845	42,31	**0.019**	0.523
DP | DP	17,85	0.059	-	-18,60	0.075	-	-27,42	0.075	-	92,38	**< .001**	0.845	96,05	**< .001**	0.828
PIR | PIR	-16,03	**0.006**	0.617	-11,09	0.241	-	-43,84	**0.001**	0.693	103,25	**< .001**	0.845	32,27	**0.003**	0.642
ENTl | ENTl	-32,29	**< .001**	0.828	28,65	**0.002**	0.7101	-41,01	**< .001**	0.829	118,23	**< .001**	0.845	25,87	**0.007**	0.591
ENTm | ENTm	-24,37	**0.011**	0.574	3,04	0.734	-	-18,59	0.140	-	125,45	**< .001**	0.845	33,56	**0.002**	0.659
ORBl | ORBl	-3,92	0.162	-	-21,33	0.063	-	-41,52	**0.002**	0.694	94,92	**< .001**	0.848	53,15	**0.001**	0.693
ORBvl | ORBvl	7,42	0.791	-	-15,22	0.075	-	-29,21	**0.014**	0.558	103,33	**< .001**	0.851	67,02	**< .001**	0.794
ORBm | ORBm	15,64	0.677	-	-14,37	**0.026**	0.507	-31,68	**0.003**	0.677	100,13	**< .001**	0.856	60,44	**< .001**	0.829
CG | MWM_{TMZ}	$GABA_{A(BZ)}R$			$GABA_BR$			α_1R			α_2R			$D_{1/5}R$		
	[%]	*p*	[r]	[%]	*p*	[r]	[%]	*p*	[r]	[%]	*p*	[r]	[%]	*p*	[r]
MOB | MOB	22,55	0.052	-	-3,11	0.075	-	6,64	0.273	-	-29,36	**0.003**	0.676	46,68	**0.017**	0.541
AOB | AOB	-0,99	0.971	-	46,12	0.002	-	4,02	0.910	-	-41,91	**0.011**	0.557	-1,95	0.344	-
AOC | AOC	58,89	**< .001**	0.726	42,48	**< .001**	0.845	0,35	0.940	-	24,51	**0.043**	0.456	-34,11	**0.038**	0.473
TTd | TTd	56,16	**< .001**	0.845	54,02	**< .001**	0.845	8,33	0.529	-	16,72	0.105	-	-35,54	0.082	-
TTv | TTv	58,14	**< .001**	0.845	23,29	**0.038**	0.473	-21,54	0.571	-	-9,09	0.684	-	-37,01	0.450	-
EPd | EPd	70,10	**< .001**	0.777	-3,85	0.460	-	35,88	**0.005**	0.642	1,09	0.791	-	-74,55	**< .001**	0.845

OT | OT	40,64	**0.035**	0.473	4,97	0.384	-	-0,48	0.850	-	-10,13	0.384	-	3,61	0.971	-
DP | DP	80,97	**< .001**	0.845	19,23	0.393	-	33,46	0.121	-	40,25	**0.005**	0.608	-34,88	**0.014**	0.558
PIR | PIR	65,15	**< .001**	0.828	6,52	0.315	-	19,45	0.089	-	-16,74	**0.035**	0.473	-43,18	**0.001**	0.744
ENTl | ENTl	97,10	**< .001**	0.845	65,46	**< .001**	0.845	30,20	**0.001**	0.693	5,27	1.000	-	17,94	0.121	-
ENTm | ENTm	72,04	**0.006**	0.625	40,33	**< .001**	0.845	37,97	**0.005**	0.642	6,60	0.315	-	43,77	**0.017**	0.541
ORBl | ORBl	78,17	**< .001**	0.846	10,92	**< .001**	0.814	7,16	**0.045**	0.457	-18,30	0.570	-	6,09	0.343	-
ORBvl | ORBvl	84,86	**< .001**	0.846	29,98	**0.017**	0.541	23,35	0.054	-	0,30	0.705	-	17,64	0.103	-
ORBm | ORBm	95,61	**< .001**	0.846	56,82	0.104	-	19,67	0.211	-	-5,86	**< .001**	0.829	7,21	0.383	-

Supp. Tab. 37: Mean receptor densities of olfactory layers (CG versus MWM_{TMZ}).

Layer-specific absolute receptor densities of the subregions of the olfactory system (mean ± SEM) for control mice (CG) and trained mice with suppressed adult neurogenesis (MWM_{TMZ}). For pairwise comparisons between regions see further Supp. Tab. 38.

CG | MWM_{TMZ}		Receptor (fmol/mg protein)									
		AMPA	kainate	NMDA	$mGlu_{2/3}$	$GABA_A$	$GABA_{A(BZ)}$	$GABA_B$	α_1	α_2	$D_{1/5}$
Main olfactory bulb											
gr	CG	764 ± 55	911 ± 72	823 ± 111	1697 ± 32	260 ± 42	976 ± 67	2062 ± 119	447 ± 22	1027 ± 31	49 ± 4
	MWM_{TMZ}	711 ± 40	1118 ± 101	366 ± 19	2725 ± 144	351 ± 31	1525 ± 49	1873 ± 43	424 ± 28	562 ± 74	81 ± 5
ipl	CG	719 ± 40	1311 ± 114	796 ± 132	1876 ± 64	375 ± 58	1025 ± 96	1920 ± 77	406 ± 23	442 ± 26	57 ± 6
	MWM_{TMZ}	729 ± 58	1596 ± 82	381 ± 18	3735 ± 185	478 ± 38	2563 ± 64	1544 ± 76	432 ± 31	191 ± 18	85 ± 4
mi	CG	678 ± 35	1087 ± 88	886 ± 168	1686 ± 33	303 ± 42	950 ± 73	1971 ± 75	404 ± 20	588 ± 44	49 ± 7
	MWM_{TMZ}	699 ± 61	1527 ± 79	364 ± 18	3303 ± 167	564 ± 44	2190 ± 60	1711 ± 80	422 ± 29	251 ± 38	85 ± 3
opl	CG	665 ± 31	1567 ± 136	975 ± 161	2369 ± 159	670 ± 86	2578 ± 255	1930 ± 31	572 ± 28	337 ± 29	68 ± 5
	MWM_{TMZ}	697 ± 48	1643 ± 100	479 ± 30	4133 ± 266	981 ± 75	3872 ± 185	1256 ± 51	471 ± 31	212 ± 26	97 ± 3
gl	CG	622 ± 45	1943 ± 155	1684 ± 211	3064 ± 215	2367 ± 336	9695 ± 533	3391 ± 296	1032 ± 92	351 ± 18	79 ± 9
	MWM_{TMZ}	642 ± 55	1674 ± 158	604 ± 33	3811 ± 164	6246 ± 505	14511 ± 201	6603 ± 145	940 ± 42	189 ± 14	100 ± 5
onl	CG	694 ± 97	1025 ± 101	672 ± 101	1986 ± 171	831 ± 96	4308 ± 227	2173 ± 254	381 ± 22	304 ± 29	73 ± 7
	MWM_{TMZ}	374 ± 44	587 ± 31	268 ± 22	1855 ± 155	1320 ± 109	4862 ± 241	1999 ± 189	207 ± 8	158 ± 15	85 ± 4
Accessory olfactory bulb											
gr	CG	942 ± 84	1189 ± 88	1183 ± 183	3320 ± 257	744 ± 214	6982 ± 579	2955 ± 340	621 ± 68	607 ± 95	106 ± 19
	MWM_{TMZ}	821 ± 59	969 ± 48	529 ± 53	4930 ± 228	1471 ± 462	1293 ± 272	2798 ± 122	548 ± 26	512 ± 94	82 ± 6
mi	CG	946 ± 98	1930 ± 45	1553 ± 25	4907 ± 617	1693 ± 312	7090 ± 868	2880 ± 100	1016 ± 67	469 ± 98	107 ± 21
	MWM_{TMZ}	1196 ± 82	2051 ± 177	650 ± 96	9180 ± 355	2078 ± 298	12455 ± 778	3033 ± 128	921 ± 79	259 ± 36	121 ± 13
gl	CG	661 ± 283	785 ± 17	1226 ± 167	1298 ± 175	462 ± 150	2910 ± 528	5087 ± 810	400 ± 81	531 ± 127	67 ± 10
	MWM_{TMZ}	1033 ± 73	1582 ± 226	568 ± 33	4215 ± 414	2949 ± 716	6672 ± 388	6037 ± 147	499 ± 80	283 ± 30	118 ± 9
Anterior olfactory cortex											
pe	CG	940 ± 124	1298 ± 29	1124 ± 98	3081 ± 321	825 ± 147	2597 ± 250	3551 ± 505	449 ± 37	1340 ± 219	161 ± 37
	MWM_{TMZ}	1050 ± 66	1026 ± 37	1019 ± 90	5878 ± 465	639 ± 40	4215 ± 189	5957 ± 279	338 ± 36	969 ± 75	146 ± 13
m	CG	1226 ± 81	1327 ± 141	1416 ± 50	2266 ± 208	545 ± 100	2073 ± 224	4608 ± 423	315 ± 10	2169 ± 176	189 ± 34
	MWM_{TMZ}	1400 ± 109	1280 ± 77	1251 ± 133	4763 ± 664	483 ± 45	3500 ± 193	5875 ± 274	325 ± 37	1984 ± 111	161 ± 17
d	CG	1040 ± 112	1454 ± 137	1668 ± 114	2420 ± 194	397 ± 99	1414 ± 146	4389 ± 374	318 ± 24	2296 ± 165	234 ± 69
	MWM_{TMZ}	1516 ± 101	1606 ± 125	1324 ± 84	6361 ± 535	497 ± 33	3121 ± 195	5624 ± 251	244 ± 23	1803 ± 116	143 ± 14
pv	CG	1078 ± 111	1783 ± 138	996 ± 62	1846 ± 115	565 ± 21	1972 ± 294	3629 ± 328	308 ± 22	1925 ± 221	137 ± 36

	MWM_{TMZ}	1406 ± 54	1477 ± 73	1212 ± 124	4960 ± 409	402 ± 53	3605 ± 370	5447 ± 269	239 ± 18	1813 ± 80	136 ± 14
I	CG	1177 ± 120	1433 ± 85	2469 ± 259	3001 ± 484	311 ± 66	2134 ± 186	4602 ± 570	327 ± 20	1925 ± 214	107 ± 4
	MWM_{TMZ}	1476 ± 37	1281 ± 64	1230 ± 97	6834 ± 572	496 ± 32	3057 ± 138	6097 ± 141	320 ± 48	1926 ± 102	125 ± 9
e	CG	910 ± 48	1246 ± 227	799 ± 23	3054 ± 653	991 ± 351	1923 ± 467	3197 ± 584	366 ± 75	1271 ± 240	42 ± 26
	MWM_{TMZ}	1215 ± 79	809 ± 78	1007 ± 148	4822 ± 685	491 ± 83	2758 ± 221	5259 ± 262	309 ± 30	1527 ± 244	141 ± 28
taenia tecta, dorsal											
I	CG	1161 ± 94	994 ± 162	2319 ± 250	3559 ± 357	1003 ± 119	3316 ± 425	4995 ± 333	300 ± 62	1362 ± 186	216 ± 44
	MWM_{TMZ}	1161 ± 80	900 ± 72	1264 ± 170	7133 ± 834	1690 ± 153	5342 ± 87	8146 ± 131	262 ± 19	1270 ± 50	184 ± 19
II	CG	1404 ± 120	1120 ± 98	2210 ± 158	3019 ± 209	888 ± 79	3731 ± 350	4999 ± 570	283 ± 38	1798 ± 135	267 ± 46
	MWM_{TMZ}	1458 ± 78	1263 ± 95	1532 ± 61	6537 ± 693	1702 ± 156	6488 ± 198	7508 ± 114	276 ± 18	1730 ± 84	190 ± 19
III	CG	1100 ± 65	1293 ± 97	2140 ± 219	2554 ± 154	914 ± 83	3967 ± 358	4922 ± 591	302 ± 25	1649 ± 181	372 ± 58
	MWM_{TMZ}	1254 ± 89	1519 ± 150	1288 ± 119	5665 ± 690	1479 ± 151	6364 ± 317	7846 ± 131	284 ± 18	1875 ± 62	210 ± 27
IV	CG	924 ± 64	1843 ± 185	1506 ± 148	2491 ± 199	730 ± 36	3633 ± 310	3377 ± 318	341 ± 43	2000 ± 180	594 ± 92
	MWM_{TMZ}	1173 ± 124	1737 ± 134	1178 ± 136	4938 ± 661	1458 ± 176	5658 ± 352	6497 ± 190	259 ± 11	1901 ± 85	264 ± 27
taenia tecta, ventral											
I	CG	1014 ± 91	699 ± 104	1665 ± 179	2767 ± 327	796 ± 142	2949 ± 375	796 ± 281	288 ± 51	1028 ± 165	201 ± 55
	MWM_{TMZ}	1013 ± 67	559 ± 65	721 ± 128	5706 ± 538	1354 ± 129	4287 ± 226	6683 ± 183	215 ± 8	724 ± 91	150 ± 23
II	CG	1477 ± 105	1067 ± 142	1814 ± 164	2948 ± 282	876 ± 118	3315 ± 334	876 ± 512	318 ± 60	1463 ± 220	251 ± 72
	MWM_{TMZ}	1331 ± 89	1151 ± 60	1125 ± 113	6009 ± 553	1492 ± 88	5851 ± 163	7668 ± 307	248 ± 22	1151 ± 101	189 ± 28
III	CG	1442 ± 93	1299 ± 163	1721 ± 116	2667 ± 174	693 ± 44	3222 ± 257	693 ± 399	338 ± 40	1638 ± 225	492 ± 151
	MWM_{TMZ}	1214 ± 33	1836 ± 61	1397 ± 55	4824 ± 432	1164 ± 68	5721 ± 197	7764 ± 207	246 ± 18	1439 ± 79	238 ± 26
Dorsal peduncular cortex											
I	CG	1092 ± 36	1154 ± 46	2067 ± 173	4126 ± 334	952 ± 93	4188 ± 588	5035 ± 648	265 ± 54	1121 ± 137	253 ± 39
	MWM_{TMZ}	1085 ± 72	997 ± 75	1153 ± 189	8934 ± 491	2292 ± 298	5949 ± 524	8057 ± 411	313 ± 25	1140 ± 79	210 ± 15
II/III	CG	1358 ± 108	1587 ± 135	2677 ± 280	3665 ± 215	1085 ± 90	4273 ± 406	5683 ± 837	343 ± 69	951 ± 65	330 ± 55
	MWM_{TMZ}	1210 ± 93	1571 ± 131	1378 ± 171	8101 ± 645	2484 ± 150	7469 ± 339	7232 ± 442	339 ± 21	1230 ± 118	262 ± 26
V	CG	992 ± 54	1611 ± 119	2245 ± 210	3126 ± 183	1154 ± 82	4364 ± 293	5251 ± 801	374 ± 74	1032 ± 85	348 ± 40
	MWM_{TMZ}	1073 ± 76	1621 ± 135	1183 ± 122	7330 ± 536	2420 ± 163	7861 ± 315	5360 ± 493	319 ± 22	1332 ± 89	274 ± 33
VI	CG	909 ± 90	1860 ± 129	1631 ± 233	2860 ± 122	963 ± 91	3715 ± 328	4224 ± 506	260 ± 34	950 ± 101	509 ± 61
	MWM_{TMZ}	888 ± 56	1560 ± 168	1252 ± 163	7513 ± 512	2307 ± 178	7357 ± 313	4996 ± 232	316 ± 22	1296 ± 98	271 ± 20
Piriform cortex											
I	CG	780 ± 32	580 ± 66	2103 ± 165	4400 ± 283	1169 ± 77	4193 ± 205	4727 ± 141	497 ± 42	832 ± 52	149 ± 18
	MWM_{TMZ}	768 ± 82	537 ± 55	940 ± 55	8867 ± 512	1712 ± 127	6757 ± 124	5577 ± 88	419 ± 30	533 ± 53	119 ± 10
II	CG	1607 ± 53	764 ± 49	1877 ± 190	3380 ± 214	1153 ± 42	3993 ± 259	5382 ± 210	467 ± 52	1116 ± 101	208 ± 21
	MWM_{TMZ}	1154 ± 32	804 ± 53	1142 ± 82	7459 ± 385	1633 ± 117	6792 ± 65	5852 ± 210	433 ± 33	846 ± 43	135 ± 11
III	CG	877 ± 38	977 ± 48	1627 ± 151	2613 ± 154	888 ± 66	3603 ± 143	4518 ± 115	381 ± 37	1159 ± 99	368 ± 51

		MWM_{TMZ}	1044	±	73	976	±	54	999	±	80	7131	±	247	1246	±	79	5914	±	168	4731	±	219	403	±	26	883	±	22	156	±	15
Entorhinal cortex, lateral																															
	I	CG	1066	±	120	407	±	61	2302	±	316	3264	±	325	1150	±	88	3197	±	448	5416	±	419	271	±	16	943	±	84	230	±	33
		MWM_{TMZ}	604	±	65	260	±	45	1309	±	80	8535	±	236	1414	±	149	4982	±	250	8916	±	414	433	±	38	998	±	75	391	±	42
	II	CG	2009	±	116	722	±	48	3401	±	274	3431	±	194	1623	±	66	3868	±	348	6602	±	331	292	±	22	1592	±	156	344	±	43
		MWM_{TMZ}	1154	±	98	545	±	35	1738	±	157	7978	±	289	1888	±	135	6952	±	205	8773	±	502	455	±	33	1584	±	68	505	±	47
	III	CG	2106	±	80	823	±	42	3628	±	281	3380	±	154	1595	±	95	3637	±	250	6719	±	374	279	±	18	1815	±	175	356	±	36
		MWM_{TMZ}	1360	±	95	737	±	51	1921	±	143	7101	±	212	2024	±	136	7190	±	147	10159	±	613	329	±	28	1652	±	60	468	±	39
	IV	CG	1966	±	101	945	±	12	3417	±	215	3242	±	269	1539	±	100	3423	±	151	6514	±	323	267	±	23	2012	±	168	312	±	24
		MWM_{TMZ}	1329	±	95	1021	±	94	1950	±	115	6810	±	400	1836	±	130	7111	±	142	9551	±	572	326	±	18	1821	±	101	447	±	36
	V	CG	1746	±	101	1206	±	74	3330	±	192	3064	±	261	1282	±	95	3371	±	136	6106	±	337	293	±	27	2061	±	168	311	±	33
		MWM_{TMZ}	1354	±	69	1407	±	126	1770	±	106	6290	±	290	1512	±	102	7256	±	147	9200	±	600	341	±	20	1753	±	115	440	±	22
	VIa	CG	1520	±	88	1710	±	112	2781	±	179	2612	±	131	1199	±	82	3928	±	148	5705	±	222	381	±	21	2020	±	135	406	±	45
		MWM_{TMZ}	1269	±	88	2300	±	236	1516	±	58	5977	±	393	1361	±	89	7666	±	159	8052	±	396	439	±	13	1730	±	118	641	±	80
	VIb	CG	1187	±	62	1616	±	100	2123	±	187	1964	±	70	995	±	85	3572	±	207	4258	±	155	430	±	34	1952	±	127	453	±	67
		MWM_{TMZ}	1109	±	113	2625	±	159	1442	±	69	4394	±	395	1173	±	87	6256	±	298	5517	±	220	509	±	32	1457	±	73	645	±	61
Entorhinal cortex, medial																															
	I	CG	1452	±	82	648	±	70	1679	±	253	3201	±	373	1116	±	58	3679	±	602	5815	±	301	271	±	39	941	±	107	212	±	30
		MWM_{TMZ}	576	±	78	293	±	33	1193	±	174	6915	±	751	1329	±	139	5613	±	221	7819	±	646	293	±	20	1071	±	85	388	±	74
	II	CG	1538	±	188	869	±	58	2698	±	163	3512	±	432	1504	±	53	3833	±	691	7038	±	286	302	±	38	1659	±	186	333	±	40
		MWM_{TMZ}	819	±	138	737	±	41	1590	±	265	7595	±	395	1691	±	92	7013	±	146	11511	±	404	384	±	35	1952	±	162	578	±	112
	III	CG	1542	±	194	1065	±	61	2602	±	137	3274	±	349	1599	±	72	3602	±	464	6677	±	272	286	±	26	1938	±	152	385	±	36
		MWM_{TMZ}	1103	±	116	902	±	76	1784	±	205	7172	±	397	1778	±	78	7292	±	227	10520	±	483	409	±	27	1693	±	117	593	±	125
	IV	CG	1564	±	93	1207	±	111	1681	±	300	3117	±	292	1458	±	42	3495	±	486	6478	±	210	259	±	28	2109	±	207	349	±	30
		MWM_{TMZ}	1293	±	50	1273	±	140	1698	±	150	6708	±	474	1754	±	96	7046	±	229	9765	±	560	381	±	30	2014	±	141	579	±	106
	V	CG	1497	±	106	1276	±	96	2383	±	304	3000	±	263	1246	±	88	3544	±	611	5921	±	280	323	±	32	2127	±	146	345	±	23
		MWM_{TMZ}	1385	±	80	1728	±	151	1512	±	192	6369	±	392	1671	±	58	6676	±	215	9119	±	548	419	±	33	1886	±	167	507	±	84
	VI	CG	1501	±	134	1309	±	107	1360	±	155	2375	±	213	905	±	86	3168	±	394	5276	±	471	377	±	31	1651	±	89	375	±	10
		MWM_{TMZ}	1214	±	91	1465	±	172	1225	±	157	5219	±	485	1218	±	74	6650	±	339	6626	±	208	459	±	32	1933	±	89	485	±	74
Orbitofrontal cortex, medial																															
	I	CG	1253	±	75	595	±	114	2741	±	237	4846	±	598	1371	±	201	4362	±	282	5681	±	365	445	±	57	700	±	54	127	±	23
		MWM_{TMZ}	1109	±	115	827	±	70	1251	±	121	11006	±	960	2448	±	126	6365	±	195	10866	±	610	506	±	35	532	±	27	189	±	23
	II	CG	1132	±	87	945	±	220	2365	±	270	4004	±	532	1537	±	231	4519	±	659	5465	±	669	536	±	91	660	±	26	166	±	30
		MWM_{TMZ}	1332	±	191	1005	±	68	1532	±	52	10459	±	904	2650	±	160	8216	±	372	10009	±	587	605	±	31	451	±	34	195	±	23
	II/III	CG	1076	±	44	1063	±	177	2041	±	249	4060	±	755	1362	±	231	4362	±	714	5046	±	429	575	±	84	573	±	34	216	±	52
		MWM_{TMZ}	1323	±	137	1213	±	143	1339	±	72	9293	±	865	2622	±	200	8718	±	353	8164	±	479	613	±	32	378	±	23	235	±	30

	V	CG	995	±	109	1300	±	66	1661	±	160	3387	±	605	1330	±	193	4088	±	679	4725	±	359	521	±	62	454	±	21	272	±	46
		MWM_{TMZ}	1092	±	76	1175	±	119	1144	±	125	8938	±	833	2451	±	225	8945	±	334	6551	±	325	555	±	39	354	±	9	254	±	46
	VI	CG	948	±	103	1518	±	43	2070	±	207	3475	±	597	1364	±	137	4140	±	649	4359	±	327	491	±	61	435	±	20	276	±	44
		MWM_{TMZ}	966	±	61	1374	±	121	1160	±	60	7819	±	746	1904	±	158	9273	±	442	6249	±	415	452	±	31	310	±	16	264	±	40
Orbitofrontal cortex, ventrolateral																															
	I	CG	1174	±	72	769	±	114	2459	±	317	4515	±	528	1578	±	136	4676	±	317	6181	±	481	505	±	52	767	±	54	77	±	23
		MWM_{TMZ}	1022	±	129	755	±	44	1095	±	111	10354	±	725	3047	±	184	8272	±	317	9802	±	567	513	±	45	551	±	40	169	±	15
	II/III	CG	991	±	77	885	±	78	2266	±	248	4088	±	532	1559	±	233	5096	±	481	6482	±	530	475	±	58	580	±	24	108	±	34
		MWM_{TMZ}	1182	±	133	814	±	38	1279	±	45	10528	±	831	3090	±	200	8581	±	218	8711	±	509	542	±	46	346	±	24	141	±	11
	V	CG	1013	±	104	1253	±	115	2200	±	254	3963	±	541	1494	±	178	5192	±	539	5653	±	437	499	±	52	535	±	40	127	±	29
		MWM_{TMZ}	1053	±	69	819	±	52	1108	±	106	9797	±	764	2886	±	338	9822	±	341	6977	±	539	558	±	39	291	±	16	151	±	15
	VI	CG	959	±	108	1470	±	81	2013	±	194	3531	±	496	1449	±	162	4083	±	619	5320	±	475	500	±	42	409	±	19	212	±	35
		MWM_{TMZ}	951	±	67	1249	±	126	1094	±	94	8172	±	677	2338	±	262	9934	±	327	5732	±	294	448	±	39	328	±	25	196	±	19
Orbitofrontal cortex, lateral																															
	I	CG	1248	±	100	702	±	102	2482	±	281	5193	±	110	1566	±	98	4732	±	324	6500	±	276	384	±	29	802	±	35	119	±	46
		MWM_{TMZ}	1096	±	105	597	±	38	1178	±	122	13218	±	971	3134	±	156	8028	±	323	8541	±	185	426	±	39	534	±	40	168	±	7
	II/III	CG	1035	±	81	973	±	173	2610	±	323	4458	±	88	1667	±	69	5491	±	443	6190	±	220	505	±	50	685	±	23	164	±	56
		MWM_{TMZ}	943	±	80	805	±	55	1253	±	54	10073	±	773	2891	±	252	9655	±	356	7283	±	524	428	±	17	394	±	19	145	±	15
	V	CG	1092	±	83	1468	±	131	2242	±	253	4083	±	288	1473	±	120	4947	±	434	5829	±	459	544	±	34	562	±	43	169	±	45
		MWM_{TMZ}	987	±	94	1105	±	105	1277	±	79	8693	±	713	2450	±	246	9707	±	332	6497	±	478	451	±	28	304	±	10	171	±	16
	VI	CG	982	±	96	1609	±	126	2240	±	243	2983	±	300	1449	±	164	4405	±	348	5744	±	561	537	±	44	534	±	31	248	±	34
		MWM_{TMZ}	953	±	69	1352	±	120	1117	±	115	7854	±	586	1947	±	155	9303	±	492	6191	±	400	488	±	40	324	±	24	206	±	20
Olfactory tubercle																															
	I	CG	757	±	44	711	±	62	1445	±	166	4837	±	283	773	±	87	2656	±	449	2131	±	286	185	±	28	589	±	100	4529	±	404
		MWM_{TMZ}	416	±	58	275	±	18	205	±	76	7981	±	204	1359	±	188	2779	±	185	3790	±	327	181	±	17	460	±	49	5767	±	235
	II	CG	1381	±	98	1100	±	101	1768	±	116	4090	±	409	973	±	91	3195	±	408	3344	±	316	201	±	25	813	±	113	6451	±	563
		MWM_{TMZ}	733	±	56	956	±	65	569	±	65	8318	±	383	1655	±	215	4740	±	394	6038	±	440	213	±	14	596	±	66	7237	±	168
	III	CG	1092	±	80	1147	±	80	1700	±	129	3487	±	248	812	±	67	3293	±	399	3508	±	286	227	±	23	909	±	116	5041	±	503
		MWM_{TMZ}	859	±	66	1268	±	61	764	±	40	6513	±	408	1290	±	204	5572	±	356	4529	±	338	236	±	22	703	±	58	6254	±	253

Supp. Tab. 38: Statistical analysis of the comparison of layer-specific receptor concentrations of CG versus MWM_{TMZ}

Significant differences between receptor densities between the olfactory layers for control mice (CG) and trained mice with suppressed adult neurogenesis (MWM_{TMZ}). Each receptor type was tested with non-parametric Mann-Whitney-U test. The percentage difference in absolute receptor concentrations (first column), Z-value (negative: group MWM_{TMZ} is significantly higher; positive: group CG is significantly higher; middle column), p-value (right column).

CG | MWM_{TMZ}	AMPA			Kainate			NMDA			$mGlu_{2/3}$			$GABA_A$		
	%	*Z*	*p-value*	%	*Z*	*p-value*	%	*Z*	*p-value*	%	*Z*	*p-value*	%	*Z*	*p-value*
MOB gr	3,63	0,00	1,00	27,18	-1,63	0,11	-51,39	2,68	0,01	52,31	-3,74	0,00	22,53	-1,40	0,17
MOB ipl	15,70	-0,72	0,48	17,97	-1,70	0,09	-36,19	0,94	0,35	67,09	-3,74	0,00	1,20	-0,11	0,91
MOB mi	6,13	-0,42	0,68	37,11	-2,83	0,00	-54,81	2,31	0,02	73,69	-3,74	0,00	57,74	-3,06	0,00
MOB opl	15,05	-1,25	0,22	11,16	-1,25	0,22	-43,14	1,70	0,09	65,28	-3,44	0,00	27,87	-2,38	0,01
MOB gl	19,07	-1,10	0,28	-11,01	1,02	0,31	-65,57	3,74	0,00	21,49	-2,08	0,04	87,45	-3,06	0,00
MOB onl	-13,03	0,79	0,44	-53,48	3,59	0,00	-67,54	3,74	0,00	-23,85	2,23	0,02	16,52	-1,17	0,25
AOB gr	-2,84	1,10	0,28	-14,77	2,23	0,02	-35,53	2,54	0,01	21,73	-1,32	0,19	228,98	-3,44	0,00
AOB mi	-8,98	0,87	0,39	-0,42	-1,25	0,22	-64,09	3,75	0,00	77,77	-3,67	0,00	5,30	0,04	1,00
AOB gl	36,49	-1,02	0,31	33,07	0,19	0,85	-60,76	3,75	0,00	96,74	-2,69	0,01	310,20	-2,01	0,04
AON pe	35,30	-2,08	0,04	-27,91	2,99	0,00	-13,41	1,40	0,17	92,91	-3,52	0,00	-23,70	1,25	0,22
AON m	32,99	-1,25	0,22	2,86	-0,64	0,53	-0,66	0,04	0,97	79,93	-3,59	0,00	-13,25	0,64	0,53
AON d	35,02	-2,00	0,04	16,98	-1,40	0,17	-3,70	-0,11	0,91	92,58	-3,76	0,00	-10,36	1,17	0,25
AON pv	55,13	-2,53	0,01	-0,50	-0,04	0,97	24,75	-2,61	0,01	154,55	-3,74	0,00	-32,30	2,31	0,02
AON l	27,92	-1,63	0,11	0,41	-0,72	0,48	-33,44	2,99	0,00	94,67	-2,99	0,00	38,77	-1,93	0,05
TTd I	-10,95	1,25	0,22	-4,36	0,11	0,91	-49,69	3,14	0,00	66,83	-3,14	0,00	29,70	-1,32	0,19
TTd II	1,56	-0,26	0,80	28,19	-1,93	0,05	-26,56	2,91	0,00	103,91	-3,74	0,00	40,83	-1,85	0,06
TTd III	17,99	-1,40	0,17	41,58	-2,38	0,01	-18,44	1,85	0,06	102,35	-3,74	0,00	19,54	-1,10	0,28
TTd IV	19,54	-1,55	0,12	8,21	-0,72	0,48	-10,43	1,10	0,28	55,39	-3,14	0,00	42,71	-2,23	0,02
TTv I	-16,12	2,69	0,01	3,19	0,72	0,48	-70,96	3,59	0,00	110,53	-2,46	0,01	57,31	-2,00	0,04
TTv II	-9,28	1,78	0,08	25,03	-0,79	0,44	-40,31	3,29	0,00	102,27	-3,29	0,00	48,89	-1,85	0,06
TTv III	-18,35	2,23	0,02	34,23	-2,38	0,01	-32,36	3,44	0,00	101,74	-3,74	0,00	59,91	-2,08	0,04
OT I	-34,27	2,76	0,00	-51,94	0,01	0,01	-79,79	3,76	0,00	62,95	-3,74	0,00	32,84	-1,55	0,12
OT II	-40,69	2,99	0,00	-3,86	0,79	0,80	-64,22	3,74	0,00	86,34	-3,74	0,00	44,05	-2,38	0,01
OT III	-37,05	3,14	0,00	1,99	0,85	0,85	-59,42	3,75	0,00	88,67	-3,74	0,00	49,24	-2,61	0,01

DP I	23,20	-2,99	0,00	-8,20	0,24	0,25	-32,78	2,84	0,00	79,07	-3,74	0,00	103,70	-3,29	0,00
DP II/III	-8,44	0,95	0,35	-7,01	0,57	0,58	-38,17	2,99	0,00	107,56	-3,74	0,00	96,99	-3,67	0,00
DP V	57,29	-3,52	0,00	-9,84	0,47	0,48	-34,85	3,44	0,00	122,05	-3,74	0,00	85,80	-3,44	0,00
DP VI	-2,33	0,19	0,85	-30,07	0,01	0,01	-36,53	1,47	0,14	63,32	-3,74	0,00	98,46	-3,59	0,00
PIR I	-22,83	2,68	0,01	-34,94	0,01	0,01	-55,06	3,74	0,00	110,50	-3,75	0,00	30,56	-2,91	0,00
PIR II	-42,72	3,74	0,00	0,17	0,79	0,80	-39,84	2,91	0,00	86,47	-3,74	0,00	24,76	-2,83	0,00
PIR III	31,05	-3,52	0,00	-2,66	0,68	0,68	-38,94	2,53	0,01	98,97	-3,74	0,00	28,38	-2,53	0,01
ENT I I	-44,06	2,83	0,00	-36,16	0,05	0,04	-37,45	2,68	0,01	173,32	-3,74	0,00	15,46	-1,02	0,31
ENT I II	-36,03	3,52	0,00	-19,79	0,02	0,02	-41,29	3,74	0,00	137,49	-3,74	0,00	11,53	-1,70	0,09
ENT I III	-36,09	3,75	0,00	-3,63	0,38	0,39	-38,81	3,74	0,00	118,57	-3,74	0,00	24,96	-2,38	0,01
ENT I IV	-37,47	3,74	0,00	20,18	0,14	0,14	-38,19	3,67	0,00	108,02	-3,74	0,00	13,39	-2,38	0,01
ENT I V	-39,68	3,59	0,00	23,89	0,06	0,06	-41,88	3,67	0,00	90,12	-2,99	0,00	29,07	-2,61	0,01
ENT I VIa	-16,41	1,63	0,11	47,60	0,01	0,01	-38,12	3,52	0,00	105,93	-3,67	0,00	29,67	-2,68	0,01
ENT I VIb	-6,78	0,87	0,39	67,47	0,00	0,00	-40,79	3,37	0,00	92,44	-3,74	0,00	31,10	-2,38	0,01
ENT m I	-55,70	3,74	0,00	-40,84	0,00	0,00	-23,47	1,55	0,12	133,54	-3,74	0,00	20,83	-2,15	0,03
ENT m II	-26,02	2,16	0,03	-8,87	0,08	0,08	-30,84	3,44	0,00	133,56	-3,74	0,00	14,85	-1,93	0,05
ENT m III	-14,88	1,32	0,19	-18,20	0,01	0,01	-17,23	2,91	0,00	124,44	-3,74	0,00	10,13	-1,85	0,06
ENT m IV	-4,58	1,10	0,28	-11,99	0,43	0,44	16,29	-1,10	0,28	123,74	-3,74	0,00	23,33	-3,06	0,00
ENT m V	-6,16	1,32	0,19	34,57	0,01	0,01	-29,28	2,38	0,01	115,59	-3,74	0,00	29,07	-2,99	0,00
ENT m VI	-25,81	2,31	0,02	39,07	0,02	0,02	0,87	0,11	0,91	113,28	-3,67	0,00	28,84	-2,31	0,02
ORB m I	3,44	-0,64	0,53	12,15	0,47	0,48	-60,01	3,74	0,00	78,15	-3,75	0,00	62,21	-2,38	0,01
ORB m II	20,87	-0,79	0,44	-19,24	0,04	0,04	-36,01	3,06	0,00	112,33	-3,75	0,00	54,98	-2,99	0,00
ORB m II/III	28,55	-2,31	0,02	-15,51	0,04	0,04	-20,66	2,46	0,01	114,59	-3,68	0,00	84,06	-3,14	0,00
ORB m V	20,81	-1,32	0,19	-30,72	0,00	0,00	-1,64	0,57	0,58	111,98	-3,60	0,00	68,21	-3,29	0,00
ORB m VIa	16,96	-0,19	0,85	-19,78	0,09	0,09	-32,31	2,76	0,00	99,19	-3,68	0,00	33,65	-2,91	0,00
ORB vl I	-0,27	0,19	0,85	-3,31	0,09	0,09	-41,81	3,21	0,00	103,17	-3,75	0,00	91,45	-3,74	0,00
ORB vl II/III	19,90	-1,32	0,19	-17,61	0,16	0,17	-31,80	2,68	0,01	119,39	-3,76	0,00	76,91	-3,29	0,00
ORB vl V	6,79	-0,42	0,68	-42,73	0,00	0,00	-30,79	2,38	0,01	104,54	-3,75	0,00	67,03	-3,29	0,00
ORB vl VIa	4,59	0,04	0,97	-20,59	0,04	0,04	-30,73	2,46	0,01	89,91	-3,68	0,00	38,62	-2,16	0,03
ORB l I	-16,90	1,32	0,19	-10,14	0,27	0,28	-45,57	3,52	0,00	84,75	-3,76	0,00	74,65	-3,74	0,00
ORB l II/III	-2,97	0,72	0,48	-32,02	0,01	0,01	-49,12	3,06	0,00	80,18	-3,76	0,00	55,72	-3,59	0,00
ORB l V	-3,97	0,87	0,39	-36,13	0,00	0,00	-38,91	2,68	0,01	71,47	-3,76	0,00	56,93	-3,74	0,00
ORB l VIa	11,63	-0,19	0,85	-24,41	0,09	0,09	-42,63	2,68	0,01	108,17	-3,75	0,00	30,14	-2,08	0,04

CG | MWM_{CG}	$GABA_{A(BZ)}$			$GABA_B$			α_1			α_2			$D_{1/5}$		
	%	*Z*	*p-value*	%	*Z*	*p-value*	%	*Z*	*p-value*	%	*Z*	*p-value*	%	*Z*	*p-value*
MOB gr	71,54	-3,44	0,00	-19,14	2,68	0,01	0,62	-0,42	0,68	-27,04	3,29	0,00	41,81	-2,76	0,00
MOB ipl	163,72	-3,74	0,00	-32,75	3,75	0,00	33,67	-2,83	0,00	-34,79	3,29	0,00	43,27	-2,46	0,01
MOB mi	147,40	-3,74	0,00	-21,67	3,06	0,00	23,02	-2,38	0,01	-32,33	3,06	0,00	74,93	-2,91	0,00
MOB opl	54,63	-2,91	0,00	-40,17	3,74	0,00	-4,52	0,57	0,58	-20,02	1,93	0,05	37,88	-2,08	0,04
MOB gl	49,98	-3,67	0,00	71,40	-3,74	0,00	15,36	-1,40	0,17	-28,87	3,36	0,00	44,75	-1,78	0,08
MOB onl	11,62	-2,99	0,00	-54,12	3,59	0,00	-38,15	3,74	0,00	-51,15	3,36	0,00	22,23	-0,42	0,68
AOB gr	-85,78	3,74	0,00	1,41	-0,04	0,97	-21,27	2,08	0,04	-61,39	3,36	0,00	-4,73	0,79	0,44
AOB mi	115,09	-3,74	0,00	-14,76	3,59	0,00	6,97	-0,79	0,44	-24,16	1,56	0,12	-4,55	0,79	0,44
AOB gl	125,04	-3,62	0,00	121,06	-3,75	0,00	24,69	0,04	1,00	-38,64	2,77	0,00	36,29	-0,27	0,80
AON pe	67,74	-3,59	0,00	60,41	-3,29	0,00	2,84	-0,64	0,53	-12,98	-0,11	0,91	-20,13	0,87	0,39
AON m	30,99	-1,78	0,08	27,46	-2,61	0,01	11,56	-1,63	0,11	22,36	-1,78	0,08	-34,69	2,00	0,04
AON d	117,20	-3,74	0,00	48,69	-3,74	0,00	-10,14	1,32	0,19	21,30	-2,15	0,03	-44,50	1,55	0,12
AON pv	48,93	-2,15	0,03	66,69	-3,74	0,00	-8,09	0,64	0,53	32,75	-2,15	0,03	-23,22	0,94	0,35
AON l	55,85	-2,84	0,00	35,03	-2,99	0,00	-8,27	2,00	0,04	28,39	-2,00	0,04	-9,31	1,33	0,19
TTd I	56,36	-3,06	0,00	55,04	-3,76	0,00	9,27	-0,64	0,53	-9,90	0,42	0,68	-15,58	0,34	0,74
TTd II	56,24	-3,06	0,00	60,44	-3,74	0,00	24,52	-1,32	0,19	5,26	-0,11	0,91	-21,33	0,42	0,68
TTd III	39,82	-3,14	0,00	51,25	-3,21	0,00	12,92	-1,47	0,14	22,47	-1,85	0,06	-32,16	1,78	0,08
TTd IV	68,22	-3,59	0,00	80,63	-3,74	0,00	-8,12	0,95	0,35	10,14	-2,38	0,01	-53,36	3,14	0,00
TTv I	51,13	-3,21	0,00	25,30	-2,69	0,01	-30,86	0,94	0,35	-11,64	0,19	0,85	-15,89	0,19	0,85
TTv II	63,56	-3,74	0,00	25,05	-1,93	0,05	-11,84	0,11	0,91	-6,17	0,11	0,91	-23,55	-0,04	0,97
TTv III	63,63	-3,75	0,00	30,88	-2,38	0,01	-14,11	1,10	0,28	-11,21	0,34	0,74	-52,52	1,32	0,19
OT I	-7,39	0,26	0,80	5,18	-0,19	0,85	-19,05	1,32	0,19	-11,70	0,64	0,53	-0,11	0,79	0,44
OT II	33,37	-1,70	0,09	9,71	-0,57	0,58	7,71	-0,72	0,48	-7,64	0,79	0,44	1,82	0,49	0,63
OT III	73,76	-3,21	0,00	0,32	-0,49	0,63	7,38	-0,95	0,35	-11,34	1,02	0,31	8,18	-0,57	0,58
DP I	43,43	-2,76	0,00	46,93	-2,68	0,01	53,02	-1,85	0,06	3,83	-0,34	0,74	-5,37	0,04	1,00
DP II/III	85,47	-3,74	0,00	16,97	-0,94	0,35	9,88	-0,57	0,58	52,63	-2,54	0,01	-29,44	1,63	0,11
DP V	90,69	-3,74	0,00	6,89	0,04	0,97	16,20	-0,72	0,48	63,26	-3,52	0,00	-39,07	3,06	0,00
DP VI	103,82	-3,67	0,00	12,67	-0,87	0,39	73,52	-3,14	0,00	71,50	-3,29	0,00	-50,18	3,21	0,00
PIR I	57,19	-3,74	0,00	8,28	-1,25	0,22	13,93	-1,10	0,28	-33,55	3,52	0,00	-20,66	1,63	0,11
PIR II	65,67	-3,67	0,00	-0,13	0,04	0,97	20,76	-1,85	0,06	-7,95	1,02	0,31	-37,01	2,61	0,01
PIR III	78,07	-3,74	0,00	10,59	-1,25	0,22	19,97	-1,78	0,08	-15,36	1,70	0,09	-55,79	3,67	0,00

ENT l I	33,20	-1,55	0,12	80,65	-3,67	0,00	34,16	-2,53	0,01	15,07	-1,02	0,31	26,85	-1,47	0,14
ENT l II	63,99	-3,44	0,00	64,53	-3,74	0,00	49,81	-3,59	0,00	10,22	-0,42	0,68	-0,99	-0,04	0,97
ENT l III	96,63	-3,74	0,00	67,19	-3,74	0,00	36,30	-3,06	0,00	13,03	-0,94	0,35	7,40	-0,26	0,80
ENT l IV	130,26	-3,74	0,00	69,77	-3,74	0,00	26,22	-2,15	0,03	10,22	-0,57	0,58	24,69	-1,70	0,09
ENT l V	134,19	-3,74	0,00	72,97	-3,74	0,00	22,49	-2,23	0,02	-1,30	0,57	0,58	21,75	-1,78	0,08
ENT l VIa	110,02	-3,74	0,00	61,76	-3,74	0,00	19,60	-2,31	0,02	3,65	-0,11	0,91	18,10	-1,32	0,19
ENT l VIb	95,33	-3,74	0,00	33,79	-3,59	0,00	24,22	-2,38	0,01	-3,51	0,19	0,85	28,69	-1,47	0,14
ENT m I	24,21	-0,34	0,74	32,79	-3,14	0,00	13,67	-0,95	0,35	29,91	-1,70	0,09	95,96	-2,53	0,01
ENT m II	66,84	-2,99	0,00	37,69	-3,60	0,00	36,64	-2,53	0,01	10,95	-0,42	0,68	59,73	-2,00	0,04
ENT m III	86,16	-3,67	0,00	44,16	-3,67	0,00	46,57	-2,68	0,01	7,44	-1,17	0,25	26,95	-1,78	0,08
ENT m IV	95,92	-3,59	0,00	45,82	-3,75	0,00	48,81	-2,16	0,03	6,88	-1,17	0,25	35,42	-2,53	0,01
ENT m V	105,97	-3,44	0,00	44,89	-3,75	0,00	42,94	-2,46	0,01	10,84	-1,25	0,22	33,92	-2,61	0,01
ENT m VI	127,75	-3,74	0,00	35,44	-2,76	0,00	45,30	-3,67	0,00	26,35	-3,29	0,00	26,44	-1,55	0,12
ORB m I	54,01	-3,52	0,00	52,00	-2,68	0,01	24,52	-1,70	0,09	-14,11	1,40	0,17	79,35	-2,31	0,02
ORB m II	88,72	-3,37	0,00	61,27	-2,99	0,00	21,38	-1,40	0,17	-10,89	1,02	0,31	28,39	-1,33	0,19
ORB m II/III	111,22	-3,67	0,00	71,44	-3,59	0,00	22,07	-1,85	0,06	-10,20	1,85	0,06	2,46	-0,49	0,63
ORB m V	114,45	-3,75	0,00	46,80	-3,14	0,00	20,84	-2,00	0,04	4,26	-0,11	0,91	-20,63	1,71	0,09
ORB m VIa	105,98	-3,59	0,00	42,14	-2,46	0,01	7,17	-0,64	0,53	3,59	-0,64	0,53	-7,53	0,49	0,63
ORB vl I	74,93	-3,67	0,00	47,50	-2,99	0,00	31,15	-2,46	0,01	-2,51	0,26	0,80	99,31	-2,16	0,03
ORB vl II/III	86,49	-3,67	0,00	32,55	-2,99	0,00	29,53	-2,08	0,04	-4,90	1,78	0,08	5,39	-0,49	0,63
ORB vl V	76,40	-3,75	0,00	25,22	-1,55	0,12	26,06	-2,38	0,01	-6,88	0,57	0,58	11,03	-1,17	0,25
ORB vl VIa	104,95	-3,67	0,00	11,54	-0,87	0,39	9,67	-0,79	0,44	-1,63	0,79	0,44	-1,95	-0,04	0,97
ORB l I	46,96	-3,21	0,00	21,56	-2,16	0,03	21,93	-2,91	0,00	-14,95	3,44	0,00	32,51	-0,72	0,48
ORB l II/III	80,54	-3,74	0,00	9,84	-1,85	0,06	11,67	-1,70	0,09	-20,87	3,14	0,00	-1,96	-0,27	0,80
ORB l V	89,83	-3,74	0,00	-2,96	0,72	0,48	-1,44	0,04	0,97	-22,69	2,38	0,01	6,52	-0,79	0,44
ORB l VIa	95,63	-3,74	0,00	5,41	-1,55	0,12	9,04	-1,33	0,19	-24,62	2,76	0,00	-1,58	0,49	0,63

Supp. Tab. 39: Region-specific receptor concentrations of CG_{TMZ} versus MWM_{TMZ}

Neurotransmitter receptor densities (fmol/mg protein) in different regions of the mouse olfactory system (Mean ± SEM) of mice with suppressed adult neurogenesis (CG_{TMZ}) and trained mice with suppressed adult neurogenesis (MWM_{TMZ}). For pairwise comparisons between regions see further Supp. Tab. 40.

CG_{TMZ} | MWM_{TMZ}		AMPA			Kainate			NMDA			$mGlu_{2/3}$			$GABA_A$		
MOB	CG_{TMZ}	727	±	54	1281	±	95	954	±	158	2180	±	121	803	±	93
	MWM_{TMZ}	742	±	77	1357	±	55	442	±	19	2961	±	117	1475	±	214
AOB	CG_{TMZ}	909	±	88	1328	±	94	1203	±	156	3948	±	376	950	±	212
	MWM_{TMZ}	892	±	92	1327	±	75	596	±	32	4746	±	426	2036	±	221
AON	CG_{TMZ}	1044	±	87	1432	±	69	1445	±	189	2365	±	165	566	±	73
	MWM_{TMZ}	1449	±	118	1329	±	61	1264	±	50	4867	±	383	430	±	28
TTd	CG_{TMZ}	1151	±	58	1356	±	124	1878	±	213	2977	±	212	906	±	64
	MWM_{TMZ}	1216	±	93	1553	±	117	1471	±	87	5283	±	339	1171	±	122
TTv	CG_{TMZ}	1361	±	86	1022	±	114	1716	±	125	2825	±	222	788	±	85
	MWM_{TMZ}	1123	±	48	1266	±	135	910	±	83	5723	±	713	1222	±	156
Epd	CG_{TMZ}	789	±	51	1480	±	75	1239	±	129	1836	±	224	695	±	61
	MWM_{TMZ}	852	±	100	1150	±	82	793	±	91	3797	±	260	886	±	102
OT	CG_{TMZ}	1079	±	88	964	±	70	1638	±	131	3964	±	346	853	±	77
	MWM_{TMZ}	668	±	70	856	±	104	529	±	44	7551	±	324	1213	±	102
DP	CG_{TMZ}	1069	±	62	1624	±	95	1909	±	255	3442	±	155	1048	±	78
	MWM_{TMZ}	1259	±	59	1322	±	111	1386	±	111	6622	±	356	2054	±	149
PIR	CG_{TMZ}	1060	±	41	785	±	48	1821	±	162	3328	±	207	1034	±	68
	MWM_{TMZ}	890	±	37	698	±	37	1023	±	77	6765	±	301	1368	±	64
ENTl	CG_{TMZ}	1664	±	59	1054	±	32	3037	±	224	3070	±	198	1297	±	84

ENTm	MWM_{TMZ}	1127	±	66	1356	±	72	1791	±	65	6699	±	308	1632	±	83
	CG_{TMZ}	1580	±	102	1040	±	71	2091	±	301	3081	±	268	1190	±	98
ORBl	MWM_{TMZ}	1195	±	109	1072	±	86	1702	±	105	6947	±	328	1590	±	83
	CG_{TMZ}	1089	±	83	1095	±	164	2292	±	278	3867	±	360	1553	±	105
ORBvl	MWM_{TMZ}	1047	±	111	862	±	78	1340	±	47	7537	±	274	2379	±	99
	CG_{TMZ}	1034	±	79	995	±	140	2101	±	236	4024	±	511	1520	±	162
ORBm	MWM_{TMZ}	1111	±	110	843	±	59	1487	±	71	8182	±	284	2539	±	124
	CG_{TMZ}	1100	±	75	1039	±	175	2168	±	209	3983	±	524	1393	±	172
	MWM_{TMZ}	1272	±	102	890	±	53	1481	±	77	7972	±	266	2235	±	131

CG_{TMZ} | MWM_{TMZ}		$GABA_{A(BZ)}$			$GABA_B$			α_1			α_2			$D_{1/5}$		
MOB	CG_{TMZ}	3867	±	577	2246	±	71	547	±	33	497	±	32	61	±	6
	MWM_{TMZ}	4739	±	349	2078	±	48	584	±	25	351	±	20	89	±	10
AOB	CG_{TMZ}	6409	±	664	3617	±	288	675	±	50	547	±	69	100	±	15
	MWM_{TMZ}	6346	±	867	5285	±	274	703	±	41	318	±	27	98	±	13
AON	CG_{TMZ}	2038	±	181	4223	±	345	338	±	19	1809	±	160	171	±	29
	MWM_{TMZ}	3238	±	176	6017	±	92	339	±	13	2252	±	103	112	±	11
TTd	CG_{TMZ}	3662	±	331	4736	±	428	308	±	36	1589	±	141	357	±	49
	MWM_{TMZ}	5718	±	287	7295	±	112	334	±	13	1854	±	82	230	±	14
TTv	CG_{TMZ}	3214	±	272	4316	±	442	321	±	45	1377	±	177	315	±	90
	MWM_{TMZ}	5083	±	198	5321	±	156	252	±	9	1251	±	123	198	±	20
EPd	CG_{TMZ}	2791	±	257	4059	±	211	238	±	23	1032	±	49	888	±	95
	MWM_{TMZ}	4747	±	377	3902	±	95	324	±	17	1043	±	44	226	±	24
OT	CG_{TMZ}	3048	±	403	2995	±	277	204	±	25	770	±	107	5340	±	439
	MWM_{TMZ}	4286	±	297	3143	±	98	203	±	16	692	±	52	5533	±	164

DP	CG_{TMZ}	4125	±	340	5048	±	674	317	±	52	1031	±	94	360	±	44
	MWM_{TMZ}	7465	±	269	6019	±	304	423	±	31	1445	±	92	234	±	22
PIR	CG_{TMZ}	3961	±	243	4853	±	158	448	±	40	1027	±	80	242	±	28
	MWM_{TMZ}	6541	±	248	5170	±	199	536	±	24	855	±	40	137	±	6
ENTl	CG_{TMZ}	3627	±	221	5894	±	254	314	±	19	1771	±	137	345	±	26
	MWM_{TMZ}	7149	±	421	9753	±	292	409	±	12	1864	±	39	406	±	20
ENTm	CG_{TMZ}	3553	±	487	6201	±	200	304	±	26	1770	±	136	330	±	17
	MWM_{TMZ}	6113	±	792	8701	±	187	419	±	26	1887	±	125	474	±	39
ORBl	CG_{TMZ}	4894	±	323	5925	±	392	502	±	38	650	±	22	175	±	43
	MWM_{TMZ}	8720	±	277	6572	±	327	538	±	10	531	±	35	186	±	12
ORBvl	CG_{TMZ}	4762	±	406	5909	±	461	495	±	48	570	±	24	131	±	28
	MWM_{TMZ}	8803	±	317	7680	±	530	610	±	15	572	±	40	154	±	10
ORBm	CG_{TMZ}	4269	±	529	5003	±	404	513	±	67	564	±	22	211	±	33
	MWM_{TMZ}	8351	±	352	7846	±	509	614	±	16	531	±	35	227	±	24

Supp. Tab. 40: Statistical analysis of the comparison of region-specific receptor concentrations of CG_{TMZ} versus MWM_{TMZ}

Significant differences between receptor densities between the olfactory regions of mice with suppressed adult neurogenesis (CG_{TMZ}) and trained mice with suppressed adult neurogenesis (MWM_{TMZ}). Each receptor type was tested with non-parametric Mann-Whitney-U test. The percentage difference in absolute receptor concentrations (first column), p-value (middle column), and correlation coefficient r (limits: weak (0.1-0.3), medium (0.3-0.5), and strong (> 0.5) to evaluate the effect size (right column).

CG_{TMZ} | MWM_{TMZ}	AMPAR			kainateR			NMDAR			$mGlu_{2/3}R$			$GABA_AR$		
	[%]	*p*	[r]	[%]	*p*	[r]	[%]	*p*	[r]	[%]	*p*	[r]	[%]	*p*	[r]
MOB | MOB	28,41	0.089	0,389	5,12	0.853	0,051	-32,62	**< .001**	0,812	48,00	**< .001**	0,811	51,33	**0.011**	0,558
AOB | AOB	10,42	0.796	0,068	-32,83	**0.002**	0,710	-14,38	0.089	0,389	22,68	0.123	0,355	98,38	**0.001**	0,727
AOC | AOC	53,42	**0.005**	0,609	-15,36	**0.034**	0,482	-20,30	**0.023**	0,507	91,42	**< .001**	0,811	-22,22	0.307	0,237
TTd | TTd	13,01	0.247	0,270	14,06	0.173	0,313	-15,13	0.089	0,389	73,78	**< .001**	0,845	-12,22	0.427	0,186
TTv | TTv	-4,50	0.677	0,101	-7,94	0.280	0,254	-41,15	**< .001**	0,811	79,71	**0.002**	0,659	13,31	0.684	0,101
EPd | EPd	16,24	1.000	0,000	-22,46	**0.007**	0,592	-24,85	**0.019**	0,524	101,91	**< .001**	0,845	2,47	0.912	0,034
OT | OT	-34,02	**0.004**	0,625	-30,03	**0.011**	0,558	-59,68	**< .001**	0,845	101,27	**< .001**	0,845	8,32	0.481	0,169
DP | DP	23,80	**0.029**	0,490	-15,66	0.123	0,355	-24,32	**0.007**	0,592	105,19	**< .001**	0,845	37,84	**0.011**	0,558
PIR | PIR	-7,33	0.173	0,313	-12,29	0.173	0,313	-26,35	**0.009**	0,575	116,40	**< .001**	0,845	14,21	0.406	0,194
ENTl | ENTl	-33,79	**< .001**	0,778	26,93	**0.015**	0,541	-9,80	0.218	0,287	133,60	**< .001**	0,845	34,14	**0.004**	0,625
ENTm | ENTm	-9,99	0.104	0,372	5,96	0.910	0,034	5,93	0.579	0,135	151,17	**< .001**	0,845	21,55	0.186	0,304
ORBl | ORBl	2,99	0.315	0,237	-15,85	0.190	0,304	-24,06	0.052	0,439	102,84	**< .001**	0,829	43,20	**0.043**	0,456
ORBvl | ORBvl	8,64	0.762	0,076	-21,78	0.123	0,355	-13,68	**0.029**	0,490	96,97	**< .001**	0,845	46,91	**0.001**	0,736
ORBm | ORBm	14,46	1.000	0,000	-27,29	0.436	0,186	-12,46	**< .001**	0,778	85,89	**< .001**	0,846	22,59	**< .001**	0,727
CG_{TMZ} | MWM_{TMZ}	$GABA_{A(BZ)}R$			$GABA_BR$			α_1R			α_2R			$D_{1/5}R$		
	[%]	*p*	[r]	[%]	*p*	[r]	[%]	*p*	[r]	[%]	*p*	[r]	[%]	*p*	[r]
MOB | MOB	31,97	0.023	0,507	-15,49	0.023	0,507	5,02	0.247	0,270	-28,85	**0.002**	0,710	43,74	**0.021**	0,525
AOB | AOB	-11,17	0.677	0,101	39,02	0.002	0,710	20,35	0.026	0,507	-40,45	**< .001**	0,761	45,75	0.014	0,559
AOC | AOC	42,48	**0.002**	0,676	13,21	**0.063**	0,423	-11,02	0.054	0,440	17,06	**0.089**	0,389	-43,87	**0.002**	0,693
TTd | TTd	37,31	**0.001**	0,693	32,98	**< .001**	0,710	-7,02	0.218	0,287	12,24	0.218	0,287	-33,02	0.014	0,558
TTv | TTv	54,98	**< .001**	0,794	-17,62	**0.004**	0,659	-25,09	0.002	0,693	-10,22	0.579	0,135	-38,02	0.009	0,592
EPd | EPd	53,44	**0.002**	0,659	-15,73	0.009	0,592	0,20	**1000**	0,000	-10,89	0.273	0,254	-30,09	**0.212**	0,288

OT | OT	36,64	**0.004**	0,625	-33,42	0.007	0,592	-26,71	0.043	0,456	-43,77	< .001	0,727	17,08	0.011	0,579
DP | DP	65,46	**< .001**	0,845	0,39	0.791	0,068	-5,31	0.677	0,101	25,61	**0.165**	0,321	-36,34	**0.002**	0,702
PIR | PIR	59,47	**< .001**	0,845	-3,07	0.684	0,101	3,97	0.496	0,161	-20,06	**0.143**	0,338	-41,18	**< .001**	0,744
ENTl | ENTl	72,92	**< .001**	0,845	27,96	**0.002**	0,676	19,23	**0.010**	0,583	1,16	0.684	0,101	0,52	0.520	0,152
ENTm | ENTm	25,23	**0.043**	0,456	26,48	**0.009**	0,575	-9,38	**0.212**	0,287	-8,31	0.315	0,237	34,71	**0.015**	0,550
ORBl | ORBl	62,82	**< .001**	0,828	-0,73	**0.280**	0,254	0,17	**0.075**	0,406	-6,90	0.165	0,321	-17,64	0.791	0,068
ORBvl | ORBvl	63,83	**< .001**	0,845	14,83	**0.280**	0,254	16,00	0.026	0,507	5,99	0.623	0,118	-20,43	0.130	0,347
ORBm | ORBm	58,47	**< .001**	0,845	10,86	0.739	0,085	15,87	0.970	0,017	-9,32	**0.054**	0,440	-0,42	0.069	0,415

Supp. Tab. 41: Mean receptor densities of olfactory layers (CG_{TMZ} versus MWM_{TMZ})

Layer-specific absolute receptor densities of the subregions of the olfactory system (mean ± SEM) of mice with suppressed adult neurogenesis (CG_{TMZ}) and trained mice with suppressed adult neurogenesis (MWM_{TMZ}). For pairwise comparisons between regions see further Supp. Tab. 42.

CG_{TMZ} | MWM_{TMZ}			Receptor (fmol/mg protein)									
			AMPA	kainate	NMDA	$mGlu_{2/3}$	$GABA_A$	$GABA_{A(BZ)}$	$GABA_B$	α_1	α_2	$D_{1/5}$
Main olfactory bulb												
	gr	CG_{TMZ}	678 ± 46	916 ± 20	587 ± 41	1553 ± 97	587 ± 41	1027 ± 41	2280 ± 104	426 ± 14	895 ± 56	53 ± 12
		MWM_{TMZ}	711 ± 40	1118 ± 101	366 ± 19	2725 ± 144	351 ± 31	1525 ± 49	1873 ± 43	424 ± 28	562 ± 74	81 ± 5
	ipl	CG_{TMZ}	523 ± 30	1367 ± 56	522 ± 22	1776 ± 142	522 ± 22	1290 ± 48	2104 ± 87	382 ± 8	438 ± 18	41 ± 7
		MWM_{TMZ}	729 ± 58	1596 ± 82	381 ± 18	3735 ± 185	478 ± 38	2563 ± 64	1544 ± 76	432 ± 31	191 ± 18	85 ± 4
	mi	CG_{TMZ}	547 ± 41	993 ± 46	488 ± 22	1597 ± 130	488 ± 22	1012 ± 47	2048 ± 87	356 ± 13	626 ± 59	39 ± 7
		MWM_{TMZ}	699 ± 61	1527 ± 79	364 ± 18	3303 ± 167	564 ± 44	2190 ± 60	1711 ± 80	422 ± 29	251 ± 38	85 ± 3
	opl	CG_{TMZ}	589 ± 38	1677 ± 83	755 ± 55	2268 ± 152	755 ± 55	2716 ± 122	1901 ± 42	584 ± 15	376 ± 21	48 ± 3
		MWM_{TMZ}	697 ± 48	1643 ± 100	479 ± 30	4133 ± 266	981 ± 75	3872 ± 185	1256 ± 51	471 ± 31	212 ± 26	97 ± 3
	gl	CG_{TMZ}	558 ± 36	2165 ± 70	987 ± 66	2899 ± 198	987 ± 66	10296 ± 406	3100 ± 460	1116 ± 37	363 ± 19	77 ± 5
		MWM_{TMZ}	642 ± 55	1674 ± 158	604 ± 33	3811 ± 164	6246 ± 505	14511 ± 201	6603 ± 145	940 ± 42	189 ± 14	100 ± 5
	onl	CG_{TMZ}	455 ± 57	887 ± 81	554 ± 62	1797 ± 84	554 ± 62	3980 ± 314	3013 ± 534	383 ± 20	274 ± 14	66 ± 6
		MWM_{TMZ}	374 ± 44	587 ± 31	268 ± 22	1855 ± 155	1320 ± 109	4862 ± 241	1999 ± 189	207 ± 8	158 ± 15	85 ± 4
Accessory olfactory bulb												
	gr	CG_{TMZ}	792 ± 99	1177 ± 57	642 ± 27	2975 ± 139	642 ± 27	6258 ± 178	3200 ± 323	527 ± 17	692 ± 96	61 ± 9
		MWM_{TMZ}	821 ± 59	969 ± 48	529 ± 53	4930 ± 228	1471 ± 462	1293 ± 272	2798 ± 122	548 ± 26	512 ± 94	82 ± 6
	mi	CG_{TMZ}	885 ± 68	2514 ± 118	819 ± 63	5185 ± 422	819 ± 63	9636 ± 714	2908 ± 296	834 ± 29	429 ± 30	72 ± 19
		MWM_{TMZ}	1196 ± 82	2051 ± 177	650 ± 96	9180 ± 355	2078 ± 298	12455 ± 778	3033 ± 128	921 ± 79	259 ± 36	121 ± 13
	gl	CG_{TMZ}	895 ± 63	2481 ± 178	604 ± 81	1263 ± 179	604 ± 81	3726 ± 490	4159 ± 1095	395 ± 96	474 ± 14	71 ± 25

		MWM_{TMZ}	1033	±	73	1582	±	226	568	±	33	4215	±	414	2949	±	716	6672	±	388	6037	±	147	499	±	80	283	±	30	118	±	9
Anterior olfactory cortex																															
	pe	CG_{TMZ}	643	±	65	1096	±	104	1381	±	130	3405	±	322	1381	±	130	2639	±	237	4653	±	286	485	±	31	1157	±	121	141	±	22
		MWM_{TMZ}	1050	±	66	1026	±	37	1019	±	90	5878	±	465	639	±	40	4215	±	189	5957	±	279	338	±	36	969	±	75	146	±	13
	m	CG_{TMZ}	1135	±	76	1651	±	108	1615	±	110	2371	±	144	1615	±	110	2517	±	302	5661	±	256	348	±	19	2211	±	147	228	±	46
		MWM_{TMZ}	1400	±	109	1280	±	77	1251	±	133	4763	±	664	483	±	45	3500	±	193	5875	±	274	325	±	37	1984	±	111	161	±	17
	d	CG_{TMZ}	1001	±	73	1622	±	118	1800	±	151	1937	±	117	1800	±	151	1929	±	271	5118	±	305	440	±	37	2366	±	172	182	±	57
		MWM_{TMZ}	1516	±	101	1606	±	125	1324	±	84	6361	±	535	497	±	33	3121	±	195	5624	±	251	244	±	23	1803	±	116	143	±	14
	pv	CG_{TMZ}	992	±	67	1978	±	87	1810	±	90	2281	±	248	1810	±	90	2394	±	270	5413	±	291	308	±	20	2121	±	182	191	±	38
		MWM_{TMZ}	1406	±	54	1477	±	73	1212	±	124	4960	±	409	402	±	53	3605	±	370	5447	±	269	239	±	18	1813	±	80	136	±	14
	l	CG_{TMZ}	1096	±	31	1538	±	56	1726	±	57	2511	±	217	1726	±	57	1859	±	44	6015	±	343	370	±	30	2328	±	177	115	±	8
		MWM_{TMZ}	1476	±	37	1281	±	64	1230	±	97	6834	±	572	496	±	32	3057	±	138	6097	±	141	320	±	48	1926	±	102	125	±	9
	e	CG_{TMZ}	571	±	58	1401	±	245	596	±	110	2259	±	406	596	±	110	1433	±	297	1920	±	268	306	±	22	1003	±	146	424	±	251
		MWM_{TMZ}	1215	±	79	809	±	78	1007	±	148	4822	±	685	491	±	83	2758	±	221	5259	±	262	309	±	30	1527	±	244	141	±	28
taenia tecta, dorsal																															
	I	CG_{TMZ}	1010	±	82	1112	±	124	1940	±	89	3977	±	269	1940	±	89	4117	±	284	6259	±	498	329	±	21	1446	±	121	240	±	32
		MWM_{TMZ}	1161	±	80	900	±	72	1264	±	170	7133	±	834	1690	±	153	5342	±	87	8146	±	131	262	±	19	1270	±	50	184	±	19
	II	CG_{TMZ}	1298	±	97	1323	±	72	1938	±	144	3096	±	243	1938	±	144	4273	±	276	6372	±	487	397	±	36	1861	±	153	257	±	25
		MWM_{TMZ}	1458	±	78	1263	±	95	1532	±	61	6537	±	693	1702	±	156	6488	±	198	7508	±	114	276	±	18	1730	±	84	190	±	19
	III	CG_{TMZ}	1070	±	68	1515	±	109	1592	±	148	2637	±	149	1592	±	148	4027	±	257	4570	±	308	343	±	17	1842	±	146	352	±	54
		MWM_{TMZ}	1254	±	89	1519	±	150	1288	±	119	5665	±	690	1479	±	151	6364	±	317	7846	±	131	284	±	18	1875	±	62	210	±	27
	IV	CG_{TMZ}	869	±	65	1629	±	93	1464	±	130	2204	±	43	1464	±	130	4265	±	340	4569	±	303	358	±	28	1461	±	129	520	±	102
		MWM_{TMZ}	1173	±	124	1737	±	134	1178	±	136	4938	±	661	1458	±	176	5658	±	352	6497	±	190	259	±	11	1901	±	85	264	±	27
taenia tecta, ventral																															
	I	CG_{TMZ}	911	±	72	895	±	86	1344	±	80	4467	±	244	1344	±	80	2651	±	315	6194	±	485	336	±	39	804	±	86	207	±	38

		MWM_{TMZ}	1013	±	67	559	±	65	721	±	128	5706	±	538	1354	±	129	4287	±	226	6683	±	183	215	±	8	724	±	91	150	±	23
	II	CG_{TMZ}	1309	±	95	1459	±	97	1622	±	112	3015	±	212	1622	±	112	3628	±	191	6484	±	440	347	±	29	1458	±	158	297	±	30
		MWM_{TMZ}	1331	±	89	1151	±	60	1125	±	113	6009	±	553	1492	±	88	5851	±	163	7668	±	307	248	±	22	1151	±	101	189	±	28
	III	CG_{TMZ}	1317	±	158	1613	±	113	1761	±	72	2542	±	108	1761	±	72	3102	±	268	6700	±	317	299	±	15	1770	±	142	456	±	80
		MWM_{TMZ}	1214	±	33	1836	±	61	1397	±	55	4824	±	432	1164	±	68	5721	±	197	7764	±	207	246	±	18	1439	±	79	238	±	26
Dorsal peduncular cortex																														
	I	CG_{TMZ}	938	±	86	1149	±	99	1834	±	91	4355	±	297	1834	±	91	4032	±	367	6697	±	801	377	±	42	1196	±	151	254	±	24
		MWM_{TMZ}	1085	±	72	997	±	75	1153	±	189	8934	±	491	2292	±	298	5949	±	524	8057	±	411	313	±	25	1140	±	79	210	±	15
	II/III	CG_{TMZ}	1282	±	132	1534	±	127	2051	±	130	3306	±	270	2051	±	130	4774	±	246	6946	±	484	448	±	42	1278	±	161	334	±	32
		MWM_{TMZ}	1210	±	93	1571	±	131	1378	±	171	8101	±	645	2484	±	150	7469	±	339	7232	±	442	339	±	21	1230	±	118	262	±	26
	V	CG_{TMZ}	984	±	33	1561	±	123	1789	±	164	2706	±	154	1789	±	164	4865	±	313	5520	±	352	480	±	48	1056	±	103	397	±	53
		MWM_{TMZ}	1073	±	76	1621	±	135	1183	±	122	7330	±	536	2420	±	163	7861	±	315	5360	±	493	319	±	22	1332	±	89	274	±	33
	VI	CG_{TMZ}	663	±	105	2172	±	194	1651	±	122	2379	±	206	1651	±	122	4377	±	271	4257	±	309	483	±	56	872	±	76	444	±	62
		MWM_{TMZ}	888	±	56	1560	±	168	1252	±	163	7513	±	512	2307	±	178	7357	±	313	4996	±	232	316	±	22	1296	±	98	271	±	20
Piriform cortex																														
	I	CG_{TMZ}	716	±	28	541	±	41	1352	±	76	4238	±	298	1352	±	76	4359	±	220	5448	±	451	575	±	29	827	±	87	140	±	24
		MWM_{TMZ}	768	±	82	537	±	55	940	±	55	8867	±	512	1712	±	127	6757	±	124	5577	±	88	419	±	30	533	±	53	119	±	10
	II	CG_{TMZ}	1597	±	16	828	±	43	1510	±	86	3122	±	261	1510	±	86	4128	±	117	5813	±	403	553	±	27	1219	±	115	209	±	19
		MWM_{TMZ}	1154	±	32	804	±	53	1142	±	82	7459	±	385	1633	±	117	6792	±	65	5852	±	210	433	±	33	846	±	43	135	±	11
	III	CG_{TMZ}	836	±	31	1018	±	63	1303	±	96	2355	±	191	1303	±	96	3776	±	167	4740	±	213	406	±	13	1162	±	92	352	±	47
		MWM_{TMZ}	1044	±	73	976	±	54	999	±	80	7131	±	247	1246	±	79	5914	±	168	4731	±	219	403	±	26	883	±	22	156	±	15
Entorhinal cortex, lateral																														
	I	CG_{TMZ}	833	±	69	420	±	18	1590	±	113	3497	±	231	1590	±	113	3663	±	342	7298	±	257	288	±	31	955	±	46	321	±	34
		MWM_{TMZ}	604	±	65	260	±	45	1309	±	80	8535	±	236	1414	±	149	4982	±	250	8916	±	414	433	±	38	998	±	75	391	±	42
	II	CG_{TMZ}	1724	±	108	743	±	47	2182	±	127	3732	±	285	2182	±	127	4989	±	274	9171	±	413	347	±	13	1502	±	126	450	±	39

	III	MWM_{TMZ}	1154	±	98	545	±	35	1738	±	157	7978	±	289	1888	±	135	6952	±	205	8773	±	502	455	±	33	1584	±	68	505	±	47
		CG_{TMZ}	2077	±	180	838	±	75	2283	±	121	3163	±	314	2283	±	121	4608	±	347	8659	±	580	301	±	8	1833	±	148	485	±	27
	IV	MWM_{TMZ}	1360	±	95	737	±	51	1921	±	143	7101	±	212	2024	±	136	7190	±	147	10159	±	613	329	±	28	1652	±	60	468	±	39
		CG_{TMZ}	2057	±	145	1051	±	87	2246	±	139	2801	±	255	2246	±	139	4172	±	257	8201	±	454	299	±	19	2057	±	165	367	±	28
	V	MWM_{TMZ}	1329	±	95	1021	±	94	1950	±	115	6810	±	400	1836	±	130	7111	±	142	9551	±	572	326	±	18	1821	±	101	447	±	36
		CG_{TMZ}	1991	±	139	1204	±	98	2102	±	115	2753	±	225	2102	±	115	3887	±	243	7713	±	370	330	±	19	2128	±	160	343	±	28
	VIa	MWM_{TMZ}	1354	±	69	1407	±	126	1770	±	106	6290	±	290	1512	±	102	7256	±	147	9200	±	600	341	±	20	1753	±	115	440	±	22
		CG_{TMZ}	1787	±	104	1809	±	203	1953	±	104	2618	±	225	1953	±	104	4149	±	285	7308	±	379	403	±	20	2273	±	157	423	±	50
	VIb	MWM_{TMZ}	1269	±	88	2300	±	236	1516	±	58	5977	±	393	1361	±	89	7666	±	159	8052	±	396	439	±	13	1730	±	118	641	±	80
		CG_{TMZ}	1400	±	94	1626	±	162	1545	±	85	1939	±	152	1545	±	85	3544	±	236	5483	±	299	479	±	14	2115	±	144	468	±	57
		MWM_{TMZ}	1109	±	113	2625	±	159	1442	±	69	4394	±	395	1173	±	87	6256	±	298	5517	±	220	509	±	32	1457	±	73	645	±	61
Entorhinal cortex, medial																														
	I	CG_{TMZ}	734	±	31	546	±	94	1207	±	98	3902	±	94	1207	±	98	4343	±	428	6908	±	485	382	±	45	1235	±	134	277	±	46
		MWM_{TMZ}	576	±	78	293	±	33	1193	±	174	6915	±	751	1329	±	139	5613	±	221	7819	±	646	293	±	20	1071	±	85	388	±	74
	II	CG_{TMZ}	1083	±	86	800	±	129	1730	±	90	3679	±	326	1730	±	90	5301	±	564	8155	±	542	443	±	46	1723	±	191	345	±	46
		MWM_{TMZ}	819	±	138	737	±	41	1590	±	265	7595	±	395	1691	±	92	7013	±	146	11511	±	404	384	±	35	1952	±	162	578	±	112
	III	CG_{TMZ}	1481	±	101	1124	±	70	1857	±	98	2841	±	379	1857	±	98	6209	±	355	8025	±	514	468	±	49	1891	±	170	375	±	47
		MWM_{TMZ}	1103	±	116	902	±	76	1784	±	205	7172	±	397	1778	±	78	7292	±	227	10520	±	483	409	±	27	1693	±	117	593	±	125
	IV	CG_{TMZ}	1569	±	125	1180	±	127	1862	±	133	2574	±	329	1862	±	133	6160	±	319	7842	±	642	499	±	54	2576	±	141	363	±	32
		MWM_{TMZ}	1293	±	50	1273	±	140	1698	±	150	6708	±	474	1754	±	96	7046	±	229	9765	±	560	381	±	30	2014	±	141	579	±	106
	V	CG_{TMZ}	1808	±	125	1484	±	186	1744	±	93	2484	±	291	1744	±	93	4559	±	453	6693	±	703	525	±	55	2855	±	160	333	±	29
		MWM_{TMZ}	1385	±	80	1728	±	151	1512	±	192	6369	±	392	1671	±	58	6676	±	215	9119	±	548	419	±	33	1886	±	167	507	±	84
	VI	CG_{TMZ}	1288	±	111	1593	±	188	1344	±	83	2049	±	190	1344	±	83	3875	±	338	5678	±	477	446	±	43	2354	±	210	403	±	62
		MWM_{TMZ}	1214	±	91	1465	±	172	1225	±	157	5219	±	485	1218	±	74	6650	±	339	6626	±	208	459	±	32	1933	±	89	485	±	74
Orbitofrontal cortex, medial																														

	I	CG_{TMZ}	1224	±	63	780	±	70	1700	±	60	5666	±	538	1575	±	148	4572	±	359	7686	±	394	481	±	32	654	±	56	91	±	12
		MWM_{TMZ}	1109	±	115	827	±	70	1251	±	121	11006	±	960	2448	±	126	6365	±	195	10866	±	610	506	±	35	532	±	27	189	±	23
	II	CG_{TMZ}	1243	±	121	865	±	103	1804	±	51	4886	±	433	2126	±	153	5588	±	252	7979	±	587	578	±	45	639	±	33	194	±	41
		MWM_{TMZ}	1332	±	191	1005	±	68	1532	±	52	10459	±	904	2650	±	160	8216	±	372	10009	±	587	605	±	31	451	±	34	195	±	23
	II/III	CG_{TMZ}	1046	±	58	1300	±	220	1720	±	79	3926	±	445	2027	±	192	5587	±	480	7063	±	480	586	±	37	595	±	40	260	±	51
		MWM_{TMZ}	1323	±	137	1213	±	143	1339	±	72	9293	±	865	2622	±	200	8718	±	353	8164	±	479	613	±	32	378	±	23	235	±	30
	V	CG_{TMZ}	1043	±	85	1465	±	235	1678	±	83	3303	±	320	1840	±	206	5614	±	549	6365	±	473	487	±	31	533	±	33	280	±	40
		MWM_{TMZ}	1092	±	76	1175	±	119	1144	±	125	8938	±	833	2451	±	225	8945	±	334	6551	±	325	555	±	39	354	±	9	254	±	46
	VI	CG_{TMZ}	999	±	95	1617	±	262	1574	±	70	2922	±	226	1672	±	188	5250	±	589	6295	±	502	500	±	53	504	±	32	245	±	25
		MWM_{TMZ}	966	±	61	1374	±	121	1160	±	60	7819	±	746	1904	±	158	9273	±	442	6249	±	415	452	±	31	310	±	16	264	±	40
Orbitofrontal cortex, ventrolateral																														
	I	CG_{TMZ}	1137	±	112	757	±	28	1892	±	46	4288	±	414	1892	±	46	5273	±	331	6877	±	632	549	±	38	693	±	58	154	±	24
		MWM_{TMZ}	1022	±	129	755	±	44	1095	±	111	10354	±	725	3047	±	184	8272	±	317	9802	±	567	513	±	45	551	±	40	169	±	15
	II/III	CG_{TMZ}	1015	±	42	789	±	59	1853	±	78	4557	±	426	1853	±	78	5052	±	220	7041	±	638	523	±	25	554	±	22	147	±	38
		MWM_{TMZ}	1182	±	133	814	±	38	1279	±	45	10528	±	831	3090	±	200	8581	±	218	8711	±	509	542	±	46	346	±	24	141	±	11
	V	CG_{TMZ}	967	±	76	1152	±	167	1660	±	115	3955	±	390	1660	±	115	5834	±	345	6804	±	550	520	±	38	475	±	26	205	±	34
		MWM_{TMZ}	1053	±	69	819	±	52	1108	±	106	9797	±	764	2886	±	338	9822	±	341	6977	±	539	558	±	39	291	±	16	151	±	15
	VI	CG_{TMZ}	941	±	68	1395	±	173	1552	±	102	3188	±	307	1552	±	102	5199	±	502	6032	±	453	512	±	42	433	±	17	270	±	18
		MWM_{TMZ}	951	±	67	1249	±	126	1094	±	94	8172	±	677	2338	±	262	9934	±	327	5732	±	294	448	±	39	328	±	25	196	±	19
Orbitofrontal cortex, lateral																														
	I	CG_{TMZ}	1077	±	102	695	±	34	1797	±	42	4781	±	312	1797	±	42	4802	±	364	6584	±	420	461	±	27	731	±	18	148	±	32
		MWM_{TMZ}	1096	±	105	597	±	38	1178	±	122	13218	±	971	3134	±	156	8028	±	323	8541	±	185	426	±	39	534	±	40	168	±	7
	II/III	CG_{TMZ}	1018	±	108	708	±	51	1808	±	87	3899	±	284	1808	±	87	5876	±	456	7363	±	535	542	±	47	608	±	52	182	±	25
		MWM_{TMZ}	943	±	80	805	±	55	1253	±	54	10073	±	773	2891	±	252	9655	±	356	7283	±	524	428	±	17	394	±	19	145	±	15
	V	CG_{TMZ}	1013	±	100	1123	±	179	1774	±	70	3339	±	272	1774	±	70	5949	±	484	6262	±	459	593	±	52	541	±	37	260	±	40

	VI	MWM_{TMZ}	987	±	94	1105	±	105	1277	±	79	8693	±	713	2450	±	246	9707	±	332	6497	±	478	451	±	28	304	±	10	171	±	16
		CG_{TMZ}	915	±	88	1329	±	157	1682	±	83	2845	±	241	1682	±	83	5007	±	441	6031	±	491	575	±	31	444	±	20	287	±	27
		MWM_{TMZ}	953	±	69	1352	±	120	1117	±	115	7854	±	586	1947	±	155	9303	±	492	6191	±	400	488	±	40	324	±	24	206	±	20
Olfactory tubercle																														
	I	CG_{TMZ}	681	±	47	890	±	74	938	±	62	4681	±	274	938	±	62	2382	±	183	3595	±	449	241	±	44	850	±	95	4979	±	564
		MWM_{TMZ}	416	±	58	275	±	18	205	±	76	7981	±	204	1359	±	188	2779	±	185	3790	±	327	181	±	17	460	±	49	5767	±	235
	II	CG_{TMZ}	1176	±	94	1287	±	84	1361	±	97	3884	±	323	1361	±	97	3533	±	249	5163	±	579	284	±	34	1246	±	138	5997	±	879
		MWM_{TMZ}	733	±	56	956	±	65	569	±	65	8318	±	383	1655	±	215	4740	±	394	6038	±	440	213	±	14	596	±	66	7237	±	168
	III	CG_{TMZ}	1072	±	70	1481	±	115	1450	±	81	2914	±	201	1450	±	81	3342	±	196	4853	±	546	271	±	13	1436	±	172	4190	±	566
		MWM_{TMZ}	859	±	66	1268	±	61	764	±	40	6513	±	408	1290	±	204	5572	±	356	4529	±	338	236	±	22	703	±	58	6254	±	253

Supp. Tab. 42: Statistical analysis of the comparison of layer-specific receptor concentrations of CG_{TMZ} versus MWM_{TMZ}

Significant differences between receptor densities between the olfactory layers of mice with suppressed adult neurogenesis (CG_{TMZ}) and trained mice with suppressed adult neurogenesis (MWM_{TMZ}). Each receptor type was tested with non-parametric Mann-Whitney-U test. The percentage difference in absolute receptor concentrations (first column), Z-value (negative: group MWM_{TMZ} is significantly higher; positive: group CG_{TMZ} is significantly higher; middle column), p-value (right column).

CG_{TMZ} | MWM_{TMZ}	AMPA			Kainate			NMDA			$mGlu_{2/3}$			$GABA_A$		
	%	*Z*	*p-value*	%	*Z*	*p-value*	%	*Z*	*p-value*	%	*Z*	*p-value*	%	*Z*	*p-value*
MOB gr	-14,33	-0,87	0,39	-20,96	-1,55	0,12	46,85	3,21	0,00	-39,93	-3,74	0,00	-10,08	-0,87	0,39
MOB ipl	-37,20	-2,53	0,01	-11,61	-2,23	0,02	2,71	0,26	0,80	-43,32	-3,74	0,00	11,56	0,72	0,48
MOB mi	-24,01	-1,70	0,09	-33,39	-3,52	0,00	21,75	2,53	0,01	-45,47	-3,59	0,00	-31,67	-3,29	0,00
MOB opl	-23,01	-1,93	0,05	-3,75	-0,11	0,91	36,04	2,53	0,01	-42,07	-3,52	0,00	-16,76	-2,68	0,01
MOB gl	-24,66	-1,93	0,05	25,22	3,06	0,00	70,29	3,29	0,00	-22,14	-2,31	0,02	-33,96	-2,68	0,01
MOB onl	-24,66	-1,10	0,28	86,10	3,29	0,00	153,81	3,52	0,00	18,87	1,55	0,12	-5,45	-0,57	0,58
AOB gr	-13,45	0,11	0,91	16,09	2,91	0,00	-15,81	-0,79	0,44	-26,38	-2,00	0,04	-87,87	-3,74	0,00
AOB mi	2,77	0,42	0,68	30,84	3,06	0,00	46,82	2,76	0,00	-40,56	-3,75	0,00	3,53	0,42	0,68
AOB gl	-0,74	-0,80	0,44	137,57	2,69	0,01	25,56	1,32	0,19	-50,56	-1,40	0,18	-64,50	-1,48	0,14
AON pe	-49,47	-3,52	0,00	17,10	1,40	0,17	41,89	3,14	0,00	-42,72	-2,99	0,00	5,58	0,04	0,97
AON m	-30,36	-1,55	0,12	20,97	2,16	0,03	14,82	1,63	0,11	-41,85	-3,67	0,00	35,14	1,17	0,25
AON d	-28,73	-2,38	0,01	-4,66	-0,94	0,35	12,06	1,55	0,12	-58,43	-3,74	0,00	32,21	1,25	0,22
AON pv	-40,68	-2,53	0,01	11,50	1,17	0,25	45,69	3,67	0,00	-51,46	-3,59	0,00	36,67	1,55	0,12
AON l	-27,26	-2,08	0,04	6,88	0,87	0,39	5,01	0,26	0,80	-57,02	-3,29	0,00	-16,42	-1,32	0,19
TTd I	-2,25	-0,04	0,97	17,04	1,02	0,31	66,32	3,29	0,00	-33,02	-2,68	0,01	2,15	0,04	0,97
TTd II	-8,94	-0,64	0,53	-7,91	-1,02	0,31	19,37	1,32	0,19	-49,71	-3,74	0,00	17,96	1,02	0,31
TTd III	-17,53	-1,55	0,12	-17,24	-1,47	0,14	-8,82	-1,10	0,28	-48,97	-3,74	0,00	24,03	1,32	0,19
TTd IV	-21,32	-1,85	0,06	-18,29	-1,63	0,11	8,52	0,64	0,53	-43,06	-3,74	0,00	13,15	0,49	0,63

TTv I	7,08	1,10	0,28	24,03	1,40	0,17	177,94	3,74	0,00	-23,32	-1,17	0,25	-9,73	-0,34	0,74
TTv II	-2,29	0,11	0,91	9,43	1,17	0,25	49,79	3,14	0,00	-49,44	-3,21	0,00	-12,73	-0,49	0,63
TTv III	11,84	0,79	0,44	-7,51	-0,79	0,44	51,30	3,52	0,00	-52,74	-3,74	0,00	-6,88	-0,34	0,74
OT I	36,75	2,08	0,04	160,54	3,06	0,00	221,08	3,74	0,00	-40,61	-3,74	0,00	11,54	1,10	0,28
OT II	43,63	1,93	0,05	21,71	0,94	0,35	115,15	3,74	0,00	-49,04	-3,74	0,00	-15,35	-0,94	0,35
OT III	56,02	3,14	0,00	26,62	1,70	0,09	110,14	3,74	0,00	-55,71	-3,74	0,00	-16,99	-1,93	0,05
DP I	-30,26	-2,91	0,00	8,47	0,94	0,35	31,97	2,15	0,03	-41,05	-3,74	0,00	-29,48	-2,53	0,01
DP II/III	3,07	0,04	0,97	3,92	0,49	0,63	23,90	1,63	0,11	-56,54	-3,74	0,00	-23,78	-2,08	0,04
DP V	-36,96	-3,75	0,00	7,49	0,57	0,58	22,32	1,63	0,11	-61,02	-3,74	0,00	-27,37	-2,31	0,02
DP VI	-25,33	-2,00	0,04	66,97	3,06	0,00	59,45	3,06	0,00	-49,08	-3,74	0,00	-18,84	-2,08	0,04
PIR I	19,05	2,31	0,02	43,47	2,23	0,02	43,00	2,99	0,00	-54,24	-3,75	0,00	-17,36	-1,17	0,25
PIR II	73,47	3,74	0,00	8,13	1,02	0,31	33,76	2,46	0,01	-50,47	-3,74	0,00	-12,62	-1,02	0,31
PIR III	-27,27	-3,59	0,00	7,07	0,72	0,48	31,17	2,08	0,04	-54,70	-3,74	0,00	-5,61	-0,34	0,74
ENT I I	39,69	2,46	0,01	61,59	3,59	0,00	10,40	1,02	0,31	-60,80	-3,74	0,00	-12,10	-1,02	0,31
ENT I II	34,17	2,91	0,00	28,26	2,61	0,01	9,29	1,25	0,22	-54,21	-3,74	0,00	-7,39	-1,47	0,14
ENT I III	54,33	3,37	0,00	5,54	0,42	0,68	2,84	0,26	0,80	-57,18	-3,74	0,00	-14,87	-2,00	0,04
ENT I IV	67,36	3,67	0,00	-7,46	-0,49	0,63	6,36	0,72	0,48	-58,47	-3,74	0,00	-18,10	-2,84	0,00
ENT I V	89,04	3,67	0,00	-19,40	-1,93	0,05	8,62	0,79	0,44	-52,74	-3,06	0,00	-27,32	-3,06	0,00
ENT I VIa	40,62	2,46	0,01	-28,36	-2,46	0,01	13,49	1,55	0,12	-51,34	-3,52	0,00	-26,66	-2,99	0,00
ENT I VIb	26,49	1,78	0,08	-39,92	-3,67	0,00	22,88	2,38	0,01	-48,71	-3,67	0,00	-29,22	-2,68	0,01
ENT m I	14,09	1,10	0,28	42,58	2,69	0,01	-6,06	-0,87	0,39	-47,81	-3,75	0,00	-25,05	-2,31	0,02
ENT m II	-4,87	-0,26	0,80	0,95	0,64	0,53	-7,30	-0,57	0,58	-55,16	-3,74	0,00	-17,48	-1,17	0,25
ENT m III	12,79	1,48	0,14	28,98	2,77	0,00	-13,76	-2,76	0,00	-61,33	-3,74	0,00	-3,18	-0,04	0,97
ENT m IV	5,11	1,32	0,19	11,08	0,64	0,53	-4,76	-0,26	0,80	-63,09	-3,74	0,00	-11,93	-0,87	0,39
ENT m V	28,69	2,23	0,02	-13,58	-1,17	0,25	3,50	0,11	0,91	-61,60	-3,74	0,00	-21,27	-1,93	0,05
ENT m VI	15,66	1,55	0,12	-12,47	-1,10	0,28	-1,99	0,11	0,91	-59,55	-3,74	0,00	-14,15	-1,93	0,05

ORB m I	-5,58	-0,57	0,58	16,84	1,25	0,22	55,09	3,74	0,00	-34,37	-3,29	0,00	-29,19	-2,38	0,01
ORB m II	-9,15	-0,34	0,74	13,24	1,10	0,28	19,16	2,46	0,01	-42,54	-3,74	0,00	-10,76	-1,17	0,25
ORB m II/III	-24,35	-2,23	0,02	44,76	1,32	0,19	6,20	0,79	0,44	-54,93	-3,74	0,00	-19,13	-1,63	0,11
ORB m V	-13,25	-0,94	0,35	62,58	1,63	0,11	2,71	-0,04	1,00	-54,00	-3,74	0,00	-17,74	-1,40	0,17
ORB m VIa	-9,89	-0,11	0,91	32,79	1,25	0,22	12,39	1,32	0,19	-57,80	-3,74	0,00	-8,28	-0,64	0,53
ORB vl I	-2,91	-0,04	0,97	1,78	0,64	0,53	32,28	3,74	0,00	-53,26	-3,74	0,00	-47,96	-3,74	0,00
ORB vl II/III	-14,56	-1,02	0,31	8,19	0,79	0,44	19,89	3,14	0,00	-49,19	-3,75	0,00	-35,50	-3,37	0,00
ORB vl V	-10,60	-0,79	0,44	60,59	1,63	0,11	9,04	1,17	0,25	-51,20	-3,74	0,00	-34,59	-2,84	0,00
ORB vl VIa	-6,19	-0,34	0,74	19,50	1,02	0,31	11,27	1,25	0,22	-52,46	-3,74	0,00	-15,38	-1,10	0,28
ORB l I	3,89	0,49	0,63	10,17	1,17	0,25	33,05	3,74	0,00	-50,17	-3,74	0,00	-46,60	-3,67	0,00
ORB l II/III	1,36	0,19	0,85	6,94	0,72	0,48	36,13	3,29	0,00	-51,47	-3,74	0,00	-35,54	-3,44	0,00
ORB l V	-3,35	0,34	0,74	19,80	0,42	0,68	29,58	3,29	0,00	-52,30	-3,74	0,00	-33,68	-3,74	0,00
ORB l VIa	-16	-0,49	0,63	9,23	0,26	0,80	30,85	2,83	0,00	-54,20	-3,74	0,00	-11,31	-0,72	0,48
CG_{TMZ} | MWM_{TMZ}	$GABA_{A(BZ)}$			$GABA_B$			α_1			α_2			$D_{1/5}$		
	%	*Z*	*p-value*	%	*Z*	*p-value*	%	*Z*	*p-value*	%	*Z*	*p-value*	%	*Z*	*p-value*
MOB gr	-38,68	-3,29	0,00	36,77	3,59	0,00	-5,26	-1,02	0,31	19,50	1,70	0,09	-24,30	-1,85	0,06
MOB ipl	-52,29	-3,74	0,00	62,96	3,74	0,00	-29,58	-3,59	0,00	51,81	3,60	0,00	-49,88	-3,53	0,00
MOB mi	-56,96	-3,74	0,00	32,71	3,52	0,00	-28,32	-3,21	0,00	57,34	2,68	0,01	-54,39	-3,53	0,00
MOB opl	-31,88	-2,99	0,00	64,65	3,75	0,00	7,02	0,64	0,53	39,47	3,06	0,00	-48,33	-3,21	0,00
MOB gl	-29,19	-3,74	0,00	-46,66	-3,59	0,00	-6,30	-1,40	0,17	45,62	3,36	0,00	-32,70	-2,16	0,03
MOB onl	-17,24	-2,68	0,01	202,23	3,36	0,00	62,58	3,74	0,00	84,90	3,59	0,00	-25,78	-0,95	0,35
AOB gr	530,39	3,74	0,00	6,81	1,10	0,28	7,76	1,47	0,14	195,06	3,59	0,00	-39,59	-2,61	0,01
AOB mi	-36,81	-3,74	0,00	18,48	2,53	0,01	-23,29	-2,69	0,01	20,66	1,17	0,25	-29,98	-0,87	0,39
AOB gl	-43,11	-3,14	0,00	-63,01	-3,74	0,00	-20,70	-0,72	0,48	45,32	3,60	0,00	-21,34	0,11	0,91
AON pe	-39,43	-3,36	0,00	-18,31	-2,76	0,00	5,00	0,04	0,97	-0,80	-0,04	0,97	9,27	0,42	0,68
AON m	-7,31	-0,72	0,48	-3,62	-0,11	0,91	-0,96	-0,04	0,97	-16,71	-1,63	0,11	85,09	2,46	0,01

AON d	-37,20	-3,06	0,00	-21,57	-3,52	0,00	54,09	2,83	0,00	-15,04	-1,78	0,08	40,40	1,63	0,11
AON pv	-18,51	-1,17	0,25	-10,51	-2,16	0,03	8,96	0,72	0,48	-16,98	-1,85	0,06	81,76	2,61	0,01
AON l	-44,12	-3,67	0,00	-3,21	-0,64	0,53	23,32	2,08	0,04	-5,79	-0,57	0,58	18,51	2,61	0,01
TTd l	-20,60	-2,00	0,04	-19,19	-2,24	0,02	0,47	-0,19	0,85	17,79	1,40	0,17	31,49	1,78	0,08
TTd II	-26,71	-2,83	0,00	-20,56	-2,76	0,00	12,51	1,10	0,28	-1,70	0,26	0,80	22,33	1,85	0,06
TTd III	-27,39	-3,29	0,00	-38,60	-3,74	0,00	0,68	0,49	0,63	-8,79	-0,87	0,39	39,58	1,63	0,11
TTd IV	-30,21	-2,99	0,00	-25,09	-3,29	0,00	14,11	1,32	0,19	-33,68	-3,06	0,00	87,70	2,61	0,01
TTv l	-40,53	-3,60	0,00	41,92	2,99	0,00	68,57	3,14	0,00	-11,52	-0,49	0,63	22,38	1,17	0,25
TTv II	-33,10	-3,74	0,00	12,49	1,63	0,11	23,59	1,78	0,08	6,17	0,34	0,74	54,53	2,76	0,00
TTv III	-41,16	-3,74	0,00	14,83	2,31	0,02	3,06	0,57	0,58	21,68	1,32	0,19	95,15	3,06	0,00
OT l	-3,16	-0,19	0,85	60,41	2,68	0,01	61,03	1,32	0,19	63,46	2,61	0,01	10,06	0,87	0,39
OT II	-17,10	-1,32	0,19	40,72	2,15	0,03	30,79	1,10	0,28	65,92	2,76	0,00	-8,69	-0,87	0,39
OT III	-41,59	-3,29	0,00	37,89	1,55	0,12	11,34	0,49	0,63	78,26	2,76	0,00	-23,18	-2,91	0,00
DP l	-32,88	-3,29	0,00	-9,48	-1,32	0,19	-7,21	-0,34	0,74	2,72	0,19	0,85	6,13	0,42	0,68
DP II/III	-39,76	-3,74	0,00	4,49	0,42	0,68	18,87	1,32	0,19	-12,01	-1,10	0,28	43,25	2,68	0,01
DP V	-41,53	-3,74	0,00	-1,64	-0,19	0,85	10,51	0,49	0,63	-37,30	-3,59	0,00	87,01	2,91	0,00
DP VI	-42,19	-3,44	0,00	-10,55	-1,10	0,28	7,08	-0,04	0,97	-46,47	-3,74	0,00	74,85	2,61	0,01
PIR l	-33,87	-3,67	0,00	6,44	0,42	0,68	1,59	0,19	0,85	49,60	2,38	0,01	18,04	0,87	0,39
PIR II	-37,60	-3,74	0,00	8,14	0,87	0,39	-2,09	-0,26	0,80	18,68	1,02	0,31	59,79	3,59	0,00
PIR III	-41,15	-3,74	0,00	-5,14	-1,25	0,22	-11,18	-1,93	0,05	18,44	1,02	0,31	116,05	3,44	0,00
ENT l l	-13,96	-1,47	0,14	-25,41	-3,29	0,00	-20,78	-1,63	0,11	-11,96	-1,63	0,11	10,28	0,79	0,44
ENT l II	-21,35	-2,76	0,00	-15,56	-2,61	0,01	-20,78	-3,52	0,00	-14,36	-1,40	0,17	32,18	2,23	0,02
ENT l III	-35,58	-3,59	0,00	-22,92	-2,76	0,00	-20,73	-3,52	0,00	-10,65	-1,10	0,28	26,90	2,31	0,02
ENT l IV	-47,07	-3,74	0,00	-25,84	-3,29	0,00	-11,41	-1,63	0,11	-7,26	-0,26	0,80	-5,60	-0,34	0,74
ENT l V	-50,76	-3,74	0,00	-26,97	-3,44	0,00	-7,89	-1,02	0,31	4,61	0,72	0,48	-9,47	-0,87	0,39

ENT l VIa	-49,70	-3,74	0,00	-20,82	-3,06	0,00	-11,39	-1,40	0,17	8,56	0,72	0,48	-11,77	-0,94	0,35
ENT l VIb	-49,21	-3,74	0,00	-3,73	-0,79	0,44	-10,16	-2,08	0,04	12,30	1,25	0,22	-19,58	-1,40	0,17
ENT m I	-4,96	0,26	0,80	-10,54	-1,32	0,19	24,13	1,55	0,12	1,03	-0,04	1,00	-33,11	-1,70	0,09
ENT m II	-17,09	-1,32	0,19	-15,85	-2,54	0,01	7,33	0,87	0,39	-6,40	-0,26	0,80	-35,13	-1,93	0,05
ENT m III	-7,40	-1,10	0,28	-16,62	-2,76	0,00	11,91	1,17	0,25	-9,22	-0,87	0,39	-23,37	-1,40	0,17
ENT m IV	-10,03	-2,00	0,04	-16,98	-2,46	0,01	29,68	1,63	0,11	14,28	1,85	0,06	-23,06	-2,68	0,01
ENT m V	-37,56	-3,29	0,00	-21,98	-2,08	0,04	13,74	1,02	0,31	21,09	2,76	0,00	-27,91	-2,53	0,01
ENT m VI	-46,29	-3,59	0,00	-20,54	-2,38	0,01	-18,40	-2,61	0,01	12,81	1,25	0,22	-15,17	-0,87	0,39
ORB m I	-31,93	-2,91	0,00	-10,99	-0,94	0,35	-13,31	-1,55	0,12	8,78	0,87	0,39	-60,19	-2,99	0,00
ORB m II	-34,48	-3,36	0,00	-9,46	-1,02	0,31	-11,16	-1,10	0,28	8,74	0,64	0,53	-9,11	-0,64	0,53
ORB m II/III	-39,36	-3,59	0,00	-18,36	-2,08	0,04	-16,52	-2,16	0,03	15,69	1,32	0,19	17,36	0,42	0,68
ORB m V	-35,97	-3,14	0,00	-8,24	-0,79	0,44	-22,60	-2,99	0,00	12,58	1,32	0,19	29,91	1,55	0,12
ORB m VIa	-38,44	-3,21	0,00	1,60	-0,11	0,91	-4,94	-0,42	0,68	11,89	0,79	0,44	-4,08	-0,19	0,85
ORB vl I	-35,53	-3,52	0,00	-24,57	-2,31	0,02	-17,12	-1,78	0,08	-7,35	-0,42	0,68	-0,21	0,42	0,68
ORB vl II/III	-46,85	-3,74	0,00	-18,05	-1,63	0,11	-14,98	-2,00	0,04	0,43	0,87	0,39	28,48	0,26	0,80
ORB vl V	-36,31	-3,67	0,00	-3,88	-0,34	0,74	-17,24	-1,85	0,06	-4,71	-0,34	0,74	46,06	1,93	0,05
ORB vl VIa	-37,87	-3,44	0,00	1,64	0,04	1,00	-6,70	-0,64	0,53	7,53	1,10	0,28	29,59	2,76	0,00
ORB l I	-30,96	-3,06	0,00	-16,67	-2,08	0,04	-1,42	-0,72	0,48	7,11	2,38	0,01	-6,61	-0,42	0,68
ORB l II/III	-40,73	-3,74	0,00	8,29	0,72	0,48	-3,94	-0,57	0,58	12,17	1,17	0,25	13,14	1,63	0,11
ORB l V	-36,66	-3,74	0,00	10,70	1,32	0,19	10,50	0,26	0,80	24,54	2,00	0,04	44,90	2,16	0,03
ORB l VIa	-41,91	-3,74	0,00	-0,39	-0,72	0,48	-1,74	-0,19	0,85	10,42	1,32	0,19	17,31	1,47	0,14